(1)

[redacted]

[redacted]

[redacted]

Volume IV: Acrylic Windows

[redacted]

J. D. Sinclair

NAVAL OCEAN SYSTEMS CENTER

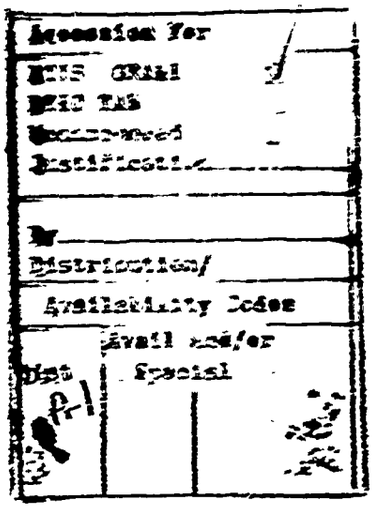

Ocean Engineering Studies

Compiled 1990

Volume IV: Acrylic Windows—
Long-Term Pressurization

J. D. Stachiw

PUBLISHED BY
NAVAL OCEAN SYSTEMS CENTER
SAN DIEGO, CALIFORNIA

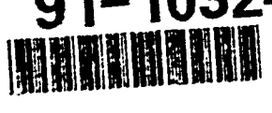

Foreword

For successful operation, all manned diving systems, submersibles, and hyperbaric chambers require pressure-resistant viewports. These viewports allow the personnel inside the diving bells and submersibles to observe the environment outside the pressure-resistant hulls. In addition, on land, operators of hyperbaric chambers can observe the behavior of patients or divers undergoing hyperbaric treatment inside the chambers.

Since the viewports form a part of the pressure-resistant envelope, they must meet or surpass the safety criteria used for designing either the metallic or plastic composite pressure envelope. The ASME Boiler and Pressure Vessel Code Section 8 provides such design criteria, and the chambers/pressure hulls designed on their basis have generated an unexcelled safety record.

The viewports, because of the unique structural properties of the acrylic plastic used in constructing the windows, could not be designed according to the same criteria as for the pressure envelopes fabricated of metallic or plastic composite materials. To preclude potential catastrophic failures of windows designed on the basis of inadequate data, in 1965, the U.S. Navy initiated a window testing program at the Naval Civil Engineering Laboratory and the Naval Ocean Systems Center. Under this program, window testing was conducted until 1975.

The objective of the window testing program was to generate test data concerning the structural performance of acrylic-plastic windows fabricated in different shapes, sizes, and thicknesses. Candidates for investigation included the effect of major design parameters, like the thickness to diameter ratio, bevel angle of bearing surfaces, and the ratio of window diameter to seat-opening diameter on the structural performance of the windows; and empirical relationships were to be formulated between these variables and the critical pressures at which windows fail. To make the test results realistic, the test conditions were varied to simulate the in-service environment that the windows were to be subjected. Thus, during testing, the windows were subjected not only to short-term pressurization at room temperature, but also to long-term sustained and repeated pressurization at different ambient temperatures.

On the basis of these data, empirical relationships were formulated between design parameters and test conditions. Committees in the Pressure Technology Codes of the American Society of Mechanical Engineers subsequently incorporated these relationships into the Safety Standard for Pressure Vessels for Human Occupancy (ASME PVHO-1 Safety Standard). Since that time, this ASME Safety Standard has formed the basis — worldwide — for designing acrylic windows in pressure chambers for human occupancy. Their performance record is excellent; since the publication of the Safety Standard in 1977, no catastrophic failures have been recorded that resulted in personal injury.

The data generated by the Navy's window testing program were originally disseminated in technical reports of the Naval Civil Engineering Laboratory and the Naval Ocean Systems Center, and were made available to the general public through the Defense Technical Information Center. To facilitate distribution of these data to users inside and outside of the Department of Defense, the technical reports have been collected and are being reissued as volumes of the U.S. Navy Ocean Engineering Studies.

These volumes, containing the collected technical reports on pressure-resistant plastic windows, will be deposited in technical libraries of Naval Laboratories and universities with ocean engineering programs. This dissemination of collected data should significantly reduce the effort currently being expended by students, engineers, and scientists in their search for data dispersed among the many reports published over a 10-year period by several Naval activities.

Volume IV of the Ocean Engineering Series is a compilation of four technical reports that focus on the structural performance of acrylic windows, shaped as conical frustums, under long-term pressurization. The deformation and crack initiation are noted and recorded as a function of pressure magnitude and duration of loading. The pressure and duration of loading described in the reports apply directly to conical frustum windows of any size, with an identical t/Di ratio; while the displacements must be multiplied by a scale factor based on the ratio of minor diameters on the test and operational windows.

J. D. Stachiw
Marine Materials Office
Ocean Engineering Division

23 * Acrylic windows, * Hemispherical shells, * Conical bodies.

A

TABLE OF CONTENTS: VOLUME IV

R645

Technical Report

WINDOWS FOR EXTERNAL OR INTERNAL HYDROSTATIC PRESSURE VESSELS—PART IV.

Conical Acrylic Windows Under Long-Term Pressure Application at 20,000 Psi

October 1969

Sponsored by

NAVAL FACILITIES ENGINEERING COMMAND

U. S. NAVAL CIVIL ENGINEERING LABORATORY

Port Hueneme, California

WINDOWS FOR EXTERNAL OR INTERNAL HYDROSTATIC PRESSURE VESSELS—PART IV. Conical Acrylic Windows Under Long-Term Pressure Application at 20,000 Psi

Technical Report R-645

YF 38.535.005.01.005

by

J. D. Stachiw

ABSTRACT

Conical acrylic windows of 30-, 60-, 90-, 120-, and 150-degree included angles have been subjected in their mounting flanges to 20,000 psi of hydrostatic pressure for up to 1,000 hours in the 32°F-to-75°F temperature range. The displacements of the windows through the flange mounting have been recorded and are graphically presented as a function of time, temperature, conical angle, and thickness-to-diameter ratio for the ready reference of the designer. A detailed study has also been made of the types of failure and of the dimensional and structural parameters that must be considered in the design of safe, operationally acceptable windows for long-term service under hydrostatic pressure of 20,000 psi.

The test results indicate that a minimum thickness to minor diameter ratio of 2 and an included conical angle of 90 degrees or larger is required to provide safe and optically acceptable windows for long-term sustained pressure loadings of 20,000 psi.

CONTENTS

INTRODUCTION

Previous studies on acrylic windows at the Naval Civil Engineering Laboratory[1-3] have shown that the short-term critical pressure of conical acrylic windows for deep-submergence applications is a function of their temperature, conical angle, as well as their thickness-to-minor-diameter ratio (hereafter referred to as t/D ratio). No effort has been made to determine what influence the duration of pressure loading has on the critical pressure of acrylic windows, although there have been indications that acrylic windows will fail when subjected to lower hydrostatic pressure for long periods of time.

Since ocean bottom structures equipped with acrylic windows will be subjected to hydrostatic pressure for long periods, it is important to generate design criteria that will permit the design of safe windows for long-term submergence. These criteria are also important in the design of windows for internal pressure vessels (Figure 1) in which long-term hydrostatic tests are performed. It was to generate such design data that the present study was conducted.

The objective of the study was to determine the following experimentally for conical acrylic windows under 20,000-psi hydrostatic loading:

1. The effect of loading duration on the initiation and propagation of cracks and fracture planes in windows of different t/D ratios and angles.

2. The effect of loading duration on the magnitude and rate of axial displacement as well as plastic deformation of low- and high-pressure faces of windows with different t/D ratios, and conical angles.

3. The effect of temperature on time-dependent displacement.

4. The dimensions required for windows of different conical angles that are to serve as optically acceptable windows for a minimum of 1,000 hours of service under 20,000-psi hydrostatic pressure.

The objectives of the study were to be met by pressurizing to 20,000 psi a series of small-scale conical acrylic windows with 30-, 60-, 90-, 120-, and 150-degree angles and $0.75 \leqslant t/D \leqslant 2.0$ ratios; that pressure would be maintained for up to 1,000 hours while the displacements of the windows

and crack growth in the acrylic were noted. It was clearly understood that some of the windows would be ejected in less than 1,000 hours, while others would still be serviceable after this period. Empirical relationships between the structural behavior of the window, duration of hydrostatic loading, and dimensional parameters could be established by comparing the magnitude of displacement, time of crack initiation, rate of crack propagation, or time to catastrophic failure at different temperatures for windows of different conical angles and t/D ratios. In addition the influence of temperature on the behavior of the acrylic under long-term loading could be determined. For some window t/D ratios that have been tested previously under short-term loading, a measure of strength degradation could be obtained by comparing the r short-term critical pressure to duration of loading prior to failure at 20,000 psi. Furthermore, by extrapolating the displacements of windows that withstood 1,000-hour pressurization, a reasonable prediction can be made on their displacement at a duration of pressure loading longer than 1,000 hours.

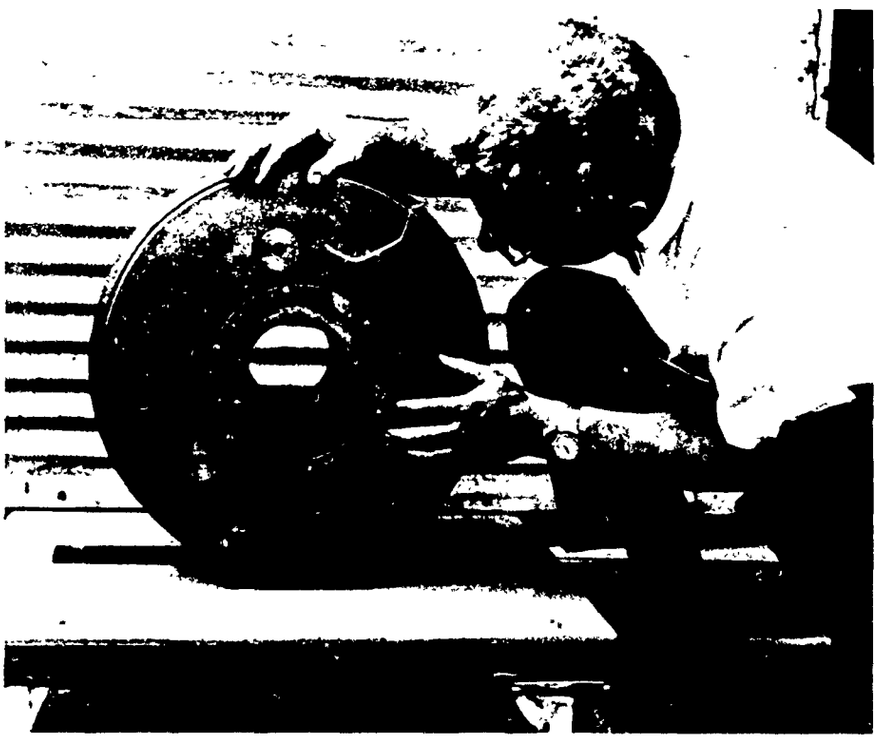

Figure 1. Window installed in end closure of 18-inch (inside diameter) pressure vessel for observation of test specimens.

TEST SPECIMENS

More than 150 model conical acrylic windows of 1-inch minor diameter (Figure 2), machined from commercial Plexiglas G grade acrylic plate stock served as test specimens. The test plan is shown in Table 1. The thickness-to-diameter ratio of these windows varied from 0.75 to 2.0, while the conical angle ranged from 30 degrees to 150 degrees in 30 degree intervals. For each thickness-to-diameter ratio and conical angle, at least five specimens were to be tested. The range of data from these tests would permit the designer utilizing this data to judge the repeatability of window behavior and specify the appropriate safety factor accordingly. The model window test specimens were made to fit the window-mounting flanges used in the previous study for the determination of critical pressure of windows under short-term pressure loading. For this reason, the minor diameter of the window (Figure 3) was selected to be 1 inch with a plus or minus 0.005-inch tolerance on the diameter. The conical angle of the windows was held to a tolerance of plus or minus 15 minutes. The actual thickness of the windows, which was the same as that of commercially supplied acrylic plates with standard manufacturing thickness tolerance, differed considerably from their nominal thickness. By utilizing the full thickness of respective acrylic plates, no machining and subsequent polishing was required on most of the windows' light-transmitting surfaces. The conical bearing surfaces, machined to a 32-rms finish, when covered with grease sealed the windows in the flange.

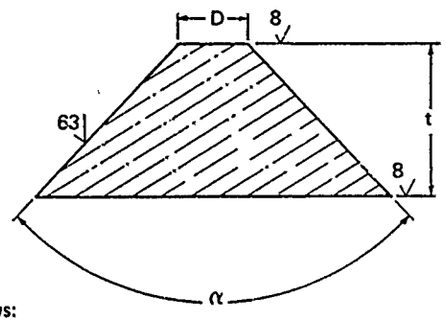

Material: Plexiglas G

Nomenclature

D = minor diameter (in.)
t = thickness (in.)
α = included conical angle (deg)

Dimensions

1. For 1-in.-diam windows:
   - D = 1.0; tolerance = ±0.005
   - t = nominal 3/4, 7/8, 1, 1-1/4, 1-1/2, 1-3/4, and 2 (manufacturer's plate thickness tolerances apply)
   - α = 30, 60, 90, 120, or 150; tolerance = ±15'
2. For 4-in.-diam windows:
   - D = 4.0; tolerance = ±0.010
   - t = nominal 4 (manufacturer's plate thickness tolerances apply)
   - α = 30, 60, or 90; tolerance = ±15'

Figure 2. Dimensions of typical conical window specimens.

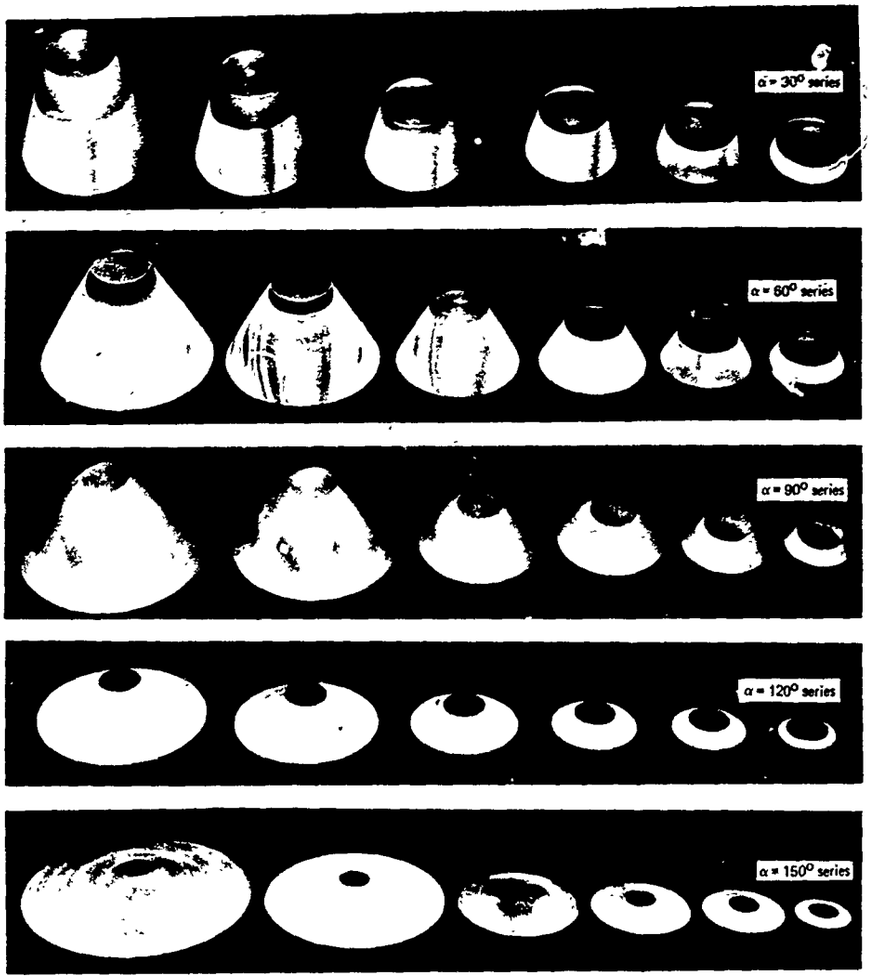

Figure 3. Typical conical acrylic windows of 1-inch minor diameter used in the experimental program.

In addition to the 1-inch-diameter model windows, 4-inch-diameter windows (30-, 60-, and 90-degree included angles) of 1.0 t/D ratio were fabricated. These full-scale windows were later subjected to a pressure loading identical to that of the 1-inch-diameter windows (Table 1). The objective was to compare the displacement and crack propagation of the large and the small windows and to determine whether the displacements and magnitudes of cracks of the large windows are in proportion to their diameter. If such a relationship is established for the 30-, 60-, and 90-degree windows, a reasonable assurance exists that the cracks and displacements of large windows with other conical angles under long-term loading can be predicted on the basis of the measured cracks and displacements of 1-inch-diameter windows of the same conical angle.

Table 1. Test Plan for Conical Acrylic Windows Subjected to 20,000 Psi of Hydrostatic Pressure for 1,000 Hours

(X represents a group of five test specimens; D = minor diameter.)

Thickness, t (in.)	Included Angle									
	30°		60°		90°		120°		150°	
	D = 1.0	D = 4.0	D = 1.0	D = 4.0	D = 1.0	D = 4.0	D = 1.0	D = 4.0	D = 1.0	D = 4.0
5/8 (0.625)			X							
3/4 (0.75)			X		X		X		X	
7/8 (0.875)	X		X		X		X		X	
1 (1.0)	X		X		X		X		X	
1-1/4 (1.25)	X		X		X		X			
1-1/2 (1.5)	X		X		X		X			
1-3/4 (1.75)	X		X		X		X			
2 (2.0)	X		X		X		X		X	
4 (4.0)		X		X		X				

TEST SETUP

Window Flanges

The test specimens with 1-inch minor diameter were mounted in steel flanges (Figures 4 and 5) designed to fit into 16-inch naval gunsheds converted to pressure vessels.[4] The flanges (Figures 6 and 7) for the 4-inch-diameter windows on the other hand were designed to fit the end closure of the 18-inch-diameter high-pressure vessel. The steel flanges were of sufficient thickness to insure that very little flange deformation occurred during application of hydrostatic pressure to the window's high-pressure face. It can, therefore, be assumed that for all practical purposes the window flanges were rigid and only the acrylic windows were deformed during the pressurization.

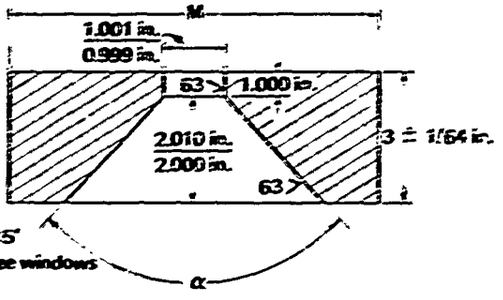

Nomenclature

M = external flange diameter (in.)
k = overall window flange thickness (in.)
α = included conical angle (deg)

Dimensions

α = 30, 60, 90, 120 and 150; tolerance = ±5°
M = 8 ± 1/64 for 30-, 60-, 90-, and 120-degree windows
17 ± 1/64 for 150-degree windows

Material: 1015 steel

Figure 4. Dimensions of typical window mounting flanges for 1-inch-diameter conical windows.

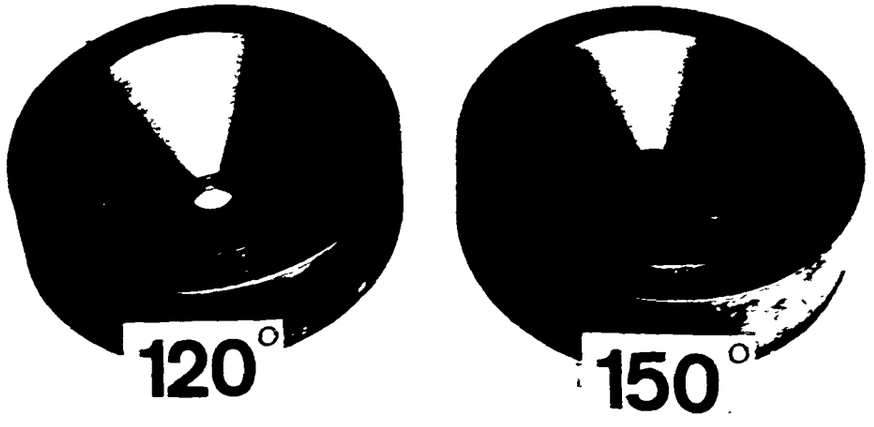

Figure 5. Typical flanges for 1-inch-diameter conical window.

Nomenclature

M = external flange diameter (in.)
L = overall flange thickness (in.)
k = cylindrical passage length (in.)
α = included conical angle (deg)

Dimensions

α = 30, 60, or 90; tolerance = ±5°
M = 9±1/64 for 30- and 60-degree windows
17-3/4±1/64 for 90-degree windows
k = 8±1/64 for 30- and 60-degree windows
1±1/64 for 90-degree windows
L = 12±1/64 for 30- and 60-degree windows
5±1/64 for 90-degree windows

Material: 4130 steel

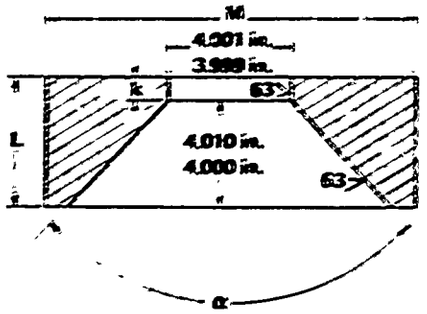

Figure 6. Dimensions of typical window mounting flanges for 4-inch-diameter conical windows.

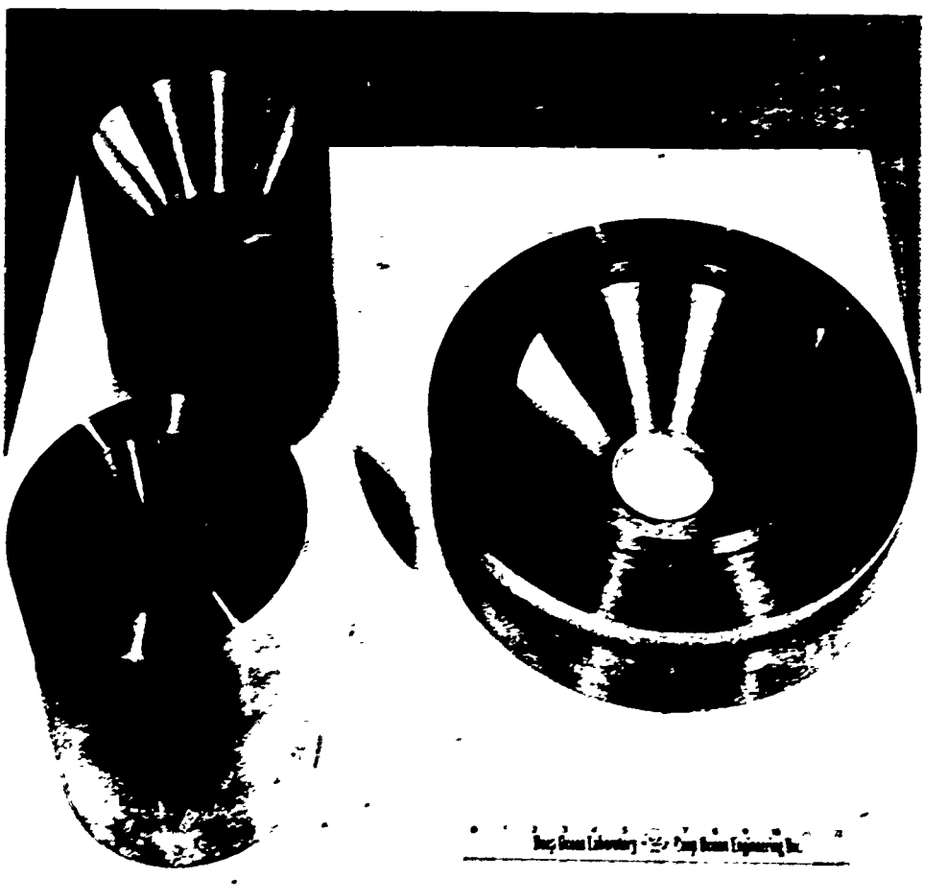

Figure 7. Typical flanges for 4-inch-diameter conical windows.

To standardize the window displacement tests, all windows and flanges were designed to have the minor diameter of the conical frustum window always equal to the minor diameter of the window cavity in the flange. Thus, the low-pressure face was flush with the bottom of the conical cavity in the flange (Figure 4), while the high-pressure face of the window extended to different elevations in the conical flange cavity, depending on the window's thickness. The special feature of these conical window flanges, designated previously as DOL 1 mounting configuration,[1] was the termination of the conical cavity in a cylindrical section that would act as a radial restraint on the extruding portion of the window (Figure 4). The length of the cylindrical section varied from flange to flange, depending on the window's angle and t/D ratio. In all cases, however, the section was designed to be long enough so that the extruded acrylic plug would be radially supported along its whole length.

The DOL 1 mounting configuration is not the only, or for that matter, the optimum configuration for conical acrylic windows under hydrostatic pressure. To date two other mounting configurations, DOL 2 and DOL 5 (Figure 8), have been conceived and briefly experimented with.[1] The difference between the two other mounting configurations and the configuration which has been selected for this study lies primarily in the degree and type of support afforded by the flange to the bearing surfaces of the window when the whole window displaces axially under hydrostatic loading. In case of DOL 1 flange configuration, the portion of the window displaced past the bottom of the conical flange seat receives radial support from the walls of the cylindrical cavity. The DOL 2 flange gives no support at all to the extruding portion of the window, while the DOL 5 flange gives both radial and axial support to the displaced portion of the window. When some short-term exploratory experiments were conducted previously with the three different types of flange configurations, it was noticed that most windows tested in DOL 5 flange had the highest implosion pressures; those tested in DOL 2 flange the lowest pressures. The magnitude of the beneficial effect associated with the DOL 5 flange varies with the position of the window in the flange, the included conical angle, t/D ratio, temperature, and type of hydrostatic loading. Since the relationship between these variables for any given window in this study is not known, the DOL 5 flange was not chosen for the study. It would be an additional variable affecting the rate of displacement and critical pressure, thus making it impossible to compare on a standard basis the structural response to long-term loading of acrylic windows with different t/D ratios and conical angles. The DOL 2 flange was not even considered for this experimental study as it is known to be inferior to the two other flange configurations.

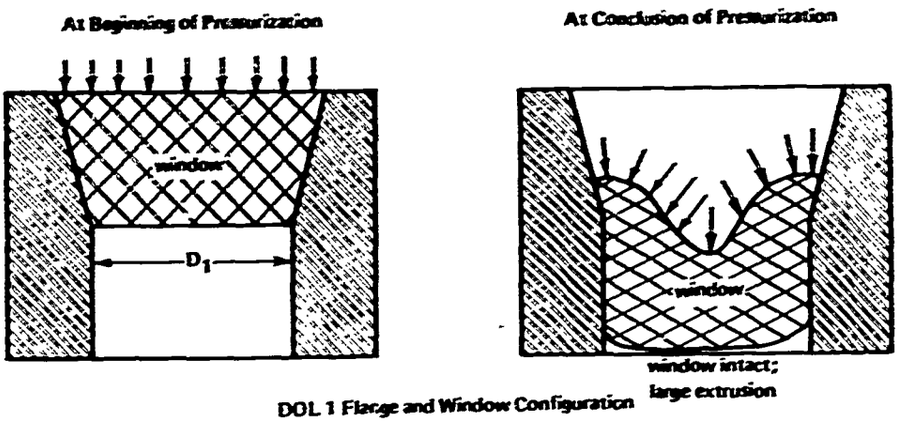

DOL 1 Flange and Window Configuration

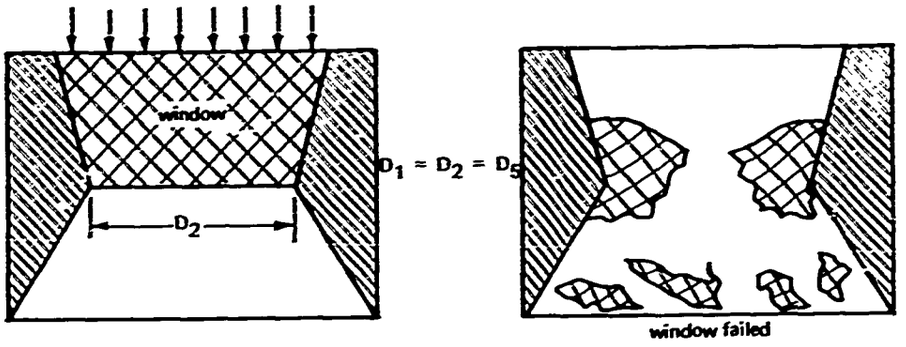

DOL 2 Flange and Window Configuration

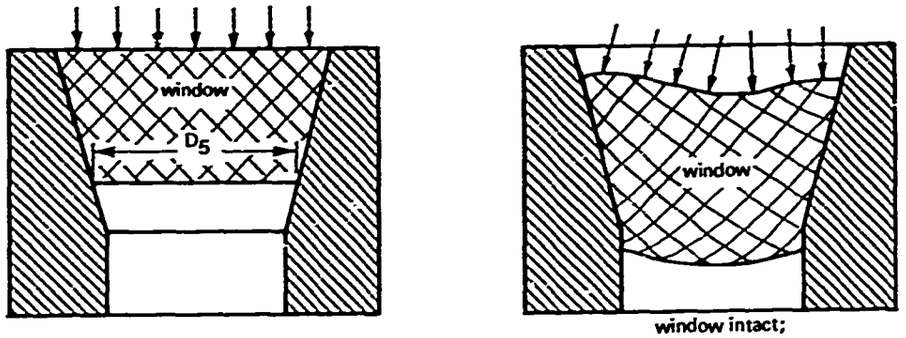

DOL 5 Flange and Window Configuration

Note: All windows of same t/D ratio pressurized to same pressure.

Figure 8. Window mounting configurations for conical windows.

PRESSURE VESSELS

The vessels used in this study were the converted 16-inch naval gun shells with a 9.4-inch internal diameter and the larger vessel with an 18-inch internal diameter. The safe operational pressure capability of both vessels is 20,000 psi, and their end closures are provided with threaded openings to which the window flanges could be attached. The flanges were mated to the end closures of pressure vessels in such a manner that the low-pressure face of the window was under the opening in the flange and thus exposed to atmospheric pressure, while the high-pressure face was acted upon by the pressurized water inside the vessel (Figure 9). By such an arrangement the same pressure differential was generated that exists on a window in a submerged structure, or on a window in an internal pressure vessel.

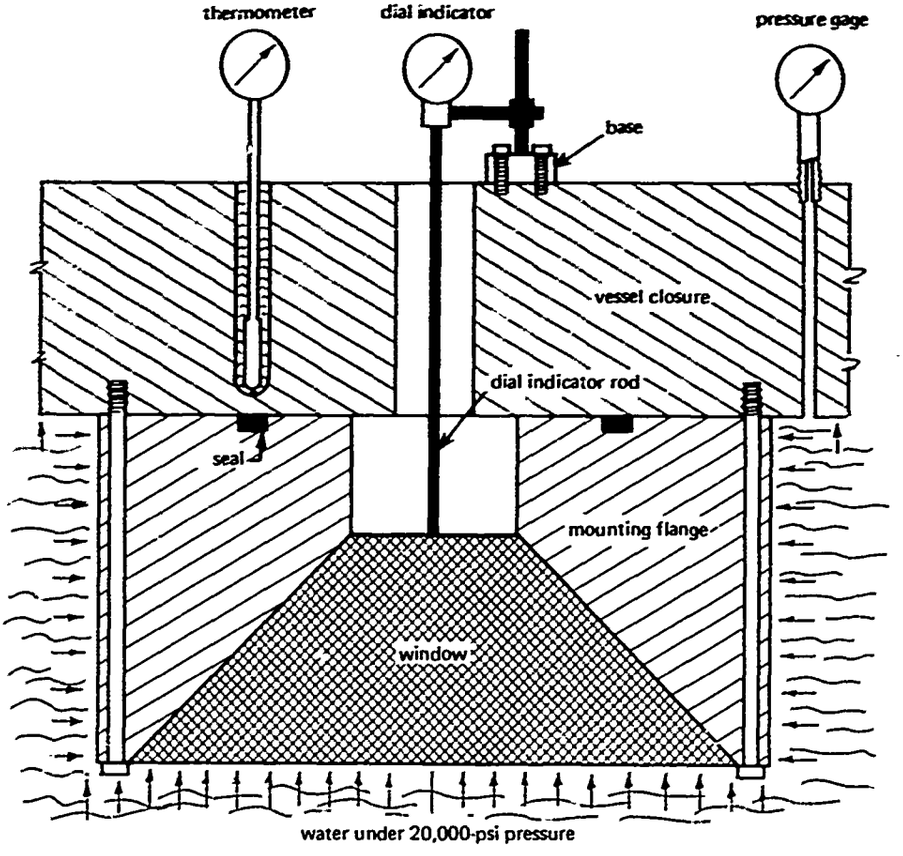

Figure 9. Schematic of window test arrangement.

All of the pressure vessels used contained a sufficient volume of compressed water at 20,000 psi to prevent the small, day-to-day displacements of the windows through the flange opening from decreasing the pressure inside the vessel by more than 50 psi. Also, the compressed water in the pressure vessel, and the stressed wall of the vessel contained sufficient potential energy to eject the window once it became so fractionated by cracks and fracture planes as to loose its structural integrity. This feature of the pressure vessels was of great importance, as it permitted locking 20,000 psi of pressure inside the vessel for unattended operation.

INSTRUMENTATION

The instrumentation for the long-term pressure testing of acrylic windows consisted of a pressure gage, a displacement indicator, and a thermometer (Figure 9). The Bourdon type pressure gage measured the hydrostatic pressure inside the vessel with ±50 psi accuracy, the mechanical dial type displacement indicator measured with 0.001-inch accuracy the displacement of the center of window's low-pressure face, while the remote-reading Bourdon tube thermometer registered with $\pm 0.5^{o}C$ accuracy the temperature of the water wetting the high-pressure face of the window.

TEST PROCEDURE

The conical bearing surfaces of the windows were liberally coated with silicone grease. After insertion of the window into the conical flange cavity (Figure 10), a force of approximately 30 pounds was applied to the window's high-pressure face to squeeze out most of the grease from between the window and the flange. Subsequently the whole test assembly, consisting of the end closure with window flange and window was placed into the proper vessel prefilled with water and locked in place. The preparations for testing were completed by mounting of the mechanical dial type displacement indicator on the end closure. The dial indicator was mounted in such a manner that the rod of the indicator protruded through the opening in the end closure and rested firmly on the center of the window's low-pressure face (Figure 11).

Figure 10. Installation of a 4-inch-diameter 90-degree conical window into flange mounted on the end closure of the 18-inch-internal-diameter vessel.

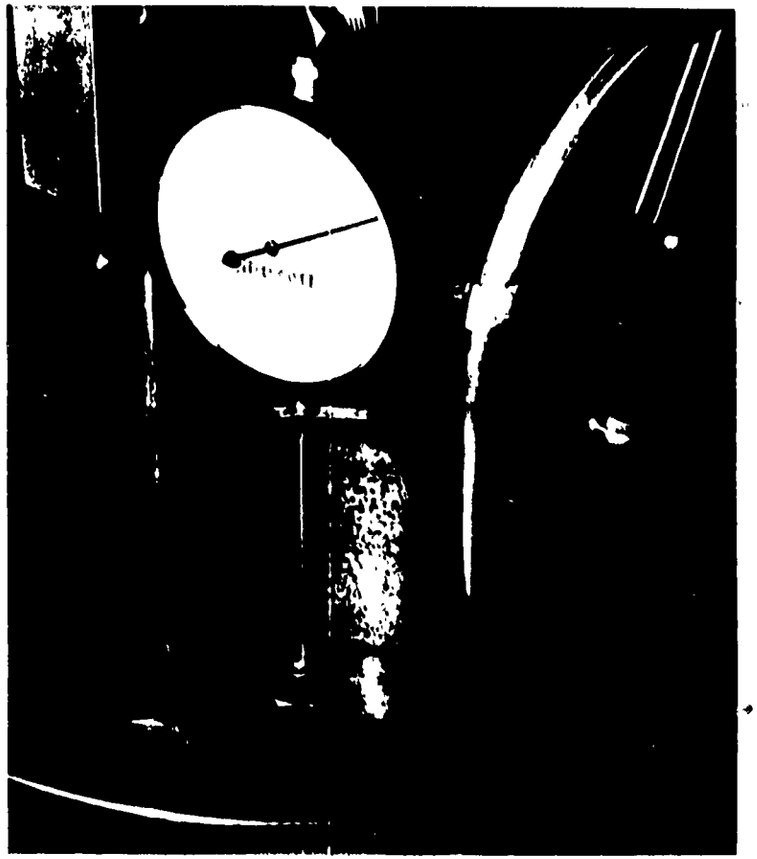

Figure 11. Typical dial indicator installation on the end closure of a converted 16-inch naval gun shell for measurement of window displacement through the flange.

The first step in the pressurization procedure of the window was to pressurize the vessel to 1,000 psi and hold it at that pressure for 1 hour. After 1 hour the pressure was dropped to zero and the dial displacement indicator was reset to zero reading. This operational procedure insured that the window was not bearing against a thick layer of grease, and that the displacements of the window recorded during following pressurization to 20,000 psi would be a measure of window deformation, rather than settlement.

The pressurization to 20,000-psi pressure level was conducted at 600-to-700-psi/min rate, and the displacement readings were taken at 1,000-psi pressure increments. After the pressure inside the vessel reached 20,000 psi, the pumps were stopped, and the valve controlling the flow of water to the vessel was closed. This operation concluded the pressurization of the windows to their long-term operational pressure.

Some of the windows were subjected to 20,000 psi of hydrostatic pressure for 500 hours, while others were kept at that pressure for 1,000 hours. In this manner the damage to the windows could be observed at two discrete time intervals, one of them being twice as long as the other. The pressure inside the vessels fluctuated as much as plus or minus 100 psi, depending on the temperature of the ambient atmosphere. Moderate effort was made to control the temperature of the water. Its temperature fluctuated from $18^{o}C$ to $23^{o}C$, depending on the season of the year, and the time of day. Displacement, pressure, and temperature readings were taken three times a day. When the readings were taken, the pressure inside the vessel was also readjusted if it differed by more than 100 psi from the set pressure of 20,000 psi. Such readjustments were very rare, and occurred either when some minor leaks occurred in a hydraulic system or a temperature change of more than $2^{o}C$ took place.

The reasons for choosing room temperature as the environment for long-term testing of windows are twofold. First, it imposes a more detrimental environment for extrusion of plastic windows because the mechanical strength and viscosity of acrylic plastic in this temperature range are less[5] than at temperatures in $32^{o}F$-to-$40^{o}F$ range generally found in the deep ocean. Second, when acrylic plastic is used as viewport material in high-pressure vessels, such vessels will probably be operated at room temperature.

However, in order to have some indication of what change in window displacement occurs when the temperature of the pressurizing medium is in the $30^{o}F$-to-$35^{o}F$ temperature range commonly found in abyssal depths, a group of 4-inch-diameter 90-degree windows with t/D = 1.0 has been subjected to 1,000 hours of pressurization at 20,000 psi at that temperature.

After the windows were maintained at 20,000-psi pressure for the desired time interval, the pressure was dropped to zero at a 100-psi/min rate. After the pressure reached the zero-psi level, the end closure was removed from the pressure vessel, and the window inspected for damage. From each group of five identical test specimens one was carefully photographed both on the low- and high-pressure faces to record the extent of cracking as well as permanent deformation of the window surfaces (Appendix A). To give the prospective window designers a feel for the magnitude of cold flow cratering on the window's high-pressure face a rectangular grid was optically superimposed on the window's face and the window was photographed. The same operation was conducted in many cases for photographing of the extended low-pressure faces.

Details on the design of window and flange systems are presented in Appendix B and window displacement histories are described in Appendix C.

DATA REDUCTION

The data resulting from testing more than 200 windows at 20,000-psi hydrostatic pressure for time periods between 500 to 1,000 hours are presented in this report pictorially (Appendix A) and graphically (Appendix C). For the hydrospace engineer designing window/flange systems, the average magnitude of window displacement for a given t/D ratio and conical angle has been plotted, as well as the scatter between the five individual window test specimens comprising each test group (Appendix C). The photographic record of crack and fracture plane location and magnitude is presented in Appendix A for all t/D ratios and angles, as it is impossible to foresee which one will be selected by an engineer for design study, or by a scientist for fracture mechanics study.

Although such detailed representation of test results is an absolute necessity for the detailed design of window/flange systems, only a general overview of window displacement as a function of t/D ratio and conical angle is needed for technical feasibility and preliminary design studies. For such applications, the details of experimental data tend to obscure the general trends of the relationship between displacements and the main structural parameters of the window/flange system.

To provide an overview, typical window deformation patterns (Figures 12-18) illustrate general trends of window behavior under long-term load. In addition, test results have been abstracted, averaged, and presented in summary form for ready reference in Figures 19 through 21. When referring to these figures, it is important to remember that they represent average displacement values without any indication of data scatter; to determine scatter one must refer to figures in Appendix C.

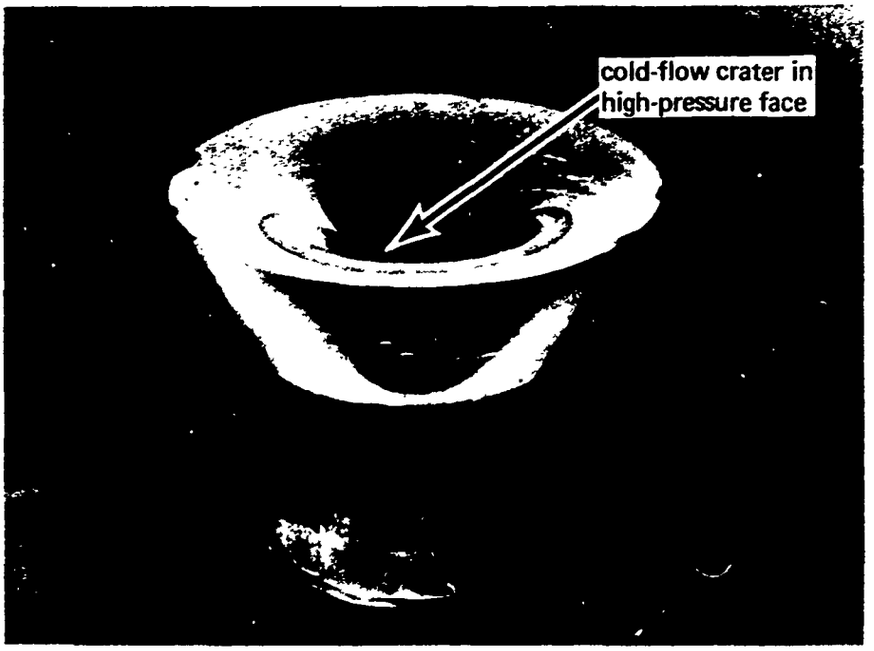

(a) Typical cold-flow cratering on window's high-pressure face.

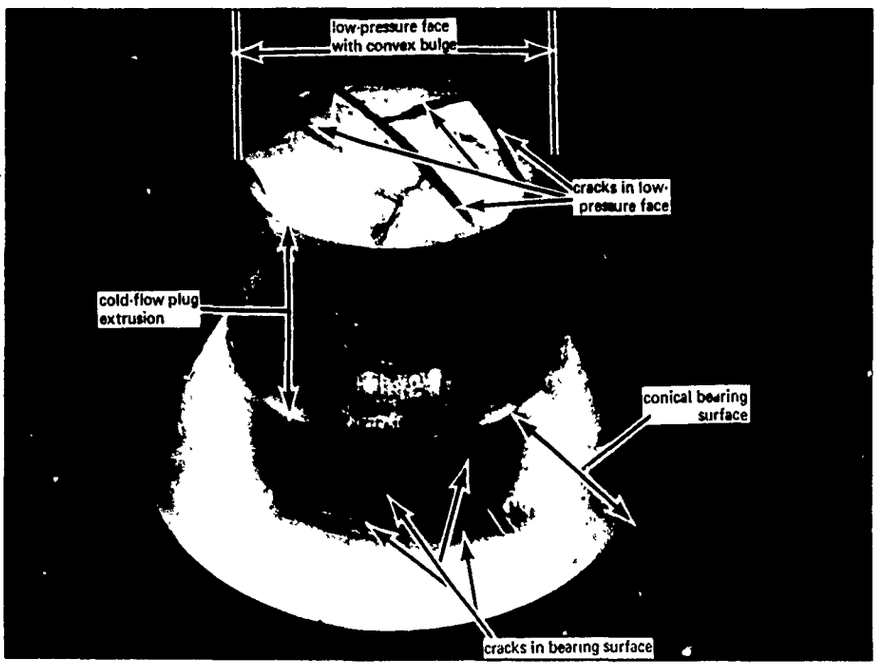

(b) Typical cold-flow plug extrusion of window's low-pressure face.

Figure 12. One-inch-diameter x 0.75-inch-thick, 60-degree conical angle window after 1,000-hour sustained pressure loading at 20,000 psi.

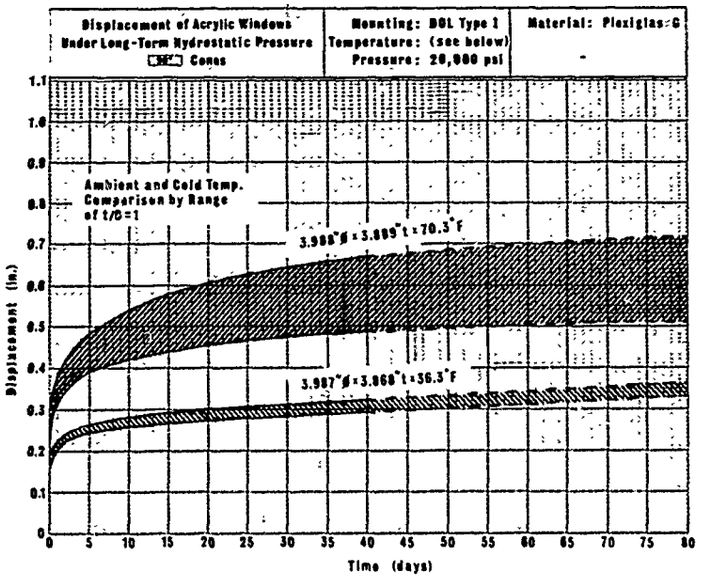

Figure 13a. Comparison of displacements on 4-inch-diameter acrylic windows of 90-degree conical angle and 1.0 t/D ratio.

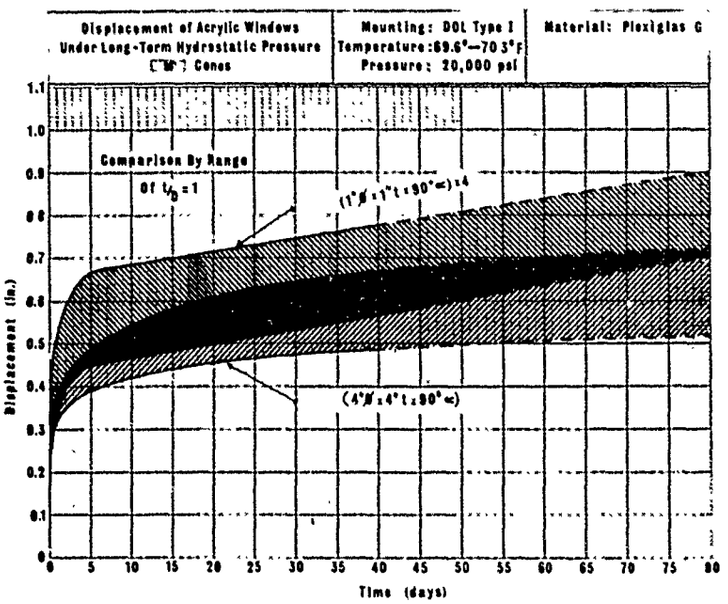

Figure 13b. Comparison of displacements on 1- and 4-inch-diameter acrylic windows of 90-degree conical angle and 1.0 t/D ratio. (Displacements of 1-inch-diameter windows have been multiplied by a factor of 4.)

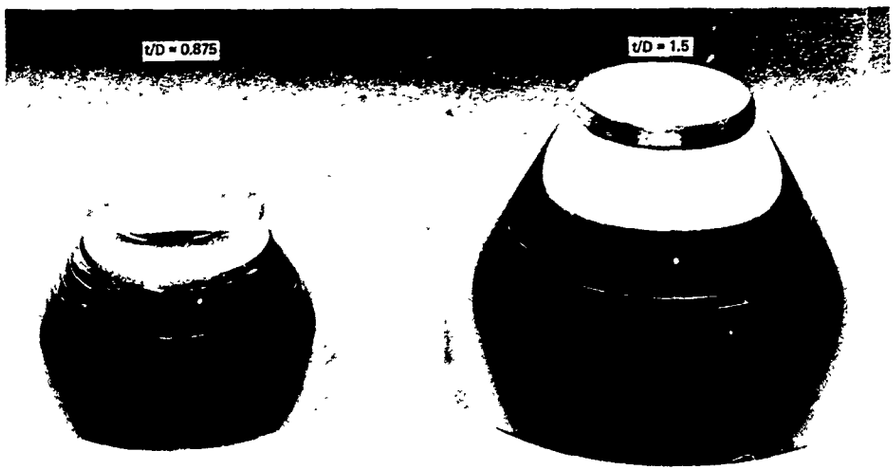

(a) Comparison of plug extrusions.

(b) Comparison of cold-flow craters.

Figure 14. One-inch-diameter, 60-degree conical windows after 500-hour sustained loading at +20,000 psi and 70°F.

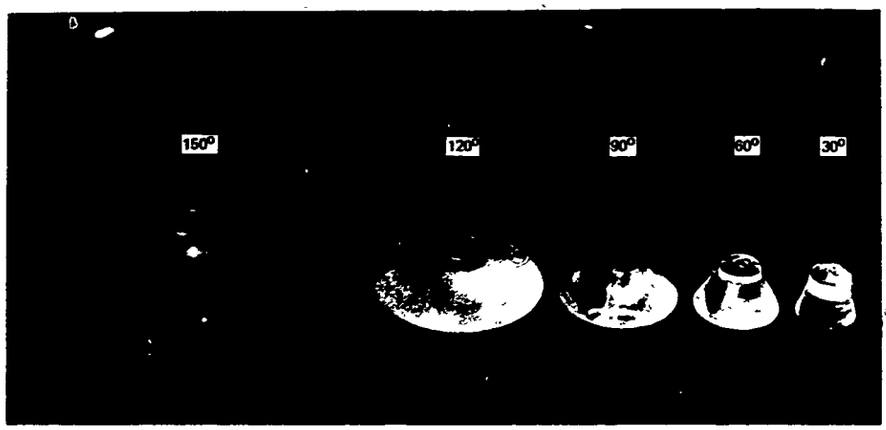

(a) Comparison of plug extrusions.

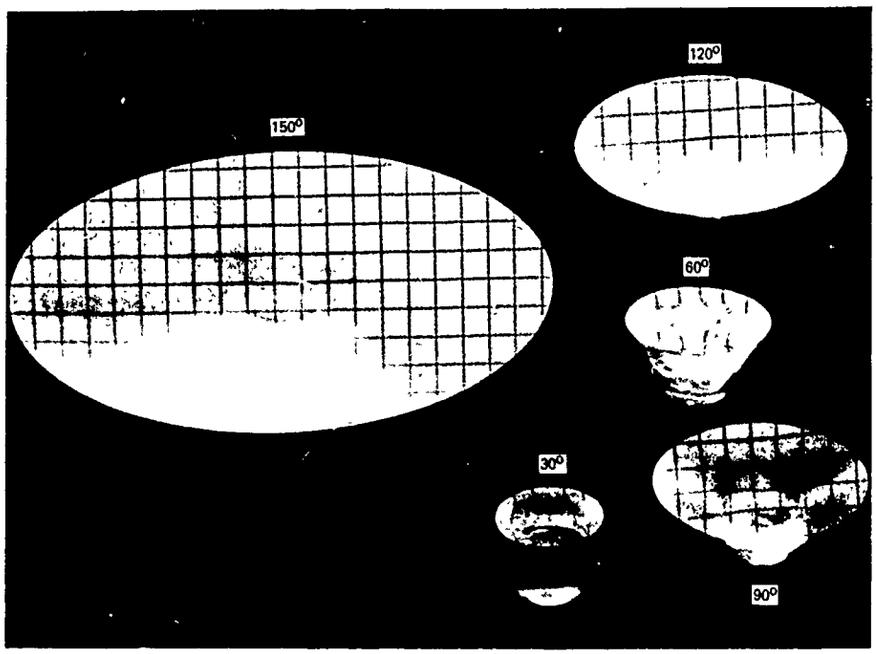

(b) Comparison of cold-flow craters.

Figure 15. One-inch-diameter windows with t/D = 1.0 and different conical angles after sustained loading at 20,000 psi for 1,000 hours in 65°F-to-75°F temperature range.

(a) Comparison of plug extrusions.

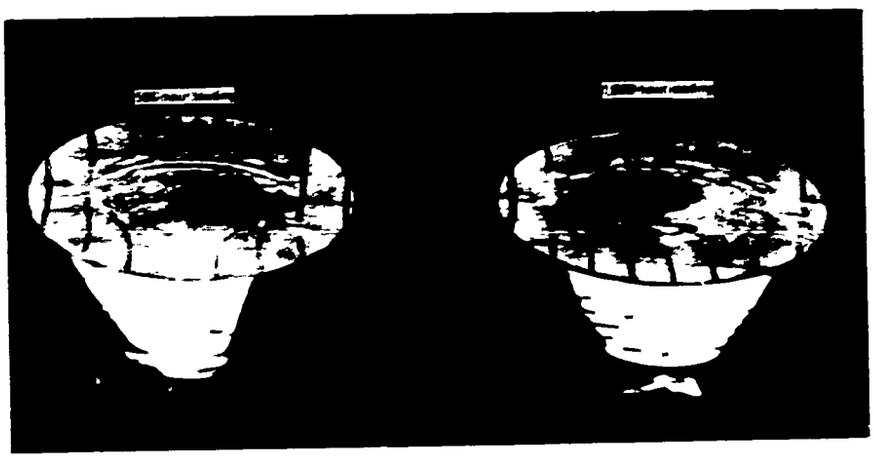

(b) Comparison of cold-flow craters.

Figure 16. One-inch-diameter, 60-degree conical windows with t/D = 0.875 subjected to different durations of loading at 20,000 psi in 65°F-to-75°F temperature range.

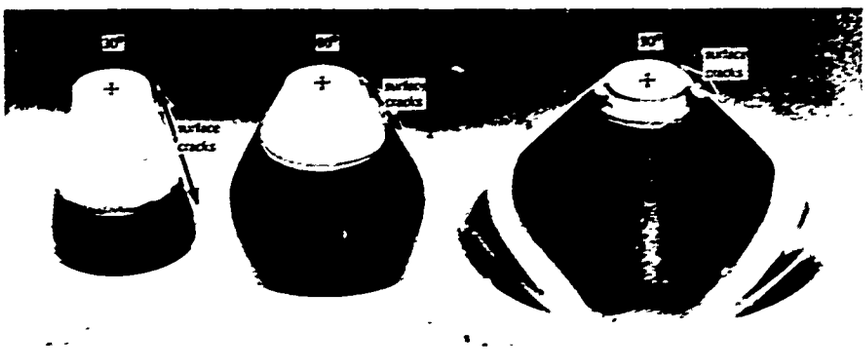

Figure 17. Comparison of crack distribution on 1-inch-diameter windows with t/D = 2.0 and 30-, 60-, and 90-degree conical angles after 1,000 hours loading under 20,000 psi in 65°F-to-75°F pressure range.

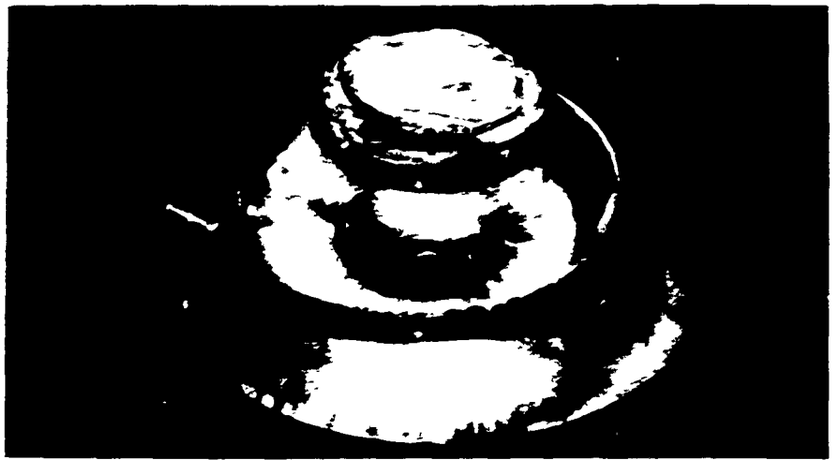

(a) Fracture surface on conical bearing surface.

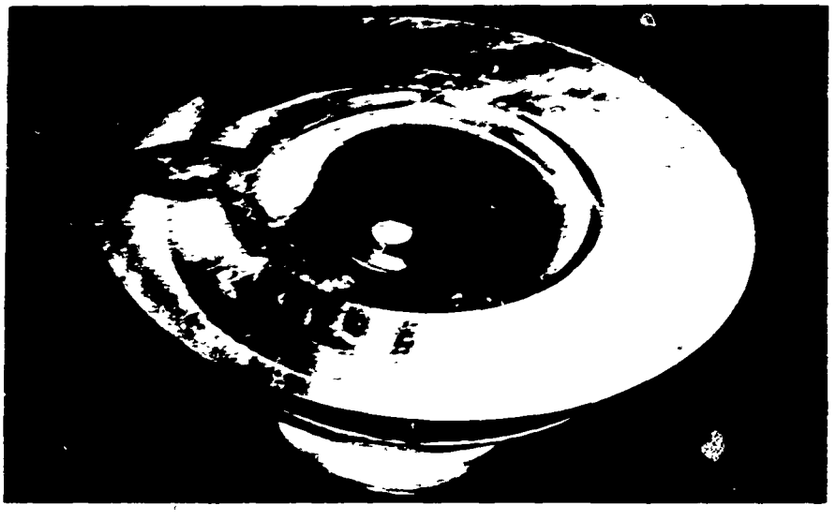

(b) High-pressure face intersected by fracture surface.

(c) Two separated fragments of the window.

Figure 18. One-inch-diameter, 90-degree window with t/D = 0.75 after 1,000 hours of loading at 20,000 psi.

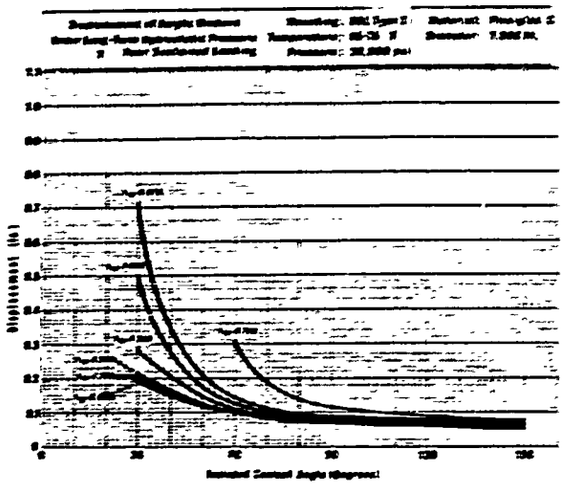

(a) 1 hour.

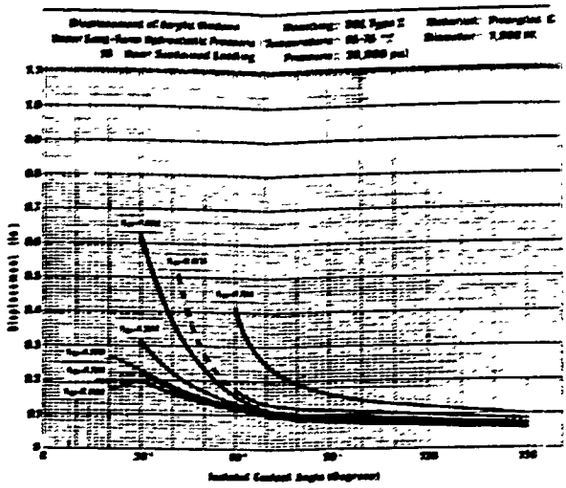

(b) 10 hours.

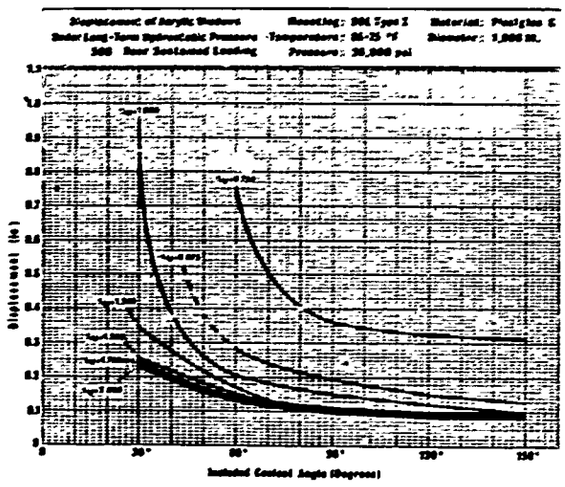

(d) 500 hours.

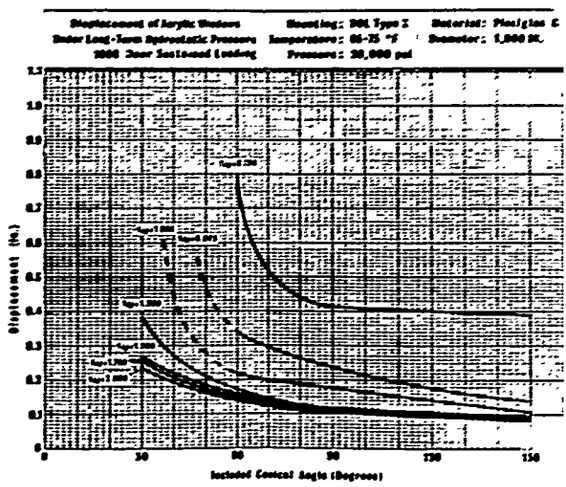

(e) 1,000 hours.

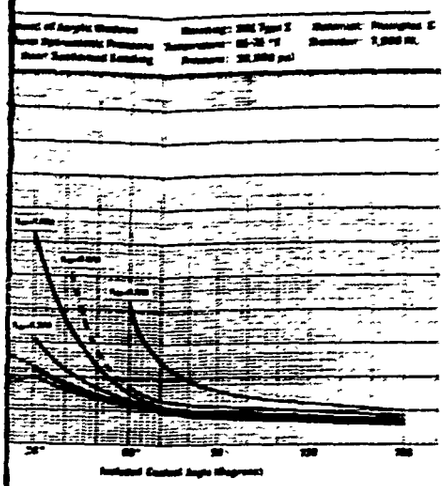

(b) 10 hours.

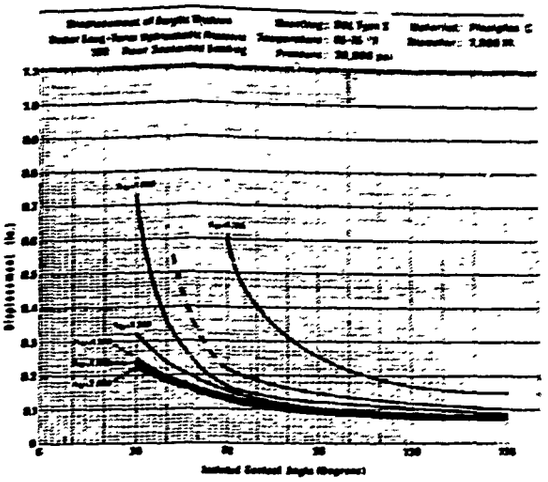

(c) 100 hours.

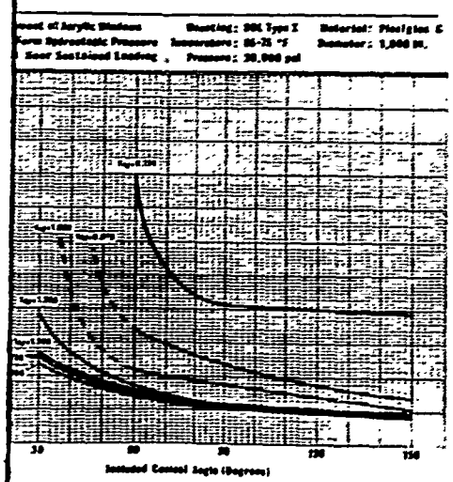

(e) 1,000 hours.

Figure 19. Axial displacement of conical windows during sustained pressure loading.

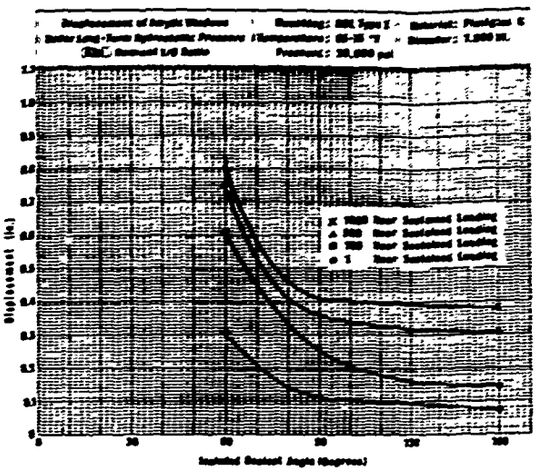

(a) t/D = 0.75.

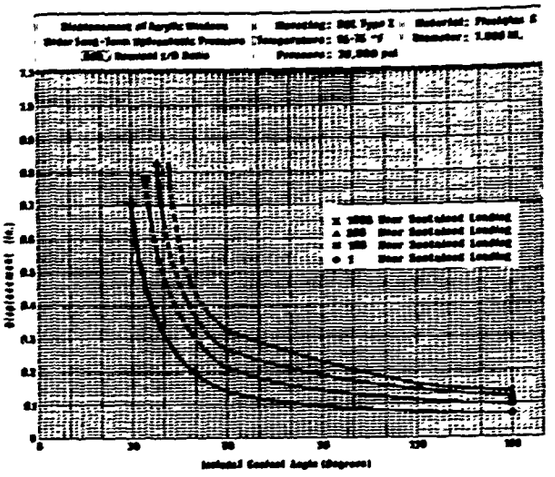

(b) t/D = 0.875.

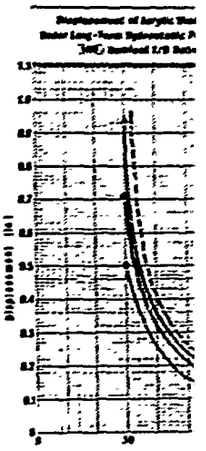

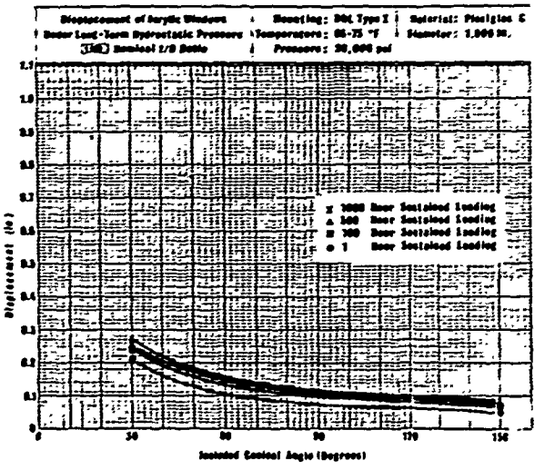

(e) t/D = 1.5.

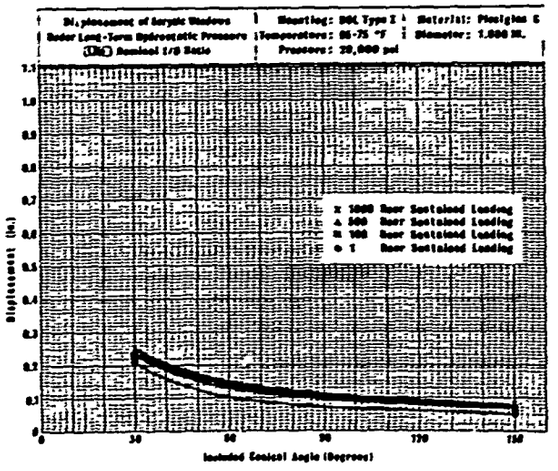

(f) t/D = 1.75.

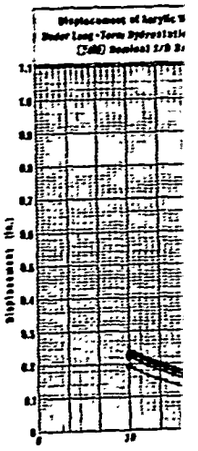

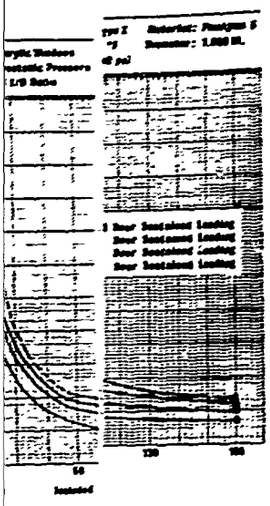

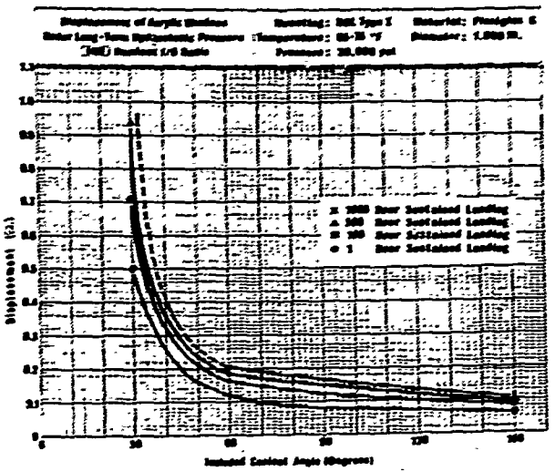

(c) t/D = 1.0.

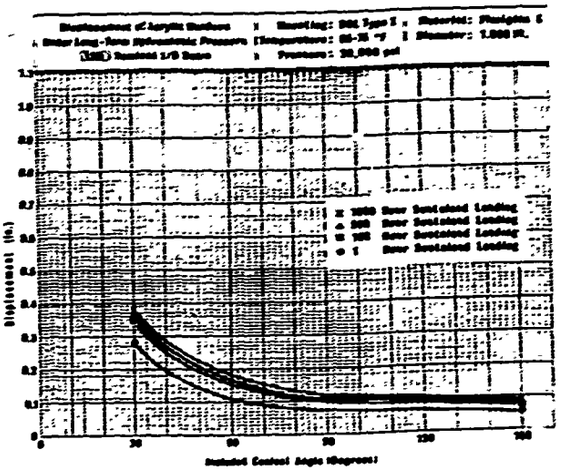

(d) t/D = 1.25.

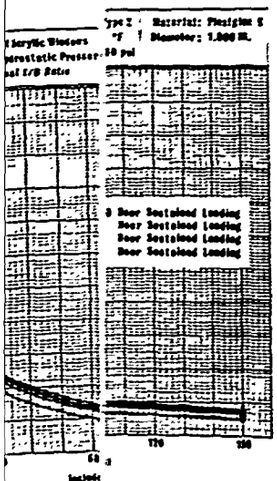

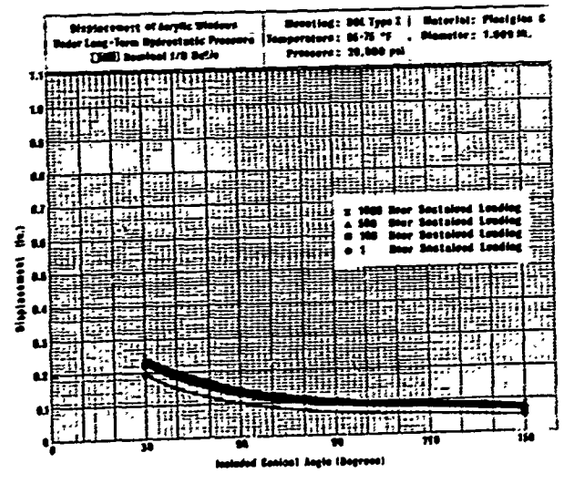

(g) t/D = 2.0.

Figure 20. Axial displacement of conical acrylic windows during sustained pressure loading.

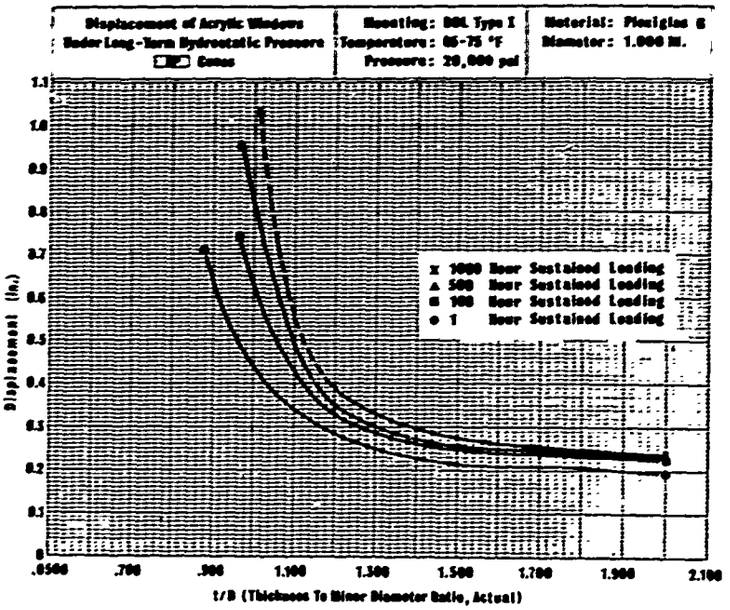

(a) 30-degree windows.

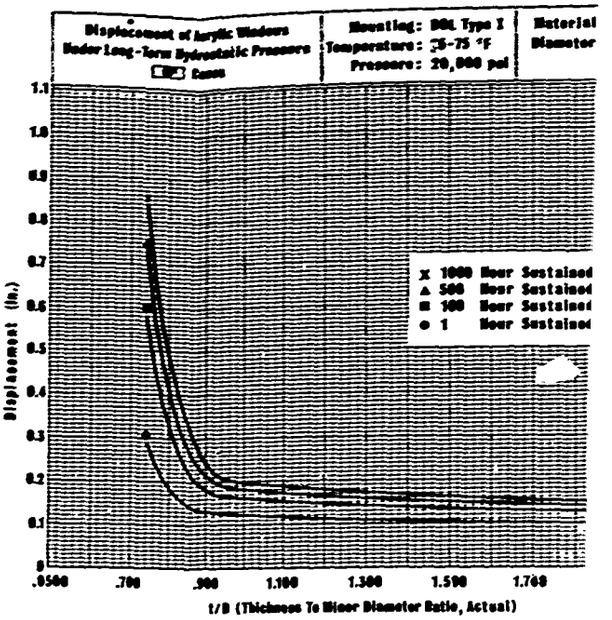

(b) 60-degree windows.

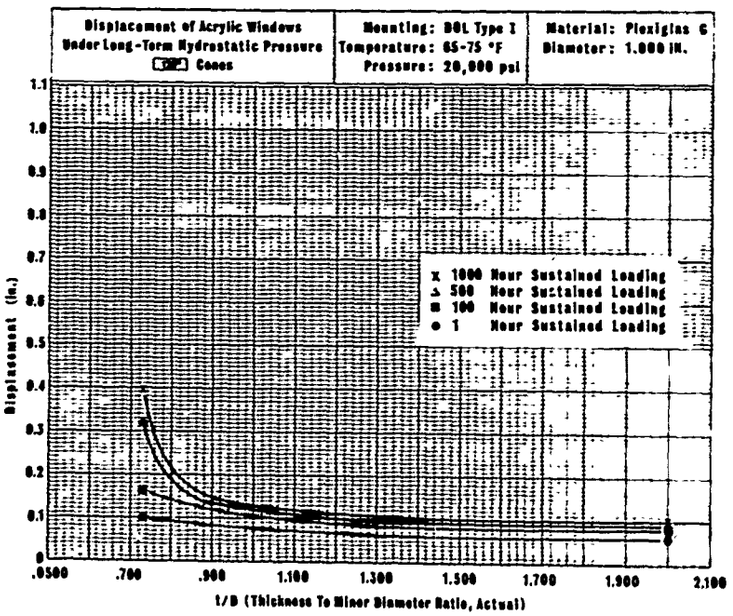

(d) 120-degree windows.

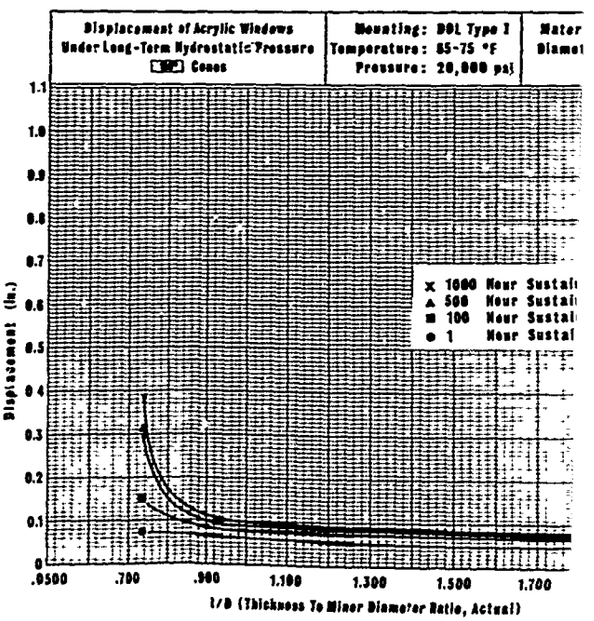

(e) 150-degree windows.

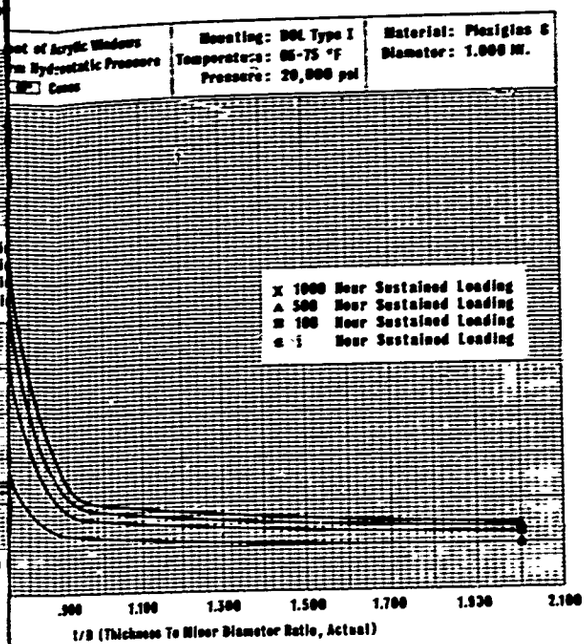

(b) 60-degree windows.

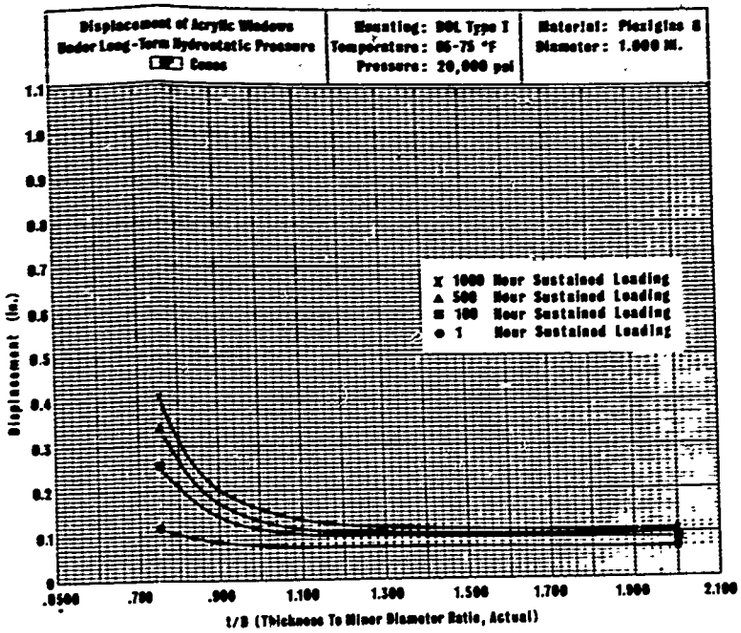

(c) 90-degree windows.

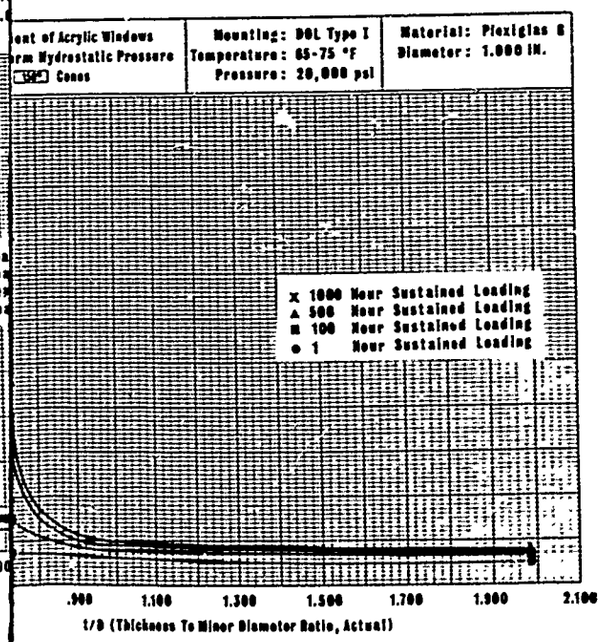

(e) 150-degree windows.

Figure 21. Axial displacement of conical windows during sustained pressure loading.

Although the experimental data are based on a time period of only 1,000 hours (the extent of maximum loading duration of windows in this study), the data are extrapolated for an additional 1,000 hours of load applications for each t/D ratio and angle (Appendix C). This should allow hydrospace window designers to predict the displacement of windows with a high degree of confidence for 2,000 hours of sustained hydrostatic load application. For 1-inch-diameter windows with a t/D ratio of 2.0 extrapolations have been made to 100,000 hours (Figure 22).

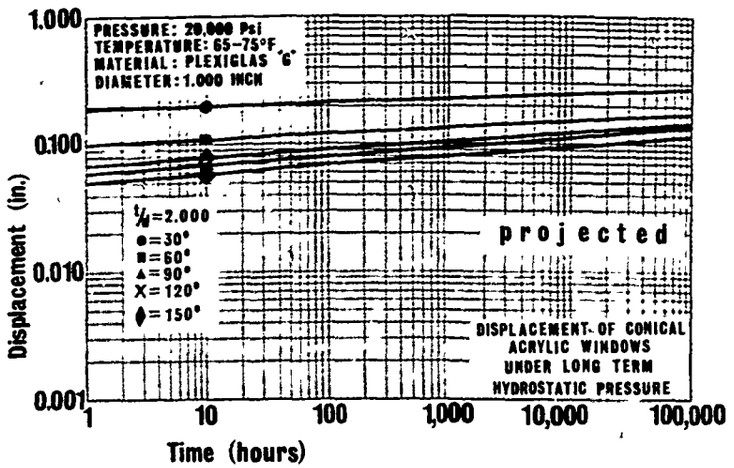

Figure 22. Extrapolation to 100,000-hour loading duration of displacements generated by 1-inch-diameter windows with t/D = 2.0 under 20,000-psi sustained pressure for 1,000 hours.

SUMMARY OF TEST OBSERVATIONS

Deformations

All of the windows subjected to long-term 20,000-psi hydrostatic loading in DOL 1 flanges underwent time-dependent elastic and/or plastic deformation; the magnitude and character of the deformation varied with the window diameter, thickness, included angle, temperature, and length of loading. Some of the windows extruded plastically through the cylindrical flange opening to such an extent that after a time they lost their ability to withstand hydrostatic pressure and failed catastrophically. The time-dependent plastic deformation of the windows consisted of cold-flow cratering on the window's high-pressure face and plug extrusion of the low-pressure face (Figure 12). This deformation was accompanied by formation of cracks on the high-pressure face, low-pressure face, and conical bearing surface. The deformation was considerably less at 32°F than at room temperature (Figure 13a).

The 20,000-psi pressure loading under which some of the windows failed was considerably lower than the pressures required to cause similar windows to fail under short-term hydrostatic loading in previous studies.[1, 2] Since in this study the failure of windows in less than 1,000 hours after pressure application took place only for two t/D ratios and angles, it is exceedingly hard to formulate general rules. It is certain, however, that the difference between critical pressures under short-term and long-term loading can be considerable. For the two groups of windows that failed in this study at 20,000 psi, the decrease in their short-term strength was 9% for the 30-degree window with t/D = 0.875, and 23% for the 60-degree window with t/D = 0.625. In the former case the average duration prior to catastrophic failure was 42 minutes, while in the latter case it was 157 minutes. This demonstrates that critical pressure of acrylic windows is intimately related to duration of hydrostatic loading. By decreasing the magnitude of hydrostatic loading, the duration of sustained load-carrying ability is increased.

Since the magnitudes of cold-flow cratering, plug extrusion and crack depth are larger for 4-inch-diameter windows than for 1-inch-diameter windows (Figure 13b) of same t/D ratio and angle, it would appear that the experimental data generated in this study by 1-inch-diameter windows are directly (without any scaling factor) applicable only to windows of 1-inch-diameter. However, because the deformation of the 4-inch-diameter windows tested in the DOL 1 flange also under 20,000-psi hydrostatic pressure is approximately four times larger than that of comparable 1-inch-diameter windows, it can be assumed that the deformation of conical acrylic windows is linearly scalable and the deformation data collected on 1-inch windows under 20,000-psi hydrostatic pressure can serve as a basis for predicting the deformation of acrylic windows of any diameter under 20,000-psi hydrostatic pressure.

The magnitude of cold-flow cratering on the high-pressure face, and the plug extrusion on the low-pressure face appears to be related to temperature, duration of sustained loading, t/D ratio, and conical angle. In general, an increase in t/D ratio (Figure 14), and conical angle (Figure 15) decreases the magnitude of extrusion and cold-flow cratering. An increase in duration of sustained load application on the other hand increases the magnitude of cold flow (Figure 16). Low temperature favors small deformations, while elevated temperature causes large deformations.

The conical bearing surfaces of the windows have been observed to harbor many fine cracks propagating into the interior of the windows at approximately a right angle to the bearing surface. The number of cracks, their depth, and pattern of distribution has been found to vary with the window's t/D ratio, conical angle, length of loading, and temperature. An increase in duration of loading and temperature, decrease in

t/D ratio, and a decrease in conical angle have been associated with an increase in number of cracks as well as their depth. An interesting phenomenon associated with the change in conical angle was that not only the number of cracks changed but also their distribution on the conical bearing surface. Generally speaking, it appears that the smaller the angle of conical windows with a given t/D ratio, the more general is the distribution of cracks over the whole bearing surface. Thus, for example for 30-degree windows the whole bearing surface is covered with cracks, while for 150-degree windows all of the cracks on the bearing surface are concentrated near the low-pressure face (Figure 17).

If the t/D ratio of the window was low and the conical angle was equal to or larger than 90 degrees, a fracture developed that divided the window into two fragments. Since the fracture originated in most cases from one of the many cracks present on the conical bearing surface, and it propagated itself at right angles to the bearing surface, the shape of resulting fracture was that of a cone with its apex intersecting the high-pressure face of the window. The resulting two fragments of the window had either the shape of an annular ring, or of a plug with two intersecting conical surfaces (Figure 18). In those cases in which the loading of the window was terminated before the window was divided by the fracture into two separate fragments, an incomplete fracture was observed.

Displacements

When the magnitudes of displacements for windows having different t/D ratios, conical angles, and duration of loading were compared, several observations were made. For all windows, regardless of their t/D ratio (Figures 19 and 20), the displacement after the same length of loading at 20,000 psi and 65°F-75°F appeared to be largest for 30-degree windows with the displacement becoming progressively smaller as the conical angle increased to 150 degrees. The largest decrease in magnitude of displacement took place between 30 degrees and 60 degrees, followed up by a smaller decrease between 60 degrees and 90 degrees (Figure 19). Some minor additional decrease took place between 90 and 150 degrees of conical angle, the magnitude of the decrease being related in some manner to the t/D ratio. When the t/D ratios were small, the differences in magnitudes of displacement between windows of same t/D ratio but different conical angles were very large (Figure 20a, b, c, and d). On the other hand, when the t/D ratios were large, the differences in magnitudes of displacement between windows of same t/D ratio but different conical angles were small for the same duration of loading (Figure 20e, f, and g).

When the magnitudes of displacement for windows of same conical angle but different t/D ratios are compared after the same loading duration (Figure 21), it appears that considerable decrease in the magnitude of extrusion occurs as the t/D ratio is increased in lower t/D ratio range, followed by very little decrease as the t/D ratio is increased in higher t/D ratio range. Thus for 30-degree windows (Figure 21a), most of the displacement decrease takes place at ratios up to t/D = 1.5; for 60-, 90-, 120-degree windows (Figure 21b, c, and d) at ratios up to t/D = 1.25; and for 150-degree windows (Figure 21e) at ratios up to t/D = 1.0.

When one compares the magnitudes of displacement for different t/D ratios of a constant conical angle at different durations of loading (Figure 19) it can be observed that the shorter the duration of loading, the less difference there is between the magnitudes of measured displacement of different t/D ratios for a given angle. Thus for 1-hour duration of loading the magnitudes of displacement for 0.75 t/D and 2.0 t/D windows with a 90-degree included angle are approximately of the same magnitude (Figure 19a), while for 1,000-hour duration of loading the displacements for those two t/D ratios are of significantly different magnitudes (Figure 19e).

Data generated by windows that failed prior to completion of the 1,000-hour sustained pressure loading indicated that under a sustained pressure loading at 65°F-to-75°F a catastrophic window failure rarely occurs before the magnitude of the window displacement is equal to at least 50% of the original window thickness. For 30-degree windows the magnitude of displacement prior to catastrophic failure under sustained loading has generally been equal to original window thickness (Figure C-1). The displacement of 60-degree windows (Figure C-2) is somewhat less than the original window thickness, but still well over 75% of original thickness. For angles larger than 60 degrees, the exact amount of displacement prior to catastrophic failure is not known but in all probability it is about 50% of original thickness. This large displacement can be used to actuate an alarm system sensor in ample time before failure takes place.

Although the experimental data generated in this study are based on the displacement of model windows under long-term loading of 1,000 hours maximum duration, a fair extrapolation of window extrusions for longer loading duration is feasible. This long-range extrapolation is possible because it has been observed that when displacement of windows is plotted versus time on log-log coordinates, a straight line results. Such an extrapolation has been prepared for all windows for t/D = 2.0; the graph has been plotted for long-term loading up to 100,000-hour duration under 20,000 psi in 65°F-to-75°F+ temperature range (Figure 22). On the basis of this extrapolated data it appears that acrylic windows of t/D = 2.0 and 30-, 60-, 90-, 120-, and 150-degree conical angles will withstand approximately

10 years of sustained pressure loading without catastrophic failure. This prediction is based on the observation that none of these windows appear to have even one-half the projected displacement in 100,000 hours which is generally considered necessary for failure of conical windows under long-term loading.

Effect of Flange Design

The displacement data generated by this study are directly applicable only when the DOL 1 flange is used for containment of windows in a pressure hull. Although only a few exploratory experiments were performed in this study on the influence of flange design, it was observed previously[1] that when DOL 2 flange is used the axial displacements become significantly larger, while when DOL 5 flange is used they become significantly smaller. Thus if the DOL 5 flange is used, the displacement data will be conservative; the actual displacements in DOL 5 flanges of any conical angle will be less. If DOL 2 flanges are used, the displacement data will be quite inapplicable; the window in this flange will be unsafe because it will displace significantly faster than the data of this report predict. The details of DOL 1 and DOL 5 flange designs are discussed at length in Appendix B.

FINDINGS

Conical acrylic windows are subject to static fatigue, which exhibits itself by time-dependent viscoelastic and viscoplastic deformation, time-dependent initiation and propagation of cracks, and time-dependent catastrophic failure. Specifically:

1. The deformation of the windows takes the form of plug extrusion through the cylindrical passage in the flange accompanied by the formation of a crater in the center of the window's high-pressure face.

2. The initiation of cracks takes place on the conical bearing surface followed by time-dependent propagation of fractures into the interior of the window at approximately a right angle to the bearing surface.

3. The displacement of the conical windows through a flange increases with the temperature, pressure, and duration of sustained hydrostatic pressure, and decreases with conical angle and t/D ratio.

4. Where specimens had a t/D ratio equal to or less than 1.0 and/or included angles of 30 or 60 degrees, catastrophic failures occurred in less than 1,000 hours of sustained loading at 20,000 psi.

5. Only windows with a t/D ratio equal to or greater than 1.25 did not fail catastrophically in 1,000 hours of sustained loading at 20,000 psi.

6. The decrease in magnitude of time-dependent displacement when t/D is increased from 1.0 to 1.25 is greater than the decrease observed when t/D is further increased from 1.25 to 2.0. The increase in t/D above 1.25, however, causes a very noticeable decrease in the number and depth of cracks on the conical bearing surface of the window.

7. The rate of displacement for windows through the flange is not a linear function of time, and as a general rule, the displacement occurring during the first hour of sustained loading is greater than the displacement taking place during the following 1,000 hours.

8. The deformation of the low- and high-pressure faces and the displacement of the window through the flange were approximately 30% less in the 32°F-to-40°F temperature range than in the 65°F-to-75°F range in which the bulk of the experimental data was generated.

CONCLUSIONS

1. When windows are to be utilized in structures subjected to long-term external or internal hydrostatic pressure, the duration of loading must be taken into consideration in selecting the t/D and angle of the conical acrylic window, since the catastrophic failure of the window under long-term sustained loading occurs at pressures invariably lower than under short-term loading.

2. It is absolutely necessary to know the magnitude of displacement, plastic surface deformation, and crack propagation as a function of time to design with confidence conical acrylic windows for long-term hydrostatic loading.

3. The time-dependent displacement curves and photographic record of cracks and plastic distortions of windows under 20,000-psi long-term hydrostatic loading from this experimental study make it possible to specify the dimensional proportions of conical acrylic windows required for safe and optically acceptable long-term service under hydrostatic pressures between 15,000 and 20,000 psi.

4. The performance of full-scale conical acrylic windows under sustained loading in terms of their deformation, displacement, and crack distribution can be predicted with reasonable accuracy on the basis of model windows.

5. For service under sustained hydrostatic loading at 20,000 psi and up to 1,000 hours duration, windows with a t/D ratio equal to or less than 1.0 and/or included angles equal to or less than 60 degrees are unsatisfactory.

Appendix A

EFFECTS OF SUSTAINED PRESSURE LOADING ON CONICAL WINDOWS

INTRODUCTION

The windows subjected to sustained loading under 20,000-psi hydrostatic pressure for time periods of 500 and 1,000 hours experienced permanent deformation, cracking, or even catastrophic failure. The extent of cracking, or duration of sustained loading prior to catastrophic failure depended on the included angle and the t/D ratio of the 1-inch-diameter windows tested, so long as the temperature of the water was held in the 65°F-to-75°F range for all the tests. At what exact time during the sustained pressure loading a certain crack or cold-flow crater was formed is unknown, as no techniques were utilized that would permit intimate observation of the interior of the window body during the hydrostatic loading.

Since all observations of damage to the tested windows were made only after the testing was completed and the windows were removed from their flanges, it cannot be stated with absolute certainty which damage to the window occurred during the pressurization phase from 0 to 20,000 psi, sustained pressure loading phase at 20,000 psi, or unloading phase from 20,000 psi to 0 psi. Some of the changes in the window (e.g. cold-flow cratering on the high-pressure face and the cold-flow extrusion on the low-pressure face) must have taken place during the hydrostatic load application. These deformations are clearly the responses of the acrylic window to hydrostatic force acting on its high-pressure face.

The time of origin of the cracks in the window is not so obvious. Some of the cracks, such as those on the low-pressure face, definitely appear during the loading of the window; they are caused by the bulging of the low-pressure face, which induces local tensile stresses in the face. Also, during some of the tests, the low-pressure faces were observed and extensive cracking and fracturing of the face was noted prior to failure. Whether the cracks at right angles to the conical seating surface occurred during the loading, or during unloading cannot be definitely ascertained. However, there is good evidence that most cracks did originate during the pressurization and sustained pressure-loading phases.

The case for this supposition rests on two observed phenomena. One is the penetration of lubricant into some very deep cracks. The lubricant, could not penetrate into the interior of the window through the

fail the cracks if it was not under very high hydrostatic pressure. But not all of the cracks were penetrated by grease, indicating either that some were formed during the depressurization phase, or that they were formed during pressurization as shear cracks, which are kept from opening into fissures by the compression forces acting at right angles to the crack surfaces. Since in explosively failed windows one can find the failure surface to be an outgrowth of just such cracks, it can be stated with a fair degree of confidence that most of the shear type cracks at right angles to the conical seating surface form when the window is being pressurized or is under sustained load and not during depressurization. The following discussion of the effects of long-term pressure loading on conical windows is based on the premise that most of the deformation and cracking did take place when the windows were being pressurized, or when they were under sustained hydrostatic loading.

DISCUSSION

1-Inch-Diameter Conical Windows

30 Degree. All 30-degree conical windows with $t/D < 0.875$ failed at levels less than 20,000 psi during raising of the hydrostatic pressure. Thus at completion of tests none of these windows were available for observation and photography. The same is true of windows with a $t/D = 0.875$, except that they failed under sustained pressure after the hydrostatic pressure of 20,000 psi was reached. Only windows with $t/D \geq 1.0$ survived the 500- or 1,000-hour sustained pressure application and remained for inspection (Figure A-1).

Cold-flow cratering was observed only on the high-pressure faces of windows with $1.0 \leq t/d \leq 1.25$, while cold-flow extrusion of the low-pressure face in the form of a plug was observed on all of the windows with $1.0 \leq t/D \leq 2.0$ (Figures A-1 through A-5). Besides the extrusion in the form of a plug, the low-pressure face also underwent some change of surface curvature. The low-pressure face changed its surface from plane to convex (Figures A-2 and A-4) with the radius of curvature on the convex surface being related to the amount of plug extrusion. Thus, windows with extremely large plug extrusions were observed to possess such a short radius of curvature that cracking of the low-pressure face surface took place (Figures A-1 and A-2), while windows with very small plug extrusions possessed convex low-pressure faces with very long radius of curvature (Figure A-4). In general it appears that the magnitude of the cold-flow cratering and of the plug extrusion on

1-inch-diameter, 30-degree conical windows is a function of the duration of sustained loading and t/D ratio when the ambient temperature is held constant. Thus 1,000-hour sustained loading and low t/D ratios result in deeper cold-flow craters and longer cold-flow plugs than 500-hour loading and high t/D ratios (not shown).

The conical seating surface of all 30-degree windows with $1.0 \leq t/D \leq 2.0$ was found to be covered with fine cracks extending into the window's interior at approximately right angles to the conical seating surface. The depth of penetration was in most cases shallow, less than 1/16 inch. In some windows a fracture plane, cutting across the whole body of the window, was observed immediately below the transition zone of the window where the cylindrical plug joins the conical window body (Figure A-3). There is a strong suspicion that this fracture separating the extruded plug from the rest of the window body occurred during depressurization when the conical part of the window body could not relax because the extruded plug was wedged tight in the cylindrical opening. Because of this restraint on relaxation, tensile forces were generated at the shape transition zone resulting in the horizontal fracture plane. In all windows tested, cracks in the conical seating surface were concentrated in the first 80% to 90% of the window's thickness, measured axially along the conical bearing surface from the minor diameter end.

From the observation of cold-flow deformations and fractures in the 30-degree conical windows it appears that no windows in the $1.0 \leq t/D \leq 2.0$ range will be optically satisfactory when subjected to 20,000 psi for duration of sustained loading equal to 1,000 hours in a DOL 1 type flange. Even windows with t/D = 2.0 exhibit excessive extrusion and conical bearing surface cracking (Figure A-5). Thus from an optical viewpoint it would appear that a 30-degree window for 20,000-psi long-term, high-grade optical service should have $t/D > 2.0$, as only then will the cold-flow extrusion and the curvature of the low-pressure face be of such small magnitude that the optical properties of the window will remain satisfactory.

60 Degree. All 60-degree windows with a $t/D \leq 0.5$ failed during raising of the hydrostatic pressure to 20,000 psi. All those with $t/D \leq 0.625$ failed some time during the sustained 20,000-psi hydrostatic loading. Thus no windows with $t/D \leq 0.625$ remained for inspection after the 1,000-hour, 20,000-psi pressure loading, and all observations are based only on windows with $t/D \geq 0.75$ (Figures A-6 through A-12).

Cold-flow *cratering* of the high-pressure face was noticeable only in 60-degree windows with $0.75 \leq t/D < 1.25$ (Figures A-6, A-7, and A-8); cold-flow *plug extrusion* has been observed on all windows in the $0.75 \leq t/D \leq 2.0$ range (Figures A-6 through A-12). The magnitude of the cold-flow

cratering and plug extrusion appears to be related to the duration of load application and the window's t/D ratio so long as the ambient temperature is constant. Small t/D ratios and 1,000-hour duration of loading produced larger cold-flow deformations than large t/D ratios, or only 500-hour load duration.

In windows with $0.75 \leq t/D < 1.25$, the cold-flow plug extrusion was accompanied by convex bulging up of the low-pressure face of such magnitude that considerable fracturing of the low-pressure surface took place (Figures A-6 and A-7). Cracks in the conical bearing surface were present in all of the windows, but those having $t/D \geq 1.75$ were found to have only very few minute cracks on the conical seating surface (Figures A-11 and A-12). These cracks on the conical seating surface were concentrated in the first 50% to 60% of window thickness measured axially along the conical bearing surface from the window's minor diameter.

From the observation of cold-flow deformations and fractures in the 60-degree conical windows, it appears that only windows with $t/D > 2.0$ will perform satisfactorily in high-grade optical systems when subjected to 20,000 psi of sustained hydrostatic loading for time periods equal to, or less than, 1,000 hours in a DOL 1 type flange.

90 Degree. All 90-degree windows with $t/D \leq 0.5$ failed during raising of the hydrostatic pressure to 20,000 psi. Most of the windows with $t/D = 0.625$ failed during the 1,000-hour loading under the sustained 20,000-psi hydrostatic pressure, thus the main body of observations is limited to windows with $t/D \geq 0.75$ (Figures A-13 through A-19).

Cold-flow cratering of the high-pressure face was observed in all of the 90-degree windows with $t/D \leq 1.0$ (Figures A-13, A-14, and A-15). It is only with $t/D > 1.0$ that the cold-flow cratering of the high-pressure face becomes so small as to be barely noticeable (Figures A-16 through A-19). Cold-flow plug extrusion has been observed on all windows with $t/D \leq 2.0$. The magnitude of the plug extrusion was found to be related to the duration of pressure application and to the window's t/D ratio so long as the ambient temperature remained constant. Both small t/D ratios and long sustained pressure loading tended to increase the magnitude of cold flow. The magnitude of cold-flow plug extrusion on windows with $t/D = 0.75$ was so great that considerable bulging and cracking of the low-pressure face took place (Figure A-13). No cracking of the low-pressure face was observed with windows in the $0.875 \leq t/D \leq 2.0$ range (Figures A-14 through A-19). The low-pressure faces of windows in the $1.0 \leq t/D \leq 2.0$ range, instead of being convex were flat with a slightly raised edge; this edge created the illusion that the surface was slightly concave.

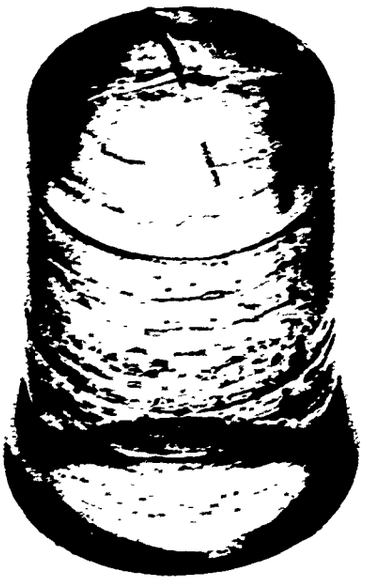

(a) Low-pressure face.

(b) High-pressure face.

Figure A-1. Conical acrylic window after constant hydrostatic pressure loading to 20,000 psi for 1,000 hours in 65°F-to-75°F temperature range; 30-degree cone, t/D = 1.0, 1-inch minor face diameter.

(a) Low-pressure face.

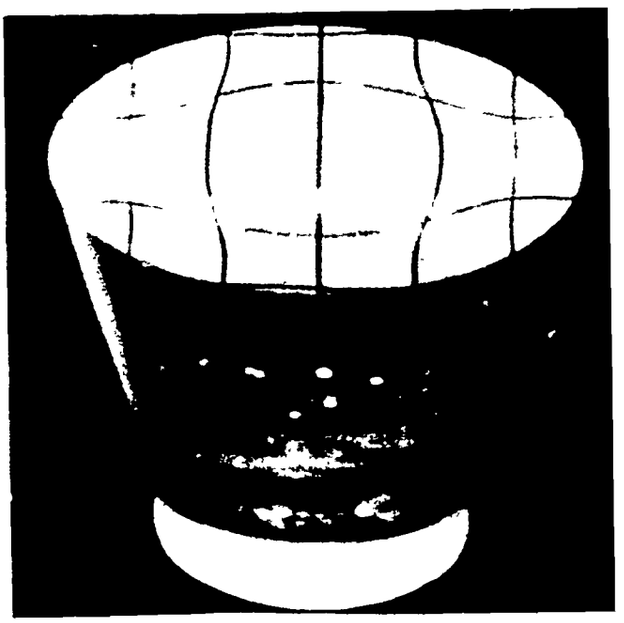

(c) High-pressure face with grid.

Figure A-2. Conical acrylic window after constant hyc temperature range; 30-degree cone, t/D =

(a) Low-pressure face.

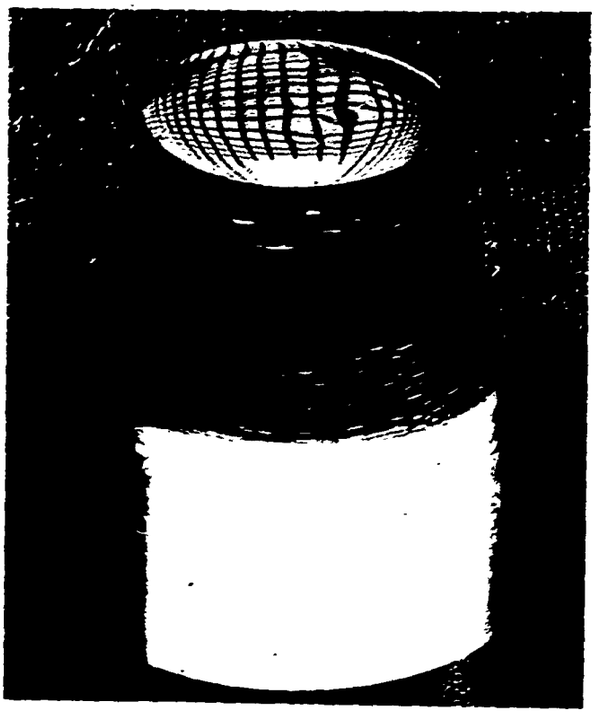

(b) Low-pressure face with grid.

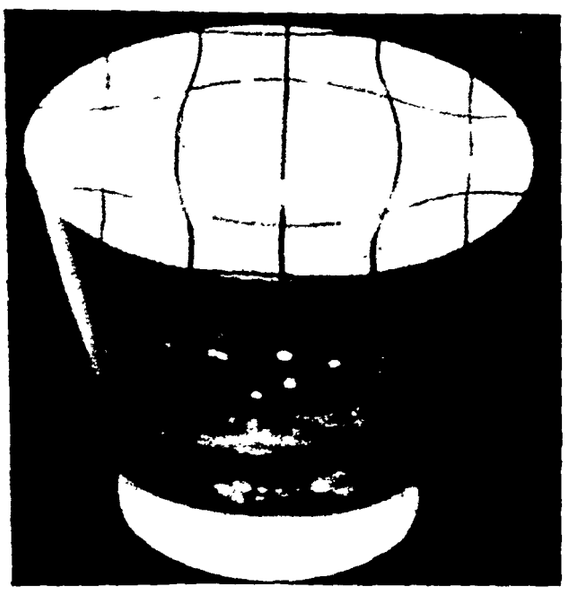

(c) High-pressure face with grid.

Figure A-2. Conical acrylic window after constant hydrostatic pressure loading to 20,000 psi for 1,000 hours in 65°F-to-75°F temperature range; 30-degree cone, t/D = 1.25, 1-inch minor face diameter.

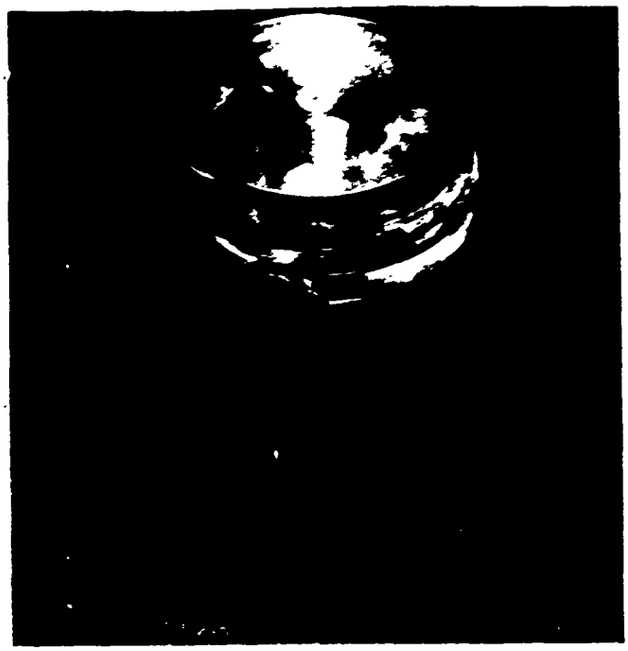

(a) Low-pressure face.

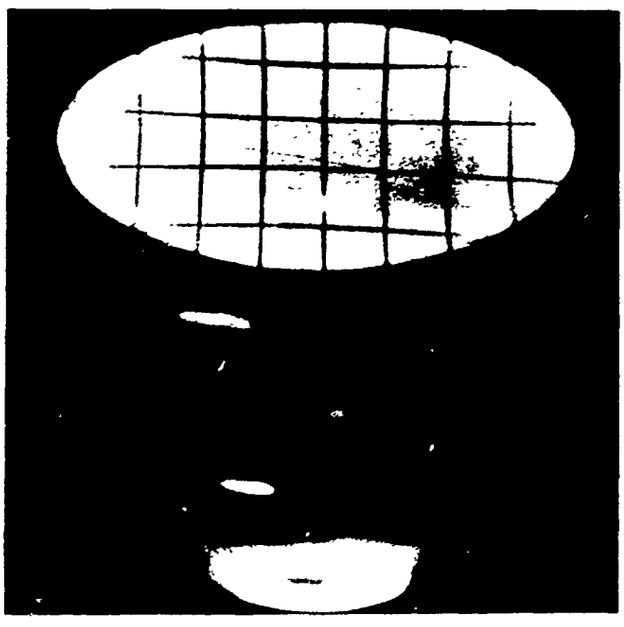

(b) High-pressure face.

Figure A-3. Conical acrylic window after constant hydrostatic pressure loading to 20,000 psi for 1,000 hours in 65°F-to-75°F temperature range; 30-degree cone, t/D = 1.5, 1-inch minor face diameter.

(a) Low-pressure face.

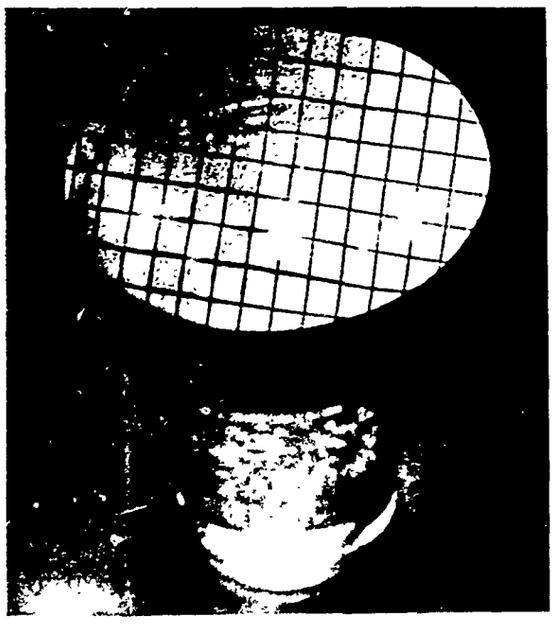

(b) High-pressure face.

Figure A-4. Conical acrylic window after constant hydrostatic pressure loading to 20,000 psi for 1,000 hours in 65°F-to-75°F temperature range; 30-degree cone, t/D = 1.75, 1-inch minor face diameter.

(a) Low-pressure face.

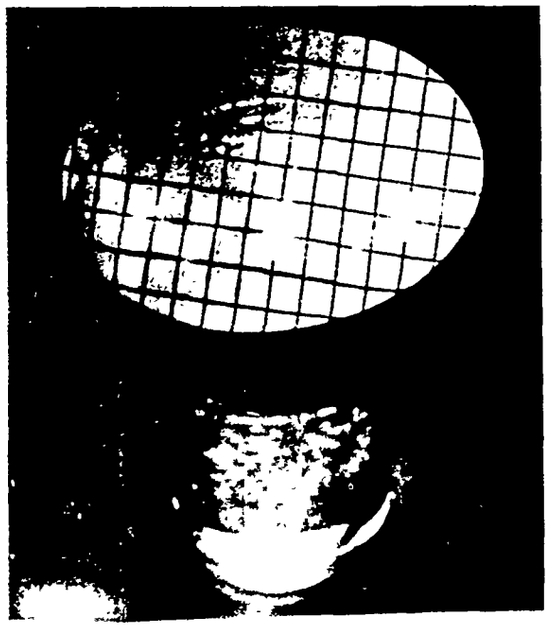

(b) High-pressure face.

Figure A-4. Conical acrylic window after constant hydrostatic pressure loading to 20,000 psi for 1,000 hours in 65°F-to-75°F temperature range; 30-degree cone, t/D = 1.75, 1-inch minor face diameter.

(a) Low-pressure face.

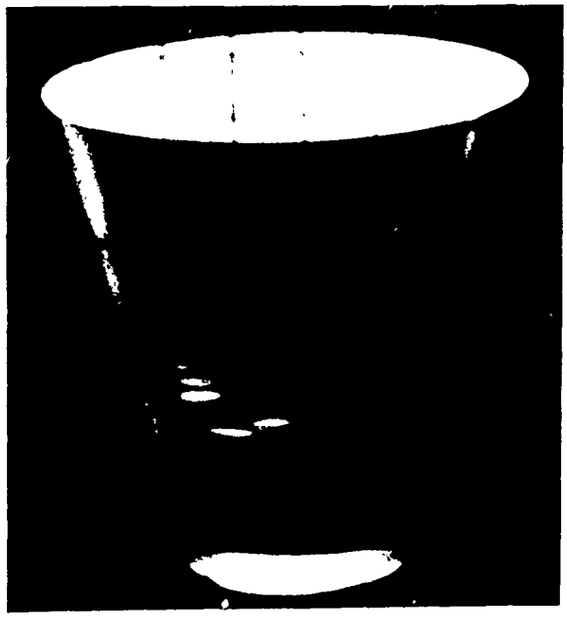

(b) High-pressure face.

Figure A-5. Conical acrylic window after constant hydrostatic pressure loading to 20,000 psi for 1,000 hours in 65°F-to-75°F temperature range; 30-degree cone, t/D = 2.0, 1-inch minor face diameter.

(a) Low-pressure face.

(b) High-pressure face.

Figure A-6. Conical acrylic window after constant hydrostatic pressure loading to 20,000 psi for 1,000 hours in 65°F-to-75°F temperature range; 60-degree cone, t/D - 0.75, 1-inch minor face diameter.

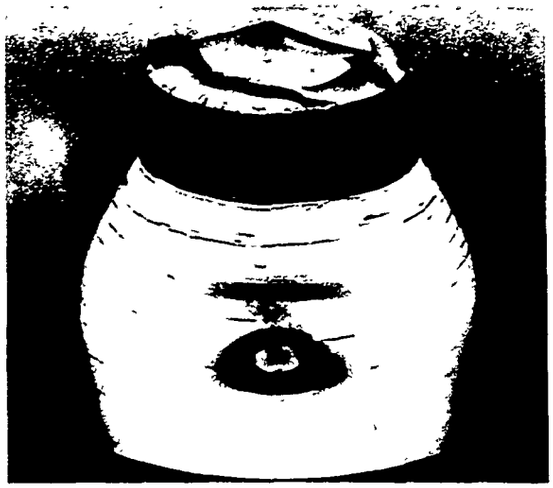

(a) Low-pressure face.

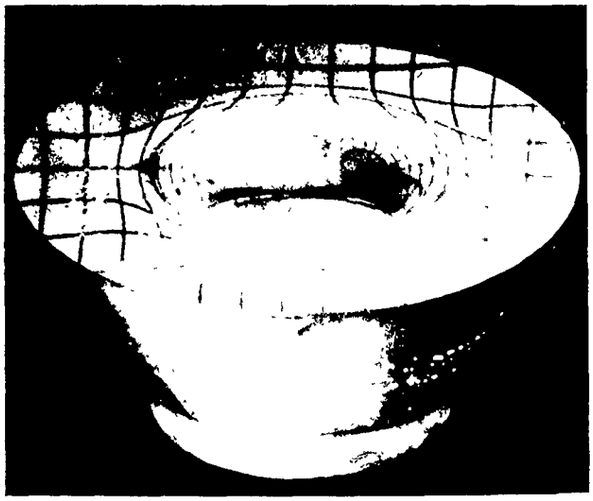

(b) High-pressure face.

Figure A-7. Conical acrylic window after constant hydrostatic pressure loading to 20,000 psi for 1,000 hours in 65°F-to-75°F temperature range; 60-degree cone, t/D = 0.875, 1-inch minor face diameter.

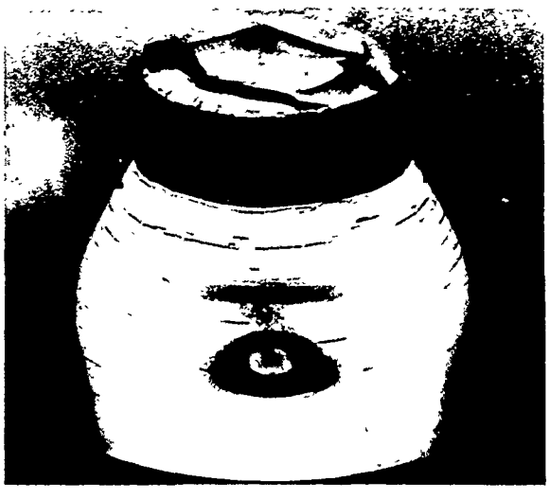

(a) Low-pressure face.

(b) High-pressure face.

Figure A-7. Conical acrylic window after constant hydrostatic pressure loading to 20,000 psi for 1,000 hours in 65°F-to-75°F temperature range; 60-degree cone, t/D = 0.875, 1-inch minor face diameter.

(a) Low-pressure face.

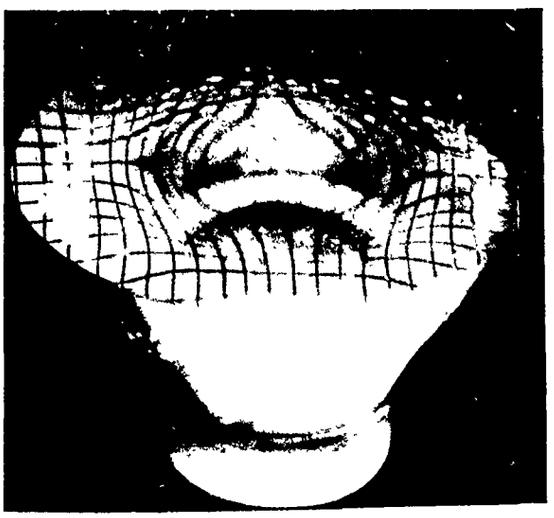

(b) High-pressure face.

Figure A-8. Conical acrylic window after constant hydrostatic pressure loading to 20,000 psi for 1,000 hours in 65°F-to-75°F temperature range; 60-degree cone, t/D = 1.0, 1-inch minor face diameter.

(a) Low-pressure face.

(b) High-pressure face.

Figure A-8. Conical acrylic window after constant hydrostatic pressure loading to 20,000 psi for 1,000 hours in 65°F-to-75°F temperature range; 60-degree cone, t/D = 1.0, 1-inch minor face diameter.

(a) Low-pressure face.

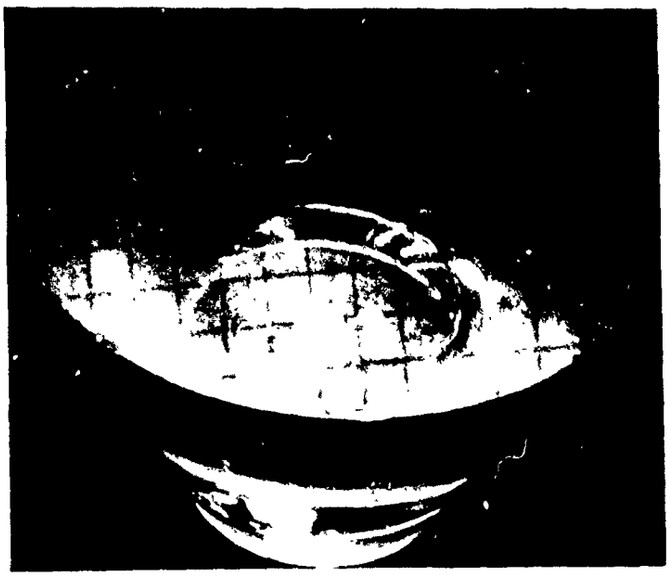

(b) High-pressure face.

Figure A-9. Conical acrylic window after constant hydrostatic pressure loading to 20,000 psi for 1,000 hours in 65°F-to-75°F temperature range; 60-degree cone, t/D = 1.25, 1-inch minor face diameter.

(a) Low-pressure face.

(b) High-pressure face.

Figure A-10. Conical acrylic window after constant hydrostatic pressure loading to 20,000 psi for 1,000 hours in 65°F-to-75°F temperature range; 60-degree cone, t/D = 1.5, 1-inch minor face diameter.

(a) Low-pressure face.

(b) High-pressure face.

Figure A-11. Conical acrylic window afte
static pressure loading to 2(
hours in 65°F-to-75°F tem
60-degree cone, t/D = 1.75,
diameter.

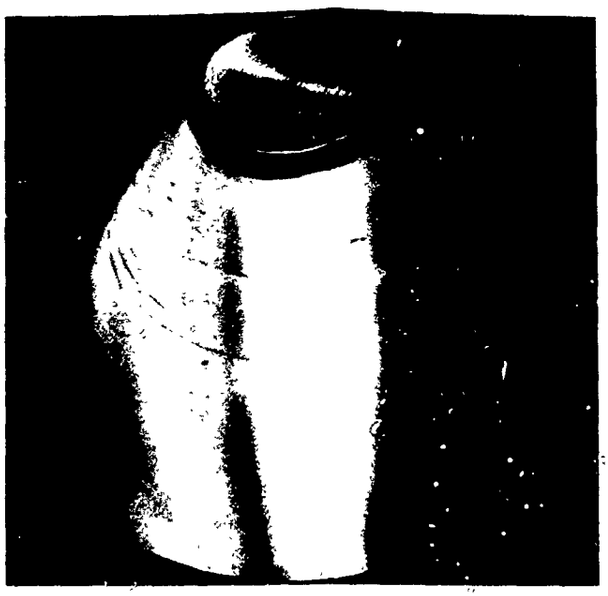

(a) Low-pressure face.

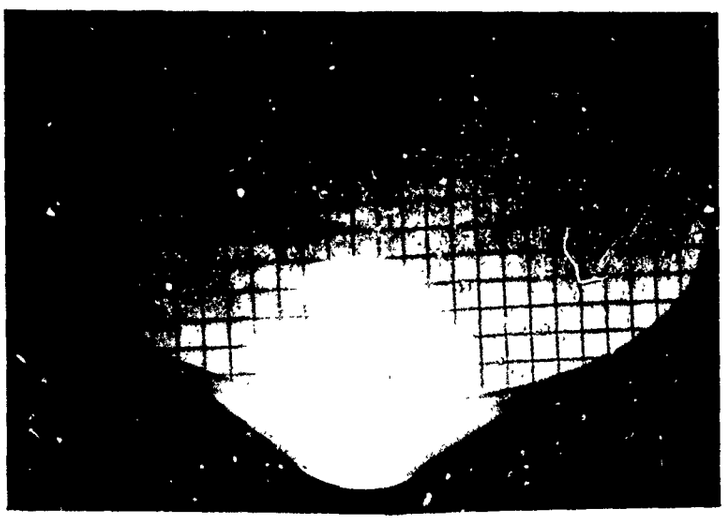

(b) High-pressure face.

Figure A-11. Conical acrylic window after constant hydrostatic pressure loading to 20,000 psi for 1,000 hours in 65°F-to-75°F temperature range; 60-degree cone, t/D = 1.75, 1-inch minor face diameter.

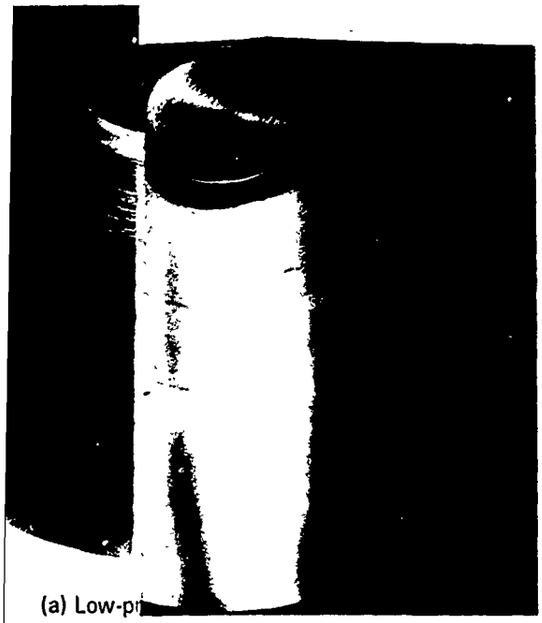

(a) Low-pr

a) Low-pressure face.

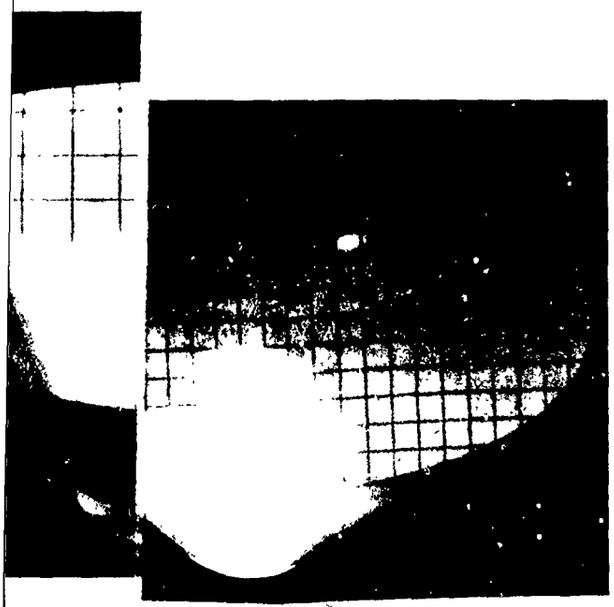

(b) Higl
Conical acry
static pressu
hours in 65°
60-degree cc
diameter.

(b) High-pressure face.
al acrylic window after constant hydro-
pressure loading to 20,000 psi for 1,000
in 65°F-to-75°F temperature range;
gree cone, t/D = 1.75, 1-inch minor face
ter.

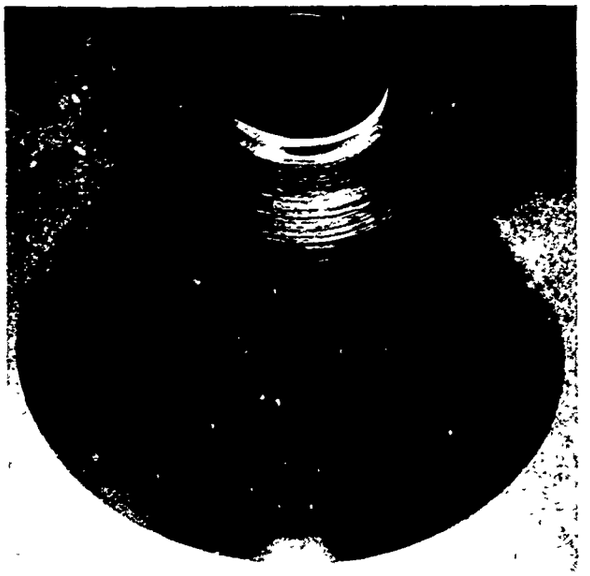

(a) Low-pressure face.

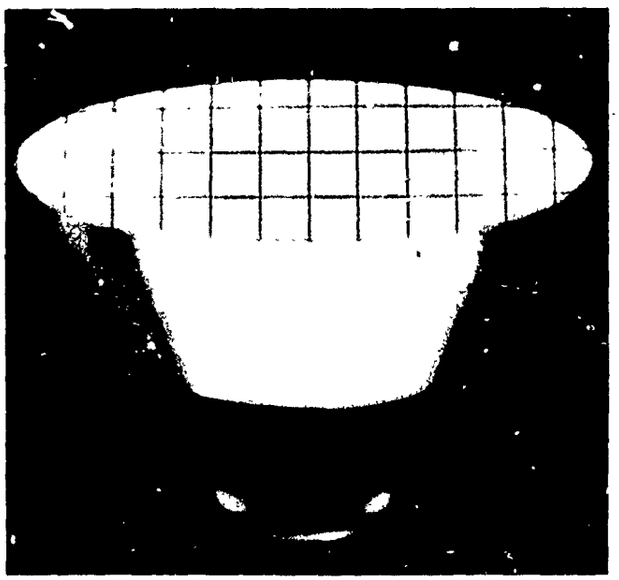

(b) High-pressure face.

Figure A-12. Conical acrylic window after constant hydrostatic pressure loading to 20,000 psi for 1,000 hours in 65°F-to-75°F temperature range; 60-degree cone, t/D = 2.0, 1-inch minor face diameter.

(a) Low-pressure face.

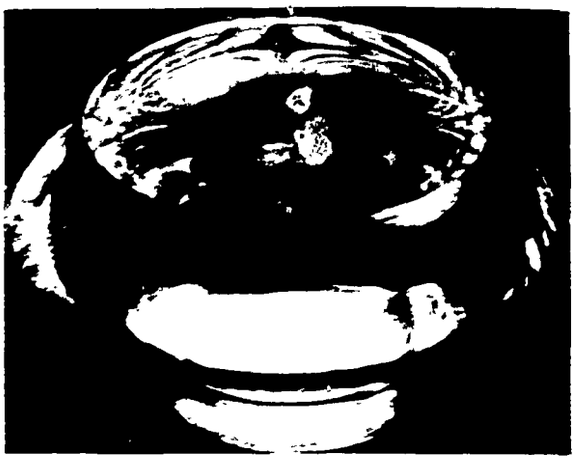

(c) View of high-pressure face showing central fragment.

(b) View of high-pressure face showing annular fragment.

Figure A-13. Conical acrylic window after constant hydrostatic pressure loading to 20,000 psi for 1,000 hours in 65°F-to-75°F temperature range; 90-degree cone, t/D = 0.75, 1-inch minor face diameter.

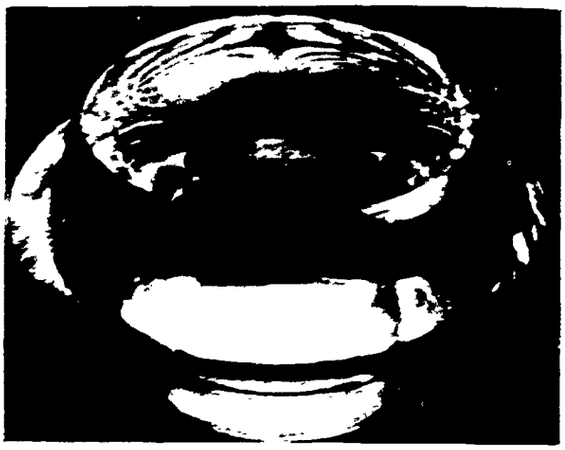

(c) View of high-pressure face showing central fragment.

(a) Low-pressure face.

(b) High-pressure face.

Figure A-14. Conical acrylic window after constant hydrostatic pressure loading to 20,000 psi for 1,000 hours in 65°F-to-75°F temperature range; 90-degree cone, t/D = 0.875, 1-inch minor face diameter.

Figure A

ressure loading to 20,000 psi for 1,000 hours in 65°F-to-75°F
ch minor face diameter.

(a) Low-pressure face.

(b) High-pressure face.

Figure A-14. Conical acrylic window after constant hydrostatic pressure loading to 20,000 psi for 1,000 hours in 65°F-to-75°F temperature range; 90-degree cone, t/D = 0.675, 1-inch minor face diameter.

(a) Low-pressure face.

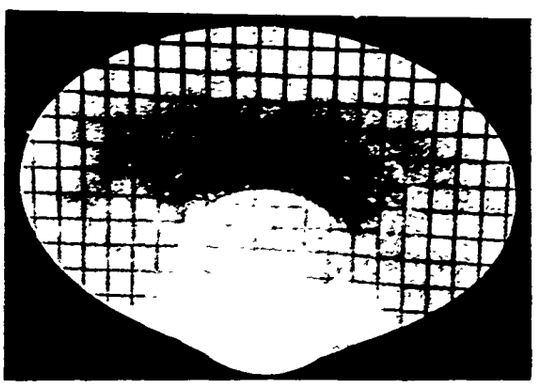

(b) High-pressure face.

Figure A-15. Conical acrylic window after constant hydrostatic pressure loading to 20,000 psi for 1,000 hours in 65°F-to-75°F temperature range; 90-degree cone, t/D = 1.0, 1-inch minor face diameter.

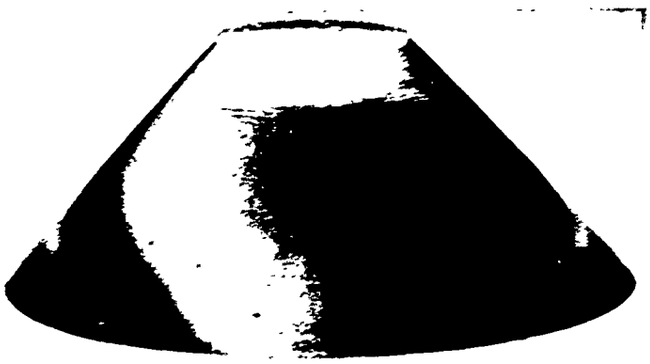

(a) Low-pressure face.

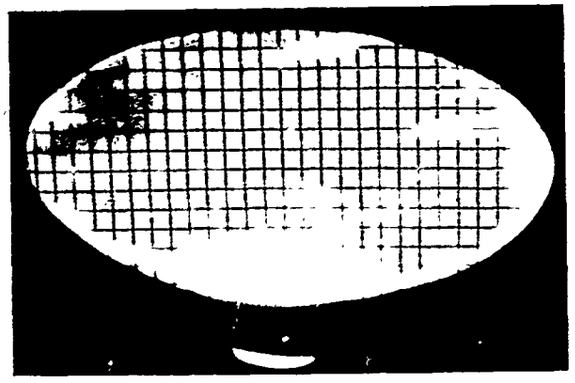

(b) High-pressure face.

Figure A-16. Conical acrylic window after constant hydrostatic pressure loading to 20,000 psi for 1,000 hours in 65°F-to-75°F temperature range; 90-degree cone, t/D = 1.25, 1-inch minor face diameter.

(a) Low-pressure face.

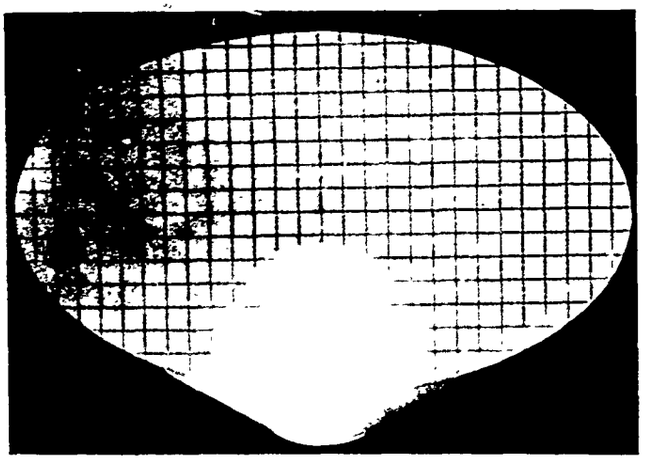

(b) High-pressure face.

Figure A-17. Conical acrylic window after constant hydrostatic pressure loading to 20,000 psi for 1,000 hours in 65°F-to-75°F temperature range; 90-degree cone, t/D = 1.5, 1-inch minor face diameter.

(a) Low-pressure face.

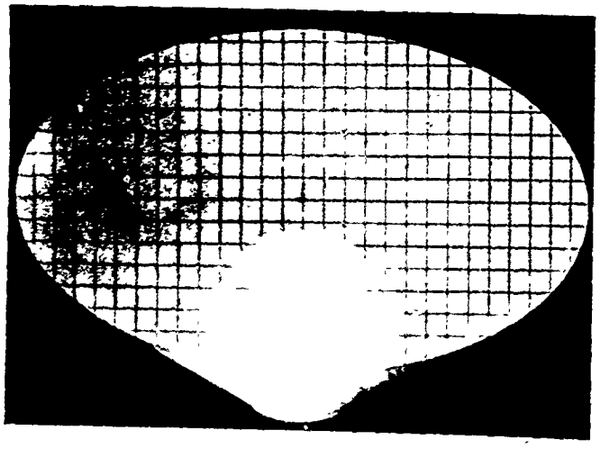

(b) High-pressure face.

Figure A-17. Conical acrylic window after constant hydrostatic pressure loading to 20,000 psi for 1,000 hours in 65°F-to-75°F temperature range; 90-degree cone, $t/D \approx 1.5$, 1-inch minor face diameter.

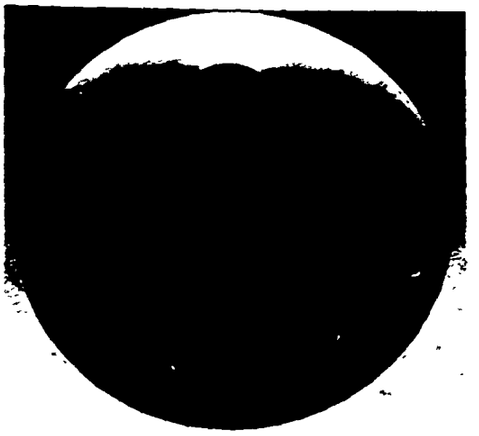

(a) Low-pressure face.

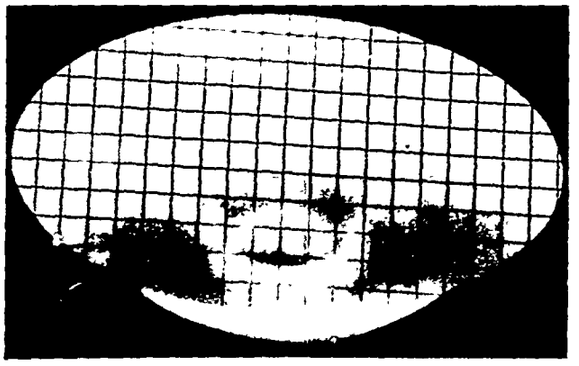

(b) High-pressure face.

Figure A-18. Conical acrylic window after constant hydrostatic pressure loading to 20,000 psi for 1,000 hours in 65°F-to-75°F temperature range; 90-degree cone, $t/D \approx 1.75$, 1-inch minor face diameter.

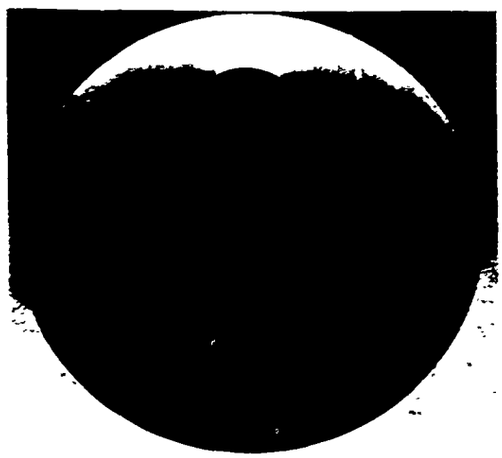

(a) Low-pressure face.

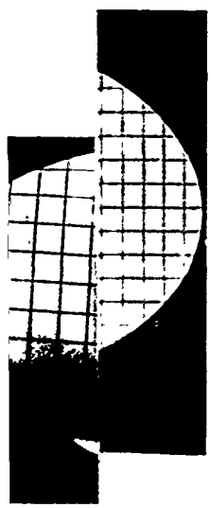

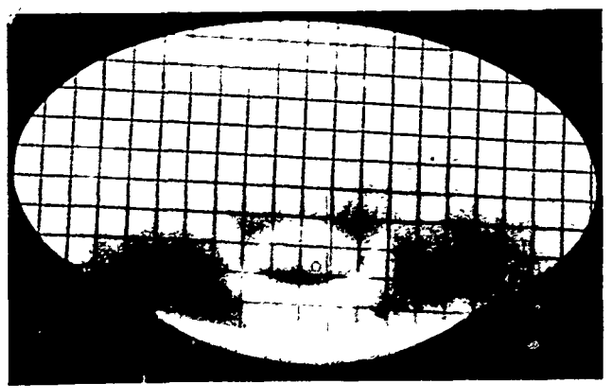

(b) High-pressure face.

Figure A-18. Conical acrylic window after constant hydrostatic pressure loading to 20,000 psi for 1,000 hours in 65°F-to-75°F temperature range; 90-degree cone, t/D = 1.75, 1-inch minor face diameter.

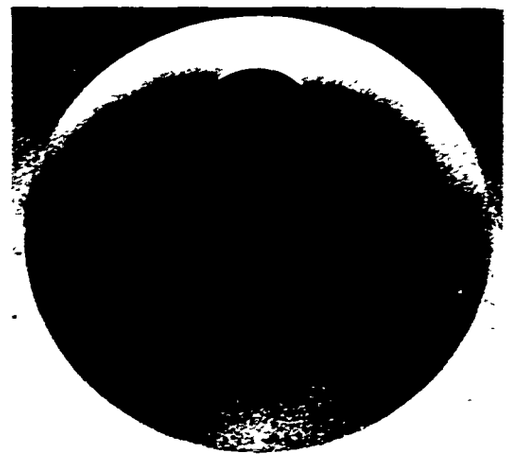

(a) Low-pressure face.

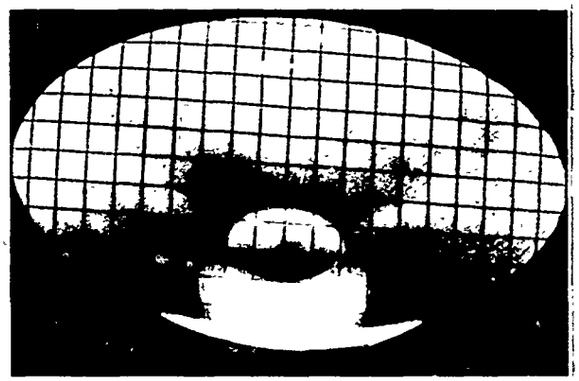

(b) High-pressure face.

Figure A-19. Conical acrylic window after constant hydrostatic pressure loading to 20,000 psi for 1,000 hours in 65°F-to-75°F temperature range; 90-degree cone, t/D = 2.0, 1-inch minor face diameter.

A number of surface cracks were observed on the conical seating surface of windows with $t/D \leq 0.875$. The conical fractures, an extension of conical seating surface cracks, were found to penetrate the body of the window and reappear on the window's high-pressure face. In windows with $t/D = 0.75$ the fractures penetrated the body of the window in less than 500 hours causing the window to be separated into two fragments (Figure A-13). The same kind of fracture was observed with windows of $t/D = 0.875$, except that in these windows the fracture did not penetrate the body of the window completely in 500 hours. In the windows with $t/D = 0.875$ it took 1,000 hours of pressure application before the fracture penetrated the whole body of the window (Figure A-14). For t/D ratios 0.75 and 0.875, the conical fracture originated on the conical seating surface and propagated into the interior of the window at approximately right angles to the conical surface. When the conical fracture penetrated the whole thickness of the window body it reappeared on the window's high-pressure face on the edge of the cold-flow crater. If the window is subjected to a sufficient loading duration, complete fragmentation of the window into two parts results (Figure A-13). One part of the window forms an annular ring and ceases to act as a load-carrying number, while the central part of the window becomes the sole load-carrying member. With time a considerable separation between originally joined surfaces takes place; the central part of the window continues to extrude through the flange opening while the annular part of the window remains in the original location with respect to the flange. Windows with $t/D \geq 1.0$ did not fracture after exposure to 20,000 psi for 1,000 hours. Surface cracks, if present, were concentrated in the first 40% to 50% of the window's thickness measured axially along the conical bearing surface from its minor diameter end.

From observation of cold-flow deformations and fractures in 90-degree conical windows, it appears that only windows with $t/D \geq 2.0$ will perform satisfactorily in a high-grade optical system when subjected to 20,000 psi of hydrostatic loading for time periods equal to or less than 1,000 hours in a DOL 1 type flange.

120 Degree. All 120-degree windows with $t/D = 0.5$ failed during raising of the pressure to 20,000 psi, while most of the windows with $t/D = 0.625$ failed during 1,000 hours of 20,000-psi hydrostatic loading. Thus, comments on windows removed from the vessel after long-term pressurization are limited to windows with $0.75 \leq t/D \leq 2.0$ (Figures A-20 through A-26).

Cold-flow cratering of the high-pressure face was observed on all 120-degree windows with $t/D \leq 1.0$ (Figures A-21 and A-22). Only windows with $t/D \geq 1.25$ did not show any noticeable cold-flow craters (Figures A-23, A-24, and A-26). Cold-flow plug extrusion was observed on all the windows

with t/D ≤ 2.0, and the magnitude of the extrusion appeared to be related to the duration of loading and window's t/D ratio so long as the temperature remained constant. Both long duration of sustained pressure loading and small t/D ratios increased the magnitude of cold flow. The magnitude of plug extrusion in windows with t/D = 0.75 was so great that deformation of the low-pressure face took place (Figure A-20). The resulting convex surface of the low-pressure face was cracked in many places. No cracks were observed on the low-pressure faces of windows with t/D ≥ 0.875 (Figures A-21 through A-26).

Considerable cracking and fracturing was observed in windows with a t/D ≤ 0.75. The conical seating surface cracks extended through the body of the window and reappeared on the window's high-pressure face. In windows with t/D = 0.75, the conical fracture penetrated the body of the window completely in less than 500 hours of load application causing the window to separate into two fragments (Figure A-20). After the window had fragmented into two parts, only the central part of the window continued to carry the load while the annular fragment remained in its original position with respect to the flange. In windows with 0.75 ≤ t/D ≤ 1.0, cracks were present on the conical seating surfaces, but did not penetrate through the whole body of the window. In some of the 0.875 and 1.0 t/D ratio windows, the conical fracture was already well initiated on the conical seating surface after the 1,000-hour loading (Figure A-22), while in windows with a t/D ≤ 1.5 only pronounced cracks were present at that location (Figures A-23 and A-24). Hairline cracks on the conical seating surface were found even in windows with t/D = 2.0 (Figure A-26). All cracks in the conical seating surface appeared in the first 10% to 20% of the window's thickness measuring axially along the conical bearing surface from the minor diameter of the window.

From the observation of cold-flow deformations and fractures in 120-degree conical windows, it appears that only windows with t/D ≥ 1.75 will perform optically in a satisfactory manner when subjected to 20,000 psi of hydrostatic loading for time periods equal to or less than 1,000 hours in a DOL 1 type flange.

150 Degree. All 150-degree windows with t/D = 0.5 failed during raising of the hydrostatic pressure to 20,000 psi. Most of the windows with t/D = 0.625 failed during the 1,000-hour, sustained 20,000-psi hydrostatic pressure. Thus, the main body of observations is limited to windows with 0.75 ≤ t/D ≤ 2.0 (Figures A-27 through A-30).

(a) Low-pressure face (assembled).

(b) Low-pressure face (disassembled).

Figure A-20. Conical acrylic window after constant hydrostatic pressure loading to 20,000 psi for 1,000 hours in 65°F-to-75°F temperature range; 120-degree cone, t/D = 0.75, 1-inch minor face diameter.

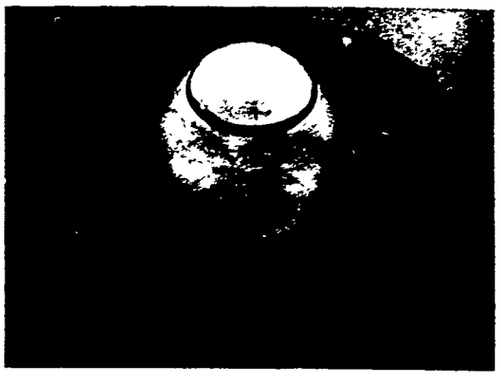

(a) Low-pressure face.

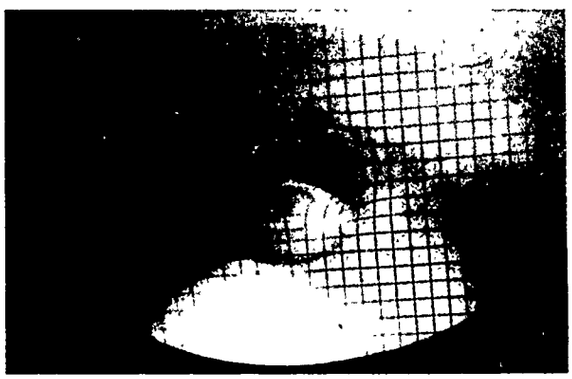

(b) High-pressure face.

Figure A-21. Conical acrylic window after constant hydrostatic pressure loading to 20,000 psi for 1,000 hours in 65°F-to-75°F temperature range; 120 degree cone, t/D = 0.875, 1-inch minor face diameter.

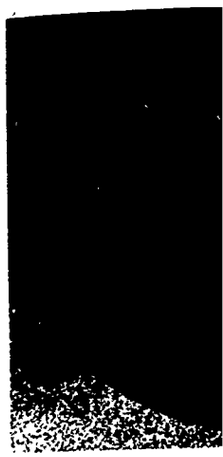

Figure A-22. Conical a
pressure l
65°F-to-
t/D = 1.0

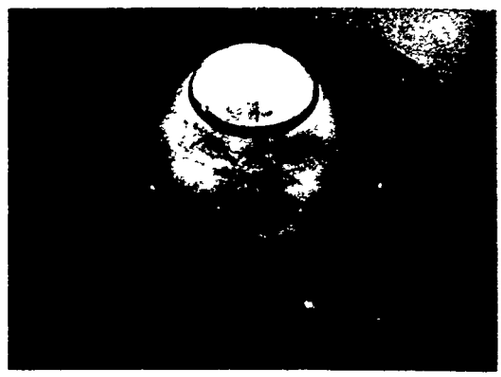

(a) Low-pressure face.

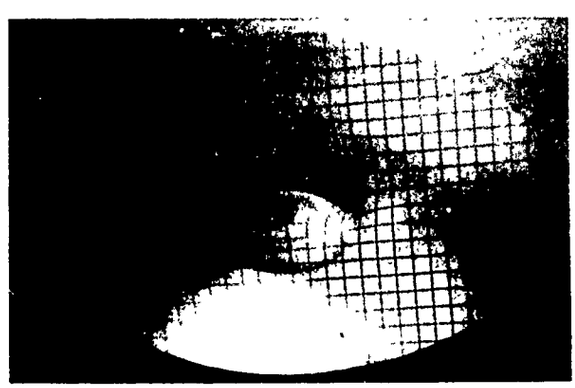

(b) High-pressure face.

Figure A-21. Conical acrylic window after constant hydrostatic pressure loading to 20,000 psi for 1,000 hours in 65°F-to-75°F temperature range; 120-degree cone, t/D = 0.875, 1-inch minor face diameter.

(a) Low-pressure face.

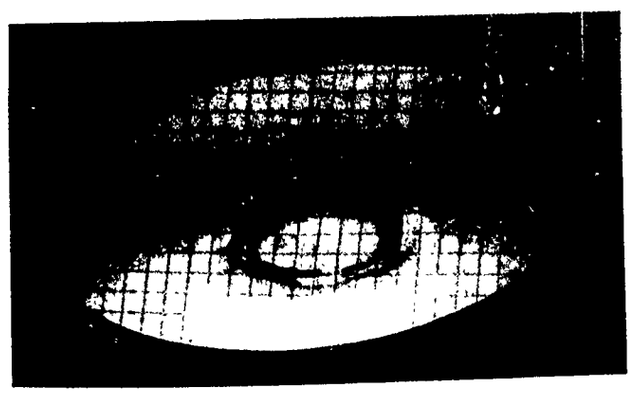

(b) High-pressure face.

Figure A-22. Conical acrylic window after constant hydrostatic pressure loading to 20,000 psi for 1,000 hours in 65°F-to-75°F temperature range; 120-degree cone, t/D = 1.0, 1-inch minor face diameter.

(a) Low-pressure face.

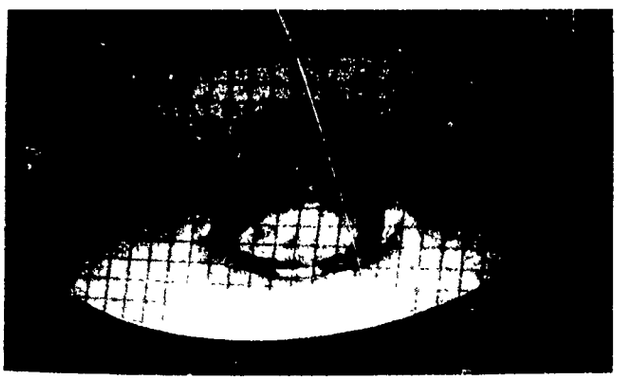

(b) High-pressure face.

Figure A-22. Conical acrylic window after constant hydrostatic pressure loading to 20,000 psi for 1,000 hours in 65°F-to-75°F temperature range; 120-degree cone, t/D = 1.0, 1-inch minor face diameter.

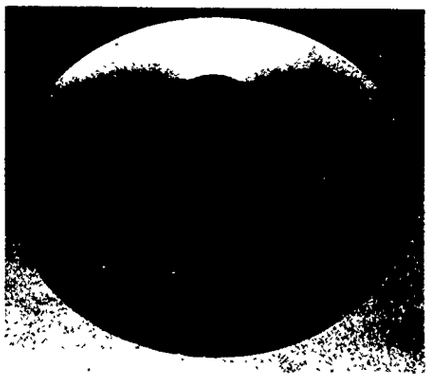

(a) Low-pressure face.

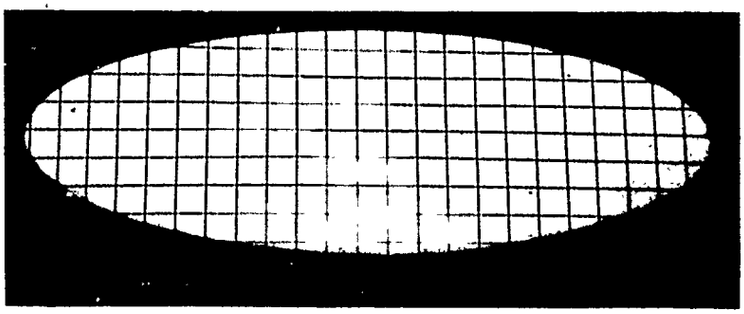

(b) High-pressure face.

Figure A-23. Conical acrylic window after constant hydrostatic pressure loading to 20,000 psi for 1,000 hours in 65°F-to-75°F temperature range; 120-degree cone, t/D = 1.25, 1-inch minor face diameter.

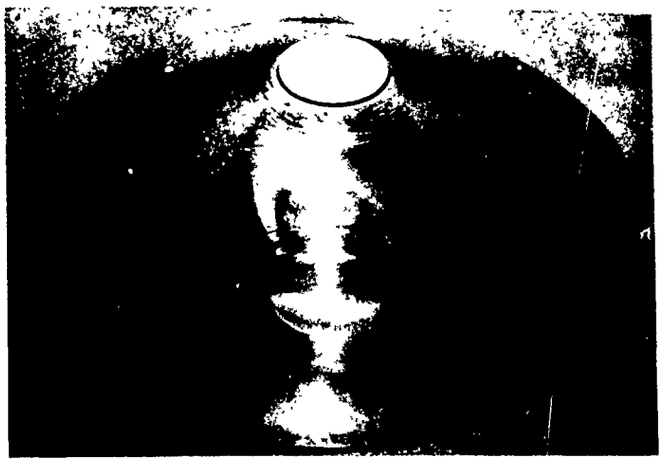

(a) Low-pressure face.

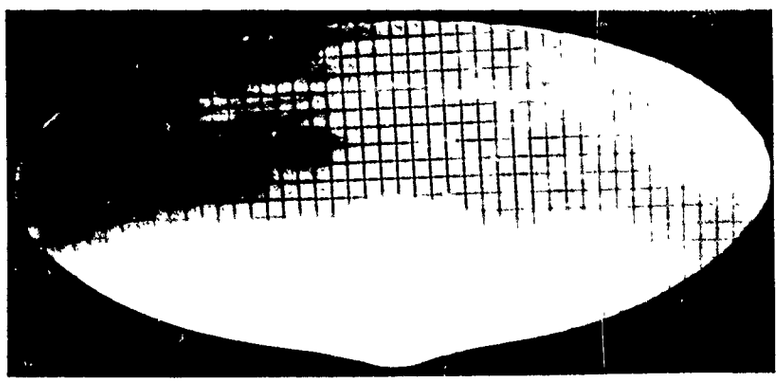

(b) High-pressure face.

Figure A-24. Conical acrylic window after constant hydrostatic pressure loading to 20,000 psi for 1,000 hours in 65°F-to-75°F temperature range; 120-degree cone, t/D = 1.5, 1-inch minor face diameter.

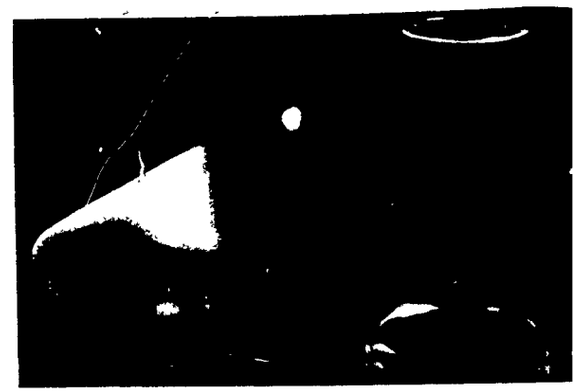

(a) Low-pressure face.

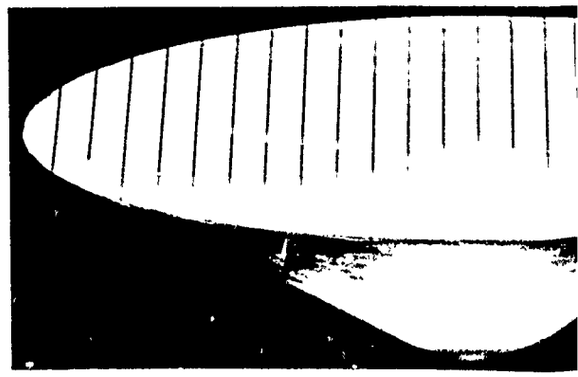

(b) High-pressure face.

Figure A-25. Conical acrylic window after consta pressure loading to 20,000 psi for 1 65°F-to-75°F temperature range; 1 t/D = 1.75, 1-inch minor face diam

(a) Low-pressure face.

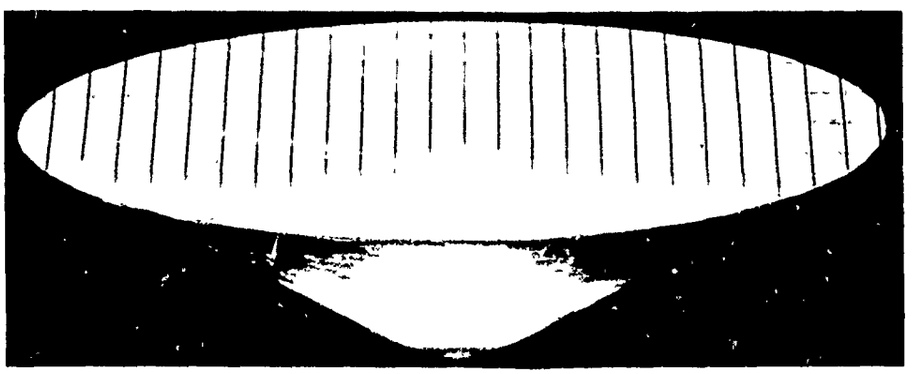

(b) High-pressure face.

Figure A-25. Conical acrylic window after constant hydrostatic pressure loading to 20,000 psi for 1,000 hours in 65°F-to-75°F temperature range; 120-degree cone, t/D = 1.75, 1-inch minor face diameter.

a) Low-pressure face.

(a) Low-pressure face.

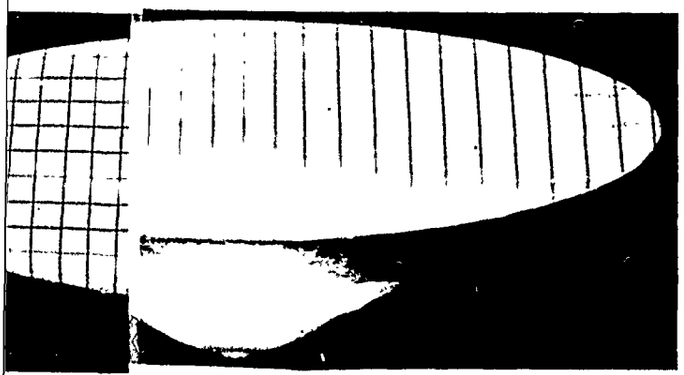

(b) High-pressure face.

igure A-26. Cor acrylic window after constant hydrostatic
pre loading to 20,000 psi for 1,000 hours in
65° -75°F temperature range; 120-degree cone,
t/D 75, 1-inch minor face diameter.

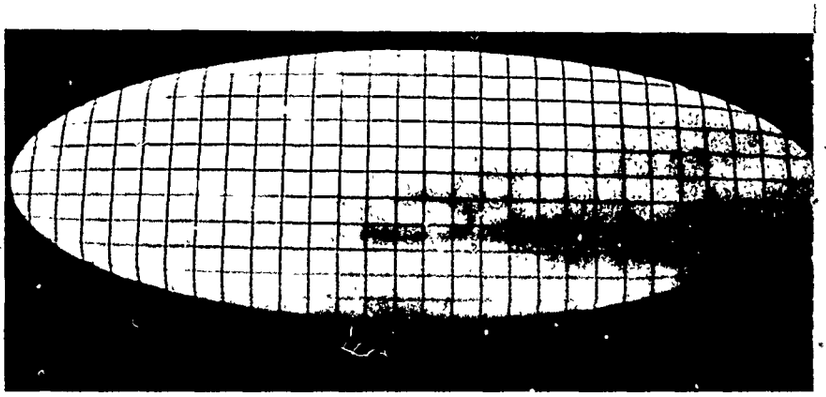

(b) High-pressure face.

Figure A-26. Conical acrylic window after constant hydrostatic pressure loading to 20,000 psi for 1,000 hours in 65°F-to-75°F temperature range; 120-degree cone, t/D = 2.0, 1-inch minor face diameter.

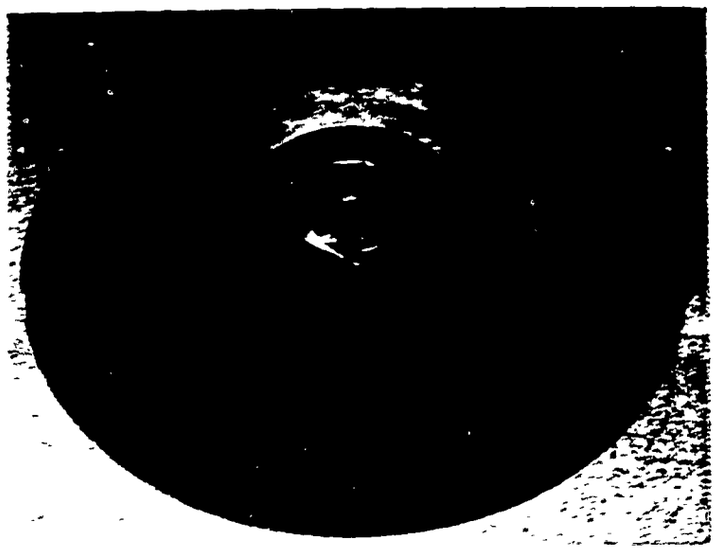

(a) Low-pressure face.

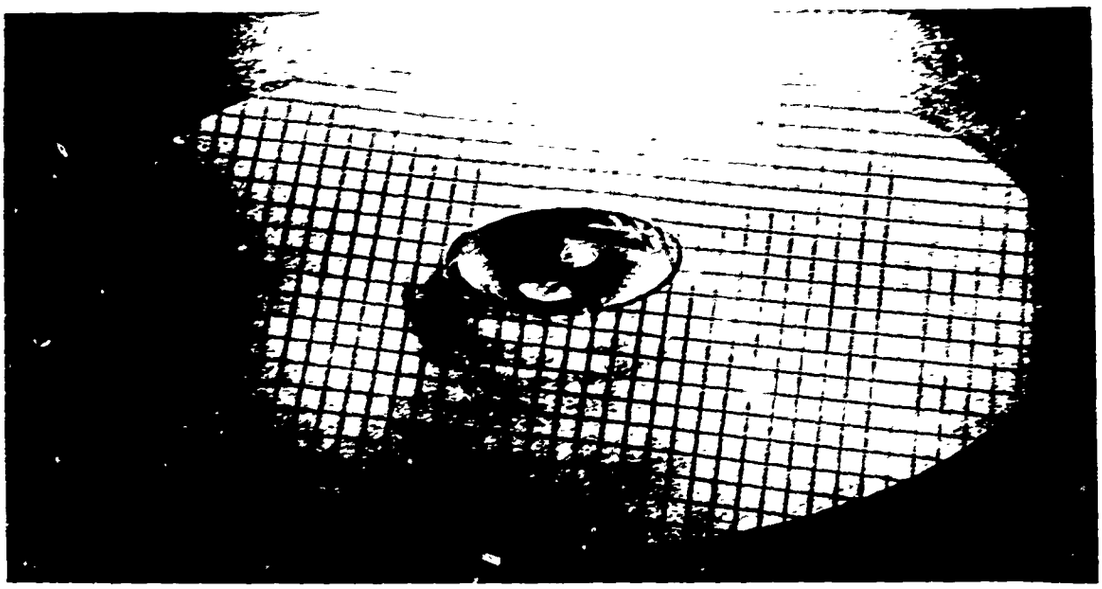

(b) High-pressure face.

Figure A-27. Conical acrylic window after constant hydrostatic pressure loading to 20,000 psi for 1,000 hours in 65°F-to-75°F temperature range; 150-degree cone, t/D = 1.0, 1-inch minor face diameter.

(a) Low-pressure face.

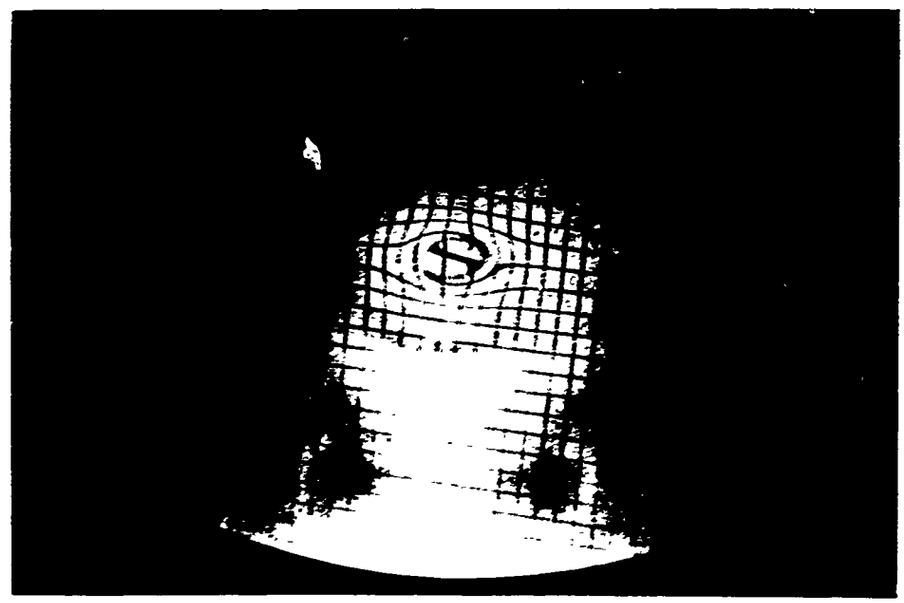

(b) High-pressure face.

Figure A-28. Conical acrylic window after constant hydrostatic pressure loading to 20,000 psi for 1,000 hours in 65°F-to-75°F temperature range; 150-degree cone, t/D = 0.875, 1-inch minor face diameter.

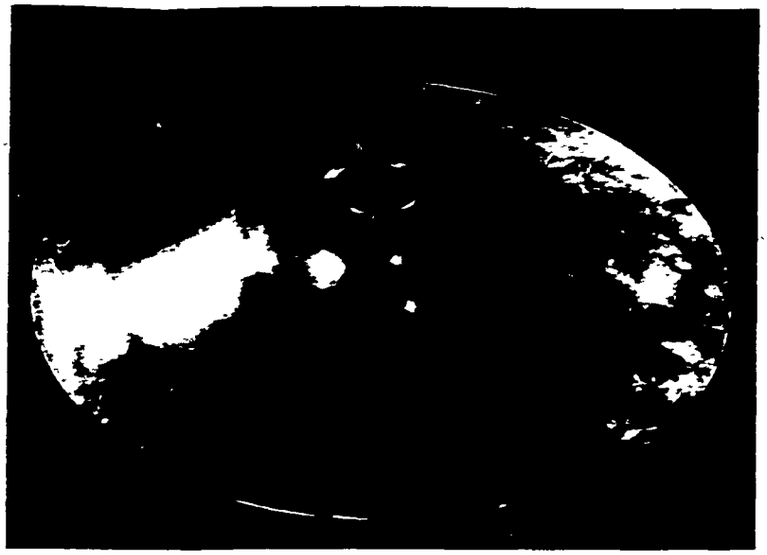

(a) Low-pressure face.

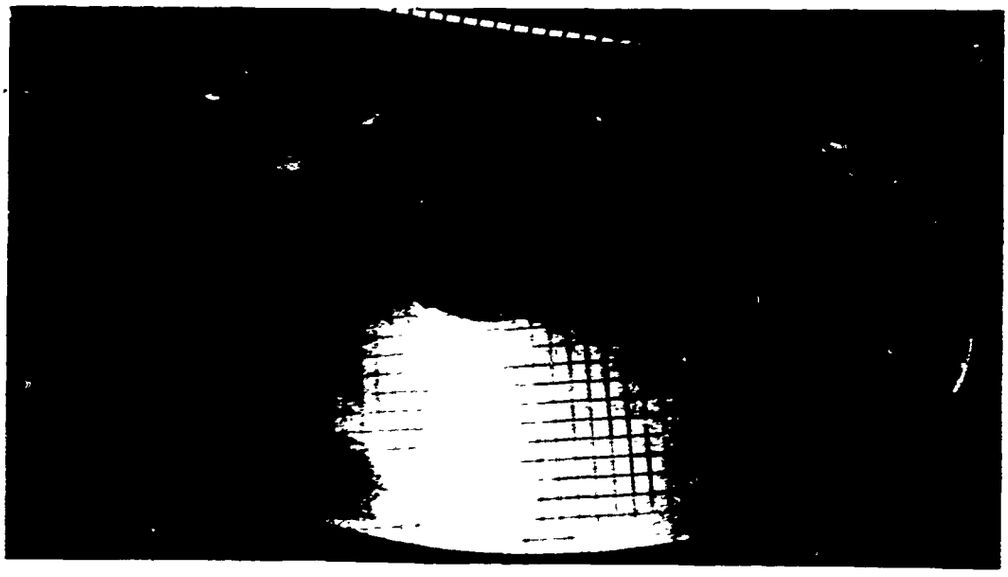

(b) High-pressure face.

Figure A-29. Conical acrylic window after constant hydrostatic pressure loading to 20,000 psi for 1,000 hours in 65°-to-75°F temperature range; 150-degree cone, t/D = 1.0, 1-inch minor face diameter.

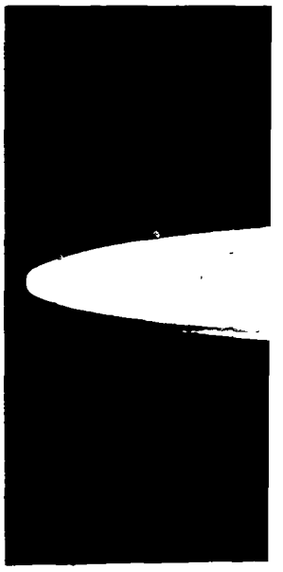

Figure A-30. Coni
1,00
mino

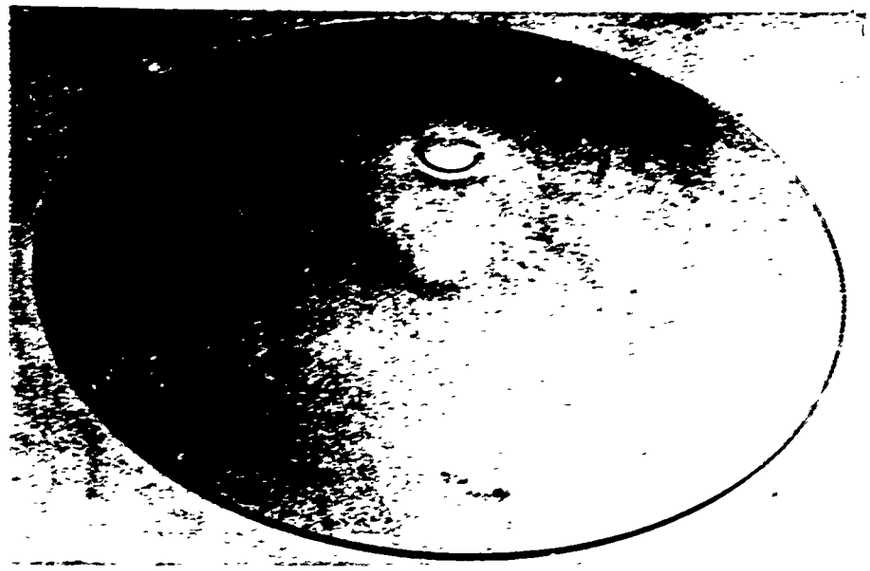

(a) Low-pressure face.

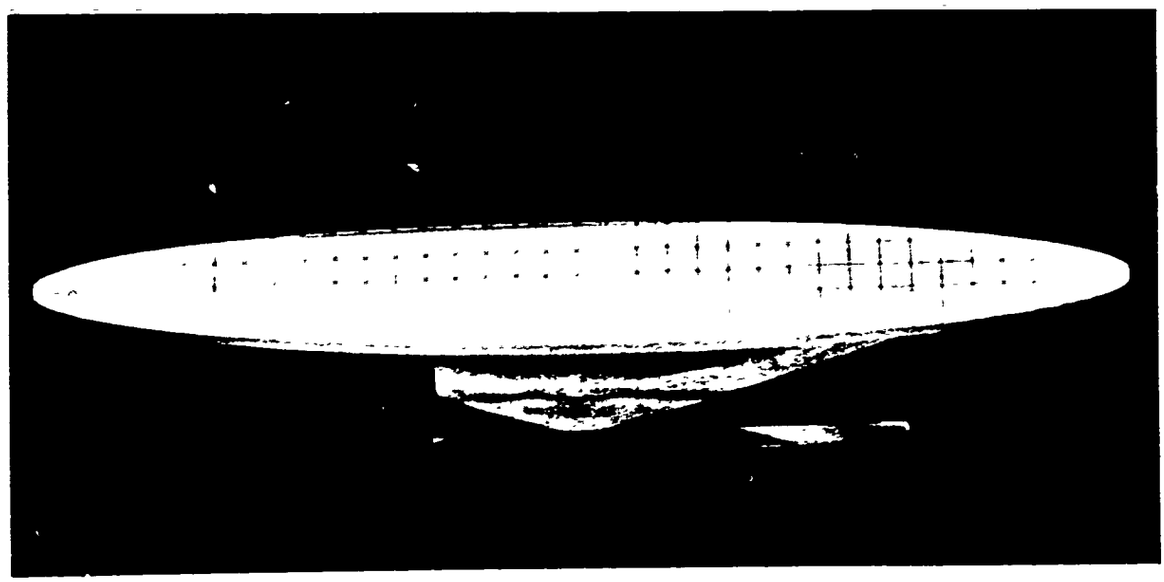

(b) High-pressure face.

Figure A-30. Conical acrylic window after constant hydrostatic pressure loading to 20,000 psi for 1,000 hours in 65°F-to-75°F temperature range; 150-degree cone, t/D = 2.0, 1-inch minor face diameter.

Cold-flow cratering of the high-pressure face was observed in all of the 150-degree windows with $t/D < 1.0$ (Figures A-27 and A-28). It is only with $t/D \geq 1.0$ that the cold-flow cratering of the high-pressure face becomes so small as to be barely noticeable (Figures A-29 and A-30).

Cold-flow plug extrusion has been observed on all windows with $t/D \leq 2.0$. The magnitude of the plug extrusion was found to be related both to the duration of pressure application and a window's t/D ratio; long pressure applications and small t/D ratios resulted in large magnitudes of cold flow. The magnitude of cold-flow plug extrusion on windows with $t/D = 0.75$ was so large that considerable cracking of the low-pressure face was observed (Figure A-27). Windows with $t/D = 0.875$ did not exhibit any cracking of the low-pressure face (Figure A-28). The low-pressure faces of windows with $0.875 \leq t/D \leq 1.0$ exhibited a raised edge around their circumference giving those faces the appearance of a slightly concave surface. The height of the raised edges was in the 0.01-to-0.02-inch range, while the diameter of the flat surface on the low-pressure face was in the 0.875-to-0.75-inch range. Only windows with $t/D = 2.0$ did not exhibit any distortion of the low-pressure face. The face of these windows was essentially flat after 1,000 hours of 20,000-psi pressure.

Considerable surface cracking and fracturing of the window body was observed on the conical seating surface of windows with $t/D \leq 0.875$. The conical fracture, an extension of cracks on the conical seating surface, penetrated the whole thickness of the window with $t/D \leq 0.75$ in less than 500 hours, reappearing on the high-pressure face (Figure A-27). In windows with $t/D = 0.875$, the conical fracture does not penetrate the whole thickness of the window even in 1,000 hours. Cracks on the conical seating surface were generally concentrated in the first 5% to 10% of the window's thickness measured axially along the conical bearing surface from the minor diameter of the window.

From the observation of cold-flow deformations and fractures in 150-degree conical windows, it appears that only windows with $t/D \geq 1.5$ will be optically satisfactory when subjected to 20,000 psi of sustained hydrostatic loading for time periods equal to, or less than 1,000 hours in a DOL 1 type flange.

4-Inch-Diameter Conical Windows

Because of limited pressure vessel time available at the Deep Ocean Laboratory for windows requiring vessels with an internal diameter of 18 inches and pressure capability of 20,000 psi, only one thickness-to-diameter

ratio (t/D = 1.0) was investigated for full-scale 4-inch-diameter windows with 30-, 60-, and 90-degree conical angles. Although the test results from full-scale windows of 30-, 60-, or 90-degree conical angle and a single t/D ratio cannot serve as an adequate statistical sample for comparison with test results obtained for model windows having 30-, 60-, 90-, 120-, and 150-degree angles in the $0.625 \leq t/D \leq 2.0$ range, they serve as a useful scaling validity indicator.

Displacements. In general the axial displacement, cold-flow cratering, plug extrusion, and distribution of cracks in the low-pressure face and conical bearing surface were found to be very similar to those found in model windows of 1-inch diameter and t/D = 1.0. Good correlation for the relative magnitude (with respect to window's low-pressure face diameter) of axial displacement was found between 1- and 4-inch-diameter windows with 60- and 90-degree conical angle and t/D = 1.0. The correlation of relative axial displacement magnitudes was only fair for the 30-degree windows. This is not surprising, as the response of t/D = 1.0 windows with this angle to 20,000-psi long-term pressure loading has been found to vary greatly from one model window test specimen to another. However, the relative magnitude of displacements in the full-scale 30-degree conical angle window falls within the range of displacements for model windows.

When one takes into consideration that the displacements of full-scale 4-inch-diameter windows with 30-, 60-, or 90-degree conical angle and $t/D_o = 1.0$ have been found to be approximately four times larger than those of corresponding 1-inch-diameter model windows, it becomes apparent that linear scaling of displacement data obtained in this study with model windows is feasible and can serve as a valuable tool in predicting the behavior of windows of any diameter. In each case, the comparison must be made between windows of same t/D ratio and conical angle that have been subjected to identical parameters of pressure, temperature, and loading duration in the DOL 1 flange configuration.

Cold-Flow Effects. The relative magnitude of permanent plug extrusion on the low-pressure face and the cold-flow cratering on the high-pressure face has been found to be approximately the same for full-scale windows as for 1-inch-diameter model windows of t/D = 1.0. Similarly, the distribution of cracks on the conical bearing surface and on the low-pressure face was about the same as for the model windows of t/D = 1.0.

The relative magnitude of crack depth was similar to model windows only for 30- and 60-degree full-scale windows (Figures A-31 and A-32). For the 90-degree full-scale windows, the relative depth of crack penetration into the body of the window was considerably greater (Figure A-33). Both

in the depth of penetration, as well as in appearance and location, the single major crack located in the bearing surface of the window had the characteristics of the crack found in model windows with $0.875 \leq t/D < 1.0$. This may indicate either that the material and/or machining of the 90-degree full-scale windows were slightly different from that of the model windows of same angle and t/D ratio, or that some unknown and unaccounted variable entered during the testing of full-scale 90-degree windows.

In general the observed deformations, cracks, and axial displacements of the full-scale windows possessed enough similarity and were of the proper relative magnitude to establish confidence in the applicability of data generated with model windows.

Low-Temperature Effects. All of the tests described thus far in this appendix were conducted at room temperature (between 65°F and 75°F). Operating in this temperature range made it unnecessary to utilize temperature-control equipment, thus considerably increasing the reliability of long-term tests. Also the results of tests conducted on temperature-sensitive acrylic windows in 65°F-to-75°F temperature range have indicated[1, 2, 3] that this temperature range represents a more severe window-deformation environment under short-term loading conditions than would be encountered in the considerably colder ocean depths, thus making the experimental data obtained at room temperature conservative for applications in the 32°F-to-40°F temperature range.

Even though the experimental data were known to be conservative, in order to define at least qualitatively the difference in magnitudes of window deformation measured in the 65°F-to-75°F range and those expected in 32°F-to-40°F range, five 4-inch-diameter, 90-degree windows with t/D = 1.0 were subjected to 20,000-psi hydrostatic pressure for 1,000 hours in the 30°F-to-35°F temperature range. The comparison of deformations in these windows tested in the low-temperature range and those previously tested in the room temperature range constitute the basis for the following discussion of temperature effects on window deformation (Figure 13a).

The deformation of the 4-inch-diameter, 90-degree windows with t/D = 1.0 after sustained pressure loading to 20,000 psi in 30°F-to-35°F temperature range for 1,000 hours was found to be less than that of comparable windows tested under identical conditions except for temperature, which was in the 65°F-to-75°F range (Figure A-33). Both the length of plug extrusion on the low-pressure face and the depth of cold-flow cratering on the high-pressure face were noticeably less than in the windows tested at room temperature. Comparison of measurements taken on the room-temperature and low-temperature test windows has shown that the plug extrusion of the low-temperature test windows was approximately 30% to

40% *less* than in room-temperature test windows. This compares quite favorably with the predicted difference of extrusion based on strains measured in acrylic tensile test specimens under different temperatures.

Slightly fewer cracks in the conical bearing surface of windows were observed in window specimens used in the low-temperature tests than in the specimens tested at room temperature. In all probability this is due to the lesser magnitude of plug extrusion found in the low-temperature test windows than in room-temperature test windows. Since the resistance to crack propagation of acrylic plastic does not decrease significantly with temperature in the 65°F-to-30°F range, the low-temperature test conditions did not impose a more severe test environment (one that would enhance the propagation of cracks) than did the room-temperature test conditions.

It appears then that the room-temperature test condition to which the windows in the main body of this program were subjected represents a more severe test condition than will be ever encountered by such windows in the 30°F-to-35°F temperature range commonly found at ocean depths in excess of 10,000 feet. However, even though the data from this study are known to be conservative, the reduction in severity of distortion in the low-temperature range for acrylic windows other than those with 90-degree included angles and t/D = 1.0 cannot be forecast in the absence of specific data.

(a) Low-pressure face.

(b) View into the window's interior through the high-pressure f

Figure A-31. Conical acrylic window after constant hydrostatic pressure loading to 20,(temperature range; 30-degree cone, t/D = 1.0, 4-inch minor face diameter.

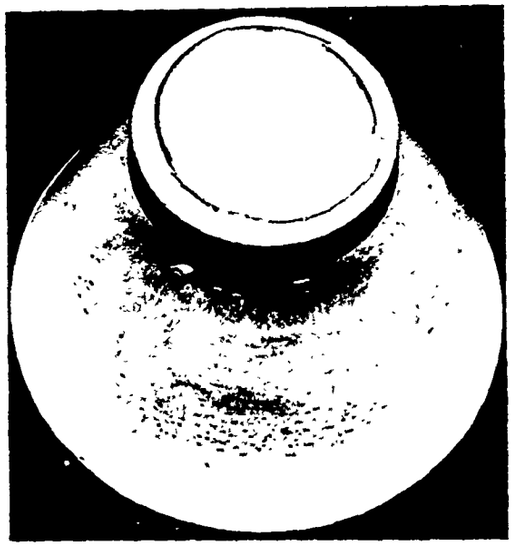

(a) Low-pressure face.

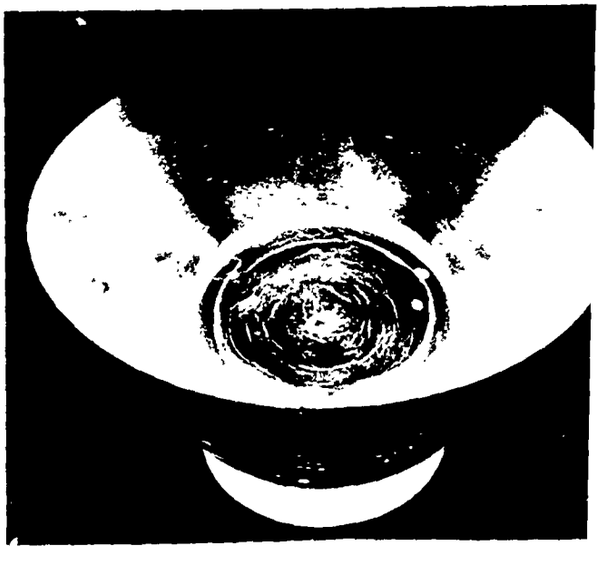

(b) View into the window's interior through the high-pressure

Figure A-32. Conical acrylic window after constant hydrostatic pressure loading to 20 temperature range; 60-degree cone, t/D = 1.0, 4-inch minor face diamete

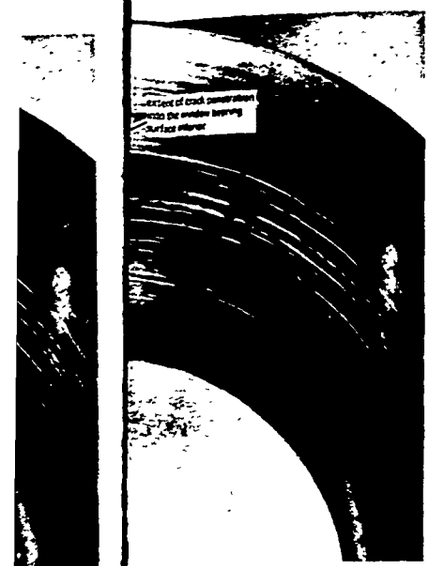

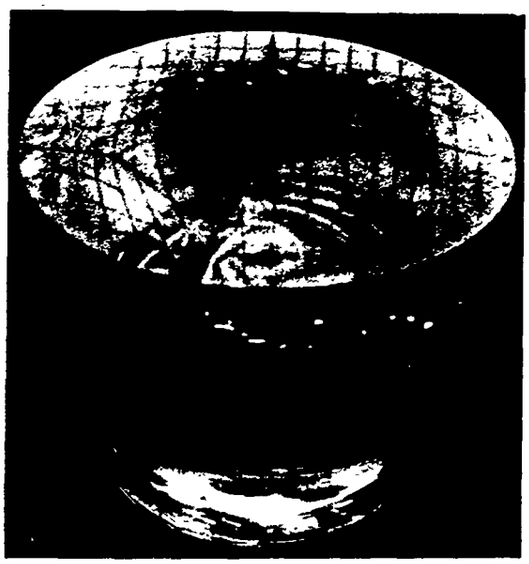

or through the high-pressure face.

(c) High-pressure face.

static pressure loading to 20,000 psi for 1,000 hours in 65°F-to-75°F
0, 4-inch minor face diameter.

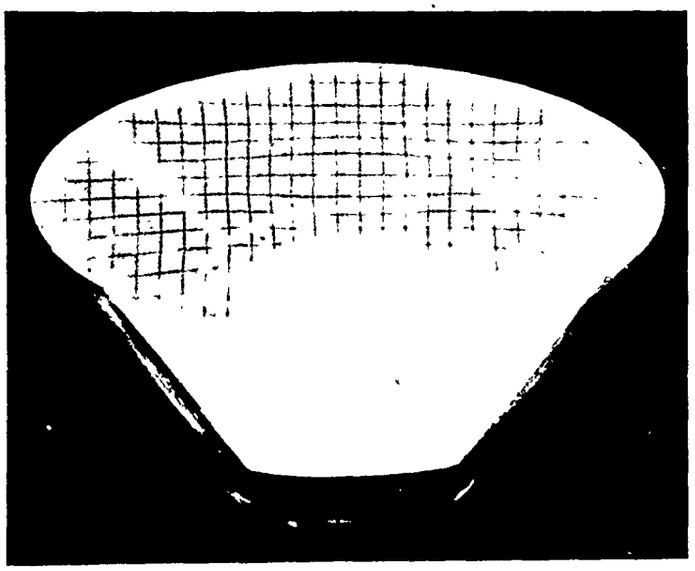

or through the high-pressure face.

(c) High-pressure face.

static pressure loading to 20,000 psi for 1,000 hours in 65°F-to-75°F
0, 4-inch minor face diameter.

(a) Low-pressure face.

(b) View into the window's interior through the high-pressure face.

Figure A-33. Conical acrylic window after constant hydrostatic pressure loading to 20,000 temperature range; 90-degree cone, t/D = 1.0, 4-inch minor face diameter.

(b) View into the window's interior through the high-pressure face.

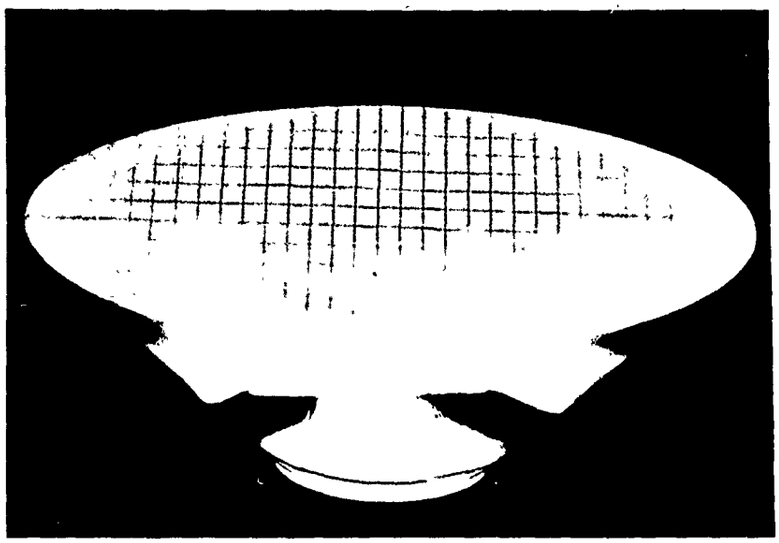

(c) High-pressure face.

,000 psi for
r.

low after constant hydrostatic pressure loading to 20,000 psi for 1,000 hours in 65°F-to-75°F
90-degree cone, t/D = 1.0, 4-inch minor face diameter.

Appendix B

DESIGN OF WINDOW AND FLANGE SYSTEMS FOR LONG-TERM LOADING AT 20,000-PSI PRESSURE

INTRODUCTION

When the data generated in this study are to be applied to the design of windows for deep-submergence systems, several design and operational parameters must be carefully evaluated. The most important operational parameter that must be considered is the type of pressure loading to which the pressure-resistant structures with windows will be subjected. For ease of discussion, hydrostatic pressure loadings can be classified into four general categories. These loading categories are (1) static short-term, (2) sustained long-term, (3) cyclical, and (4) dynamic.

The short-term static pressure loading has been defined as a continuous pressure rise at some arbitrarily set pressure rise rate until a predetermined pressure is reached, upon which the pressure is released at the same rate. The pressure rise rate selected for NCEL window studies[1, 2, 3] was 650 psi/min.

Long-term sustained pressure loading is defined here as raising the pressure at some set rate to a predetermined pressure level and holding it there for the whole duration of the mission. Depending on the duration of the constant pressure application, the long-term pressure loading is further defined by the number of hours, or days that it is maintained on the window.

Cyclical pressure loading is defined as varying the pressure between arbitrary maximum and minimum pressure levels with the period of pressure fluctuation being either constant or variable.

Dynamic pressure loading depends for its definition on the arbitrary dividing line between short-term static and dynamic pressure rise rate, which for windows used in submersibles probably can be placed at 5,000 psi/min. The dynamic pressure application may be short-term if applied once or cyclical if applied repeatedly.

WINDOWS

Selection of t/D Ratios

The data that have been generated in this study are applicable directly with some extrapolation *only to design of truncated cone acrylic windows under short-term or long-term loading at 20,000 psi*, since the test specimens

in this study underwent short-term pressurization at the rate of 650 psi/min followed by long-term steady pressure loading at 20,000 psi. On the basis of this data some guidelines can be suggested for the benefit of the engineer designing acrylic hydrospace windows of truncated cone shape for a one-time, long-term-pressurization to 20,000 psi in the 32°F-to-75°F temperature range.

Design Guideline 1. The recommended t/D ratios tabulated below are for mechanical applications in which the acrylic truncated cone is utilized simply as a ***self-energizing long-term timing device*** whose time-dependent displacement under external hydrostatic pressure is utilized to actuate mechanical, hydraulic, or electric devices that in turn cause the pressurized structure to perform some function. These t/D ratios have been selected to provide maximum time-dependent axial displacement without catastrophic failure in the indicated duration of loading.

Flange	Included Conical Angle (deg)	t/D Ratio for Sustained Loading Period of—			
		1 Hour	100 Hours	1,000 Hours	100,000 Hours
(See Design Guideline 4)	30	1.25	1.25	1.25	1.25
	60	0.75	0.875	0.875	1
	90*				
	120*				
	150*				

* Note recommended for time-dependent device actuator applications because of insufficient axial displacement for high t/D ratios and considerable fracturing at low t/D ratios.

The 30-degree included angle is considered to be the most desirable as it causes the acrylic plug to have a very large axial displacement without the considerable internal fracturing that is generally accompanied by jerkiness in the rate of displacement. The magnitude of axial displacement for t/D ratios chosen at 75°F and 20,000 psi ranges between 0.2 and 0.6 of the diameter at the end of the recommended loading periods. After each pressurization, the acrylic plugs must be replaced with new ones.

When acrylic truncated cone plugs are used as time-dependent device actuators for unmanned structures placed in the deep ocean, the displacement curves presented in this report for the DOL 1 flange should be modified by a factor that takes into consideration the effect of low temperatures at the place of submergence. Without such a factor, the actual displacements of acrylic plugs under low ambient temperatures will be found to be significantly less than those shown in the report.

If the acrylic plugs are used under pressures less than 20,000 psi, new displacement curves will have to be developed that will take the lesser pressure level into account. Pressure levels lower than 15,000 psi will also require the selection of lesser t/D ratios and/or conical angles to permit the plug to displace sufficiently to serve as a time-dependent device actuator.

Design Guideline 2. When the acrylic window is to serve only as an *illumination transmitter* for unmanned capsules and not as a high-grade optical lens, less displacement is desired than for time-dependent actuators. However, more displacement can be tolerated in illumination applications than for high-grade optical applications. When used to illuminate, considerable distortion of the window's high-pressure and low-pressure faces as well as axial displacement is permissible, so long as fracturing does not take place in the window's interior that would seriously impede the transmission of light. At the 20,000-psi pressure level in the 32°F-to-75°F temperature range, the acceptable minimum t/D ratios have displacements of less than 0.15 D for 90-degree, 0.2 D for 60-degree, and 0.3 D for 30-degree windows in a specified time span.

Flange	Included Conical Angle (deg)	t/D Ratio for Sustained Loading Period of—			
		1 Hour	100 Hours	1,000 Hours	100,000 Hours
(See Design Guideline 5)	30	≥1.5	≥1.5	≥1.75	≥2.0
	60	≥1.0	≥1.0	≥1.25	≥1.5
	90	≥1.0	≥1.0	≥1.25	≥1.25
	120*				
	150*				

* Not recommended for illumination transmission because of considerable fracturing at low t/D ratios, while high t/D ratios make windows too bulky.

After each pressurization of the structure fitted with acrylic windows, the windows must be replaced as otherwise they may fail at pressures less than 20,000 psi upon repressurization.

The t/D ratios acceptable for 20,000-psi long-term loading of specified duration are also applicable without any modification as desirable conservative ratios for long-term pressure loading in the $15{,}000 \leq p \leq 20{,}000$-psi pressure range and the 32°F-to-75°F temperature range.

Design Guideline 3. When the truncated cone acrylic windows serve as *high-grade optical lenses* for visual observation of hydrospace outside a submersible's pressure hull or the observation of simulated hydrospace inside a pressure vessel, only minute distortion of viewing surfaces can be tolerated. Because of these tolerance limitations, the acceptable t/D ratios are drastically different from those appropriate for the time-dependent device actuator and illumination transmitter described in guidelines 1 and 3.

Flange	Included Conical Angle (deg)	t/D Ratio for Sustained Loading Period of—			
		1 Hour	100 Hours	1,000 Hours	100,000 Hours
(See Design Guideline 6)	30	3.0	3.5	4.0	6.0
	60	2.0	2.5	3.25	4.75
	90	1.5	1.75	2.0	3.5
	120	1.25	1.5	1.75	2.5
	150	1.0	1.25	1.5	2.0

The t/D ratios acceptable for optical applications of truncated cone acrylic windows have been selected after a thorough consideration of three parameters of importance in operational window performance: (1) magnitude of axial displacement during the long-term pressure loading, (2) deformation of high- and of low-pressure faces, and (3) magnitude of penetration and location of cracks on the conical surface during the sustained loading. Since it is virtually impossible, regardless of t/D ratio and angle chosen, to completely eliminate time-dependent cold flow of the acrylic plastic at 20,000-psi hydrostatic pressure, an engineering judgement was made on what constitutes the minimum acceptable performance of the acrylic window from the optical and safety viewpoints.

A window is considered to be safe for manned operation if during a single sustained pressure loading of 20,000 psi in the 32^{o}F-to-75^{o}F range for the specified maximum duration no cracks or crazing were present on the high- and low-pressure faces, while the conical bearing surface exhibited only minor crazing, or cracking less than 0.010-inch deep. Total axial displacement in the range of 0.05 D to 0.1 D at the end of the specified period of loading presents no operational difficulties for the observer. The window is optically acceptable if it causes no distortion of viewed objects in hydrospace for an observer whose eyes are within 10 inches of the low-pressure face.

The t/D ratios acceptable for windows in optical applications under long-term pressure loading of 20,000 psi in 32^{o}F-to-75^{o}F range are also applicable without any modification as desirable conservative ratios for long-term pressure loading in the $15{,}000 \leq p \leq 20{,}000$-psi range pressure and 32^{o}F-to-75^{o}F temperature range.

It is understood, of course, that design guideline 3 can be applied to dimensioning of illumination transmission windows used in unmanned capsules if the designer so desires, resulting in illumination transmission windows with very little optical distortion.

Applicability of Data to Other Loading Conditions

As previously mentioned, the experimental data generated in this study is applicable with reasonable extrapolation only to a single short-, or long-term static pressure loading at 20,000 psi. However, since very little data is now available for the design of windows subjected to long-term loading at other pressures than those used in this study, some designers may be tempted to base their selections of window proportions on the data from this study. ***This is not recommended.*** The factors for adjusting t/D ratios from this study for other pressure levels have not yet been developed. Studies are underway at NCEL that will provide this information for 10,000-psi applications. The results of long-term pressure study at 10,000 psi will be published in late 1969, while the results from study at 5,000 psi will be available in early 1970.

It is recommended as operationally desirable that the minimum t/D ratios acceptable for 20,000-psi long-term pressure loading also be used for pressures in the 15,000-to-20,000-psi range. This change in long-term operational static pressure magnitude will make it possible to proof-test such windows to 20,000 psi without damaging the windows.

The experimental data of this report also should not be used for the direct selection of window proportions for applications where the window is subjected to cyclic short-term or long-term pressurizations. Caution is advised here because the relationship between the effect of cyclic and long-term loading conditions on the initiation of fracture in acrylic windows is not known. However, in view of the fact that cyclic pressurization data for windows operating in the abyssal depth range is either nonexistent or very scarce, designers may also be tempted to use long-term pressure loading data contained in this report for the design of windows for cyclic pressure service. Designers who do this are advised that the window proportions recommended for 1,000-hour sustained loading at 20,000 psi will *probably* perform quite satisfactory at 15,000-psi cyclic loading so long as the maximum duration of the pressure cycle is less than 10 hours. If window proportions are selected for cyclic service on this basis, extensive evaluation of the prototype full-scale window under simulated operational conditions is recommended.

Window Fabrication

Since the windows rely on intimate contact with the conical flange cavity surface for their high-pressure sealing as well as for their restraint against axial displacement, an accurate fit with that cavity is of great

importance. For this reason the maximum allowable machining tolerances on the window must not exceed ±0.005 inch on the minor diameter, 0.010 inch in thickness, and ±15 minutes of included conical angle.

The windows are fabricated by machining acrylic stock having the mechanical and physical properties of Plexiglas G plate. Four-inch-thick commercially available plate, a custom cast block, or a block made up by bonding of several standard acrylic plates can serve as machining stock. In the case of custom cast or bonded blocks, the end product must have the same mechanical and physical properties as a monolithic, commercially available 4-inch-thick Plexiglas G plate. It is particularly important that the tensile strength of the bonds in the bonded acrylic block be equal to or approach that of the parent material (Table B-1).

Regardless of the machining stock used, the window should be annealed twice during its fabrication: once after rough machining when it is within approximately 0.125 inch of finished dimensions, and a second time when it has been machined to its final dimensions and the surfaces have been polished. Without annealing, the conical bearing surfaces of the window will craze and crack sooner under operational service.

The finish of the conical bearing surface of the window should be a 32-rms machined surface followed by polishing. If the surface finish is rougher, crazing and cracking of the conical bearing surface could initiate sooner under operational service.

Proof-Testing of Windows

When the experimental data contained in this report are used for the design of windows, care must be taken not to damage the windows with excessive overpressure proof-testing. The basic ground rule for windows selected on the basis of long-term tests described in this report is that *conical acrylic windows should never be subjected to pressures above 20,000 psi, regardless whether this occurs during the operational life of the window or during the proof-test that precedes it*. Because of this if the operational service of the windows is to be at 20,000 psi, the proof pressure preceding the operational use of the windows must only be equal to operational pressure. If for some reason the proof pressure must be in excess of operational pressure, then accordingly the operational pressure rating must be reduced below the 20,000-psi pressure level. Thus, for example, windows selected for long-term loading condition in habitats or capsules with 15,000-psi operational depth capability cannot be proof-tested to pressures higher than 1.25 x operational pressure, as otherwise the proof pressure will exceed 20,000 psi.

Table B-1. Properties of Acrylic Window Material

Physical Properties		
Property	Requirement	Test Method
Hardness, Rockwell M	90 (minimum)	ASTM-D785-62
Hardness, Barcol	90 (minimum)	ASTM-D2583
Specific gravity	1.19 ± 0.01 (2 tests within 0.005)	ASTM-D792-64T
Refractive index; 1/8 inch	1.50 ± 0.01	ASTM-D542-50
Luminous transmittance; 1/8 inch	91% (minimum)	ASTM-D1003-61
Haze, 1/8 inch	2.3 (maximum)	ASTM-D1003-61
Heat distortion temperature +3.5°F/min at 264 psi +3.6°F/min at 66 psi	 200°F 220°F	ASTM-D648-56
Thermal expansion/°F at 20°F	35×10^{-6} (maximum)	Federal Standard 406 Method 2031
Water absorption; 1/8 inch (a) 25 hours at 73°F (b) to saturation	 0.3% (maximum) 1.9% (maximum)	ASTM-D570-63T
Mechanical Properties*		
Tensile strength, rupture (0.2 in./min)	9,000 psi	ASTM-D638-64T
Tensile elongation, rupture	2% (minimum)—6% (maximum)	ASTM-D638-64T
Modulus of elasticity, tension	425,000 psi	ASTM-D638-64T
Compressive strength, (0.2 in./min)	16,000 psi	ASTM-D695-63T
Flexural strength, rupture	16,000 psi	ASTM-D790-63
Shear strength, rupture	9,000 psi	ASTM-D732-46
Impact strength, 1 rod (per inch of notch)	0.4 ft-lb	ASTM-D256-56
Compressive deformation under load (4,000 psi at 122°F for 24 hours)	0.6% (maximum)	ASTM-D621-64

* The requirements are minimum values.

Since the proof-test to 20,000 psi prior to placement of the window in actual service constitutes a loading cycle, it is important to make it as brief as possible so that it does not substantially reduce the rated long-term life of the window in subsequent operation under service conditions. Because of this it is recommended that if the window will operate in service at 15,000 psi the application of 20,000-psi proof pressure should be limited to 1 hour.

Ideally, proof-testing of each window slated for long-term service operation at 20,000 psi should not take place at all, as it has a negative influence on the long-term life of the window. Instead of proof-testing each window, it is more advantageous to rely on quality control in the procurement of acrylic stock, and machining, annealing, and bonding of the window. When this quality control in fabrication is augmented by the testing under simulated service conditions of a window selected at random from the same group of windows on the production line, very reliable windows for long-term loading can be obtained. In this manner even though one window is sacrificed to nondestructive and possibly to destructive proof-testing, the remaining windows from the same production batch retain all of their potential pressure-resisting capability for actual service operation.

FLANGES

Configurations

Although all the bulk of experimental data of this study has been generated in the DOL 1 flange and window configuration (Figure B-1), a minor modification of this configuration is recommended for full-size hydrospace windows to give the user an added margin of safety for windows whose proportions have been selected on the basis of this study.

The recommended modification to the DOL 1 flange and window configuration consists of locating the window's low-pressure face further away from the cylindrical passage in the flange to provide not only radial but axial restraints for the extruding portion of the window. Such a flange and window configuration, designated as DOL 5 flange (Figure B-2), should permit the windows to extrude somewhat less than the windows described in this study and thus give the designer extra margin of safety and optical performance.

A group of windows with t/D = 1.5 and conical angle of 60 degrees has been tested in the DOL 5 flange to determine whether the predicted decrease in axial displacement actually takes place. Comparison of axial displacements measured on windows in the DOL 5 flange with displacements of windows in the DOL 1 flange showed that the windows tested in the DOL 5

flange displace less than similar windows tested in the DOL 1 flange. The difference in magnitude of displacement was on the order of 10%. What the difference may be for other t/D ratios and angles is unknown. It is certain however, from basic considerations of the structural parameters controlling the window displacement that the displacement of windows in the DOL 5 flange will never be more than in the DOL 1 flange. Furthermore, these exploratory tests have shown that when pressure is relieved the extruded plugs of conical windows tend to become wedged in the cylindrical passage of the DOL 1 flange causing some portions of the window to be placed under tensile loading. Such wedging does not take place in the DOL 5 flange, precluding the possibility of having the window under tensile loading when the hydrostatic pressure is zero. On the basis of these findings it is felt that the recommendation to utilize DOL 5 flanges instead of DOL 1 flanges has been experimentally validated and that the use of DOL 5 flanges constitutes an added margin of safety for use of conical acrylic windows under long-term loading. Determination of the magnitude of this margin of safety will be the subject of a future study.

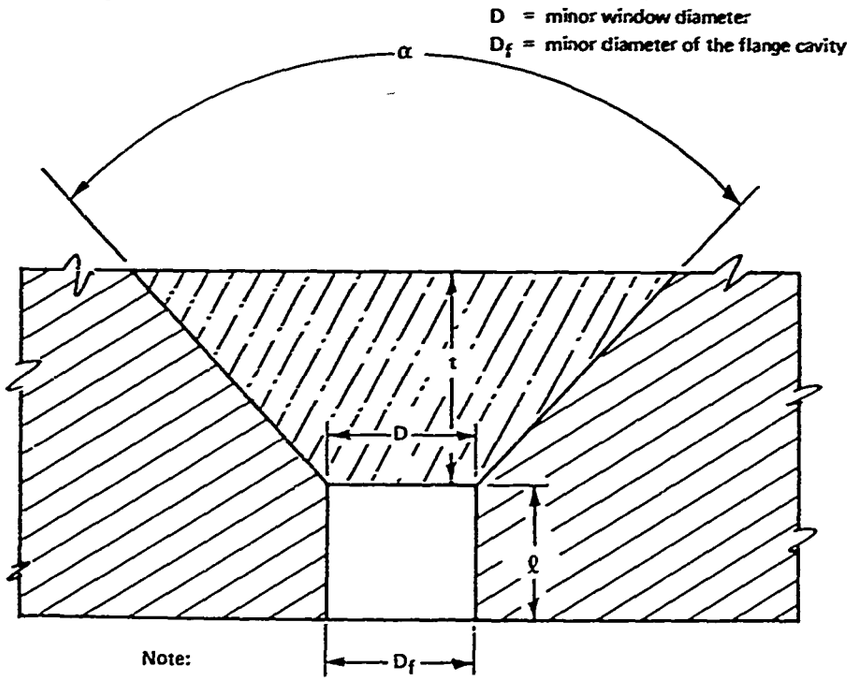

Figure B-1. Characteristics of DOL 1 flange and window assembly used in the current study.

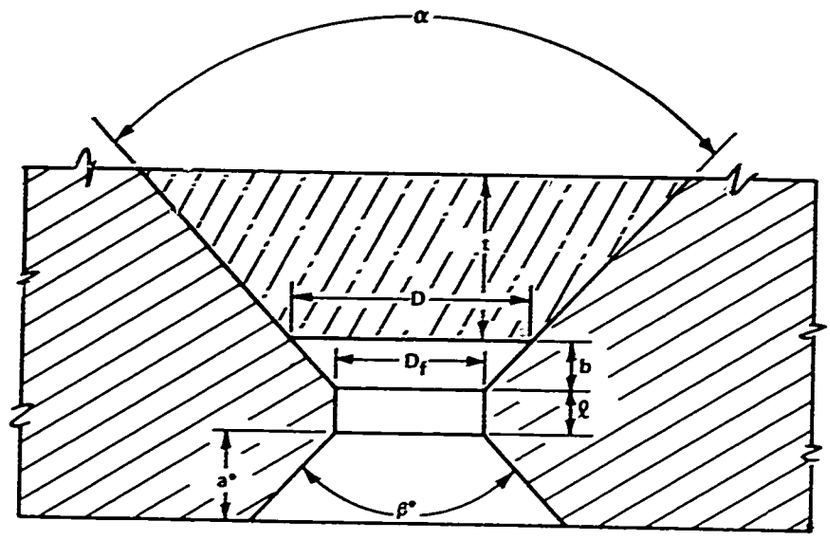

DOL 5 Assembly

Note:

1. a° — To be chosen by designer on basis of stress field evaluation in the flange
2. β° — To be chosen by designer on basis of optical viewing requirements
3. ℓ ≥ b for all t/D ratios and conical angles (α)
4. b ≥ displacement of window during the sustained pressure loading for specified period of time
5. D > D_f for all t/D ratios and conical angles α

Figure B-2. Characteristics of DOL 5 flange and window assembly (the assembly recommended for long-term 20,000-psi pressure).

In order to minimize the displacement of the window under sustained operational pressure, as well as to provide a necessary margin of safety for overpressures to which the windows may be accidentally or intentionally (as in proof-testing) exposed, the engineer must design the window flange opening with required radial and axial support for the window. The dimensions of DOL 5 window flanges have been calculated and are presented in guidelines 5 and 6. These calculations are based on two assumptions. The first is that the distance b between the window's low-pressure face in the conical flange cavity and the bottom of the conical cavity must be approximately the same as the displacement of the window with recommended t/D ratio during the specified duration of sustained loading at 20,000 psi. The second is that either an overpressure or extension of rated loading duration may be encountered by the structure during its life and therefore an additional allowance, ℓ, equal at least to b should be made for window displacement in the cylindrical flange cavity.

The first assumption must be taken into account. The second one should be considered, but in many cases no pressures higher than operational will be encountered, and thus no provisions have to be made for displacements caused by overpressure or for duration of loading past the originally specified time span.

When the acrylic truncated conical plug is used as a time-dependent device actuator, the DOL 1 flange is preferred because in this application a decrease in axial displacement is not desirable. In actuator applications no allowance is made for overpressures or loading duration past specified time span.

Design Guideline 4. For applications in which the acrylic truncated cone is simply a mechanical self-energizing long-term time-dependent device actuator for sustained service at 20,000 psi and 32°F-to-75°F temperature range, the following flange cavity proportions, which tend to favor large displacements are recommended:*

Window	Flange	Included Angle (deg)	D/D_f Ratio	Cylindrical Passage Length, ℓ
(See Design Guideline 1)	DOL 1	30 60	1.0 1.0	0.75 D 0.5 D

Design Guideline 5. For applications in which the acrylic window is to serve only as an illumination transmitter for unmanned capsules under 20,000-psi sustained service in 35°-to-75°F temperature range and not as a high-grade optical lens, the following flange cavity proportions are recommended.**

Window	Flange	Included Angle (deg)	D/D_f Ratio	Cylindrical Passage Length, ℓ
(See Design Guideline 2)	DOL 5	30 60 90	1.19 1.41 1.43	$\geq$0.3 D $\geq$0.25 D $\geq$0.15 D

Design Guideline 6. For applications in which the truncated cone acrylic windows serve as high-grade optical lenses for manned capsules under sustained pressure loading of 20,000 psi in 32°F-to-75°F temperature range the following flange cavity proportions are recommended.**

---

* No allowances for overpressures above 20,000 psi have been made.

** Allowance has been made for minor overpressure and/or extension of loading duration past the rated time span of the window.

Window	Flange	Included Angle (deg)	D/D_f Ratio	Cylindrical Passage Length, ℓ
(See Design Guideline 3)	DOL 5	30	1.05	$\geqslant$0.1 D
		60	1.14	$\geqslant$0.1 D
		90	1.25	$\geqslant$0.1 D
		120	1.54	$\geqslant$0.1 D
		150	4.0	$\geqslant$0.1 D

Finishes and Tolerances

The experimental data relating flange-seat surface roughness to crack initiation in the bearing surface of conical acrylic windows under long-term loading is inconclusive. Therefore, no definite recommendation based on scientific facts can be made for a particular surface finish at this time. It can be only stated that so long as the surface finish is in the range of 32 to 125 rms, the acrylic conical windows will perform satisfactory. The surface finish of the flanges used in this study was 63 rms; it performed quite acceptably and can be considered a happy compromise between the more expensive 32-rms finish and the rough 125-rms finish.

Although exploratory experimental data indicate that an angle mismatch between the acrylic plug and the conical flange seat of 1 to 2 degrees magnitude does not noticeably affect the critical pressure of the window, the mismatch should be kept to a minimum to eliminate high-pressure sealing problems. To minimize leaking, deviation of the conical flange cavity from the specified angle should be in the ±5-to-±15 minute range, easily attained with ordinary machine shop practice.

The effect of variation in the minor diameter of the conical cavity on the displacement and critical pressure of the conical acrylic windows varies with the type of window–flange system used. The effect of variation is most pronounced for the DOL 2 window/flange system and least pronounced for the DOL 5 system. Since DOL 5 system (Figure B-1) is the one recommended for windows under long-term hydrostatic loading, the diametral tolerance for minor diameter of conical flange cavity may be in the range ±0.001 to ±0.005 inch. These tolerances are readily achieved with ordinary machining processes.

SEALS

Requirements

One of the major problems encountered in the design of window systems for long-term loading is the design of seals. The difficulty in the design of seals for such a system stems from the fact that there are three separate operational requirements that the seals must satisfy:

1. The window system must be watertight at low pressures while the capsule, or habitat, is being towed to its location.

2. The window system must be watertight at the maximum operational pressure during the projected duration of the mission on the ocean bottom.

3. The window system must be watertight upon return of the capsule, or habitat, to the ocean surface, and during the subsequent towing to dock.

It is relatively easy to satisfy the first two requirements. Any ordinary gasket will seal the high-pressure face of the window against the window-retaining ring at low hydrostatic pressure, while the greased surface of the window acts as a seal itself under high external hydrostatic pressure. It is much more difficult to satisfy the third requirement because the window has experienced permanent yielding during its long-term service under operational pressure in 15,000-to-20,000-psi range. Upon return of the capsule to the ocean surface there is a tendency for the windows to leak; because permanent axial displacement of the window has taken place, the gasket between the window-retaining ring and the window is no longer compressed. There are many design approaches that will mitigate or completely eliminate the problem of window leakage upon return of the capsule or habitat to the ocean surface after its long-term submergence. Seals of several designs have been built and their performance noted.

Seal Designs

The five different types of seals (Figure B-3) investigated for sealing windows under long-term loading were designed primarily to satisfy requirement 3, but in the process of satisfying that requirement, in every case they also satisfied sealing requirements 1 and 2. The simplest seal investigated was the standard gasket compression seal of 60-durometer hardness held against the window's high-pressure face by a retaining ring. Its thickness was selected to permit the necessary precompression during installation without causing permanent set to the gasket. The precompression was

selected to accommodate the largest predicted displacement of the window in the flange and yet maintain sufficient contact pressure with the window and the retaining ring to permit the gasket to function as a seal when the capsule or habitat is brought back to the ocean surface.

A little more complex was the seal utilizing an O-ring in radial compression. For this design, as well as the elastomeric channel-seal design discussed later, both the window and the flange cavity had to be enlarged to accommodate the seal without reducing the window's critical dimensions. Because the O-ring was designed to be under radial compression, the yielding of the window material under long-term hydrostatic pressure in the 15,000-to-20,000-psi operational range would tend to make the seal more pressure resistant; the clearance between the edge of the window and the flange cavity surface would decrease with time. In addition, the axial movement of the window in the flange did not present any problems in this O-ring seal arrangement, as the radially compressed O-ring slides with the window along the cylindrical surface of the cavity in the flange without any loss of compression. In this design the window is held in the flange cavity by means of a single flat annular spring compressed against the high-pressure face of the window by a retaining ring.

The channel-type seal operates on basically the same principle as the radial O-ring seal. However, the seal, which slides along the cylindrical cavity surface (Figure B-3) with axial displacement of the window, is an elastomeric channel pressed against the window and the cavity surface by two split rings. The window is held in the flange cavity by means of several helical springs held in compression by a retaining ring.

The wiper-type seal in the form of an elastomeric wedge with triangular cross section was designed to operate on the same surface-wiping principle as the two preceding seals except that during axial displacement of the window in the flange cavity the seal wipes a conical surface, not a cylindrical one as is the case in the two previous seals. Because of this, the flange cavity and window may be the same size and shape as for the standard gasket design. The window-retaining ring acting upon the seal wiper ridge also serves the secondary function of preventing the window from moving excessively outward upon surfacing.

The axial O-ring seal was designed like the wiper seal to maintain constant contact with the conical flange surface under large axial displacements of the window. The window is held in positive contact with the cavity surface by the flat annular spring compressed by the retaining ring against the window's high-pressure face.

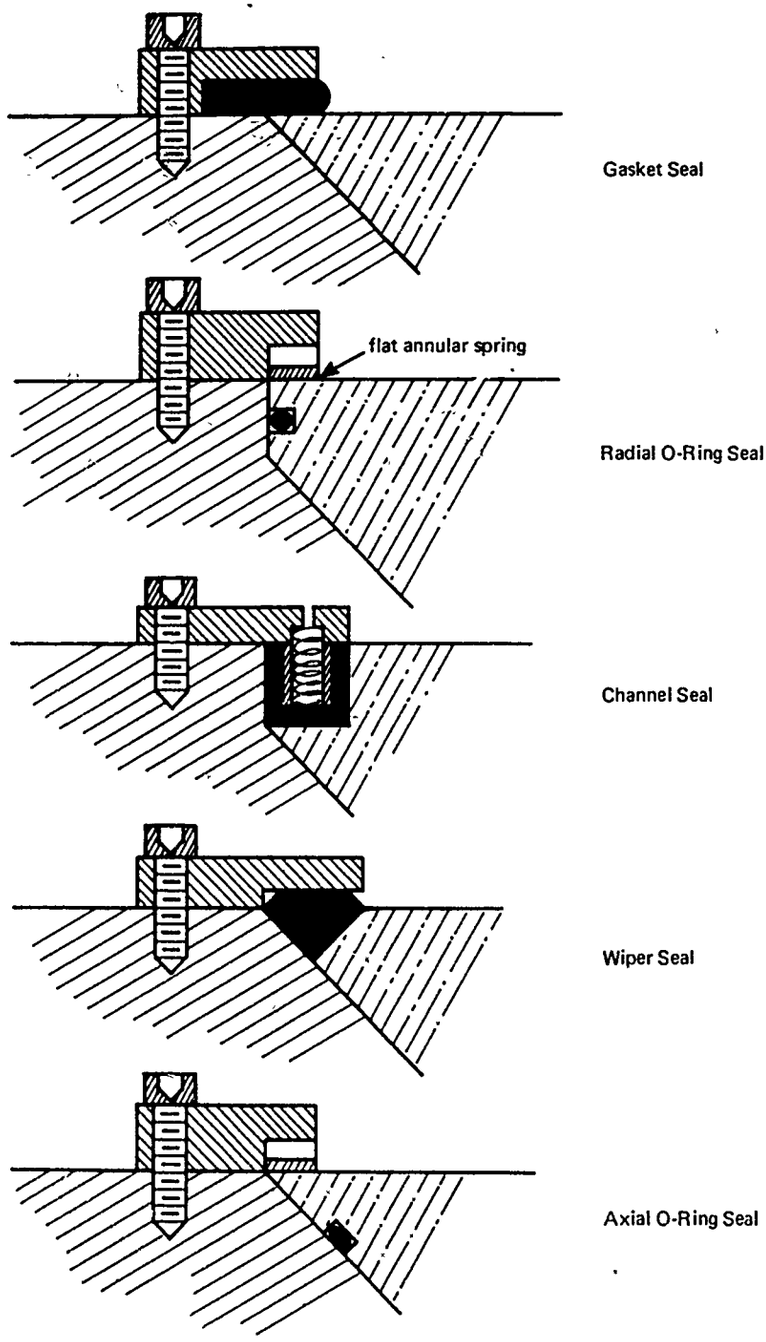

Figure B-3. Seals applicable to windows under long-term pressure loading.

Seal Evaluation

Tests performed on windows of nominal t/D = 2.0, 90-degree conical angle, and 1-inch diameter under 20,000 psi for 1,000 hours have shown that all of these seals performed their sealing function satisfactorily. However, some appear to be more desirable than others for hydrospace windows under long-term loading on the basis of economic, structural, or space considerations.

From the aspect of space required to contain the window and its seal system, the compressed gasket, the elastomeric wiper ring of triangular cross section, and the axially compressed O-ring called for the least space. They required a conical flange cavity whose depth was only somewhat greater than the window's thickness. Thus it would appear that in hydrospace window applications where the depth of the conical flange cavity in the pressure hull must be kept to a minimum because of limited hull thickness such seal designs are attractive.

One shortcoming of these two designs is that for low-pressure sealing capability at the termination of the long-term pressure loading they both rely on the elastomeric properties of the gaskets that initially were axially compressed at least 0.1 D. If, due to the action of seawater, hydrostatic pressure, low temperature, and high initial compression, a permanent set of the elastomer occurs, it will lose its ability to force the window into contact with the flange cavity surface and thus prevent sealing at low pressures.

From the aspect of sealing ability after long-term pressure loading during which the elastomers in the seals acquire a considerable permanent set, the seal designs incorporating an elastomeric O-ring or the channel seal are the most desirable. The latter seals maintain contact with the flange cavity surface even with permanent set in the elastomeric seal as a result of the force exerted on the window by precompressed metallic springs. Between these two types of seals, the ones incorporating the elastomeric O-ring are more desirable because they utilize only off-the-shelf commercial elastomeric rings that are available in many formulations.

A major shortcoming of these sealing systems is the stress raiser effect introduced into the window bearing surface by the presence of grooves machined for the placement of seals. This stress raiser effect is most severe in the groove cut for the axial O-ring seal, particularly in windows with a 30-degree included angle.

In terms of window displacement, the radial O-ring seal is the most desirable one as the window is approximately 25% thicker than designs incorporating plain gasket, wiper type seal, or axial O-ring seals; at the same time the radial O-ring design does not have the serious stress raiser

effect of the channel seal groove. Because of the added window thickness that the radial O-ring seal requires and the low stress raiser effect, it is considered to be the most conservative window seal system.

Seal Selection

In view of the considerations discussed in the section on seal design evaluation, it can be postulated that for long-term loading at a hydrostatic pressure of 20,000 psi only two seal designs are attractive. Where the window cavity in the flange is to have the least axial length possible and where the economics of window–seal system fabrication are important the simple gasket seal design is preferable.

Design Guideline 7. For the ***simple gasket seal***, the design guidelines for selecting the magnitude of elastic gasket precompression under the window retainer ring depend on the design guidelines used in the selection of window t/D ratios.

Selection of Window t/D	Corresponding Conical Cavity Dimensions	Corresponding Gasket Compressions Under Retainer Ring(s) for Included Angles—				
		30^o	60^o	90^o	120^o	150^o
Guideline 2	Guideline 5	0.3 D	0.25 D	0.15 D	—	—
Guideline 3	Guideline 6	0.1 D	0.1 D	0.1 D	0.1 D	0.1 D

If the gaskets are compressed (Figure B-4) as recommended, and no permanent set of the elastomeric gasket occurs, the seal should perform adequately prior to the long-term pressure loading, during the sustained long-term loading of 20,000 psi, and in low-pressure service encountered by the window when the ocean bottom habitat or capsule returns to the ocean's surface.

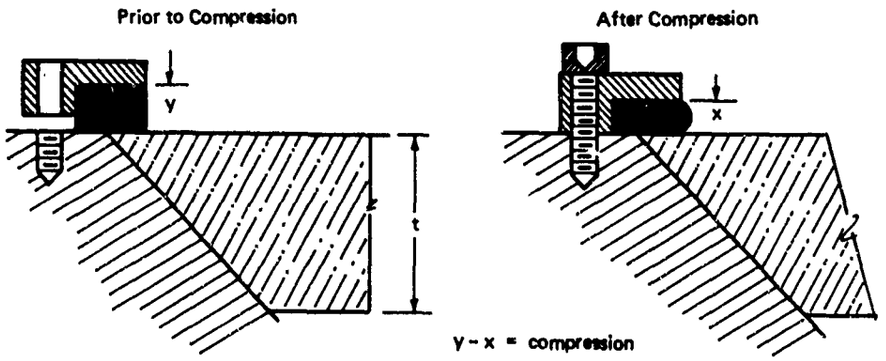

Figure B-4. Parameters for selection of gasket seal compression according to Design Guideline 7.

In applications in which (1) a deeper flange cavity can be tolerated, (2) off-the-shelf commercial O-rings are available for that particular window diameter, (3) some pressure cycling will be present, and (4) a more conservative window design is preferred, the radial O-ring seal is recommended.

Design Guideline 8. For the ***radial O-ring seal***, the design guidelines for selecting the magnitude of the cylindrical lip on the window and the corresponding cylindrical recess in the flange depend on the design guidelines used in the selection of window t/D ratios.

Selection of Window t/D	Corresponding Conical Cavity Dimensions	Corresponding Dimensions of Lower Cylindrical Windows Lip (k) for Included Angles—				
		30°	60°	90°	120°	150°
Guideline 2	Guideline 5	0.4 D	0.3 D	0.2 D	–	–
Guideline 3	Guideline 6	0.2 D	0.2 D	0.2 D	0.2 D	0.2 D

The foregoing description of dimensions (Figure B-5) recommended for the lower cylindrical window lip does not describe the overall thickness of the lip, but just its lower portion below the O-ring groove. In order to specify the window, however, one must also know the overall thickness of the lip. To arrive at that dimension K, one must add to k the width of the O-ring groove w and the upper cylindrical window lip n. Both of these dimensions do not depend on the magnitude of the external pressure to which the window will be subjected but on the size of the O-ring, which in many cases is chosen solely on the basis of the window diameter.

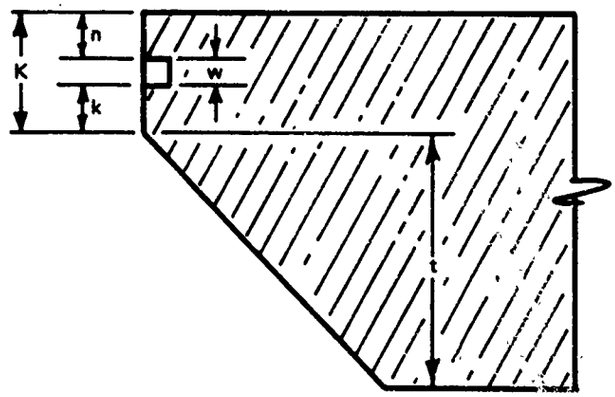

Figure B-5. Parameters for selection of window lip dimensions according to Design Guideline 8.

In general, the width of the groove should be >0.15 inch for 1/8-inch O-rings associated with small windows and >0.3 inch for 1/4-inch O-rings used in large windows. The upper cylindrical window lip should be at least equal in thickness to the groove width, or may be even thicker to prevent its chipping during handling of windows at installation. The resulting window, because of its added thickness is quite conservative and therefore particularly recommended if the long-term pressure service will be at 20,000 psi.

SUMMARY

To tie the many design guidelines together that are spelled out in Appendix B, two typical windows will be designed and dimensioned.

Case A

Requirements

Pressure:	20,000 psi
Type of loading:	Sustained, 1,000 hours
Type of service:	Optical observation of hydrospace
Cone angle:	90 degrees
Type of seal:	Radial O-ring
Minor diameter:	1 inch

Dimensioning

Optical service requires that Design Guideline 3 be used for window t/D selection (in this case t/D = 2.0), Design Guideline 6 for flange cavity D/D_f selection (in this case $D/D_f = 1.25$ and $\ell = 0.1\ D$), and Design Guideline 8 for radial O-ring seal and window lip thickness selection ($k = 0.2\ D$, $w = 0.19$, $n = 0.19$).[3] The configuration of the window and flange is shown in Figures B-6, B-7, and B-8.

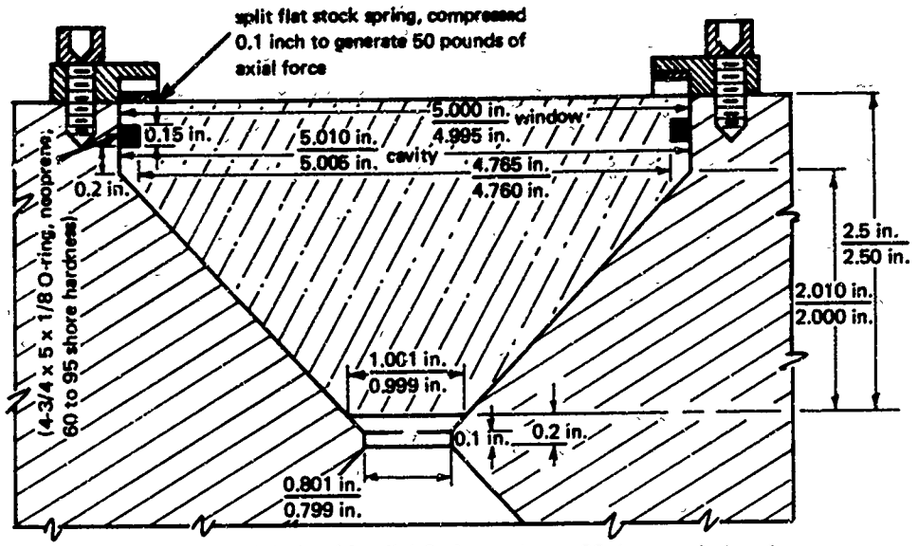

Figure B-6. Typical design of radial O-ring seal on a 90-degree window for 1,000 hours of service at sustained 20,000-psi pressure in 32°F-to-75°F temperature range.

Figure B-7. Window with a radially compressed O-ring seal after 1,000 hours of service at sustained 20,000-psi hydrostatic loading in 65°F-to-75°F temperature range (D = 1.0 in., t/D = 2.0 α = 90).

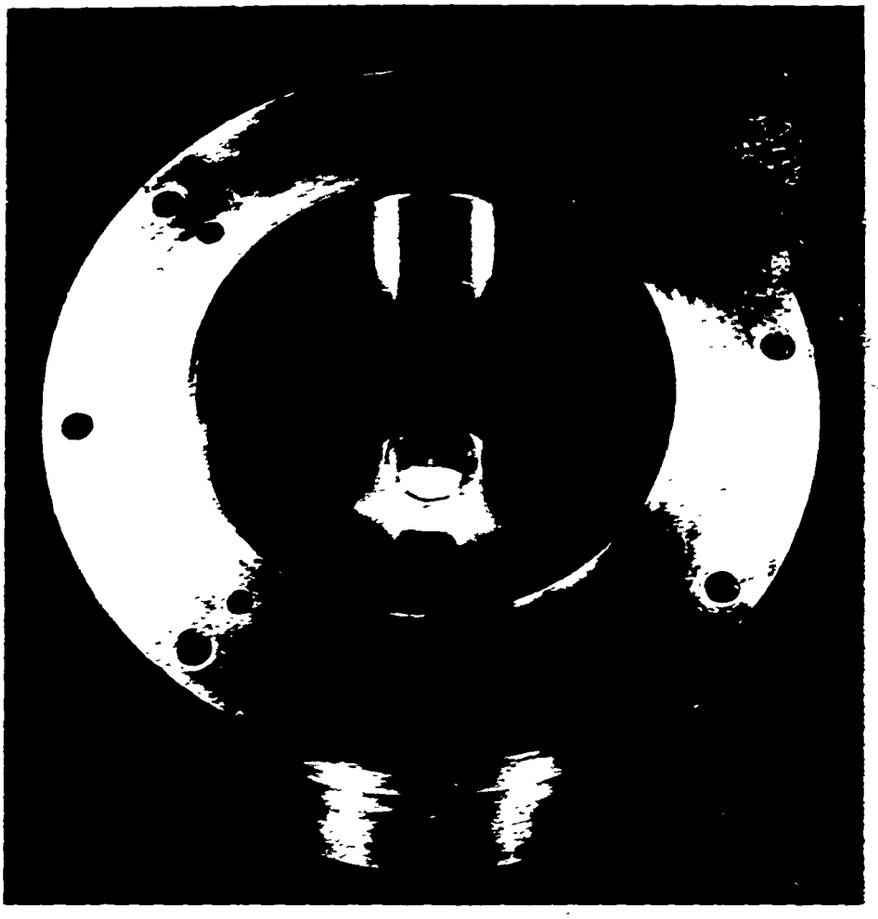

Figure B-8. Flange and window assembly. (The dimensions of this DOL 5 assembly are shown in Figure B-6 and the window configuration in Figure B-7.)

Case B

Requirements

Pressure:	20,000 psi
Type of loading:	Sustained, 1,000 hours
Type of service:	Optical observation of hydrospace
Cone angle:	90 degrees
Type of seal:	Gasket seal
Minor diameter	1 inch

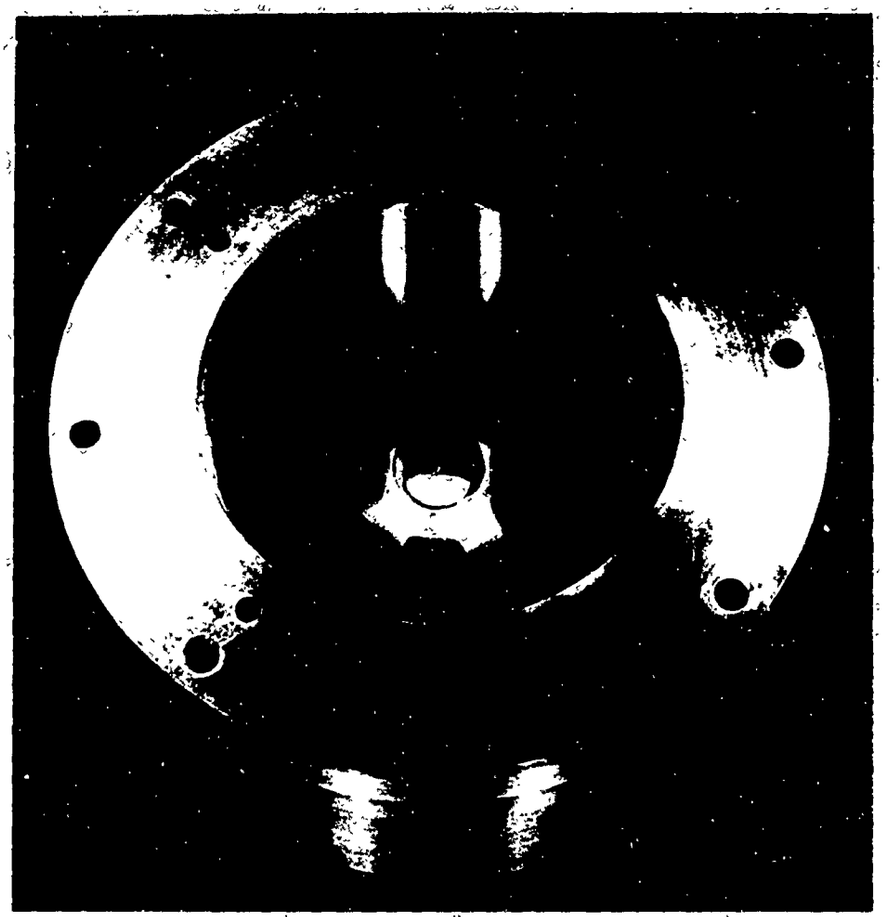

Figure B-8. Flange and window assembly. (The dimensions of this DOL 5 assembly are shown in Figure B-6 and the window configuration in Figure B-7.)

Case B

Requirements

Pressure:	20,000 psi
Type of loading:	Sustained, 1,000 hours
Type of service:	Optical observation of hydrospace
Cone angle:	90 degrees
Type of seal:	Gasket seal
Minor diameter:	1 inch

Dimensioning

Optical observation service requires that Design Guideline 3 be used for window t/D selection (in this case t/D = 2.0), Design Guideline 6 for flange cavity D/D_f selection (in this case $D/D_f = 1.25$, $\ell = 0.1$ D), and Design Guideline 7 for gasket seal precompression specification (in this case 0.1 D). The configuration of the window is shown in Figure B-9.

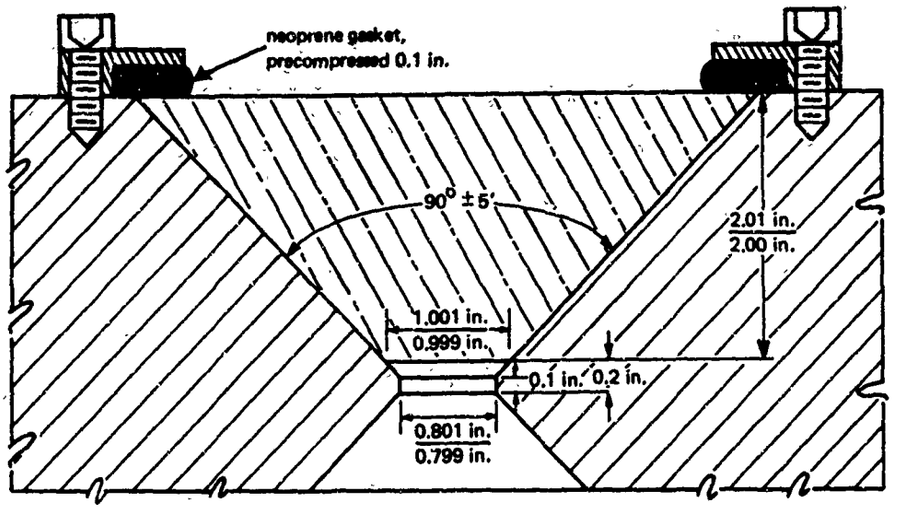

Figure B-9. Typical design of gasket seal on a 90-degree window for 1,000 hours of service at sustained 20,000-psi pressure in 32°F-to-75°F temperature range.

Since all of the design guidelines discussed in Appendix B had as their objective a window that performs reliably and safely in 15,000-to-20,000-psi pressure range and 32°F-to-75°F temperature range, an approach to dimensioning was used that always assumed the windows would be used at the most severe loading condition. Thus it can be expected that when a radial-O-ring-sealed optical service window is operated at 15,000 psi and 34°F temperature for less than the whole span of its rated life, the displacements of the window will be much less than provided for by the design guidelines. On the other hand if a gasket-sealed optical service window is operated at 20,000 psi and 75°F temperature for the whole span of its sustained loading rating, the displacements will probably be equal to those foreseen by the design guidelines, but still will be on the safe side. Because of these built-in safety margins, there is no need for the designer to incorporate additional safety factors so long as the windows will not operate outside their rated performance parameter ranges.

Appendix C

DISPLACEMENTS OF CONICAL ACRYLIC WINDOWS UNDER SUSTAINED HYDROSTATIC LOADING AT 20,000 PSI

Each of the conical acrylic windows subjected to sustained 20,000-psi hydrostatic loading experienced axial displacement through the flange opening. There were three distinct phases in the axial displacement of each window. The **first phase** took place when the pressure was raised at a 650-psi/min rate from 0 to 20,000 psi. The **second phase** was relatively rapid axial displacement of the window through the flange immediately after the 20,000-psi sustained pressure loading was reached. The second phase lasted for approximately 12 to 24 hours. The **third phase** of axial displacement was the relatively slow axial displacement of the window during the remaining duration of sustained pressure loading at 20,000 psi. To emphasize and delineate the three distinct phases of axial displacement, two different scales were used for plotting the displacements. Log-log scales with 0.001-inch displacement and 1-minute time units were selected to show the rapid rate of displacement of the windows during phases 1 and 2. Linear scales with 0.01-inch displacement and 1-day time units were chosen to show the slow rate of displacement during phase 3. To permit rapid visual comparison of the two different displacement phases, they are grouped together in Figures C-1 through C-6 for each different window configuration.

When one observes the graphs depicting phases 1, 2, and 3 one immediately notes that the relationship between time and magnitude of axial displacement is not shown graphically by a narrow line but by a wide band whose width and shape varies from one figure to another. There are several reasons for this.

1. Each curve represents the range of displacements shown by a group of five window specimens which were not of identical dimensions, but varied by the magnitude of dimensional machining tolerances.

2. All of the five windows comprising a single t/D ratio group for a given angle were not tested in the same flange, but in several flanges that differed from each other by the magnitude of dimensional machining tolerances.

3. All five windows in a group were not tested at an identical temperature. The average temperature varied several degrees from one long-term test to another.

4. All of the five windows were not machined from the same piece of material, or for that matter at the same material removal rate.

There are several general observations that can be made about the scatter of recorded displacement data. **First**, that the width of the plotted displacement range appears to be in a large measure a function of absolute displacement magnitude; i.e. small variations in material and dimensional parameters of windows result in large displacements. **Second**, displacements of windows that are accompanied by extensive cracking and fracturing of the acrylic material (**t/D** = 0.75 for 60, 90, 120, and 150 degrees) vary more from one specimen in the same group to another than the displacements of windows not accompanied by extensive cracking. This phenomenon in all probability is caused by the randomness of crack initiation and propagation, as compared to the nonrandomness of typical stress–strain behavior of material before cracking.

Since in some of the **t/D** ratio groups all of the windows failed prior to the termination of the 1,000-hour tests, no graphs exist depicting phase 3 of window displacement. In other groups of windows only some of the windows failed prior to 1,000 hours at sustained 20,000-psi pressure loading. For those groups of windows only the lower boundary of the phase 3 displacement range has been shown since the upper boundary is undefined. (See, for example, 30-degree windows with **t/D** = 1.0.)

When the data contained in Figures C-1 through C-6 is used for design of operational windows, the upper boundary of displacement ranges should be utilized. It represents a conservative approach to sizing of window flange cavities for containment of windows during their displacement under sustained hydrostatic pressure of 15,000 to 20,000 psi. For design of windows that will be used at a sustained pressure of less than 15,000 psi, the lower boundary of the displacement range should be utilized as otherwise the design of flange cavity becomes too conservative.

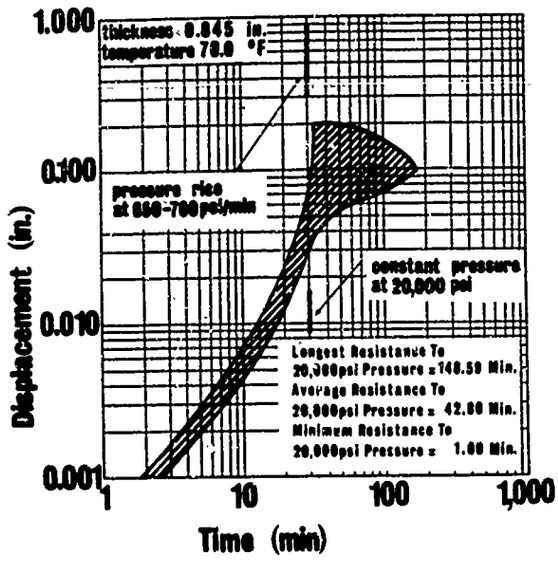

(a) t/D = 0.875.

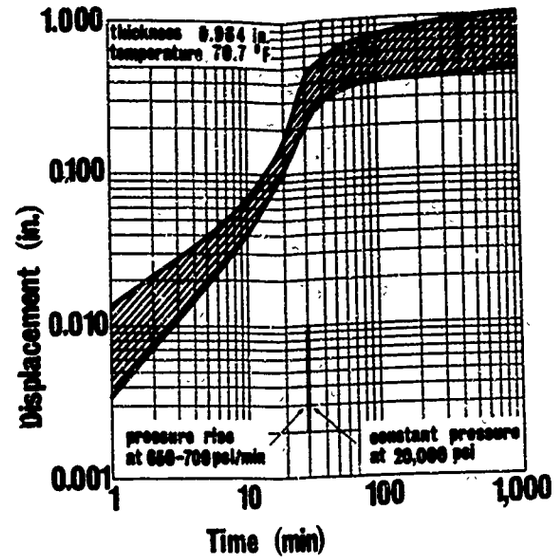

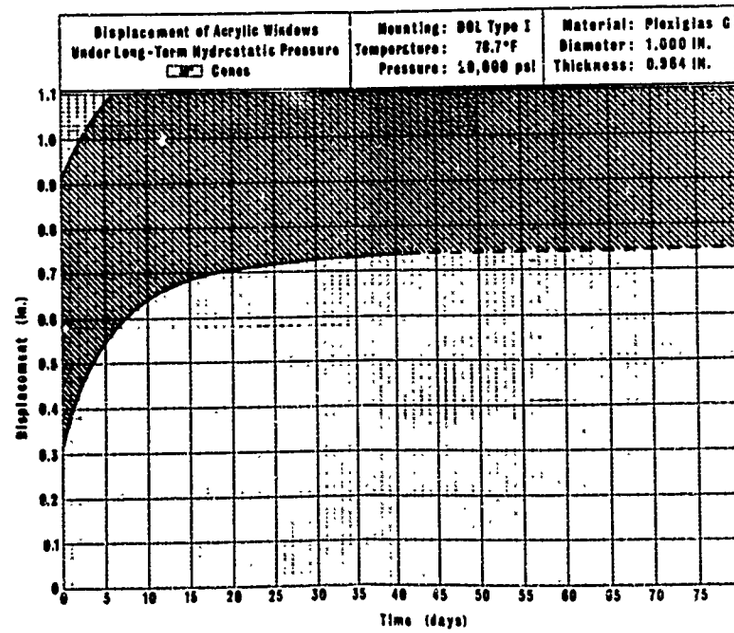

(b) t/D = 1.0.

Figure C-1. Range of displacements for five model windows of 30-degr e included cone a room temperature.

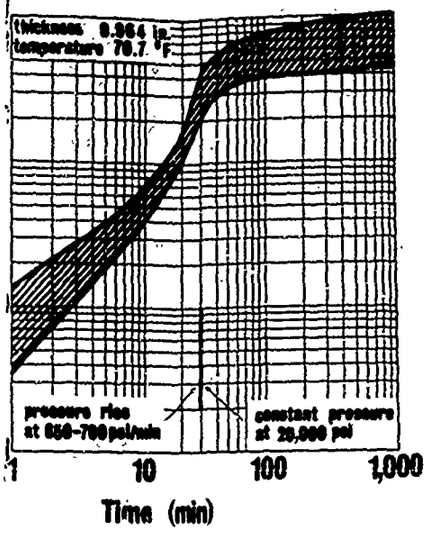

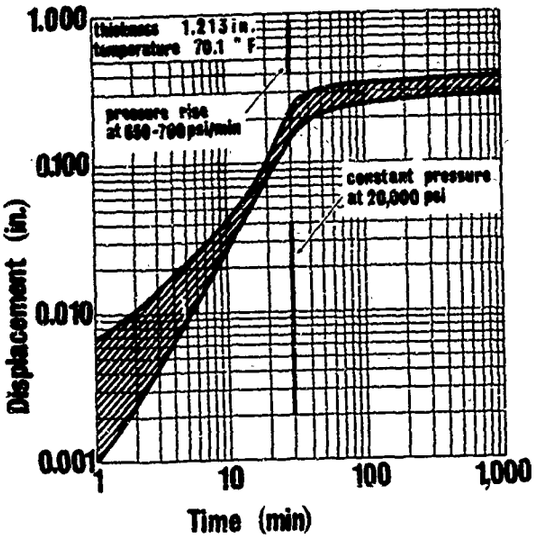

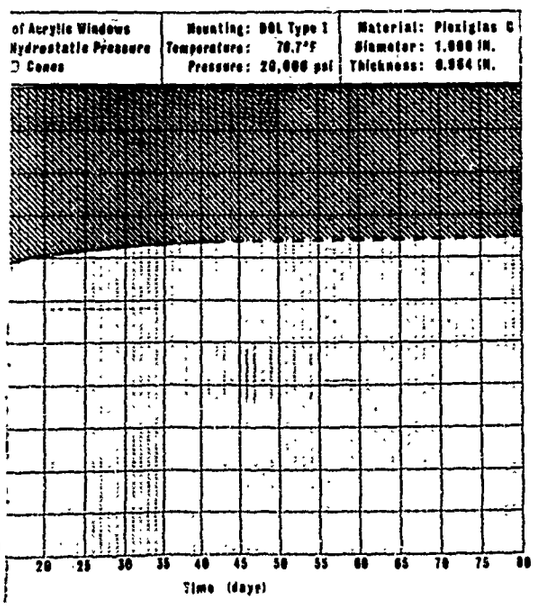

(b) t/D = 1.0.

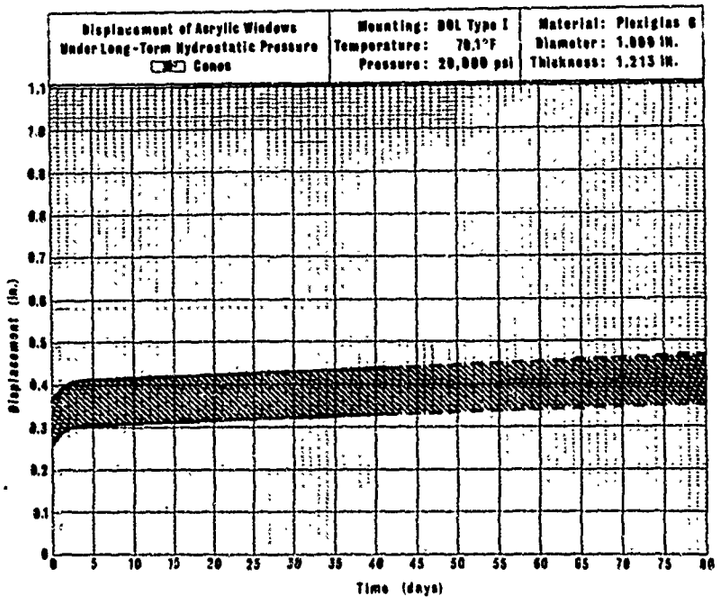

(c) t/D = 1.25

one and

ts for five model windows of 30-degree included cone angle under sustained 20,000-psi pressure at

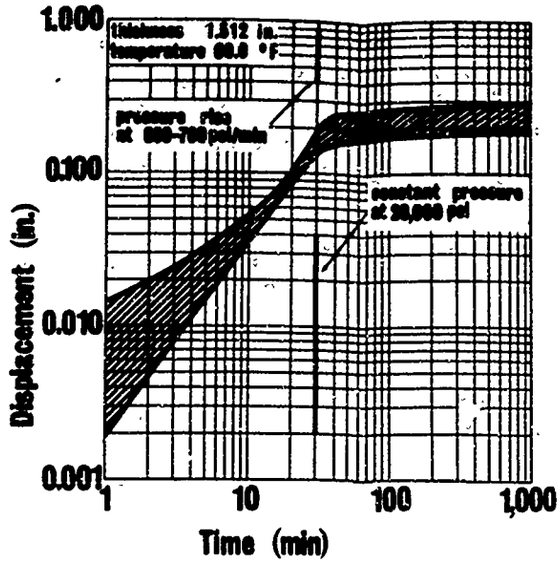

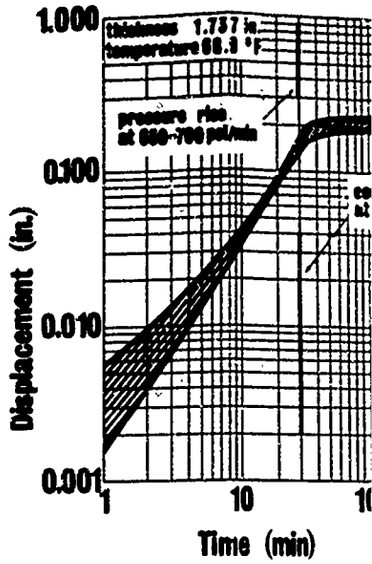

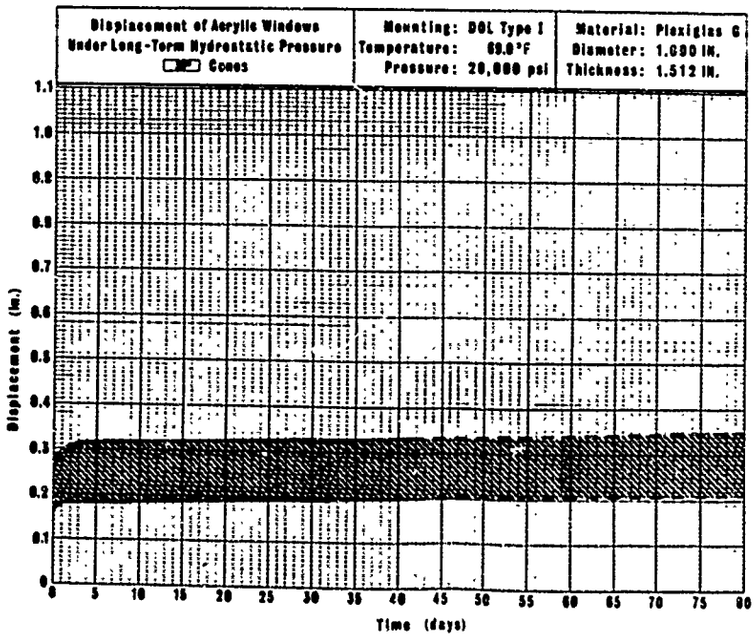

(d) t/D = 1.5.

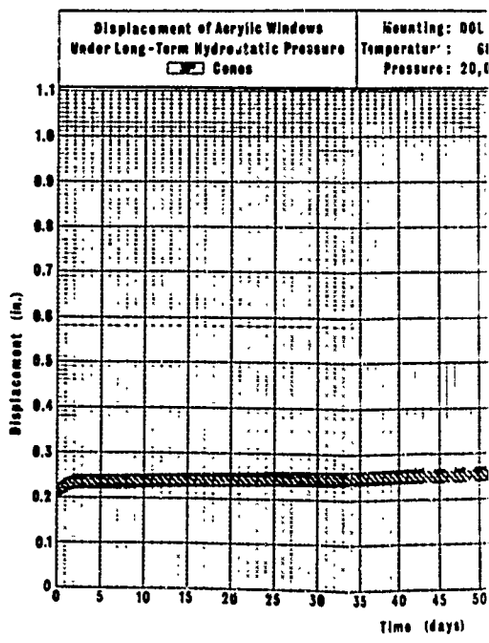

(e) t/D = 1.75.

Figure C-1. Continue

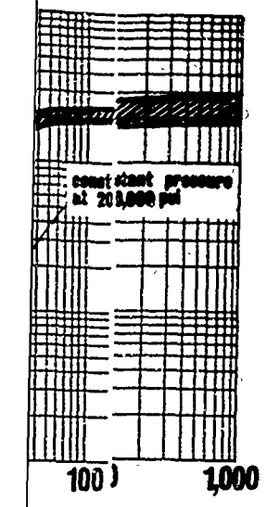

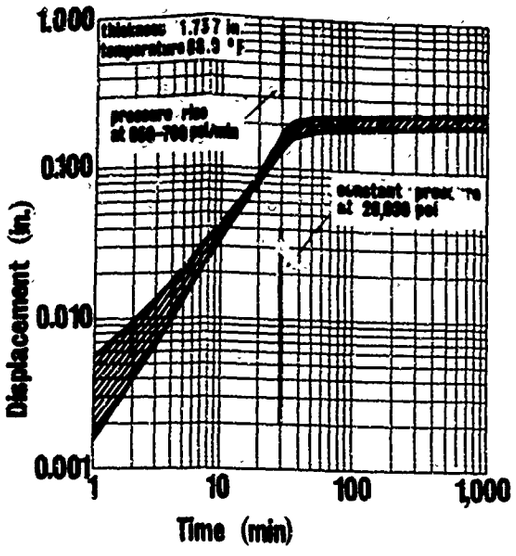

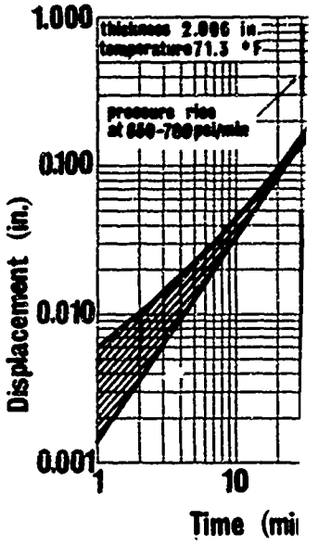

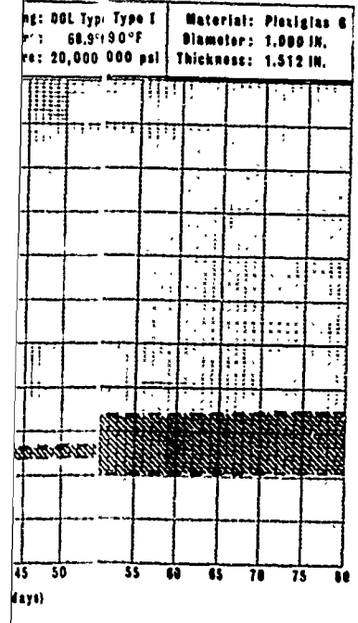

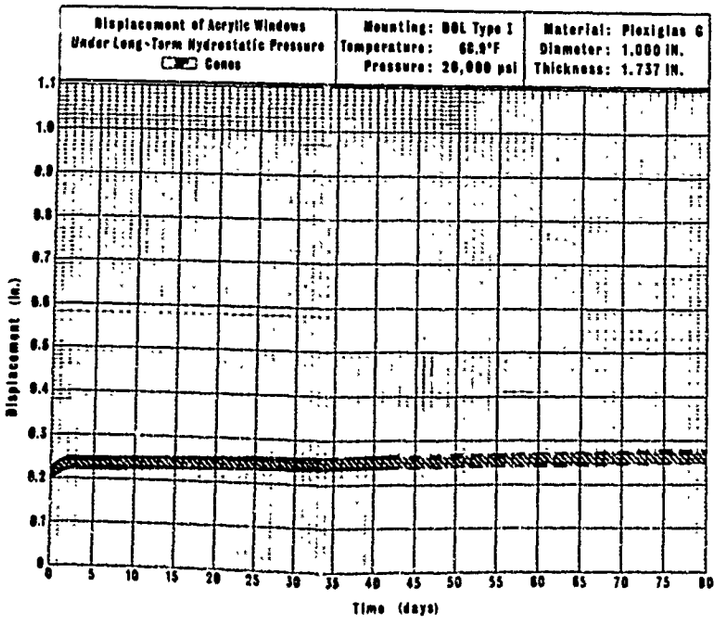

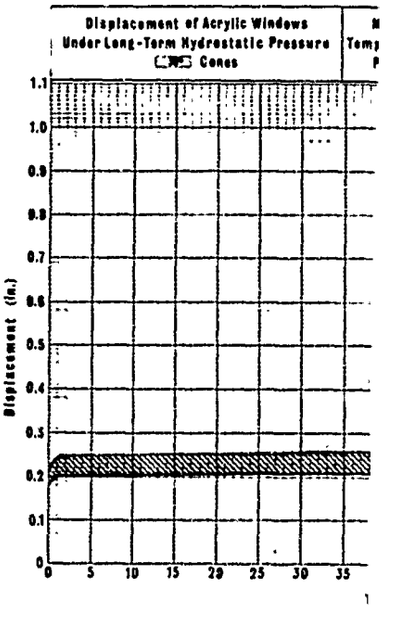

75.

(e) t/D = 1.75.

(f) t/

ntinued.

Figure C-1. Continued.

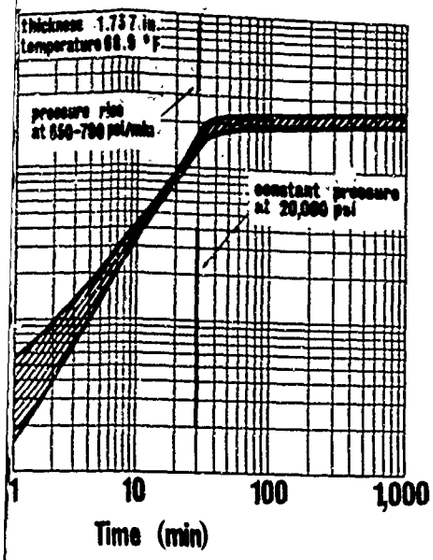

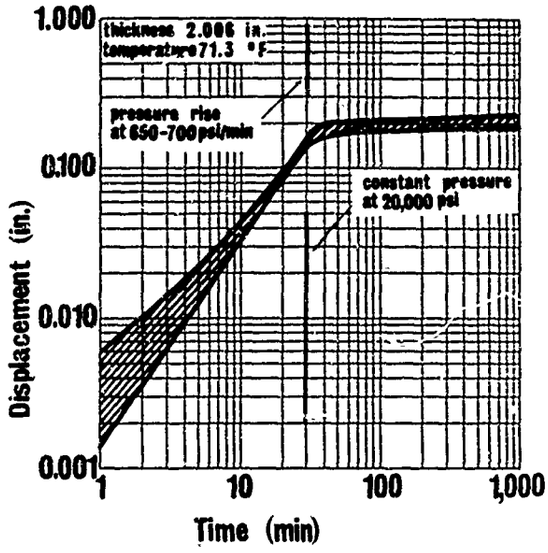

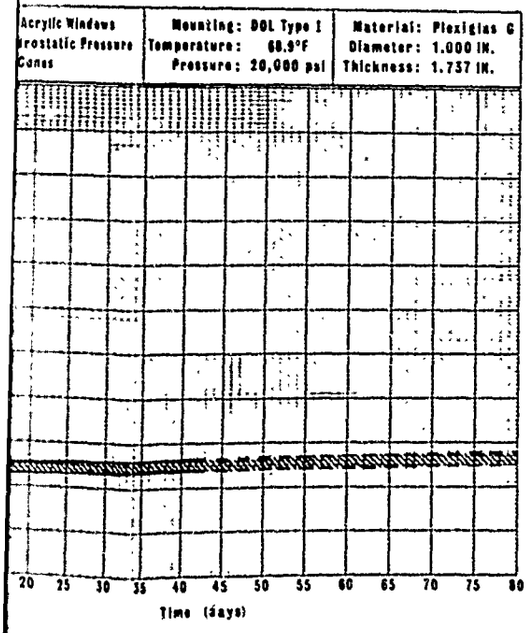

(e) t/D = 1.75.

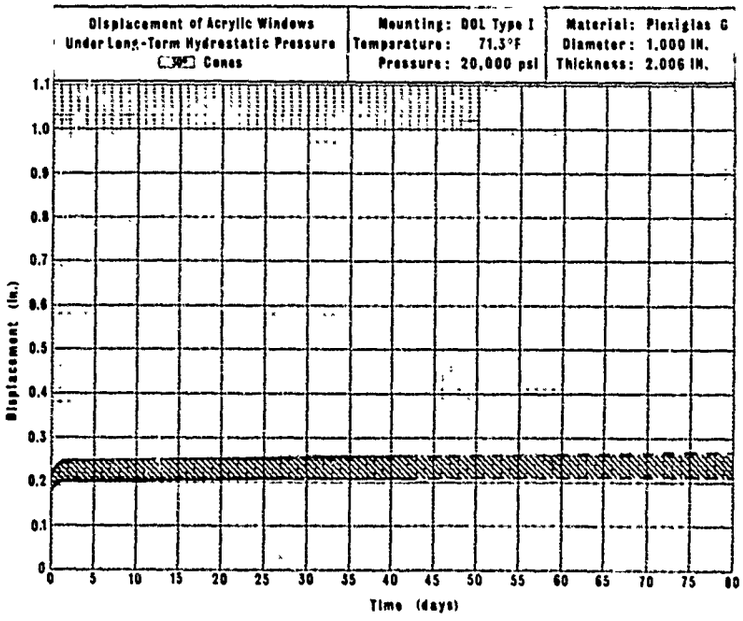

(f) t/D = 2.0.

Figure C-1. Continued.

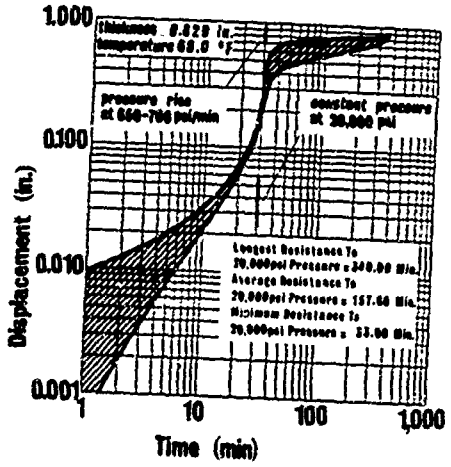

(a) t/D = 0.625.

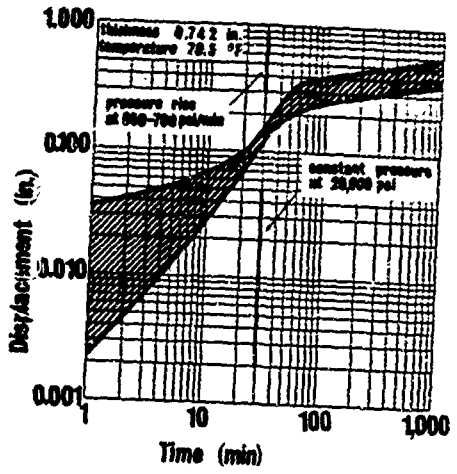

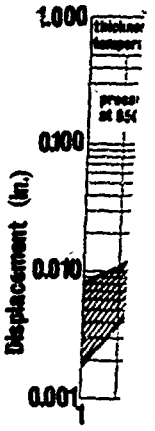

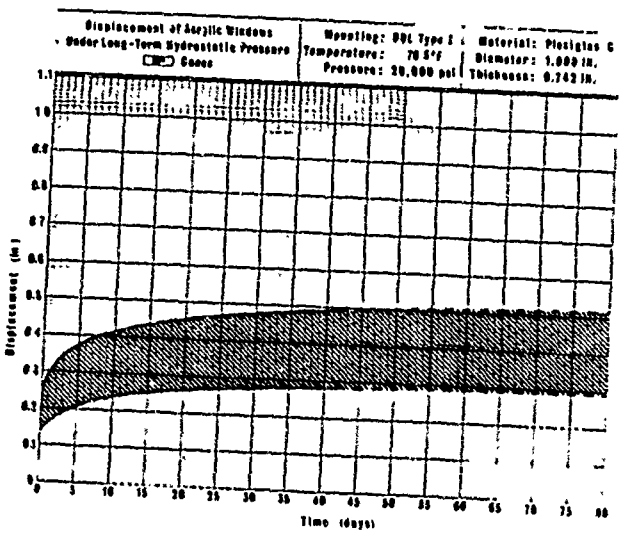

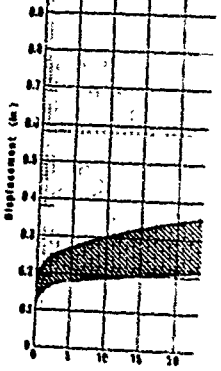

(b) t/D = 0.75.

Figure C-2. Range of displacements for five model windows of 60-degree included cone an room temperature.

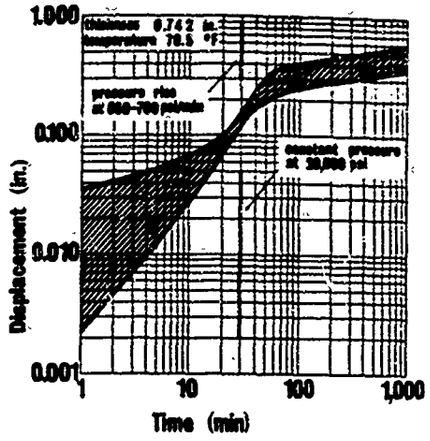

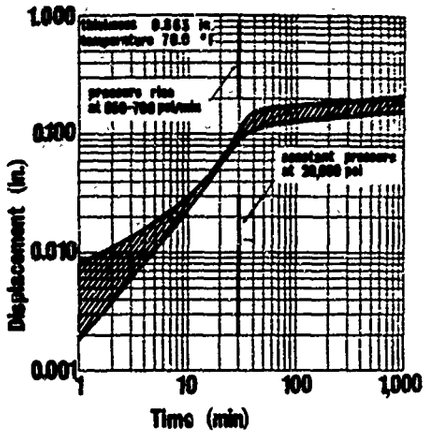

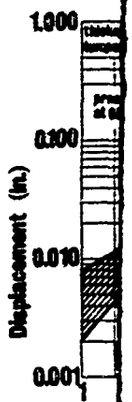

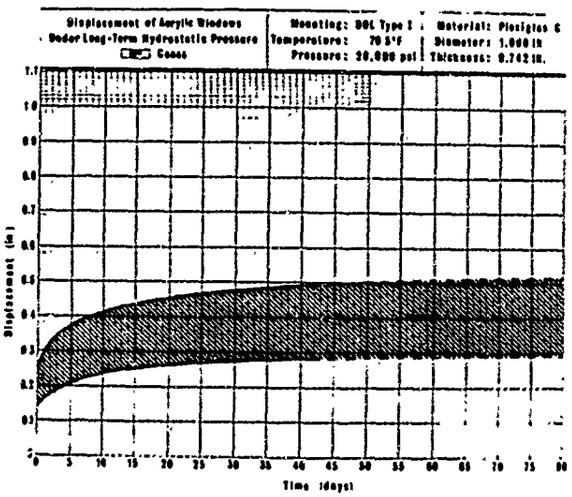

(b) t/D = 0.75.

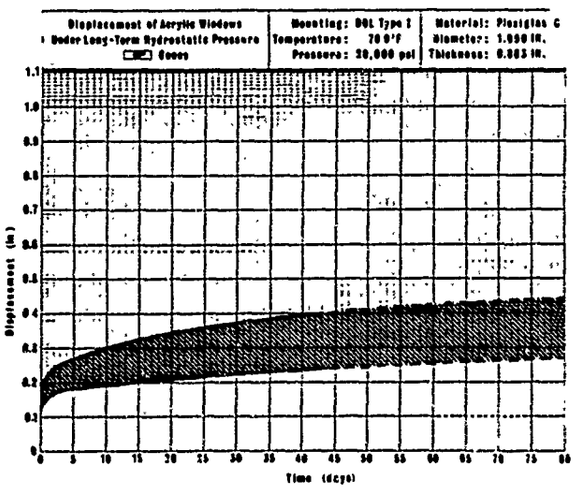

(c) t/D = 0.875.

Figure C-2. Range of displacements for five model windows of 60-degree included cone angle under sustained 20,000-psi pressure at room temperature.

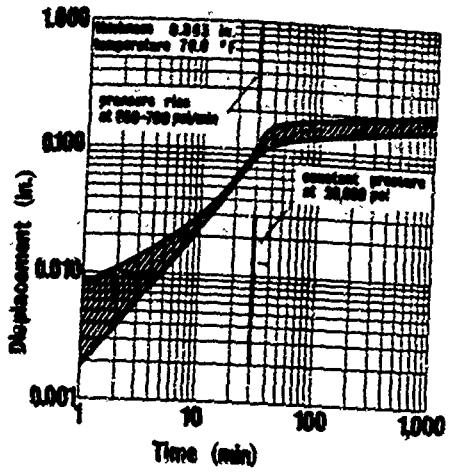

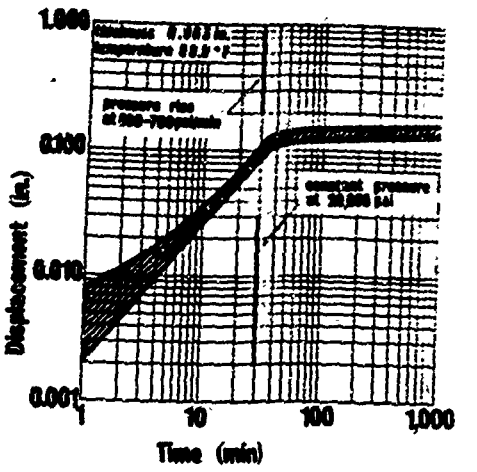

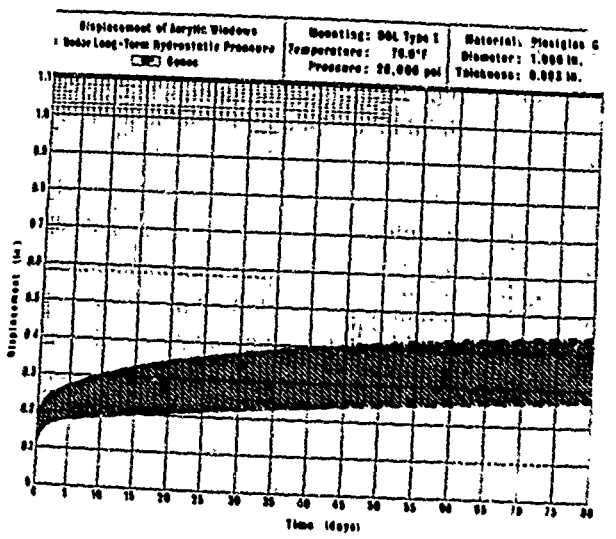

(c) t/D = 0.875.

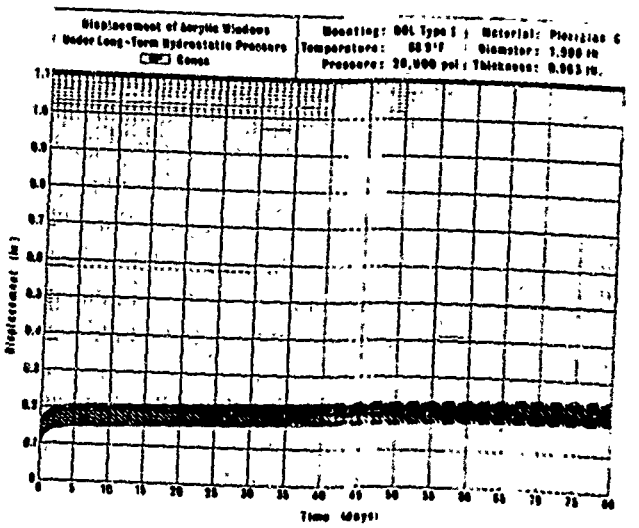

(d) t/D = 1.0.

s of 60-degree included cone angle under sustained 20,000-psi pressure at

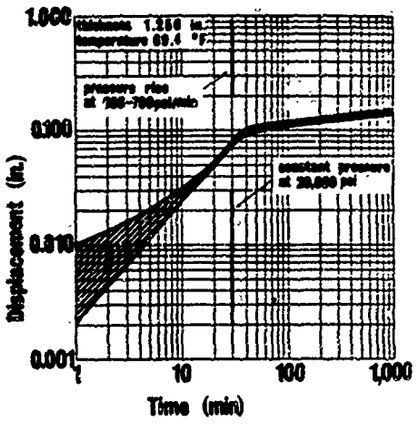

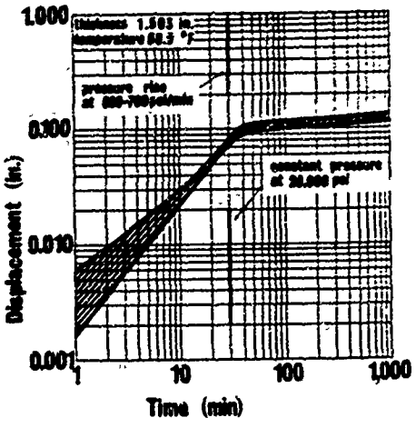

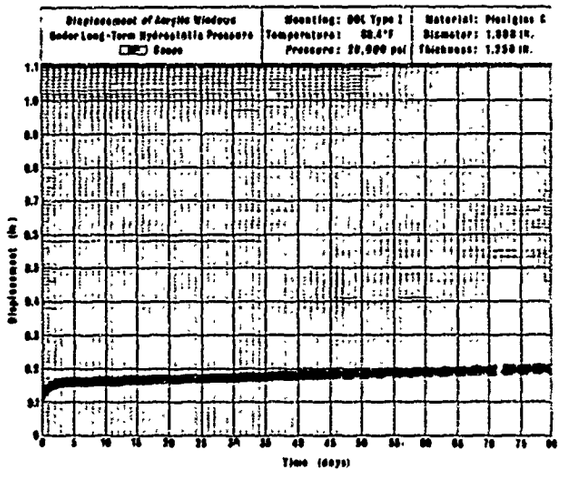

(e) t/D = 1.25.

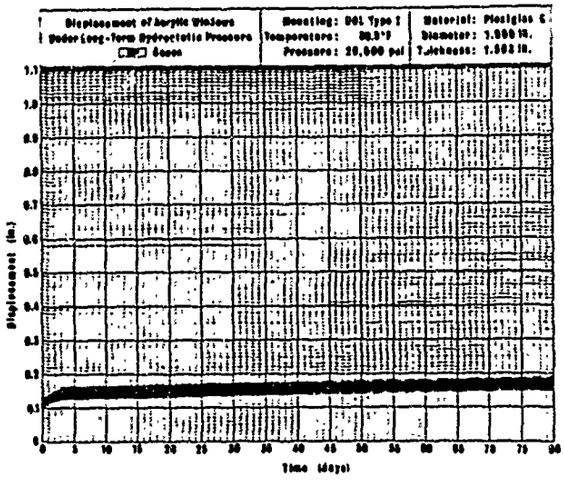

(f) t/D = 1.5.

Figure C-2. Continued.

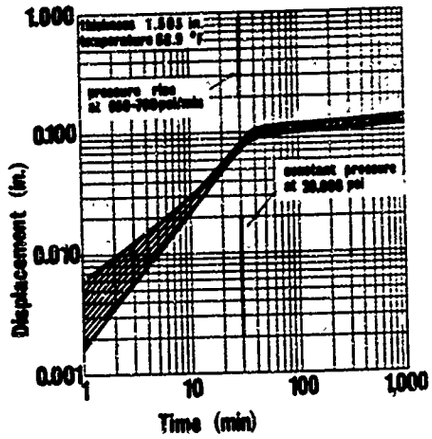

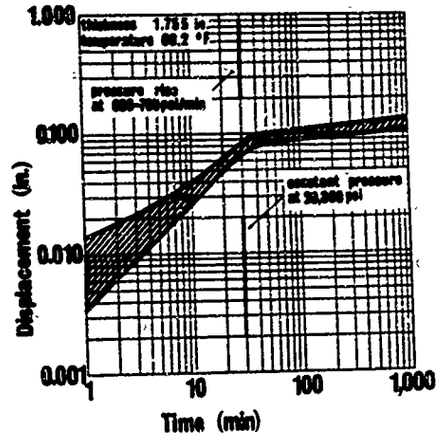

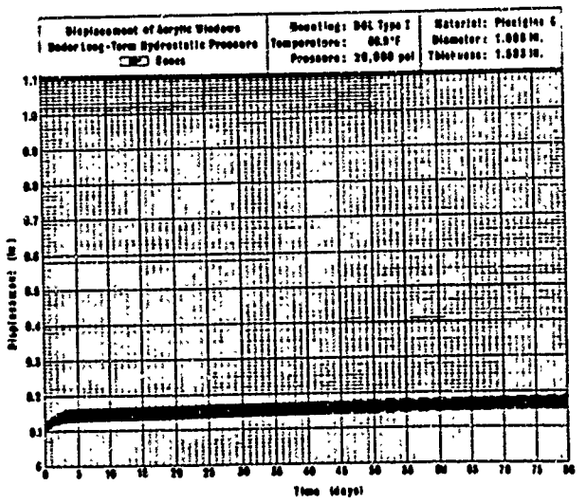

(f) t/D = 1.5.

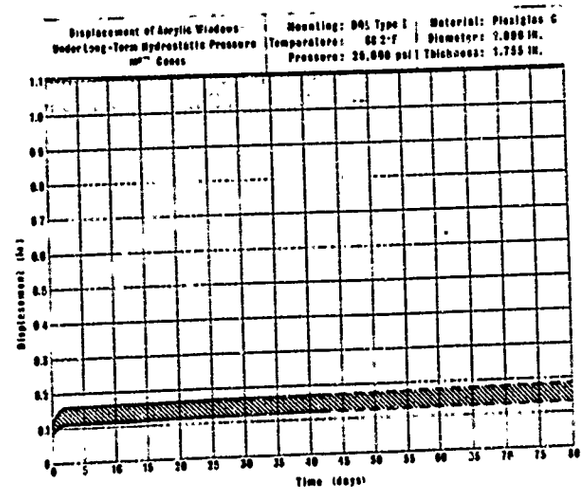

(g) t/D = 1.75.

Figure C-2. Continued.

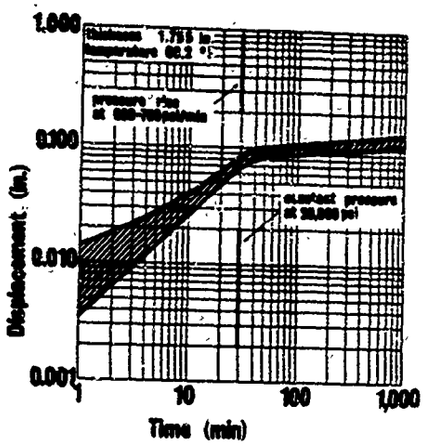

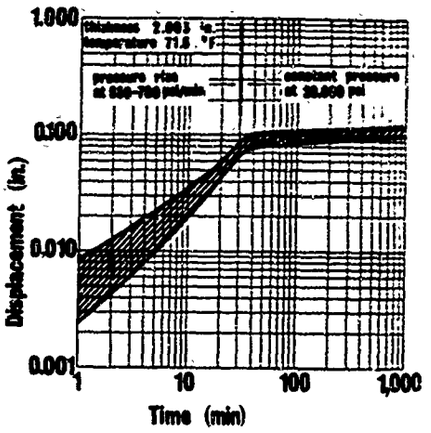

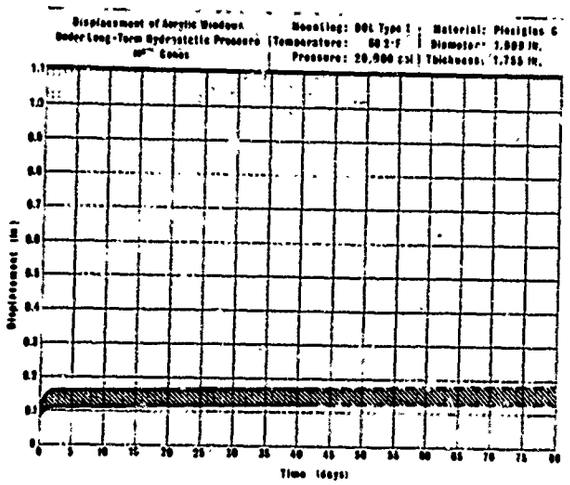

(g) t/D = 1.75.

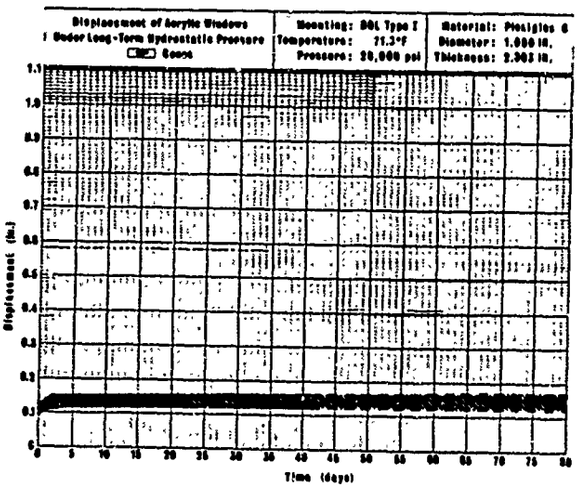

(h) t/D = 2.0.

igure C-2. Continued.

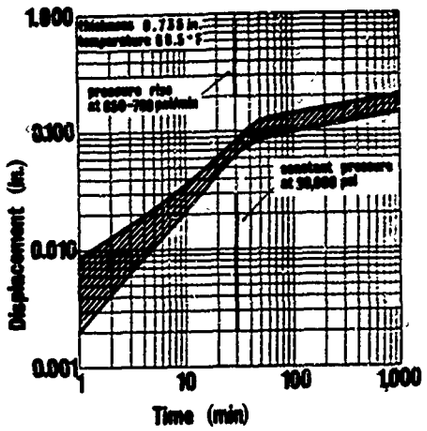

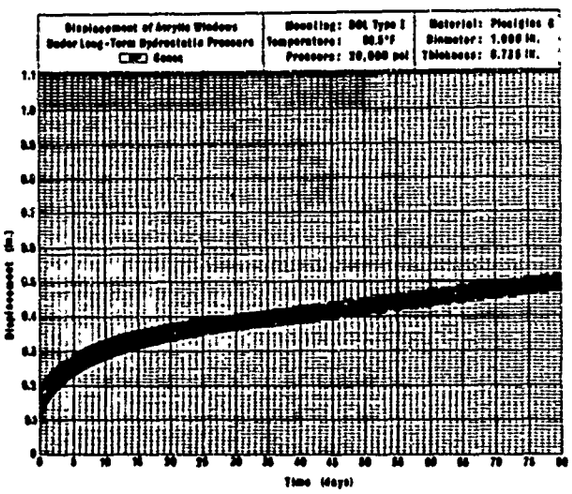

(a) t/D = 0.75.

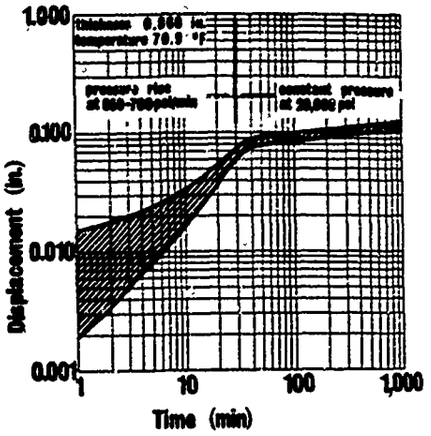

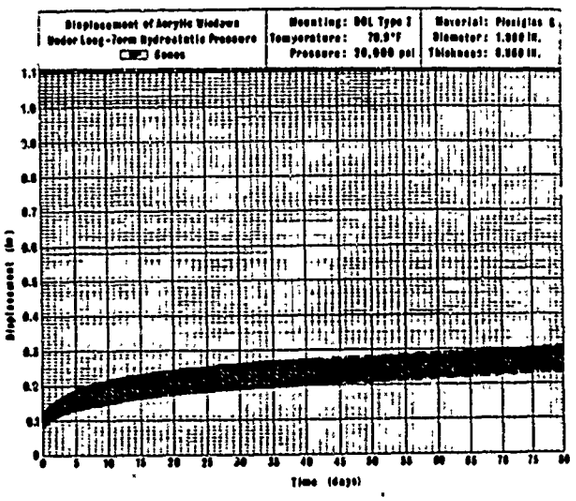

(b) t/D = 0.875.

Figure C-3. Range of displacements for five model windows of 90-degree included cone at room temperature.

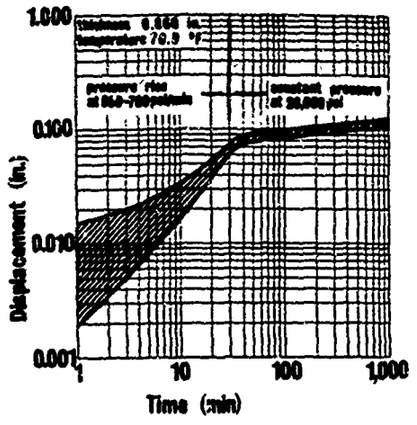

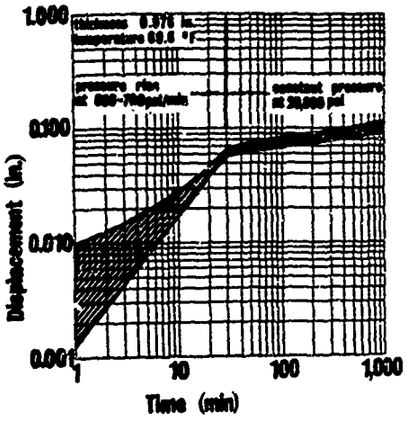

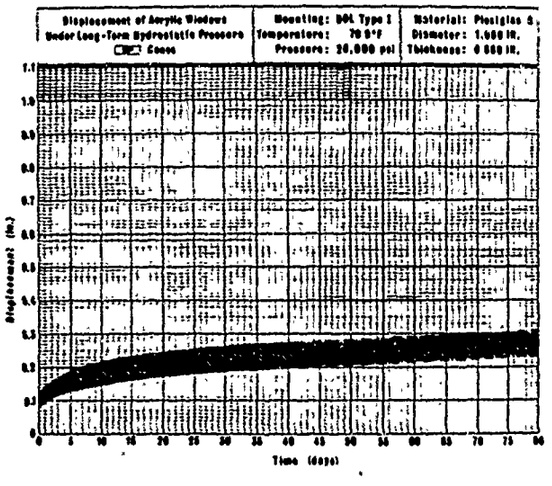

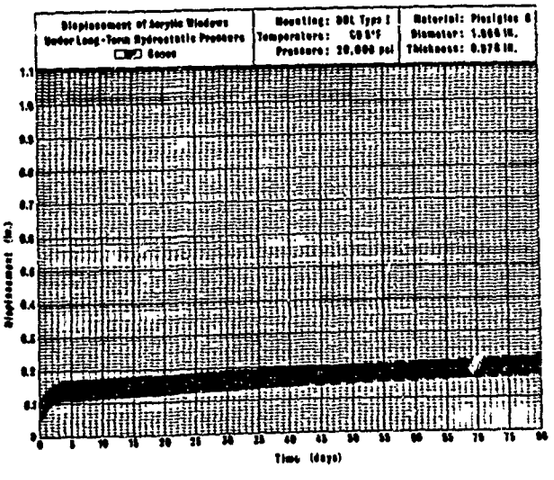

(b) t/D = 0.875.

(c) t/D = 1.0.

Figure C-3. Range of displacements for five model windows of 90-degree included cone angle under sustained 20,000-psi pressure at room temperature.

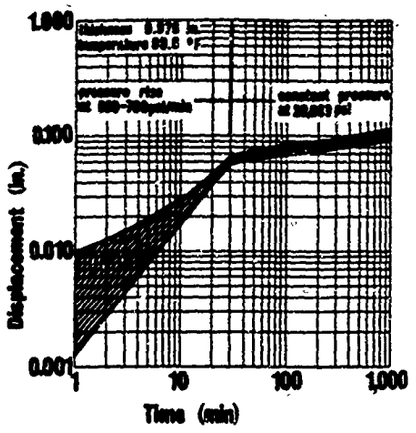

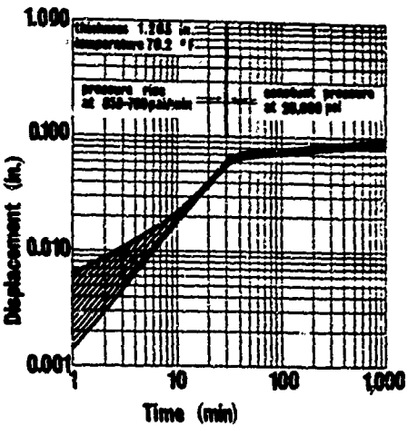

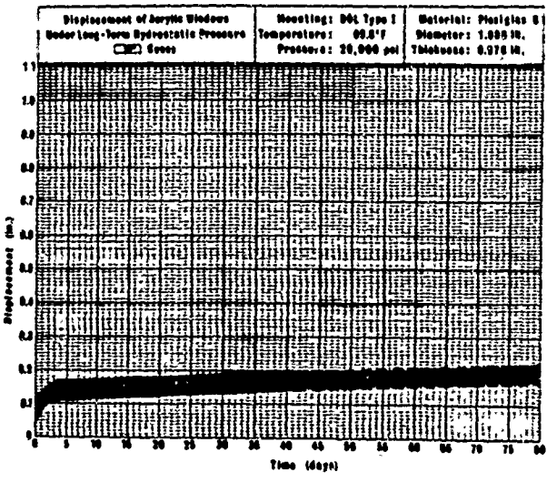

(c) t/D = 1.0.

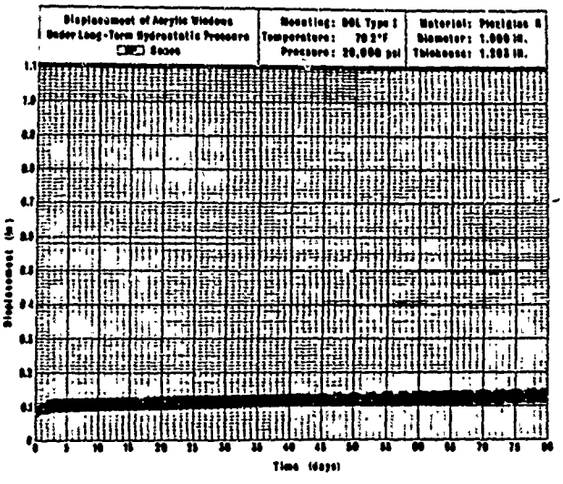

(d) t/D = 1.25.

windows of 90-degree included cone angle under sustained 20,000-psi pressure

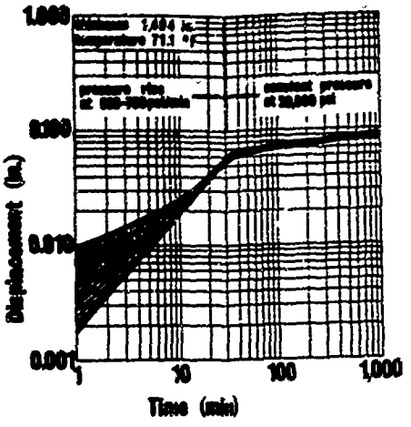

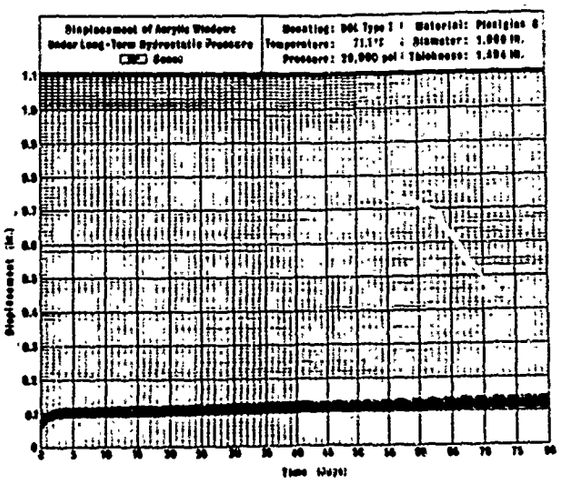

(e) t/D = 1.5.

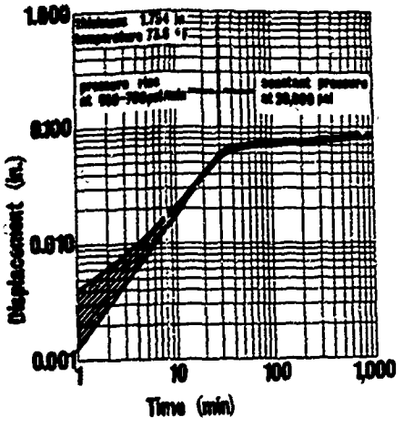

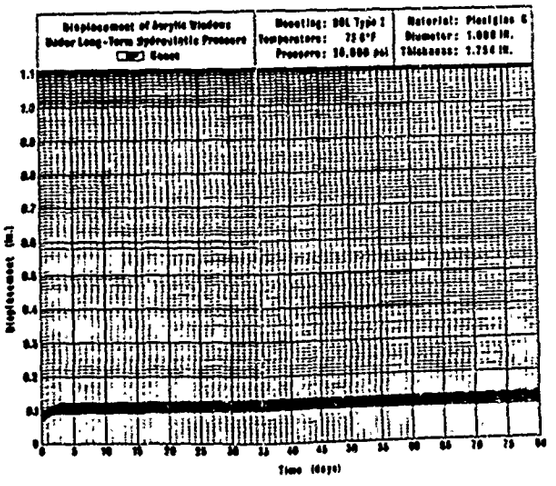

(f) t/D = 1.75.

Figure C-3. Continued.

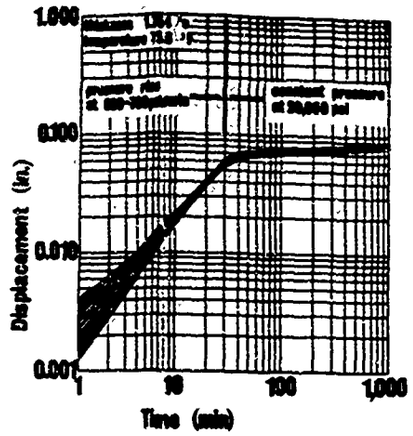

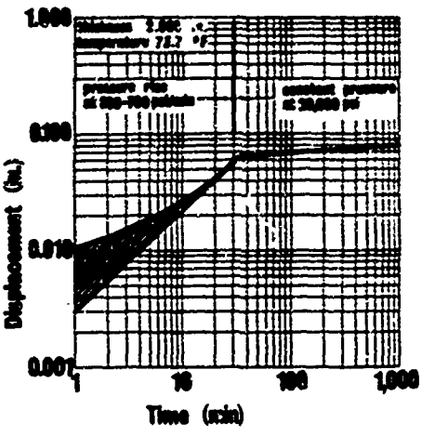

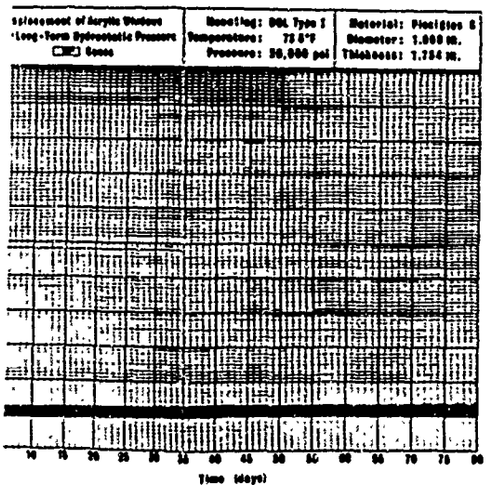

(f) t/D = 1.75.

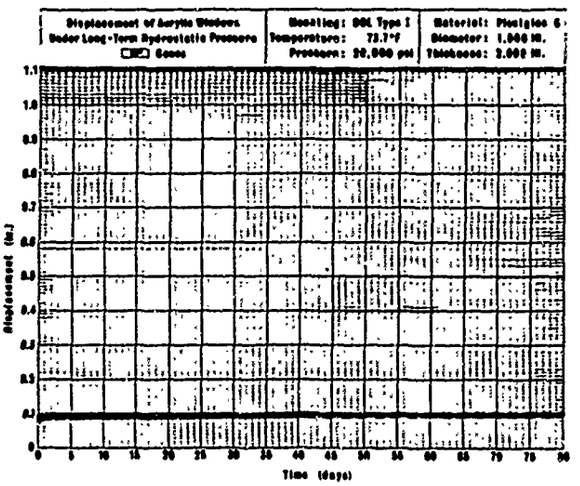

(g) t/D = 2.0.

Figure C-3. Continued.

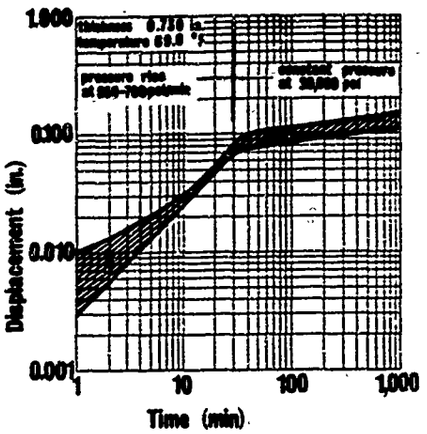

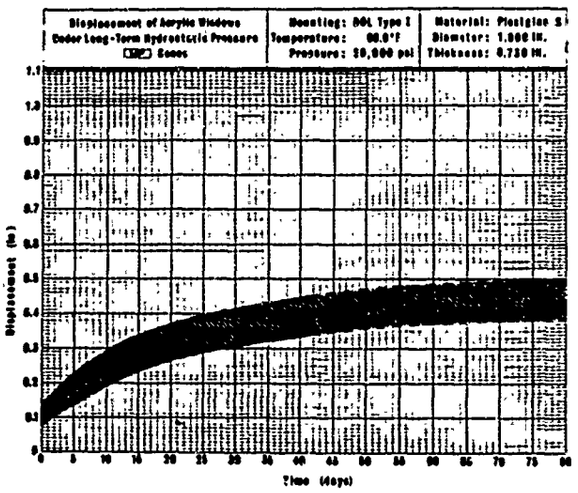

(a) t/D = 0.75.

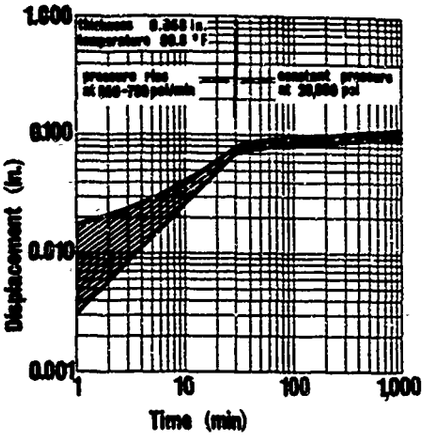

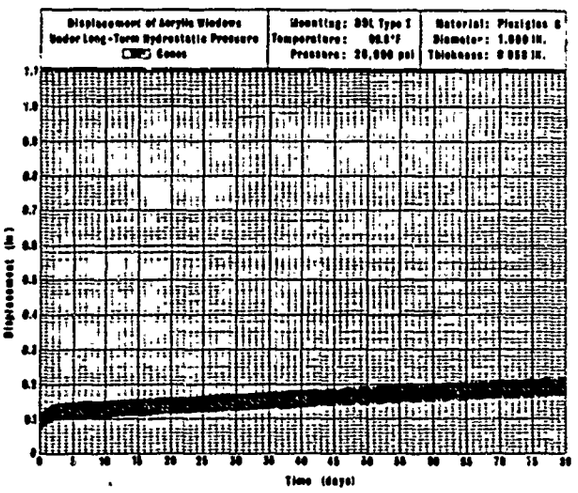

(b) t/D = 0.875.

Figure C-4. Range of displacements for five model windows of 120-degree included con at room temperature.

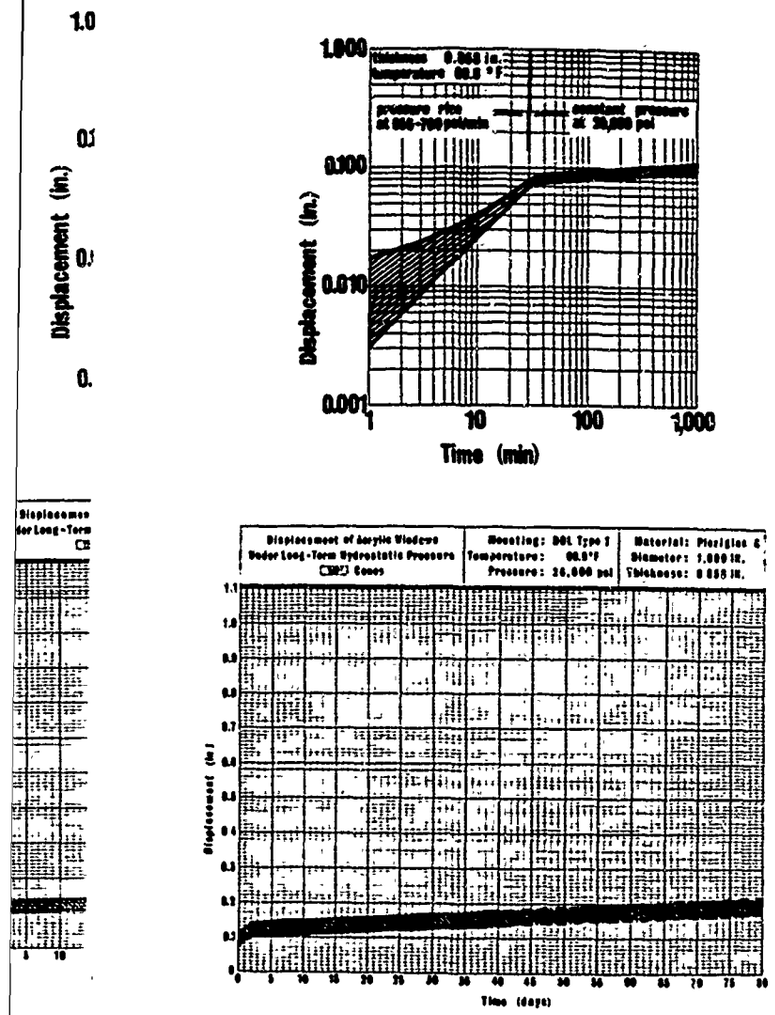

(b) t/D = 0.875.

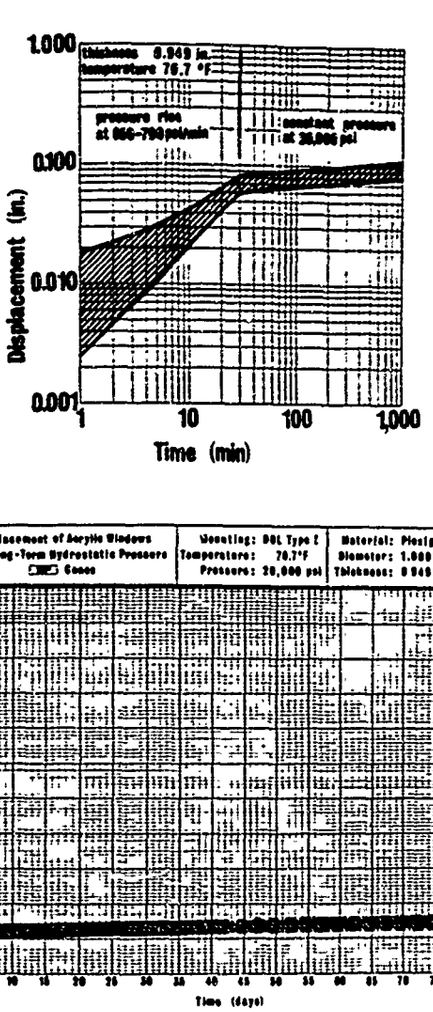

(c) t/D = 1.0.

Figure C-4. Range of displacements for five model windows of 120-degree included cone angle under sustained 20,000-psi pressure at room temperature.

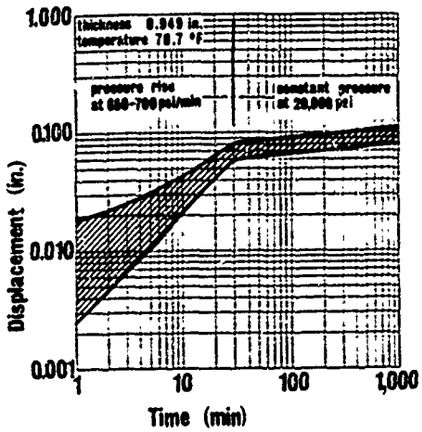

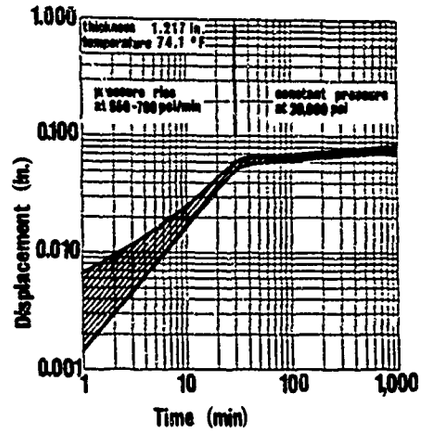

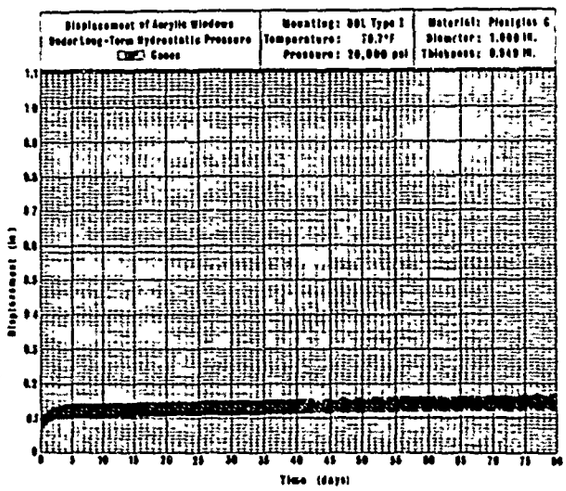

(c) t/D = 1.0.

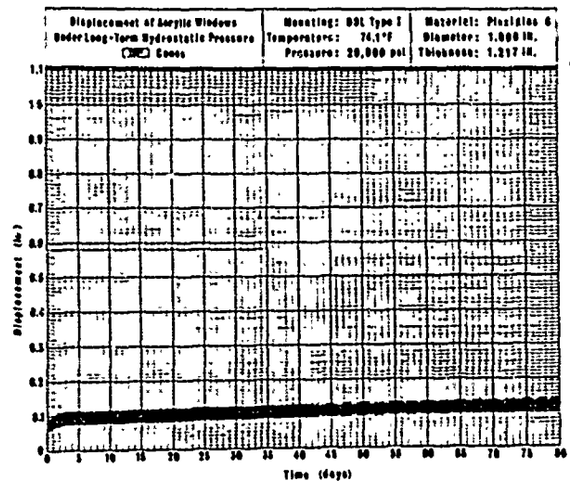

(d) t/D = 1.25.

s of 120-degree included cone angle under sustained 20,000-psi pressure

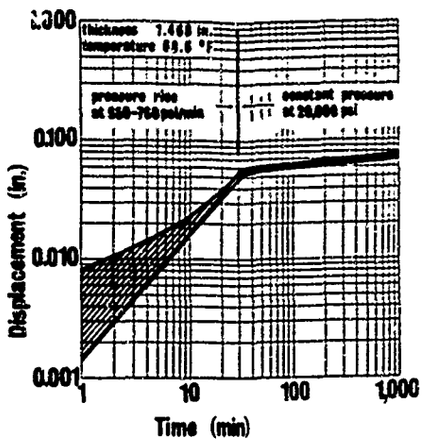

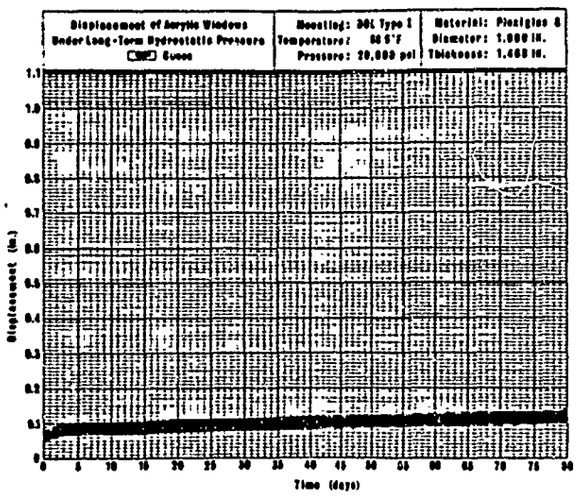

(e) t/D = 1.5.

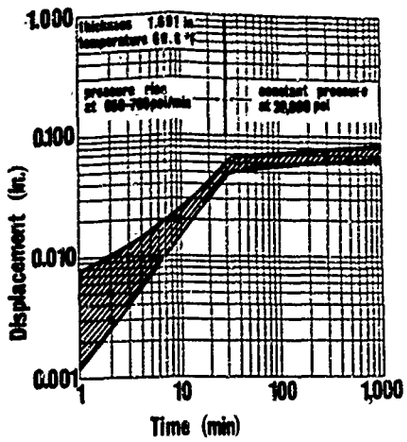

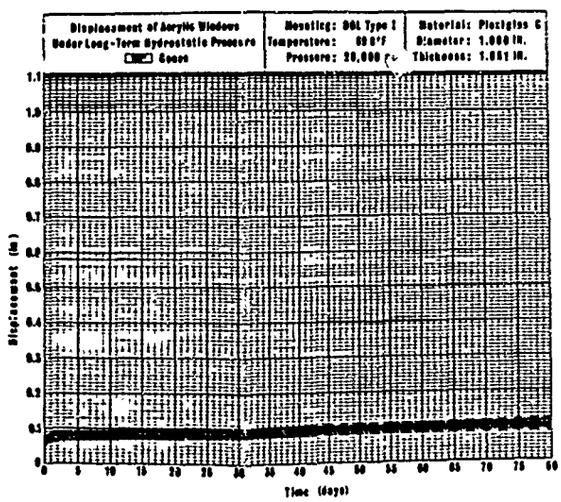

(f) t/D = 1.75.

Figure C-4. Continued.

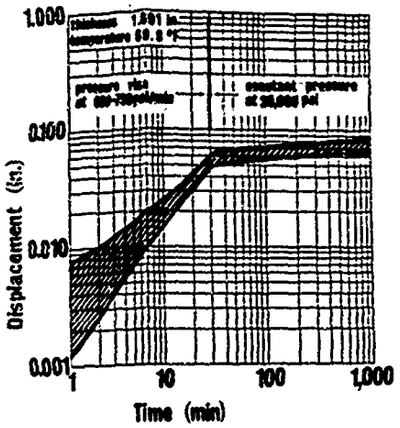

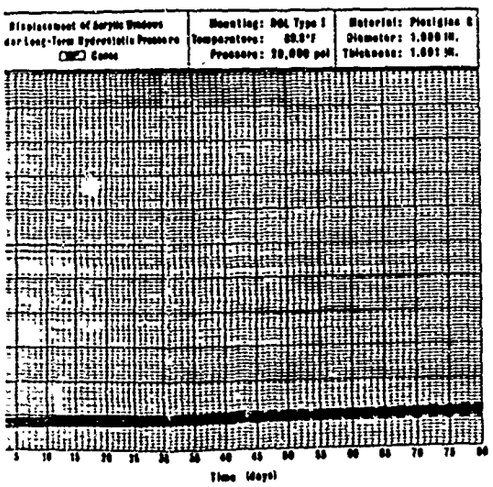

(f) t/D = 1.75.

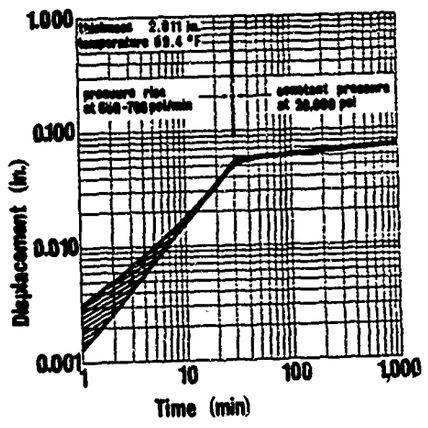

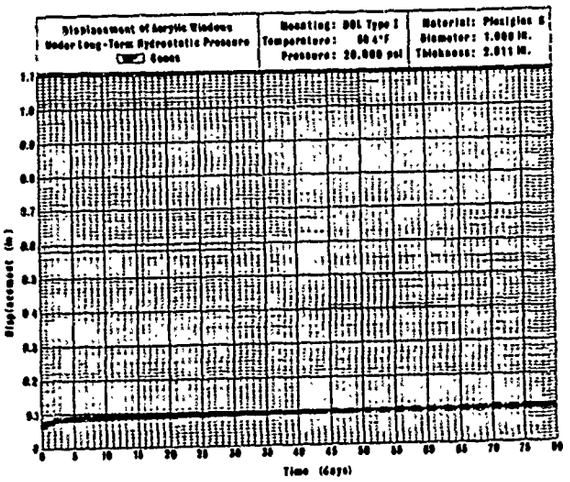

(g) t/D = 2.0.

Figure C-4. Continued.

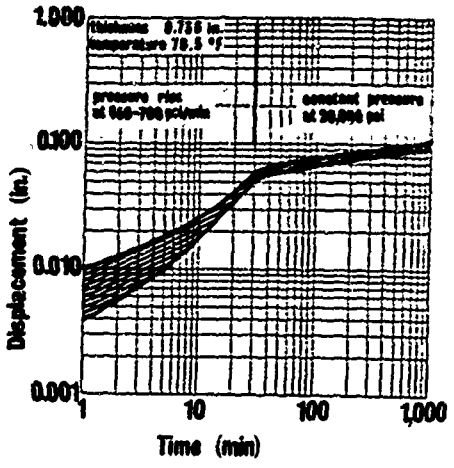

(a) t/D = 0.75.

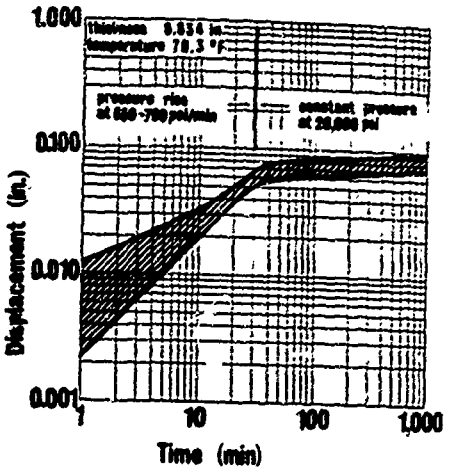

(b) t/D = 0.875.

Figure C-5. Range of displacements for five model windows of 150-degree included cone a at room temperature.

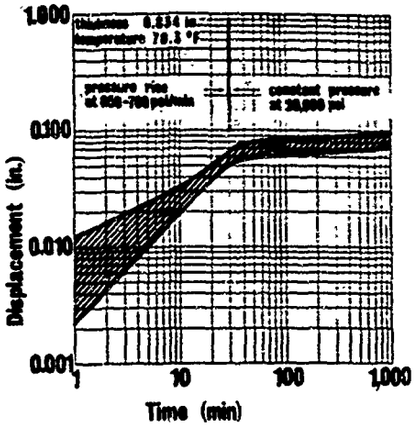

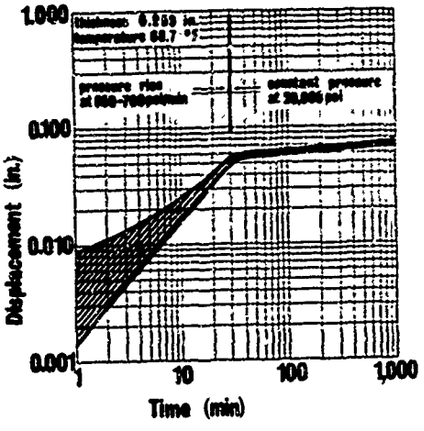

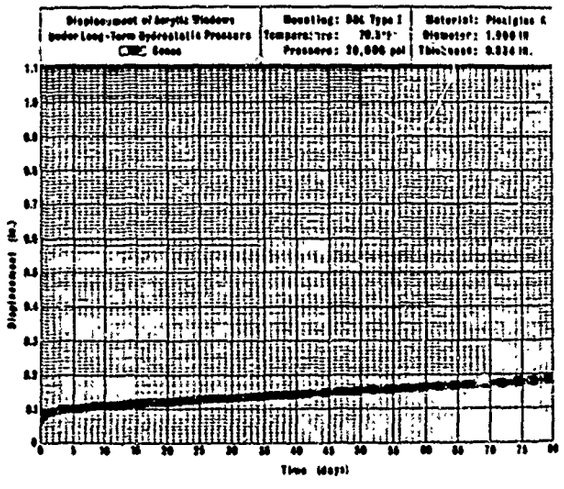

(b) t/D = 0.875.

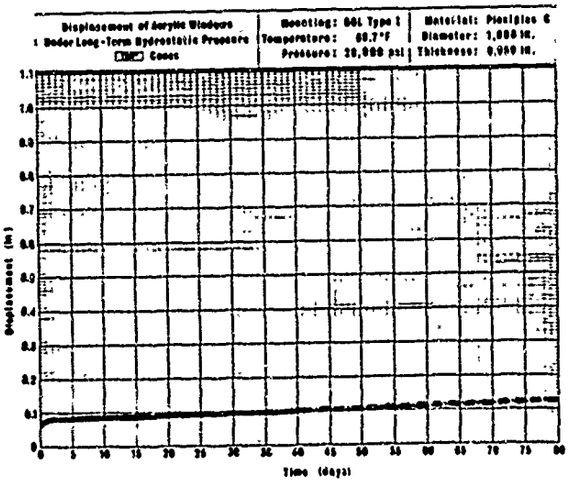

(c) t/D = 1.0.

Figure C-5. Range of displacements for five model windows of 150-degree included cone angle under sustained 20,000-psi pressure at room temperature.

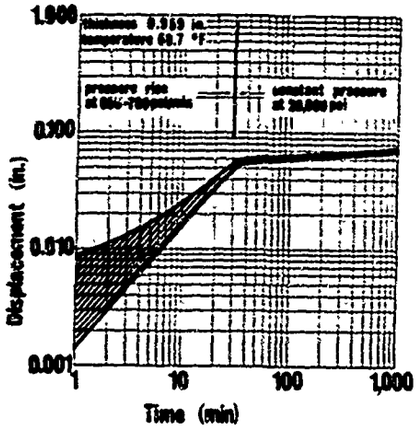

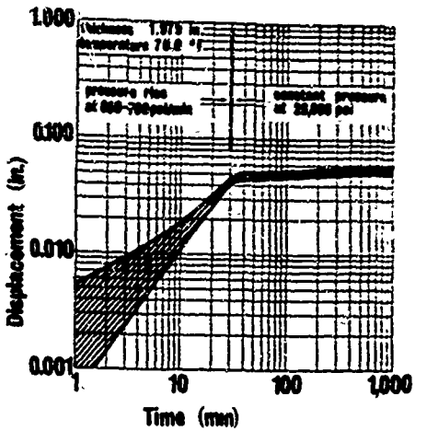

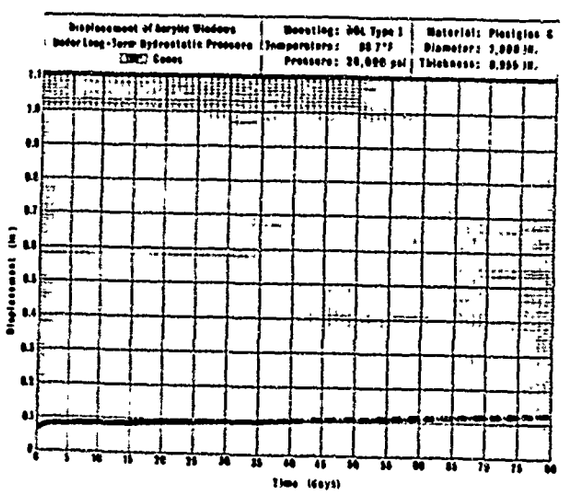

(c) t/D = 1.0.

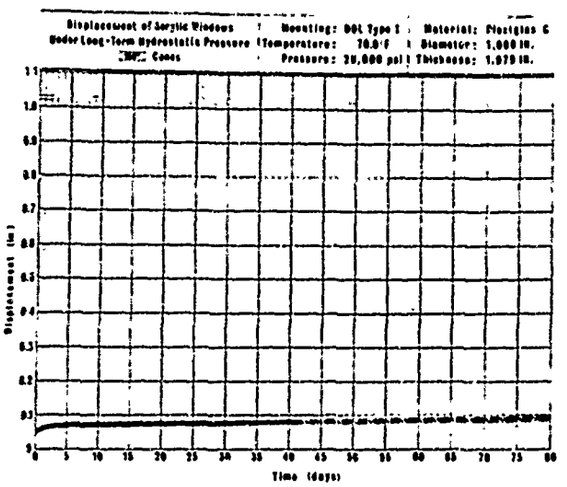

(d) t/D = 2.0.

of 150-degree included cone angle under sustained 20,000-psi pressure

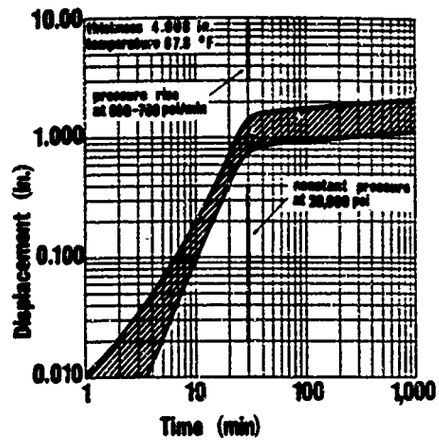

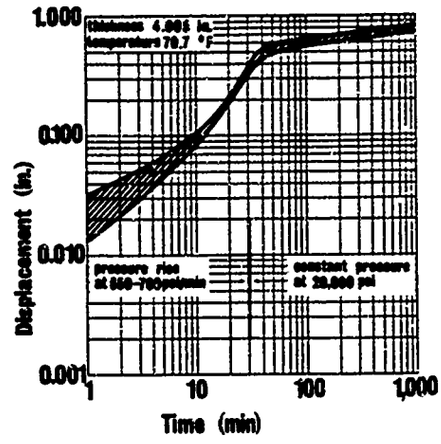

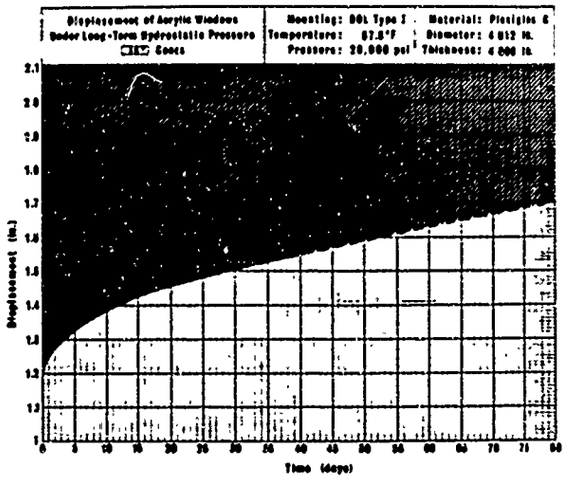

(a) 30-degree included cone angle.

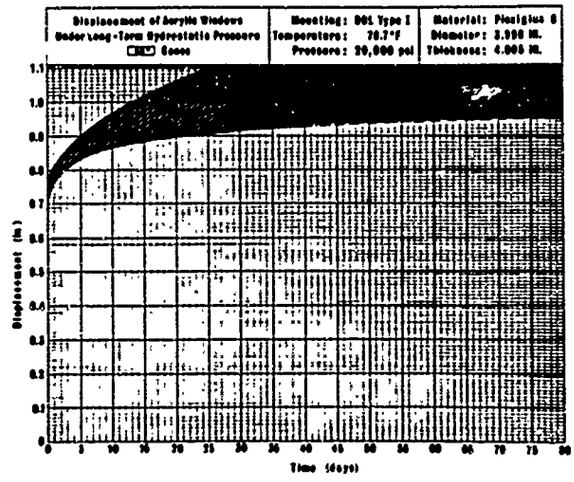

(b) 60-degree included cone angle.

Figure C-6. Range of displacements for five full-scale windows with t/D = 1.0 und

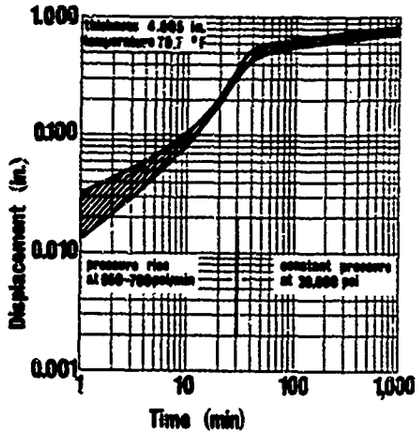

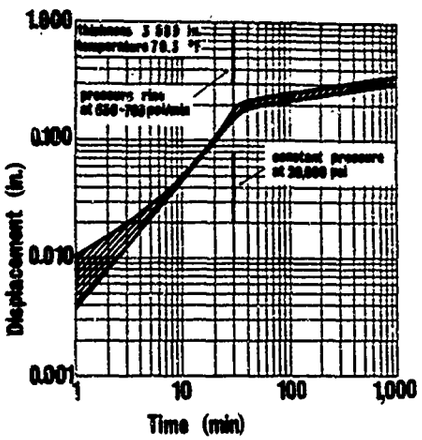

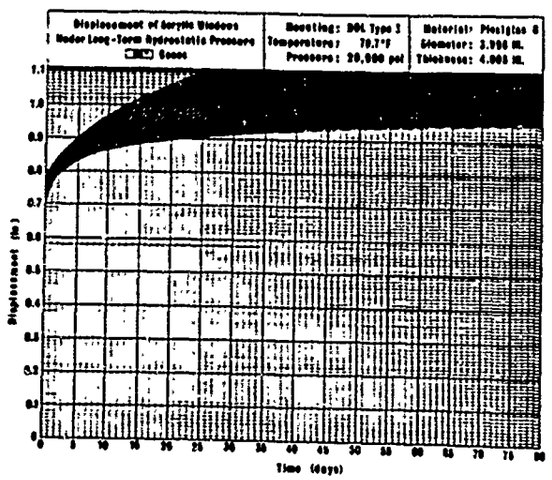

(b) 60-degree included cone angle.

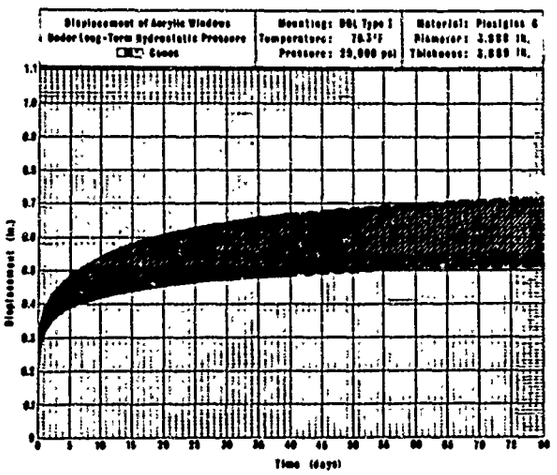

(c) 90-degree included cone angle.

Figure C-6. Range of displacements for five full-scale windows with t/D = 1.0 under sustained 20,000-psi pressure at room temperature.

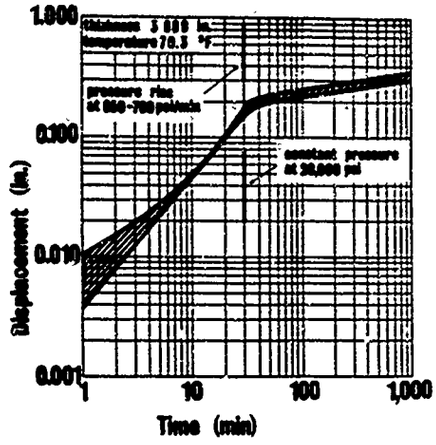

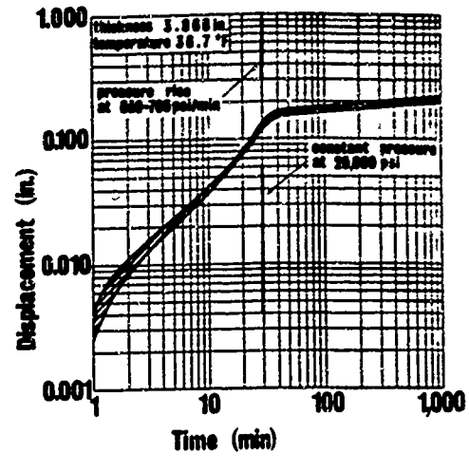

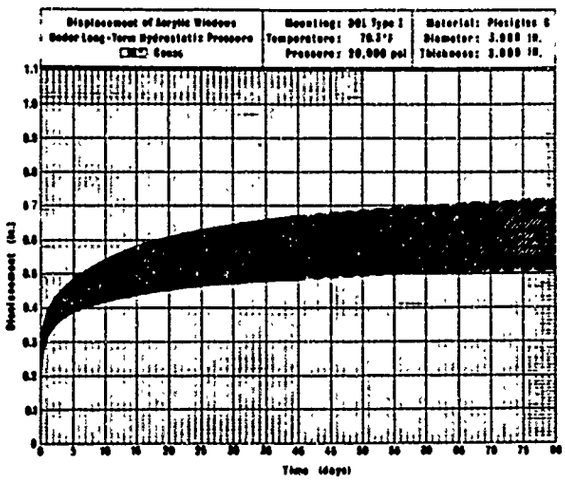

(c) 90-degree included cone angle.

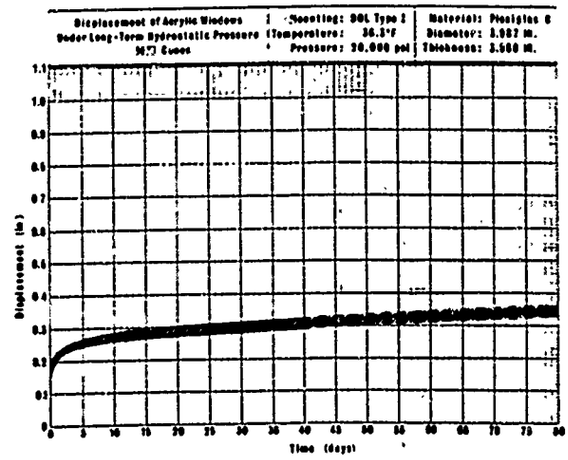

(d) 90-degree included cone angle.

e windows with t/D = 1.0 under sustained 20,000-psi pressure at room temperature.

REFERENCES

1. Naval Civil Engineering Laboratory. Technical Report R-512: Windows for external or internal hydrostatic pressure vessels, pt. I. Conical acrylic windows under short-term pressure application, by J. D. Stachiw and K. O. Gray. Port Hueneme, Calif., Jan. 1967. (AD 646882)

2. ———. Technical Report R-527: Windows for external or internal hydrostatic pressure vessels, pt. II. Flat acrylic windows under short-term pressure application, by J. D. Stachiw, G. M. Dunn, and K. O. Gray. Port Hueneme, Calif., May 1967. (AD 652343)

3. ———. Technical Report R-631: Windows for external or internal hydrostatic pressure vessels, pt. III. Spherical shell acrylic windows under short-term pressure application, by J. D. Stachiw and F. Brier. Port Hueneme, Calif., June 1969.

4. ———. Technical Note N-755: The conversion of 16-inch projectiles to pressure vessels, by K. O. Gray and J. D. Stachiw. Port Hueneme, Calif., June 1965. (AD 625950)

5. Armed Forces Supply Support Center. Military Handbook MIL-HDBK-17: Plastics for flight vehicles, pt. II. Transparent glazing materials. Washington, D. C., Aug. 1961.

DISTRIBUTION LIST

SNDL Code	No. of Activities	Total Copies	
—	1	20	Defense Documentation Center
FKAIC	1	10	Naval Facilities Engineering Command
FKNI FKN5	13	13	NAVFAC Engineering Field Divisions
FKN5	9	9	Public Works Centers
FA25	1	1	Public Works Center
—	15	15	RDT&E Liaison Officers at NAVFAC Engineering Field Divisions and Construction Battalion Centers
—	311	311	NCEL Special Distribution List No. 9 for persons and activities interested in reports on Deep Ocean Studies

Naval Civil Engineering Laboratory
WINDOWS FOR EXTERNAL OR INTERNAL HYDROSTATIC PRESSURE VESSELS—PART IV. Conical Acrylic Windows Under Long-Term Pressure Application at 20,000 Psi, by J. D. Stachiw

TR-645 88 p. illus October 1969 Unclassified

1. Conical acrylic windows—External or internal pressurization I. YF 38.535.005.01.005

Conical acrylic windows of 30-, 60-, 90-, 120-, and 150-degree included angles have been subjected in their mounting flanges to 20,000 psi of hydrostatic pressure for up to 1,000 hours in the 32°F-to-75°F temperature range. The displacements of the windows through the flange mounting have been recorded and are graphically presented as a function of time, temperature, conical angle, and thickness-to-diameter ratio for the ready reference of the designer. A detailed study has also been made of the types of failure and of the dimensional and structural parameters that must be considered in the design of safe, operationally acceptable windows for long-term service under hydrostatic pressure of 20,000 psi.

The test results indicate that a minimum thickness to minor diameter ratio of 2 and an included conical angle of 90 degrees or larger is required to provide safe and optically acceptable windows for long-term sustained pressure loadings of 20,000 psi.

Naval Civil Engineering Laboratory
WINDOWS FOR EXTERNAL OR INTERNAL HYDROSTATIC PRESSURE VESSELS—PART IV. Conical Acrylic Windows Under Long-Term Pressure Application at 20,000 Psi, by J. D. Stachiw

TR-645 88 p. illus October 1969 Unclassified

1. Conical acrylic windows—External or internal pressurization I. YF 38.535.005.01.005

Conical acrylic windows of 30-, 60-, 90-, 120-, and 150-degree included angles have been subjected in their mounting flanges to 20,000 psi of hydrostatic pressure for up to 1,000 hours in the 32°F-to-75°F temperature range. The displacements of the windows through the flange mounting have been recorded and are graphically presented as a function of time, temperature, conical angle, and thickness-to-diameter ratio for the ready reference of the designer. A detailed study has also been made of the types of failure and of the dimensional and structural parameters that must be considered in the design of safe, operationally acceptable windows for long-term service under hydrostatic pressure of 20,000 psi.

The test results indicate that a minimum thickness to minor diameter ratio of 2 and an included conical angle of 90 degrees or larger is required to provide safe and optically acceptable windows for long-term sustained pressure loadings of 20,000 psi.

Naval Civil Engineering Laboratory
WINDOWS FOR EXTERNAL OR INTERNAL HYDROSTATIC PRESSURE VESSELS—PART IV. Conical Acrylic Windows Under Long-Term Pressure Application at 20,000 Psi, by J. D. Stachiw

TR-645 88 p. illus October 1969 Unclassified

1. Conical acrylic windows—External or internal pressurization I. YF 38.535.005.01.005

Conical acrylic windows of 30-, 60-, 90-, 120-, and 150-degree included angles have been subjected in their mounting flanges to 20,000 psi of hydrostatic pressure for up to 1,000 hours in the 32°F-to-75°F temperature range. The displacements of the windows through the flange mounting have been recorded and are graphically presented as a function of time, temperature, conical angle, and thickness-to-diameter ratio for the ready reference of the designer. A detailed study has also been made of the types of failure and of the dimensional and structural parameters that must be considered in the design of safe, operationally acceptable windows for long-term service under hydrostatic pressure of 20,000 psi.

The test results indicate that a minimum thickness to minor diameter ratio of 2 and an included conical angle of 90 degrees or larger is required to provide safe and optically acceptable windows for long-term sustained pressure loadings of 20,000 psi.

Naval Civil Engineering Laboratory
WINDOWS FOR EXTERNAL OR INTERNAL HYDROSTATIC PRESSURE VESSELS—PART IV. Conical Acrylic Windows Under Long-Term Pressure Application at 20,000 Psi, by J. D. Stachiw

TR-645 88 p. illus October 1969 Unclassified

1. Conical acrylic windows—External or internal pressurization I. YF 38.535.005.01.005

Conical acrylic windows of 30-, 60-, 90-, 120-, and 150-degree included angles have been subjected in their mounting flanges to 20,000 psi of hydrostatic pressure for up to 1,000 hours in the 32°F-to-75°F temperature range. The displacements of the windows through the flange mounting have been recorded and are graphically presented as a function of time, temperature, conical angle, and thickness-to-diameter ratio for the ready reference of the designer. A detailed study has also been made of the types of failure and of the dimensional and structural parameters that must be considered in the design of safe, operationally acceptable windows for long-term service under hydrostatic pressure of 20,000 psi.

The test results indicate that a minimum thickness to minor diameter ratio of 2 and an included conical angle of 90 degrees or larger is required to provide safe and optically acceptable windows for long-term sustained pressure loadings of 20,000 psi.

Unclassified

Security Classification

DOCUMENT CONTROL DATA - R & D

(Security classification of title, body of abstract and indexing annotation must be entered when the overall report is classified)

1. ORIGINATING ACTIVITY (Corporate author)

Naval Civil Engineering Laboratory
Port Hueneme, California 93041

2a. REPORT SECURITY CLASSIFICATION

Unclassified

2b. GROUP

3. REPORT TITLE

WINDOWS FOR EXTERNAL OR INTERNAL HYDROSTATIC PRESSURE VESSELS—PART IV. Conical Acrylic Windows Under Long-Term Pressure Application at 20,000 Psi

4. DESCRIPTIVE NOTES (Type of report and inclusive dates)

Not final; July 1, 1967—June 30, 1968

5. AUTHOR(S) (First name, middle initial, last name)

J. D. Stachiw

6. REPORT DATE	7a. TOTAL NO. OF PAGES	7b. NO. OF REFS
October 1969	88	5

8a. CONTRACT OR GRANT NO.	9a. ORIGINATOR'S REPORT NUMBER(S)
b. PROJECT NO. YF 38.535.005.01.005	TR-645
c.	9b. OTHER REPORT NO(S) (Any other numbers that may be assigned this report)
d.	

10. DISTRIBUTION STATEMENT

This document has been approved for public release and sale; its distribution is unlimited.

11. SUPPLEMENTARY NOTES	12. SPONSORING MILITARY ACTIVITY
	Naval Facilities Engineering Command Washington, D. C.

13. ABSTRACT

Conical acrylic windows of 30-, 60-, 90-, 120-, and 150-degree included angles have been subjected in their mounting flanges to 20,000 psi of hydrostatic pressure for up to 1,000 hours in the 32°F-to-75°F temperature range. The displacements of the windows through the flange mounting have been recorded and are graphically presented as a function of time, temperature, conical angle, and thickness-to-diameter ratio for the ready reference of the designer. A detailed study has also been made of the types of failure and of the dimensional and structural parameters that must be considered in the design of safe, operationally acceptable windows for long-term service under hydrostatic pressure of 20,000 psi.

The test results indicate that a minimum thickness to minor diameter ratio of 2 and an included conical angle of 90 degrees or larger is required to provide safe and optically acceptable windows for long-term sustained pressure loadings of 20,000 psi.

DD FORM 1 NOV 65 1473 (PAGE 1)

S/N 0101-807-6801

Unclassified

Security Classification

14 KEY WORDS	LINK A		LINK B		LINK C	
	ROLE	WT	ROLE	WT	ROLE	WT
Windows						
Pressure vessels						
Submarines						
Undersea habitats						
Ocean engineering						
Acrylic plastics						
External pressurization						
Internal pressurization						
Short-term pressurization						
Long-term pressurization						
Failure modes						
Included angle						
Thickness/diameter ratio						
Axial displacement						

Technical Report

R 708

WINDOWS FOR EXTERNAL OR INTERNAL HYDROSTATIC PRESSURE VESSELS—PART V.

Conical Acrylic Windows Under Long-Term Pressure Application of 10,000 Psi

January 1971

Sponsored by

NAVAL FACILITIES ENGINEERING COMMAND

NAVAL CIVIL ENGINEERING LABORATORY

Port Hueneme, California

WINDOWS FOR EXTERNAL OR INTERNAL HYDROSTATIC PRESSURE VESSELS—PART V. Conical Acrylic Windows Under Long-Term Pressure Application of 10,000 Psi

Technical Report R-708

YF 38.535.005.01.005

by

J. D. Stachiw and W. A. Moody

ABSTRACT

Conical acrylic windows of 30-, 60-, 90-, and 120- and 150-degree included angle and 0.500 to 1.250 t/D (thickness to minor diameter ratio) have been subjected in their mounting flanges to 10,000 psi of hydrostatic pressure for 500 and 1,000 hours at ambient room temperature. The displacement of the windows through the flange mounting has been recorded as a function of time and plotted for the ready reference of the designer. The magnitude of the window displacement has been found to be a function of time, angle, temperature, t/D ratio and pressure.

It is recommended that for safe single sustained operation of 1,000 hour duration at 10,000 psi hydrostatic loading at ambient temperature the windows should have an included conical angle $\geq 90^{o}$ and a minimum t/D ratio of 0.750. For sustained loadings in excess of 1,000 hours the minimum t/D ratio is 1.000.

CONTENTS

INTRODUCTION

Previous studies[1-3] conducted at NCEL with the objective of comparing the structural efficiency of different window shapes have shown that although the spherical acrylic plastic shell windows are the most efficient, conical windows approach them in efficiency, particularly if the included conical angle is large. Since widespread use of conical viewports in submersibles and hyperbaric chambers has made them something of a standard, this particular shape was chosen for further studies.

Because ocean floor installations are primarily subjected only to sustained long-term submersion, the investigation of windows focused on long-term sustained loading so that the data generated in this program could be directly applied to the design of habitat windows. The first study[4] in the conical window long-term testing program investigated the behavior of windows at 20,000 psi. The magnitude of window displacement through the mounting flange was found to be a function of conical angle, thickness to minor diameter ratio, and temperature, as well as time. No effort was made to determine the relationship between pressure and window displacement under long-term loading, although it was known that the displacement of windows would be less if they were subjected to a lower pressure for the same period of time.

In the previous studies no effort was made to investigate the ability of acrylic material to return in time to its original form as the pressure is decreased to 1 atmosphere, although this property is known to exist.

Since the operational depth of permanent ocean bottom installations equipped with acrylic windows varies from one habitat to another, the windows are subjected to different levels of hydrostatic pressure for extended periods of time. Therefore, it is important to develop criteria that will permit the design of acrylic windows for any operational depth. This will allow the designer more flexibility when considering variables such as field of view, amount of space available for mounting windows and expense, while still maintaining a high degree of safety. A similar case presents itself in the design of windows for internal pressure vessels in which long-term hydrostatic tests are performed (Figure 1). It is to generate such design data that the present study has been sponsored by the Naval Facilities Engineering Command.

Figure 1. Window installed in end closure of 18-inch (inside diameter) pressure vessel for observation of test specimens.

The objective of the study was to determine experimentally the relationship between the axial displacement of conical windows, their conical angle, thickness-to-minor-diameter ratio (t/D), and duration of sustained loading at 10,000 psi hydrostatic pressure. This relationship was to be determined by (1) pressurizing a series of conical acrylic windows with 30-, 60-, 90-, 120-, and 150-degree angles and 0.500 to 1.250 t/D ratios at a constant rate to 10,000 psi, (2) maintaining that pressure for up to 1,000 hours, and (3) recording the displacements of the windows. It was clearly understood that some of these would be ejected in less than 1,000 hours, while others would still be serviceable after this time.

Also the relationship between the displacement during pressurization and the retraction during depressurization were to be investigated by dropping the pressure at the same constant rate used during pressurization. By examining the window's ability to approach its original shape as the pressure is relieved after long-term loading at 10,000 psi, a fair indication would be obtained on the window's relaxation capability.

TEST SPECIMENS

The test specimens (Figures 2 and 3) were machined from commercial Plexiglas G acrylic plate (Table 1). The bulk of the window test specimens were made to fit the same window mounting flanges used in the previous study for windows under long-term loading of 20,000 psi.

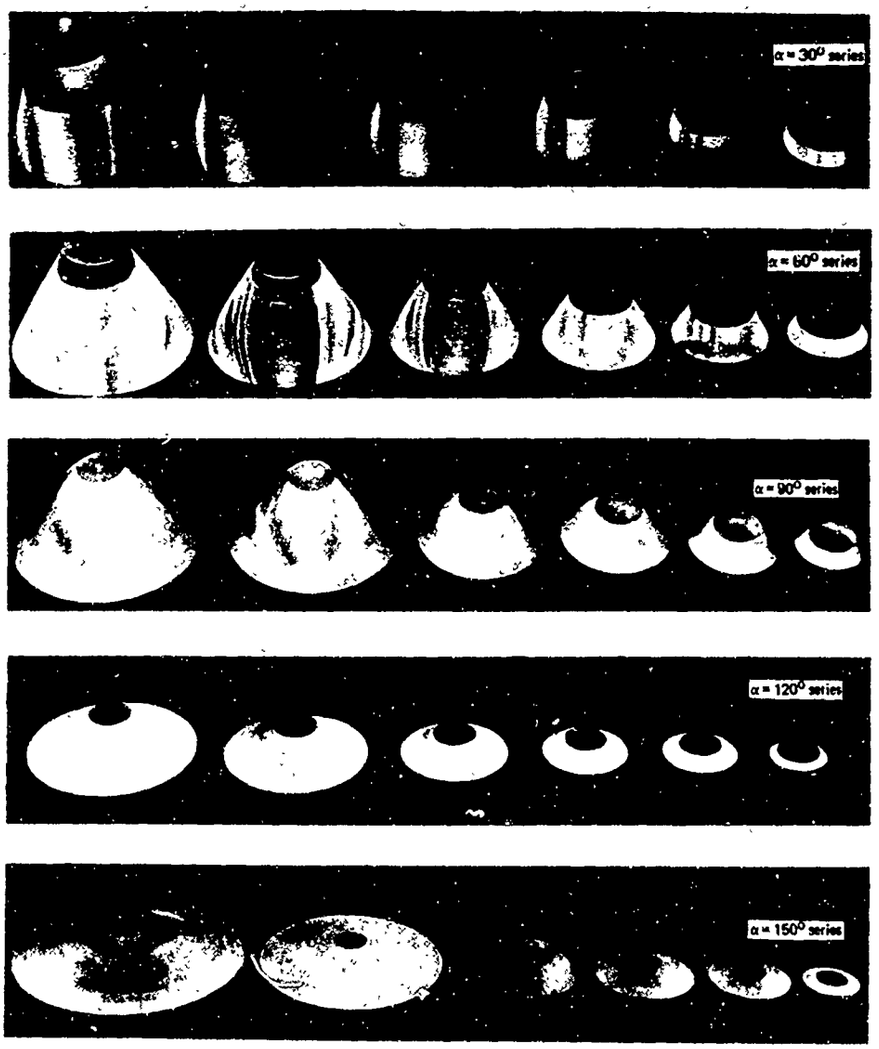

Figure 2. Typical conical acrylic windows of 1-inch minor diameter used in the experimental program.

Table 1. Properties of Acrylic Window Material

Physical Properties		
Property	Typical	Test Method
Hardness, Rockwell M	90	ASTM-D785-62
Hardness, Barcol	90	ASTM-D2583
Specific gravity	1.19 ± 0.01 (2 tests within 0.005)	ASTM-D792-64T
Refractive index; 1/8 inch	1.50 ± 0.01	ASTM-D542-50
Luminous transmittance; 1/8 inch	91%	ASTM-D1003-61
Haze, 1/8 inch	2.3	ASTM-D1003-61
Heat distortion temperature +3.6°F/min at 264 psi +3.6°F/min at 66 psi	 200°F 220°F	ASTM-D648-56
Thermal expansion/°F at 20°F	35×10^{-6}	Federal Standard 406 Method 2031
Water absorption; 1/8 inch (a) 25 hours at 73°F (b) to saturation	 0.3% 1.9%	ASTM-D570-63T
Mechanical Properties		
Tensile strength, rupture (0.2 in./min)	9,000 psi (min)	ASTM-D638-64T
Tensile elongation, rupture	2% (min) – 7% (max)	ASTM-D638-64T
Modulus of elasticity, tension	400,000 psi (min)	ASTM-D638-64T
Compressive strength, (0.2 in./min)	15,000 psi (min)	ASTM-D695-63T
Flexural strength, rupture	14,000 psi (min)	ASTM-D790-63
Shear strength, rupture	8,000 psi (min)	ASTM-D732-46
Impact strength, 1 zod (per inch of notch)	0.4 ft-lb (min)	ASTM-D256-56
Compressive deformation under load (4,000 psi at 122°F for 24 hours)	2% (max)	ASTM-D621-64

Material: Plexiglas G

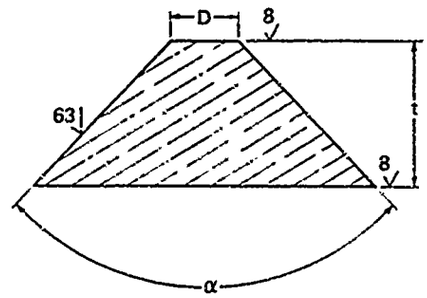

Nomenclature

D = minor diameter (in.)
t = thickness (in.)
α = included conical angle (deg)

Dimensions

1. For 1-in.-diam windows:

   D = 1.0 in.; tolerance = ±0.005
   t = nominal 1/2, 5/8, 3/4, 7/8, 1, 1-1/4 in. (manufacturer's plate thickness tolerances apply)
   α = 30, 60, 90, 120, or 150 degrees; tolerance = ±15'

2. For 4-in.-diam windows:

   D = 4.0 in.; tolerance = ±0.010
   t = nominal 4 in. (manufacturer's plate thickness tolerances apply)
   α = 90 degrees; tolerance = ±15'

Figure 3. Dimensions of typical conical window specimens.

The diameter of the window was selected to be 1 inch with a plus or minus 0.005-inch tolerance (Table 2). The conical angle of the windows was held to a plus or minus 15-minute tolerance. The actual thickness of the windows differed considerably (up to 10%) from their nominal thickness, which was the same as that of the commercially supplied acrylic plates with standard manufacturing thickness tolerance. The conical bearing surfaces were machined to a 63-rms finish, which subsequently when polished and covered with silicone grease, served as a sealing surface in contact with the flange.

In addition to the 1-inch diameter windows of 30-, 60-, 90-, 120-, and 150-degree included angle with 0.625 to 1.250 t/D ratios, a series of 4-inch diameter 90-degree included angle windows were fabricated. The reason for making larger scale windows and subjecting them to test conditions identical to those of the smaller windows was to compare the displacement of the large windows to that of the smaller windows so that the scaling factor for window displacements established in previous studies[1-4] could be reconfirmed.

TEST SETUP

Window Flanges

The test specimens with 1-inch minor diameter were mounted in flanges designed to fit into the Mk I and Mk II modified 16-inch naval gun shell end-closures (Figures 4 and 5). The flanges for the 4-inch-diameter,

90-degree windows were designed to fit the end-closure of the Deep Ocean Laboratory's 18-inch-diameter, high-pressure vessel (Figures 6 and 7). The mild steel flanges were of sufficient thickness to insure that very little deformation of the flanges occurred during application of hydrostatic pressure to the window's high-pressure face. For all practical purposes the window flanges were rigid, and only the acrylic windows were deformed during pressurization.

To standardize the window displacement tests, all windows and flanges were designed to have the minor diameter of the window always equal to the minor diameter of the conical window cavity in the flange. Because of this, the low-pressure face of every window tested was set flush with the bottom of the conical cavity in the flange (Figure 8). The special feature of these conical window flanges designated as DOL No. 1 mounting configuration was the termination of the conical cavity in a long cylindrical passage that would restrain the extruding portion of the window radially. The length of cylindrical passage varied from flange to flange, depending on the window's angle and t/D ratio, however, it was designed to be long enough so that the extruded acrylic plug would be radially supported along its whole length. (For discussion of other DOL flange mounting configurations see Reference 4 and Appendix A.)

Pressure Vessels

The DOL No. 1 window flanges, as mentioned previously, were designed either to fit the end-closure of Mk I and Mk II conversions of 16-inch naval gun shells, or the 18-inch diameter DOL pressure vessel. The flanges were attached to the end-closures in such a manner that the low-pressure face of the window was exposed to atmospheric pressure, while the high pressure face was acted upon by the pressurized water inside the vessel. By such an arrangement the pressure differential was simulated that exists on a window in a submerged structure, or on a window in an internal pressure vessel. The Mk I, Mk II, and 18-inch chamber pressure vessels contained a sufficient volume of compressed water at 10,000 psi that the small day to day extrusions of the windows through the flange opening would not decrease the pressure inside the vessel by more than 50 psi. Also, the compressed water in the pressure vessel and the stressed walls of the vessel contained sufficient amount of potential energy to carry through the ejection of windows when the critical moment arrived. This feature of the pressure vessels was of great importance, as it permitted the locking in of 10,000 psi pressure inside the vessel for unattended operation.

Table 2. Test Plan for Conical Acrylic Windows Subjected to 10,000 Psi of Hydrostatic Pressure for 1,000 Hours

[● represents a group of five test specimens; D = minor diameter (in.)]

Thickness, t (in.)	Included Angle (deg)									
	30		60		90		120		150	
	D = 1.0	D = 4.0	D = 1.0	D = 4.0	D = 1.0	D = 4.0	D = 1.0	D = 4.0	D = 1.0	D = 4.0
1/2 (0.500)	●		●		●		●		●	
5/8 (0.625)	●		●		●		●		●	
3/4 (0.75)	●		●		●		●		●	
7/8 (0.875)	●		●		●		●		●	
1 (1.0)	●		●		●		●		●	
1-1/4 (1.25)	●		●		●		●			
4 (4.0)						●				

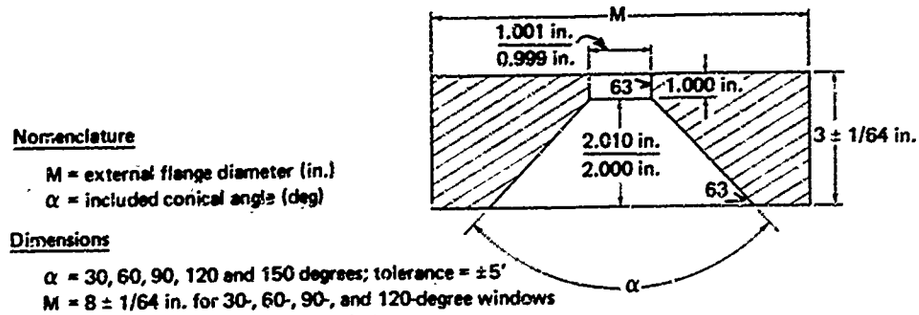

Nomenclature

M = external flange diameter (in.)
α = included conical angle (deg)

Dimensions

α = 30, 60, 90, 120 and 150 degrees; tolerance = ±5'
M = 8 ± 1/64 in. for 30-, 60-, 90-, and 120-degree windows
17 ± 1/64 in. for 150-degree windows

Material: 1015 steel

Figure 4. Dimensions of typical window mounting flanges for 1-inch-diameter conical windows.

Figure 5. Typical flanges for 1-inch-diameter conical window.

Instrumentation

The instrumentation for the long-term pressure testing of acrylic windows consisted of a pressure gage, a displacement indicator, and a thermometer (Figure 8). The Bourdon-type pressure gage measured the hydrostatic pressure inside the vessel with ±50-psi accuracy, the mechanical dial type displacement indicator measured with ± 0.001-in. accuracy the displacement of the center of the windows' low-pressure face, while the Bourdon-type thermometer registered with ± 0.5°C accuracy the temperature of the water wetting the high-pressure face of the window.

Nomenclature

M = external flange diameter (in.)
L = overall flange thickness (in.)
k = cylindrical passage length (in.)
α = included conical angle (deg)

Dimensions

α = 90 degrees; tolerance = ±5'
M = 17-3/4 ± 1/64 in.
k = 1 ± 1/64 in. for 90-degree windows
L = 5 ± 1/64 in. for 90-degree windows

Material: 4130 steel

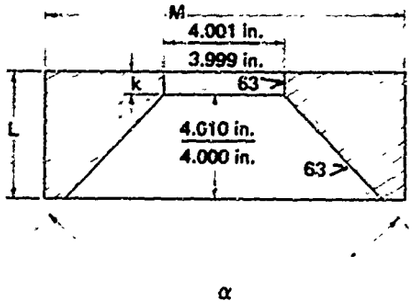

Figure 6. Dimensions of typical window mounting flange for 4-inch-diameter conical windows.

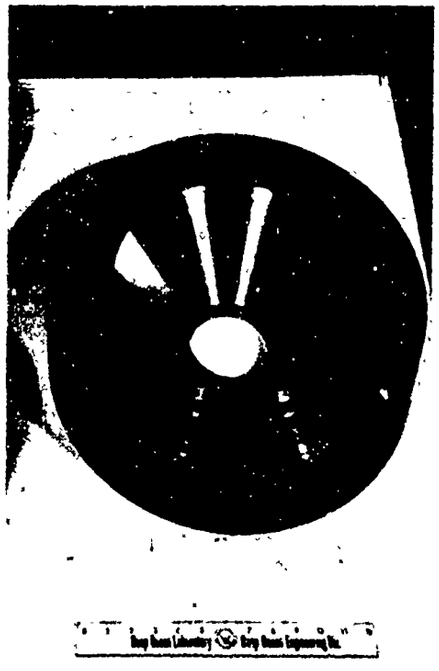

Figure 7. Typical flange for 4-inch-diameter conical windows.

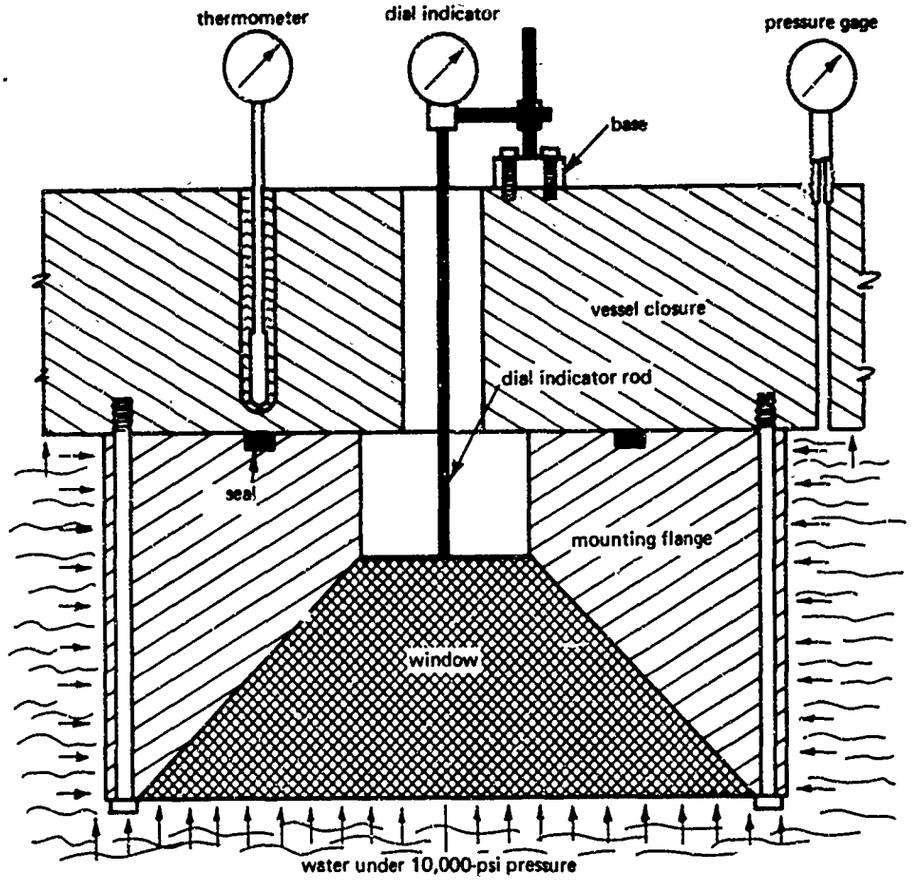

Figure 8. Schematic of window test arrangement.

TEST PROCEDURE

Mounting of Windows

The windows were liberally coated with silicone grease on their conical bearing surface prior to placement into the conical flange cavity. After inserting the window into the conical flange cavity, a force of approximately 20 to 25 pounds was applied to window's high-pressure face to squeeze out most of the grease from between the window and the flange (Figure 9). Subsequently, the flange was bolted to the vessel end-closure, the closure was then placed into the appropriate pressure vessel prefilled with fresh water and locked into place. The preparations for testing were completed by mounting of the mechanical dial-type displacement indicator on the end closure. The dial indicator was mounted in such a manner that the rod of the indicator protruded through the opening in the end closure and rested firmly on the center of the window's low-pressure face.

Figure 9. Installation of a 4-inch-diameter, 90-degree conical window into flange mounted on the end closure of the 18-inch internal-diameter vessel.

Pressurization of Windows

The first step was to pressurize the vessel to 1,000 psi and hold it for 10 minutes, after which the pressure was reduced to zero and the dial displacement indicator was adjusted to zero reading. This operational procedure insured that the window was bearing against the steel flange and not against a thick layer of grease, and that the displacement readings recorded during and following pressurization to 10,000 psi would be a measure of the window's displacement, rather than grease extrusion.

The pressurization to the 10,000-psi pressure level was conducted at a 600-to-700-psi/min rate, and the displacement readings were taken at 1,000-psi increments. After the pressure inside the vessel reached 10,000 psi, the pumps were stopped and the valve controlling the flow of water to the vessel was closed. This operation concluded the pressurization of the windows to their long-term operational pressure.

Long-Term Pressure Loading

Some of the windows were subjected to 10,000 psi of hydrostatic pressure for 500 hours, while others were kept at that pressure for 1,000 hours. In this manner, the damage to the windows could be observed at discrete time intervals, one of them being twice as long as the other. The pressure inside the vessels fluctuated as much as ±100 psi, depending on the temperature of the ambient atmosphere. No effort was made to control the temperature of the water. Its temperature fluctuated between 18°C to 22°C depending on the season of the year, and the time of day. Displacement, pressure, and temperature readings were taken three times a day. At that time the pressure inside the vessel was also readjusted if it differed by more than 100 psi from the set pressure of 10,000 psi. Such readjustments were rare, and occurred only in cases where minor leaks occurred in the hydraulic system servicing that particular vessel, or if the air temperature changed sharply.

Depressurization

After the window specimens had been maintained under 10,000-psi hydrostatic pressure for a period of 500 or 1,000 hours, the pressure was lowered to zero following the same procedure used during pressurization. When all the pressure was relieved and the magnitude of the window's displacement relaxation was noted, the end-closure was removed from the vessel and the window extracted from its flange seat. The window was inspected for any crazing and/or damage and set aside for later reference.

TEST OBSERVATIONS

Catastrophic Failures

Only a few test specimens failed when subjected to 10,000-psi loading. The windows that failed during pressurization were those with a t/D of 0.500 and an included angle of 30 degrees. The windows that failed under a sustained load of 10,000 psi in a period of less than 1,000 hours were (1) those with a t/D of 0.500 and an included angle of 60, 90, 120, and 150 degrees, and (2) those with a t/D of 0.625 with an included angle of 30 degrees.

The windows failed in one of two ways depending upon the included angle. The specimens with 30, 60, and 90 degrees included angle broke into very small fragments and ejected entirely from the flange seat upon failure. Windows with the 120- and 150-degree included angle sheared along a conical surface that intersected the window's bearing surface at a location nearly equidistant from the low and high pressure faces. The section including the low-pressure face was then ejected thorugh the 1-inch opening in the flange while the remainder of the high-pressure face remained in the flange seat in the form of an annular fragment.

Incipient Failures

Cracks were observed on many windows after termination of the 500- and 1,000-hour pressure loadings at 10,000 psi hydrostatic pressure. Their occurrence was limited to windows with $t/D \leq 0.625$ for 150- and 120-degree conical angle windows, $t/D \leq 0.625$ for 90-degree, $t/D \leq 1.250$ for 60-degree and 30-degree windows. The cracks always originated on the conical bearing surface and appeared to propagate into the interior of the window at right angles to the conical bearing surface.

The cracks were not evenly distributed along the bearing surface but tended to congregate at the low-pressure face end of the windows. The width of the band where the cracks were observed was an inverse function of the conical angle. Thus for the 150-degree conical angle windows, the band of cracks on the conical bearing surface was only about 0.060-inch wide and was located adjacent to the low-pressure face of the window. For the 30-degree conical angle windows the band of cracks was almost as wide as the width of the bearing surface. Only a very narrow band of the bearing surface adjacent to the window's high-pressure face was free of cracks or crazing.

One of the cracks on the bearing surface initiated the fracture plane if the 10,000-psi hydrostatic loading was sustained sufficiently long or if the window was pressure-cycled to 10,000 psi many times in succession (Figure 10).

The conical fracture surfaces observed in conical windows that failed under sustained long-term loading in this study bear out the postulate that the fracture plane originates at one of the many cracks on the bearing surface.

Some of the windows showed no cracking on their bearing surfaces. These windows were with t/D $\geq$ 0.750 and 90-, 120-, and 150-degree conical angles (Appendix B).

Plastic Deformation

High-Pressure Face. The plastic deformation of the windows took place in three different locations on the window (Figures 10 and 11). On the high-pressure face there appeared a concave cold-flow crater whose diameter and depth were a function of angle, t/D ratio, temperature, and duration of loading. In some of the windows, particularly those with the 150-degree conical angle, the periphery of the cold flow crater was bounded by a crack running the full circumference of the crater.

Low-Pressure Face. This face also experienced plastic deformation whose form depended on the conical angle of the window (Figure 10 and 11). For windows with 30- and 60-degree angles the low-pressure face became convex. Depending on the radius of curvature and tensile flexure, cracks were either present or absent around the circumference of the low-pressure face. Windows with conical angles > 60 degrees experienced a different deformation on the low-pressure face. Whereas with the 30- and 60-degree windows the low-pressure face became convex, with the 90-, 120-, and 150-degree windows the low-pressure face generally became slightly concave. The concave appearance of the low-pressure face was caused by the formation of a narrow, low ridge around the face's circumference.

Window Body. Besides plastic deformation of the high- and low-pressure faces, there was also deformation of the window's body. This deformation took the form of a cylindrical plug being extended through the cylindrical passage in which the conical window cavity in the flange terminated. The length of plastic plug extension was measured (1) immediately after termination of the long-term pressurization, and (2) 1,000 hours after termination of the long-term pressurization (Table 3). A significant difference in magnitude was observed between these two measurements, the magnitude of plug extension immediately after termination of long-term pressurization being the larger one. This indicates that the total plug extension of the window is the sum of three deformations, (1) the elastic, (2) the viscoelastic, and (3) the plastic.

(a) Fracture surface on conical bearing surface.

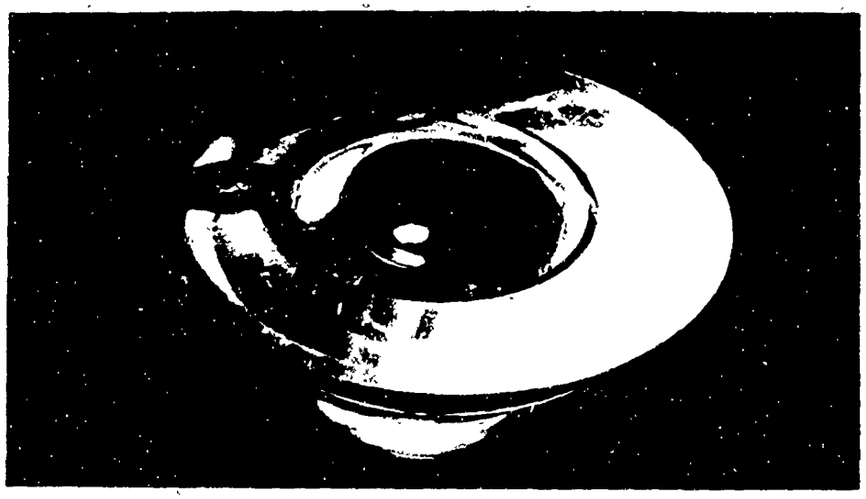

(b) High-pressure face intersected by fracture surface.

(c) Two separated fragments of the window.

Figure 10. Typical deformation and fracture pattern for conical acrylic windows with included conical angles of 90, 120, and 150 degrees under sustained hydrostatic loading.

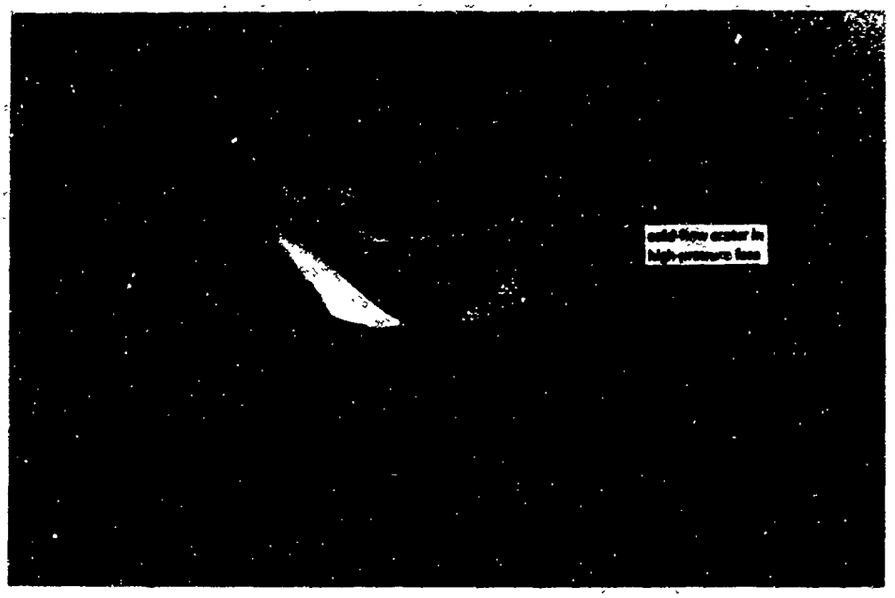

(a) Typical cold-flow cratering on window's high-pressure face.

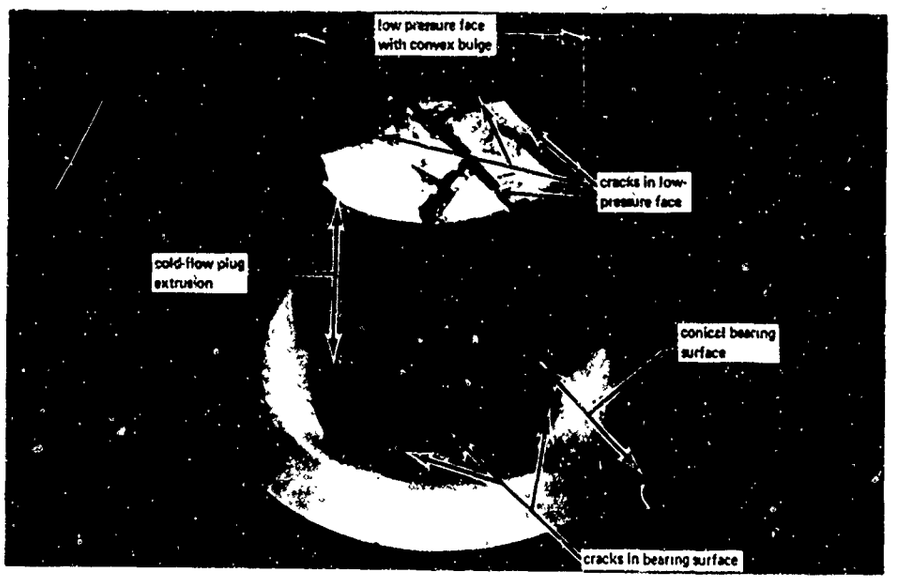

(b) Typical cold-flow plug extrusion of window's low-pressure face.

Figure 11. Typical deformation and fracture pattern of conical acrylic windows with 30- and 60-degree included angles.

Table 3. Displacement of Windows After Depressurization From Sustained Long-Term Hydrostatic Loading at 10,000 Psi

t/D	Included Conical Angle (deg)	Displacement* (in.)		
		Prior to Depressurization	Immediately After Depressurization	1,000 Hours After Depressurization
500-Hour Loading Duration				
0.625	30	–	–	–
	60	0.078	0.026	0.000
	90	0.057	0.009	0.001
	120	0.050	0.015	0.001
	150	0.044	0.009	0.001
0.750	30	0.119	0.109	0.001
	60	0.071	0.003	0.001
	90	0.050	0.006	0.000
	120	0.041	0.006	0.001
	150	0.037	0.003	0.001
0.875	30	0.097	0.066	0.001
	60	0.053	0.011	0.000
	90	0.045	0.004	0.000
	120	0.036	0.006	0.001
	150	0.042	0.004	0.000
1.000	30	0.077	0.046	0.001
	60	0.054	0.015	0.001
	90	0.046	0.004	0.001
	120	0.036	0.006	0.001
	150	0.037	0.004	0.000
1.250	30	0.078	0.046	0.002
	60	0.052	0.010	0.000
	90	0.041	0.003	0.000
	120	0.036	0.002	0.000
	150	0.034	0.004	0.000

continued

Table 3. Continued

t/D	Included Conical Angle (deg)	Displacement* (in.)		
		Prior to Depressurization	Immediately After Depressurization	1,000 Hours After Depressurization
1,000-Hour Loading Duration				
0.625	30	–	–	–
	60	0.083	0.027	0.000
	90	0.064	0.016	0.000
	120	0.0473	0.015	0.001
	150	0.049	0.012	0.000
0.750	30	0.121	0.105	0.003
	60	0.070	0.003	0.000
	90	0.050	0.006	0.001
	120	0.043	0.007	0.001
	150	0.038	0.004	0.001
0.875	30	0.116	0.097	0.001
	60	0.054	0.015	0.000
	90	0.044	0.007	0.000
	120	0.037	0.008	0.001
	150	0.039	0.005	0.001
1.000	30	0.080	0.058	0.003
	60	0.050	0.016	0.000
	90	0.047	0.004	0.001
	120	0.039	0.007	0.001
	150	0.041	0.006	0.000
1.250	30	0.080	0.055	0.002
	60	0.052	0.016	0.000
	90	0.041	0.002	0.000
	120	0.037	0.005	0.000
	150	0.036	0.005	0.000

* Displacements shown are not average values for groups of five windows but are values measured on a few individual windows.

The maximum extent of *elastic plug deformation* is obtained by subtracting from the axial displacement just prior to depressurization the displacement reading immediately upon reaching zero psi. The magnitude of *viscoelastic* plug deformation, on the other hand, is determined by subtracting from the displacement reading immediately after depressurization the displacement reading after 1,000 hours of relaxation. The magnitude of *plastic* plug deformation is, of course, the difference between the zero displacement reading prior to pressurization and the reading 1,000 hours after termination of long-term pressure loading at 10,000 psi.

Displacements

Axial displacements measured during the long-term sustained loading of the windows varied with t/D ratio, conical angle, and duration of loading (Figures 12 and 13 and Appendix C). The magnitude of displacement appeared to be directly related to time while inversely related to t/D ratio and conical angle (Table 4). As the t/D ratio was increased for windows of any angle, the magnitude of displacement for the same duration of sustained loading decreased. The decrease of displacement did not appear to be, however, a linear function of the t/D ratio. With each increase in t/D ratio the decrease in displacement became less, until an asymptotic displacement value was reached that could not be decreased further by increases in t/D ratios. At 1,000 hours after initiation of sustained loading, the asymptotic displacement values for 1-inch minor diameter windows were as follows:

Conical Angle (deg)	t/D Ratio	Displacement (in.)
30	1.250	0.085
60	1.000	0.054
90	0.875	0.045
120, 150	0.875	0.036

The rate of displacement was also observed to be a function of t/D ratio, conical angle, and duration of sustained loading. In general, the rate of displacement was inversely proportional to all of the above-mentioned parameters. The rate of displacement is so high immediately after pressurization to 10,000 psi and drops off so rapidly thereafter that the magnitude of displacement reached by windows 1 hour after pressurization represents generally more than 50% of the total displacement observed on the window after 1,000 hours of sustained loading.

Table 4. Average Displacement of Conical Acrylic Windows During Sustained Loading at 10,000 Psi

t/D	Included Conical Angle (deg)	Average Displacement (in.) After —				
		1 Hour	10 Hours	100 Hours	500 Hours	1,000 Hours
0.500	30	–	–	–	–	–
	60	0.146	–	–	–	–
	90	0.062	0.102	–	–	–
	120	0.050	0.066	0.195	–	–
	150	0.050	0.064	0.194	–	–
0.625	30	0.180	0.197	0.340	0.524	–
	60	0.057	0.066	0.076	0.081	0.084
	90	0.046	0.047	0.054	0.058	0.062
	120	0.036	0.038	0.045	0.049	0.053
	150	0.032	0.038	0.041	0.045	0.048
0.750	30	0.120	0.126	0.133	0.138	0.140
	60	0.052	0.059	0.065	0.069	0.071
	90	0.042	0.044	0.048	0.051	0.052
	120	0.035	0.036	0.039	0.041	0.042
	150	0.031	0.033	0.038	0.039	0.040
0.875	30	0.085	0.092	0.103	0.106	0.108
	60	0.046	0.048	0.055	0.055	0.057
	90	0.038	0.038	0.044	0.044	0.045
	120	0.034	0.035	0.036	0.039	0.040
	150	0.030	0.030	0.035	0.037	0.038
1.000	30	0.076	0.078	0.078	0.081	0.082
	60	0.042	0.043	0.048	0.052	0.053
	90	0.033	0.035	0.042	0.043	0.044
	120	0.030	0.030	0.034	0.038	0.039
	150	0.028	0.029	0.034	0.036	0.037
1.250	30	0.074	0.076	0.077	0.077	0.079
	60	0.041	0.041	0.047	0.051	0.053
	90	0.032	0.034	0.041	0.042	0.043
	120	0.029	0.029	0.034	0.037	0.038
	150	0.027	0.028	0.033	0.035	0.036

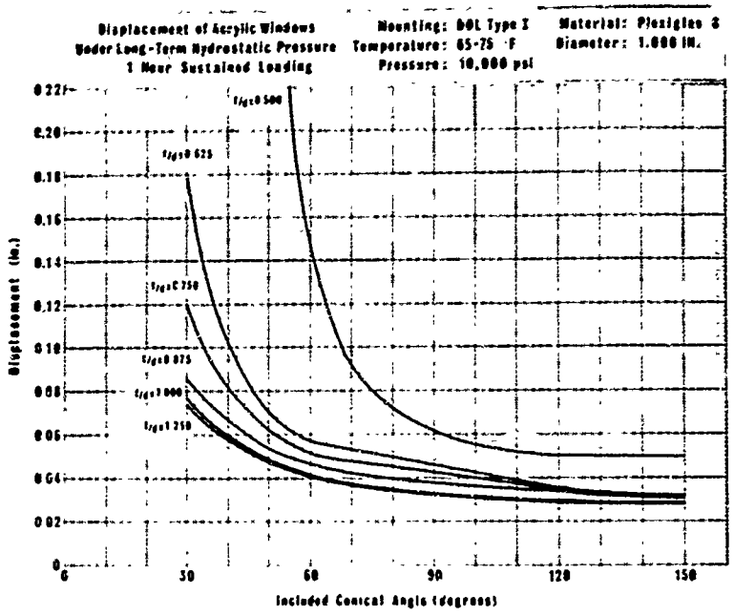

(a) After 1 hour of sustained loading.

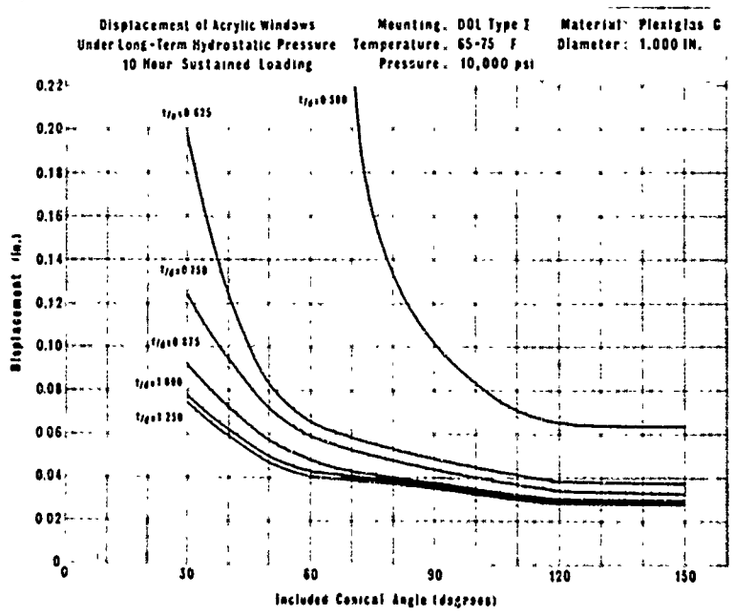

(b) After 10 hours of sustained loading.

Figure 12. Displacement of conical acrylic plastic windows under sustained pressure loading as a function of window's in conical angle.

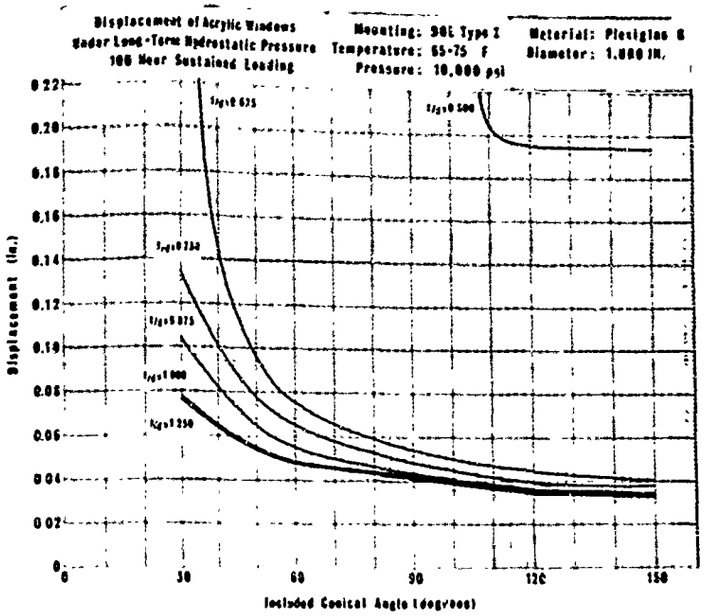

(c) After 100 hours of sustained loading.

nder 1
w's inc Displacement of conical acrylic plastic windows under 10,000 psi sustained pressure loading as a function of window's included conical angle.

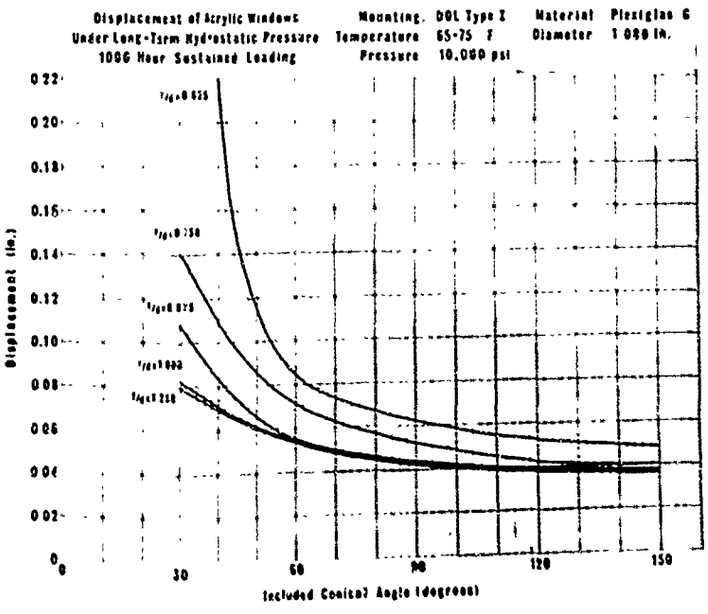

(d) After 1,000 hours of sustained loading.

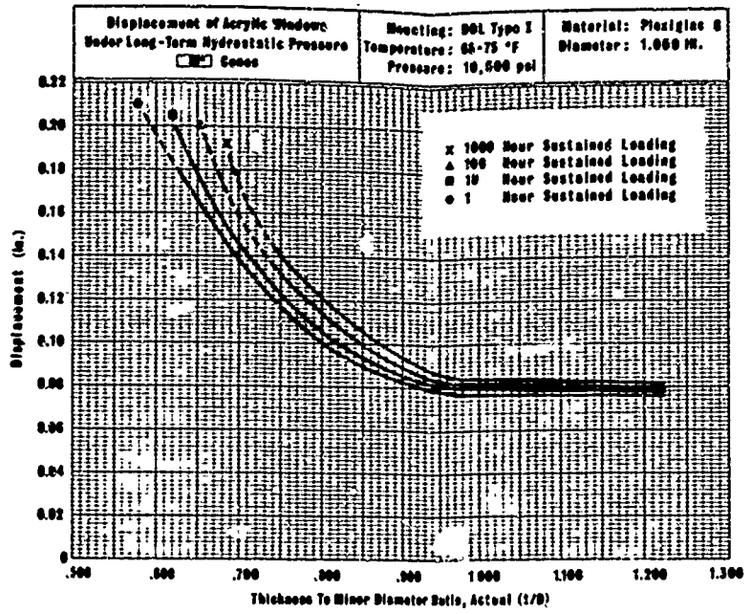

(a) Windows with 30-degree included conical angle.

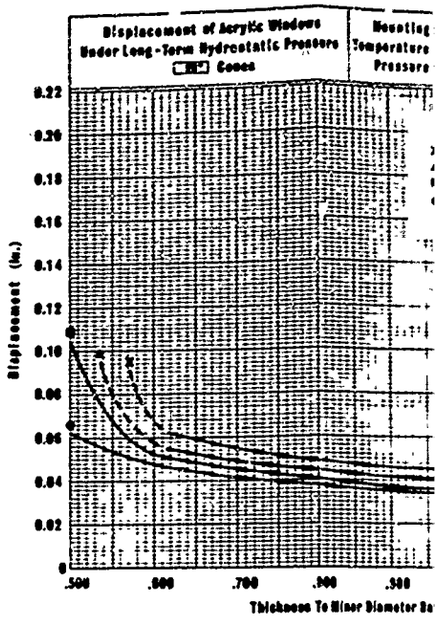

(c) Windows with 90-degree inc

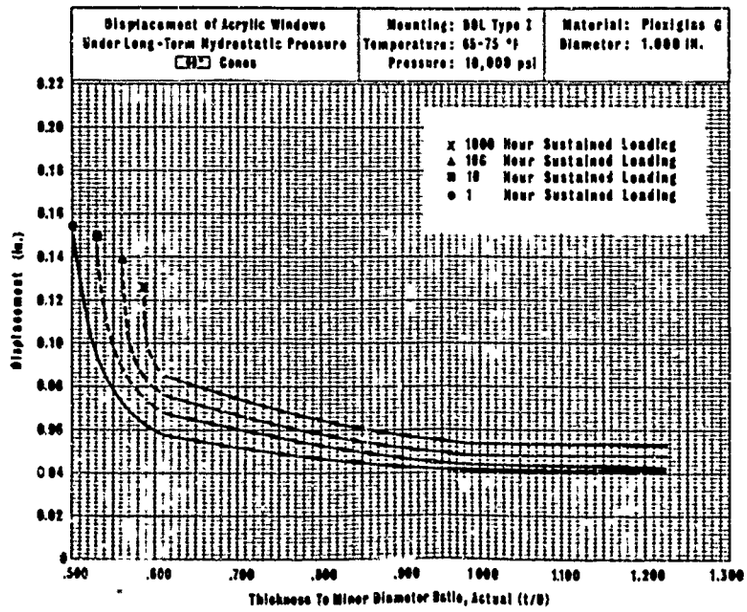

(b) Windows with 60-degree included conical angle.

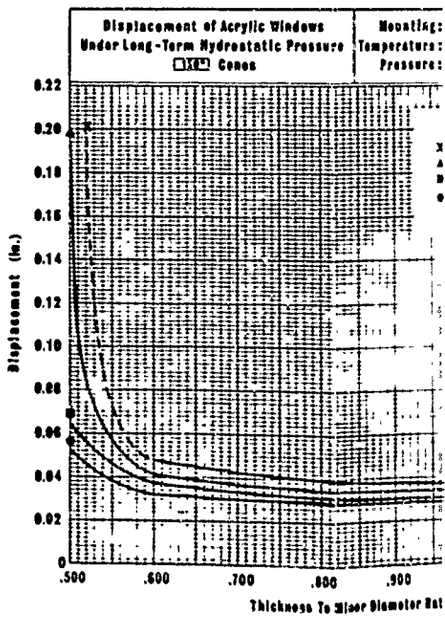

(d) Windows with 120-degree incl

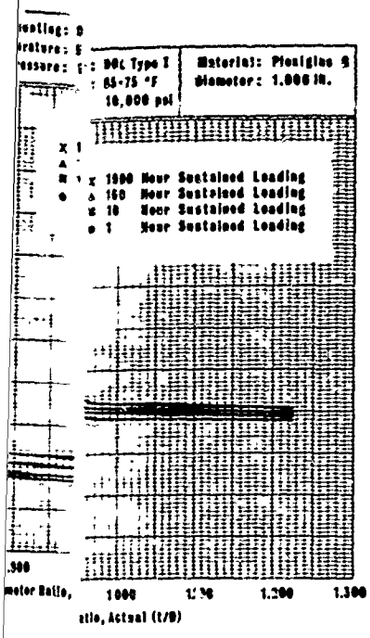

ree incl

ded conical angle.

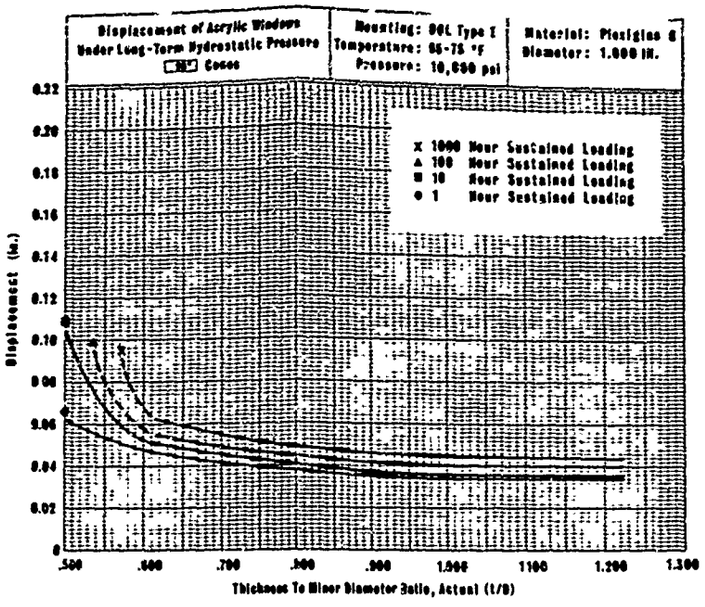

(c) Windows with 90-degree included conical angle.

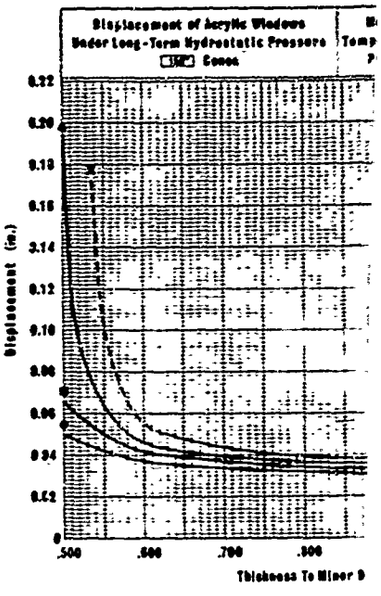

(e) Windows with 150-d

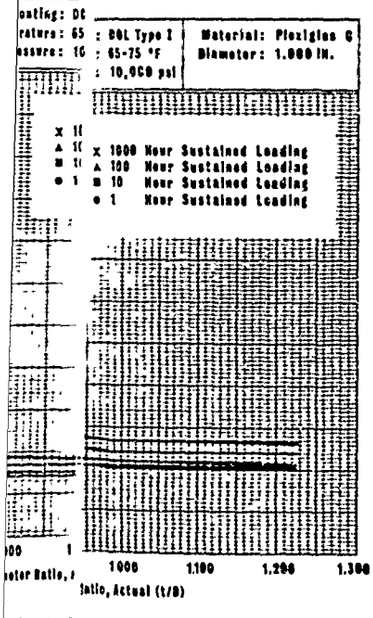

e includ luded conical angle.

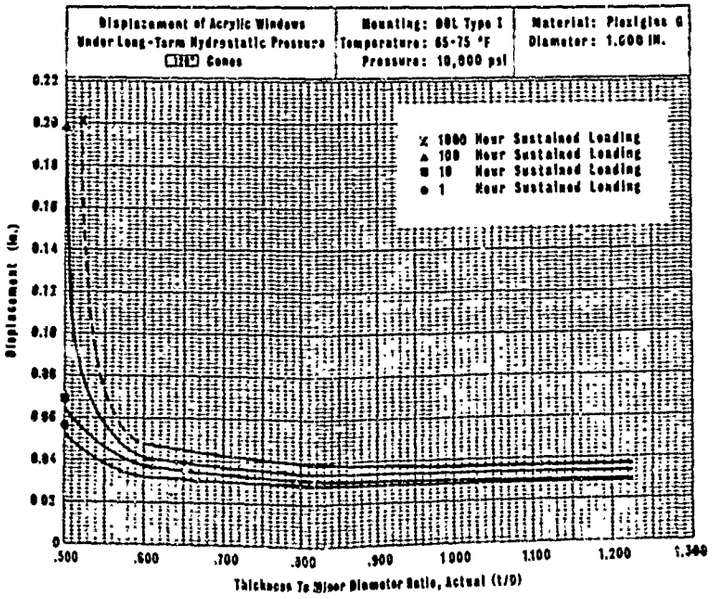

(d) Windows with 120-degree included conical angle.

Figure 13. Displacements of conical acr
sustained pressure loading as

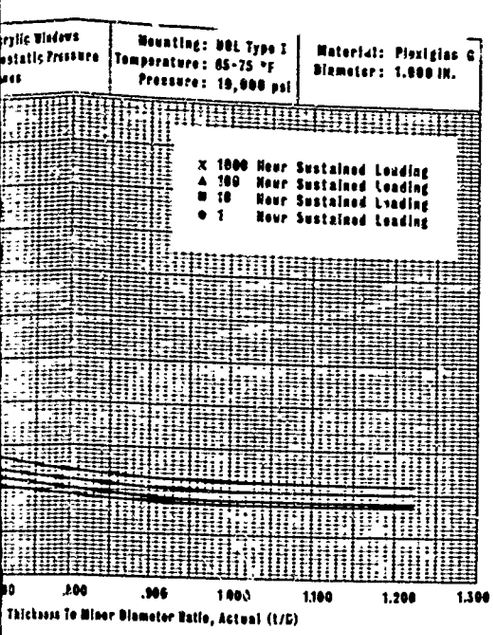

ws with 90-degree included conical angle.

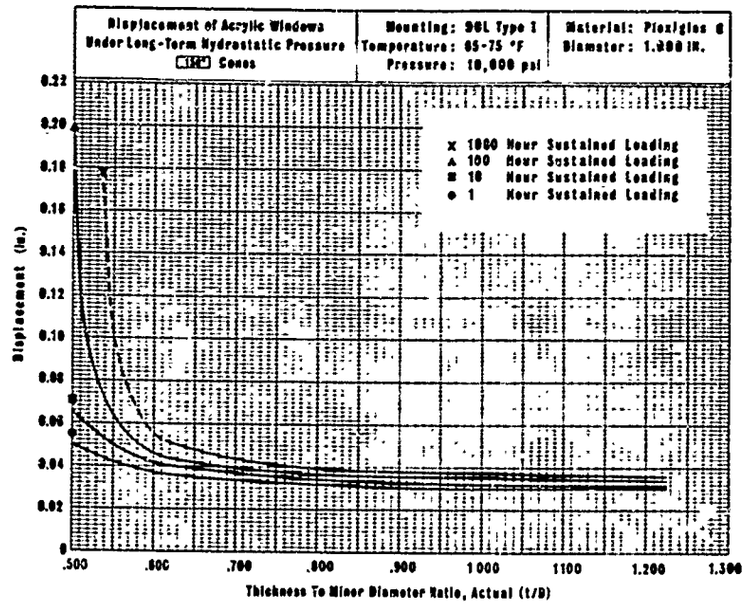

(e) Windows with 150-degree included conical angle.

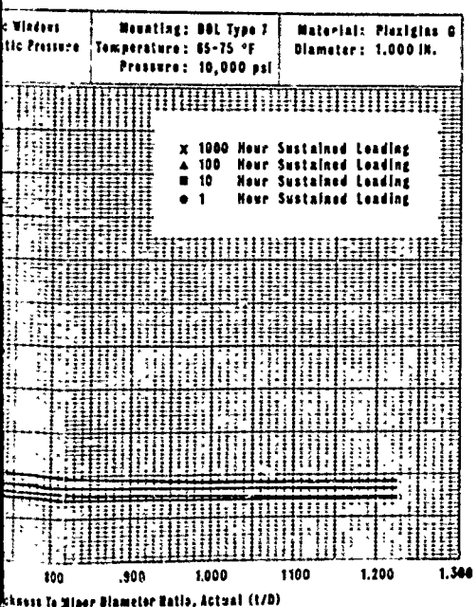

th 120-degree included conical angle.

Figure 13. Displacements of conical acrylic plastic windows under 10,000 psi sustained pressure loading as a function of window's t/D ratio.

The magnitudes of displacement observed on full-scale windows with t/D = 1.00, a 90-degree conical angle, and 4.00-inch minor diameter were approximately four times larger than the displacement of model windows with ide. tical t/D ratios and conical angles but only 1.00-inch minor diameters. This confirms the findings made in previous studies that the magnitude of axial displacement scales linearly with the minor diameter of the window providing t/D, conical angle, temperature, pressure loading and duration of loading remain the same.

FINDINGS

1. Conical acrylic windows under 10,000-psi long-term hydrostatic loading deform either viscoelastically, or viscoplastically, the mode depending on the conical angle, thickness-to-diameter ratio, duration of loading, and ambient temperature.

2. The deformation of the windows is in the form of a cylindrical plug on the low-pressure side and a craterlike depression on the high-pressure face.

3. The deformation is a direct function of temperature and duration of loading, and an inverse function of conical angle and t/D ratio.

4. The windows that experienced no permanent deformation (as determined by measurements after a single 1,000-hour sustained loading at 10,000 psi followed by a relaxation period of 1,000 hours) were (1) 30-degree windows with $t/D \geq 0.750$ and (2) 60-, 90-, 120-, and 150-degree windows with $t/D \geq 0.625$.

5. No cracks were observed in 90-, 120-, and 150-degree windows with $t/D \geq 0.750$. Windows with 30- and 60-degree angles had cracks in the whole $0.625 \leq t/D \leq 1.250$ range of ratios.

6. The magnitude of axial displacement of windows through the opening in the flange is a direct function of the temperature and duration of loading, and an inverse function of conical angle and t/D ratio.

7. For each conical angle of windows under 1,000-hour sustained loading at 10,000-psi pressure, there is a corresponding t/D ratio at which any further increase in t/D ratio ceases to produce any further decrease in magnitude of displacement:

t/D Ratio	Conical Angle (deg)
1.250	30
1.000	60
0.875	90, 120, 150

8. The asymptotic displacement values for conical acrylic windows with t/D ratios equal to or larger than those enumerated in Finding 7 are at 1,000-hour loading approximately:

Displacement (in.)	Conical Angle (deg)
0.085	30
0.054	60
0.045	90
0.036	120, 150

9. The rate of displacement is a direct function of temperature and an inverse function of t/D ratio, conical angle, and duration of loading.

CONCLUSIONS

Conical acrylic windows are suitable for applications under long-term sustained hydrostatic loading of 10,000 psi providing the proper t/D ratio for a given conical angle is chosen. Windows with conical angles ≥ 90 degrees require a minimum t/D ratio of 0.75 for crack-free life of 1,000 hours under a single sustained pressure loading.

RECOMMENDATIONS

For design and fabrication of conical acrylic windows under long-term hydrostatic loading of 10,000 psi detailed information and specifications contained in Appendixes A, B, and C should be taken into consideration.

Appendix A

DESIGN OF WINDOW AND FLANGE SYSTEMS FOR LONG-TERM LOADING AT 10,000-PSI PRESSURE

INTRODUCTION

When the data generated in this study are to be applied to the design of windows for deep-submergence systems, several design and operational parameters must be carefully evaluated. The most important operational parameter that must be considered is the type of pressure loading to which the pressure-resistant structures with windows will be subjected. For ease of discussion, hydrostatic pressure loadings can be classified into four general categories. These loading categories are (1) static short-term, (2) sustained long-term, (3) cyclical, and (4) dynamic.

The short-term static pressure loading has been defined as a continuous pressure rise at some arbitrarily set pressure rise rate until a predetermined pressure is reached; at this point, the pressure is released at the same rate. The pressure rise rate selected for NCEL window studies[1,2,3] was 650 psi/min.

Long-term sustained pressure loading is defined here as raising the pressure at some set rate to a predetermined pressure level and holding it there for the whole duration of the mission. Depending on the duration of the constant pressure application, the long-term pressure loading is further defined by the number of hours, or days that it is maintained on the window.[4]

Cyclical pressure loading is defined as varying the pressure between arbitrary maximum and minimum pressure levels with the period of pressure fluctuation being either constant or variable.

Dynamic pressure loading depends for its definition on the arbitrary dividing line between short-term static and dynamic pressure rise rate, which for windows used in submersibles probably can be placed at 5,000 psi/min. The dynamic pressure application may be short-term if applied once or cyclical if applied repeatedly.

WINDOWS

Selection of t/D Ratios

The data that have been generated in this study are applicable directly with some extrapolation *only to design of truncated cone acrylic windows under short-term or long-term loading at 10,000 psi,* since the test specimens

in this study underwent short-term pressurization at the rate of 650 psi/min followed by long-term steady pressure loading at 10,000 psi. On the basis of this data a guideline can be suggested for the benefit of the engineer designing acrylic hydrospace windows of truncated cone shape for a one-time, long-term pressurization to 10,000 psi in the 32°F-to-75°F temperature range.

Design Guideline 1. For applications in which the truncated cone acrylic windows serve as high-grade optical lenses for manned capsules under a *single sustained pressure loading* of 10,000 psi in 32°F-75°F temperature range, the following *minimum* window dimensions are recommended:

Flange	Included Conical Angle (deg)	t/D Ratio for Sustained Loading Period of—			
		1 Hour	100 Hours	1,000 Hours	100,000 Hours
(See Design Guideline 2)	30	1.500	1.750	2.000	2.500
	60	1.000	1.250	1.500	2.000
	90	0.625	0.625	0.750	1.000
	120	0.625	0.625	0.750	1.000
	150	0.625	0.625	0.750	1.000

The t/D ratios acceptable for optical applications of truncated cone acrylic windows have been selected after a thorough consideration of three parameters of importance in operational window performance: (1) magnitude of axial displacement during the long-term pressure loading, (2) deformation of high- and of low-pressure faces, and (3) magnitude of penetration and location of cracks on the conical surface during the sustained loading. Since it is virtually impossible, regardless of t/D ratio and angle chosen, to completely eliminate time-dependent cold flow of the acrylic plastic at 10,000-psi hydrostatic pressure, an engineering judgment was made on what constitutes the minimum acceptable performance of the acrylic window from the optical and safety viewpoints.

A window is considered to be safe for manned operation if during a single sustained pressure loading of 10,000 psi in the 32°F-to-75°F range for the specified maximum duration *no cracks or crazing* were present on the high- and low-pressure faces, while the conical bearing surface exhibited only minor crazing, if any. Total axial displacement in the range of 0.04 D to 0.08 D at the end of the specified period of loading presents no operational difficulties for the observer. The window is optically acceptable if it causes no distortion of viewed objects in hydrospace for an observer whose eyes are within 10 inches of the low-pressure face.

Applicability of Data to Other Loading Conditions

As previously mentioned, the experimental data generated in this study is applicable with reasonable extrapolation only to a single short- or long-term static pressure loading at 10,000 psi. However, since very few data are now available for the design of windows subjected to long-term loading at pressures other than those used in this study, some designers may be tempted to base their selection of window proportions on the data from this study. *This is not recommended.* The factors for adjusting t/D ratios from this study for other pressure levels have not yet been developed. Studies, however, have been completed that provide this information for 20,000-psi applications.[4] The results of long-term pressure study at 5,000 psi will be published in late 1971.

It is recommended as operationally desirable that the minimum t/D ratios acceptable for 10,000-psi long-term pressure loading also be used for pressures in the 5,000-to-10,000-psi range. This change in long-term operational static pressure magnitude will make it possible to proof-test such windows to 10,000 psi without damaging them.

The experimental data of this report also should not be used for the direct selection of window proportions for applications where the window is subjected to cyclic short-term or long-term pressurizations. Caution is advised here because the relationship between the effect of cyclic and long-term loading conditions on the initiation of fractures in acrylic windows is not known. However, in view of the fact that cyclic pressurization data for windows operating at 10,000 psi are either nonexistent or very scarce, designers may also be tempted to use long-term pressure loading data contained in this report for the design of windows for cyclic pressure service. Designers who do this are advised that the window proportions recommended for 100,000-hour sustained loading at 10,000 psi will *probably* perform quite satisfactorily at 10,000-psi cyclic loading so long as the maximum duration of the pressure cycle is less than 100 hours. If window proportions are selected for cyclic service on this basis, evaluation of the prototype full-scale window under simulated operational conditions is recommended.

Window Fabrication

Since the windows rely on intimate contact with the conical flange cavity surface for their high-pressure sealing as well as for their restraint against axial displacement, an accurate fit with that cavity is of great importance. For this reason the maximum allowable machining tolerances on the window must not exceed ±0.005 inch on the minor diameter, 0.010 inch in thickness, and ±15 minutes of included conical angle.

The windows are fabricated by machining acrylic stock having the mechanical and physical properties of Plexiglas G plate. Four-inch-thick commercially available plate, a custom cast block, or a block made up by bonding of several standard acrylic plates can serve as machining stock. In the case of custom cast or bonded blocks, the end product must have the same mechanical and physical properties as a monolithic, commercially available 4-inch-thick Plexiglas G plate. It is particularly important that the tensile strength of the bonds in the bonded acrylic block be equal to or approach (6,000-psi minimum) that of the parent material (Table 1).

Regardless of the machining stock used, the window should be annealed twice during its fabrication: once after rough machining when it is within approximately 0.125 inch of finished dimensions, and a second time when it has been machined to its final dimensions and the surfaces have been polished. Without annealing, the conical bearing surfaces of the window will craze and crack sooner under operational service.

The machined surface of the conical bearing surface of the window should have a smoothness of at least 63 rms followed by polishing. If the surface finish is rougher, crazing and cracking of the conical bearing surface *could* initiate sooner in operational service.

Proof-Testing of Windows

When the experimental data contained in this report are used for the design of windows, care must be taken not to damage the windows with excessive overpressure proof-testing. The basic ground rule for windows selected on the basis of long-term tests described in this report is that *conical acrylic windows should not be subjected to pressures above 10,000 psi, regardless whether this occurs during the operational life of the window or during the proof-test that precedes it.* Because of this, if the operational service of the windows is to be at 10,000 psi, the proof pressure preceding the operational use of the windows must only be equal to operational pressure. If for some reason the proof pressure must be in excess of operational pressure, then accordingly the operational pressure rating must be reduced below the 10,000-psi pressure level.

Since the proof-test to 10,000 psi prior to placement of the window in actual service constitutes a loading cycle, it is important to make it as brief as possible so that it does not substantially reduce the rated long-term life of the window in subsequent operation under service conditions. In addition to proof-testing each window, quality control in the procurement of acrylic stock, and in machining, annealing, and bonding of the window is required. If this quality control in fabrication is augmented by the destructive testing under short-term conditions of a window selected at random from the same group of windows on the production line, very reliable windows for long-term

loading can be obtained. In this manner even though one window is sacrificed to destructive proof-testing, the remaining windows from the same production batch retain most of their potential pressure-resisting capability for actual service.

If the proof-testing of operational windows to 10,000 psi is a firm requirement for certification, the t/D ratio of windows for sustained service at 10,000 psi should be based on design guideline 1 for 100,000 hours sustained loading duration.

FLANGES

Configurations

Although all the bulk of experimental data of this study has been generated in the DOL 1 flange and window configuration (Figure A-1), a minor modification of this configuration is recommended for full-size hydrospace windows to give the user an added margin of safety for windows whose proportions have been selected on the basis of this study.

The recommended modification to the DOL 1 flange and window configuration consists of locating the window's low-pressure face further away from the cylindrical passage in the flange to provide not only radial but axial restraints for the extruding portion of the window. Such a flange and window configuration, designated as DOL 5 flange (Figure A-2), permits the windows to extrude somewhat less than the windows described in this study and thus give the designer extra margin of safety and optical performance.

In order to minimize the displacement of the window under sustained operational pressure, as well as to provide a necessary margin of safety for overpressures to which the windows may be accidentally or intentionally (as in proof-testing) exposed, the engineer must design the window flange opening with required radial and axial support for the window. The dimensions of DOL 5 window flanges have been calculated and are presented in guideline 2. These calculations are based on two assumptions. The **first** is that the distance b between the window's low-pressure face in the conical flange cavity and the bottom of the conical cavity must be approximately the same as the displacement of the window with recommended t/D ratio during the specified duration of sustained loading at 10,000 psi. The **second** is that either an overpressure or extension of rated loading duration may be encountered by the structure during its life and therefore an additional allowance, ℓ, equal at least to b should be made for window displacement in the cylindrical flange cavity.

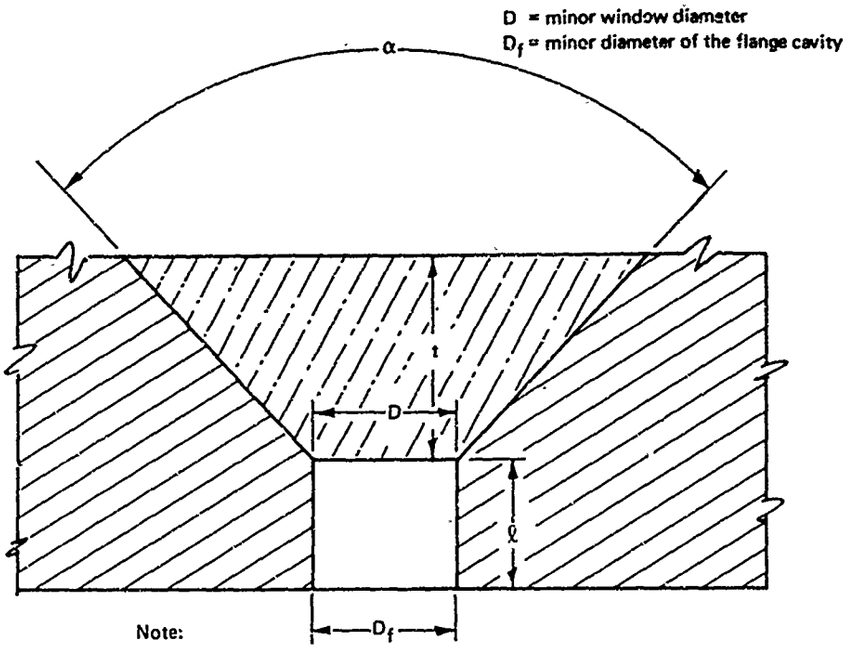

Figure A-1. Characteristics of DOL 1 flange and window assembly used in the current study.

The first assumption **must** be taken into account. The second one **should** be considered, but in many cases no pressures higher than operational will be encountered, and thus no provisions have to be made for displacements caused by overpressure or for duration of loading past the originally specified time span.

Design Guideline 2. For applications in which the truncated cone acrylic windows serve as high-grade optical lenses for manned capsules under sustained pressure loading of 10,000 psi in 32°F-to-75°F temperature range, the following minimum flange cavity proportions are recommended:

Window	Flange	Included Angle (deg)	D/D_f Ratio	Cylindrical Passage Length, ℓ
(See Design Guideline 1)	DOL 5	30	1.05	≥0.1 D
		60	1.10	≥0.1 D
		90	1.15	≥0.1 D
		120	1.20	≥0.1 D
		150	1.42	≥0.1 D

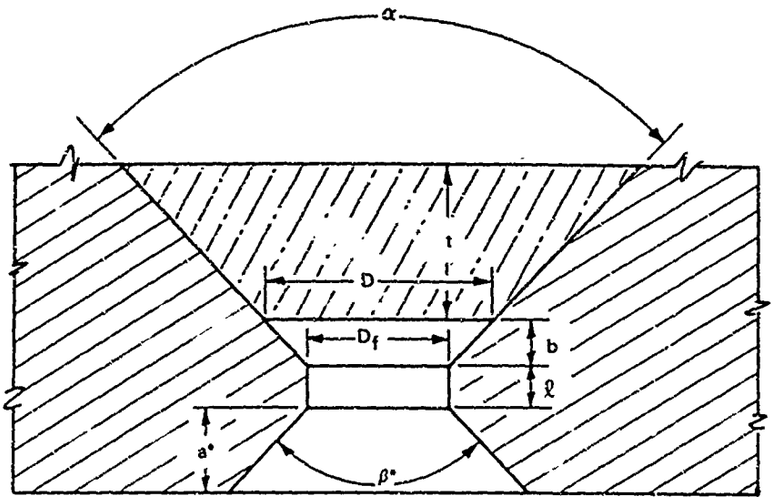

DOL 5 Assembly

Note:

1. a° — To be chosen by designer on basis of stress field evaluation in the flange
2. β° — To be chosen by designer on basis of optical viewing requirements
3. ℓ ≥ b for all t/D ratios and conical angles (α)
4. b ≥ displacement of window during the sustained pressure loading for specified period of time
5. $D > D_f$ for all t/D ratios and conical angles α

Figure A-2. Characteristics of DOL 5 flange and window assembly (the assembly recommended for long-term 10,000-psi pressure).

Finishes and Tolerances

The experimental data relating flange-seat surface roughness to crack initiation in the bearing surface of conical acrylic windows under long-term loading is inconclusive. Therefore, no definite recommendation that would be applicable to all t/D ratios and angles can be made for a particular surface finish at this time. It can be only stated that so long as the surface finish is in the range of 32 to 125 rms, the acrylic conical windows will perform satisfactorily. The surface finish of the flanges used in this study was 63 rms, it performed quite acceptably and can be considered a happy compromise between the more expensive 32-rms finish and the rough 125-rms finish.

Although exploratory experimental data indicate that an angle mismatch between the acrylic plug and the conical flange seat of 1 to 2 degrees magnitude does not noticeably affect the critical pressure of the window, the mismatch should be kept to a minimum to eliminate high-pressure sealing

problems. To minimize leaking, deviation of the conical flange cavity from the specified angle should be in the ±5-to-±15-minute range, easily attained with ordinary machine shop practice.

The effect of variation in the minor diameter of the conical cavity on the displacement and critical pressure of the conical acrylic windows varies with the type of window–flange system used. The effect of variation is most pronounced for the DOL 2 window/flange system and least pronounced for the DOL 5 system. Since DOL 5 system (Figure A-2) is the one recommended for windows under long-term hydrostatic loading, the diametral tolerance for minor diameter of conical flange cavity may be in the range ±0.001 to ±0.005 inch. These tolerances are readily achieved with ordinary machining processes.

SEALS

Requirements

One of the major problems encountered in the design of window systems for long-term loading is the design of seals. The difficulty in the design of seals for such a system stems from the fact that there are three separate operational requirements that the seals must satisfy.

1. The window system must be watertight at low pressures while the capsule, or habitat, is being towed to its location.
2. The window system must be watertight at the maximum operational pressure during the projected duration of the mission on the ocean bottom.
3. The window system must be watertight upon return of the capsule, or habitat, to the ocean surface, and during the subsequent towing to dock.

It is relatively easy to satisfy the first two requirements. Any ordinary gasket will seal the high-pressure face of the window against the window-retaining ring at low hydrostatic pressure, while the greased surface of the window acts as a seal itself under high external hydrostatic pressure. It is much more difficult to satisfy the third requirement because the window has experienced viscoelastic deformation during its long-term service under operational pressure of 10,000 psi. Upon return of the capsule to the ocean surface there is a tendency for the windows to leak; because viscoelastic displacement of the window has taken place, the gasket

between the window-retaining ring and the window is no longer compressed. There are many design approaches that will mitigate or completely eliminate the problem of window leakage upon return of the capsule or habitat to the ocean surface after its long-term submergence.

Seal Evaluation

From *the aspect of space* required to contain the window and its seal system, the compressed gasket, the elastomeric wiper ring of triangular cross section, and the axially compressed O-ring (Figure A-3) called for the least space. They required a conical flange cavity whose depth was only somewhat greater than the window's thickness. Thus it would appear that in hydrospace window applications in which the depth of the conical flange cavity in the pressure hull must be kept to a minimum because of limited hull thickness, such seal designs are attractive.

One shortcoming of the compressed gasket and the wiper seal designs is that for low-pressure sealing capability at the termination of the long-term pressure loading they both rely on the elastomeric properties of the gaskets that initially were axially compressed at least 0.1 D. If, due to the action of seawater, hydrostatic pressure, low temperature, and high initial compression, a permanent set of the elastomer occurs, it will lose its ability to force the window into contact with the flange cavity surface and thus not provide sealing at low pressures.

From the aspect of *sealing ability* after long-term pressure loading during which the elastomers in the seals acquire a considerable permanent set, the seal designs incorporating an elastomeric O-ring or the channel seal are the most desirable. The latter seals maintain contact with the flange cavity surface even with permanent set in the elastomeric seal as a result of the force exerted on the window by precompressed metallic springs. Of these two types of seals, the ones incorporating the elastomeric O-ring are more desirable because they utilize only off-the-shelf commercial elastomeric rings that are available in many formulations.

A major shortcoming of these sealing systems is the stress raiser effect introduced into the window bearing surface by the presence of grooves machined for the placement of seals. This stress raiser effect is most severe in the groove cut for the axial O-ring seal, particularly in windows with a 30-degree included angle. The stress raiser effect of the axial O-ring seal, however, has negligible influence on the critical pressure or life of the window if the groove is located not further than t/3 from the high-pressure face of the window (Figure A-1), since in that area the stresses generated by hydrostatic loading of a conical window are generally low.

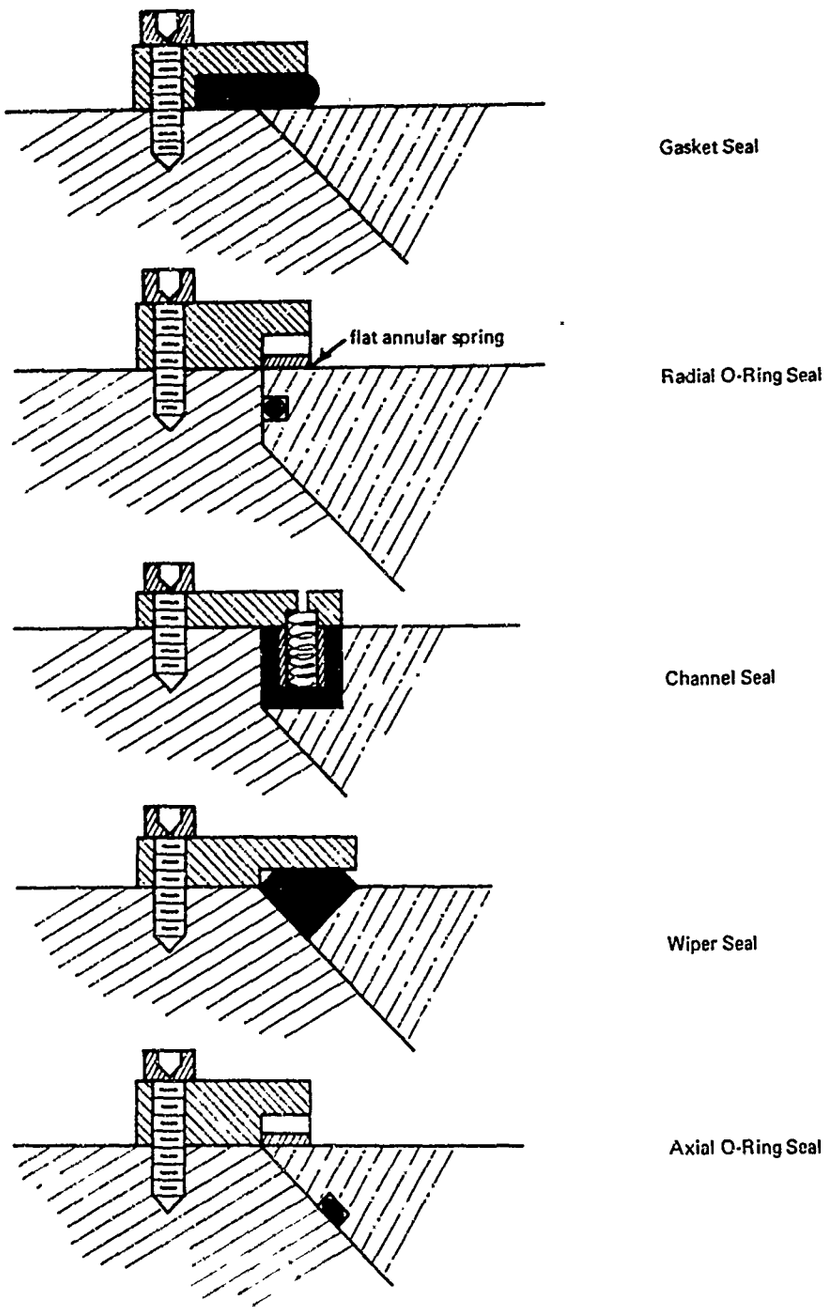

Figure A-3. Seals applicable to windows under long-term pressure loading.

In terms of *window displacement*, the radial O-ring seal is the most desirable one as the window is approximately 25% thicker than designs incorporating plain gasket, wiper type seal, or axial O-ring seals; at the same time the radial O-ring design does not have the serious stress raiser effect of the channel seal groove. Because of the added window thickness that the radial O-ring seal requires and the low stress raiser effect, it is considered to be the most conservative window seal system.

Seal Selection

In view of the considerations discussed in the section on seal design evaluation, it can be postulated that for long-term loading at a hydrostatic pressure of 10,000 psi only two seal designs are attractive. Where the window cavity in the flange is to have the *least axial length* possible and where the *economics* of window–seal system fabrication are important, the simple gasket seal design is preferable.

Design Guideline 3. For the *simple gasket seal*, the design guidelines for selecting the magnitude of elastic gasket precompression under the window retainer ring depend on the design guidelines used in the selection of window t/D ratios.

Selection of Window t/D	Corresponding Conical Cavity Dimensions	Corresponding Gasket Compressions[a] Under Retainer Ring(s) for Included Angles—				
		30°	60°	90°	120°	150°
Guideline 1	Guideline 2	0.08 D	0.06 D	0.06 D	0.05 D	0.05 D

[a] Minimum precompression.

If the gaskets are compressed (Figure A-4) as recommended, and no permanent set of the elastomeric gasket occurs, the seal should perform adequately prior to the long-term pressure loading, during the sustained long-term loading of 10,000 psi, and in low-pressure service encountered by the window when the ocean bottom habitat or capsule returns to the ocean's surface.

In applications in which (1) a deeper flange cavity can be tolerated, (2) off-the-shelf commercial O-rings are available for that particular window diameter, (3) some pressure cycling will be present, and (4) a more conservative window design is preferred, the radial O-ring seal is recommended.

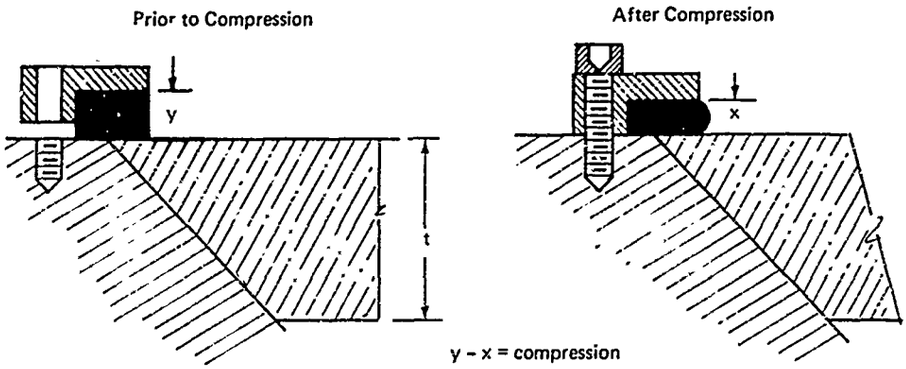

Figure A-4. Parameters for selection of gasket seal compression according to Design Guideline (Appendix A).

Design Guideline 4. For the *radial O-ring seal*, the design guidelines for selecting the magnitude of the cylindrical lip on the window and corresponding cylindrical recess in the flange depend on the design guidelines used in the selection of window t/D ratios.

Selection of Window t/D	Corresponding Conical Cavity Dimensions	Corresponding Dimensions[a] of Lower Cylindrical Windows Lip (k) for Included Angles—				
		30°	60°	90°	120°	150°
Guideline 1	Guideline 2	0.2 D	0.2 D	0.2 D	0.2 D	0.2 D

[a] Minimum thickness.

The foregoing description of dimensions (Figure A-5) recommended for the lower cylindrical window lip does no describe the overall thickness of the lip, but just its lower portion below the O-ring groove. In order to specify the window, however, one must also know the overall thickness of the lip. To arrive at that dimension K, one must add to k the width of the O-ring groove w and the upper cylindrical window lip n. Both of these dimensions do not depend on the magnitude of the external pressure to which the window will be subjected but on the size of the O-ring, which in many cases is chosen solely on the basis of the window diameter.

In general, the width of the groove should be > 0.15 inch for 1/8-inch O-rings associated with small windows and > 0.3 inch for 1/4-inch O-rings used in large windows. The upper cylindrical window lip should be at least equal in

thickness to the groove width, or may be even thicker to prevent its chipping during handling of windows at installation. The resulting window, because of its added thickness is quite conservative for service at 10,000 psi.

SUMMARY

To tie the many design guidelines together that are spelled out in Appendix A, two typical windows will be designed and dimensioned.

Case A

Requirements

Pressure:	10,000 psi
Type of loading:	Sustained, 1,000 hours
Type of service:	Optical observation of hydrospace
Cone angle:	90 degrees
Type of seal:	Radial O-ring
Minor diameter:	1 inch

Dimensioning

Optical service requires that Design Guideline 1 be used for window t/D selection (in this case t/D = 0.750), Design Guideline 2 for flange cavity D/D_f selection (in this case $D/D_f = 1.15$ and $\ell = 0.1\ D$), and Design Guideline 4 for radial O-ring seal and window lip thickness selection ($k = 0.2\ D$, $w = 0.15$, $n = 0.15$).[3] The configuration of the window and flange is shown in Figure A-6.

Case B

Requirements

Pressure:	10,000 psi
Type of loading:	Sustained, 1,000 hours
Type of service:	Optical observation of hydrospace
Cone angle:	90 degrees
Type of seal:	Gasket seal
Minor diameter:	1 inch

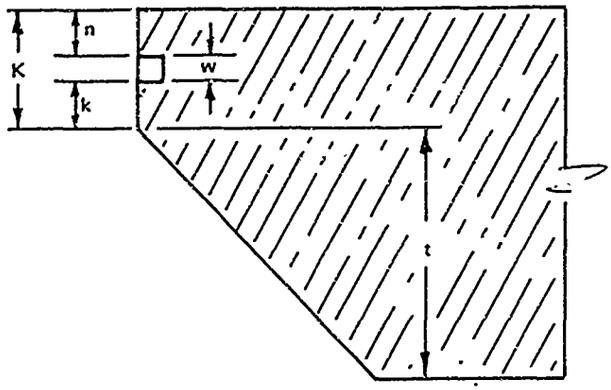

Figure A-5. Parameters for selection of window lip dimensions according to Design Guideline 4.

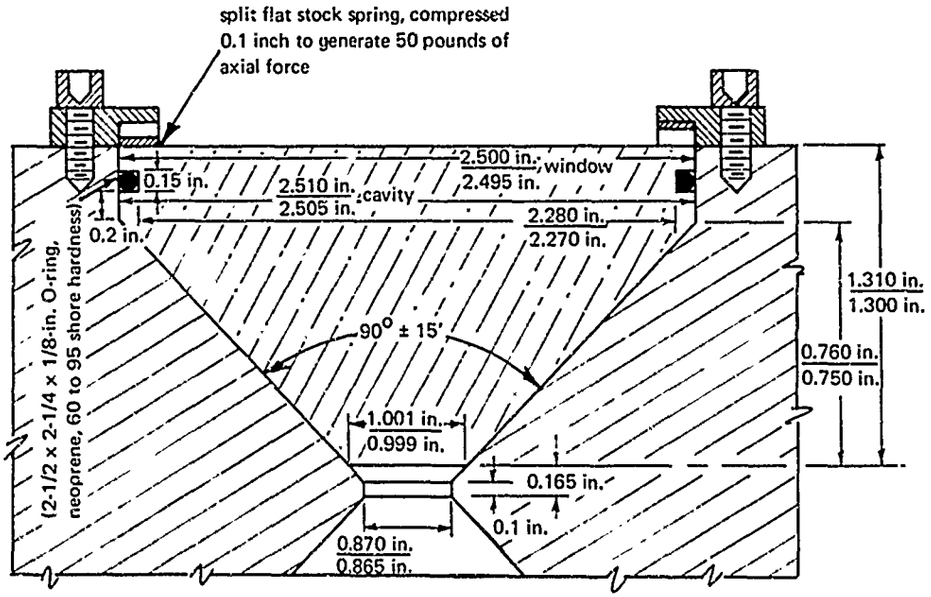

Figure A-6. Typical design of radial O-ring seal on a 90-degree window for 1,000 hours of service at sustained 10,000-psi pressure in 32°F-to-75°F temperature range.

Dimensioning

Optical observation service requires that Design Guideline 1 be used for window t/D selection (in this case t/D = 0.75), Design Guideline 3 for flange cavity D/D_f selection (in this case $D/D_f = 1.15$, $\ell = 0.1$ D), and Design Guideline 3 for gasket seal precompression specification (in this case 0.06 D). The configuration of the window is shown in Figure A-7.

Since all of the design guidelines discussed in Appendix A had as their objective a window that performs reliably and safely in 5,000-to-10,000-psi pressure range and 32°F-to-75°F temperature range, an approach to dimensioning was used that always assumed the windows would be used at the most severe loading condition. Thus it can be expected that when an optical service window sealed with a radial O-ring is operated at 6,000 psi and 34°F temperature for less than the whole span of its rated life, the displacements of the window will be much less than provided for by the design guidelines. On the other hand if a gasket-sealed optical service window is operated at 10,000 psi and 75°F temperature for the whole span of its sustained loading rating, the displacements will probably be equal to those foreseen by the design guidelines, but not larger. If the windows may during their life be subjected to (1) pressures above 10,000 psi (like dynamic overpressures), (2) temperatures above 75°F (as windows in deep ocean simulation facilities on land), (3) cyclic loading to 10,000 psi, or (4) if optical requirements are especially stringent, then window thicknesses for 100,000-hour sustained service must be chosen even though the length of actual sustained loading may be on the order of only several hours.

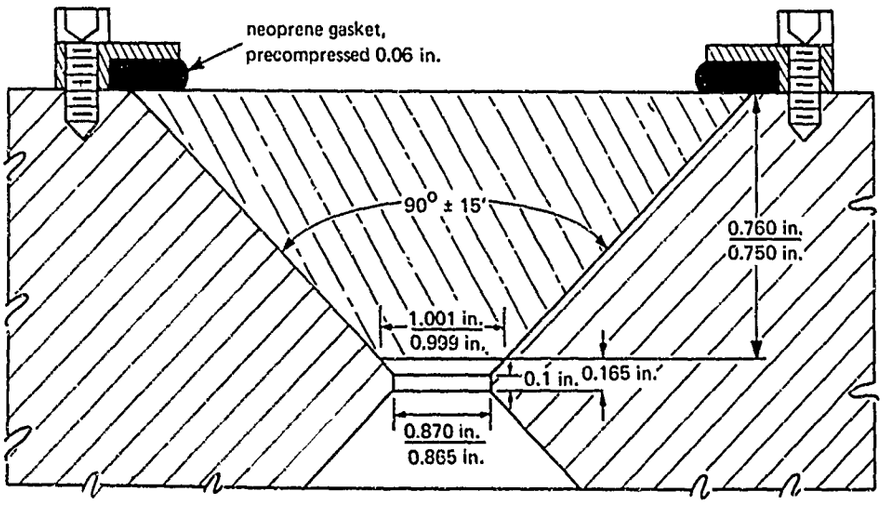

Figure A-7. Typical design of gasket seal on a 90-degree window for 1,000 hours of service at sustained 10,000-psi pressure in 32°F-to-75°F temperature range.

Appendix B

EFFECTS OF SUSTAINED PRESSURE LOADING ON CONICAL WINDOWS

INTRODUCTION

The windows subjected to sustained loading under 10,000-psi hydrostatic pressure for time periods of 500 and 1,000 hours experienced permanent deformation, cracking, or even catastrophic failure. The extent of cracking, or duration of sustained loading prior to catastrophic failure depended on the included angle and the t/D ratio of the 1-inch-diameter windows tested, so long as the temperature of the water was held in the 65°F-to-75°F range for all the tests. At what exact time during the sustained pressure loading a certain crack or cold-flow crater was formed is unknown, as no techniques were utilized that would permit intimate observation of the interior of the window body during the hydrostatic loading.

Since all observations of damage to the tested windows were made only after the testing was completed and the windows were removed from their flanges, it cannot be stated with absolute certainty which damage to the window occurred during the pressurization phase from 0 to 10,000 psi, sustained pressure loading phase at 10,000 psi, or unloading phase from 10,000 psi to 0 psi. Some of the changes in the window (e.g. cold-flow cratering on the high-pressure face and the cold-flow extrusion on the low-pressure face) must have taken place during the hydrostatic load application. These deformations are clearly the responses of the acrylic window to hydrostatic force acting on its high-pressure face.

The time of origin of the cracks in the window is not so obvious. Some of the cracks, such as those on the low-pressure face, definitely appear during the loading of the window; they are caused by the bulging of the low-pressure face, which induces local tensile stresses in the face. Also, during some of the tests, the low-pressure faces were observed and extensive cracking and fracturing of the face was noted prior to failure. Whether the cracks at right angles to the conical seating surface occurred during the loading, or during unloading cannot be definitely ascertained. However, there is good evidence that most cracks did originate during the pressurization and sustained pressure-loading phases.

The case for this supposition rests on two observed phenomena. One is the penetration of lubricant into some very deep cracks. The lubricant, could not penetrate into the interior of the window through the

hairline cracks if it was not under very high hydrostatic pressure. But not all of the cracks were penetrated by grease, indicating either that some were formed during the depressurization phase, or that they were formed during pressurization as shear cracks, which are kept from opening into fissures by the compression forces acting at right angles to the crack surfaces. Since in explosively failed windows one can find the failure surface to be an outgrowth of just such cracks, it can be stated with a fair degree of confidence that most of the shear type cracks at right angles to the conical seating surface form when the window is being pressurized or is under sustained load and not during depressurization. Because description of cracks or crazing in individual windows would be quite lengthy, and at best only a poor substitute for visual information, it has been omitted in this report. Instead, photographs of all the tested windows have been included that will permit the designer to judge for himself the extent of damage, if any, that the windows have incurred during the long-term sustained loading of 1,000 hours at 10,000 psi hydrostatic loading in ambient room temperature environment (Figures B-1 through B-5).

(a) Windows with t/D ratios of 0.625, 0.750, 0.875, 1.000, and 1.250.

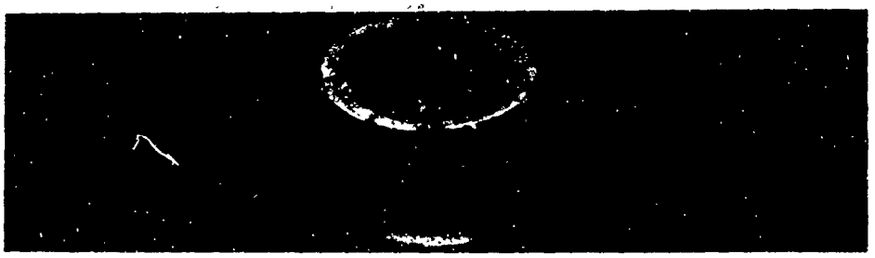

(b) Cold-flow crater on high-pressure face of window with t/D = 0.625.

Figure B-1. Effect of 1,000-hour sustained loading under 10,000-psi pressure on 30-degree conical acrylic plastic windows.

(a) Windows with t/D ratios of 0.500, 0.625, 0.750, 0.875, 1.000, and 1.250.

(b) Cold-flow crater on high-pressure face of window with t/D = 0.500.

Figure B-2. Effect of 1,000-hour sustained loading under 10,000-psi pressure on 60-degree conical acrylic plastic windows.

(a) Windows with t/D ratios of 0.500, 0.625, 0.750, 0.875, 1.000, and 1.250.

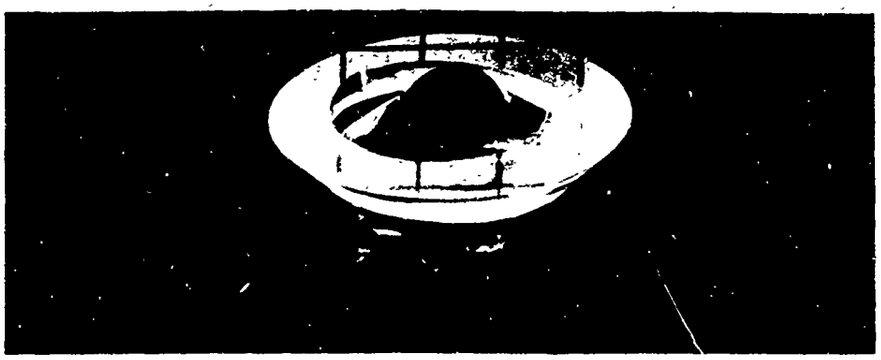

(b) Cold-flow crater on high-pressure face of window with t/D = 0.500.

Figure B-3. Effect of 1,000-hour sustained loading under 10,000-psi pressure on 90-degree conical acrylic plastic windows.

(a) Windows with t/D ratios of 0.500, 0.625, 0.750, 0.875, 1.000, and 1.250.

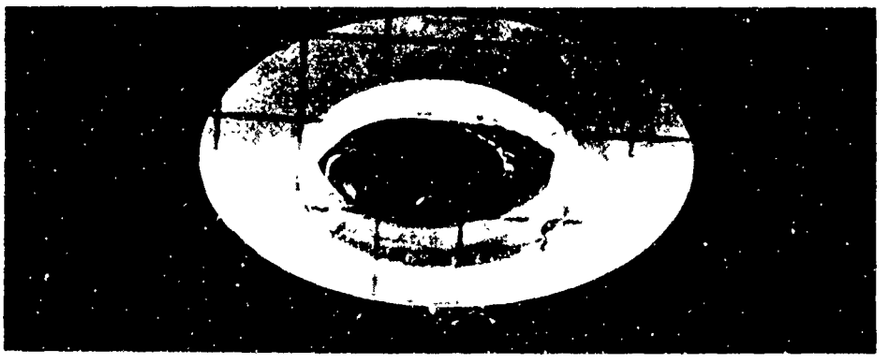

(b) Cold-flow crater on high-pressure face of window with t/D = 0.500.

Figure B-4. Effect of 1,000-hour sustained loading under 10,000-psi pressure on 120-degree conical acrylic plastic windows.

(a) Windows with t/D ratios of 0.500, 0.625, 0.750, 0.875, 1.000, and 1.250.

(b) Cold-flow crater on high-pressure face of window with t/D = 0.500.

Figure B-5. Effect of 1,000-hour sustained loading under 10,000-psi pressure on 150-degree conical acrylic plastic windows.

Appendix C

DISPLACEMENTS OF CONICAL ACRYLIC WINDOWS UNDER SUSTAINED HYDROSTATIC LOADING AT 10,000 PSI

Each of the conical acrylic windows subjected to sustained 10,000-psi hydrostatic loading experienced axial displacement through the flange opening. There were three distinct phases in the axial displacement of each window. The **first phase** took place when the pressure was raised at a 650-psi/min rate from 0 to 10,000 psi. The **second phase** was relatively rapid axial displacement of the window through the flange immediately after the 10,000-psi sustained pressure loading was reached. The second phase lasted for approximately 12 to 24 hours. The **third phase** of axial displacement was the relatively slow axial displacement of the window during the remaining duration of sustained pressure loading at 10,000 psi. To emphasize and delineate the three distinct phases of axial displacement, two different scales were used for plotting the displacements. Log-log scales with 0.001-inch displacement and 1-minute time units were selected to show the rapid rate of displacement of the windows during phases 1 and 2. Linear scales with 0.01-inch displacement and 1-day time units were chosen to show the slow rate of displacement during phase 3. To permit rapid visual comparison of the two different displacement phases, they are grouped together in Figures C-1 through C-6 for each different window configuration.

When one observes the graphs depicting phases 1, 2, and 3 one immediately notes that the relationship between time and magnitude of axial displacement is not shown graphically by a narrow line but by a wide band whose width and shape varies from one figure to another. There are several reasons for this.

1. Each curve represents the range of displacements shown by a group of five window specimens which were not of identical dimensions, but varied by the magnitude of dimensional machining tolerances.

2. All of the five windows comprising a single t/D ratio group for a given angle were not tested in the same flange, but in several flanges that differed from each other by the magnitude of dimensional machining tolerances and slight differences in machining finish.

3. All five windows in a group were not tested at an identical temperature. The average temperature varied several degrees from one long-term test to another.

4. All of the five windows were not machined from the same piece of material, or for that matter at the same material removal rate.

There are several general observations that can be made about the scatter of recorded displacement data. **First**, the width of the plotted displacement range appears to be in a large measure a function of absolute displacement magnitude; (that is, at small displacements the range is narrow, while for large displacements the range is large). **Second**, displacements of windows that are accompanied by extensive cracking and fracturing of the acrylic material (t/D = 0.500 for 60, 90, 120, and 150 degrees) vary more from one specimen in the same group to another than the displacements of windows not accompanied by extensive cracking. This phenomenon in all probability is caused by the randomness of crack initiation and propagation, as compared to the nonrandomness of typical stress–strain behavior of material before cracking.

Since in some of the t/D ratio groups all of the windows failed prior to the termination of the 1,000-hour tests, no graphs exist depicting phase 3 of window displacement. In other groups of windows only some of the windows failed prior to 1,000 hours at sustained 10,000-psi pressure loading. For those groups of windows, only the lower boundary of the phase 3 displacement range has been shown since the upper boundary is undefined. (See, for example, 30-degree windows with t/D = 0.625.)

When the data contained in Figures C-1 through C-6 are used for design of operational windows, the upper boundary of displacement ranges should be utilized. It represents a conservative approach to sizing of window flange cavities for containment of windows during their displacement under sustained hydrostatic pressure of 7,500 to 10,000 psi. For design of windows that will be used at a sustained pressure in 5,000-to-7,500-psi range the lower boundary of the displacement range should be utilized as otherwise the design of flange cavity becomes too conservative.

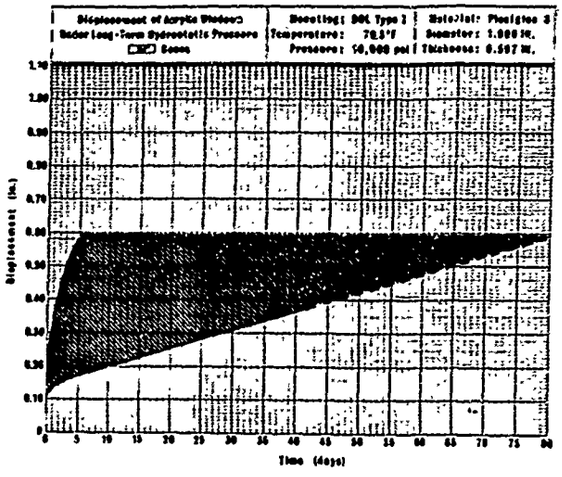

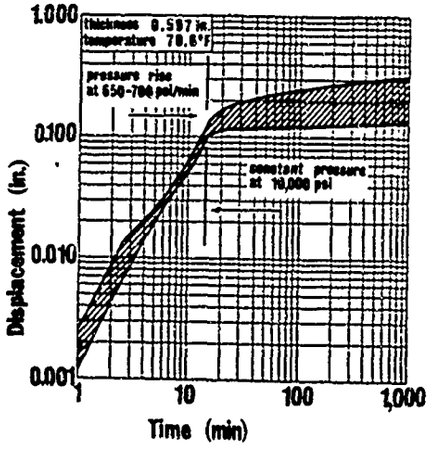

Figure C-1a. Displacement of conical acrylic plastic windows under 10,000-psi sustained pressure loading; 30-degree included angle with t/D ratio = 0.597.

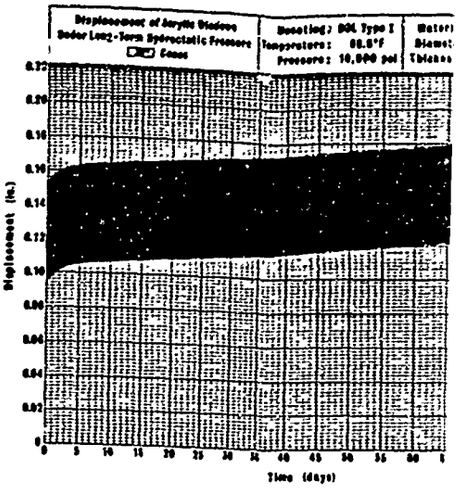

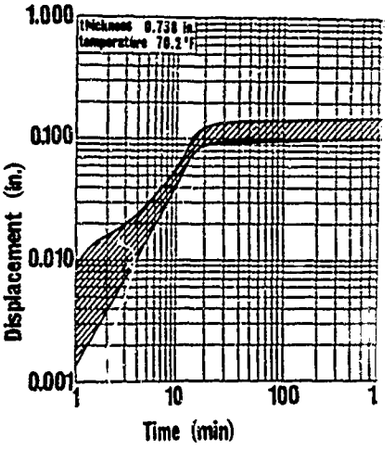

Figure C-1b. Displacement of conical acrylic plastic windo 10,000-psi sustained pressure loading; 30-degr angle with t/D ratio = 0.738.

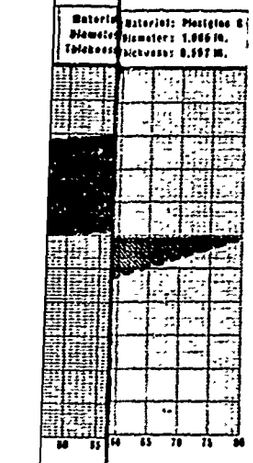

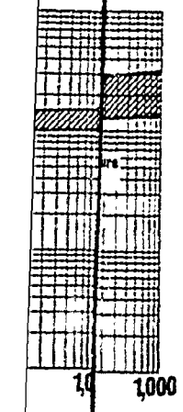

windows under
30-degree included

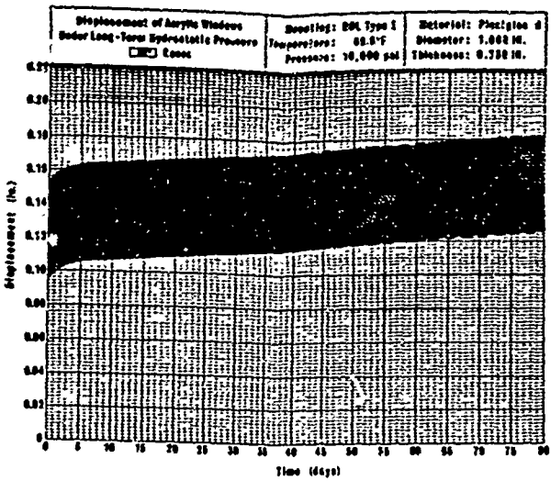

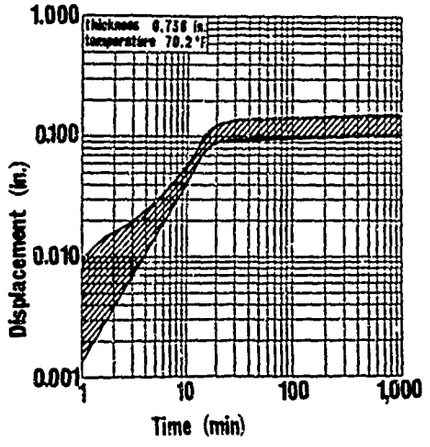

Figure C-1b. Displacement of conical acrylic plastic windows under 10,000-psi sustained pressure loading; 30-degree included angle with t/D ratio = 0.738.

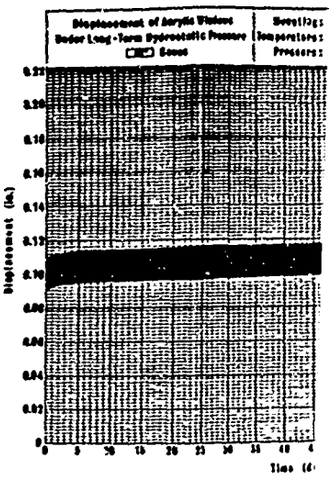

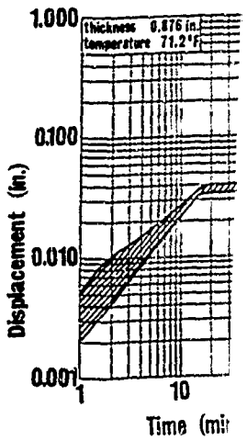

Figure C-1c. Displacement of conic
10,000-psi sustained p
angle with t/D ratio =

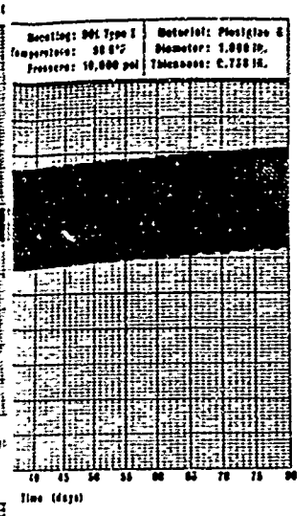

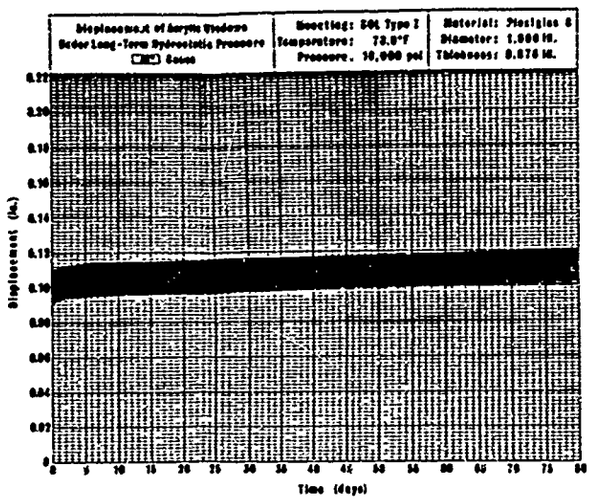

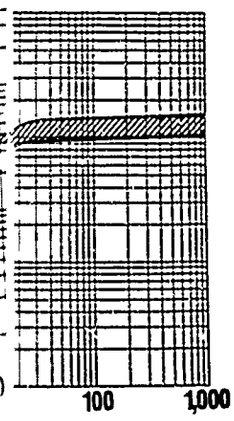

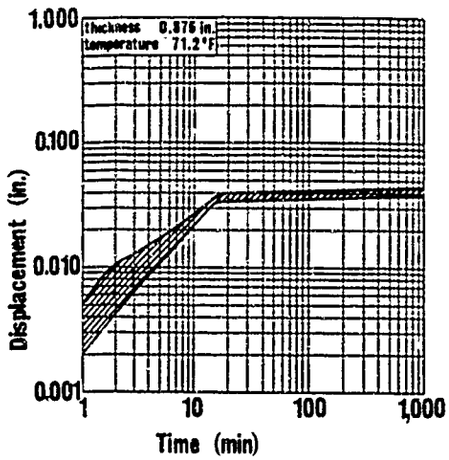

al acrylic plastic windows under
ressure loading; 30-degree included
0.738.

Figure C-1c. Displacement of conical acrylic plastic windows under 10,000-psi sustained pressure loading; 30-degree included angle with t/D ratio = 0.876.

Continued

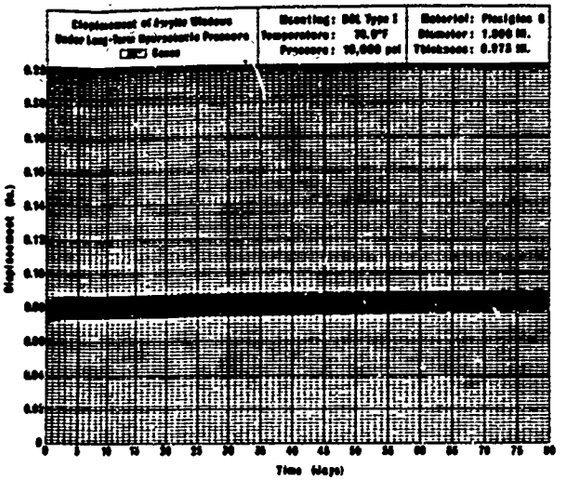

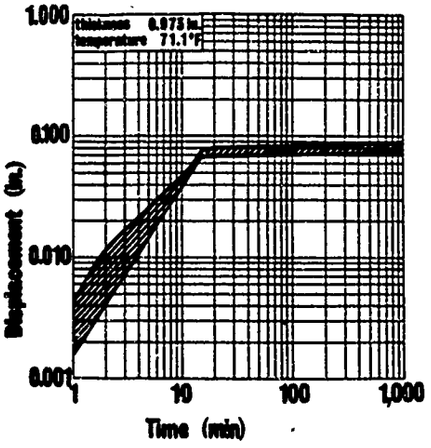

Figure C-1d. Displacement of conical acrylic plastic windows under 10,000-psi sustained pressure loading; 30-degree included angle with t/D ratio = 0.973.

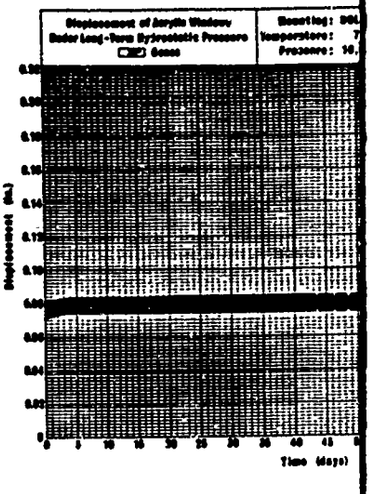

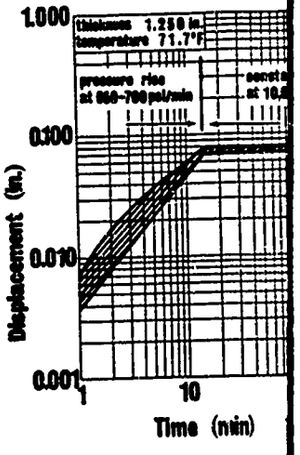

Figure C-1e. Displacement of conical acrylic
10,000-psi sustained pressure lo
angle with t/D ratio = 1.250.

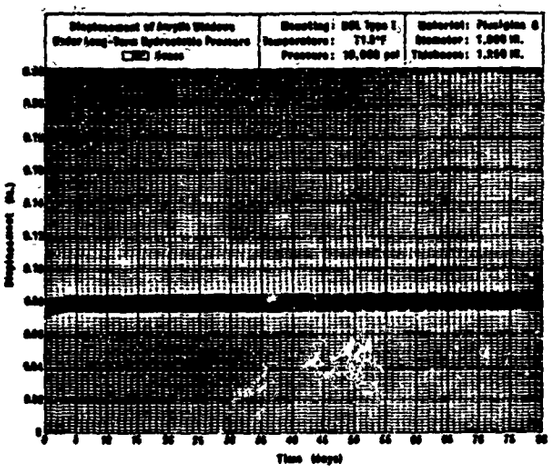

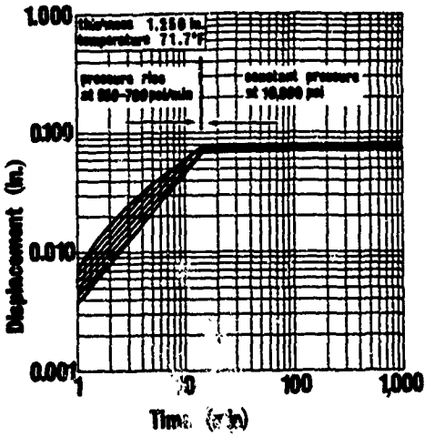

Figure C-1e. Displacement of conical acrylic plastic windows under 10,000-psi sustained pressure loading; 30-degree included angle with t/D ratio = 1.250.

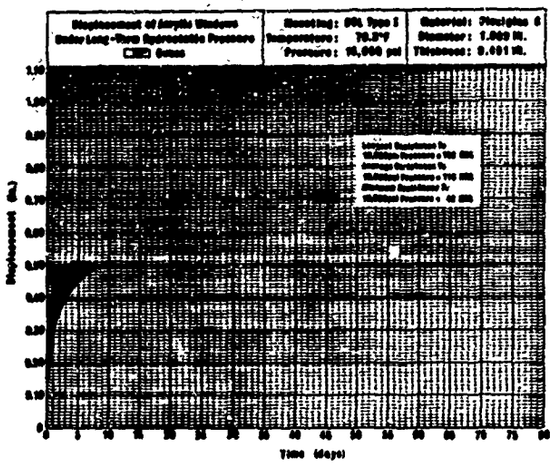

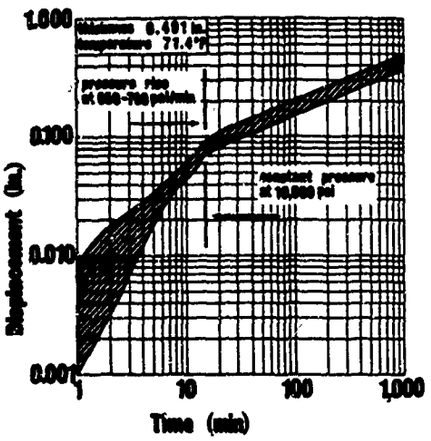

Figure C-2a. Displacement of conical acrylic plastic windows under 10,000-psi sustained pressure loading; 60-degree included angle with t/D ratio = 0.491.

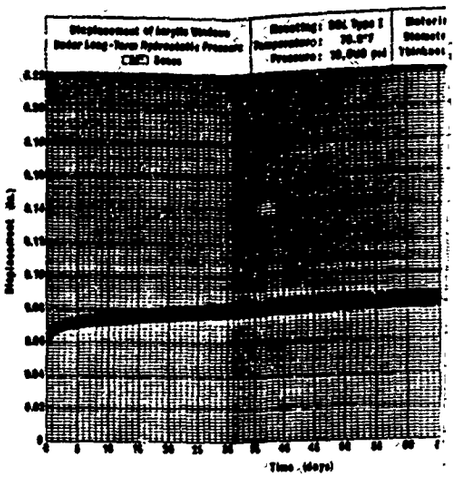

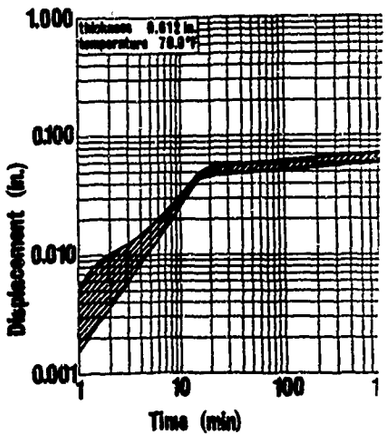

Figure C-2b. Displacement of conical acrylic plastic win 10,000-psi sustained pressure loading; 60-d angle with t/D ratio = 0.612.

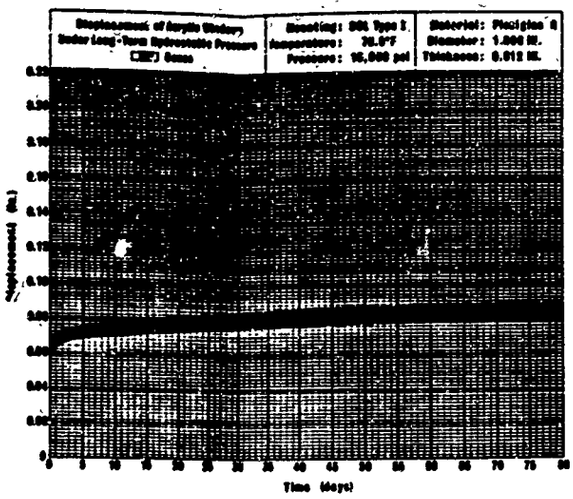

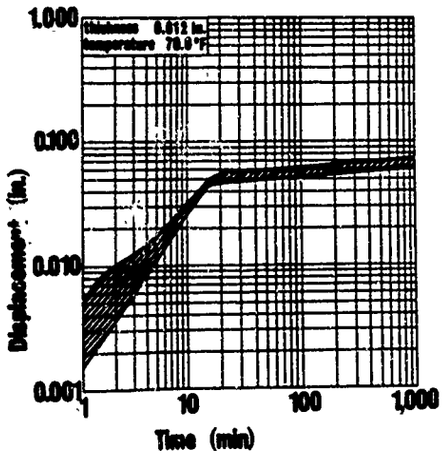

Figure C-2b. Displacement of conical acrylic plastic windows under 10,000-psi sustained pressure loading; 60-degree included angle with t/D ratio = 0.612.

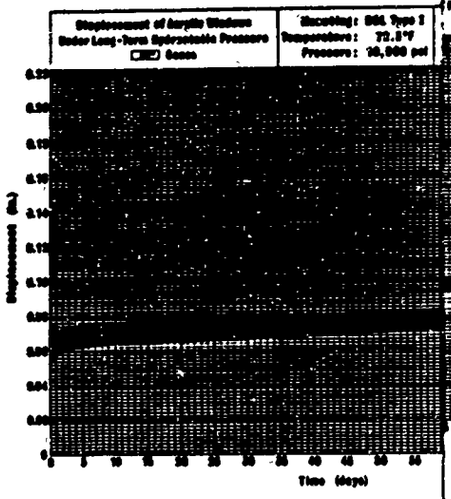

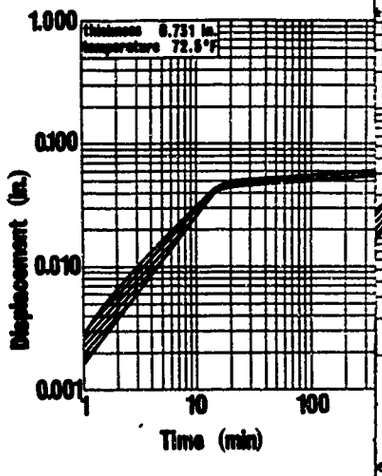

Figure C-2c. Displacement of conical acrylic plast 10,000-psi sustained pressure loading angle with t/D ratio = 0.731.

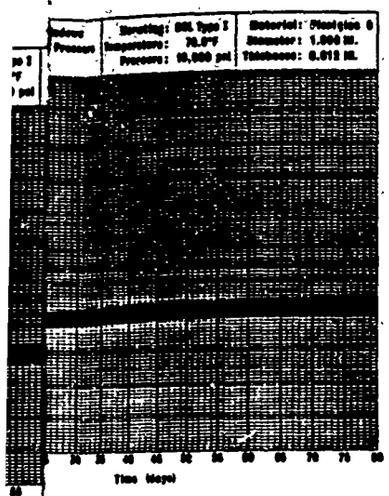

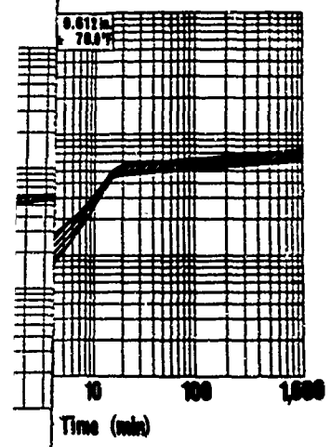

ent of conical acrylic plastic windows under
sustained pressure loading; 60-degree included
t/D ratio = 0.612.

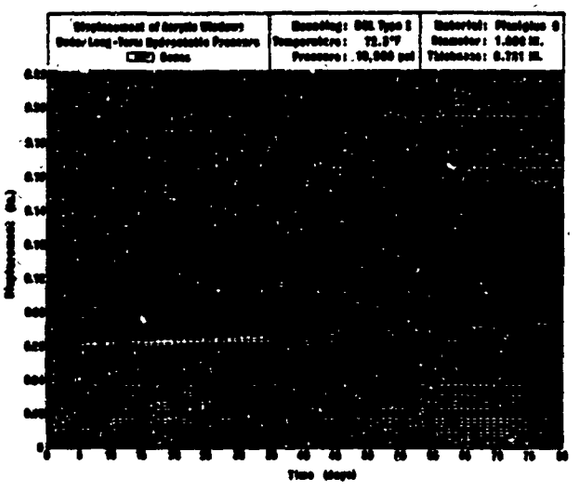

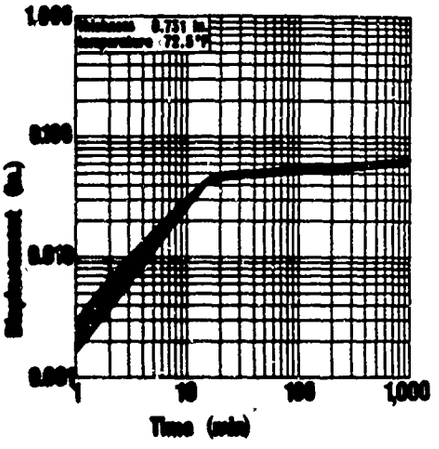

Figure C-2c. Displacement of conical acrylic plastic windows under 10,000-psi sustained pressure loading; 60-degree included angle with t/D ratio = 0.731.

Continued

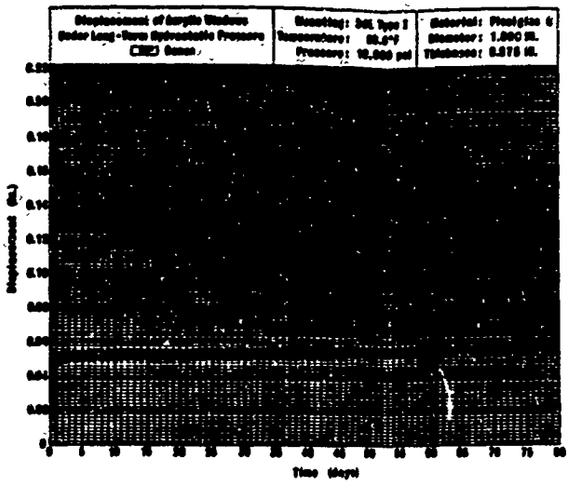

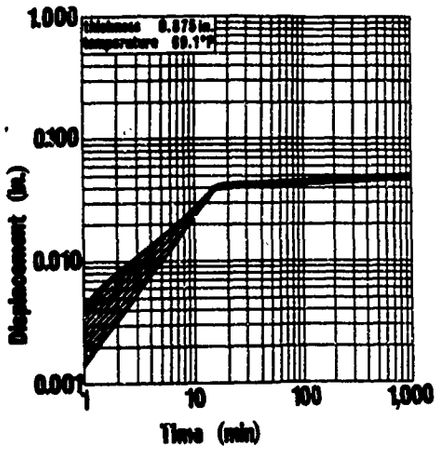

Figure C-2d. Displacement of conical acrylic plastic windows under 10,000-psi sustained pressure loading; 60-degree included angle with t/D ratio = 0.875.

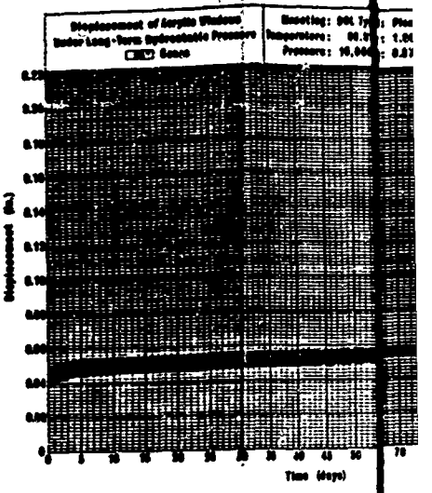

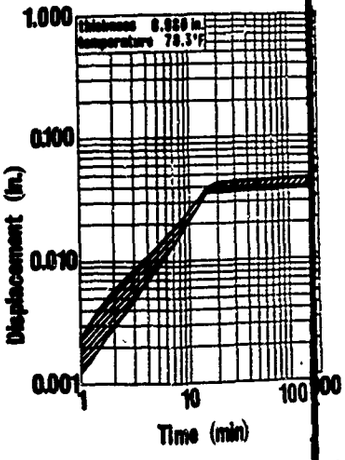

Figure C-2e. Displacement of conical acrylic plas nder 10,000-psi sustained pressure loadi nclu angle with t/D ratio = 0.980.

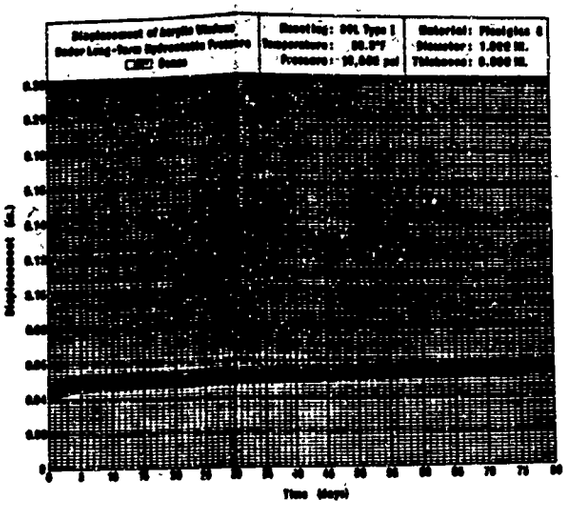

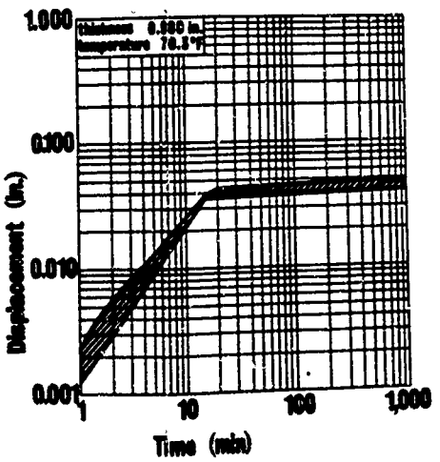

Figure C-2e. Displacement of conical acrylic plastic windows under 10,000-psi sustained pressure loading; 60-degree included angle with t/D ratio = 0.990.

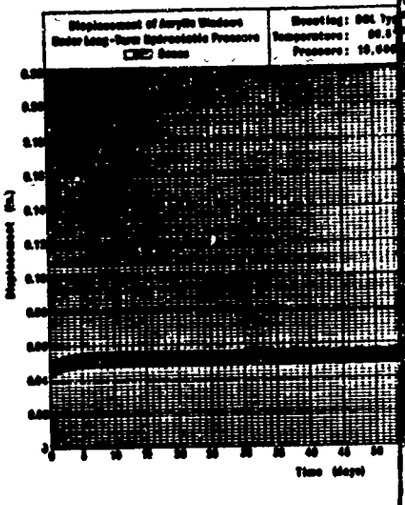

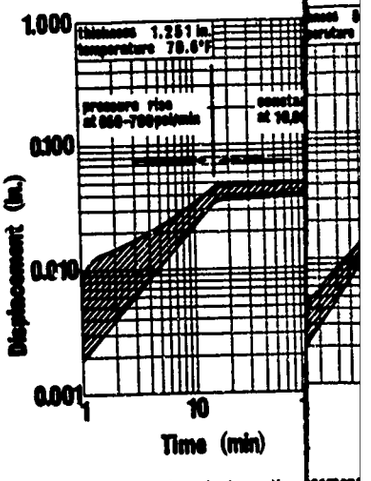

Figure C-2f. Displacement of conical acrylic p
10,000-psi sustained pressure loa
angle with t/D ratio = 1.251.

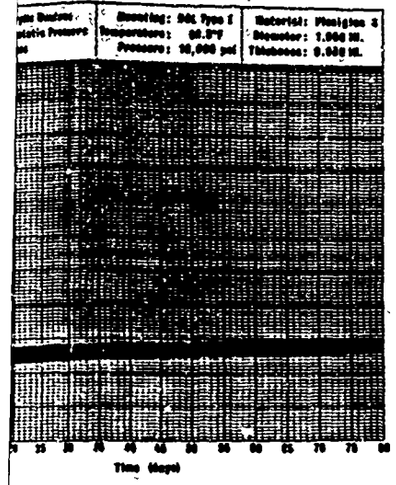

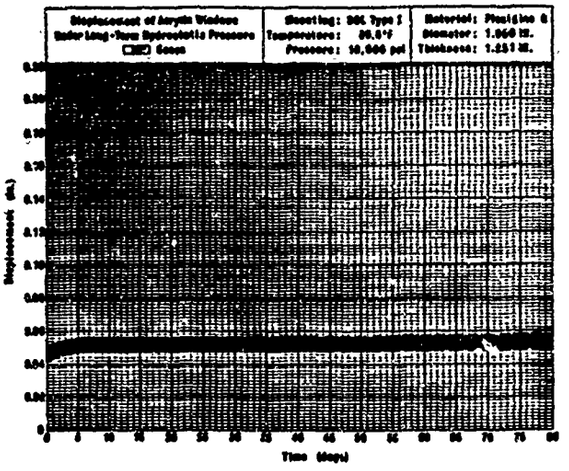

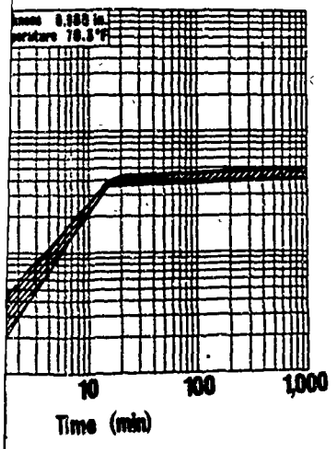

cement of conical acrylic plastic windows under
0-psi sustained pressure loading; 60-degree included
with t/D ratio = 0.980.

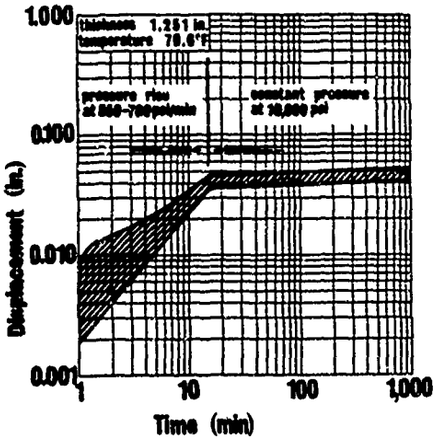

Figure C-2f. Displacement of conical acrylic plastic windows under 10,000-psi sustained pressure loading; 60-degree included angle with t/D ratio = 1.251.

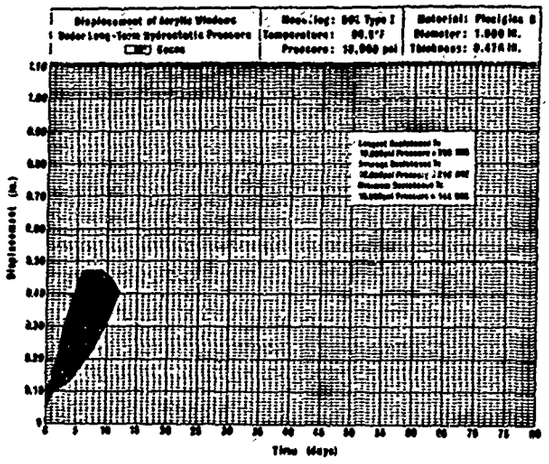

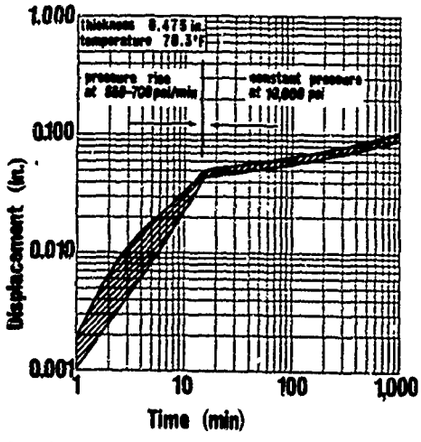

Figure C-3a. Displacement of conical acrylic plastic windows under 10,000-psi sustained pressure loading; 90-degree included angle with t/D ratio = 0.476.

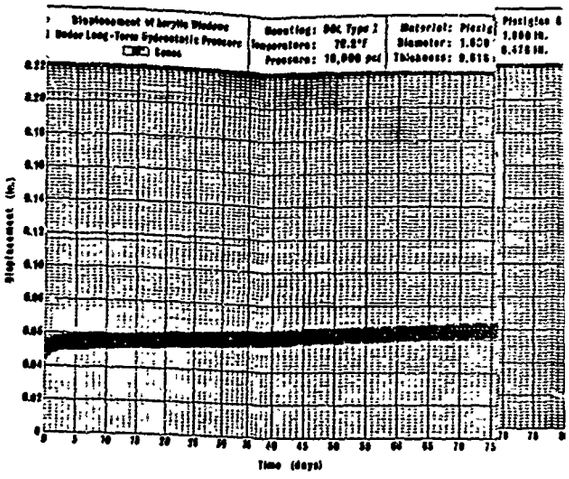

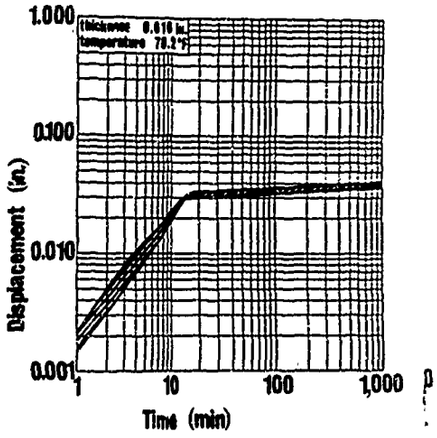

Figure C-3b. Displacement of conical acrylic plastic windows under 10,000-psi sustained pressure loading; 90-degree included angle with t/D ratio = 0.616.

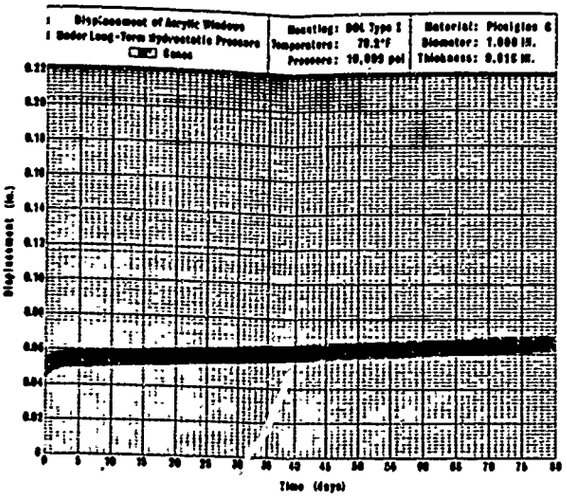

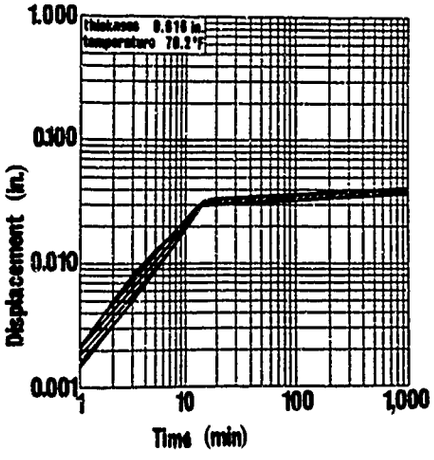

Figure C-3b. Displacement of conical acrylic plastic windows under 10,000-psi sustained pressure loading; 90-degree included angle with t/D ratio = 0.616.

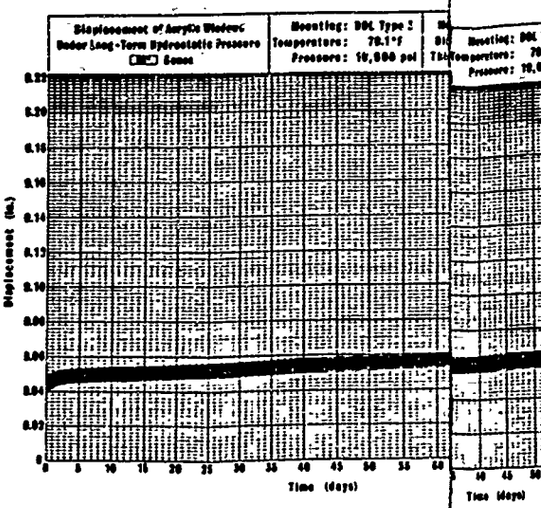

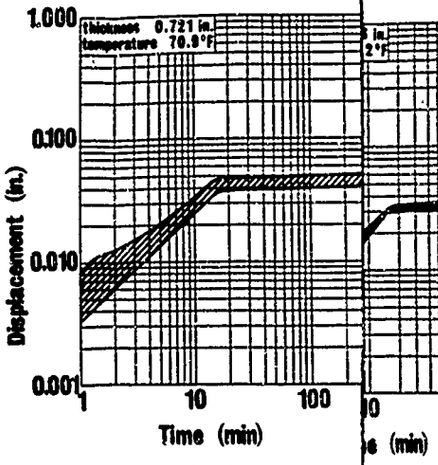

Figure C-3c. Displacement of conical acrylic plasti
10,000-psi sustained pressure loading;
angle with t/D ratio = 0.721.

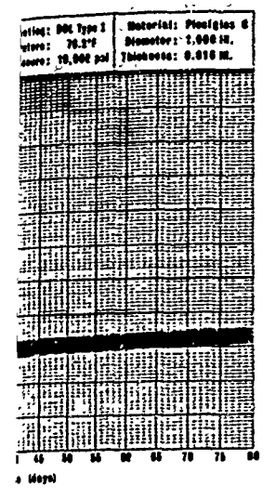

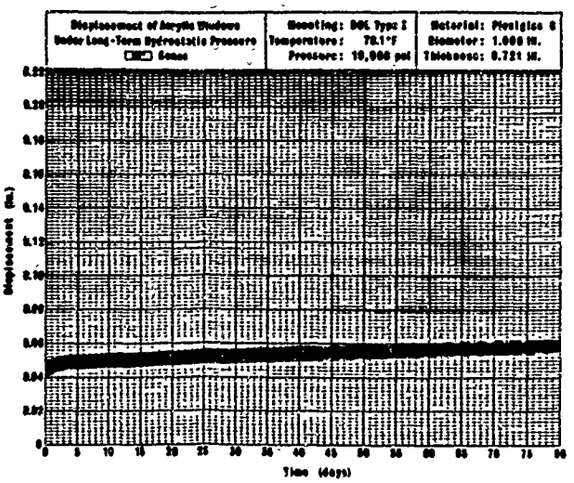

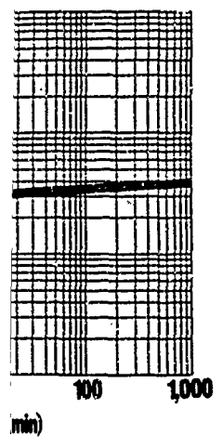

ical acrylic plastic windows under
pressure loading; 90-degree included
= 0.616.

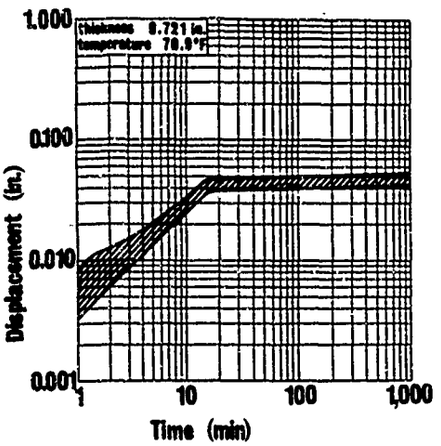

Figure C-3c. Displacement of conical acrylic plastic windows under 10,000-psi sustained pressure loading; 90-degree included angle with t/D ratio = 0.721.

Continued

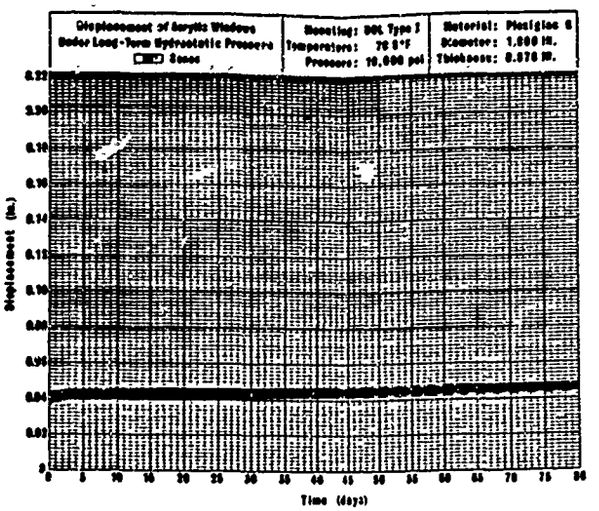

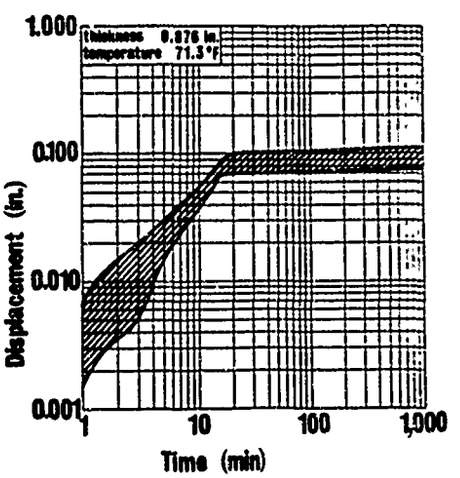

Figure C-3d. Displacement of conical acrylic plastic windows under 10,000-psi sustained pressure loading; 90-degree included angle with t/D ratio = 0.876.

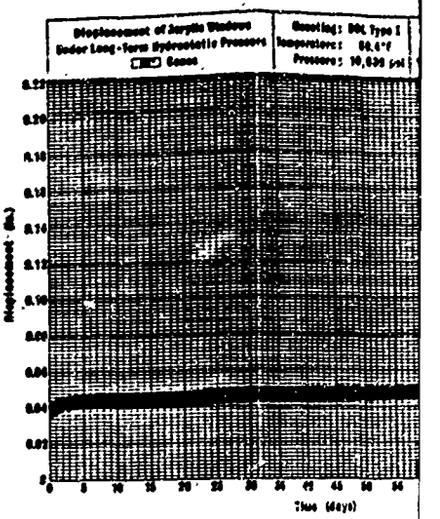

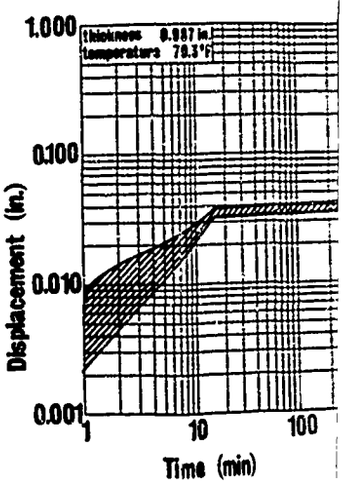

Figure C-3e. Displacement of conical acrylic plastic
10,000-psi sustained pressure loading;
angle with t/D ratio = 0.987.

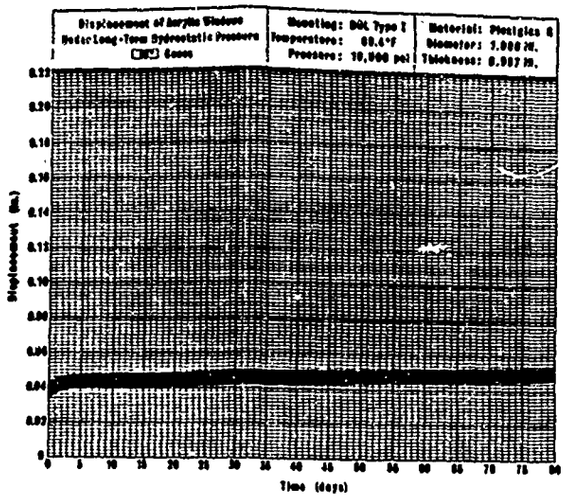

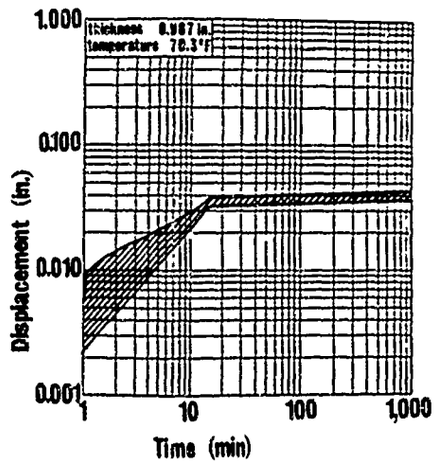

Figure C-3e. Displacement of conical acrylic plastic windows under 10,000-psi sustained pressure loading; 90-degree included angle with t/D ratio = 0.987.

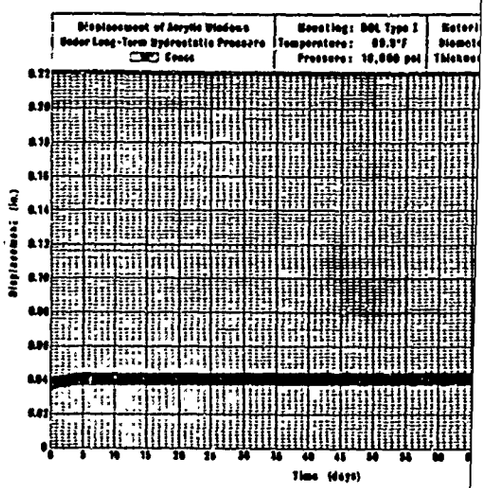

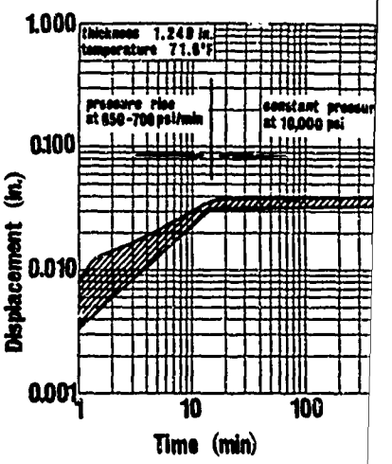

Figure C-3f. Displacement of conical acrylic plastic windo 10,000-psi sustained pressure loading; 90-de angle with t/D ratio = 1.249.

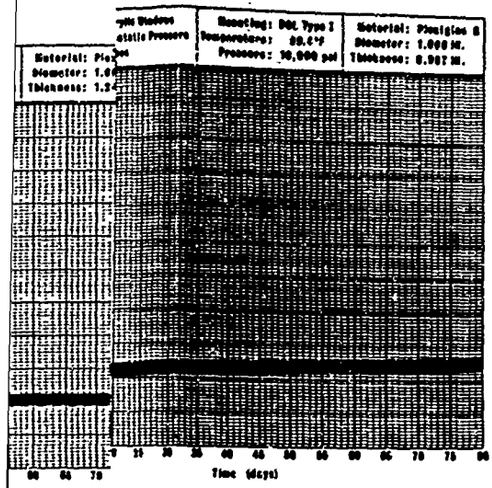

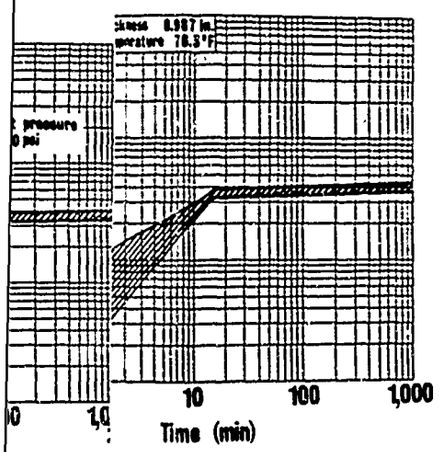

cement of conical acrylic plastic windows under
ic windows un-psi sustained pressure loading; 90-degree included
; 90-degree in with t/D ratio = 0.987.

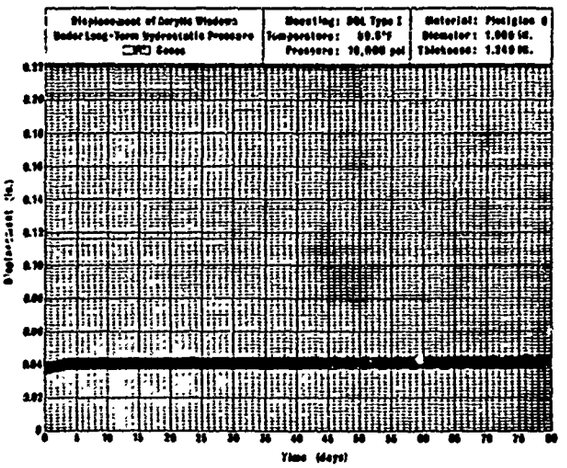

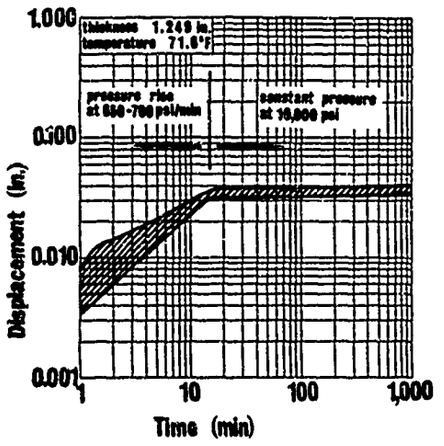

Figure C-3f. Displacement of conical acrylic plastic windows under 10,000-psi sustained pressure loading; 90-degree included angle with t/D ratio = 1.249.

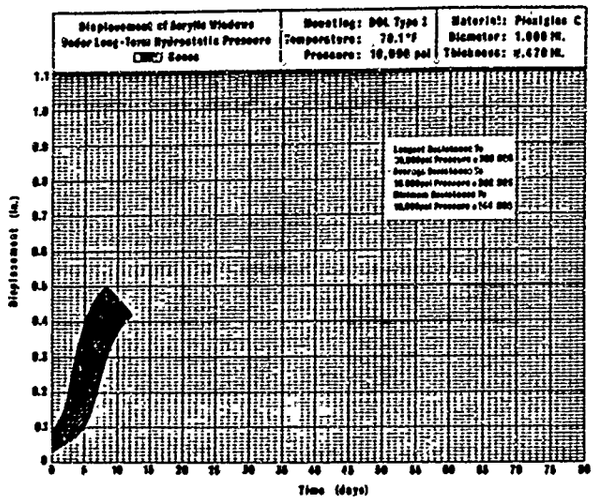

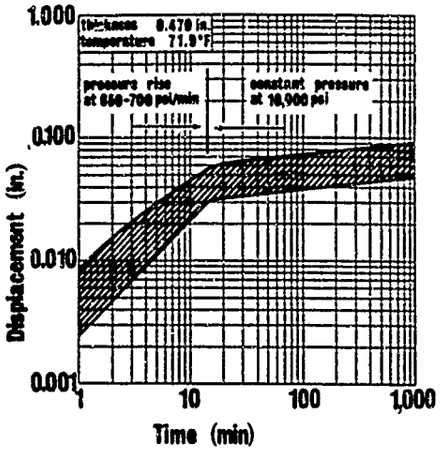

Figure C-4a. Displacement of conical acrylic plastic windows under 10,000-psi sustained pressure loading; 120-degree included angle with t/D ratio = 0.470.

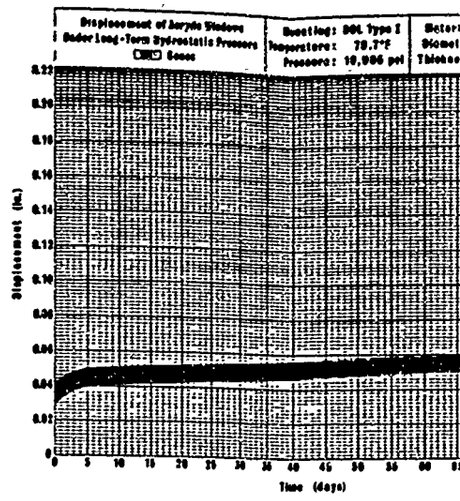

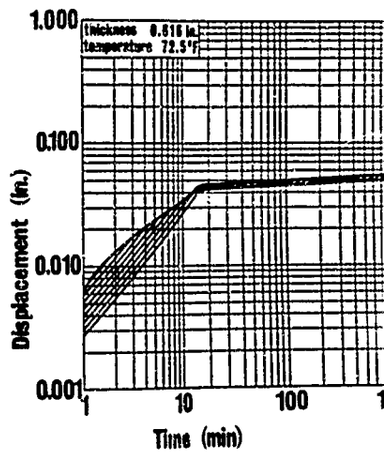

Figure C-4b. Displacement of conical acrylic plastic windows u 10,000-psi sustained pressure loading; 120-degree angle with t/D ratio = 0.616.

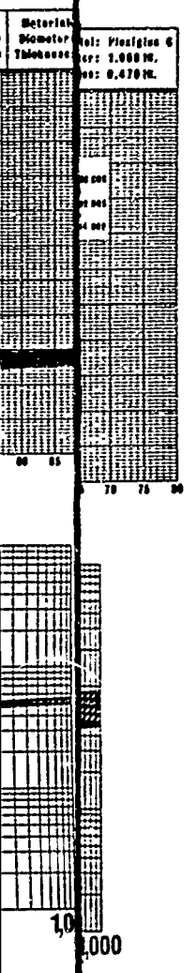

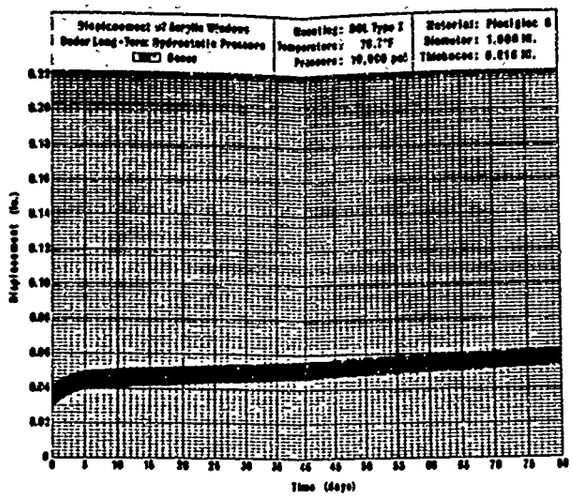

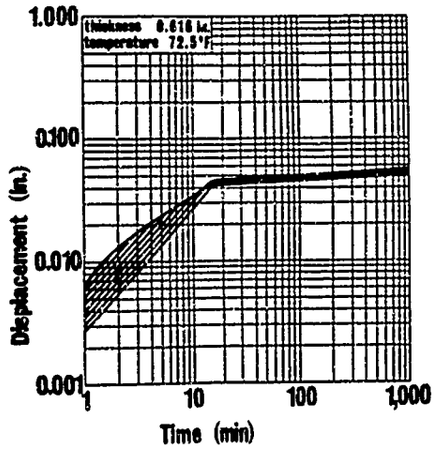

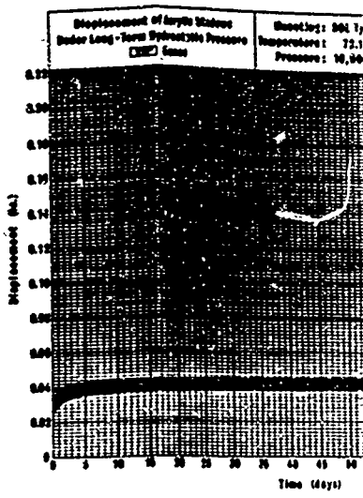

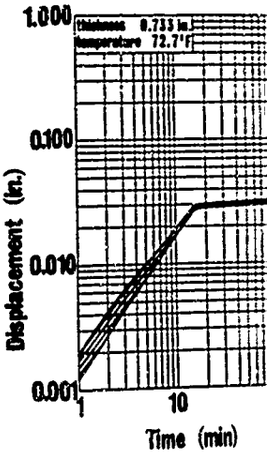

ndows und
-degree in
s under
ee included

Figure C-4b. Displacement of conical acrylic plastic windows under 10,000-psi sustained pressure loading; 120-degree included angle with t/D ratio = 0.616.

Figure C-4c. Displacement of conical acrylic
10,000-psi sustained pressure lo
angle with t/D ratio = 0.733.

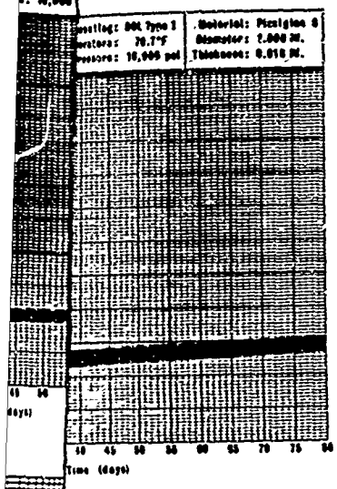

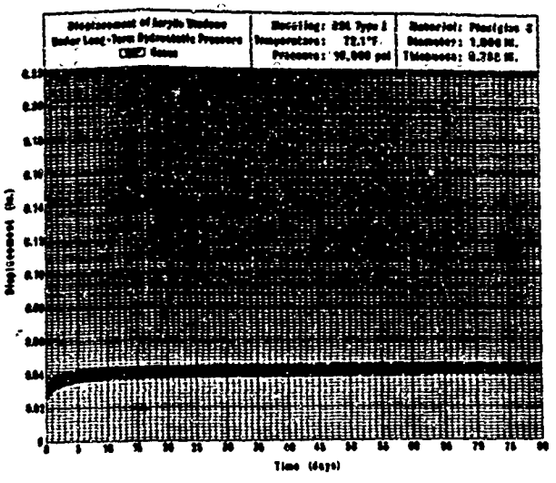

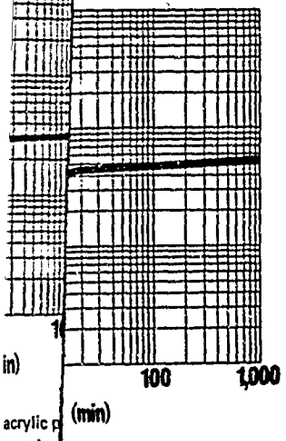

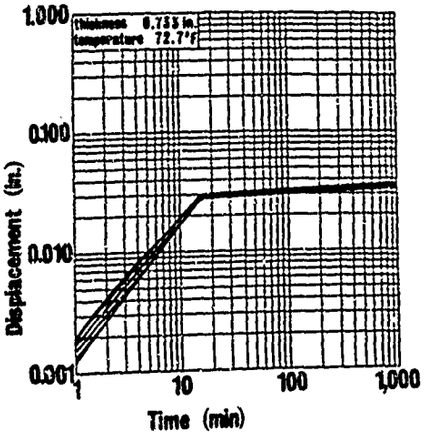

acrylic plastic windows under
ssure loading; 120-degree included
.616.

Figure C-4c. Displacement of conical acrylic plastic windows under 10,000-psi sustained pressure loading; 120-degree included angle with t/D ratio = 0.733.

Continued

53

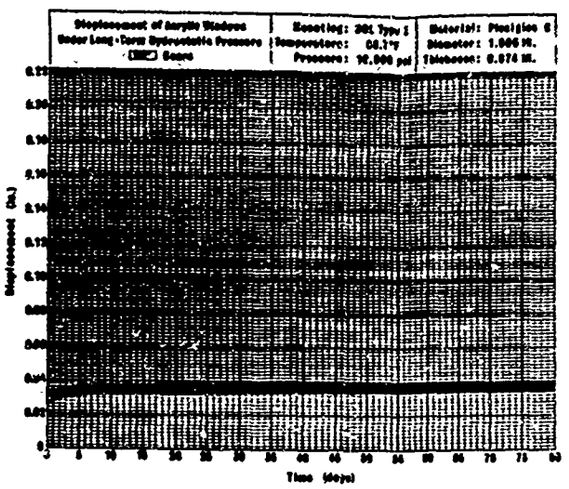

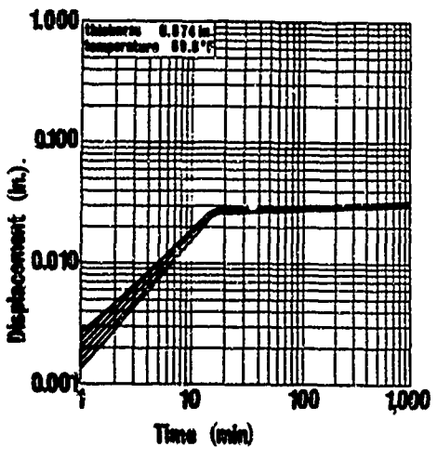

Figure C-4d. Displacement of conical acrylic plastic windows under 10,000-psi sustained pressure loading; 120-degree included angle with t/D ratio = 0.874.

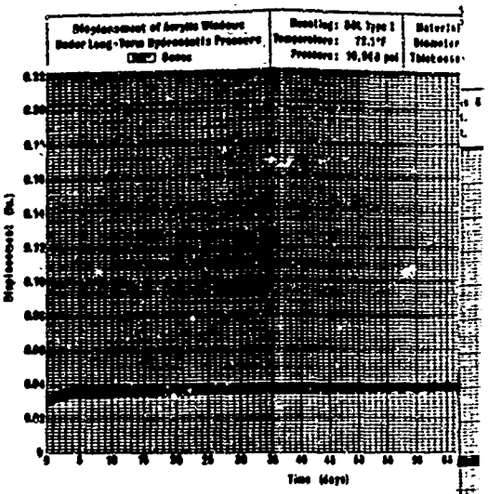

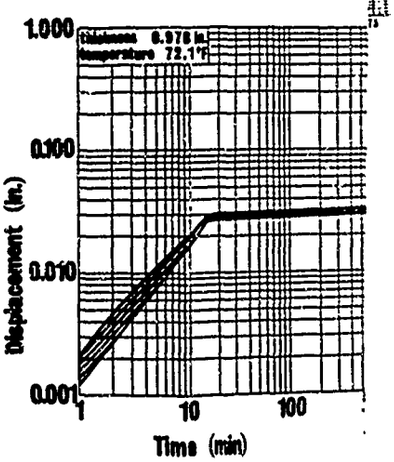

Figure C-4e. Displacement of conical acrylic plastic wind 10,000-psi sustained pressure loading; 120-d angle with t/D ratio = 0.978.

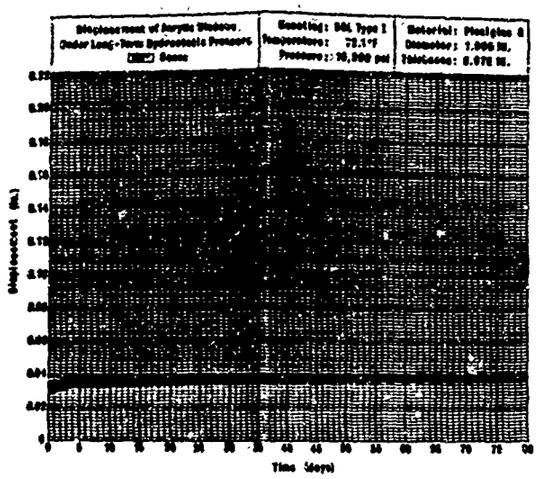

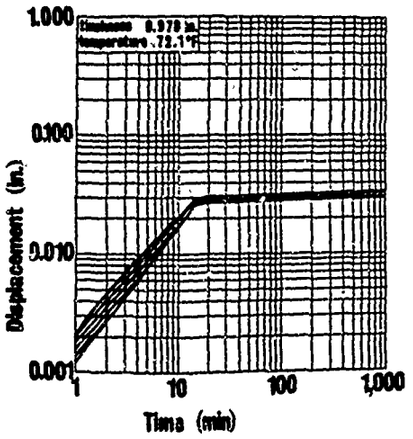

Figure C-4e. Displacement of conical acrylic plastic windows under 10,000-psi sustained pressure loading; 120-degree included angle with t/D ratio = 0.978.

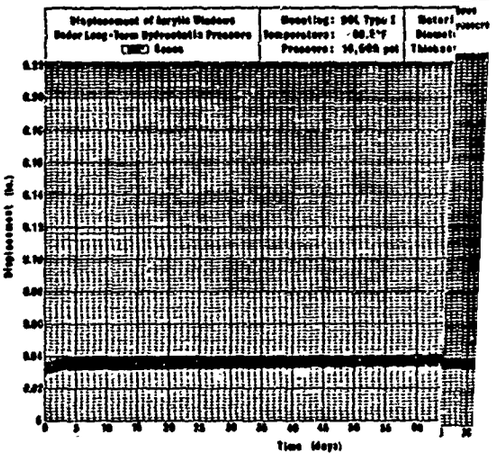

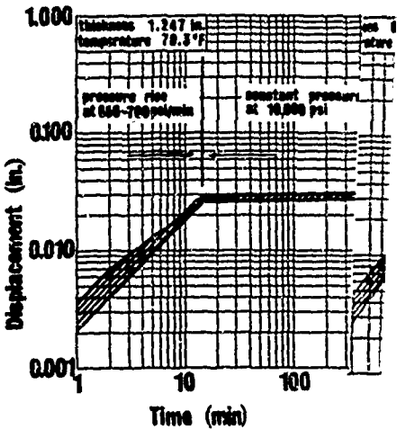

Figure C-4f. Displacement of conical acrylic plastic 10,000-psi sustained pressure loading; angle with t/D ratio = 1.247.

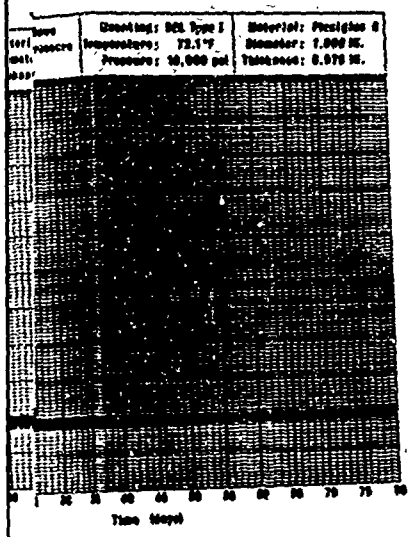

Time (days)

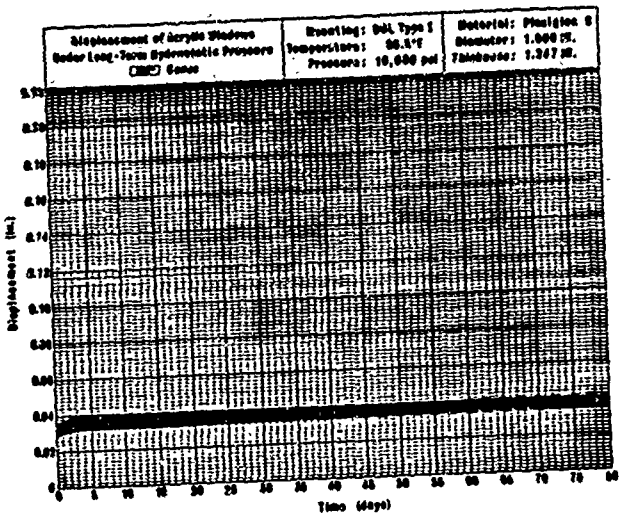

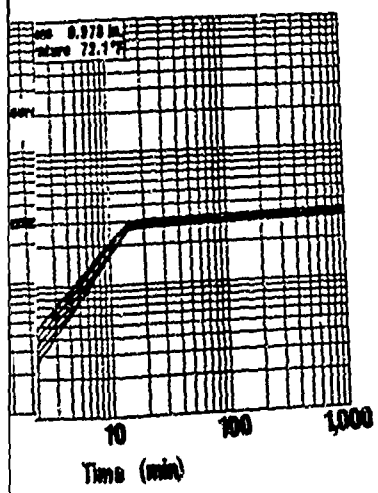

stic ement of conical acrylic plastic windows under
ng: psi sustained pressure loading; 120-degree included
ith t/D ratio = 0.978.

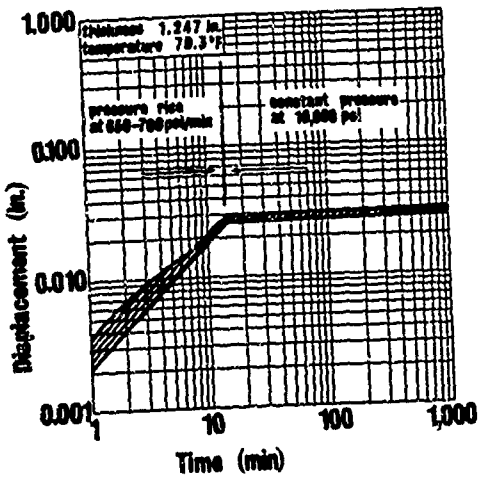

Figure C-4f. Displacement of conical acrylic plastic windows under 10,000-psi sustained pressure loading; 120-degree included angle with t/D ratio = 1.247.

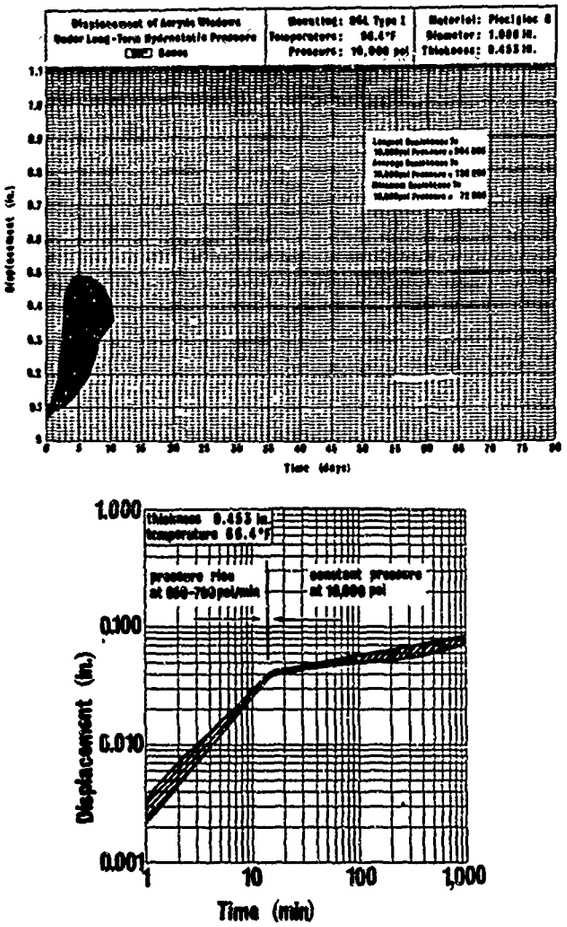

Figure C-5a. Displacement of conical acrylic plastic windows under 10,000-psi sustained pressure loading; 150-degree included angle with t/D ratio = 0.453.

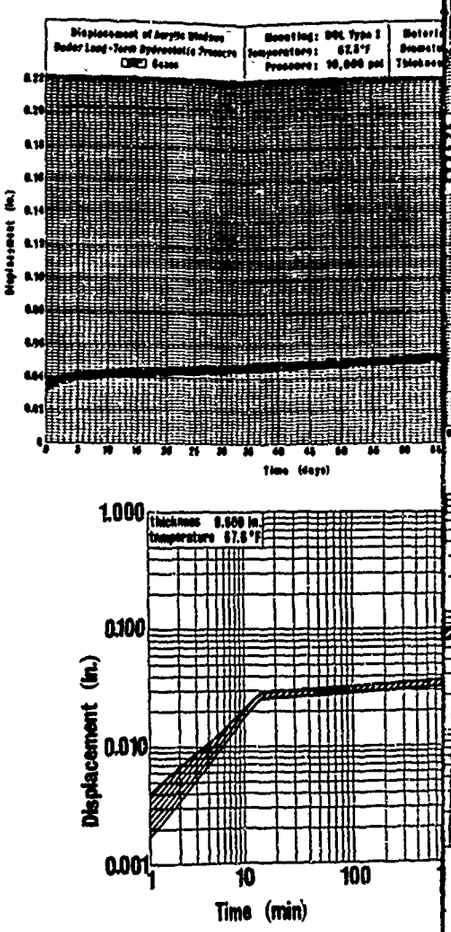

Figure C-5b. Displacement of conical acrylic plastic windo
10,000-psi sustained pressure loading; 150-de
angle with t/D ratio = 0.600.

ndows under
0-degree included

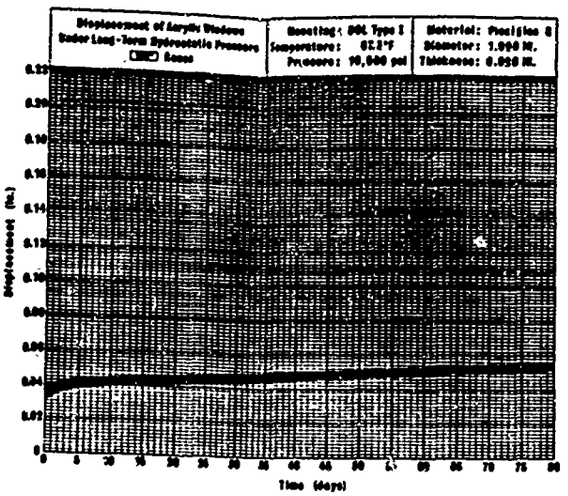

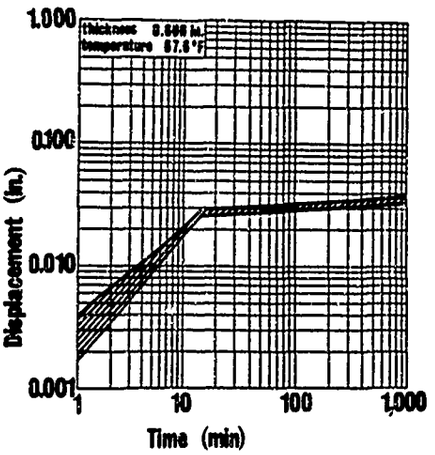

Figure C-5b. Displacement of conical acrylic plastic windows under 10,000-psi sustained pressure loading; 150-degree included angle with t/D ratio = 0.600.

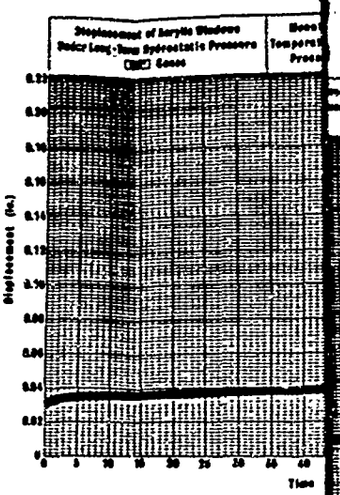

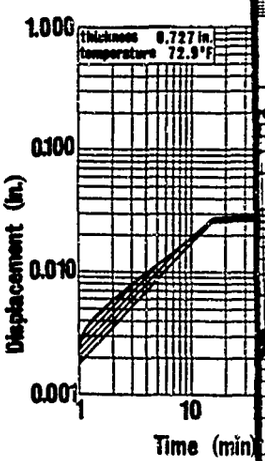

Figure C-5c. Displacement of conical acry
10,000-psi sustained pressure
angle with t/D ratio = 0.727.

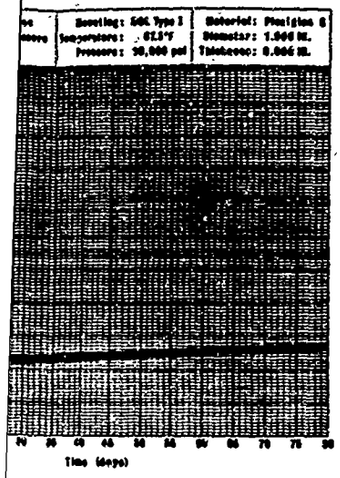

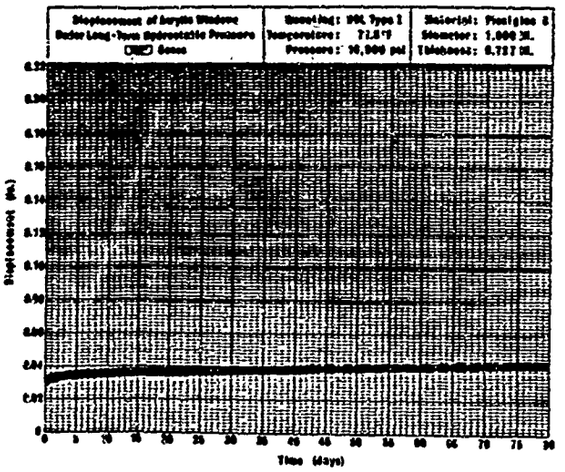

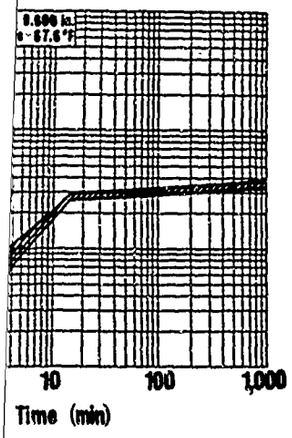

nt of conical acrylic plastic windows under sustained pressure loading; 150-degree included /D ratio = 0.600.

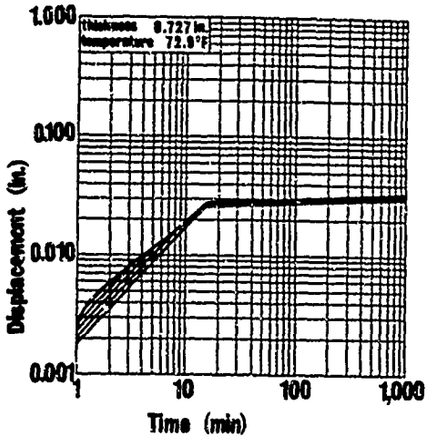

Figure C-5c. Displacement of conical acrylic plastic windows under 10,000-psi sustained pressure loading; 150-degree included angle with Y/D ratio = 0.727.

Continued

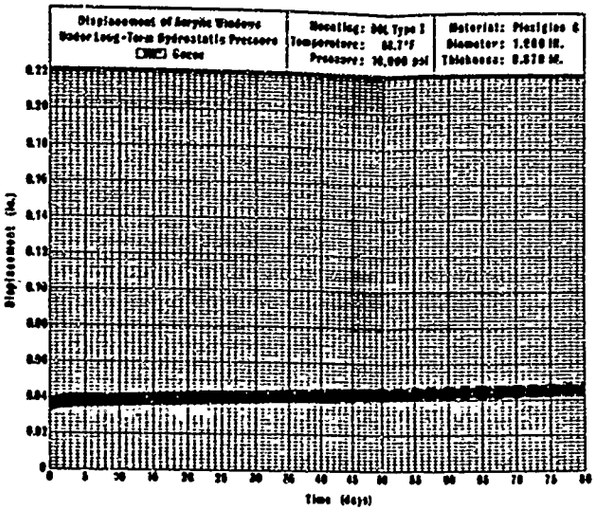

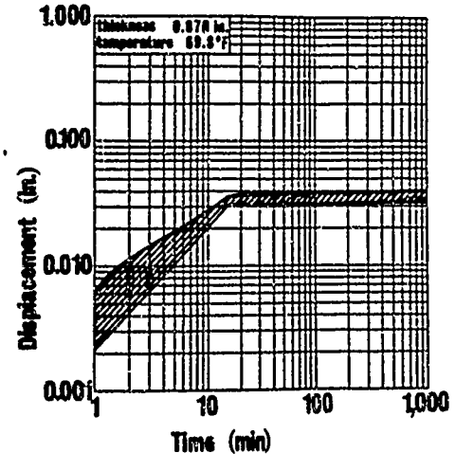

Figure C-5d. Displacement of conical acrylic plastic windows under 10,000-psi sustained pressure loading; 150-degree included angle with t/D ratio = 0.870.

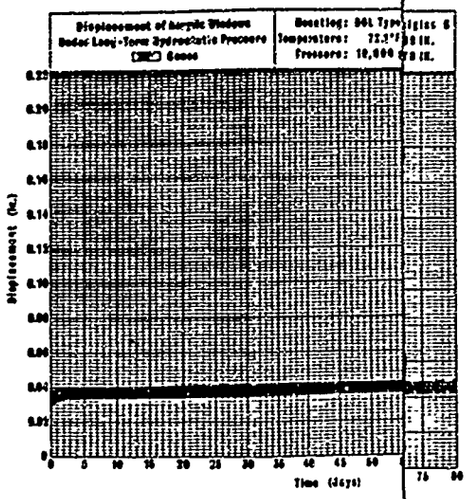

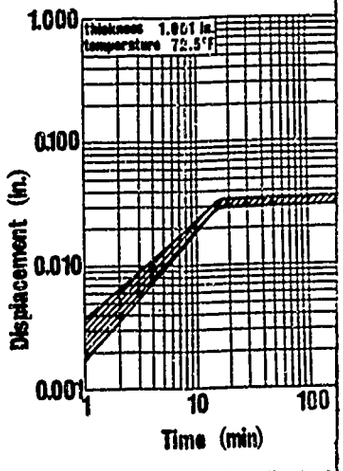

Figure C-5e. Displacement of conical acrylic plastic ed 10,000-psi sustained pressure loading; angle with t/D ratio = 1.001.

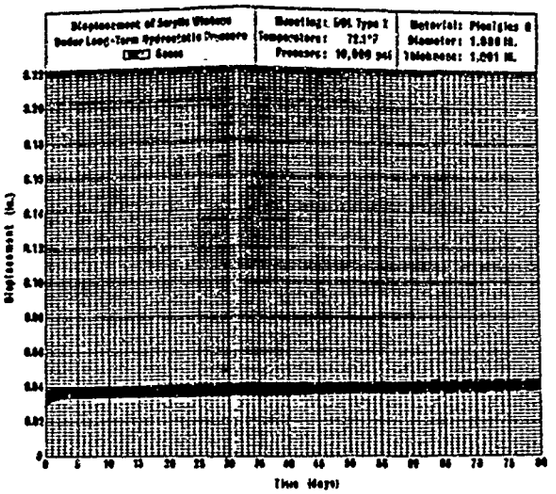

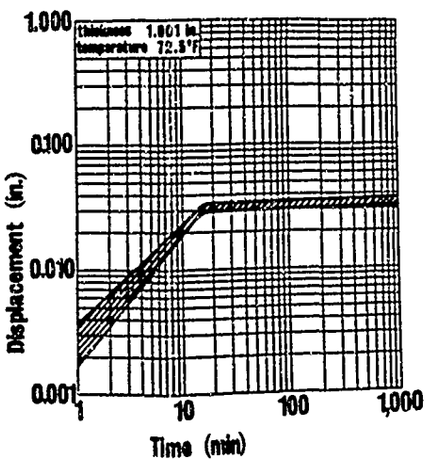

Figure C-5e. Displacement of conical acrylic plastic windows under 10,000-psi sustained pressure loading; 150-degree included angle with t/D ratio = 1.001.

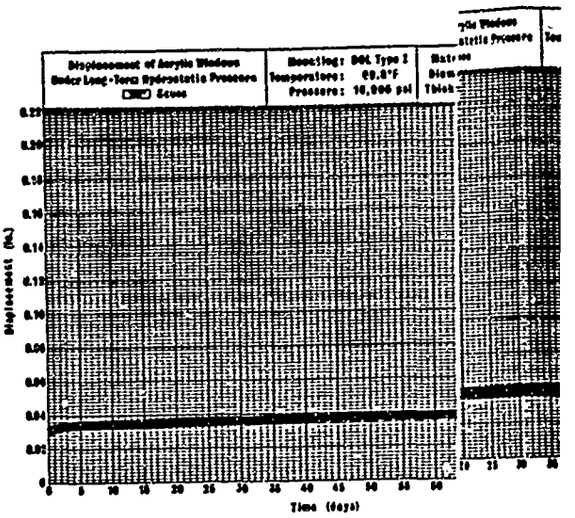

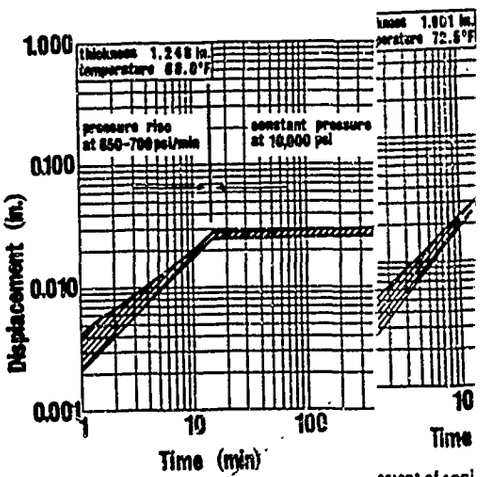

Figure C-5f. Displacement of conical acrylic plastic wi 10,000-psi sustained pressure loading; 150 angle with t/D ratio = 1.248.

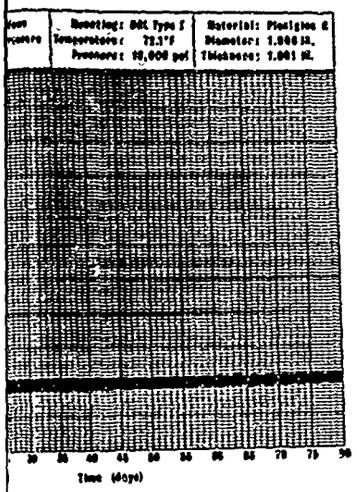

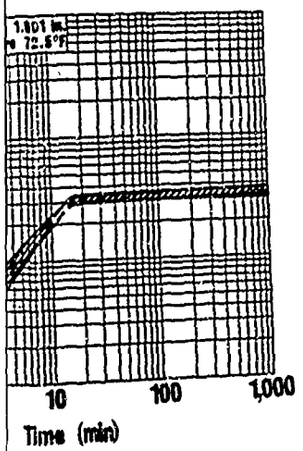

t of conical acrylic plastic windows under
ustained pressure loading; 150-degree included
D ratio = 1.001.

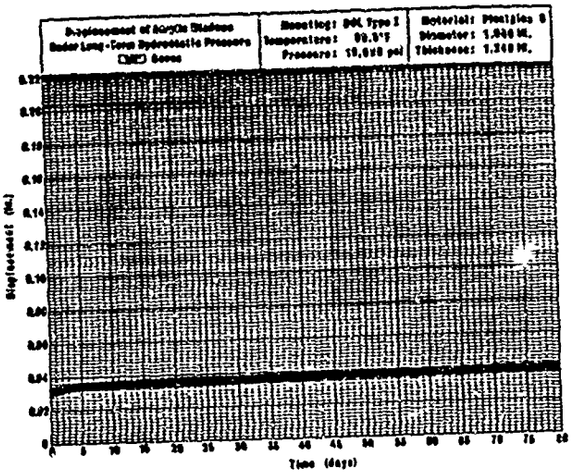

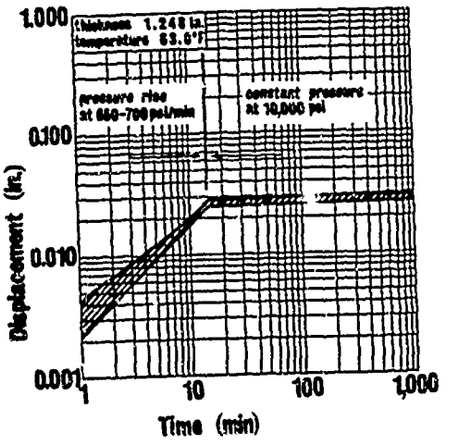

Figure C-5f. Displacement of conical acrylic plastic windows under 10,000-psi sustained pressure loading; 150-degree included angle with t/D ratio = 1.248.

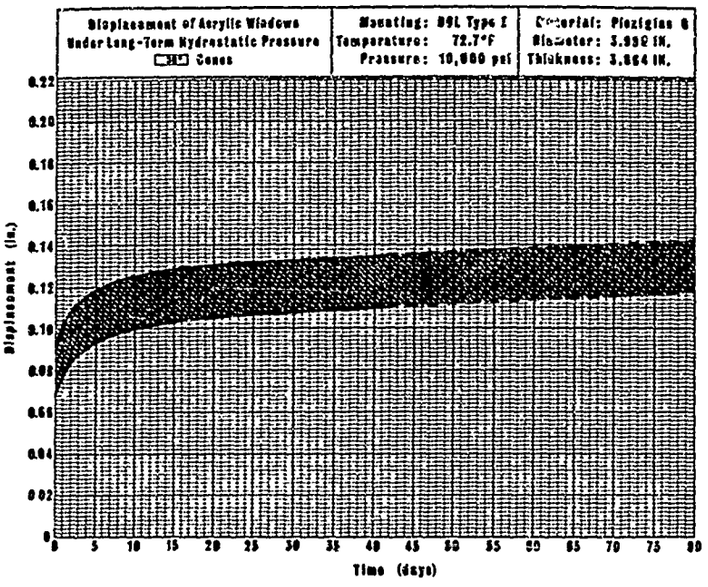

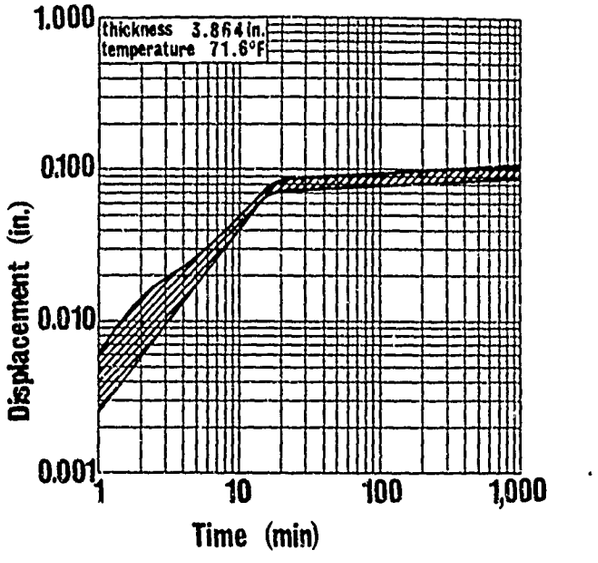

Figure C-6. Displacement of conical acrylic plastic windows under 10,000-psi sustained pressure loading; 150-degree included angle with t/D ratio = 0.967.

REFERENCES

1. Naval Civil Engineering Laboratory. Technical Report R-512: Windows for external or internal hydrostatic pressure vessels, pt. I. Conical acrylic windows under short-term pressure application, by J. D. Stachiw and K. O. Gray. Port Hueneme, Calif., Jan. 1967. (AD 646882)

2.———. Technical Report R-527: Windows for external or internal hydrostatic pressure vessels, pt. II. Flat acrylic windows under short-term pressure application, by J. D. Stachiw, G. M. Dunn, and K. O. Gray. Port Hueneme, Calif., May 1967. (AD 652343)

3.———. Technical Report R-631: Windows for external or internal hydrostatic pressure vessels, pt. III. Critical pressure of acrylic spherical shell windows under short-term pressure applications, by J. D. Stachiw and F. W. Brier. Port Hueneme, Calif., June 1969. (AD 689789)

4.———. Technical Report R-645: Windows for external or internal hydrostatic pressure vessels, pt. IV. Conical acrylic windows under long-term pressure application at 20,000 psi, by J. D. Stachiw. Port Hueneme, Calif., Oct. 1969. (AD 697272)

DISTRIBUTION LIST

SNDL Code	No. of Activities	Total Copies	
—	1	20	Defense Documentation Center
FKAIC	1	10	Naval Facilities Engineering Command
FKN1	6	6	NAVFAC Engineering Field Divisions
FKN5	9	9	Public Works Centers
FA25	1	1	Public Works Center
—	9	9	RDT&E Liaison Officers at NAVFAC Engineering Field Divisions and Construction Battalion Centers
—	298	298	NCEL Special Distribution List No. 9 for persons and activities interested in reports on Deep Ocean Studies

Unclassified
Security Classification

DOCUMENT CONTROL DATA - R & D

(Security classification of title, body of abstract and indexing annotation must be entered when the overall report is classified)

1. ORIGINATING ACTIVITY (Corporate author)
Naval Civil Engineering Laboratory
Port Hueneme, California 93041

2a. REPORT SECURITY CLASSIFICATION
Unclassified

2b. GROUP

3. REPORT TITLE
WINDOWS FOR EXTERNAL OR INTERNAL HYDROSTATIC PRESSURE VESSELS—Part V. Conical Acrylic Windows Under Long-Term Pressure Application of 10,000 Psi

4. DESCRIPTIVE NOTES (Type of report and inclusive dates)
Final; July 1969 – June 1970

5. AUTHOR(S) (First name, middle initial, last name)
J. D. Stachiw and W. A. Moody

6. REPORT DATE	7a. TOTAL NO. OF PAGES	7b. NO. OF REFS
January 1971	59	4

8a. CONTRACT OR GRANT NO.	9a. ORIGINATOR'S REPORT NUMBER(S)
b. PROJECT NO. YF 38.535.005.01.005	TR-708
c.	9b. OTHER REPORT NO(S) (Any other numbers that may be assigned this report)
d.	

10. DISTRIBUTION STATEMENT
This document has been approved for public release and sale; its distribution is unlimited.

11. SUPPLEMENTARY NOTES	12. SPONSORING MILITARY ACTIVITY
	Naval ~~Civil~~ Facilities Engineering Command Washington, D. C. 20390

13. ABSTRACT

Conical acrylic windows of 30-, 60-, 90-, 120- and 150-degree included angle and 0.500 to 1.250 t/D (thickness to minor diameter ratio) have been subjected in their mounting flanges to 10,000 psi of hydrostatic pressure for 500 and 1,000 hours at ambient room temperature. The displacement of the windows through the flange mounting has been recorded as a function of time and plotted for the ready reference of the designer. The magnitude of the window displacement has been found to be a function of time, angle, temperature, t/D ratio and pressure.

It is recommended that for safe single sustained operation of 1,000 hour duration at 10,000 psi hydrostatic loading at ambient temperature the windows should have an included conical angle $\geq 90^0$ and a minimum t/D ratio of 0.750. For sustained loadings in excess of 1,000 hours the minimum t/D ratio of 1.000.

DD FORM 1 NOV 65 1473 (PAGE 1)
S/N 0101-807-6801

Unclassified
Security Classification

14 KEY WORDS	LINK A		LINK B		LINK C	
	ROLE	WT	ROLE	WT	ROLE	WT
Pressure vessel windows						
Acrylic plastic						
Conical						
Short-term pressurization						
Long-term pressurization						
Failure modes						
Displacement						
Deformation						
Fracture patterns						
Window flange designs						
Submersible windows						
Undersea habitat windows						
Deep-submergence windows						

R 747

Technical Report

WINDOWS FOR EXTERNAL OR INTERNAL HYDROSTATIC PRESSURE VESSELS—PART VI.

Conical Acrylic Windows Under Long-Term Pressure Application at 5,000 Psi

November 1971

Sponsored by

NAVAL FACILITIES ENGINEERING COMMAND

NAVAL CIVIL ENGINEERING LABORATORY

Port Hueneme, California 93043

WINDOWS FOR EXTERNAL OR INTERNAL HYDROSTATIC PRESSURE VESSELS—PART VI. Conical Acrylic Windows Under Long-Term Pressure Application at 5,000 Psi

Technical Report R-747

YF 51.543.008.01.001

by

J. D. Stachiw and K. O. Gray

ABSTRACT

Conical acrylic windows with five included angles (α) from 30 to 150 degrees and thickness-to-minor-diameter (t/D) ratios from 0.375 to 1.00 have been subjected to 5,000 psi of sustained hydrostatic loading for up to 1,000 hours in the temperature range from 65°F to 75°F while the axial displacement of the windows through the flange has been monitored. The magnitude of axial displacement was found to be a function of α, t/D ratio, temperature, and duration of loading. Only windows with t/D ratios $\geq$1.000, 0.625, 0.500, and 0.500 for 30-, 60-, 90-, 120-, and 150-degree conical angles, respectively, were found to be free of cracks. Minimum axial displacements of the windows can be achieved only with t/D ratios of >1.000, 1.000, 0.750, 0.750, and 0.625 for 30-, 60-, 90-, 120-, and 150-degree conical angles, respectively. The minimum axial displacements of D = 1.000-inch windows with these t/D ratios and conical angles are 0.042, 0.023, 0.023, 0.019, and 0.019 inch, respectively. It is recommended that only windows with t/D ratios $\geq$0.625 and $\alpha \geq$60 degrees be used for sustained hydrostatic loading of 5,000 psi at temperatures $\leq$80°F.

CONTENTS

INTRODUCTION

Previous studies[1-3] conducted at the Naval Civil Engineering Laboratory (NCEL) have shown that although the spherical shell sector windows represent the most efficient structural shape for acrylic windows, the conical frustum windows are also fairly efficient, particularly if the included conical angle is very large. Because widespread use of conical windows has made them a somewhat standard shape, they were chosen first for further investigation in preference to spherical shell windows.

Because the viscoelastic nature of acrylic makes the duration of sustained hydrostatic loading a crucial operational factor, it was chosen as the first of the candidate materials to be studied in greater detail. In view of the multitude of variables involved, it was decided to investigate the effect of long-term loading on conical acrylic windows in three distinct phases. The first phase in the long-term loading program was to focus on the behavior of conical windows under long-term 20,000-psi hydrostatic loading, while the succeeding two phases addressed themselves to 10,000-psi and 5,000-psi hydrostatic loadings. The first two phases of the research program have been already completed.[4,5]

The test results from the previous two studies have shown that although the viscoelastic nature of acrylic makes time-dependent axial displacement of acrylic windows under long-term loading inevitable, the windows are operationally safe for hydrostatic pressures up to 20,000 psi providing proper thickness-to-minor-diameter (t/D) ratios and included conical angles (α) are chosen. Furthermore, it was shown that the axial displacement of the window through the flange is a function of pressure, temperature, t/D ratio, conical angle α, and duration of sustained loading. Since the interrelationship between the many variables is very complex and the analytical tools for analyzing them were not available at that time without a lengthy and expensive development program, an empirical approach was chosen for providing the engineer with the necessary data (Appendix A) for design of windows applicable to ocean bottom habitats or ocean simulation facilities (Figure 1). Thus, the experimental data have been presented (1) in graphical form as sets of curves where the axial displacement of the windows through the flange at a given hydrostatic pressure is plotted versus time, t/D ratio, and included angle α, (2) in pictorial form in which the cracks and fractures in the windows are related to the window dimensions and length of loading. Such

sets of curves and photographs are already available for the 20,000-psi and 10,000-psi long-term pressure loadings. This report presents the results of study on the long-term loading of acrylic windows at 5,000-psi hydrostatic pressure.

The scope of the investigation of the behavior of conical acrylic windows under sustained long-term hydrostatic loading of 5,000 psi was limited to model windows with 30-, 60-, 90-, 120-, and 150-degree included conical angles and 1.000, 0.750, 0.625, 0.500, and 0.375 t/D ratios (Table 1). All of the tests were conducted in the ambient room temperature range from 65° to 75°F, and the duration of loading was either 500 or 1,000 hours. The effect of temperature was not investigated, as its effect on the axial displacement and critical pressures of conical acrylic windows under long-term loading was already established in the first phase[4] of the long-term window loading program. The effect of temperature was found to be that critical pressure increased and axial displacement decreased as the temperature decreased. The effect of dimensional scaling on the axial displacement of windows under long-term loading was also not investigated as it was established in the first[4] and second[5] phases of the long-term window loading program that for windows with identical t/D and α the displacements vary linearly with D.

Figure 1. Window installed in end closure of 18-inch (inside diameter) pressure vessel for observation of test specimens.

Table 1. Test Plan for Conical Acrylic Windows Subjected to 5,000 Psi of Hydrostatic Pressure for 1,000 Hours

(● represents a group of five test specimens, each with a minor diameter of 1.0 inch.)

Thickness, t (in.)	Included Angle (deg)				
	30	60	90	120	150
3/8 (0.375)	●	●	●	●	●
1/2 (0.500)	●	●	●	●	●
5/8 (0.625)	●	●	●	●	●
3/4 (0.750)	●	●	●	●	●
1 (1.000)	●	●	●	●	●

TEST SPECIMENS

The test specimens (Figure 2) were machined from commercial Plexiglas G stock (Table 2) by turning in a horizontal lathe. Accepted machine shop practices were used to maintain dimensional tolerances of ±0.005 inch on the specified minor diameter of 1.000 inch and ±30 minutes on the included conical angle for all the test specimens (Figure 3). Since the thickness of commercially available acrylic plate stock varied from the nominal thickness because of fabrication tolerances, the actual thickness of the finished windows also deviated from the nominal thickness. However, since all of the windows for a given t/D ratio and conical angle were machined from the same acrylic plate, their thicknesses were within ±0.010 inch of each other. The finish on the conical surface was 32 rms.

TEST SETUP

Window Flanges

The window flanges used for the testing were the same that were used in the long-term loadings of windows to 20,000-psi and 10,000-psi pressure (Figures 4 and 5). The ±0.001-inch tolerance on the 1.000-inch minor diameter and the ±15-minute tolerance on the conical angle assured close fit between the windows and the flange. Because the minor diameter of the window matched

that of the flange, the low-pressure face of the window was flush with the bottom of the conical cavity in the flange. This type of window seating in the flange and the cylindrical passage in the flange through which the window had to displace are the characteristics of the DOL 1 window mounting arrangement used in the prior studies on long-term loading at NCEL. Because the mounting arrangement was the same for all the long-term loading studies, the resulting data can be compared without resorting to any special conversion factors.

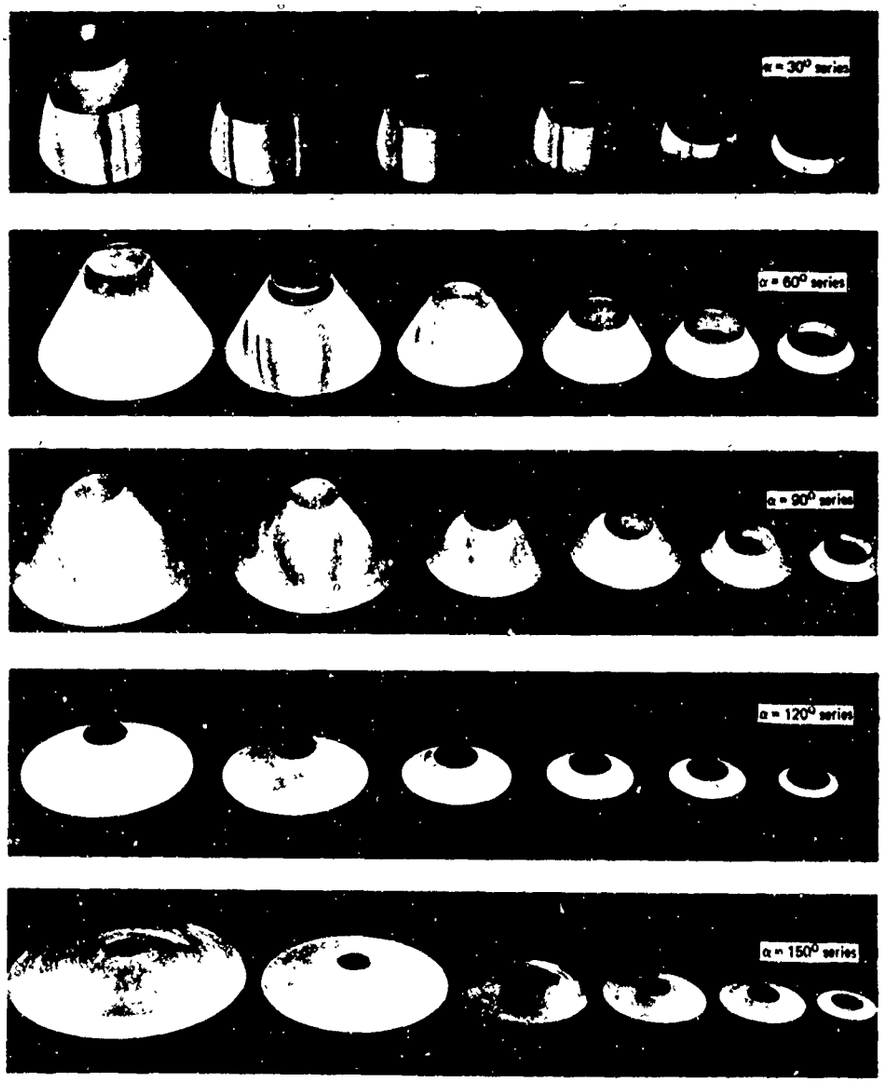

Figure 2. Typical conical acrylic windows of 1-inch minor diameter used in NCEL experimental programs.

Table 2. Properties of Acrylic Window Material

Property	Typical	Test Method
Physical Properties		
Hardness, Rockwell M	90	ASTM-D785-62
Hardness, Barcol No.	47	ASTM-D2583
Specific gravity	1.19 ± 0.01 (2 tests within 0.005)	ASTM-D792-64T
Refractive index	1.50 ± 0.01	ASTM-D542-50
Luminous transmittance (1/8-inch material)	91% (min)	ASTM-D1003-61
Haze (1/8-inch material)	2.3 (max)	ASTM-D1003-61
Heat distortion temperature		ASTM-D648-56
+3.6°F/min at 264 psi	200°F	
+3.6°F/min at 66 psi	220°F	
Thermal expansion/°F at 20°F	35×10^{-6}	Federal Standard 406 Method 2031
Water absorption (1/8-inch material)		ASTM-D570-63T
(a) 25 hours at 73°F	0.3% (max)	
(b) to saturation	1.9% (max)	
Mechanical Properties		
Tensile strength, rupture (0.2 in./min)	9,000 psi (min)	ASTM-D638-64T
Tensile elongation, rupture	2% (min) to 7% (max)	ASTM-D638-64T
Modulus of elasticity, tension	400,000 psi (min)	ASTM-D638-64T
Compressive strength, (0.2 in./min)	15,000 psi (min)	ASTM-D695-63T
Flexural strength, rupture	14,000 psi (min)	ASTM-D790-63
Shear strength, rupture	8,000 psi (min)	ASTM-D732-46
Impact strength, Izod (per inch of notch)	0.4 ft-lb (min)	ASTM-D256-56
Compressive deformation under load (4,000 psi at 122°F for 24 hours)	2% (max)	ASTM-D621-64

Material: Plexiglas G

Nomenclature

D = minor diameter (in.)
t = thickness (in.)
α = included conical angle (deg)

Dimensions

D = 1.0 in.; tolerance = ±0.005 in.
t = nominal 0.375, 0.500, 0.625, 0.750, 1.000 in. (manufacturer's plate thickness tolerances apply)
α = 30, 60, 90, 120, or 150 deg; tolerance = ±15 min

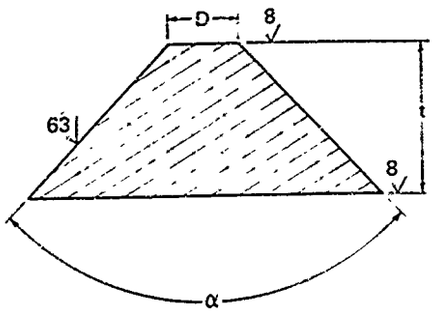

Figure 3. Dimensions of typical conical window specimens.

Material: 1015 steel

Nomenclature

M = external flange diameter (in.)
k = overall window flange thickness (in.)
α = included conical angle (deg)

Dimensions

α = 30, 60, 90, 120 and 150 deg; tolerance = ± 5 min
M = 8 ± 1/64 in. for 30-, 60-, 90-, and 120-deg windows
17 ± 1/64 in. for 150-deg windows

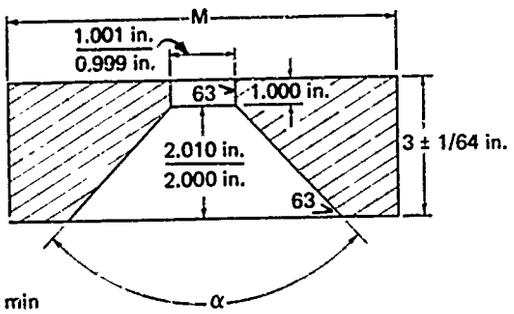

Figure 4. Dimensions of typical window mounting flanges for 1-inch-diameter conical windows.

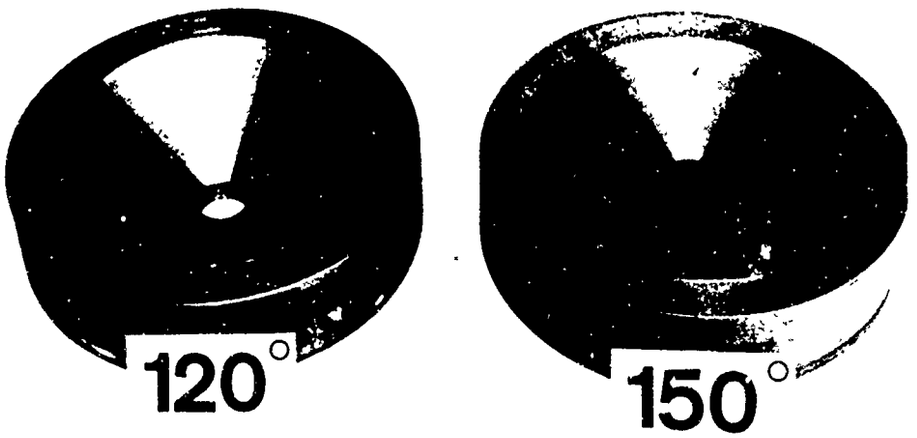

Figure 5. Typical flanges for 1-inch-diameter conical window.

Pressure Vessels

The vessels used for the testing of windows were 16-inch naval gun shells converted by NCEL to serve as internal pressure vessels. The window test flanges were attached to the vessel end closures by special adapters that permitted the cylindrical passage in the window mounting flange to line up with the opening in the end closure. With the help of this arrangement, it was possible to maintain atmospheric pressure on the low-pressure face of the windows and also to allow the fragments of the window to be ejected from the vessel if the window failed during the long-term test (Figure 6).

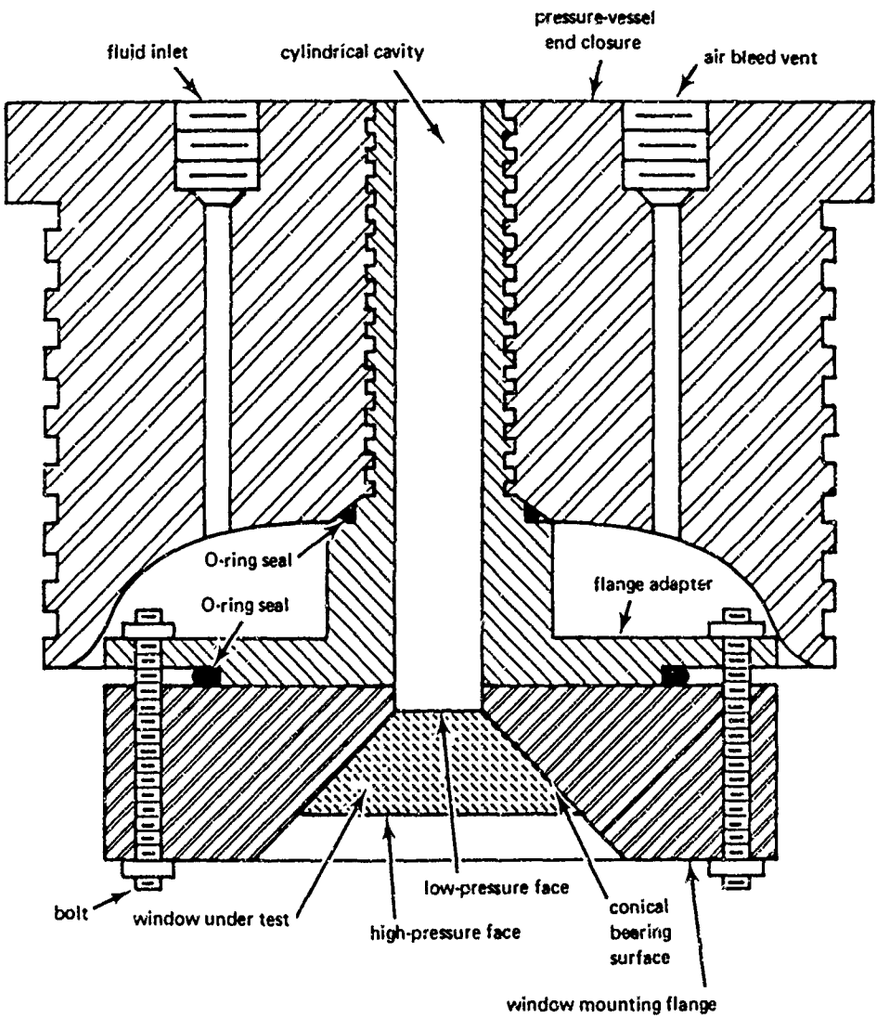

Figure 6. Typical window/flange assembly used in testing 1-inch-diameter conical windows in converted 16-inch naval gun shells.

The vessels were equipped with an electrically heated jacket to maintain the temperature of the water above 65°F even if the ambient temperature in the vicinity of the vessels dropped to 40°F during the winter months. No provisions existed for preventing the temperature from rising above 70°F when the ambient air temperature increased during hot spells in the summer months.

Instrumentation

The instrumentation for the long-term testing of windows consisted of a Bourdon-type pressure gage, a mechanical-type dial indicator (Figure 7), and a remote-reading thermometer. The pressure gage could be read within 50-psi intervals, the dial indicator within 0.001 inch, and the thermometer within 1°F. All of the instruments were calibrated prior to each test on an individual window.

TEST PROCEDURE

Placement of Windows

Prior to placement into the flange, the windows were accurately measured and subsequently liberally coated with silicone grease. To insure good sealing, the windows were forced into the flange cavity with 20 to 30 pounds of force and rotated several times in place. The placement and locking of the end closure, with flange attached, to the vessel completed the preparation of the vessel for the test. Now the vessel was ready for insertion of the dial indicator rod into the cylindrical passage between the low-pressure face of the window and the exterior of the vessel. The position of the dial indicator on the pressure vessel end closure was adjusted until the tip of the dial indicator rod touched the center of the window's low-pressure face.

The presence of a thick layer of silicone grease trapped between the bearing surface of the window and the flange caused erroneous displacement readings when the grease squeezed out during initial hydrostatic loading. This problem was solved by preloading the window with 1,000-psi hydrostatic pressure for 1 hour, depressurizing it to zero, and readjusting the dial indicator to read zero displacement. This procedure effectively removed the excess grease from the window in each test and insured that axial window displacement readings taken during the long-term loading reflected only the displacement of the windows and not the squeezing out of grease.

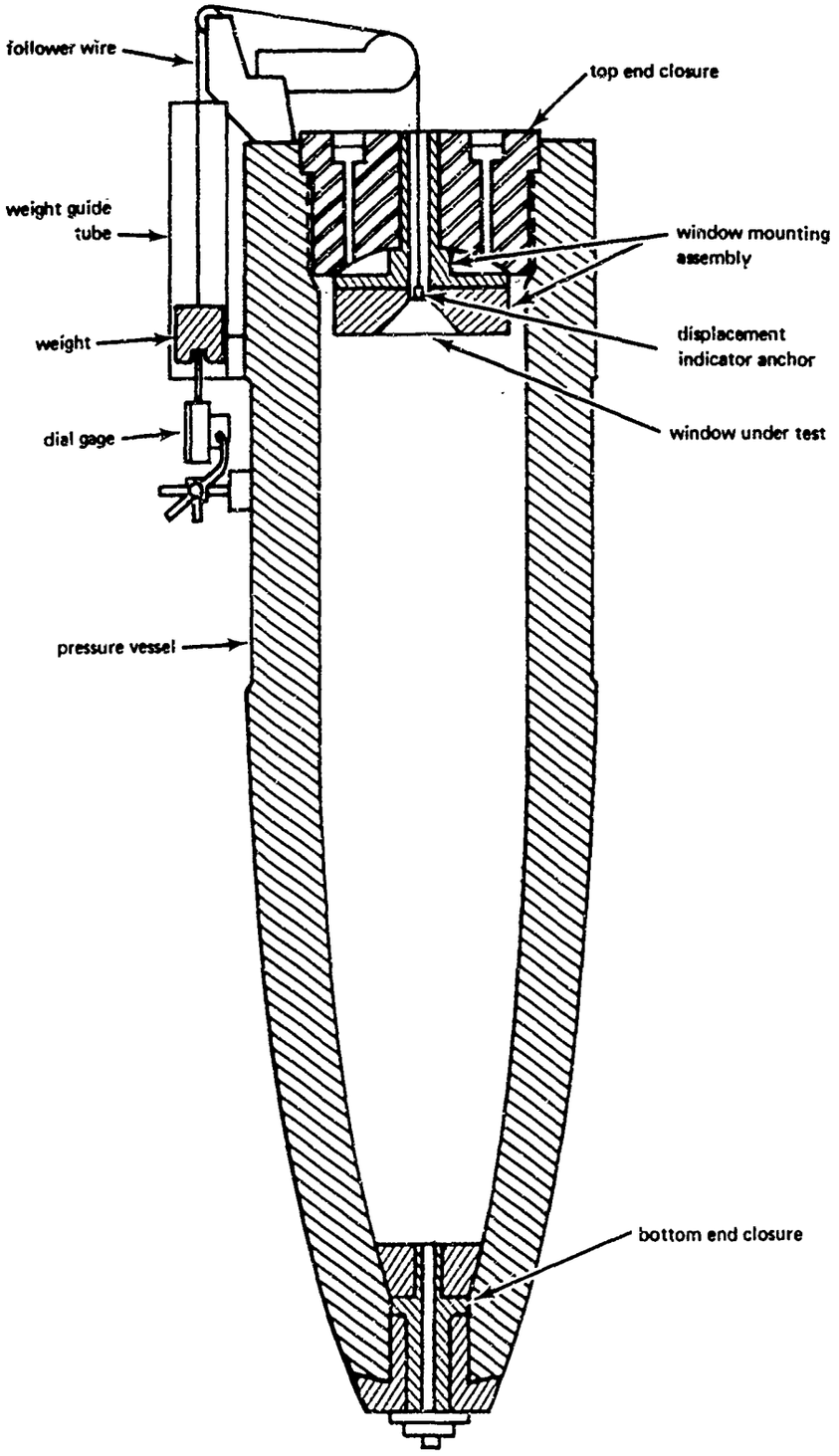

Figure 7. Axial window displacement measuring device attached to exterior of converted 16-inch naval gun shell.

Pressure Loading

The pressurization of windows from 0 psi to the 5,000-psi level proceeded at a rate of 650 psi/min. Tap water, which was used as the pressurization medium, was pumped into the vessels by means of a positive displacement, air-operated pump. Window displacement readings were taken at every 1,000-psi pressure interval. When the pressure inside the vessel reached 5,000 psi, the vessel was isolated from the pressurization system.

The long-term sustained pressure loading of 5,000 psi was maintained inside the vessel by means of daily pressure checks. If the pressure inside the vessel was found to deviate in excess of ±100 psi from the specified 5,000 psi, the shutoff valve at the vessel was opened, and the pressure inside the vessel was raised by pumping in additional water, or lowered by bleeding some water. The adjusting of pressure, which took place infrequently, was required only when either excessive window displacement or variation in ambient atmospheric temperature occurred. Readings of window displacements were taken three times daily during the duration of sustained long-term loading.

Depressurization of windows after the specified time period was accomplished by bleeding the water from the vessel interior through a partially open valve. Depressurization was conducted at a rate of 650 psi/min, the same rate as the pressurization. Axial displacement readings were taken every 1,000 psi as the pressure was lowered from 5,000 psi to the 0-psi level.

TEST RESULTS

Data generated by the long-term tests at 5,000 psi are presented below graphically, pictorially, and descriptively to answer the varying needs of different users.

Graphical Data

The axial displacement of the windows through the window flange are in graphical form, since graphical presentation has been found to be the most efficient way of summarizing the experimental data generated by the study. Because these data are of interest not only to window designers, but also to research engineers studying the relationship between the many structural, physical, and mechanical parameters determining the performance of hydrospace windows, the same data have been presented graphically in two different ways.

One set of graphs presented for the benefit of researchers is the summary of all experimental parameters that determined the axial displacement of windows in this study (Figures 8 and 9). Since the objective of these graphs is to show the interrelationships between the many experimental parameters, only *average displacement* values were plotted, as otherwise the graphs would become too cluttered, and the message they carry would become lost.

A different set of graphs is presented for the use of the designer who is not so much interested in the relationship between the experimental variables as in the reproducibility and reliability of displacement measurements for windows of a given set of dimensions. For this reason, the displacement data have been also shown (Appendix A) in a series of graphs depicting the ranges of axial displacements for each group of five windows of a given t/D and α. After noting the range of displacements for a given t/D ratio and α, the designer will be in a better position to predict what magnitude of axial displacement the window that he has selected for particular application may experience during sustained hydrostatic loading.

Pictorial Data

The *permanent deformation* of windows and magnitude of cracks are presented in pictorial form, as there are no quantitative means of recording the permanent effects of sustained loading upon conical acrylic windows (Figures 10 through 13). Since the permanent effect of sustained loading on windows is visually best observed on the high-pressure face, low-pressure face, and conical bearing surface of the window, the photographs focused upon these areas. Thus one set of photographs shows the plastic deformations and cracks on the low-pressure faces and conical bearing surfaces of windows, while the other set shows the permanent deformations in high-pressure faces. To bring out the permanent deformations of high-pressure faces, a grid pattern has been optically superimposed on them. At locations where the surface of the window is not perfectly flat, distortions of the square grid become visible, the severity of distortion being directly related to the magnitude of deformation.

Descriptive Data

The condition of windows after long-term loading is described in words, because the evaluation of condition is a matter of judgment that takes into account everything observable or measurable on the window. Basically, the assessment of the condition of a window depends on whether a window

of given t/D ratio and included angle has withstood the long-term loadings sufficiently well to recommend it for operational service under similar loading conditions.

TEST OBSERVATIONS

Window Deformation

The conical acrylic windows deformed both viscoelastically and viscoplastically under sustained hydrostatic pressure. The magnitude of viscoplastic deformation varied directly with the duration of loading and temperature, while it varied inversely with the t/D ratio and included conical angle. The window deformation included (1) a cold-flow crater on its high-pressure face, (2) a cylindrical extrusion plug at the minor diameter of the body, and (3) an outward curvature on the low-pressure face (Figures 10 and 11). The depth of the cold-flow crater and length of extrusion plug were found to be *inversely* related to the conical angle and t/D ratio, and *directly* related to duration of loading and temperature.

The deformation of the windows was in many cases accompanied by crazing and cracking of the window surfaces. The severity of cracking was generally directly related to the magnitude of deformation or displacement. The crazing (or in more severe cases, cracks) appeared first on the conical bearing surface of the window for 30- and 60-degree conical angles *only* (Figure 12). For $\alpha \geq 90$ degrees, the cracks appeared first on the low-pressure face of the window (Figure 13).

The circumferential cracks at right angle to the bearing surface (Figure 12) were indicative of shear stresses associated with large-scale displacement of the window. As the t/D ratio of 30- and 60-degree windows was increased, the number and severity of these cracks decreased until at t/D = 0.625 for $\alpha = 60$ degrees and t/D = 1.000 for $\alpha = 30$ degrees, they disappeared completely.

The star-shaped crack on the low-pressure face of windows (Figure 13) was indicative of severe flexure stress at the center of the low-pressure face for windows with $\alpha \geq 90$ degrees and t/D $\leq$ 0.375. As the t/D ratio of windows with $\alpha \geq 90$ degrees was increased, the depth of the star-shaped crack decreased until for windows with t/D $\geq$ 0.500, it disappeared altogether. The shear-type cracks were not observed on windows with $\alpha \geq 90$ degrees, even at t/D = 0.375 ratio.

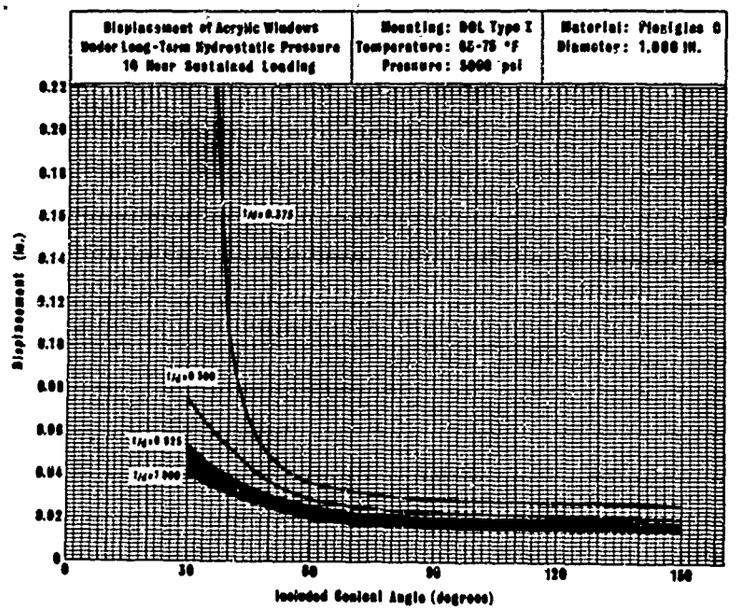

(a) After 10 hours of sustained loading.

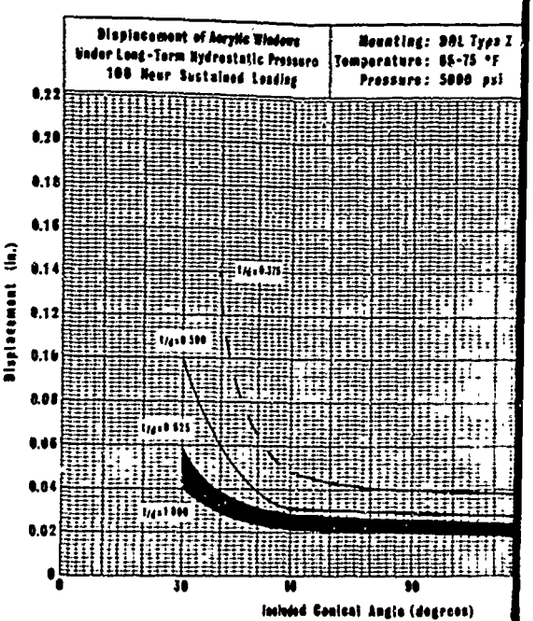

(b) After 100 hours of sustained load

Figure 8. Displacement of conical acrylic plastic win
sustained pressure loading as function of w
conical angle.

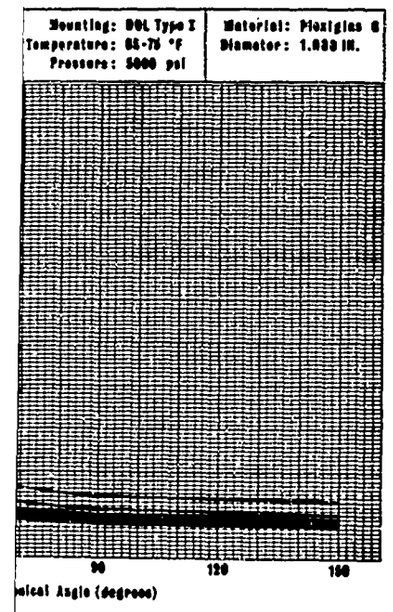

s of sustained loading.

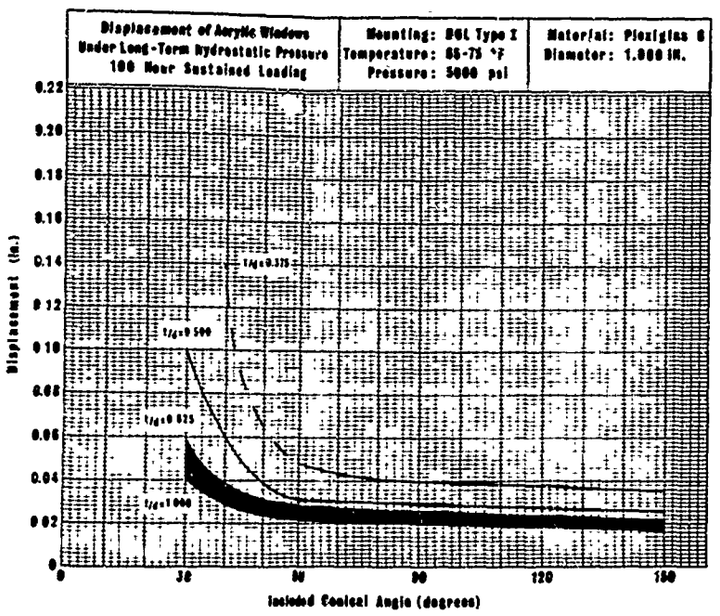

(b) After 100 hours of sustained loading.

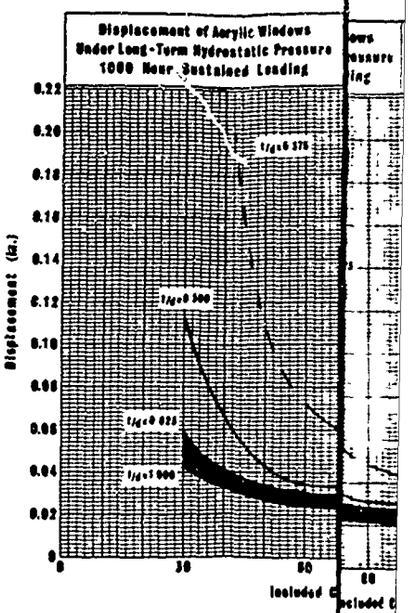

(c) After 1,000 ho 00 hou

Figure 8. Displacement of conical acrylic plastic windows under 5,000-psi sustained pressure loading as function of window's included conical angle.

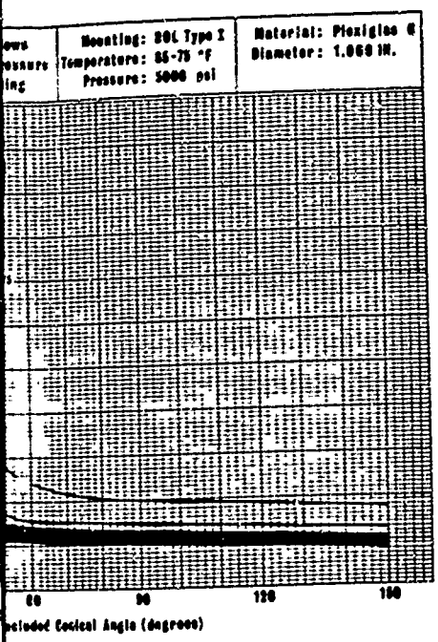

00 hours of sustained loading.

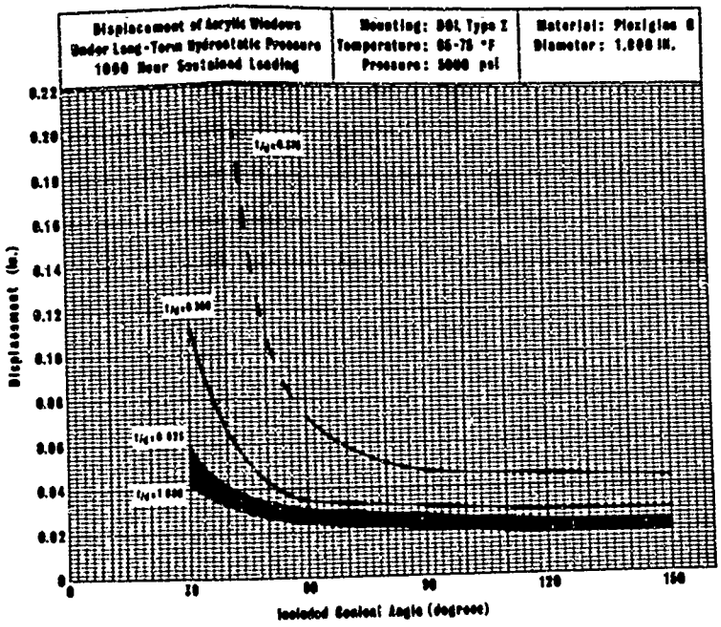

(c) After 1,000 hours of sustained loading.

conical acrylic plastic windows under 5,000-psi
loading as function of window's included

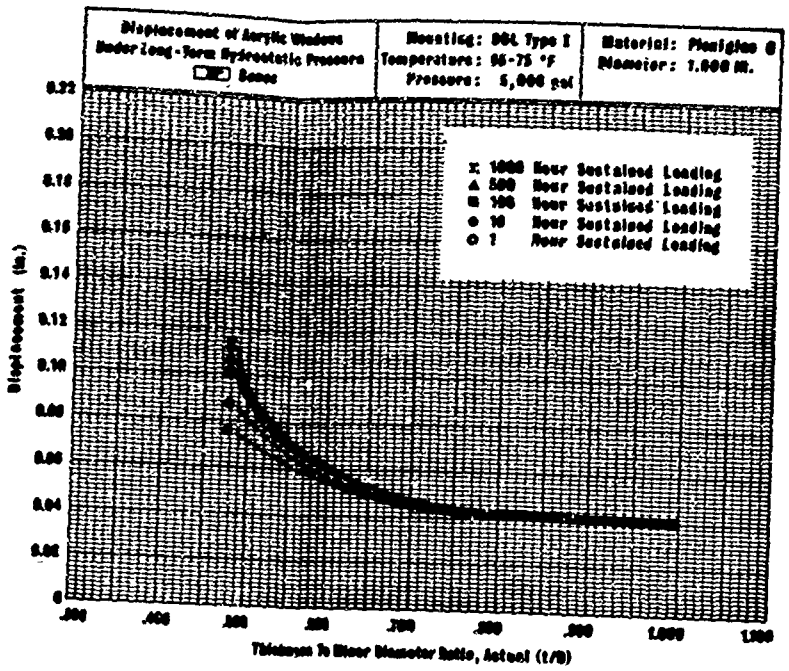

(a) Windows with 30-degree included conical angle.

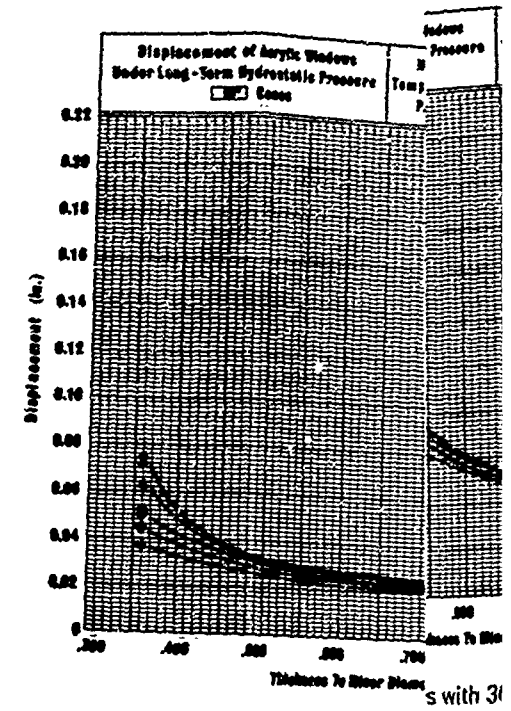

(b) Windows with 60-degre

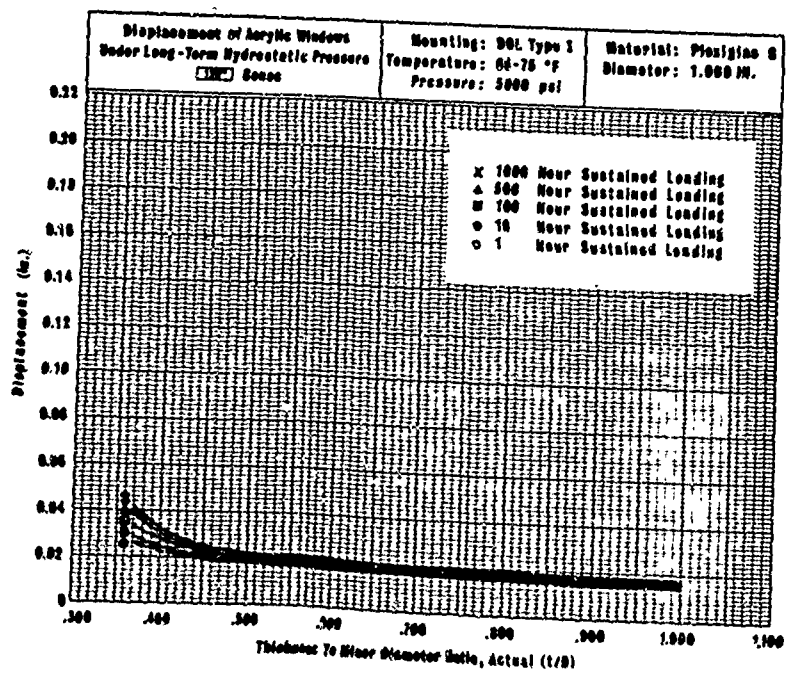

(d) Windows with 120-degree included conical angle.

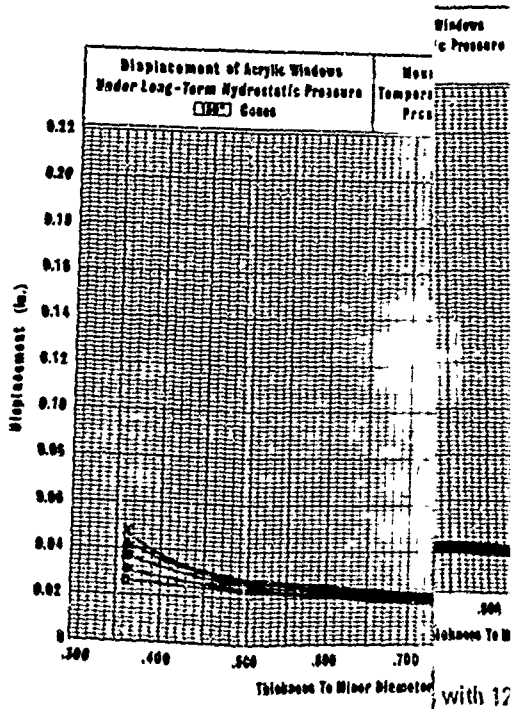

(e) Windows with 150-degree i

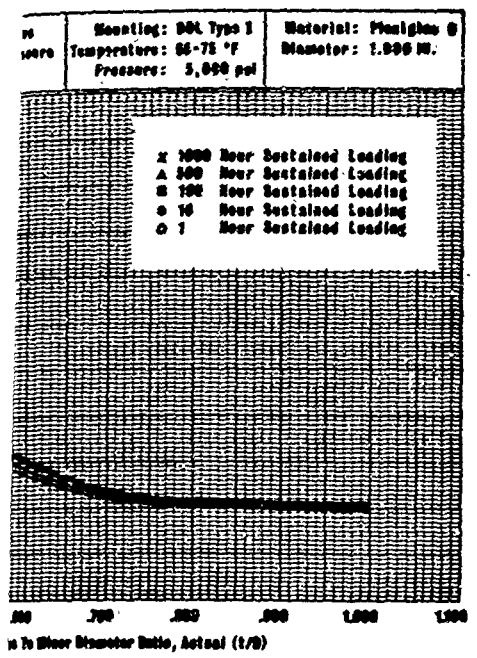

with 30-degree included conical angle.

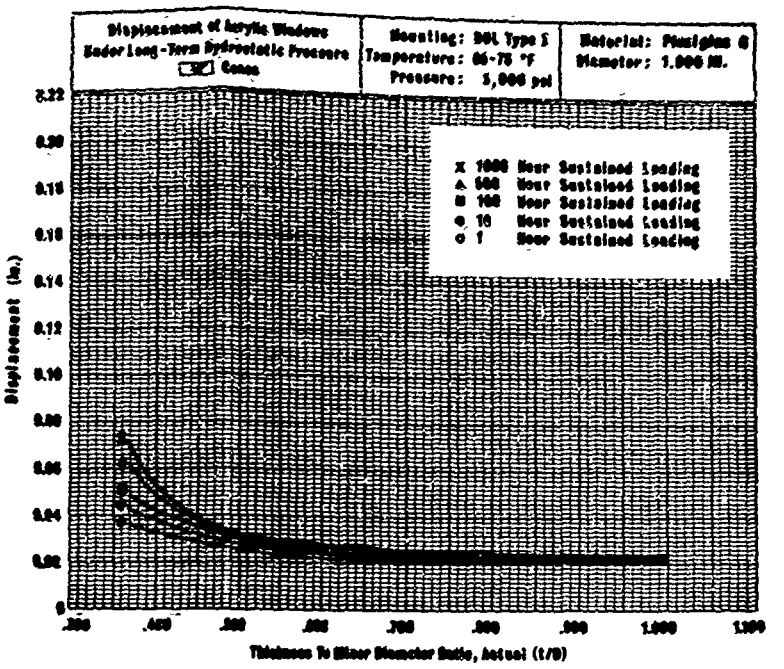

(b) Windows with 60-degree included conical angle.

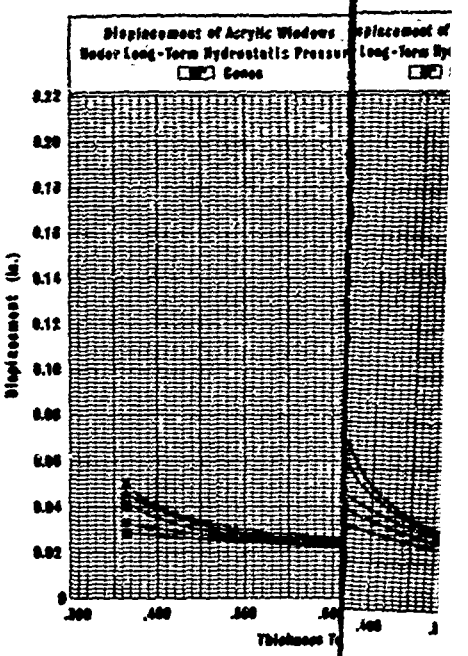

(c) Windows with

(b) Win

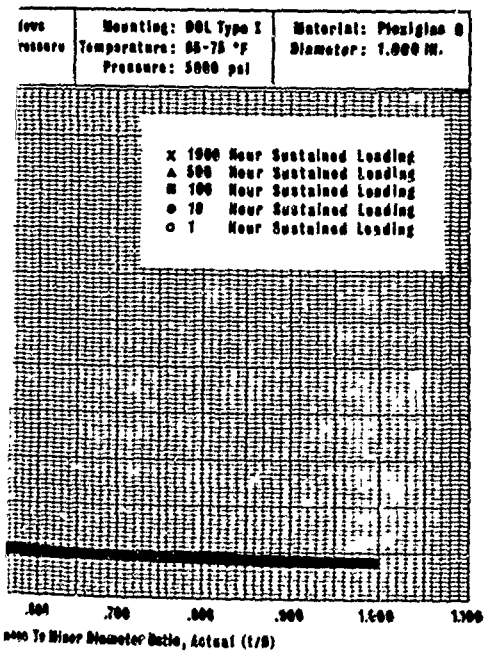

ith 120-degree included conical angle.

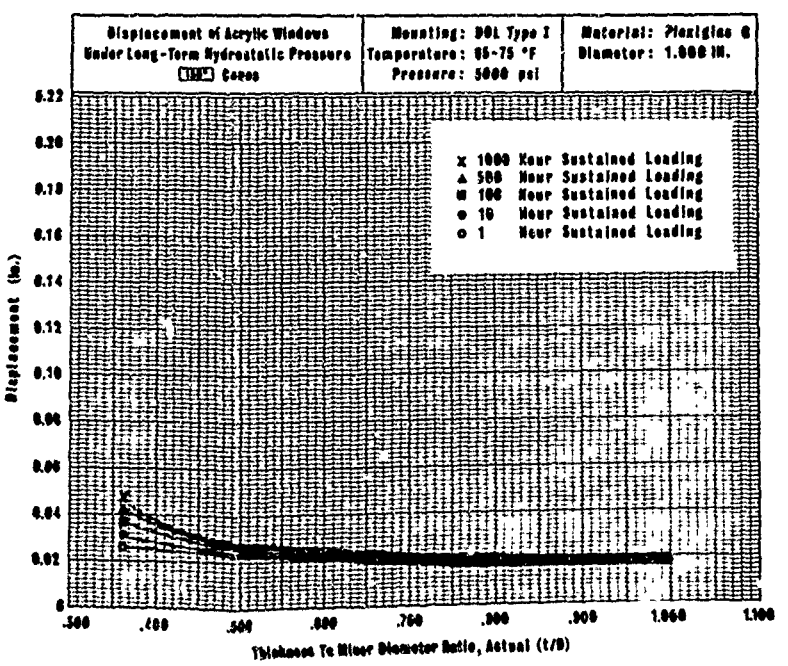

(e) Windows with 150-degree included conical angle.

Figure 9. Displacement o
sustained press

) Windo

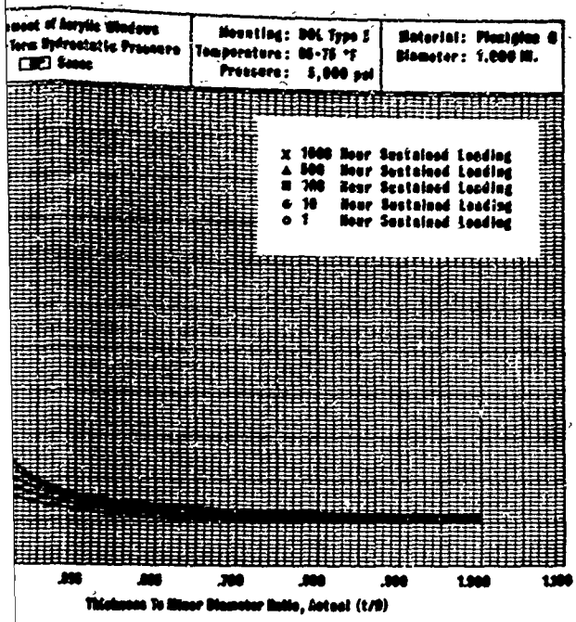

) Windows with 60-degree included conical angle.

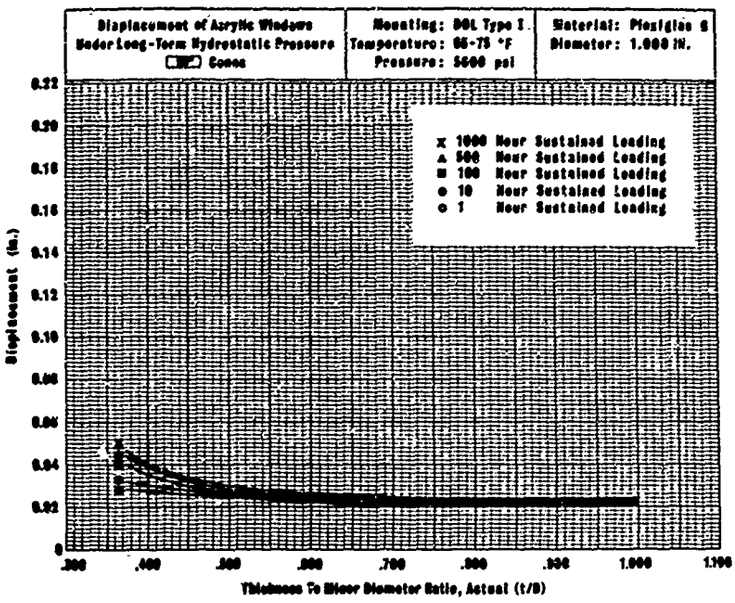

(c) Windows with 90-degree included conical angle.

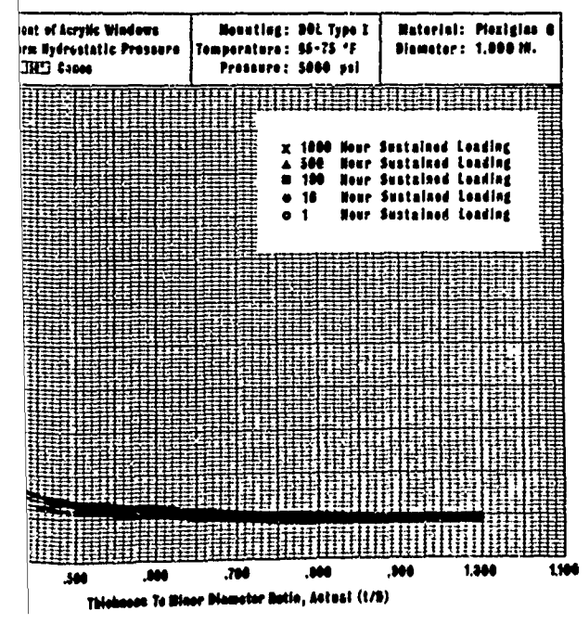

indows with 150-degree included conical angle.

Figure 9. Displacement of conical acrylic plastic windows under 5,000-psi sustained pressure loading as function of window's t/D ratio.

Figure 10. Effect of 5,000-psi sustained loading on conical acrylic windows with t/D ratio = 0.375 and 60-, 90-, 120-, and 150-degree included angles. Note star-shaped cracks in the centers of low-pressure faces of 90-, 120-, and 150-degree windows.

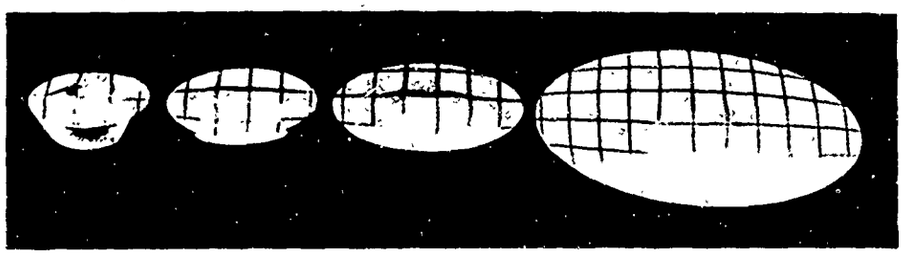

Figure 11. High-pressure faces of windows shown in Figure 10. Note cold-flow cratering. Grid on the window faces is a mirror reflection of a grid with uniform squares.

Window Displacement

All windows experienced axial displacement through the flange opening. Since the axial displacement at any time is the sum of elastic, viscoelastic, and viscoplastic deformations, it is not known how much of the axial displacement (Table 3) at any time was due to elastic deformation and how much due to plastic deformation. The magnitude of axial displacement was directly related to duration of loading and inversely related to t/D ratio and conical angle (Figures 8 and 9). It is known from previous test programs that the magnitude of axial displacement is also directly related to (1) ambient temperature, (2) the hydrostatic pressure level, and (3) diameter of the window D.

Although the magnitude of axial displacement under 5,000-psi sustained loading decreased as the t/D ratio of the windows was increased, a minimum was reached beyond which no further significant decrease in displacement was achieved by further increases in t/D ratios. The t/D ratios at which the displacements remained relatively constant under 5,000-psi sustained loading varied with the conical angle. These t/D ratios were >1.000, 1.000, 0.750, 0.750, and 0.625 for 30-, 60-, 90-, 120-, and 150-degree conical angles, respectively.

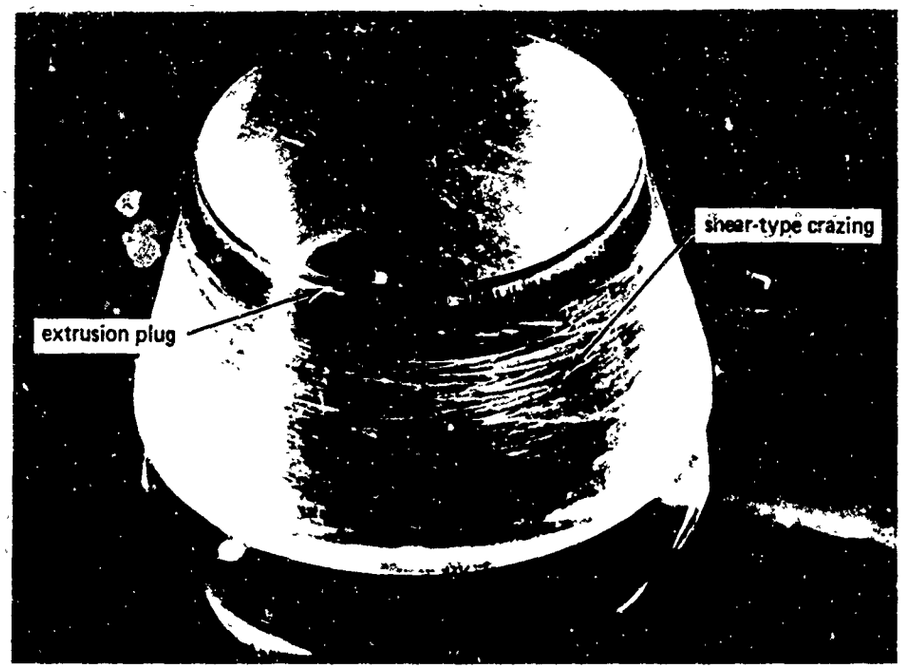

Figure 12. Shear-type crazing found on conical bearing surface of 30-degree acrylic windows with t/D ratio = 0.375 after sustained loading at 5,000 psi for 1,000 hours.

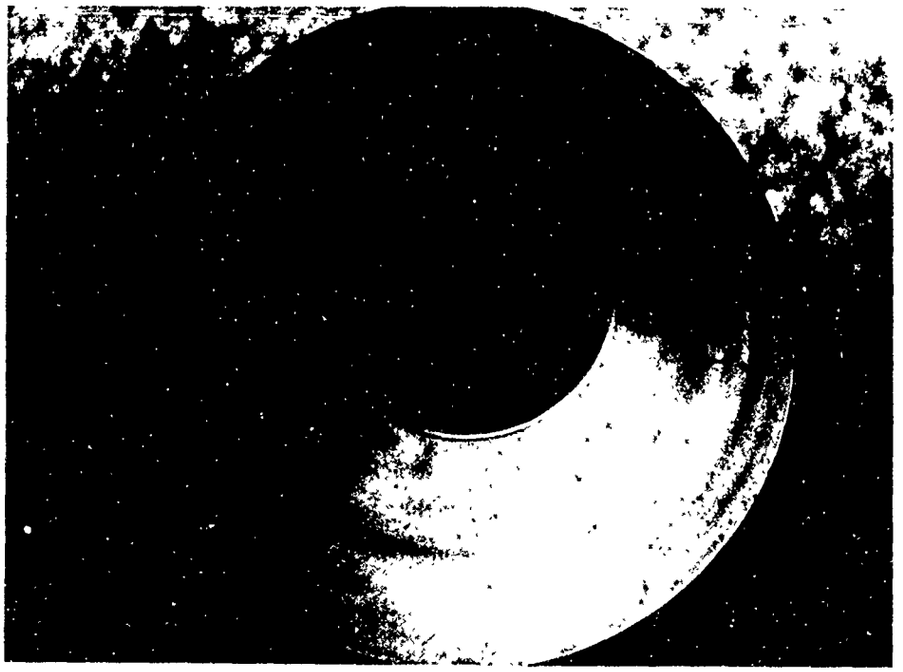

Figure 13. Flexure-type star-shaped crack found in center of low-pressure face on 90-degree conical window with t/D ratio = 0.375 after sustained loading at 5,000 psi for 1,000 hours.

Table 3. Average Displacement of Conical Acrylic Windows Measured After 1-, 10-, 100-, 500-, and 1,000-Hour Intervals During Sustained Loading at 5,000 Psi

Thickness-to-Minor-Diameter Ratio, t/D	Included Conical Angle, α (deg)	Average Displacement (in.) After—				
		1 Hour	10 Hours	100 Hours	500 Hours	1,000 Hours
0.375	30	0.345	–	–	–	–
	60	0.036	0.042	0.048	0.062	0.072
	90	0.028	0.032	0.040	0.044	0.047
	120	0.026	0.029	0.034	0.039	0.041
	150	0.026	0.029	0.036	0.041	0.044
0.500	30	0.074	0.086	0.100	0.106	0.112
	60	0.025	0.028	0.030	0.031	0.032
	90	0.024	0.025	0.027	0.028	0.030
	120	0.020	0.021	0.024	0.025	0.028
	150	0.023	0.024	0.026	0.027	0.028
0.625	30	0.054	0.056	0.058	0.058	0.059
	60	0.024	0.025	0.027	0.028	0.029
	90	0.023	0.024	0.026	0.027	0.028
	120	0.021	0.021	0.023	0.024	0.025
	150	0.015	0.016	0.017	0.018	0.019
0.750	30	0.042	0.046	0.048	0.049	0.050
	60	0.022	0.023	0.023	0.024	0.025
	90	0.020	0.021	0.022	0.023	0.023
	120	0.016	0.016	0.018	0.018	0.019
	150	0.017	0.018	0.019	0.020	0.021
1.000	30	0.040	0.040	0.041	0.041	0.042
	60	0.020	0.021	0.021	0.022	0.023
	90	0.023	0.023	0.024	0.024	0.024
	120	0.014	0.015	0.016	0.017	0.017
	150	0.018	0.019	0.020	0.021	0.022

FINDINGS

1. The axial displacement of the conical acrylic window through the flange opening, the deformation of the high- and low-pressure faces, and the severity of surface cracks are direct functions of time under sustained 5,000-psi hydrostatic loading and inverse functions of t/D ratio and included conical angle.

2. Cracking was observed only on the conical bearing surface of windows with $\alpha \leq 60$ degrees, while star-shaped cracks in the center of the window's low-pressure face were seen only on windows with $\alpha \geq 90$ degrees.

3. No cracks were observed after a single sustained loading of 1,000 hours at 5,000 psi in windows with adequately large t/D ratios. These ratios were $\geq$1.000, 0.625, 0.500, 0.500, and 0.500 for 30-, 60-, 90-, 120-, and 150-degree included angles, respectively.

4. No further decrease in axial displacement was achieved by the selection of windows with t/D ratios larger than >1.000, 1.000, 0.750, 0.750, 0.625, for 30-, 60-, 90-, 120-, and 150-degree included angles, respectively.

5. The minimum axial displacements after 1,000-hour sustained loading at 5,000 psi that could be achieved by increasing the t/D of windows with D = 1.000 inch were: 0.042, 0.023, 0.023, 0.019, and 0.019 inch for 30-, 60-, 90-, 120-, and 150-degree included angles, respectively.

CONCLUSIONS

Conical acrylic windows are suitable for applications under long-term sustained hydrostatic loading of 5,000 psi providing the proper t/D ratio for a given conical angle is chosen. Only windows with $\alpha \geq 60$ degrees and t/D $\geq$ 0.625, or $\alpha \geq 90$ degrees and t/D $\geq$ 0.500 will provide safe and crack-free service for sustained loading of 1,000 hours duration where maximum operational pressure is 5,000 psi.

RECOMMENDATIONS

For the design and fabrication of conical acrylic windows under long-term hydrostatic loading of 5,000 psi, detailed information and specifications contained in Appendixes A and B should be taken into consideration.

Appendix A

DISPLACEMENT OF CONICAL ACRYLIC WINDOWS UNDER SUSTAINED HYDROSTATIC LOADING AT 5,000 PSI

Each of the conical acrylic windows subjected to sustained 5,000-psi hydrostatic loading experienced axial displacement through the flange opening. There were three distinct phases in the axial displacement of each window. The first phase took place when the pressure was raised at a 650-psi/minute rate from 0 to 5,000 psi. The second phase was relatively rapid axial displacement of the window through the flange immediately after the 5,000-psi sustained pressure loading was reached. The second phase lasted for approximately 12 to 24 hours. The third phase of axial displacement was the relatively slow axial displacement of the window during the remaining duration of sustained pressure loading at 5,000 psi. To emphasize and delineate the three distinct phases of axial displacement, two different scales were used for plotting the displacements. Log-log scales with 0.001-inch displacement and 1-minute time units were selected to show the rapid rate of displacement of the windows during phases 1 and 2. Linear scales with 0.002-inch displacement and 1-day time units were chosen to show the slow rate of displacement during phase 3. To permit rapid visual comparison of the two different displacement phases, they are grouped together in Figures A-1 through A-5 for each different window configuration.

When one observes the graphs depicting phases 1, 2, and 3, one immediately notes that the relationship between time and magnitude of axial displacement is not shown graphically by a narrow line but by a wide band whose width and shape varies from one figure to another. There are several reasons.

1. Each curve represents the range of displacements shown by a group of five window specimens which were not of identical dimensions, but varied by the magnitude of dimensional machining tolerances.

2. All of the five windows comprising a single t/D ratio group for a given angle were not tested in the same flange, but in several flanges that differed from each other by the magnitude of dimensional machining tolerances and surface finish.

3. All five windows in a group were not tested at an identical temperature. The average temperature varied several degrees from one long-term test to another.

4. All of the five windows were not machined from the same piece of material, or for that matter at the same machining rate.

There are several general observations that can be made about the scatter of recorded displacement data. First, the width of the plotted displacement range appears to be in a large measure a function of absolute displacement magnitude; (that is, at small displacements the range is narrow, while for large displacements the range is large). Second, displacements of windows that are accompanied by extensive cracking and fracturing of the acrylic material vary more from one specimen in the same group to another than the displacements of windows not accompanied by extensive cracking. This phenomenon in all probability is caused by the randomness of crack initiation and propagation, as compared to the nonrandomness of typical stress–strain behavior of material before cracking.

For some t/D ratio groups (Figure A-1a) there are no graphs depicting phase 3 of window displacement because all of the windows in that group failed prior to the termination of the 1,000-hour tests.

When the data contained in Figures A-1 through A-5 are used for design of operational windows, the upper boundary of displacement ranges should be utilized. It represents a conservative approach to sizing of window flange cavities for containment of windows during their displacement under sustained hydrostatic pressure of 5,000 psi. For design of windows that will be used at a sustained pressure of less than 5,000 psi, the lower boundary of the displacement range should be utilized, as otherwise the design of flange cavity becomes too conservative.

Since the axial displacements shown in Figures A-1 through A-5 have been experimentally generated by testing of model scale windows with 1-inch minor diameter, the data can be applied *directly* without any modification *only* to prediction of displacements for windows with D = 1.000 inch. The displacements of windows with diameters larger than 1.000 inch can be predicted also, but the displacements shown in Figures A-1 through A-5 have to be modified by a linear scaling factor which is a function of D. Thus, for example, the displacements of 90-degree windows with t/D = 0.500 and D = 6.000 inch will be larger by a factor of six than those shown in Figure A-3b for 90-degree windows with t/D = 0.500 and D = 1.000 inch. The validity of the linear scaling factor for prediction of axial displacement of windows under short-term and long-term hydrostatic loadings has been experimentally proved in previous studies.[1,4,5]

Note: Day scale not present as window blew out.

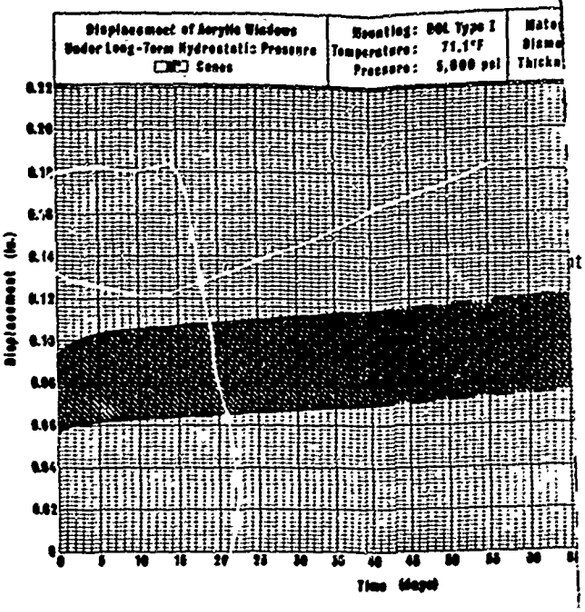

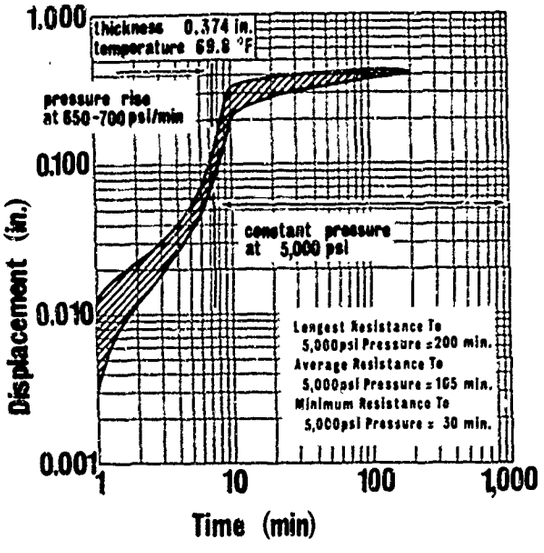

Figure A-1a. Displacement of conical acrylic plastic windows under 5,000-psi sustained pressure loading; 30-degree included angle with t/D ratio = 0.375.

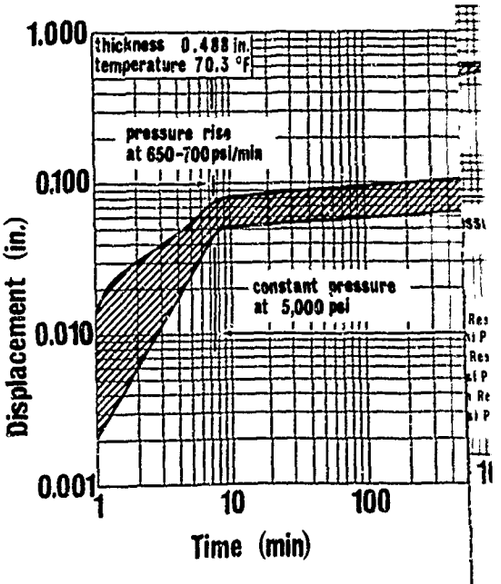

Figure A-1b. Displacement of conical acrylic plastic wi
5,000-psi sustained pressure loading; 30-d
angle with t/D ratio = 0.500.

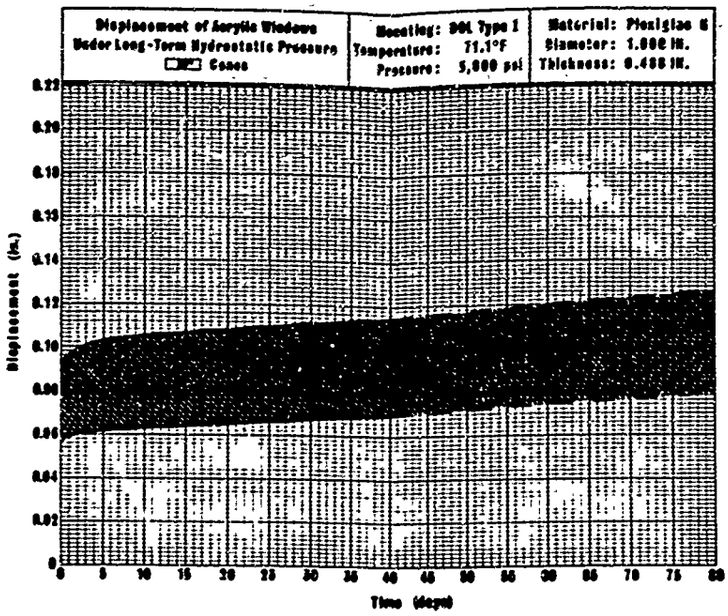

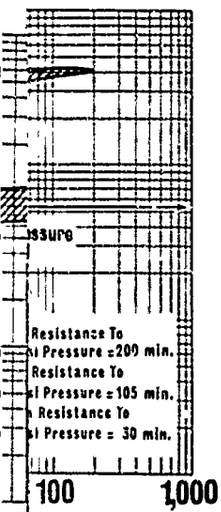

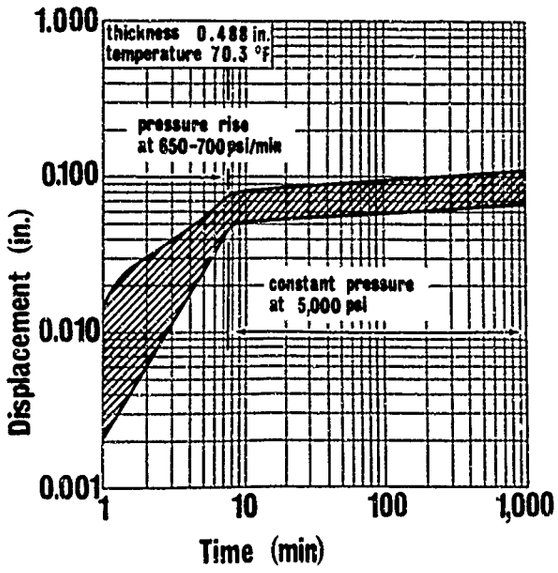

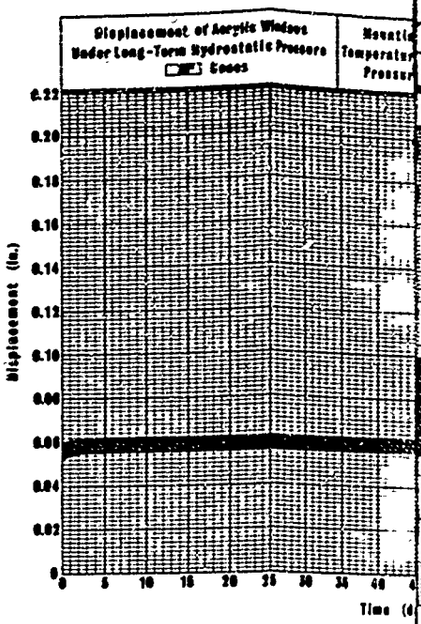

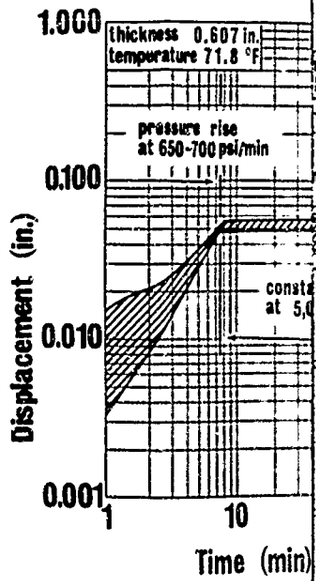

ic plastic windows under
wi pading; 30-degree included
-de

Figure A-1b. Displacement of conical acrylic plastic windows under 5,000-psi sustained pressure loading; 30-degree included angle with t/D ratio = 0.500.

Figure A-1c. Displacement of conical ac
5,000-psi sustained pressur
angle with t/D ratio = 0.62

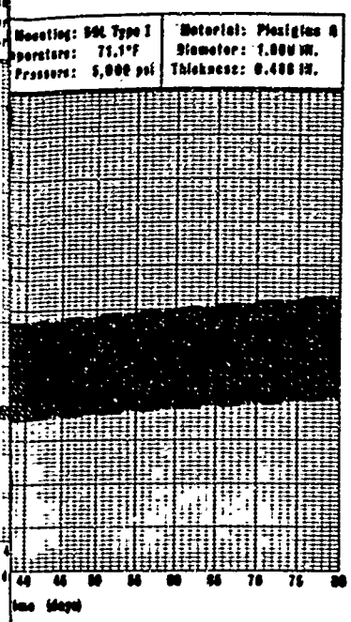

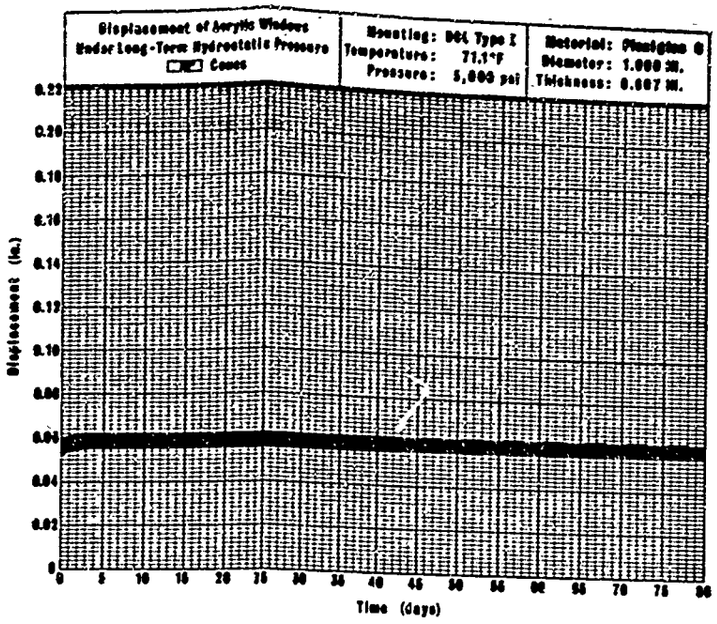

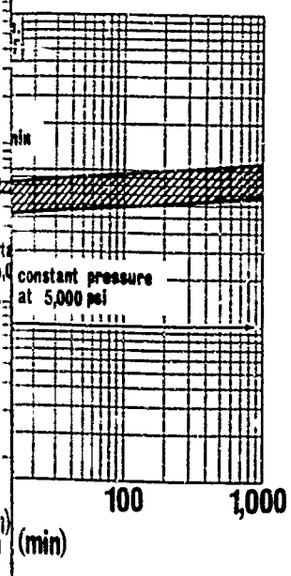

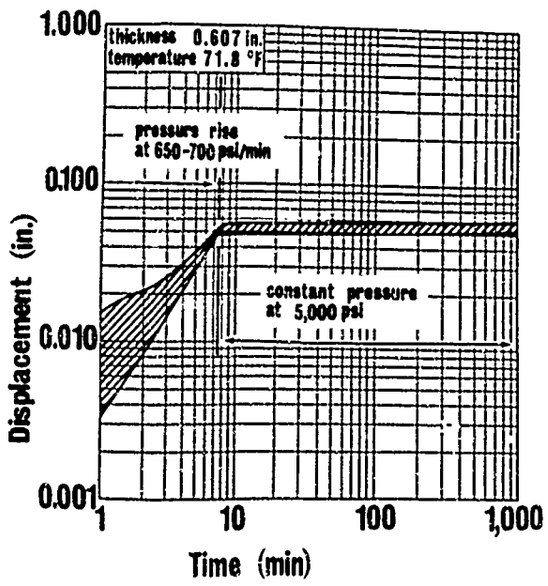

nical acrylic plastic windows under
pressure loading; 30-degree included
= 0.500.

Figure A-1c. Displacement of conical acrylic plastic windows under 5,000-psi sustained pressure loading; 30-degree included angle with t/D ratio = 0.625.

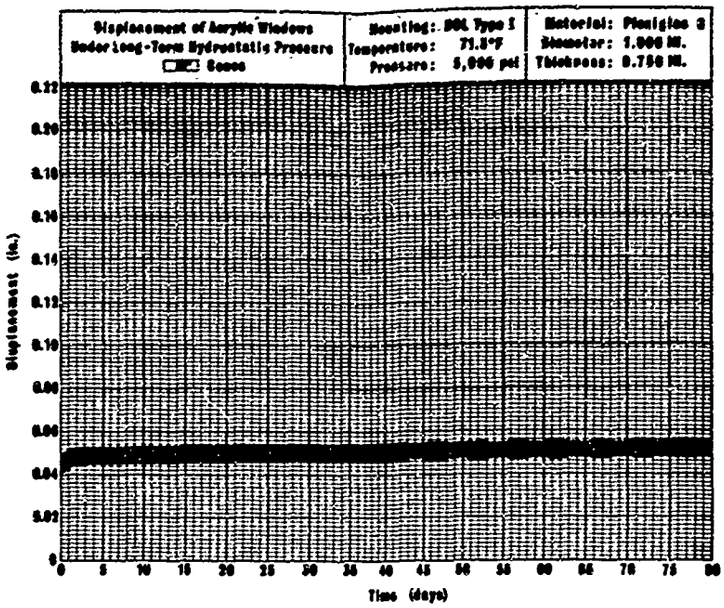

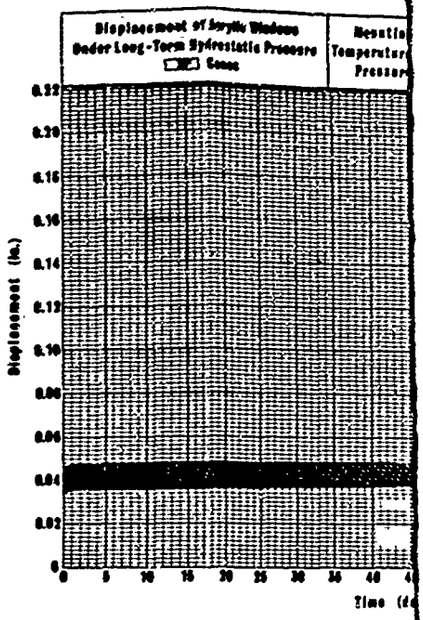

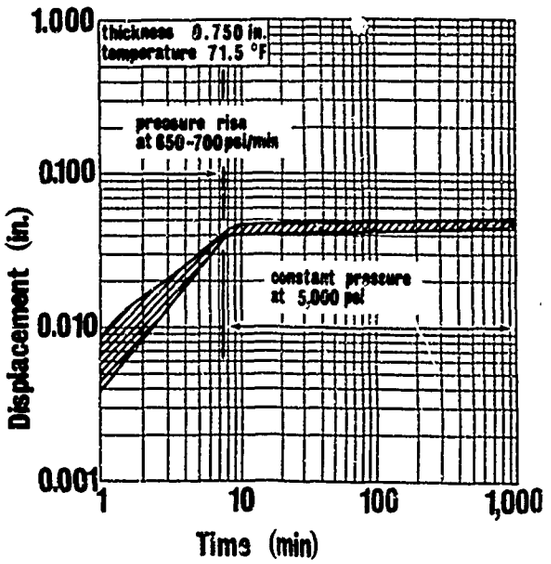

Figure A-1d. Displacement of conical acrylic plastic windows under 5,000-psi sustained pressure loading; 30-degree included angle with t/D ratio = 0.750.

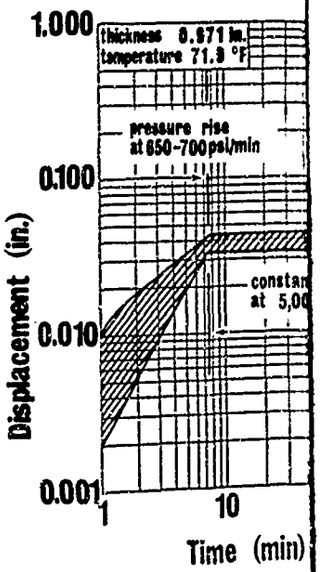

Figure A-1e. Displacement of conica
5,000-psi sustained pre
angle with t/D ratio =

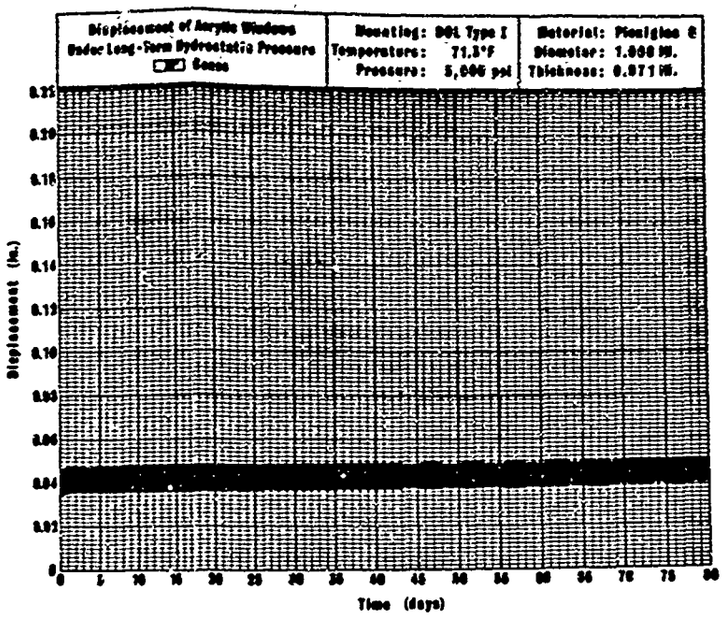

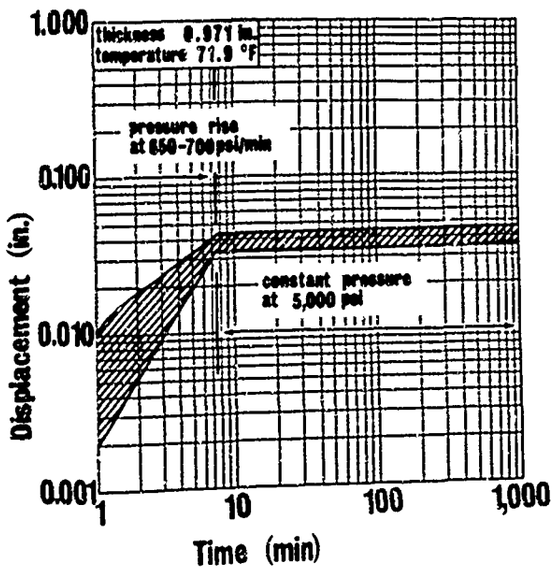

Figure A-1e. Displacement of conical acrylic plastic windows under 5,000-psi sustained pressure loading; 30-degree included angle with t/D ratio = 1.000.

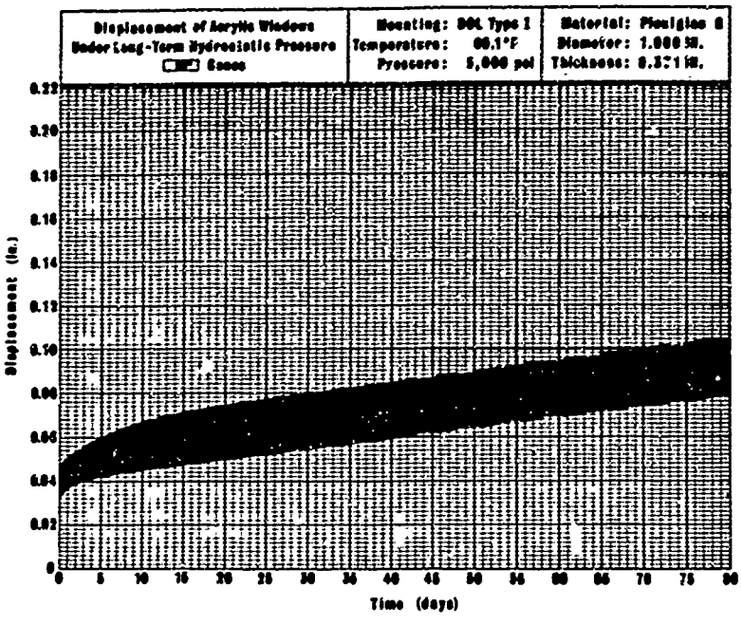

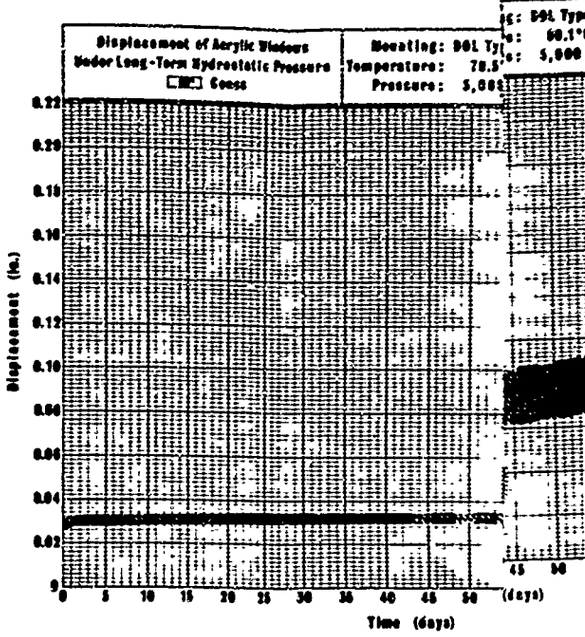

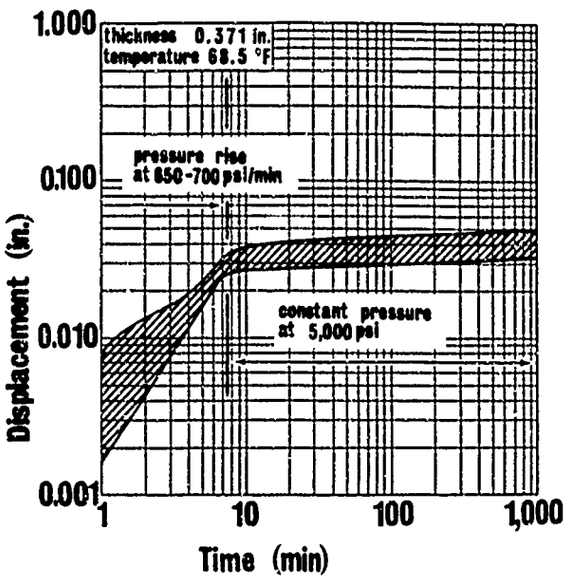

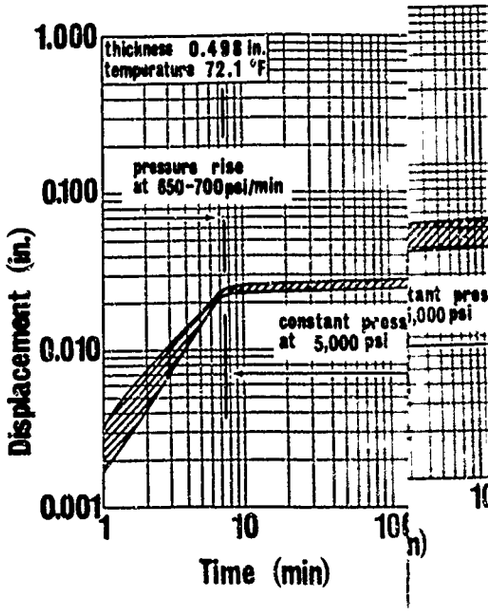

Figure A-2a. Displacement of conical acrylic plastic windows under 5,000-psi sustained pressure loading; 60-degree included angle with t/D ratio = 0.375.

Figure A-2b. Displacement of conical acrylic plastic windows under 5,000-psi sustained pressure loading; 60-degree included angle with t/D ratio = 0.500.

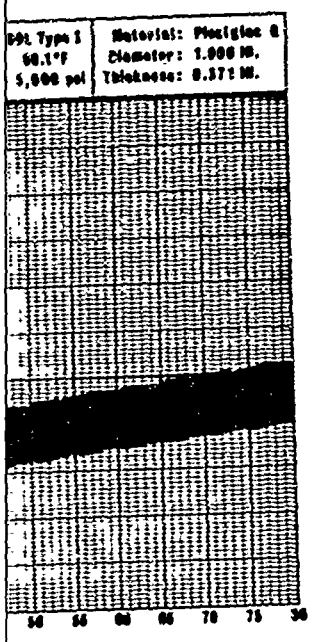

a)

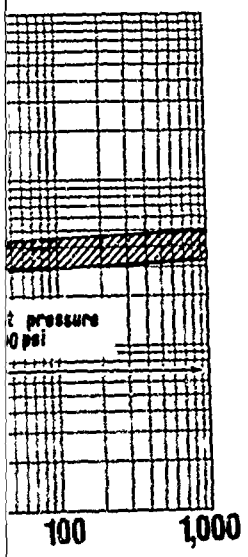

rylic plastic windows under
e loading; 60-degree included
75.

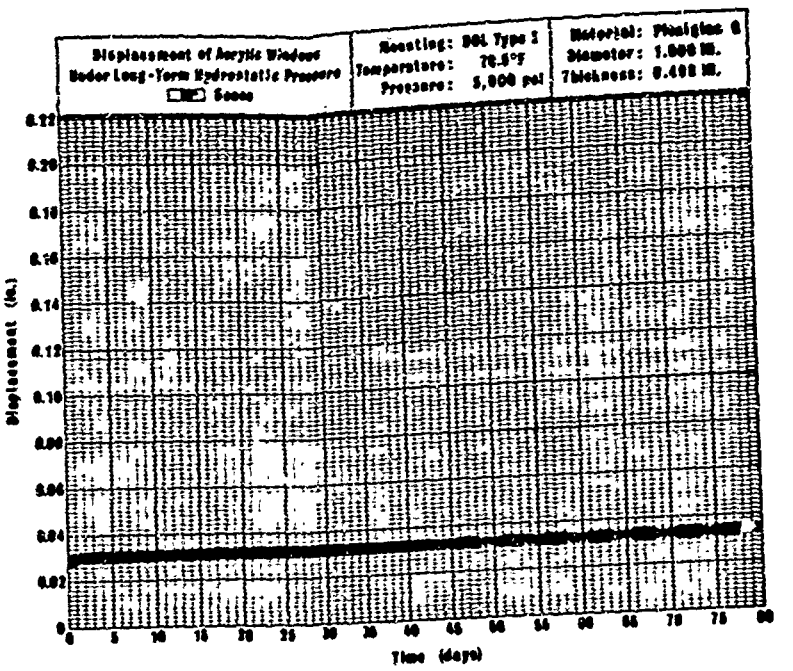

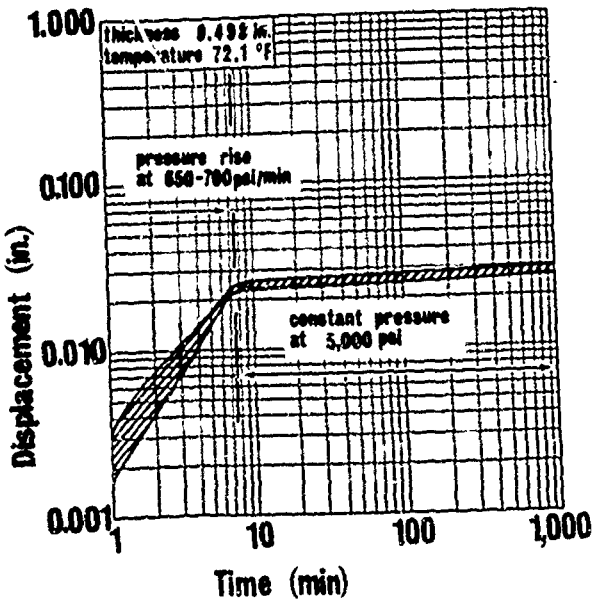

Figure A-2b. Displacement of conical acrylic plastic windows under 5,000-psi sustained pressure loading; 60-degree included angle with t/D ratio = 0.500.

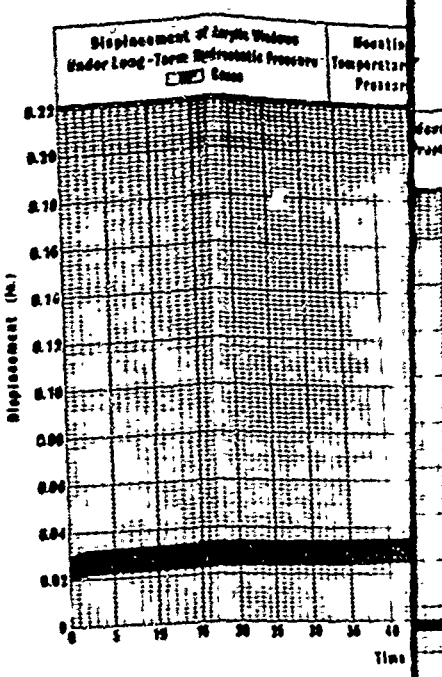

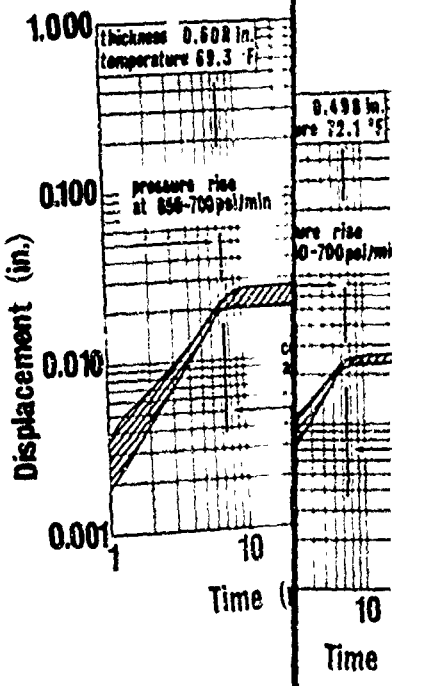

Figure A-2c. Displacement of conic
5,000-psi sustained p
angle with t/D ratio =

ent of cor
sustained
t/D ratio

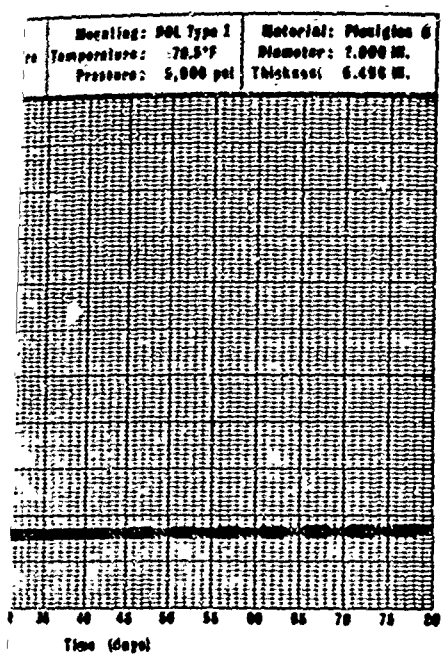

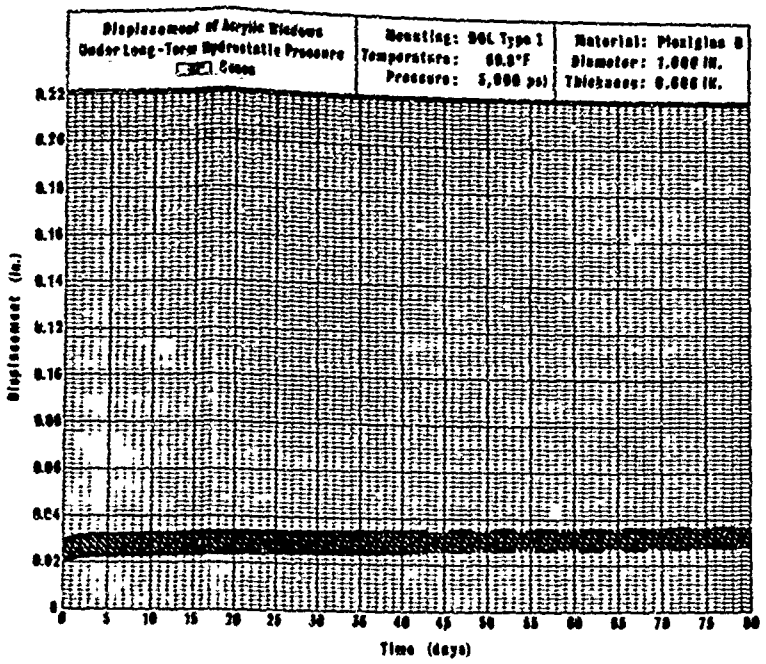

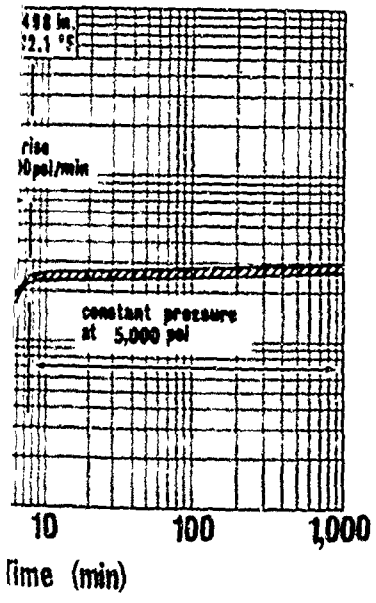

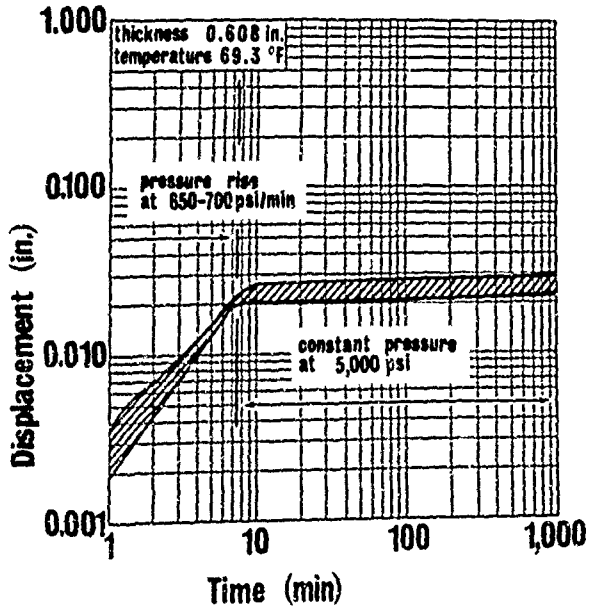

of conical acrylic plastic windows under
ained pressure loading; 60-degree included
) ratio = 0.500.

Figure A-2c. Displacement of conical acrylic plastic windows under 5,000-psi sustained pressure loading; 60-degree included angle with t/D ratio = 0.625.

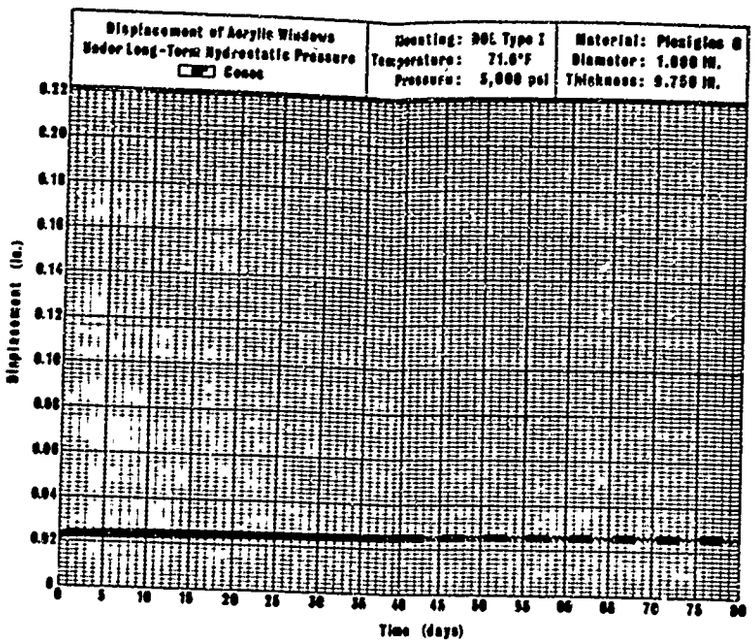

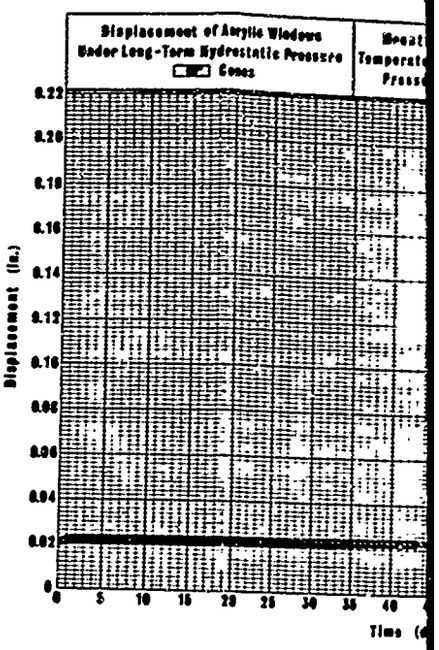

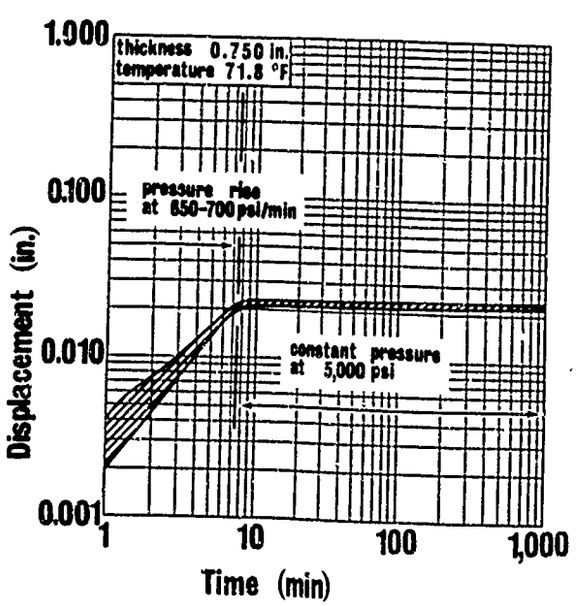

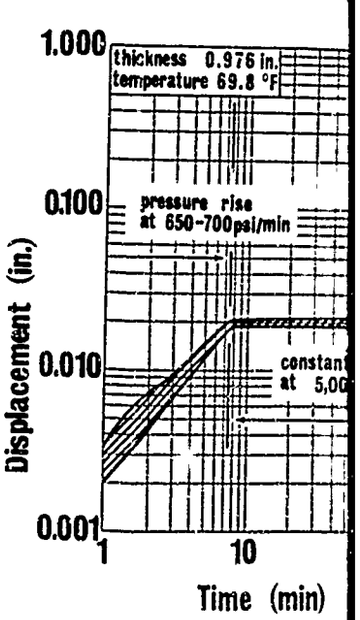

Figure A-2d. Displacement of conical acrylic plastic windows under 5,000-psi sustained pressure loading; 60-degree included angle with t/D ratio = 0.750.

Figure A-2e. Displacement of conical acry
5,000-psi sustained pressure
angle with t/D ratio = 1.000.

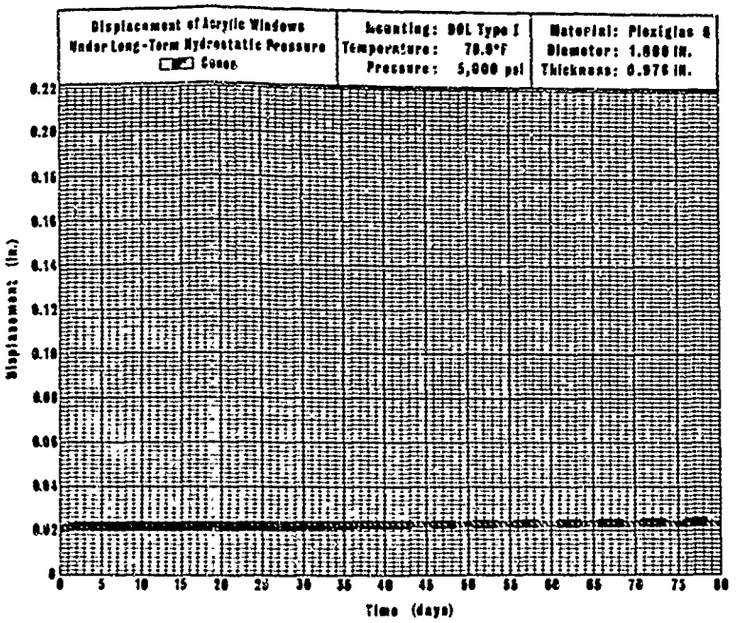

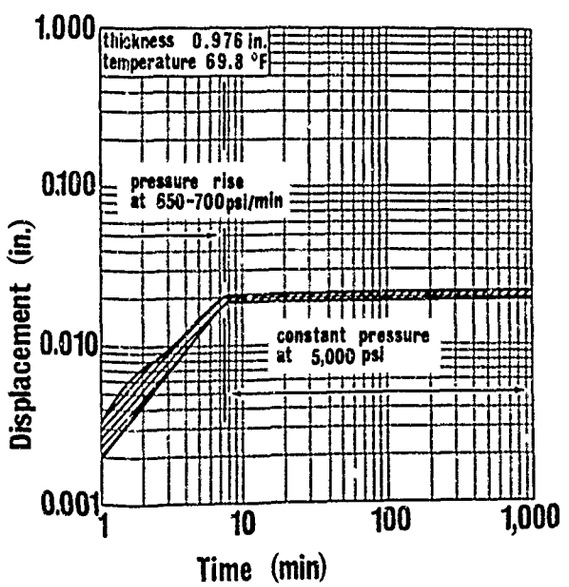

Figure A-2e. Displacement of conical acrylic plastic windows under 5,000-psi sustained pressure loading; 60-degree included angle with t/D ratio = 1.000.

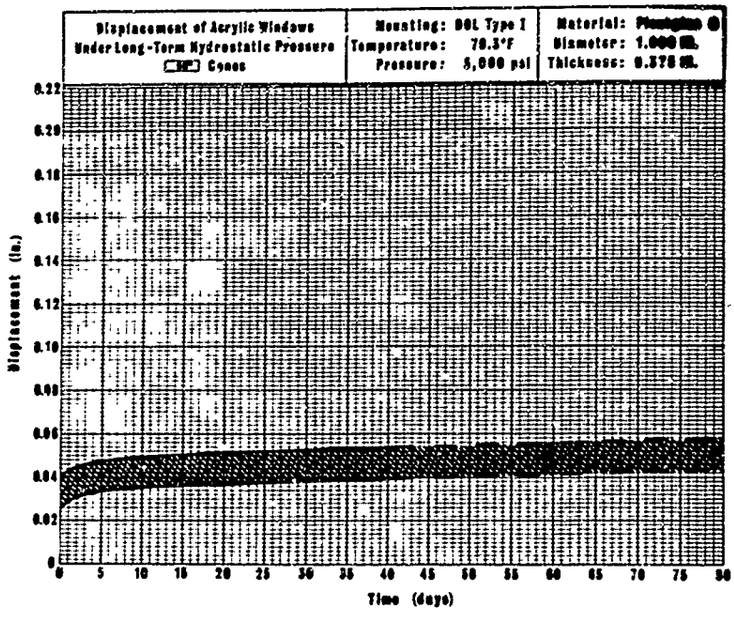

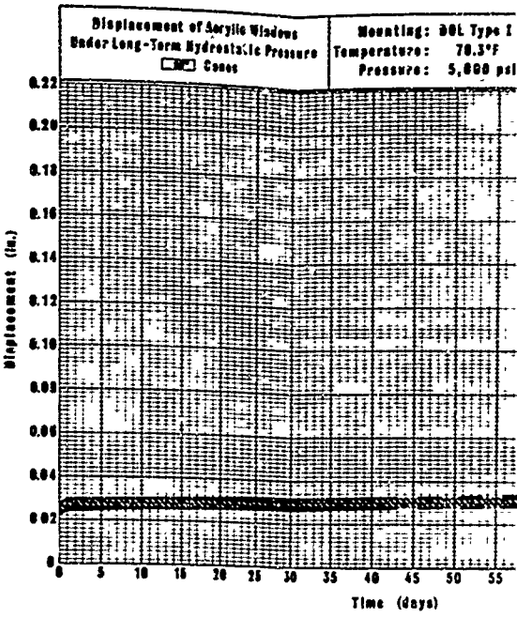

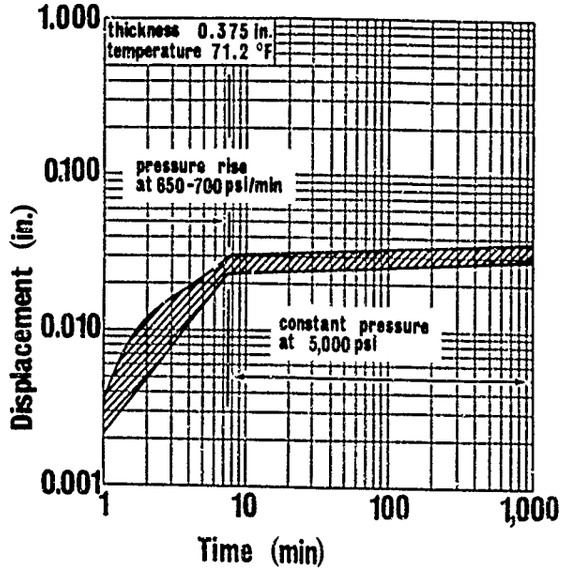

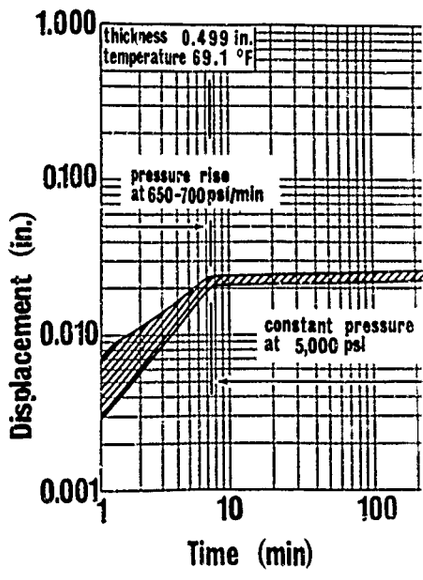

Figure A-3a. Displacement of conical acrylic plastic windows under 5,000-psi sustained pressure loading; 90-degree included angle with t/D ratio = 0.375.

Figure A-3b. Displacement of conical acrylic plastic 5,000-psi sustained pressure loading; 9 angle with t/D ratio = 0.500.

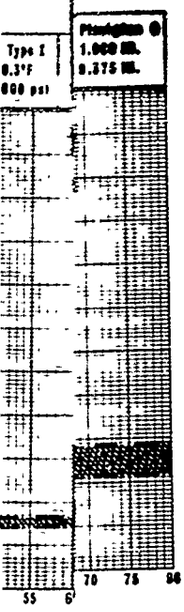

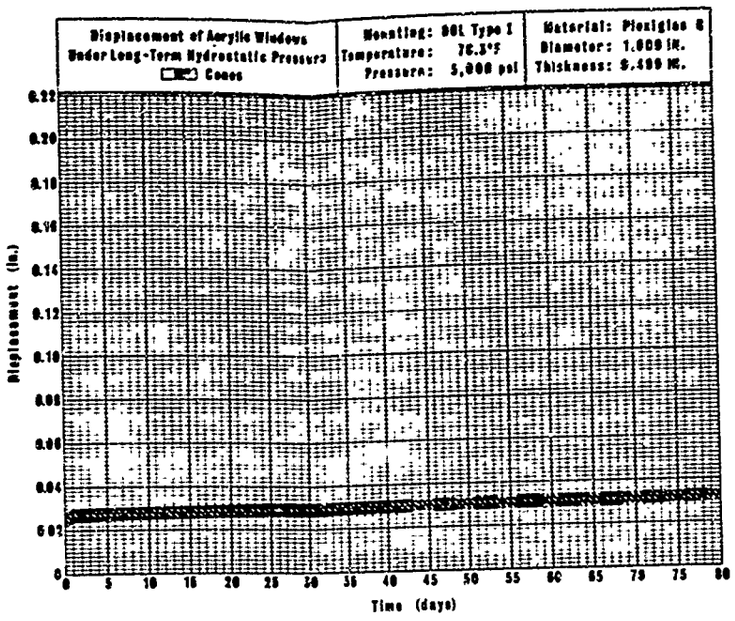

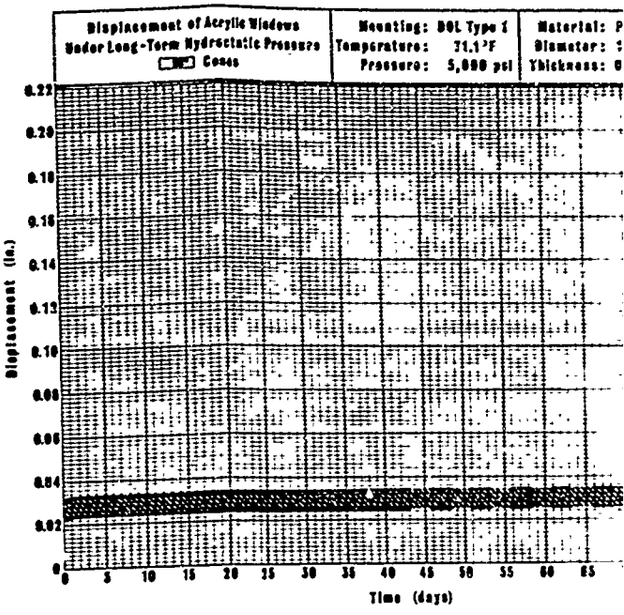

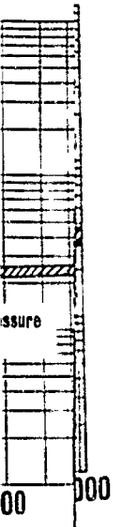

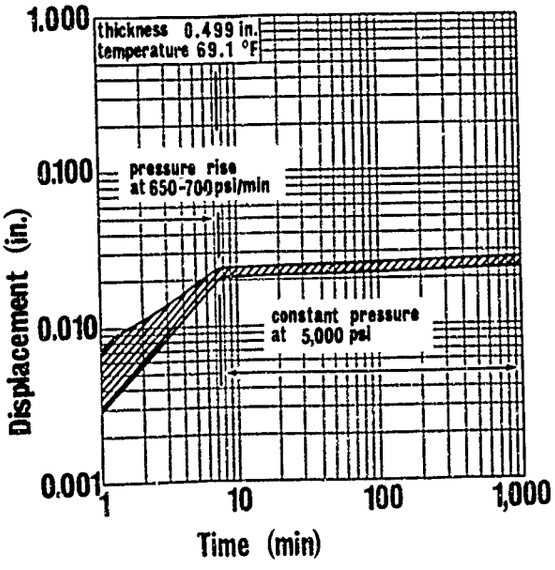

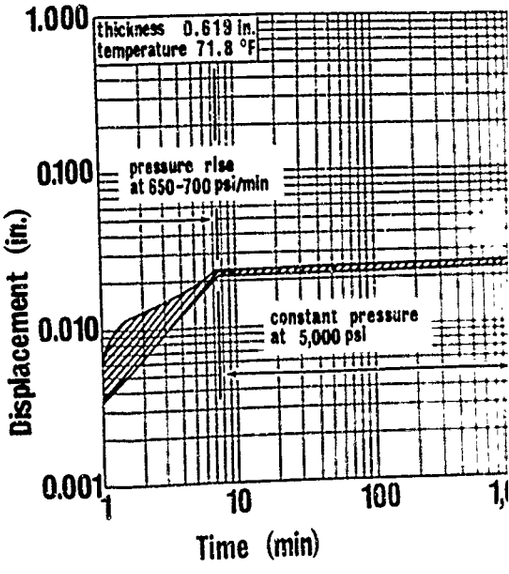

lastic w ws under
ing; 90- e included

Figure A-3b. Displacement of conical acrylic plastic windows under 5,000-psi sustained pressure loading; 90-degree included angle with t/D ratio = 0.500.

Figure A-3c. Displacement of conical acrylic plastic wind 5,000-psi sustained pressure loading; 90-deg angle with t/D ratio = 0.625.

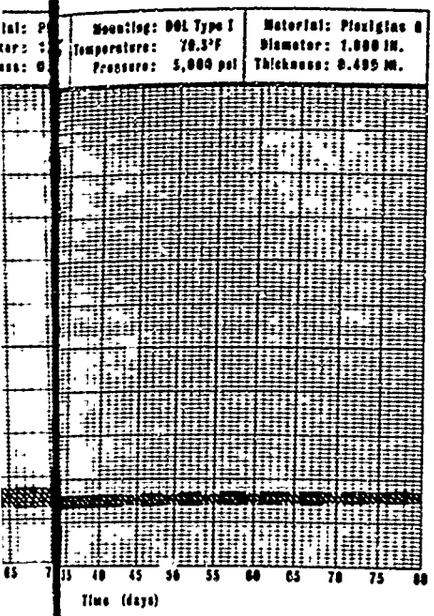

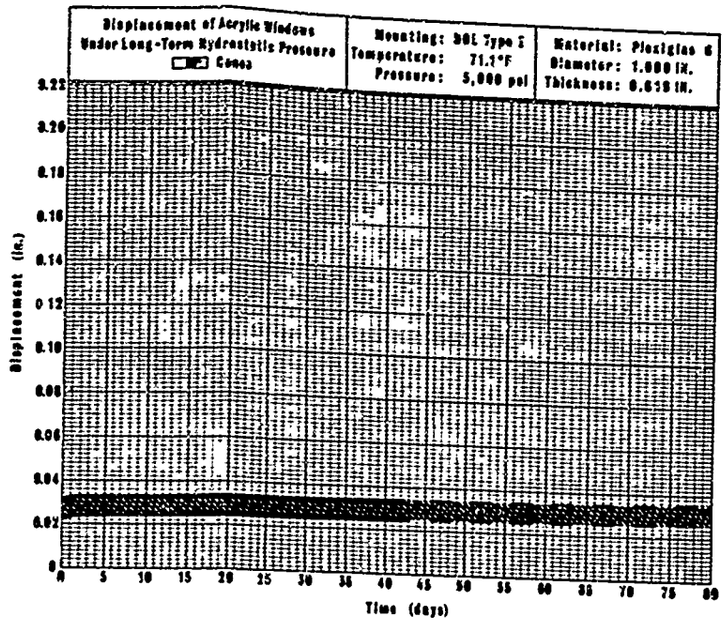

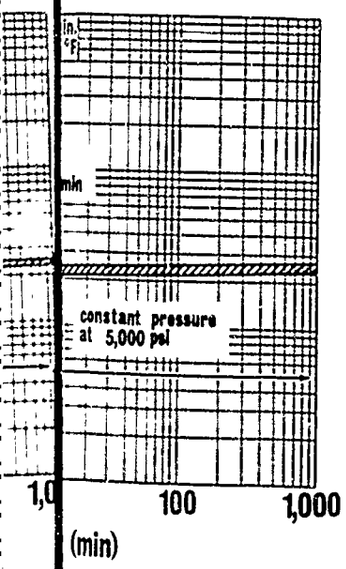

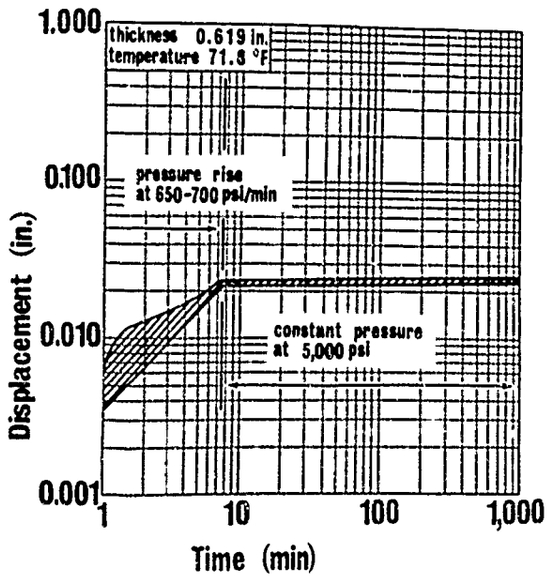

cal acrylic plastic windows under
essure loading; 90-degree included
0.500.

Figure A-3c. Displacement of conical acrylic plastic windows under 5,000-psi sustained pressure loading; 90-degree included angle with t/D ratio = 0.625.

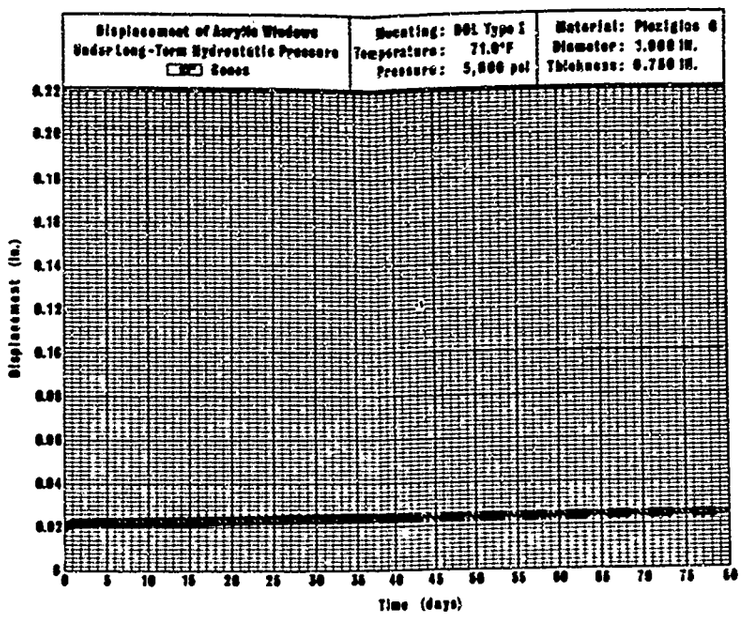

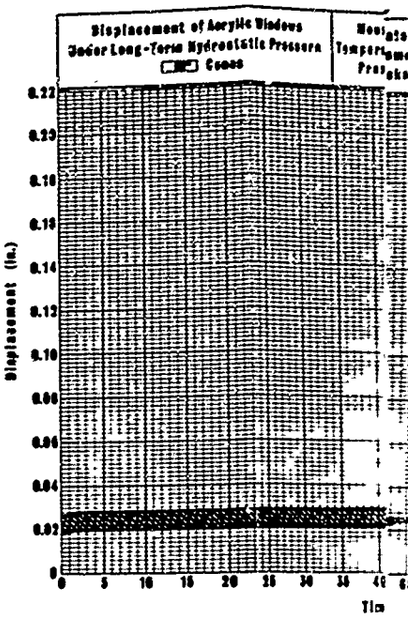

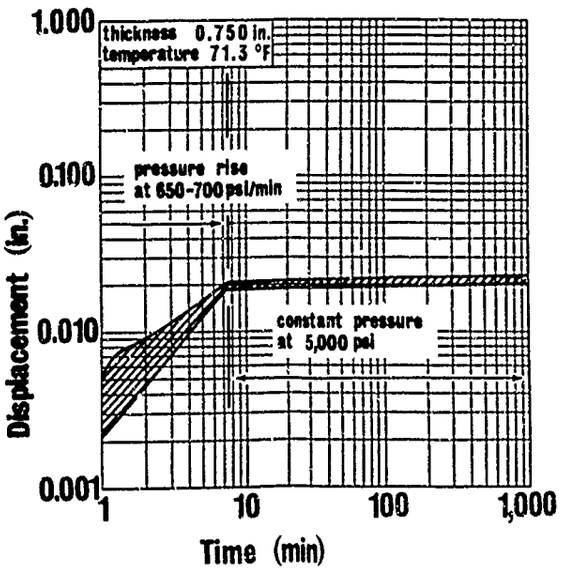

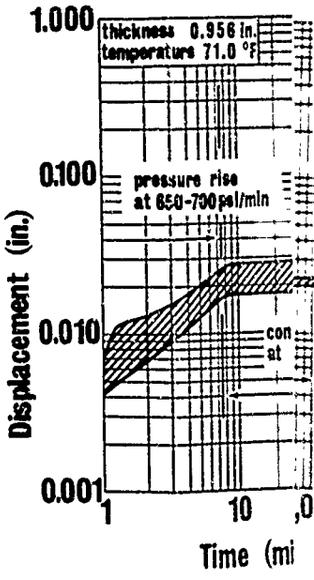

Figure A-3d. Displacement of conical acrylic plastic windows under 5,000-psi sustained pressure loading; 90-degree included angle with t/D ratio = 0.750.

Figure A-3e. Displacement of conical ov
5,000-psi sustained pressu
angle with t/D ratio = 1

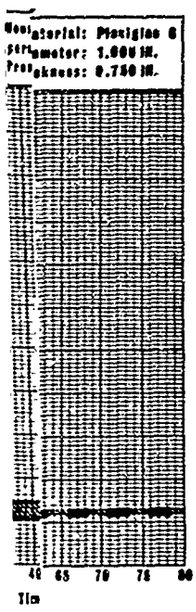

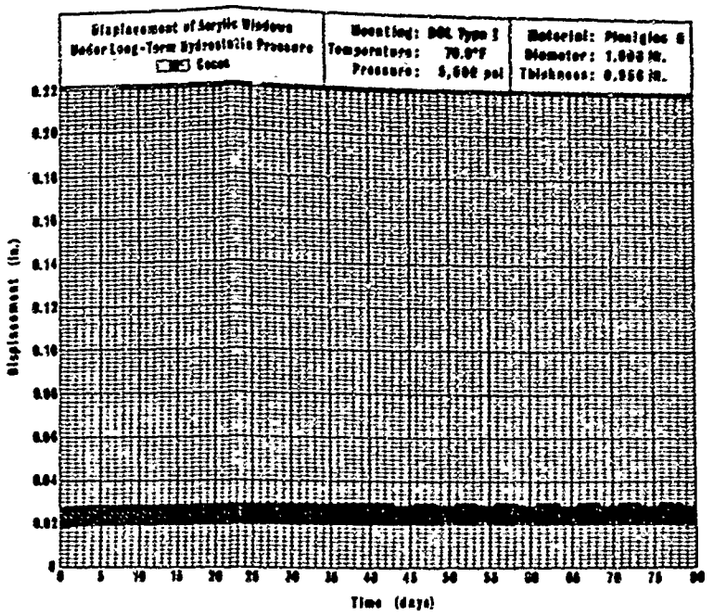

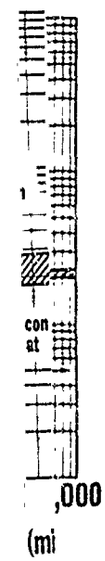

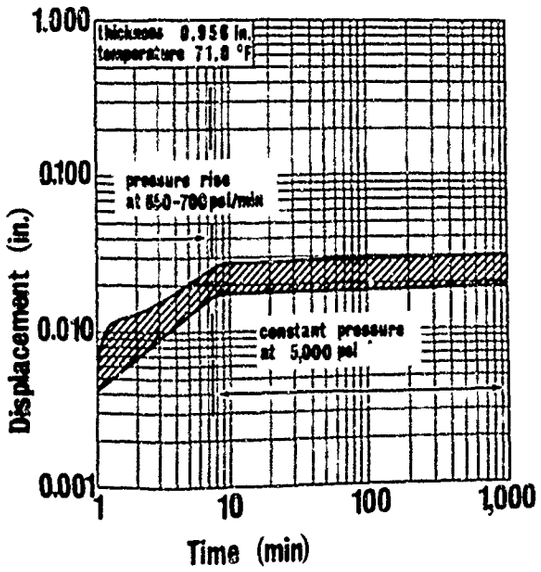

ical ows under
ressee included
= 1

Figure A-3e. Displacement of conical acrylic plastic windows under 5,000-psi sustained pressure loading; 90-degree included angle with t/D ratio = 1.000.

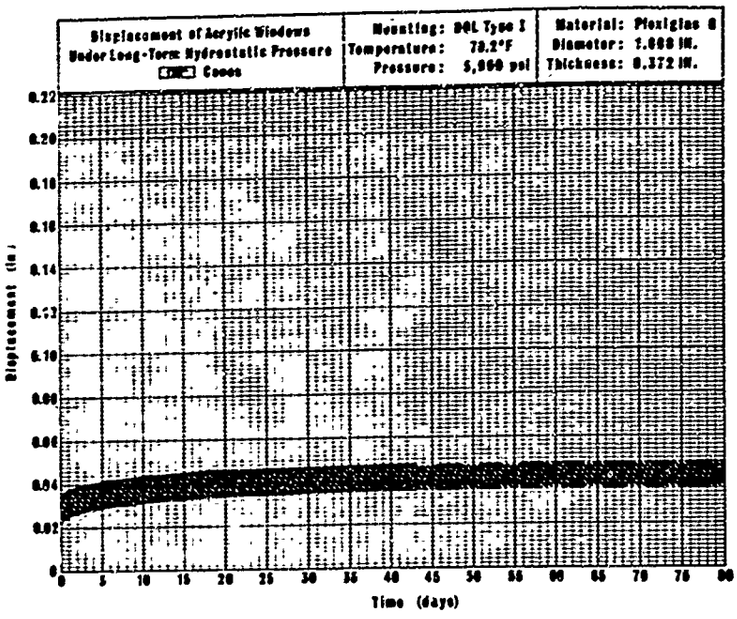

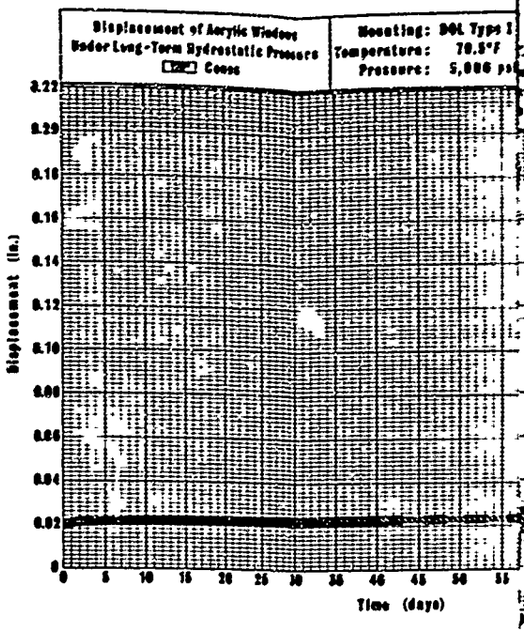

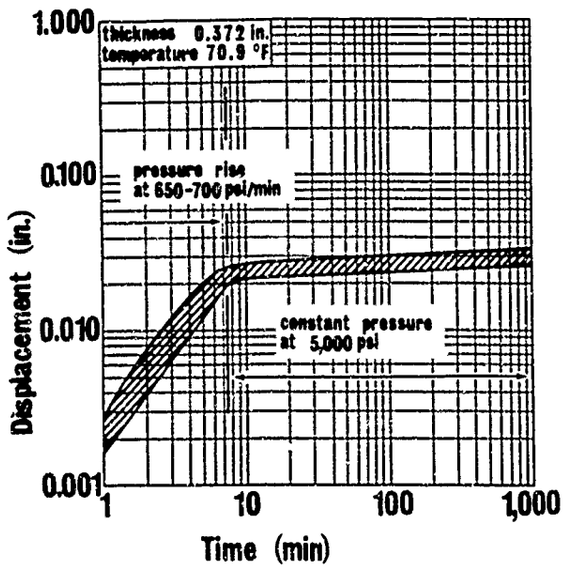

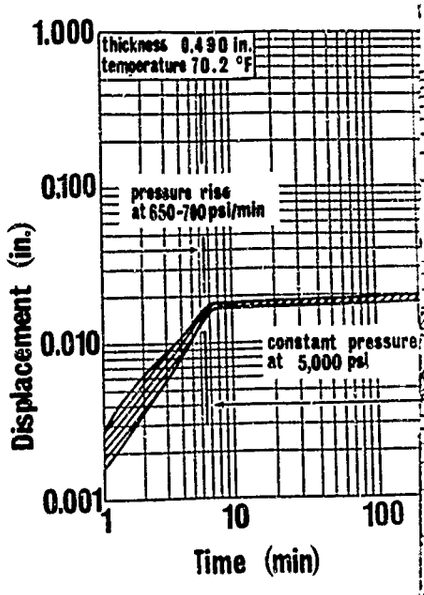

Figure A-4a. Displacement of conical acrylic plastic windows under 5,000-psi sustained pressure loading; 120-degree included angle with t/D ratio = 0.375.

Figure A-4b. Displacement of conical acrylic plasti 5,000-psi sustained pressure loading; angle with t/D ratio = 0.500.

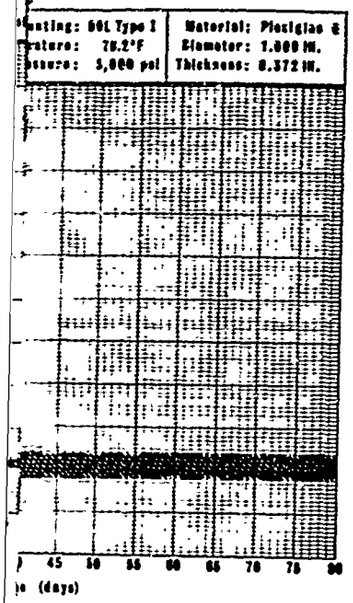

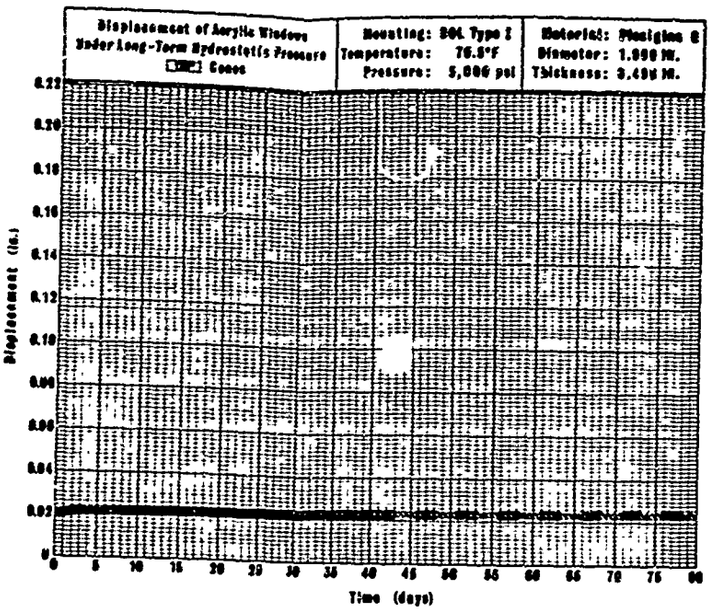

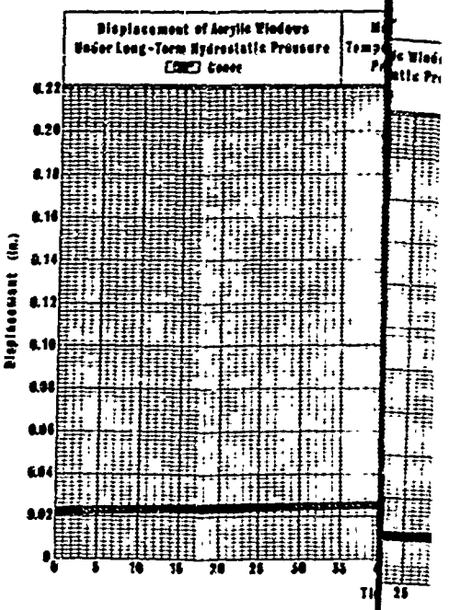

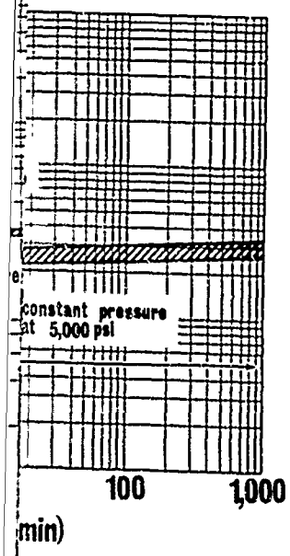

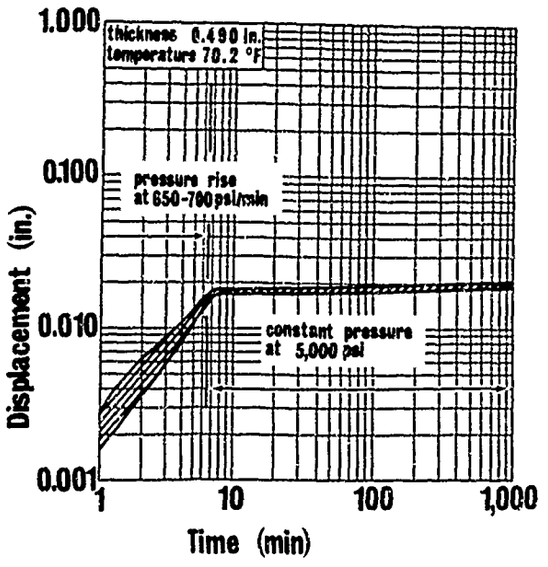

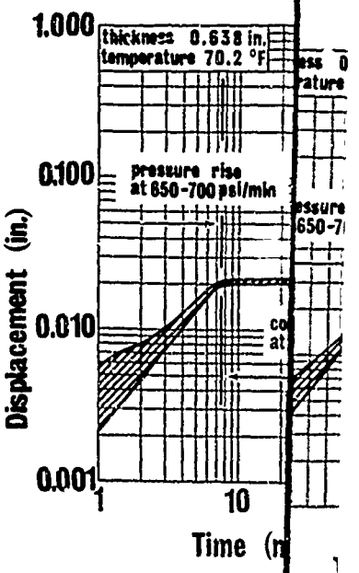

acrylic plastic windows under
ure loading; 120-degree included
375.

Figure A-4b. Displacement of conical acrylic plastic windows under 5,000-psi sustained pressure loading; 120-degree included angle with t/D ratio = 0.500.

Figure A-4c. Displacement of conica
5,000-psi sustained pres ent
angle with t/D ratio = susta
t/D

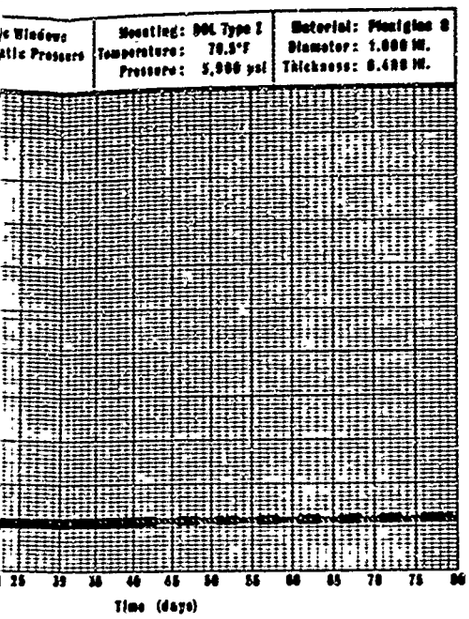

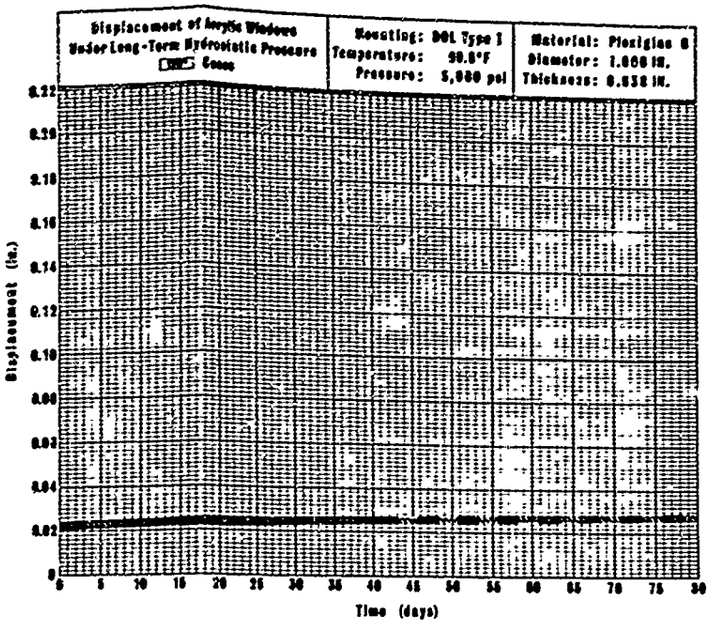

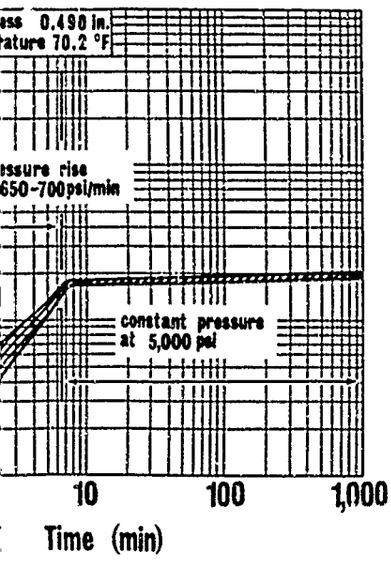

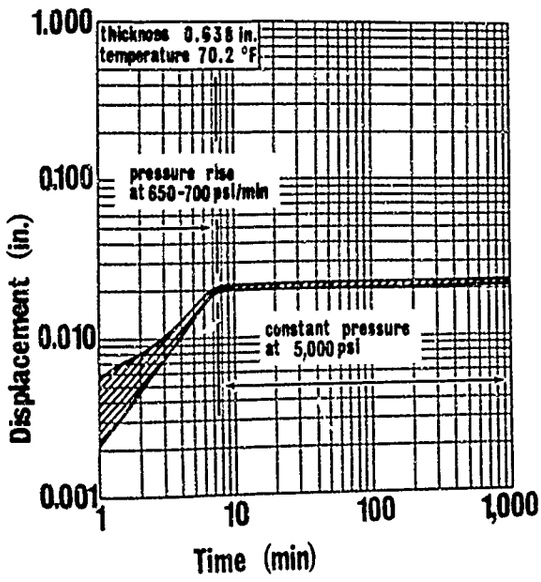

ent of conical acrylic plastic windows under
sustained pressure loading; 120-degree included
t/D ratio = 0.500.

Figure A-4c. Displacement of conical acrylic plastic windows under 5,000-psi sustained pressure loading; 120-degree included angle with t/D ratio = 0.625.

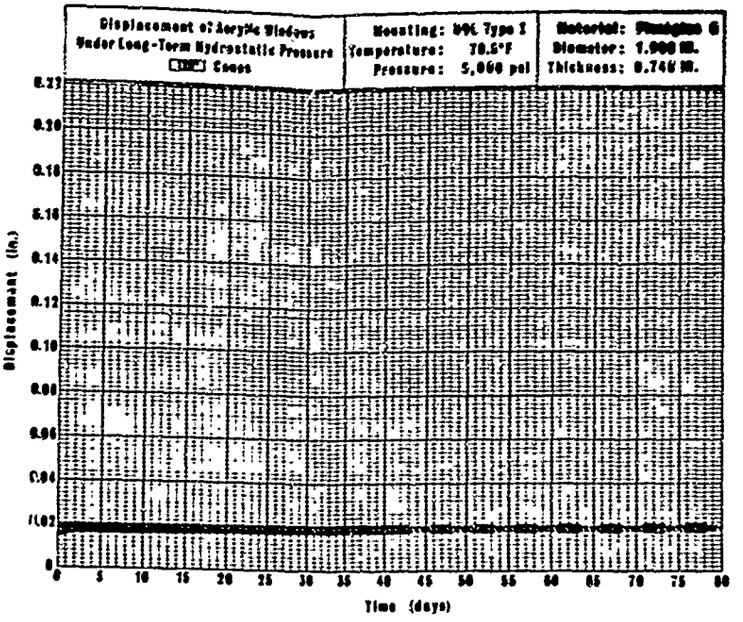

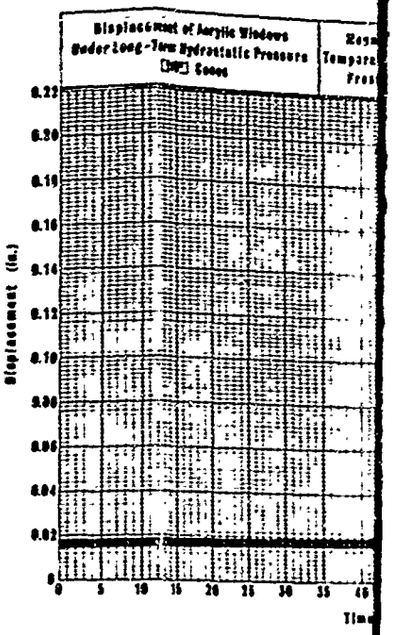

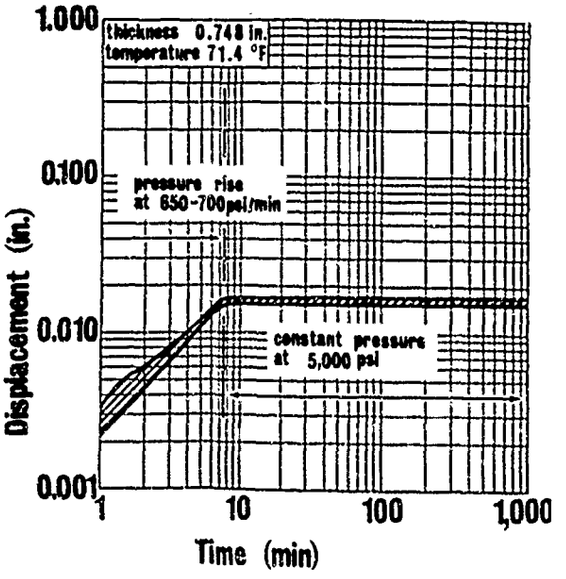

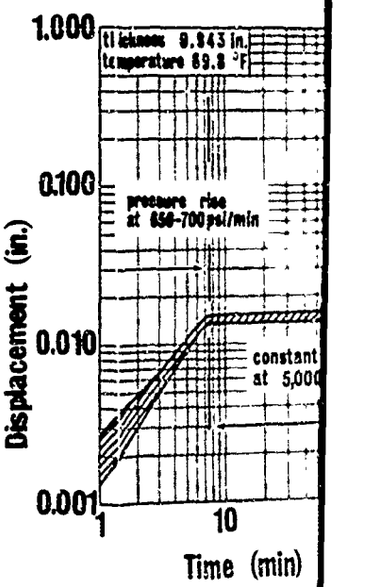

Figure A-4d. Displacement of conical acrylic plastic windows under 5,000-psi sustained pressure loading; 120-degree included angle with t/D ratio = 0.750.

Figure A-4e. Displacement of conical a
5,000-psi sustained pressu
angle with t/D ratio = 1.0

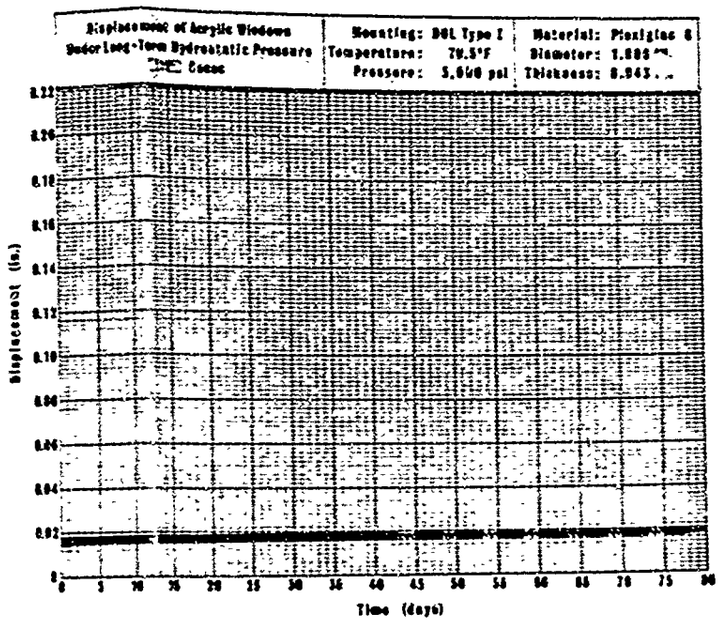

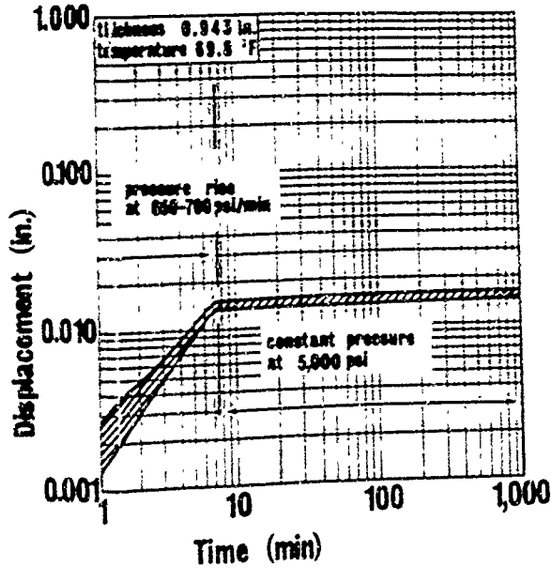

Figure A-4e. Displacement of conical acrylic plastic windows under 5,000-psi sustained pressure loading; 120-degree included angle with t/D ratio = 1.000.

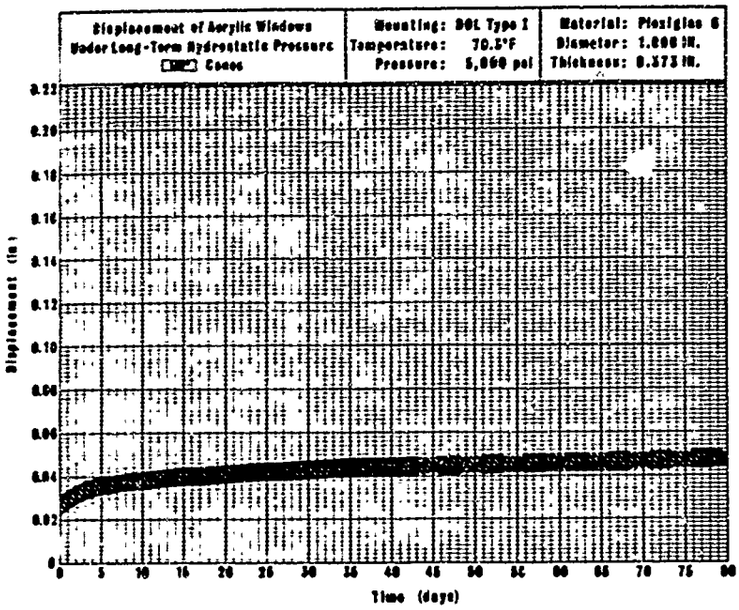

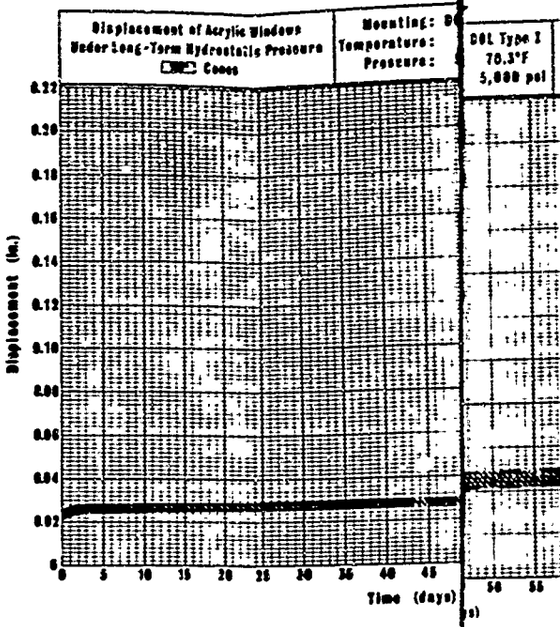

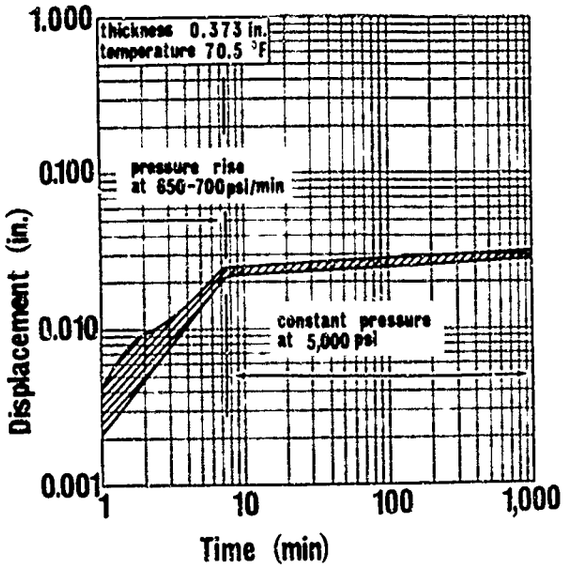

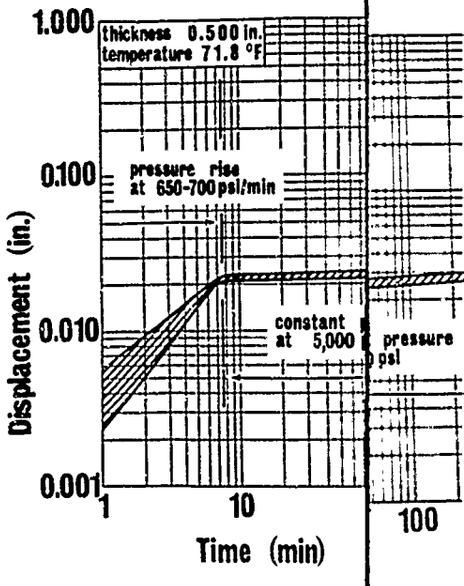

Figure A-5a. Displacement of conical acrylic plastic windows under 5,000-psi sustained pressure loading; 150-degree included angle with t/D ratio = 0.375.

Figure A-5b. Displacement of conical acry ylic plasti 5,000-psi sustained pressure loading; angle with t/D ratio = 0.500.

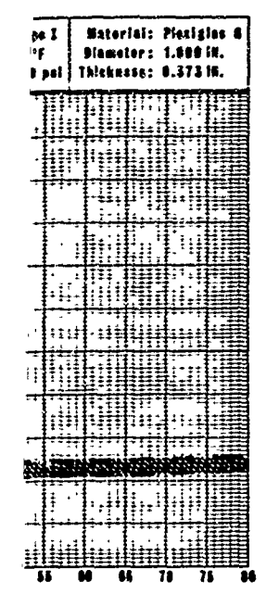

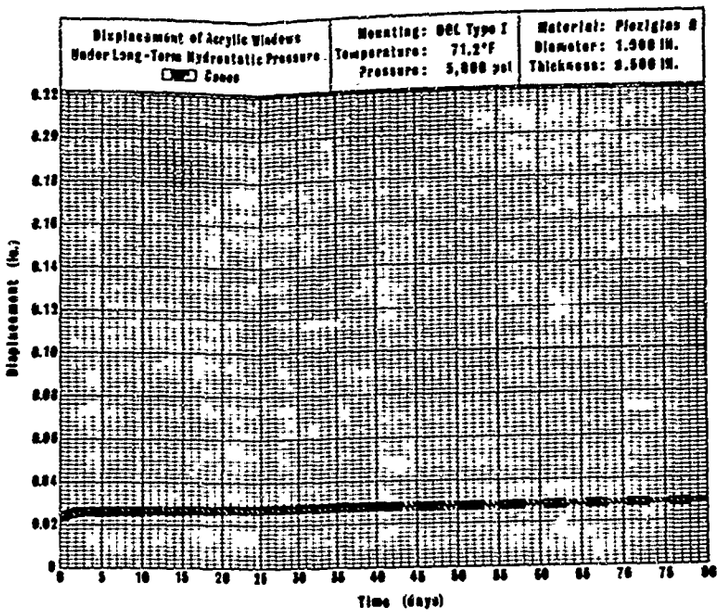

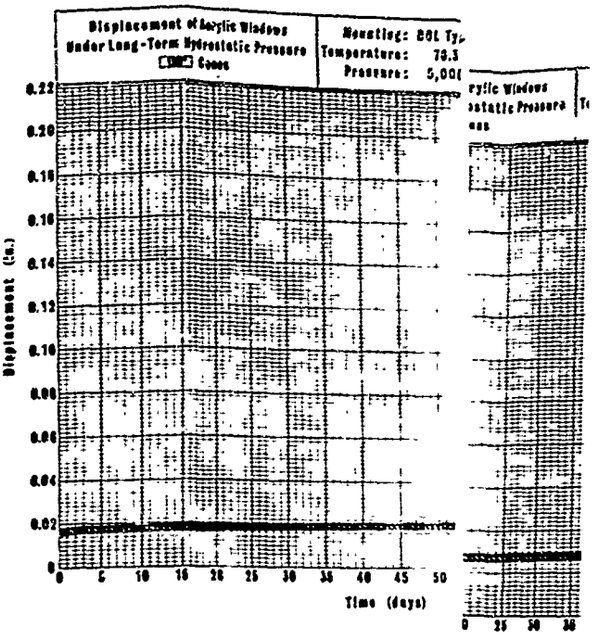

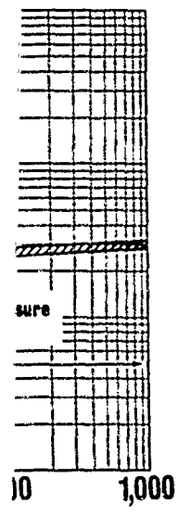

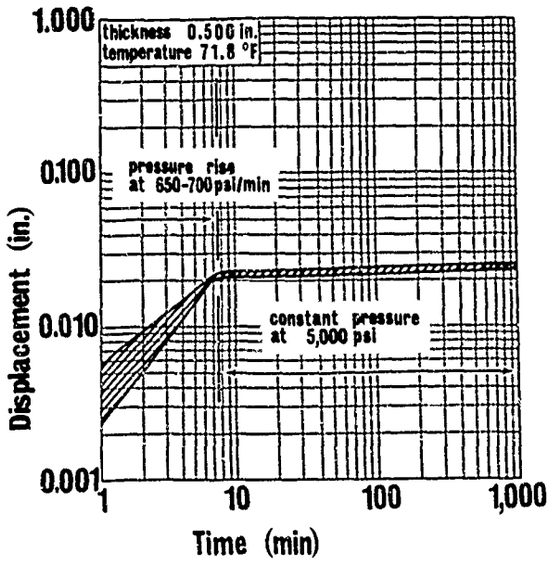

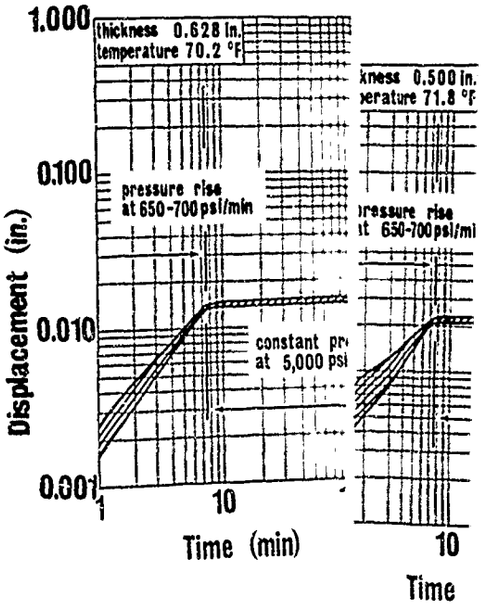

plastic windows under
ing; 150-degree included

Figure A-5b. Displacement of conical acrylic plastic windows under 5,000-psi sustained pressure loading; 150-degree included angle with t/D ratio = 0.500.

Figure A-5c. Displacement of conical acryli
5,000-psi sustained pressure lo
angle with t/D ratio = 0.625

acement of co
)-psi sustained
with t/D ratio

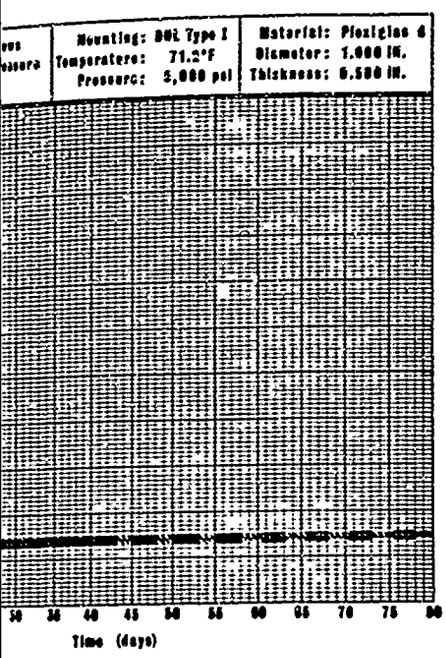

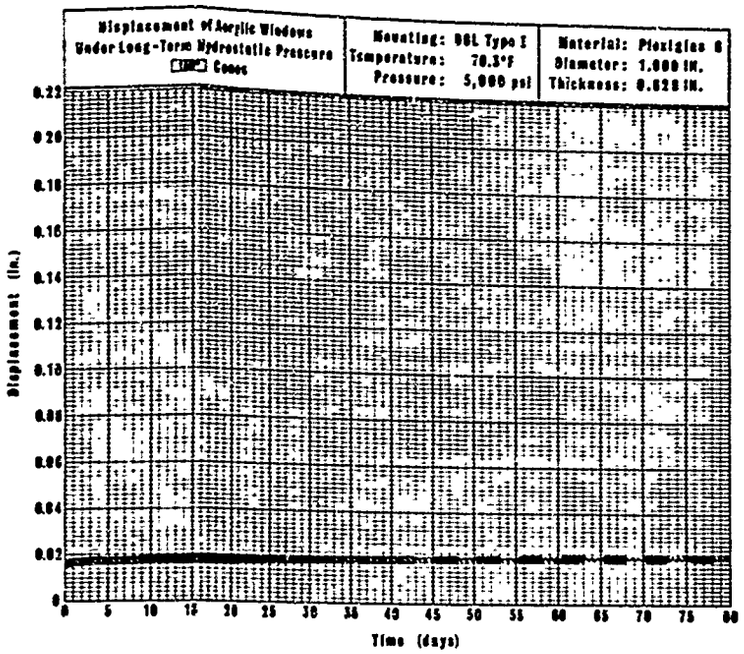

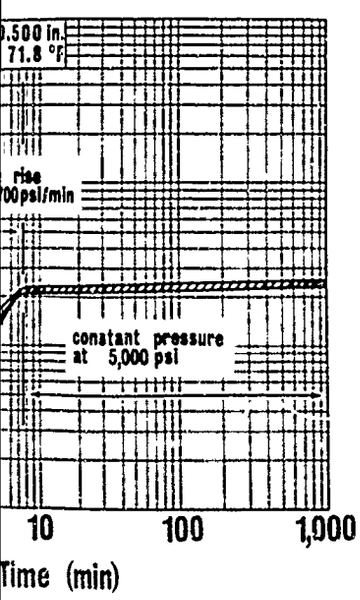

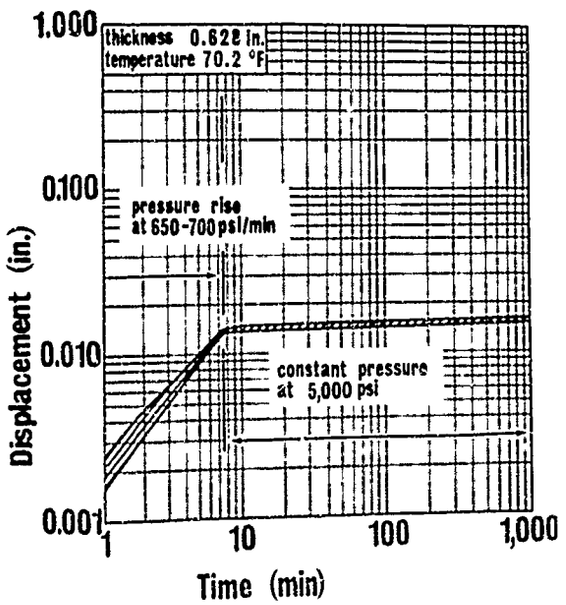

nt of conical acrylic plastic windows under
stained pressure loading; 150-degree included
/D ratio = 0.500.

Figure A-5c. Displacement of conical acrylic plastic windows under 5,000-psi sustained pressure loading; 150-degree included angle with t/D ratio = 0.625.

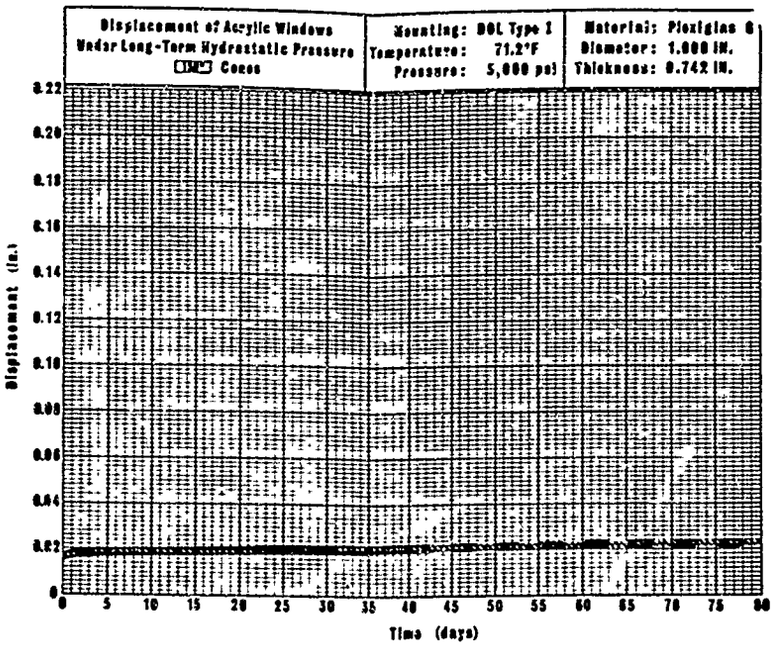

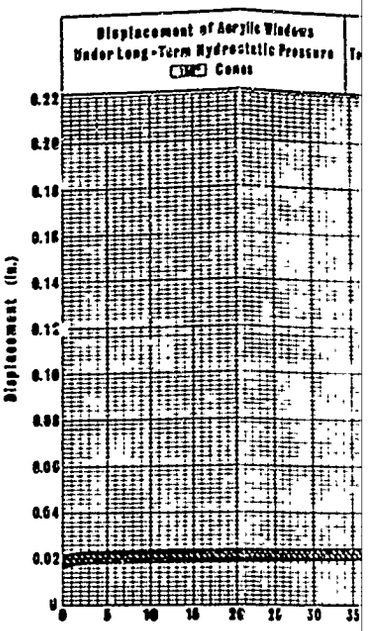

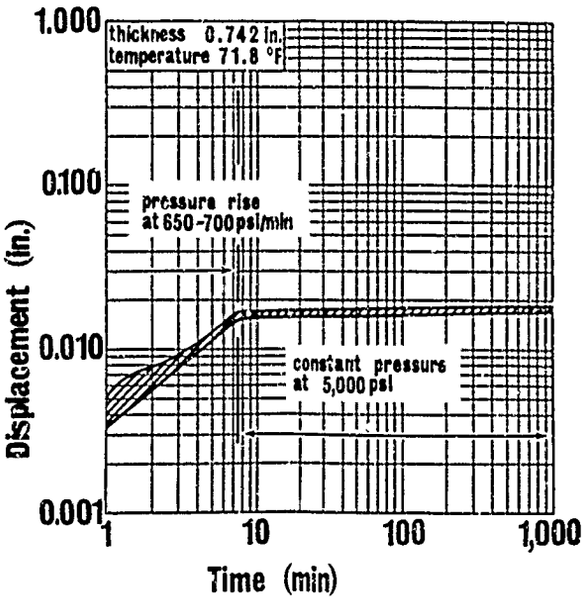

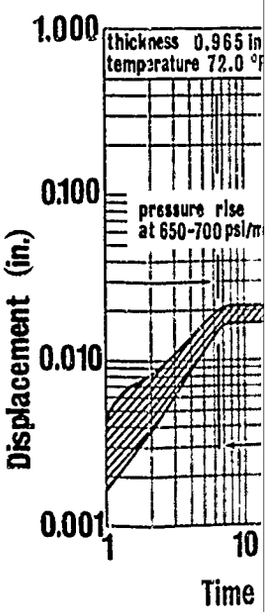

Figure A-5d. Displacement of conical acrylic plastic windows under 5,000-psi sustained pressure loading; 150-degree included angle with t/D ratio = 0.750.

Figure A-5e. Displacement of con
5,000-psi sustained p
angle with t/D ratio =

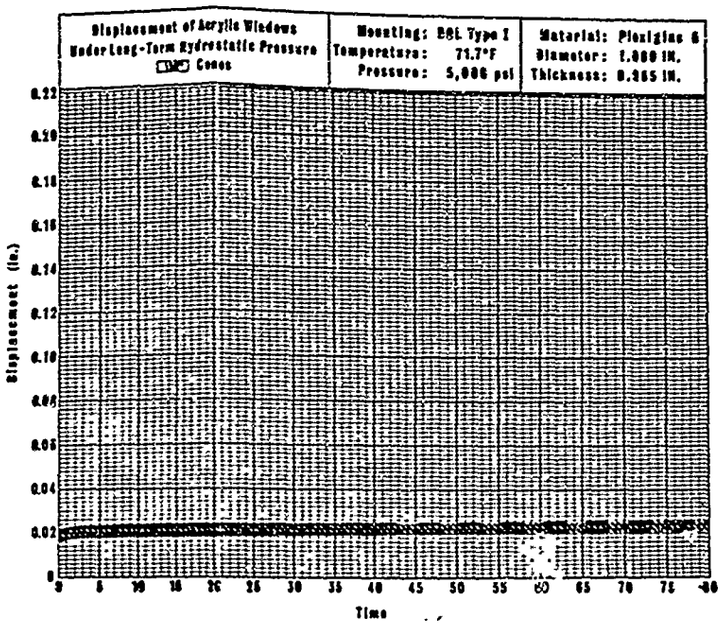

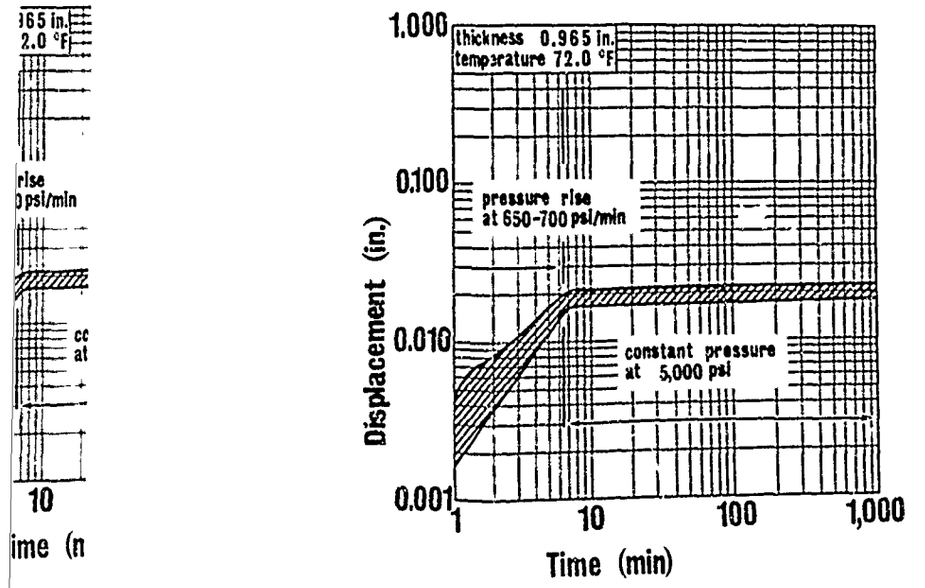

Figure A-5e. Displacement of conical acrylic plastic windows under 5,000-psi sustained pressure loading; 150-degree included angle with t/D ratio = 1.000.

Appendix B

DESIGN OF WINDOW AND FLANGE SYSTEMS FOR LONG-TERM LOADING AT 5,000 PSI

INTRODUCTION

When the data generated in this study are to be applied to the design of windows for deep-submergence systems, several design and operational parameters must be carefully evaluated. The most important operational parameter that must be considered is the type of pressure loading to which the pressure-resistant structures with windows will be subjected. For ease of discussion, hydrostatic pressure loadings can be classified into four general categories: (1) static short-term, (2) sustained long-term, (3) cyclical, and (4) dynamic.

The short-term static pressure loading has been defined as a continuous pressure rise at some arbitrarily set pressure rise rate until a predetermined pressure is reached; at this point, the pressure is released at the same rate. The pressure rise rate selected for NCEL window studies[1-3] was 650 psi/min.

Long-term sustained pressure loading is defined here as raising the pressure at some set rate to a predetermined pressure level and holding it there for the duration of the mission. Depending on the duration of the constant pressure application, the long-term pressure loading is further defined by the number of hours or days that it is maintained on the window.

Cyclical pressure loading is defined as varying the pressure between arbitrary maximum and minimum pressure levels, with the period of pressure fluctuation being either constant or variable.

Dynamic pressure loading depends for its definition on the arbitrary dividing line between short-term static and dynamic pressure rise rate, which for windows used in submersibles probably can be placed at 5,000 psi/min. The dynamic pressure application may be short-term if applied once, or cyclical if applied repeatedly.

WINDOWS

Selection of t/D Ratios

The data that have been generated in this study are directly applicable *only to design of truncated cone acrylic windows under short-term or long-term loading at 5,000 psi*, since the test specimens in this study underwent short-term pressurization at the rate of 650 psi/min followed by long-term steady pressure loading at 5,000 psi. On the basis of these data, a guideline can be suggested for the benefit of the engineer designing acrylic hydrospace windows of truncated cone shape for a one-time, long-term pressurization to 5,000 psi in the 32°F-to-75°F temperature range.

Design Guideline 1. For applications in which the truncated cone acrylic windows serve as high-grade optical lenses for manned submersibles under a *single sustained pressure loading* of 5,000 psi in the 32°F-to-75°F temperature range, the following *minimum* window dimensions are recommended:

Flange	Included Conical Angle (deg)	t/D Ratio for Sustained Loading Period of—			
		1 Hour	100 Hours	1,000 Hours	100,000 Hours
(See Design Guideline 2)	30	0.750	1.000	1.000	1.250
	60	0.500	0.625	0.625	0.750
	90	0.375	0.500	0.500	0.625
	120	0.375	0.500	0.500	0.625
	150	0.375	0.500	0.500	0.625

The t/D ratios acceptable for optical applications of truncated cone acrylic windows have been selected after a thorough consideration of three parameters of importance in operational window performance: (1) magnitude of axial displacement during the long-term pressure loading, (2) deformation of high- and of low-pressure faces, and (3) magnitude of penetration and location of cracks on the conical surface during the sustained loading. Since it is virtually impossible, regardless of t/D ratio and angle chosen, to *completely* eliminate time-dependent cold flow of the acrylic plastic at 5,000-psi hydrostatic pressure, an engineering judgment was made on what constitutes the minimum acceptable performance of the acrylic window from the optical and safety viewpoints.

A window is considered to be safe for manned operation if during a single sustained pressure loading of 5,000 psi in the 32°F-to-75°F range for the specified maximum duration *no cracks or crazing* were present on the

high- and low-pressure faces or the conical bearing surface. Total axial displacement in the range of 0.02D to 0.05D at the end of the specified period of loading presents no operational difficulties for the observer. The window is optically acceptable if it causes no distortion of viewed objects in hydrospace for an observer whose eyes are within 10 inches of the low-pressure face.

Applicability of Data to Other Loading Conditions

As previously mentioned, the experimental data generated in this study are applicable with reasonable extrapolation only to a single short- or long-term static pressure loading at 5,000 psi. However, since very few data are now available for the design of windows subjected to long-term loading at pressures other than those used in this study, some designers may be tempted to base their selections of window proportions on the data from this study. *This is not recommended.* The factors for adjusting t/D ratios from this study for other pressure levels have not yet been developed. Studies, however, have been completed that provide this information for 20,000-psi[4] and 10,000-psi[5] applications.

It is recommended as operationally desirable that the minimum t/D ratios acceptable for 5,000-psi long-term pressure loading also be used for pressures in the 0-to-5,000-psi range. This change in long-term operational static pressure magnitude will make it possible to proof-test such windows to 5,000 psi without damaging them.

The experimental data of this report should not be used for the direct selection of window proportions for applications where the window is subjected to *cyclic* short-term or long-term pressurizations. Caution is advised here because the relationship between the effect of cyclic and long-term loading conditions on the initiation of fractures in acrylic windows is not known. However, because cyclic pressurization data for windows operating at 5,000 psi are either nonexistent or very scarce, designers may also be tempted to use long-term pressure loading data contained in this report for the design of windows for cyclic pressure service. Designers who do this are advised that the window proportions recommended for 100,000-hour sustained loading at 5,000 psi will *probably* perform quite satisfactory at 5,000-psi cyclic loading so long as the maximum duration of the pressure cycle is less than 100 hours. If window proportions are selected for cyclic service on this basis, evaluation of the prototype full-scale window under simulated operational conditions is recommended. For applications at 5,000-psi hydrostatic loading where the ambient temperature is in excess of 80°F but less than

120°F, the t/D and D/D_f ratios* should be chosen on the basis of recommendations published previously for 10,000-psi service.[4] Where the ambient temperature exceeds 120°F but is less than 150°F, the t/D and D/D_f ratios should be chosen on the basis of recommendations published previously for 20,000-psi service.[5]

Window Fabrication

Since the windows rely on intimate contact with the conical flange cavity surface for their high-pressure sealing as well as for their restraint against axial displacement, an accurate fit with that cavity is of great importance. For this reason the maximum allowable machining tolerances on the window must not exceed ±0.005 inch on the minor diameter, 0.010 inch in thickness, and ±15 minutes of included conical angle.

The windows are fabricated by machining acrylic stock having the mechanical and physical properties of Plexiglas G plate. Commercially available 4-inch-thick plate, a custom cast block, or a block made up by bonding of several standard acrylic plates can serve as machining stock. In the case of custom cast or bonded blocks, the end product must have the same mechanical and physical properties as a monolithic, commercially available 4-inch-thick Plexiglas G plate. It is particularly important that the tensile strength of the bonds in the bonded acrylic block be equal to or approach (6,000 psi minimum) that of the parent material (Table 2).

Regardless of the machining stock used, the window should be annealed twice during its fabrication: once after rough machining when its within approximately 0.125 inch of finished dimensions, and a second time when it has been machined to its final dimensions and the surfaces have been polished. Without annealing, the conical bearing surfaces of the window will craze and crack sooner under operational service.

The finish of the conical bearing surface of the window should be at least 63 rms followed by polishing. If the surface finish is rougher, crazing and cracking of the conical bearing surface *could* initiate sooner under operational service.

Proof-Testing of Windows

When the experimental data contained in this report are used for the design of windows, care must be taken not to damage the windows with excessive overpressure proof-testing. *The basic ground rule for windows*

* D/D_f ratio is the ratio of the minor diameter of the window to the minor diameter of the flange cavity.

selected on the basis of long-term tests is that they should never be subjected to pressures in excess of those used to generate the basic data, regardless whether this occurs during the operational life of the window or during the proof-test that precedes it. Because of this, if the operational service of the windows is to be at 5,000-psi, the proof pressure preceding the operational use of the windows must only be equal to operational pressure. If for some reason the proof pressure must be in excess of operational pressure, then accordingly either (1) the operational pressure rating must be reduced below the 5,000-psi pressure level, or (2) the t/D and D/D_f ratios of windows must be chosen on the basis of recommendations published previously[4] for windows operating at 10,000 psi.

Since the proof-test to 5,000 psi prior to placement of the window in actual service constitutes a loading cycle, it is important to make it as brief as possible so that it does not substantially reduce the rated long-term life of the window in subsequent operation under service conditions. Unless there are some special reasons for it, the duration of the proof-test should not exceed 1 hour.

Ideally, proof-testing of each window slated for long-term service operation at 5,000 psi should not take place at all, as it has a negative influence on the long-term life of the window. Instead of proof-testing each window, it is more advantageous to rely on quality control in the procurement of acrylic stock and in machining, annealing, and bonding of the window. When this quality control in fabrication is augmented by the testing under simulated service conditions of a window selected at random from the same group of windows on the production line, very reliable windows for long-term loading can be obtained. In this manner even though one window is sacrificed to nondestructive and possibly to destructive proof-testing, the remaining windows from the same production batch retain all of their potential pressure-resisting capability for actual service.

If the proof-testing of operational windows to 5,000 psi is a firm requirement for certification, the t/D ratio of windows for sustained service at 5,000 psi should be based on design guideline 1 for 100,000 hours sustained loading duration.

FLANGES

Configurations

Although all the experimental data of this study have been generated in the DOL 1 flange and window configuration (Figure B-1), a minor modification of this configuration is recommended for full-size hydrospace windows to give the user an added margin of safety for windows whose proportions have been selected on the basis of this study.

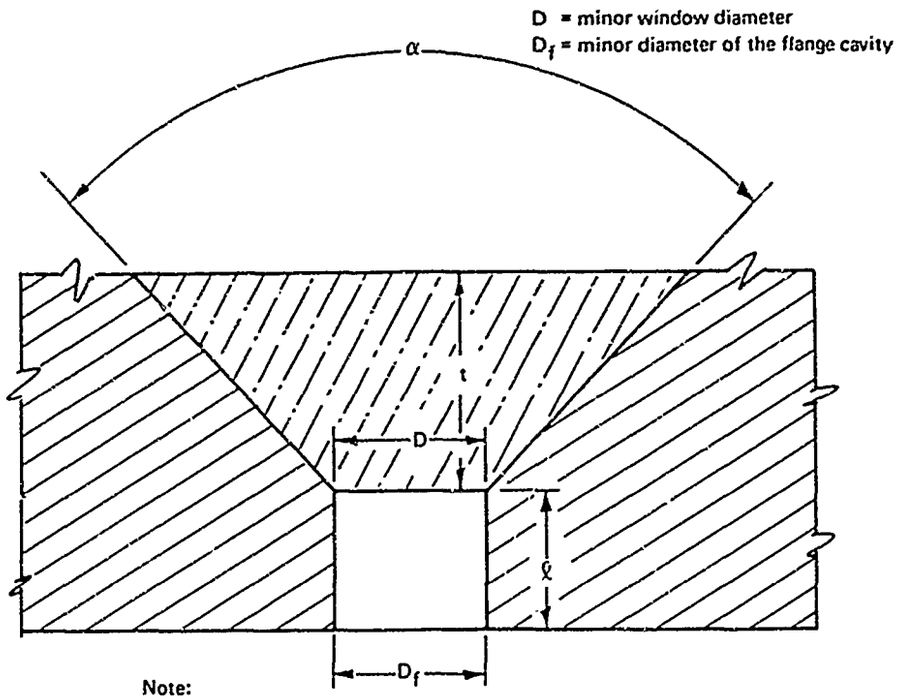

Note:

1. $D = D_f$ for all t/D ratios and conical angles (α)
2. ℓ > 2 x displacement of window during the sustained pressure loading for specified period of time

Figure B-1. Characteristics of DOL 1 flange and window assembly (used in the current study).

The recommended modification to the DOL 1 flange and window configuration consists of locating the window's low-pressure face farther away from the cylindrical passage in the flange to provide not only radial but axial restraints for the extruding portion of the window. Such a flange and window configuration, designated as DOL 5 flange (Figure B-2), should permit the windows to extrude somewhat less than the windows described in this study and thus give the designer an extra margin of safety and improved optical performance.

In order to minimize the displacement of the window under sustained operational pressure, as well as to provide a necessary margin of safety for overpressures to which the windows may be accidentally or intentionally (as in proof-testing) exposed, the engineer must design the window flange opening with required radial and axial support for the window. The dimensions of DOL 5 window flanges have been calculated and are presented in guideline 2. These calculations are based on two assumptions. The first is that the distance b between the window's low-pressure face in the conical flange cavity and the bottom of the conical cavity must be approximately

the same as the displacement of the window with recommended t/D ratio during the specified duration of sustained loading at 5,000 psi. The second is that either an overpressure or extension of rated loading duration may be encountered by the structure during its life and therefore an additional allowance, ℓ, equal at least to b should be made for window displacement in the cylindrical flange cavity.

The first assumption must be taken into account. The second one should be considered, but in many cases no pressures higher than operational will be encountered, and thus no provisions have to be made for displacements caused by overpressure or for duration of loading past the originally specified time span.

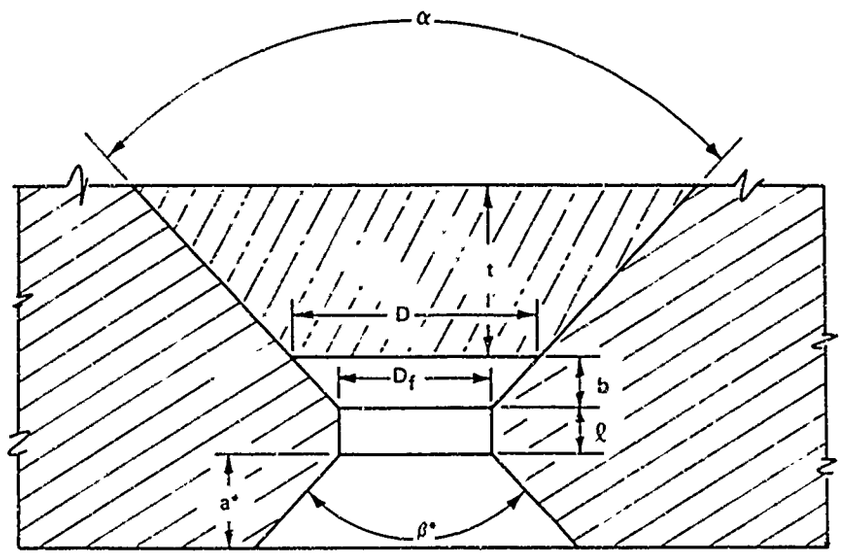

Note:

1. a° — To be chosen by designer on basis of stress field evaluation in the flange
2. β° — To be chosen by designer on basis of optical viewing requirements
3. ℓ ≥ b for all t/D ratios and conical angles (α)
4. b ≥ displacement of window during the sustained pressure loading for specified period of time
5. $D > D_f$ for all t/D ratios and conical angles α

Figure B-2. Characteristics of DOL 5 flange and window assembly (the assembly recommended for long-term 5,000-psi pressure application).

Design Guideline 2. For applications in which the truncated cone acrylic windows serve as high-grade optical lenses for manned capsules under sustained pressure loading of 5,000 psi in the 32°F-to-75°F temperature range, the following flange cavity proportions are recommended:

Window	Flange	Included Angle (deg)	D/D_f Ratio	Cylindrical Passage Length, ℓ
(See Design Guideline 1)	DOL 5	30	1.03	$\geq 0.1D$
		60	1.04	$\geq 0.1D$
		90	1.06	$\geq 0.1D$
		120	1.12	$\geq 0.1D$
		150	1.28	$\geq 0.1D$

Finishes and Tolerances

The experimental data relating flange-seat surface roughness to crack initiation in the bearing surface of conical acrylic windows under long-term loading are inconclusive. Therefore, no definite recommendation based on test data can be made for a particular surface finish at this time. It can be only stated that so long as the surface finish is in the range of 32 to 125 rms, the acrylic conical windows will perform satisfactorily. The surface finish of the flanges used in this study was 63 rms; it performed quite acceptably and can be considered a compromise between the more expensive 32-rms finish and the rough 125-rms finish.

Although exploratory experimental data indicate that an angle mismatch between the acrylic plug and the conical flange seat of 1 to 2 degrees magnitude does not noticeably affect the critical pressure of the window, the mismatch should be kept to a minimum to eliminate low-pressure sealing problems. To minimize leaking, deviation of the conical flange cavity from the specified angle should be in the ±5-to-±15-minute range, easily attained with ordinary machine shop practice.

The effect of variation in the minor diameter of the conical cavity on the displacement and critical pressure of the conical acrylic windows varies with the type of window—flange system used. The effect of variation is most pronounced for the DOL 2 window—flange system (Figure B-3) and least pronounced for the DOL 5 system. Since the DOL 5 system (Figure B-2) is the one recommended for windows under long-term hydrostatic loading, the diametral tolerance for minor diameter of conical flange cavity may be in the range ±0.001 to ±0.005 inch. These tolerances are readily achieved with ordinary machining processes.

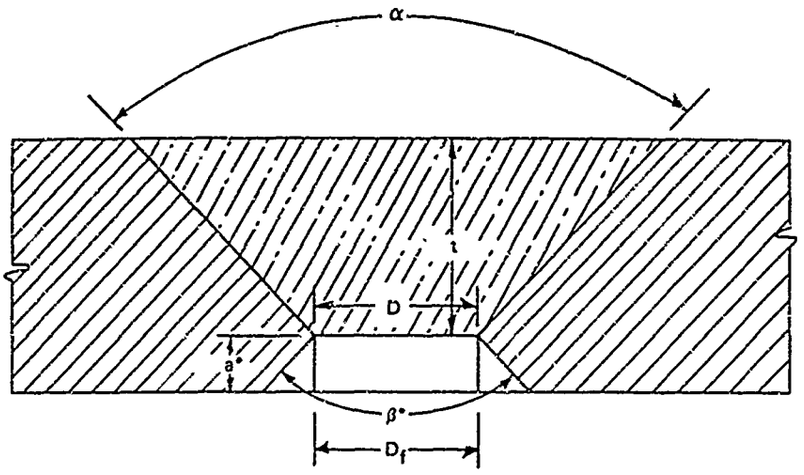

Note:

1. D = D_f for all t/D ratios and conical angles (α)
2. a° – To be chosen by designer on basis of stress field evaluation in the flange
3. β° – To be chosen by designer on basis of optical viewing requirements

Figure B-3. Characteristics of DOL 2 flange and window assembly (the assembly *not* recommended for long-term 5,000-psi pressure application).

SEALS

Requirements

One of the major problems encountered in the design of window systems for long-term loading is the design of seals. The difficulty in the design of seals for such a system stems from the fact that there are three separate operational requirements that the seals must satisfy:

1. The window system must be watertight at low pressures while the capsule or habitat is being towed to its location.
2. The window system must be watertight at the maximum operational pressure during the projected duration of the mission on the ocean bottom.
3. The window system must be watertight upon return of the capsule or habitat to the ocean surface, and during the subsequent towing to dock.

It is relatively easy to satisfy the first two requirements. Any ordinary gasket will seal the high-pressure face of the window against the window-retaining ring at low hydrostatic pressure, while the greased surface of the window acts as a seal itself under high external hydrostatic pressure. It is much more difficult to satisfy the third requirement because the window has experienced viscoelastic deformation during its long-term service under operational pressure of 5,000 psi. Upon return of the capsule to the ocean surface there is a tendency for the windows to leak; because viscoelastic displacement of the window has taken place, the gasket between the window-retaining ring and the window is no longer compressed. There are many design approaches that will mitigate or completely eliminate the problem of window leakage upon return of the capsule or habitat to the ocean surface after its long-term submergence. Seals of several designs have been built and their performance noted.

Seal Designs

The five different types of seals (Figure B-4) investigated for sealing windows under long-term loading were designed primarily to satisfy sealing requirement 3, but in the process of satisfying that requirement in every case they also satisfied requirements 1 and 2. The simplest seal investigated was the standard gasket compression seal of 60-durometer hardness held against the window's high-pressure face by a retaining ring. Its thickness was selected to permit the necessary precompression during installation without causing permanent set to the gasket. The precompression was selected to accommodate the largest predicted displacement of the window in the flange and yet maintain sufficient contact pressure with the window and the retaining ring to permit the gasket to function as a seal when the capsule or habitat is brought back to the ocean surface.

The seal utilizing an O-ring in radial compression was a little more complex. For this design, as well as the elastomeric channel seal design discussed later, both the window and the flange cavity had to be enlarged to accommodate the seal without reducing the window's critical dimensions. Because the O-ring was designed to be under radial compression, the deformation of the window material under long-term hydrostatic pressure would tend to make the seal more pressure resistant; the clearance between the edge of the window and the flange cavity surface would decrease with time. In addition, the axial movement of the window in the flange did not present any problems in this O-ring seal arrangement, as the radially compressed O-ring slides with the window along the cylindrical surface of the cavity in the flange without any loss of compression. In this design, the window is held in the flange cavity by means of a single flat annular spring compressed against the high-pressure face of the window by a retaining ring.

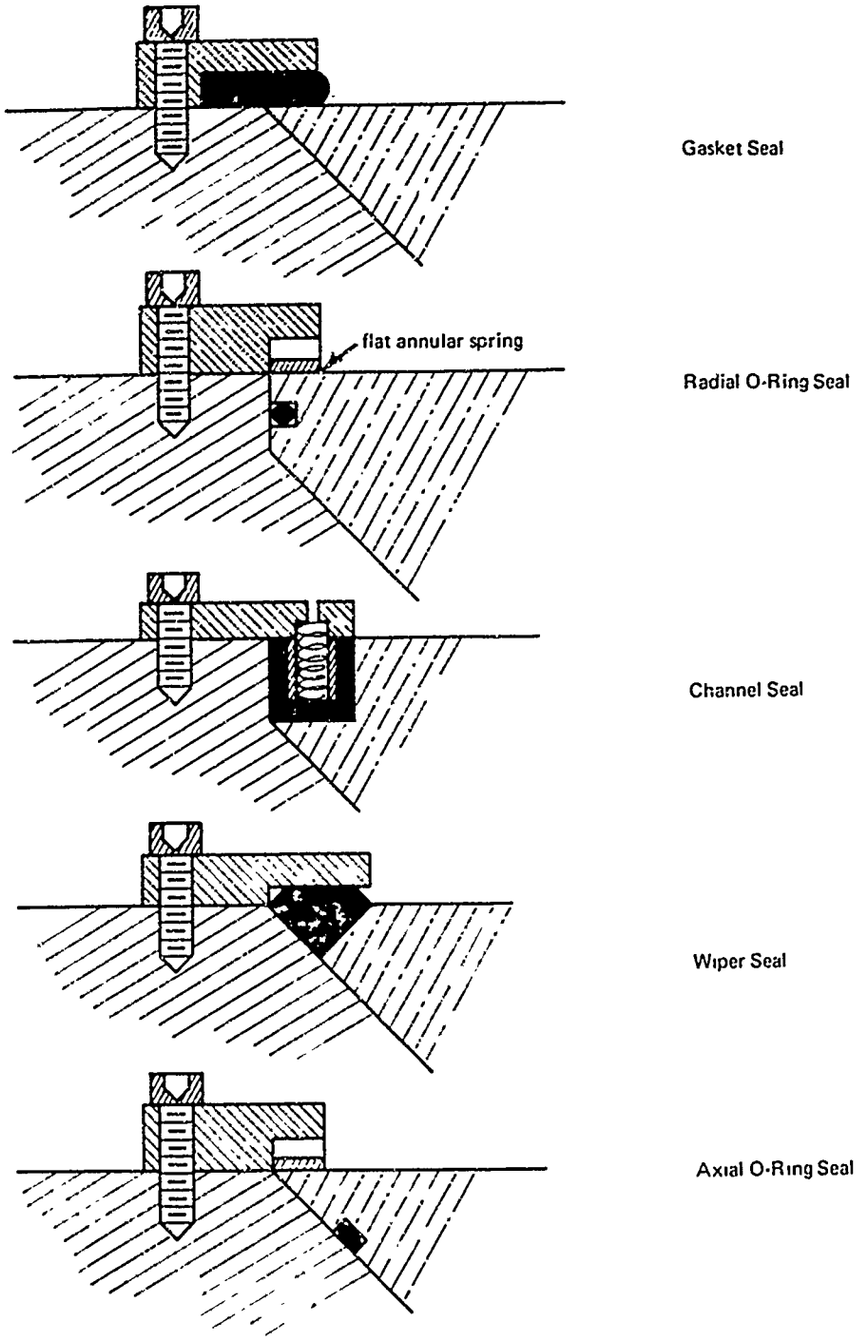

Figure B-4. Seals applicable to windows under long-term pressure loading.

The channel seal operates on basically the same principle as the radial O-ring seal. However, the seal, which slides along the cylindrical cavity surface (Figure B-4) with axial displacement of the window, is an elastomeric channel pressed against the window and the cavity surface by two split rings. The window is held in the flange cavity by means of several helical springs held in compression by a retaining ring.

The wiper seal, in the form of an elastomeric wedge with triangular cross section, was designed to operate on the same surface-wiping principle as the two preceding seals except that during axial displacement of the window in the flange cavity the seal wipes a conical surface, not a cylindrical one as is the case in the two previous seals. Because of this, the flange cavity and window may be the same size and shape as for the standard gasket design. The window-retaining ring acting upon the seal wiper ridge also serves the secondary function of preventing the window from moving excessively outward upon surfacing.

The axial O-ring seal was designed like the wiper seal to maintain constant contact with the conical flange surface under large axial displacements of the window. The window is held in positive contact with the cavity surface by a flat annular spring or rubber gasket compressed by the retaining ring against the window's high-pressure face.

Seal Evaluation

All of the seals shown in Figure B-4 performed equally well under sustained or cyclic 5,000-psi hydrostatic loading. The reason for the satisfactory performance of all seal configurations is the relatively low hydrostatic pressure to which they were subjected in this study. While in previous tests,[4,5] where the hydrostatic pressures were 10,000 or 20,000 psi, the axial displacement and deformation of the windows were large ($\geq$0.050 inch for windows with D = 1.000 inch), in the current tests they were small ($\leq$0.050 inch). Because of the rather small displacements and viscoelastic deformations in windows under 5,000-psi hydrostatic loading, there is no need to use the rather complex seal systems used in the 10,000- and 20,000-psi loading studies, since the simple more economical seal systems will do just as well.

Seal Selection

In view of the considerations discussed in the section on seal design evaluation, it can be postulated that for long-term loading at a hydrostatic pressure of 5,000 psi only two seal designs (simple gasket and O-ring) are attractive.

Where the window cavity in the flange is to have the least axial length possible and where the economics of window–seal system fabrication are important, the simple gasket seal design is preferable.

Design Guideline 3. For the ***simple gasket seal,*** the design guidelines for selecting the magnitude of elastic gasket precompression under the window-retaining ring depend on the design guidelines used in the selection of window t/D ratios.

Selection of Window t/D	Corresponding Conical Cavity Dimensions	Corresponding Gasket Compressions[a] Under Retaining Ring(s) for Included Angles—				
		30°	60°	90°	120°	150°
Guideline 1	Guideline 2	0.06D	0.04D	0.030D	0.030D	0.030D

[a] Minimum precompression.

If the gaskets are compressed (Figure B-5) as recommended, and no permanent set of the elastomeric gasket occurs, the seal should perform adequately prior to the long-term pressure loading, during the sustained long-term loading of 5,000 psi, and in low-pressure service encountered by the window when the ocean bottom habitat or capsule returns to the ocean's surface.

In applications in which economy is not of prime consideration and off-the-shelf commercial O-rings are available for that particular window diameter, the axial O-ring seal can be utilized instead of the gasket seal.

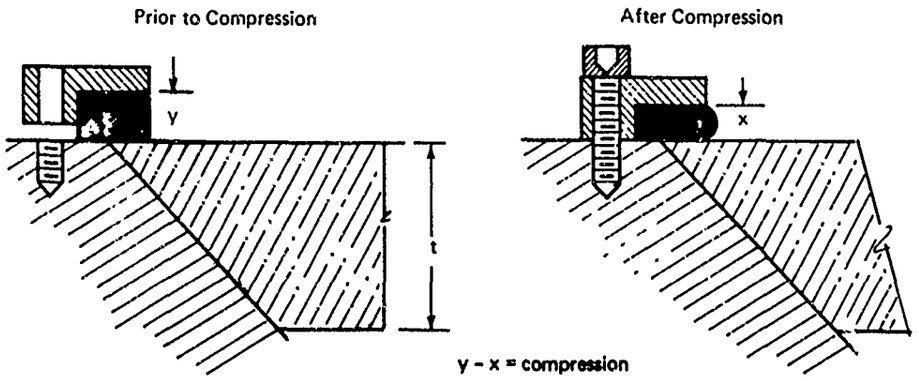

Figure B-5. Parameters for selection of gasket seal compression according to Design Guideline 3.

Design Guideline 4. For the *axial O-ring seal*, the design guidelines for selecting the size of the groove in the window and its location depend on the design guidelines used in the selection of window t/D ratios.

Selection of Window t/D	Corresponding Conical Cavity Dimensions	Corresponding Dimensions of Window Lip (k) for Included Angle—				
		30°	60°	90°	120°	150°
Guideline 1	Guideline 2	0.2D	0.2D	0.3D	0.3D	0.3D

The foregoing list dimensions (defined in Figure B-6) recommended for the window lip describes the maximum permissible thickness of the lip. In order to specify the window, however, one must also know the minimum permissible thickness of the lip. The minimum dimensions do not depend on the magnitude of the external pressure to which the window will be subjected or the conical angle but on (1) the size of the O-ring, which in many cases is chosen solely on the basis of the window diameter, and (2) the rigidity of the lip, which varies with k rather than D.

In general, the width of the groove[6] should be >0.15 inch for 1/8-inch O-rings associated with small windows and >0.3 inch for 1/4-inch O-rings used in large windows. The window lip should be at least equal in thickness to the groove width, or preferably twice as thick to prevent its chipping during handling of windows at installation.

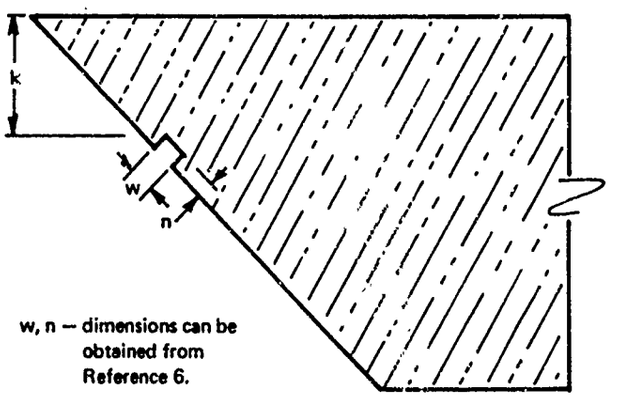

Figure B-6. Parameters for selection of window lip dimensions according to Design Guideline 4.

SUMMARY

To tie together the many design guidelines spelled out in Appendix B, two typical windows will be designed and dimensioned.

Case A

Requirements.

Pressure:	5,000 psi
Type of loading:	Sustained, 100,000 hours
Type of service:	Optical observation of hydrospace
Cone angle:	90 degrees
Type of seal:	Axial O-ring
Minor diameter:	1 inch

Dimensioning. Optical service requires that Design Guideline 1 be used for window t/D selection (in this case t/D = 0.625), Design Guideline 2 for flange cavity D/D_f selection (in this case $D/D_f = 1.06$ and $\ell = 0.1D$), and Design Guideline 4 for axial O-ring seal and window lip thickness selection ($k \leq 0.3D$, $w = 0.100$, $n = 0.05$). The configuration of the window and flange is shown in Figure B-7.

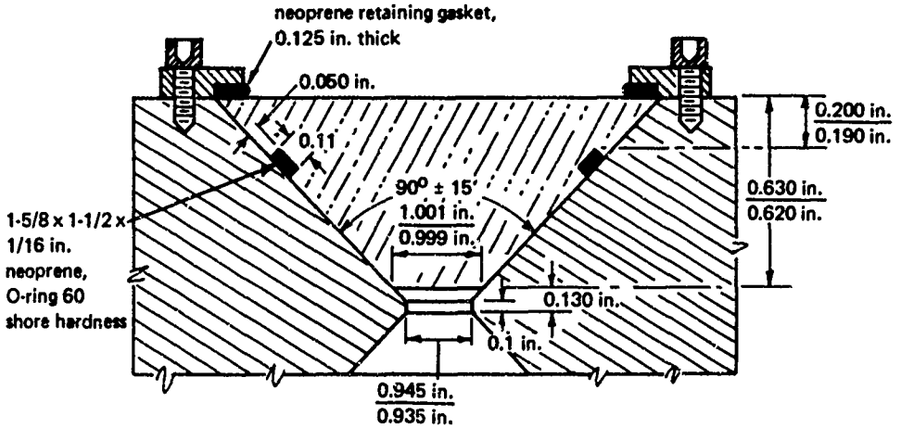

Figure B-7. Typical design of axial O-ring seal on a 90-degree window for 100,000 hours of service at sustained 5,000-psi pressure in 32°F-to-75°F temperature range.

Case B

Requirements.

Pressure:	5,000 psi
Type of loading:	Sustained, 1,000 hours
Type of service:	Optical observation of hydrospace
Cone angle:	90 degrees
Type of seal:	Gasket seal
Minor diameter:	1 inch

Dimensioning. Optical observation service requires that Design Guideline 1 be used for window t/D selection (in this case t/D = 0.5), Design Guideline 2 for flange cavity D/D_f selection (in this case $D/D_f = 1.06$, $\ell = 0.1D$), and Design Guideline 3 for gasket seal precompression specification (in this case 0.03D). The configuration of the window is shown in Figure B-8.

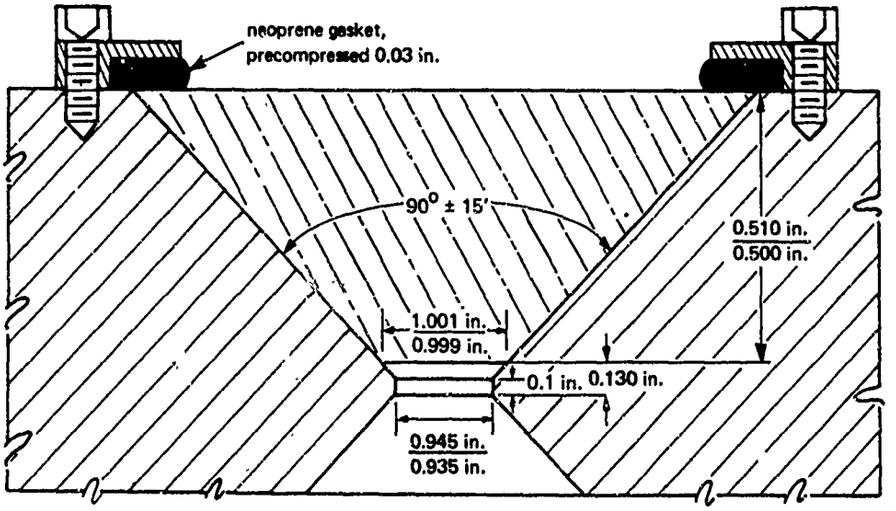

Figure B-8. Typical design of gasket seal on a 90-degree window for 1,000 hours of service at sustained 5,000-psi pressure in 32°F-to-75°F temperature range.

Since all of the design guidelines discussed in Appendix B had as their objective a window that performs reliably and safely in 0 to 5,000 psi pressure range and 32°F-to-75°F temperature range, an approach to dimensioning was used that always assumed the windows would be used at the most severe loading condition. Thus, it can be expected that when an axial O-ring-sealed optical service window is operated at 3,000 psi and 34°F temperature

for less than the whole span of its rated life, the displacements of the window will be much less than provided for by the design guidelines. On the other hand if a gasket-sealed optical service window is operated at 5,000 psi and 75°F temperature for the whole span of its sustained loading rating, the displacements will probably be equal to those foreseen by the design guidelines.

Although both of the typical windows shown (Figures B-7 and B-8) have a minor diameter of only 1.000 inch, the same design criteria can be successfully utilized for dimensioning of windows with larger minor diameters. This has been facilitated by giving all the dimensions in Design Guidelines 1 through 4, in terms of the minor window diameter, **D**. Thus, regardless of whether **D** is specified by the designer in terms of inches, centimeters, or feet, the dimensions called out by the design guidelines of Appendix B will be in the same terms, since all of the dimensions given in the guidelines are linear functions of **D**.

REFERENCES

1. Naval Civil Engineering Laboratory. Technical Report R-512: Windows for external or internal hydrostatic pressure vessels, pt. I: Conical acrylic windows under short-term pressure application, by J. D. Stachiw and K. O. Gray. Port Hueneme, Calif., Jan. 1967. (AD 646882)

2.——. Technical Report R-527: Windows for external or internal hydrostatic pressure vessels, pt. II. Flat acrylic windows under short-term pressure application, by J. D. Stachiw, G. M. Dunn, and K. O. Gray. Port Hueneme, Calif., May 1967. (AD 652343)

3.——. Technical Report R-631: Windows for external or internal hydrostatic pressure vessels, pt. III. Critical pressure of acrylic spherical shell windows under short-term pressure applications, by J. D. Stachiw and F. Brier. Port Hueneme, Calif., June 1969. (AD 689789)

4. ——. Technical Report R-645: Windows for external or internal hydrostatic pressure vessels, pt. IV: Conical acrylic windows under long-term pressure application at 20,000 psi, by J. D. Stachiw. Port Hueneme, Calif., Oct. 1969. (AD 697272)

5.——. Technical Report R-708: Windows for external or internal hydrostatic pressure vessels, pt. V. Conical acrylic windows under long-term pressure application at 10,000 psi, by J. D. Stachiw and W. A. Moody. Port Hueneme, Calif., Jan. 1971. (AD 718812)

6. Parker Seal Company. Publication OR 5700: O-ring handbook. Culver City, Calif., Jan. 1970.

DISTRIBUTION LIST

SNDL Code	No. of Activities	Total Copies	
—	1	12	Defense Documentation Center
FKAIC	1	10	Naval Facilities Engineering Command
FKNI	6	6	NAVFAC Engineering Field Divisions
FKN5	9	9	Public Works Centers
FA25	1	1	Public Works Center
—	9	9	RDT&E Liaison Officers at NAVFAC Engineering Field Divisions and Construction Battalion Centers
—	304	304	NCEL Special Distribution List No. 9 for persons and activities interested in reports on Deep Ocean Studies

Naval Civil Engineering Laboratory
WINDOWS FOR EXTERNAL OR INTERNAL HYDROSTATIC PRESSURE VESSELS—PART VI. Conical Acrylic Windows Under Long-Term Pressure Application at 5,000 Psi, by J. D. Stachiw and K. O. Gray
TR-747 49 p. illus November 1971 Unclassified

1. Pressure vessel windows—Conical acrylic plastic I. YF 51.543.008.01.001

Conical acrylic windows with five included angles (α) from 30 to 150 degrees and thickness-to-minor-diameter (t/D) ratios from 0.375 to 1.00 have been subjected to 5,000 psi of sustained hydrostatic loading for up to 1,000 hours in the temperature range from 65°F to 75°F while the axial displacement of the windows through the flange has been monitored. The magnitude of axial displacement was found to be a function of α, t/D ratio, temperature, and duration of loading. Only windows with t/D ratios ≥1.000, 0.625, 0.500, 0.500, and 0.500 for 30-, 60-, 90-, 120-, and 150-degree conical angles, respectively, were found to be free of cracks. Minimum axial displacements of the windows can be achieved only with t/D ratios of >1.000, 1.000, 0.750, 0.750, and 0.625 for 30-, 60-, 90-, 120-, and 150-degree conical angles, respectively. The minimum axial displacements of D = 1.000-inch windows with these t/D ratios and conical angles are 0.042, 0.023, 0.023, 0.019, and 0.019 inch, respectively. It is recommended that only windows with t/D ratios ≥0.625 and α ≥60 degrees be used for sustained hydrostatic loading of 5,000 psi at temperatures ≤80°F.

Naval Civil Engineering Laboratory
WINDOWS FOR EXTERNAL OR INTERNAL HYDROSTATIC PRESSURE VESSELS—PART VI. Conical Acrylic Windows Under Long-Term Pressure Application at 5,000 Psi, by J. D. Stachiw and K. O. Gray
TR-747 49 p. illus November 1971 Unclassified

1. Pressure vessel windows—Conical acrylic plastic I. YF 51.543.008.01.001

Conical acrylic windows with five included angles (α) from 30 to 150 degrees and thickness-to-minor-diameter (t/D) ratios from 0.375 to 1.00 have been subjected to 5,000 psi of sustained hydrostatic loading for up to 1,000 hours in the temperature range from 65°F to 75°F while the axial displacement of the windows through the flange has been monitored. The magnitude of axial displacement was found to be a function of α, t/D ratio, temperature, and duration of loading. Only windows with t/D ratios ≥1.000, 0.625, 0.500, 0.500, and 0.500 for 30-, 60-, 90-, 120-, and 150-degrees conical angles, respectively, were found to be free of cracks. Minimum axial displacements of the windows can be achieved only with t/D ratios of >1.000, 1.000, 0.750, 0.750, and 0.625 for 30-, 60-, 90-, 120-, and 150-degree conical angles, respectively. The minimum axial displacements of D = 1.000-inch windows with these t/D ratios and conical angles are 0.042, 0.023, 0.023, 0.019, and 0.019 inch, respectively. It is recommended that only windows with t/D ratios ≥0.625 and α ≥60 degrees be used for sustained hydrostatic loading of 5,000 psi at temperatures ≤80°F.

Naval Civil Engineering Laboratory
WINDOWS FOR EXTERNAL OR INTERNAL HYDROSTATIC PRESSURE VESSELS—PART VI. Conical Acrylic Windows Under Long-Term Pressure Application at 5,000 Psi, by J. D. Stachiw and K. O. Gray
TR-747 49 p. illus November 1971 Unclassified

1. Pressure vessel windows—Conical acrylic plastic I. YF 51.543.008.01.001

Conical acrylic windows with five included angles (α) from 30 to 150 degrees and thickness-to-minor-diameter (t/D) ratios from 0.375 to 1.00 have been subjected to 5,000 psi of sustained hydrostatic loading for up to 1,000 hours in the temperature range from 65°F to 75°F while the axial displacement of the windows through the flange has been monitored. The magnitude of axial displacement was found to be a function of α, t/D ratio, temperature, and duration of loading. Only windows with t/D ratios ≥1.000, 0.625, 0.500, 0.500, and 0.500 for 30-, 60-, 90-, 120-, and 150-degree conical angles, respectively, were found to be free of cracks. Minimum axial displacements of the windows can be achieved only with t/D ratios of >1.000, 1.000, 0.750, 0.750, and 0.625 for 30-, 60-, 90-, 120-, and 150-degree conical angles, respectively. The minimum axial displacements of D = 1.000-inch windows with these t/D ratios and conical angles are 0.042, 0.023, 0.023, 0.019, and 0.019-inch, respectively. It is recommended that only windows with t/D ratios ≥0.625 and α ≥60 degrees be used for sustained hydrostatic loading of 5,000 psi at temperatures ≤80°F.

Naval Civil Engineering Laboratory
WINDOWS FOR EXTERNAL OR INTERNAL HYDROSTATIC PRESSURE VESSELS—PART VI. Conical Acrylic Windows Under Long-Term Pressure Application at 5,000 Psi, by J. D. Stachiw and K. O. Gray
TR-747 49 p. illus November 1971 Unclassified

1. Pressure vessel windows—Conical acrylic plastic I. YF 51.543.008.01.001

Conical acrylic windows with five included angles (α) from 30 to 150 degrees and thickness-to-minor-diameter (t/D) ratios from 0.375 to 1.00 have been subjected to 5,000 psi of sustained hydrostatic loading for up to 1,000 hours in the temperature range from 65°F to 75°F while the axial displacement of the windows through the flange has been monitored. The magnitude of axial displacement was found to be a function of α, t/D ratio, temperature, and duration of loading. Only windows with t/D ratios ≥1.000, 0.625, 0.500, 0.500, and 0.500 for 30-, 60-, 90-, 120-, and 150-degree conical angles, respectively, were found to be free of cracks. Minimum axial displacements of the windows can be achieved only with t/D ratios of >1.000, 1.000, 0.750, 0.750, and 0.625 for 30-, 60-, 90-, 120-, and 150-degree conical angles, respectively. The minimum axial displacements of D = 1.000-inch windows with these t/D ratios and conical angles are 0.042, 0.023, 0.023, 0.019, and 0.019 inch, respectively. It is recommended that only windows with t/D ratios ≥0.625 and α ≥60 degrees be used for sustained hydrostatic loading of 5,000 psi at temperatures ≤80°F.

Unclassified

Security Classification

DOCUMENT CONTROL DATA - R & D

(Security classification of title, body of abstract and indexing annotation must be entered when the overall report is classified)

1. ORIGINATING ACTIVITY (Corporate author) Naval Civil Engineering Laboratory Port Hueneme, California 93043	2a. REPORT SECURITY CLASSIFICATION Unclassified 2b. GROUP

3. REPORT TITLE

WINDOWS FOR EXTERNAL OR INTERNAL HYDROSTATIC PRESSURE VESSELS—PART VI. Conical Acrylic Windows Under Long-Term Pressure Application at 5,000 Psi

4. DESCRIPTIVE NOTES (Type of report and inclusive dates)

Not final; March 1969 – October 1970

5. AUTHOR(S) (First name, middle initial, last name)

J. D. Stachiw and K. O. Gray

6. REPORT DATE	7a. TOTAL NO. OF PAGES	7b. NO. OF REFS
November 1971	49	6

8a. CONTRACT OR GRANT NO. b. PROJECT NO. YF 51.543.008.01.001 c. d.	9a. ORIGINATOR'S REPORT NUMBER(S) TR-747 9b. OTHER REPORT NO(S) (Any other numbers that may be assigned this report)

10. DISTRIBUTION STATEMENT

Approved for public release; distribution unlimited.

11. SUPPLEMENTARY NOTES	12. SPONSORING MILITARY ACTIVITY
	Naval Facilities Engineering Command Washington, D. C. 20390

13. ABSTRACT

Conical acrylic windows with five included angles (α) from 30 to 150 degrees and thickness-to-minor-diameter (t/D) ratios from 0.375 to 1.00 have been subjected to 5,000 psi of sustained hydrostatic loading for up to 1,000 hours in the temperature range from 65°F to 75°F while the axial displacement of the windows through the flange has been monitored. The magnitude of axial displacement was found to be a function of α, t/D ratio, temperature, and duration of loading. Only windows with t/D ratios $\geq$1.000, 0.625, 0.500, 0.500, and 0.500 for 30-, 60-, 90-, 120-, and 150-degree conical angles, respectively, were found to be free of cracks. Minimum axial displacements of the windows can be achieved only with t/D ratios of $>$1.000, 1.000, 0.750, 0.750, and 0.625 for 30-, 60-, 90-, 120-, and 150-degree conical angles, respectively. The minimum axial displacements of D = 1.000-inch windows with these t/D ratios and conical angles are 0.042, 0.023, 0.023, 0.019, and 0.019 inch, respectively. It is recommended that only windows with t/D ratios $\geq$0.625 and $\alpha \geq$60 degrees be used for sustained hydrostatic loading of 5,000 psi at temperatures $\leq$80°F.

DD FORM 1 NOV 68 1473 (PAGE 1)

S/N 0101-807-6801

Unclassified

Security Classification

Unclassified

Security Classification

14 KEY WORDS	LINK A		LINK B		LINK C	
	ROLE	WT	ROLE	WT	ROLE	WT
Pressure vessel windows						
Acrylic plastic						
Conical						
Short-term pressurization						
Long-term pressurization						
Failure modes						
Displacement						
Deformation						
Fracture patterns						
Window flange designs						
Submersible windows						
Undersea habitat windows						
Deep-submergence windows						
Viewports						
Hyperbaric chamber windows						

R 686

Technical Report

STRUCTURAL DESIGN OF CONICAL ACRYLIC VIEWPORTS

June 1970

Sponsored by

NAVAL FACILITIES ENGINEERING COMMAND

NAVAL CIVIL ENGINEERING LABORATORY

Port Hueneme, California

STRUCTURAL DESIGN OF CONICAL ACRYLIC VIEWPORTS

Technical Report R-686

YF 38.535.005.01.005

by

M. R. Snoey and M. G. Katona

ABSTRACT

The purpose of this report is to establish a rational engineering approach for the design of conical acrylic viewports. To achieve this goal, a time-dependent, yield-failure criterion was developed and utilized in the analysis of a variety of viewport configurations. Specifically, a range of thickness/minor diameter (t/d) ratios from 0.25 to 1.75 and included angles from 60^{o} to 120^{o} were analyzed by the finite element technique. Using the viewport structural analysis in conjunction with the yield-failure criterion for acrylic, time-dependent operating depths were determined as a function of viewport configuration.

Paralleling the above, an experimental investigation was performed to validate the analytical results. Six full-scale viewports were tested for a year under simulated operational conditions that included simultaneous cycling of pressure and temperature, 0 to 4,000 psi and 70 to 35^{o}F, respectively.

Comparison of analytical and experimental results indicated excellent agreement for the physical location of viewport failure at specified loading histories.

Design recommendations are presented in the form of design curves which enable the design of a conical acrylic viewport for a specified operating pressure and duration under load. To complete the recommendations, design information is given also on sealing with a conventional O-ring, as well as guidelines for elevating a viewport in its flange.

CONTENTS

INTRODUCTION

Objectives

1. Accumulate experimental test data on full-scale viewports under simulated operational conditions.
2. Develop a rational failure criterion for conical acrylic viewports.
3. Develop parametric design curves based on the failure criterion.

Purpose

The presence of viewports in practically every undersea vehicle is indicative of their importance for visibility in undersea research. Piccard[1] first introduced conical acrylic viewports in 1939 and, presently, 18 submersibles, or about half the total number, utilize Piccard's 90° conical frustum design for a wide range of operating depths. Figure 1 shows full-scale, 90° conical viewports while Reference 2 contains a historical background on viewports along with a summary of viewport designs for about 40 vehicles.

This study is intended to satisfy a need in the design of conical viewports that has existed and has seen no improvement for the past 30 years. The need was to develop parametric design curves based on the viewports functional use and to include time effects (creep) in the design curves.

A thorough structural analysis of a conical viewport was not even available until just recently.[3,4,5] All three of these references provide good insight into the structural response of a conical viewport, however, they do not provide any information for the designer.

Although acrylic viewports have accumulated a large amount of operational time, thereby generating some confidence in the material, trepidations still do exist. Design curves based on accurate experimental material tests, a rational failure theory, and complete structural analysis should relieve these fears and provide more confidence in viewport design.

Design recommendations for conical acrylic viewports would not be complete without a section on sealing. Therefore, Appendix A contains information on methods of sealing and how they affect the viewport design economically, operationally, and structurally.

Figure 1. Full-scale, 90° conical acrylic viewports.

SCOPE OF INVESTIGATION

The investigation was divided into two sections: (1) the experimental phase which will be discussed first followed by (2) the analytical phase.

Experimental Phase

The objective of the experimental tests was to accumulate data on full-scale, 90^{o} conical viewports with a range of thickness to minor diameter ratios, **t/d**. Figure 2 shows a cross section of a typical viewport. The test conditions simulated actual operational conditions as nearly as possible so that the results could be used to provide insight on the type and location of failures occurring during operation. More importantly, the data would serve to test the validity of the analytical results.

Tests were conducted on six viewports of three sizes as listed in Table 1. The viewports were all machined from a 4-inch-thick commercial cast sheet of Plexiglas G acrylic plastic. The minor diameters were approximately 4, 6, and 8 inches which gave t/d ratios of 0.92, 0.61, and 0.45, respectively.

Table 1. Full-Scale Experimental Viewport Dimensions

Included Angle, α (±5')	Major Diameter, D (in.)	Minor Diameter, d (in.)	Thickness, t (in.)	t/d
90^{o} 0'	11.863	4.193	3.835	0.915
90^{o} 0'	11.854	4.180	3.837	0.916
90^{o} 0'	13.969	6.299	3.835	0.610
90^{o} 0'	13.950	6.292	3.829	0.608
90^{o} 0'	16.013	8.411	3.801	0.453
90^{o} 0'	16.025	8.431	3.797	0.451

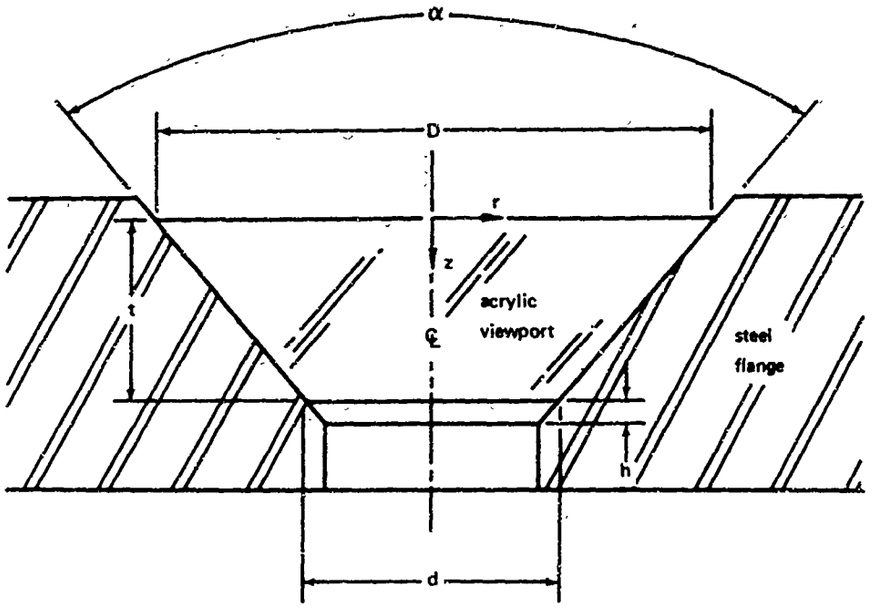

Figure 2. Cross section of a typical viewport.

The six viewports were tested simultaneously in three refrigerated pressure vessels. Displacements and post-test observations served as the recordable data. Details on the equipment and test procedure used are in Appendix B.

Inasmuch as an undersea vehicle might make many dives, cycling of the pressure load was included as part of the test procedure. The simulation of actual dives required simultaneous changes in pressure and temperature. As the pressures were changed from 0 to 4,000 psi, the temperature simultaneously was changed from 70 to 35°F. It was believed that the most severe test of the viewports would be to cycle the maximum creep strains occurring in each viewport under the 4,000 psi load. Therefore, the period of the cycle for all viewports was determined by loading the least conservative design, $t/d = 0.45$, and letting the viewport displace until the displacement-time curve was asymptotic within the accuracy of the measuring system. This resulted in a "load-on" time period of 500 hours with a "load-off" or relaxation period of 100 hours; the time necessary to completely relax all the strains so the viewport would return to zero displacement. The tests were conducted over a 1-year period which resulted in 13 total cycles.

Analytical Phase

General. The knowledge gained from the experimental tests was utilized as a basis for performing an analytical study on viewport designs. In particular, analytical investigation for a spectrum of viewport parameters, t/d and α ranging from 0.25 to 1.75 and 60^{o} to 120^{o}, respectively, was accomplished by means of the finite element technique.

In order to develop rational design recommendations, it is necessary to define the capacity of the system, i.e., what constitutes failure. Since the failure mode definition and failure criteria influence the assumptions made in an analytical study, the concept of failure is discussed prior to the analytical method of attack.

Concept of Failure. Failure must be considered from two viewpoints: (1) the structural level and (2) the material level. First, at the structural level, the investigator must define failure. In the past, structural viewport failure has been taken as the complete collapse of the system, often called the upper limit or ultimate strength, which is typified by large plastic flow and rupture. Another definition of failure is the lower limit capacity of a system which is defined as that load which causes initial plastic yielding in any local region of the system.

The authors have chosen the lower limit or "yield criterion" as the definition for failure of acrylic viewports based on the following considerations. (1) The functional use of a viewport is to transmit undistorted and undiminished light to the viewer, however, earlier experimental results have shown that this function is seriously impaired when the viewport is loaded into the plastic range which results in crazing and distortion of the acrylic. (2) The pressure that causes yielding is much lower than the load causing ultimate collapse failure; consequently, a built-in safety factor for the hazardous environment is intrinsic in the lower limit design, in addition to the standard safety factor used for the functional aspect.

The second major consideration in establishing a failure criterion belongs to the realm of the material itself independent of the particular structure configuration and functional use.

Since, by definition, the structure fails when local yielding occurs, this dictates that a yield criterion for acrylic must be established which will adequately predict yield states under combined stresses. Fortunately, much research has been accomplished in this area and it has been shown that the Huber-von Mises-Hencky or distortion energy theory of failure[6] predicts combined-stress yield-states extraordinarily well for acrylic.[7,8] However, this flow law is complicated by the anisotropic response of yielding in tension

and compression with tensile strength being lower than the compressive. A conservative approach was used to circumvent this problem. The tensile strength was applied to combined states of stress at any time when at least one principal stress was significantly in a tension zone, and the higher compressive strength was used strictly in the all-compression failure octant.

Because acrylic is a typical thermoplastic, two additional variables significantly affect its material properties: temperature and time.

In general, when temperatures are increased, acrylic material properties decrease in value. This feature of acrylic makes it an ideal material for its proposed use as a viewport for an undersea vehicle because the ocean provides a low-temperature environment which enhances properties over those measured at room temperature.

The design recommendations set forth in this report are based upon material response at room temperature, thus allowing the additional strength of the acrylic due to lower temperatures at operational depths to increase the margin of safety.

The second variable, time, is not as easily dealt with as temperature, but is certainly important due to the creep properties of acrylic. For this reason every effort has been made to rationally treat the effect of time on the stress distributions of the viewport and the yield strength of the acrylic. The details of this approach are given in Appendix C as a separate topic because this treatment is not limited to viewports; the approach may be used for any structure utilizing acrylic.

Briefly, the approach is to choose the "worst" stress distribution and utilize this for any value of the parameter time, while the development of a yield-stress versus load-duration curve provides the factor of time in the design parameters. Appendix C deals with the concepts in a straightforward and rational manner.

Method of Analysis. As discussed in Appendix C, the highest stress concentrations result from the viscoelastic solution when time is equal to zero. This is identical to elastic solutions; consequently, elastic solutions based on all the classical assumptions of linear, infinitesimal-strain, elastic theory were assumed and the solutions were obtained by the finite element program for an axisymmetric solid written by Wilson.[9] References 4 and 5 verify the capability of using a finite element analysis on conical acrylic viewports.

The sequence of analysis was as follows: for each viewport configuration, the finite element program computed the local state of stress at every element and the corresponding effective stress defined as

$$\sigma_o = \sqrt{\frac{(\sigma_1 - \sigma_2)^2 + (\sigma_2 - \sigma_3)^2 + (\sigma_3 - \sigma_1)^2}{2}}$$

where σ_o = effective stress at an element per unit of applied pressure

$\sigma_1, \sigma_2, \sigma_3$ = principal stresses at each element per unit of applied pressure

Thus the relationship for yielding becomes

$$p = \frac{\sigma_y}{\sigma_o}$$

where

KNOWN BY FINITE ELEMENT SOLUTION

- σ_o = the maximum effective stress of all elements with all the principal stresses in compression

or

- σ_o = the maximum effective stress of all elements with any tension in the principal stresses

KNOWN BY YIELD-STRESS VS TIME CURVES

- σ_y = material yield strength in compression for a particular loading duration

or

- σ_y = material yield strength in tension for a particular loading duration

DESIGN REQUIREMENT

- p = the maximum pressure that can be applied to the viewport which initiates yielding in any zone with all the principal stresses in compression

or

- p = the maximum pressure that can be applied to the viewport which initiates yielding in any zone with tension in the principal stresses

The above format explicitly sets forth the procedure used to determine the capacity of the various viewport geometries.

A further point of concern was in specifying the boundary condition between the viewport and the flange. In order to account for all practical contingencies, two extreme boundary conditions were applied to each viewport configuration as shown in Figure 3: (1) the boundary was fixed, representing maximum friction between the acrylic viewport and its flange; and (2) the boundary was allowed to be frictionless, representing perfectly smooth, greased interfacing. Of these two boundary conditions, the one resulting in the controlling failure as outlined above, was chosen as the governing boundary condition.

A structural response discovered during the course of the analysis was that an arbitrarily high stress concentration existed in the element at the corner of the low-pressure face for all viewport configurations and boundary conditions. This phenomenon correlated with experimental findings where it was discovered that the low-pressure face corner underwent deformation or "rounding" for even the smallest load magnitudes (see Figure 4).

An intensive analytical investigation, outlined in Appendix C, revealed that the spiked stress concentration was relieved by deforming the corner of the mathematical model as was suggested by the experimental models. Thus, the viewport geometries considered in this report were all analyzed with a predeformed corner characterizing an actual viewport after its initial loading.

The last analytical refinement considered was to investigate the response from an O-ring groove machined in the acrylic. The analytical results along with the experimental tests are presented in Appendix A.

Input to Wilson's code[9] required material properties for acrylic. Reference 5 describes experimental tests performed to determine these necessary values at room temperature as: modulus of elasticity, 444,000 psi; and Poisson's ratio, 0.4.

RESULTS AND DISCUSSION

Experimental

Post-test visual observations and displacements at the center of the viewport low-pressure face served as experimental data. Since the viewports were all exposed to the same pressure loading and environment, the cause of any post-test effects would be the differences in structural design (all other variables considered equal).

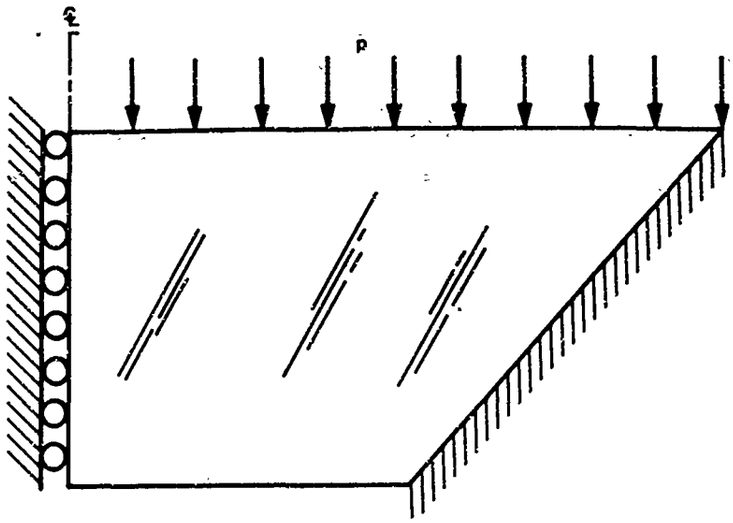

(a) Fixed boundary.

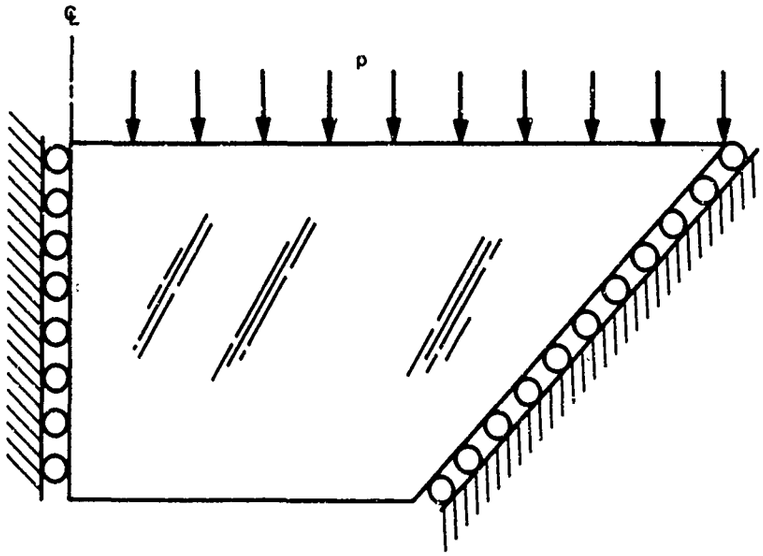

(b) Free boundary.

Figure 3. Boundary conditions for finite element analysis.

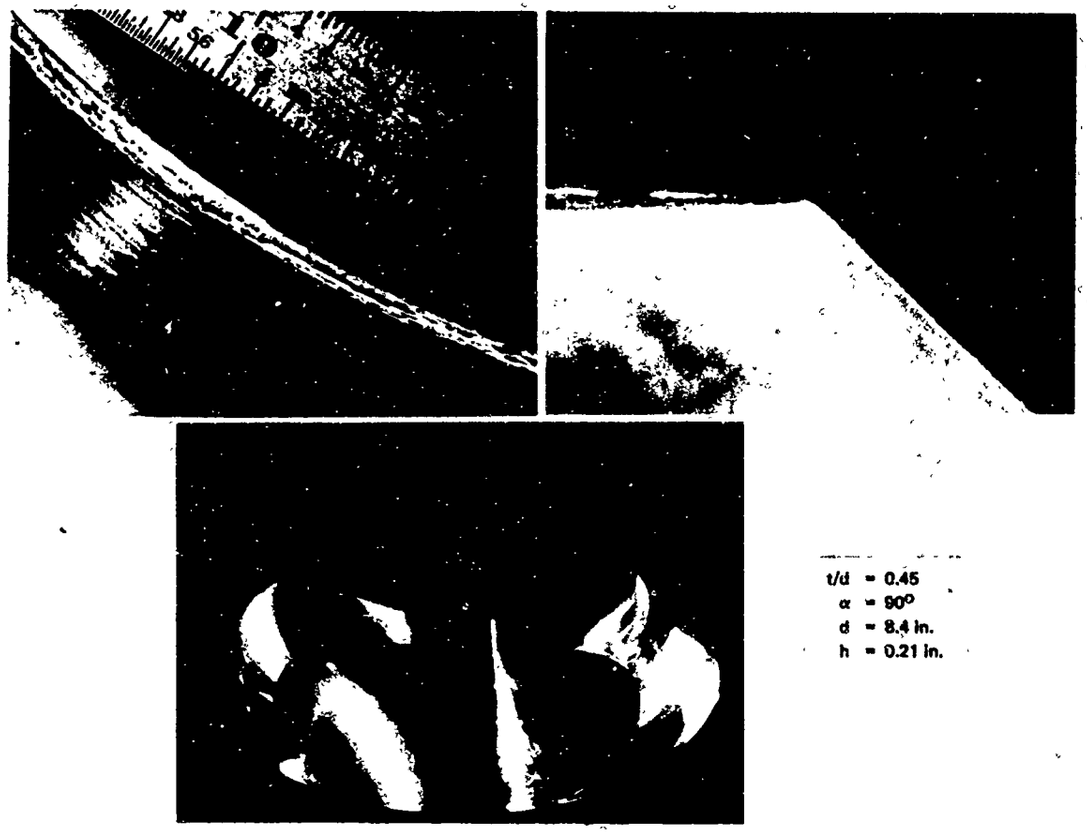

Figure 4. Post-test physical condition of t/d = 0.45 viewport after thirteen cycles.

Post-Test Observations. Failure results on the six viewports are contained in Table 2. From Table 2, it is shown that as the t/d ratio decreased, the frequency of stress crazing and cracks increased. Figures 4, 5, and 6 provide a visual supplement to Table 2. The least conservative design or the lowest t/d ratio (0.45) is shown in Figure 4. The resulting cracks and deformation at the low-pressure face corner are clearly shown. There was no visible damage anywhere else on the viewport. Collection of condensate around the low-pressure face resulted in an accumulation of rust on the flange which caused the ragged surface on the rounded corner of the viewport.

Table 2. Results of Test on Full-Scale Viewports

t/d Ratio	Maximum Width of Crack Pattern (in.)	$\frac{\text{Creep Displacement}}{\text{Total Displacement}} \times 100$ (%)
0.92	0 0	14
0.61	1/16 0	20
0.45	3/32 1/16	26

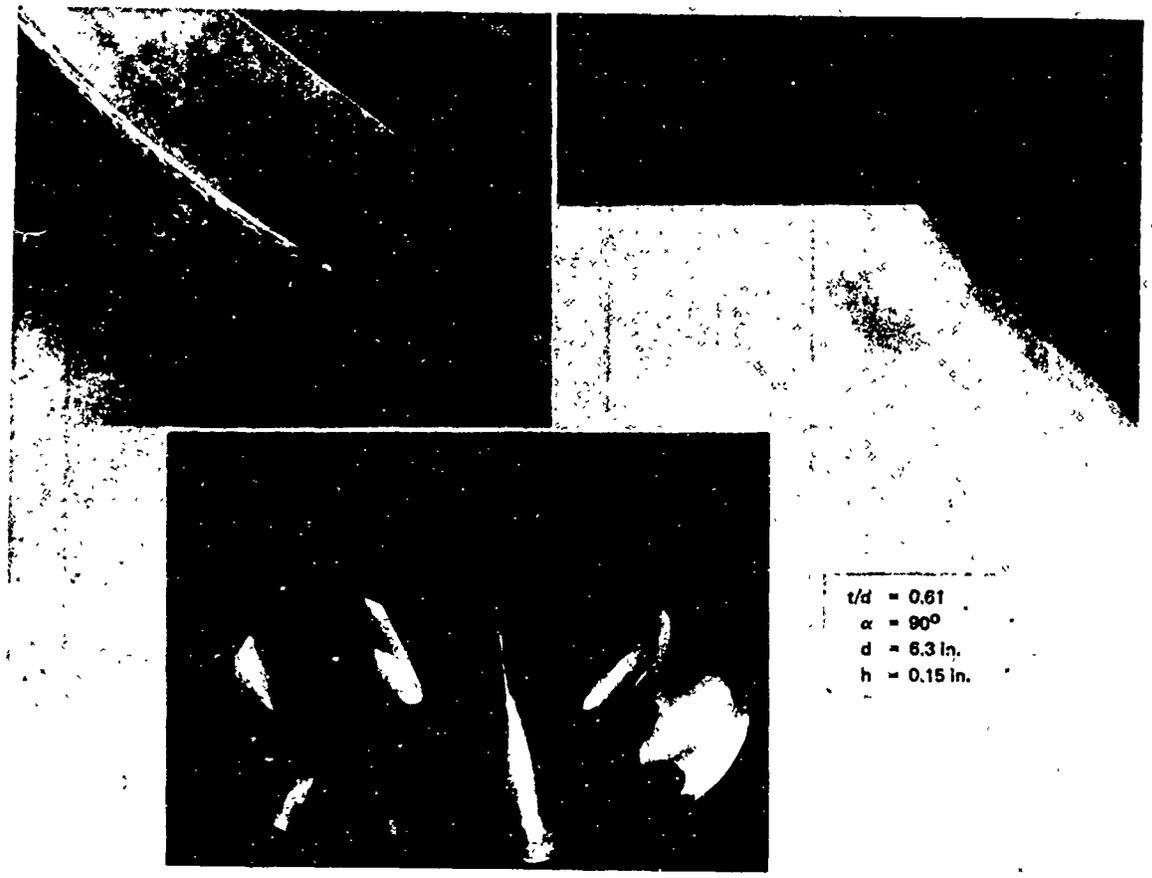

Figure 5. Post-test physical condition of t/d = 0.61 viewport after thirteen cycles.

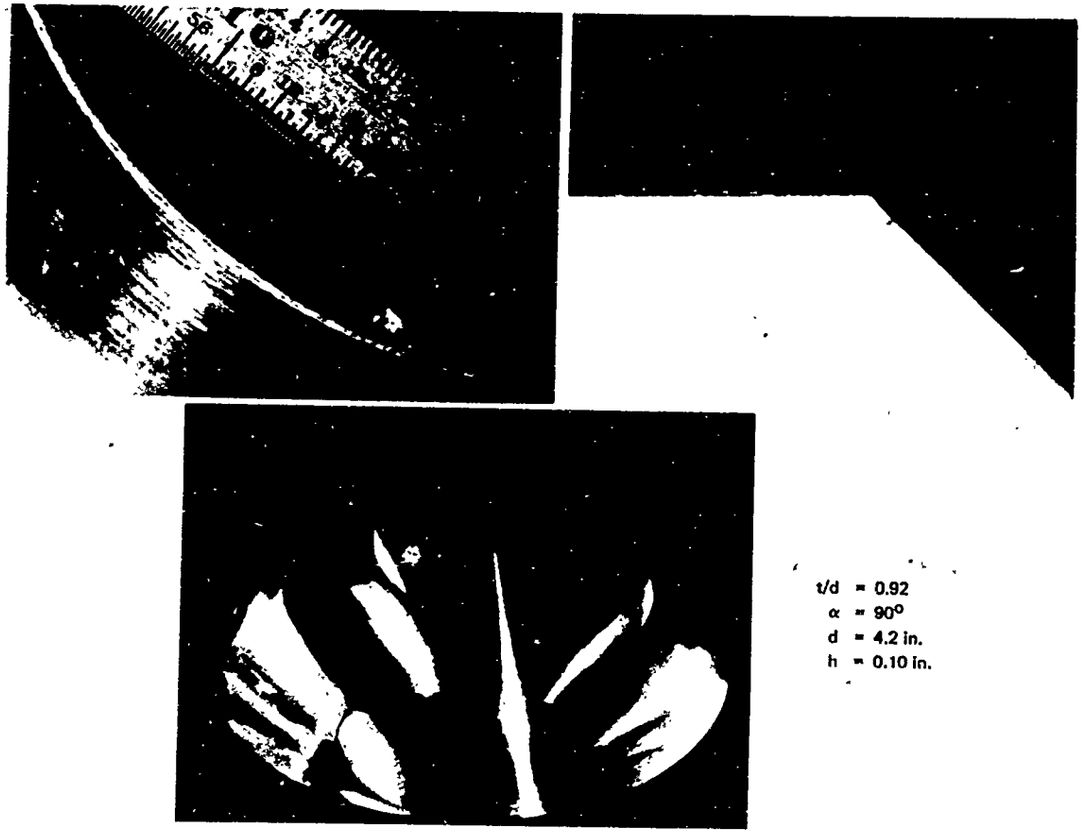

Figure 6. Post-test physical condition of t/d = 0.92 viewport after thirteen cycles.

The t/d = 0.61 viewport with its crazing cracks is shown in Figure 5. These cracks are much smaller than the ones in Figure 4 and the crack band is much narrower. The corner did not deform as much as in the previous case.

In the most conservative design, t/d = 0.92, there were no cracks visible anywhere. In fact, the corner rounding even appeared to be at a minimum.

Displacements. Figure 7 contains the absolute displacements of the three pairs of experimental viewports which are presented in this case to provide the designer with a good feel for maximum viewport displacements. The pressure and temperature cycling periods are also shown in Figure 7. Table 2 gives the percentage of the total displacement due to creep.

To simulate a dive, the pressure was increased at a rate of 50 psi/min, and the cooling of the system was initiated. It should be noted that at the operating depth or highest pressure, the temperature is the lowest. The total time period for a typical cycle was 600 hours. As was expected, the least conservative design, t/d = 0.45, had the highest absolute displacement (Figure 7) and the highest percentage of creep (Table 2).

Analytical

Analytical results consist of pertinent plots and data extracted from the finite element analysis results. The data are divided into two areas: (1) stresses and (2) displacements. Both results demonstrate the variations in structural response due to changes in the following parameters: t/d ratio, included angle, and boundary condition.

Stresses. Figures 8 through 13 include both a contour and surface plot of the effective stresses for each of the 24 computer runs; four t/d ratios, three included angles, and two boundary conditions were used. The stress contour plots provide visual quantitative data, whereas, the surface plots provide visual qualitative data. Figures 8, 9, and 10 present the results for the fixed boundary condition, and Figures 11, 12, and 13 present the results for the free boundary case. In all of the plots, the stress concentration is apparent at the corner of the low-pressure face. For either the fixed or free boundary condition, the strength of the viewport is seen to increase with an increase in either the t/d ratio and/or the included angle. This agrees with data developed in Reference 3.

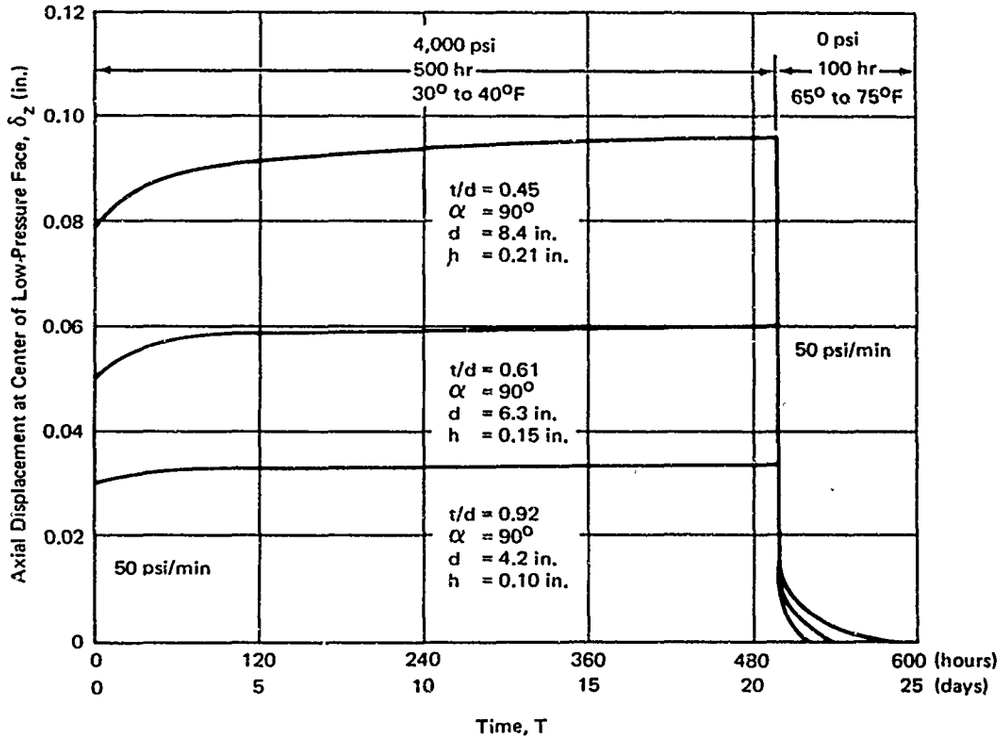

Figure 7. Typical displacement responses during one of thirteen cycles.

Two items of interest are apparent from the surface plots: (1) the flexural bending behavior exhibited by the t/d = 0.25 viewports and the absence of bending exhibited by the t/d ratios of 0.75, 1.25, and 1.75; and (2) the absence of high effective stresses at the high-pressure face corner. Generally speaking, this latter area appears to be in almost a hydrostatic stress state which means that some structural modification could be made in this region (refer to Appendix A).

Displacements. Figure 14 illustrates the displacements at the center of the low-pressure face. The results are presented in nondimensional form for use with any diameter viewport. Generally speaking, the difference in displacement between the fixed and free boundary condition is the gross distance that the viewport moves. Thus, the 60^{O} included angle viewport displaces much more in the free case, which causes the higher effective stress at the low-pressure face corner. The 90^{O} and 120^{O} viewports displace less and thus, the effective stress is less. The transition to flexural behavior is evident in Figure 14 by the knee in the curve at about t/d = 0.6. Two additional points (t/d = 0.45) from the analysis in Appendix A are included in Figures 14, 15, 16, and 17.

Figure 14 is also used in the Design Recommendations section of the report for calculating elevation of the viewport in the flange.

Comparison of Experimental and Analytical Results

Figures 15 and 16 provide a comparison of experimental and analytical results. Figure 15 is based on the operating pressure and shows an excellent comparison. The experimental data is based on post-test observations of the six experimental viewports, while the analytical data is based on the magnitude of the effective stress at the low-pressure face corner. Cracks determined the presence of failure in the experimental viewports, while the controlling factor in the analytical analysis was the pressure required to equate effective stress with yield stress in the compression-compression-compression octant. Note that the free boundary condition controls for the range of the t/d ratios and that the analytical curves were shifted to the left by 20% in accordance with the low temperature.[4,10] Although the 35^{O}F sea water is on the high-pressure face, it is a fair assumption that the steel flange has a low-temperature-gradient throughout and thus, provides a 35^{O}F interface with the viewport.

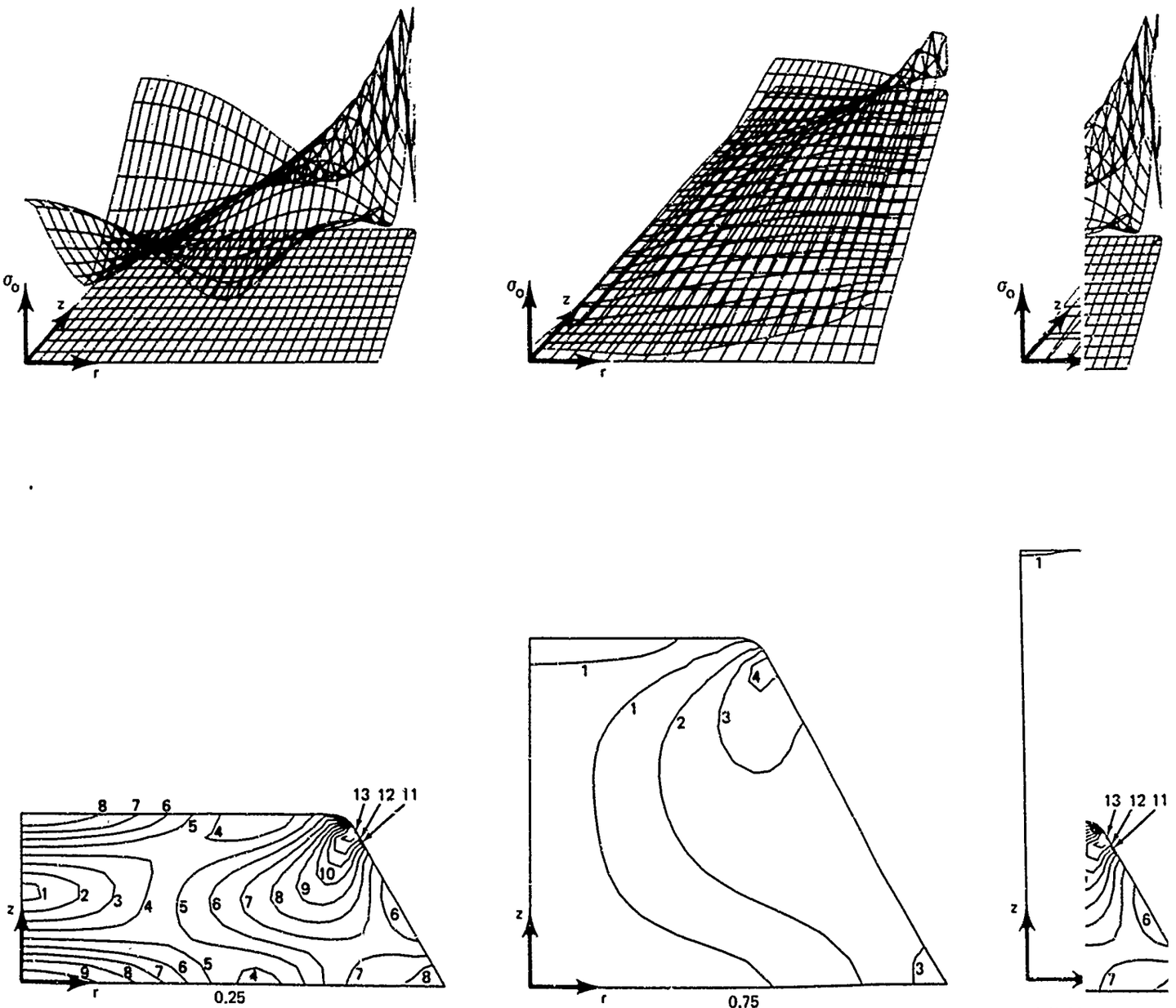

Figure 8. Effective stress contour and surface plots for 60°

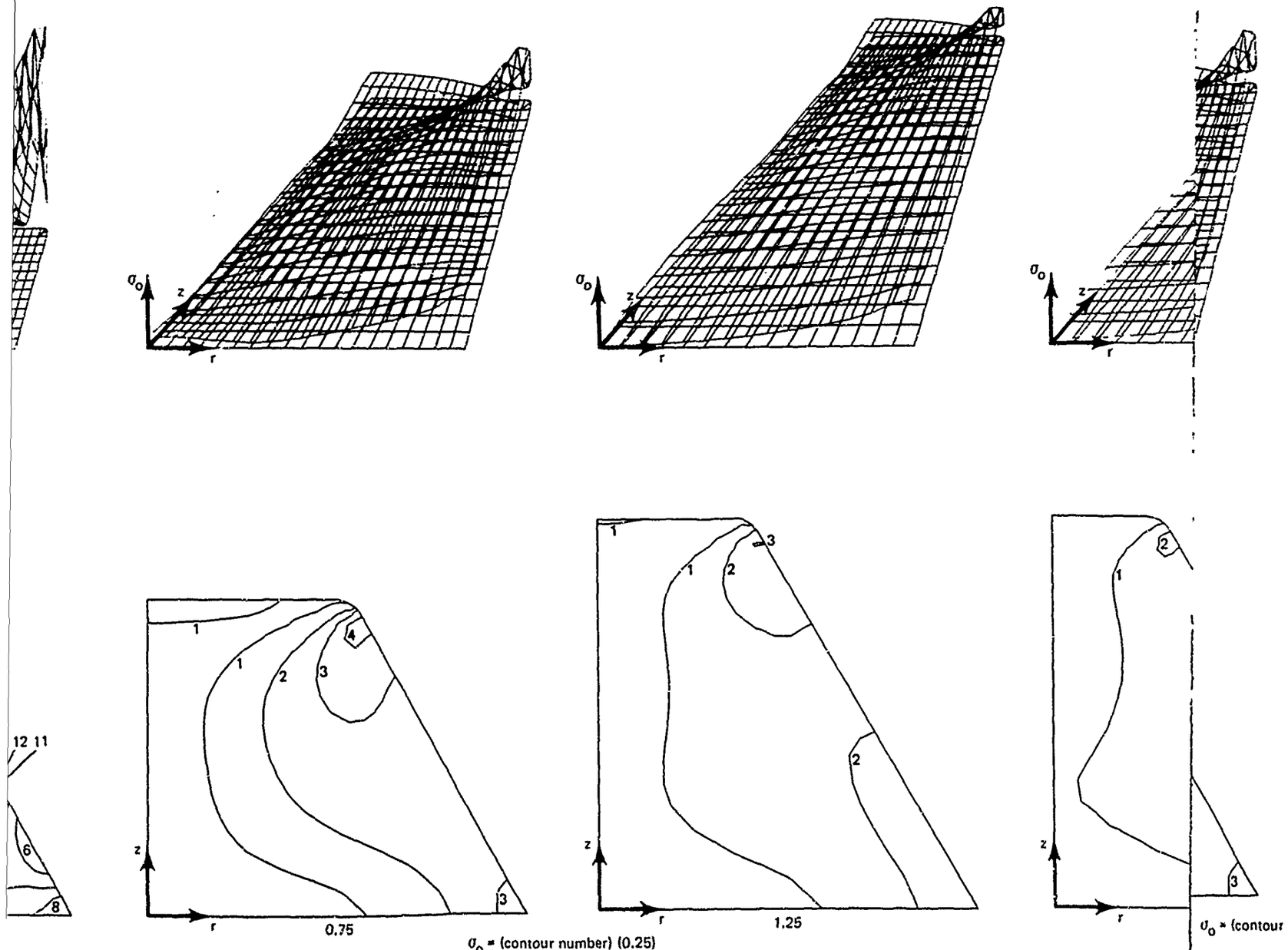

Figure 8. Effective stress contour and surface plots for 60° angle and fixed boundary condition.

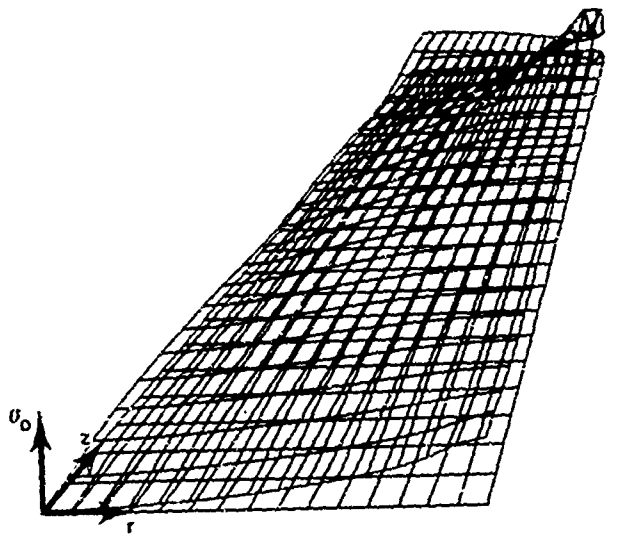

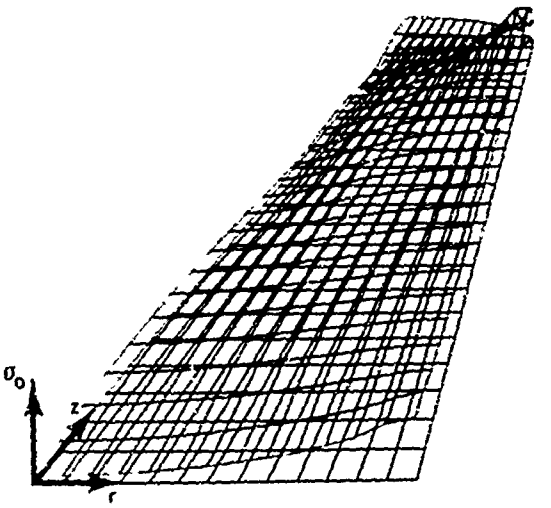

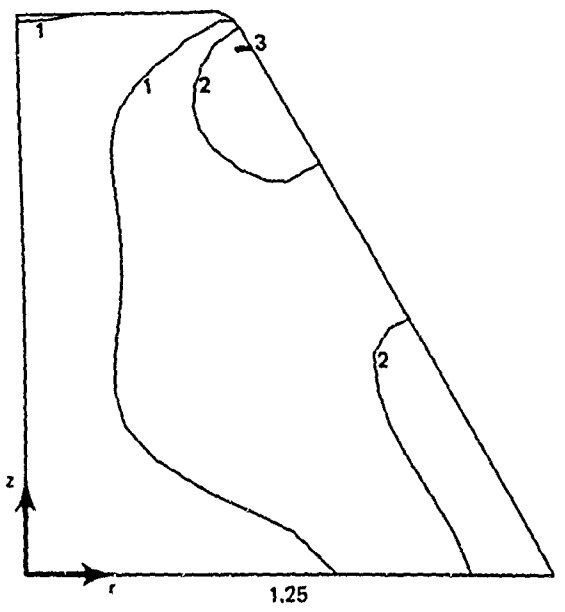

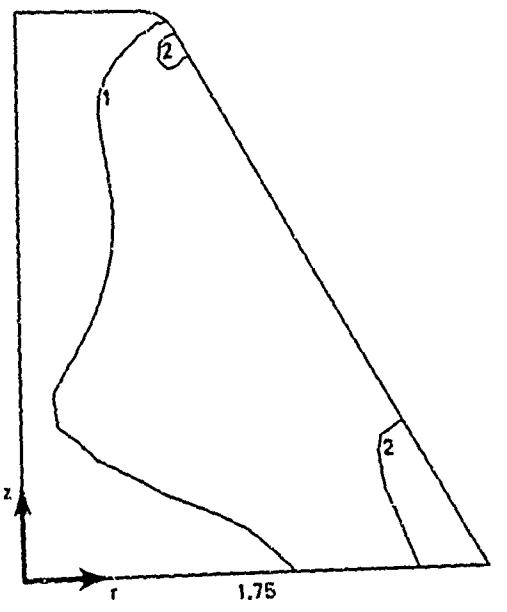

ontour number) (0.25)

Minor Diameter Ratio, t/d

rface plots for 60^{o} angle and fixed boundary condition.

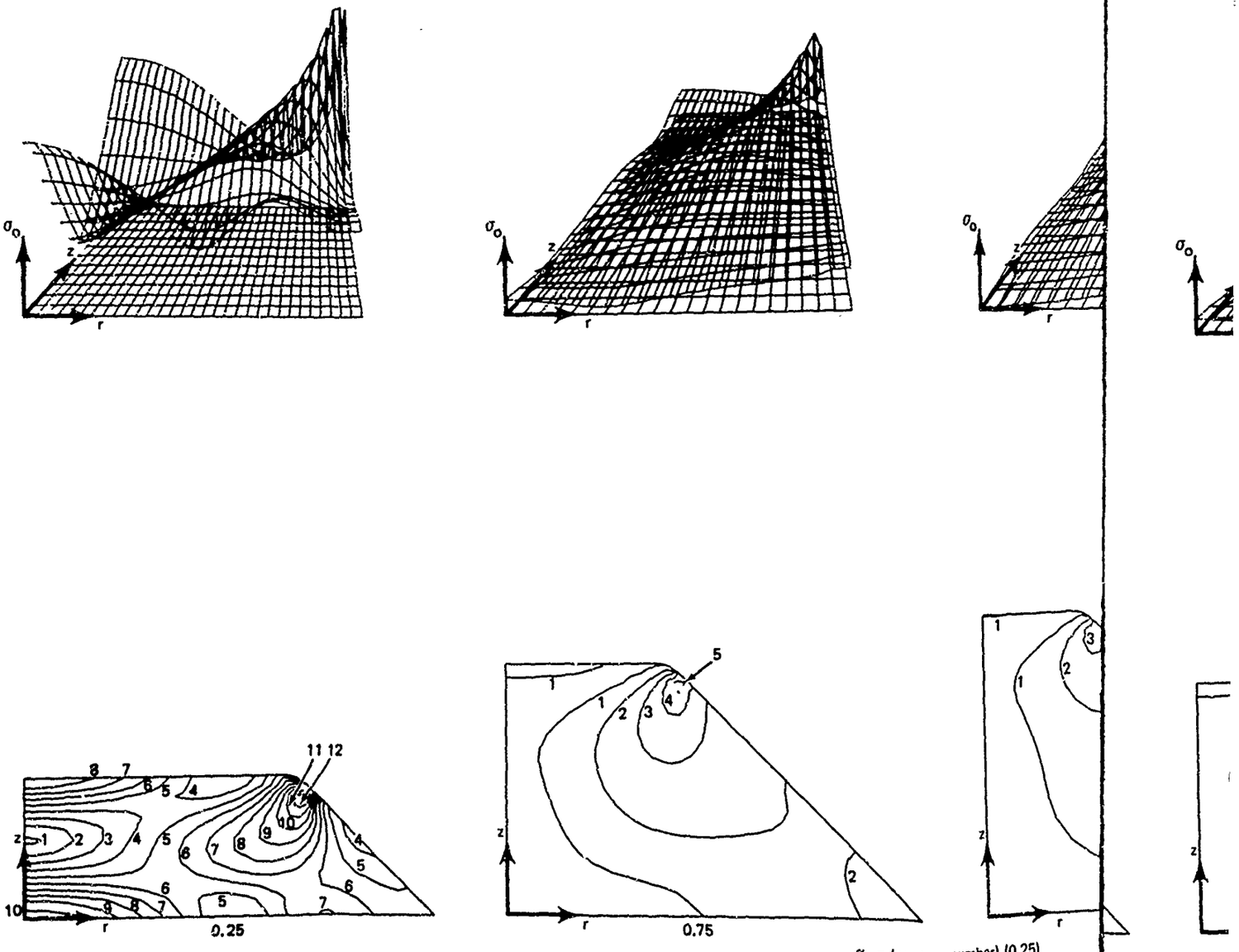

Figure 9. Effective stress contour and surface plots for 90° angle and

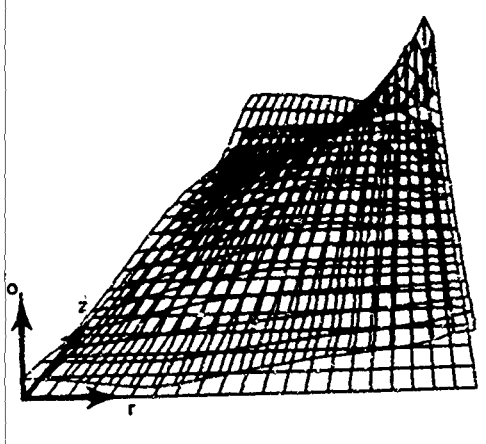

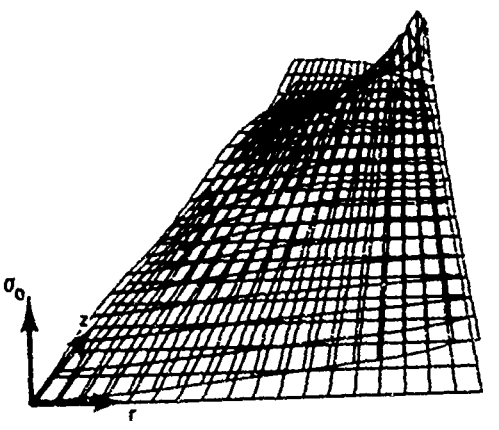

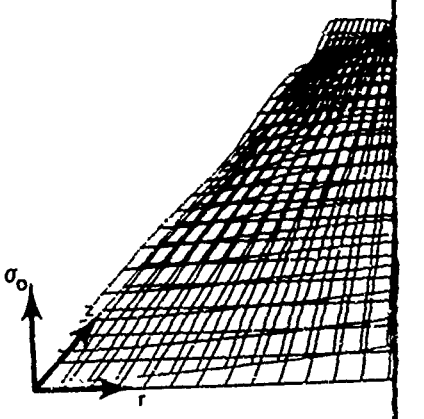

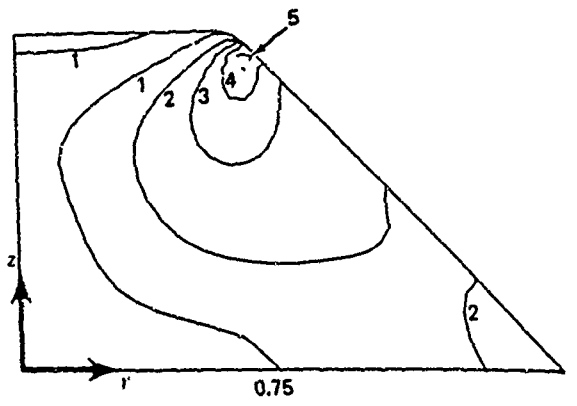

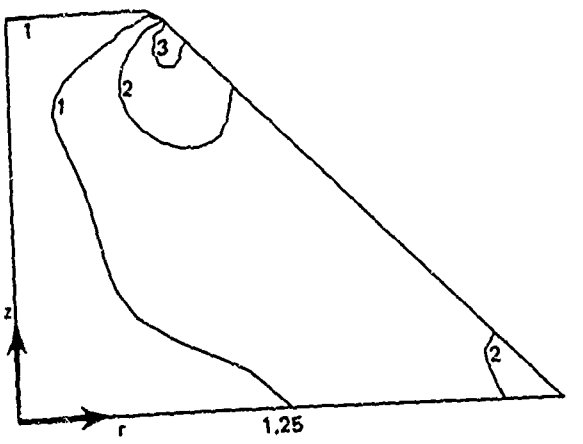

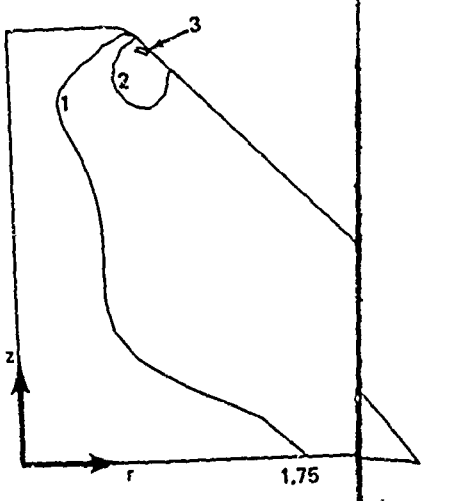

σ_o = (contour number) (0.25)

Thickness/Minor Diameter Ratio, t/d

Figure 9. Effective stress contour and surface plots for 90° angle and fixed boundary condition.

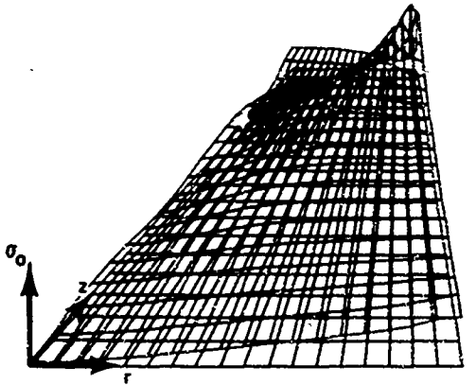

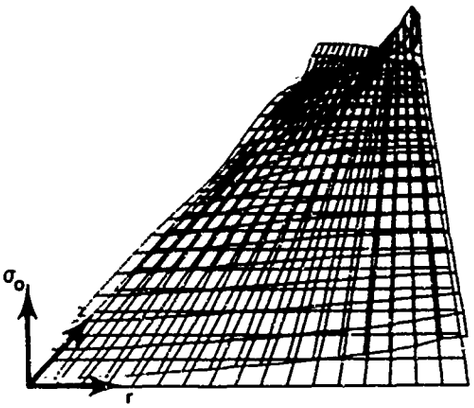

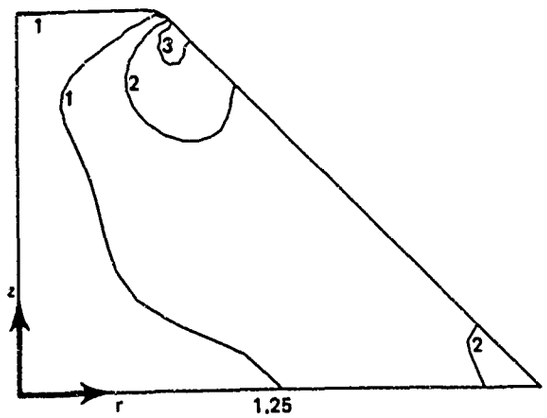

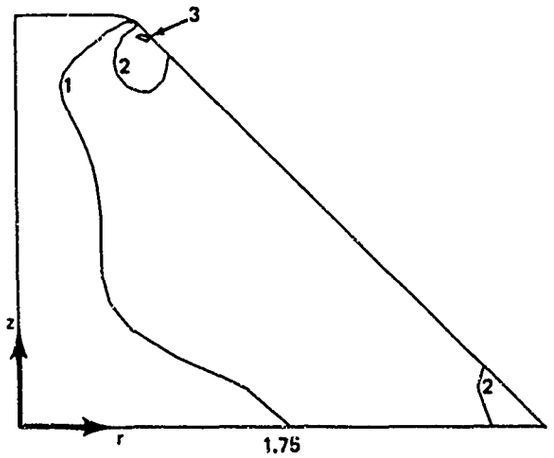

mber) (0.25)

meter Ratio, t/d

ts for 90° angle and fixed boundary condition.

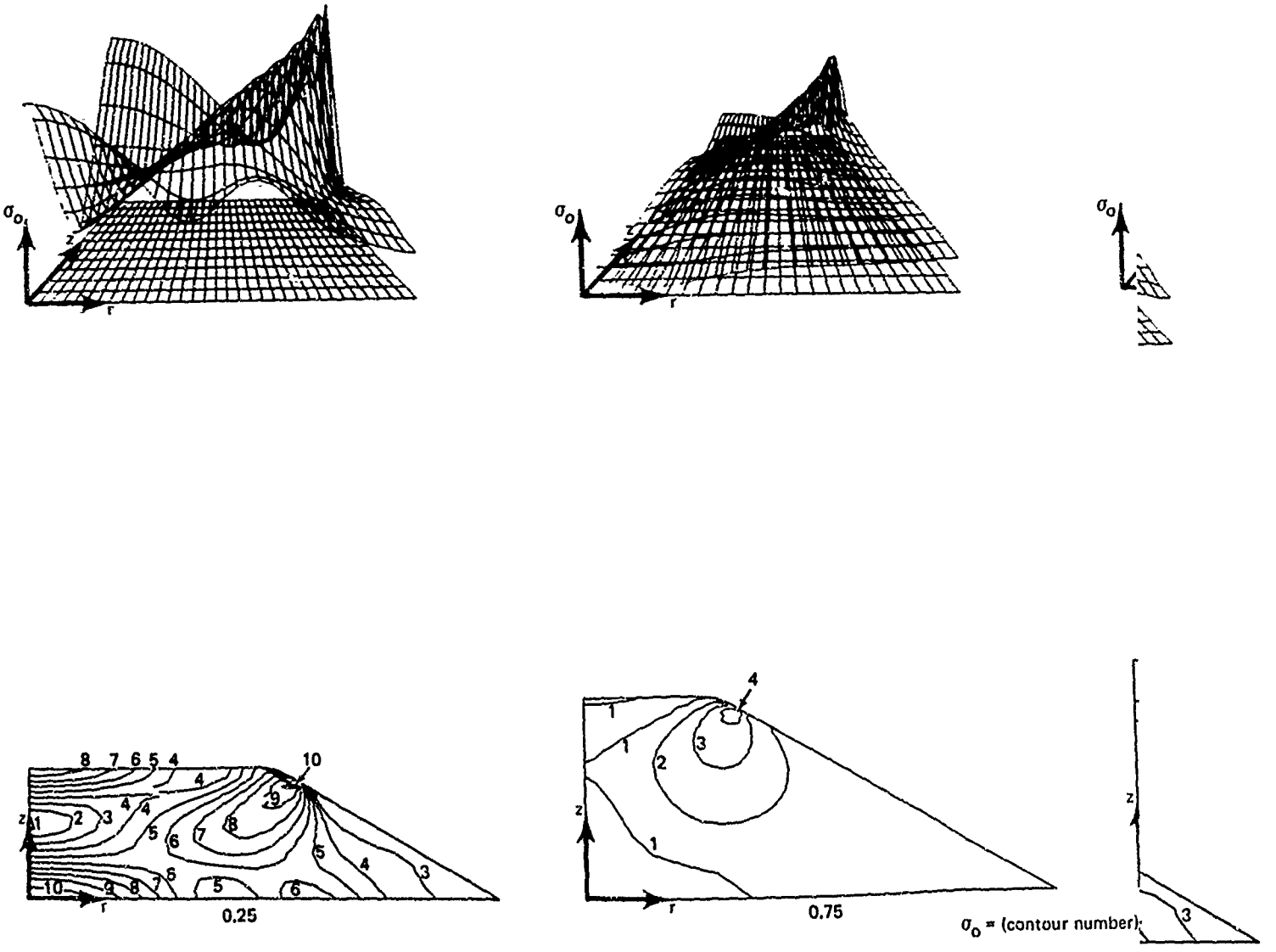

Figure 10. Effective stress contour and surface plots fo

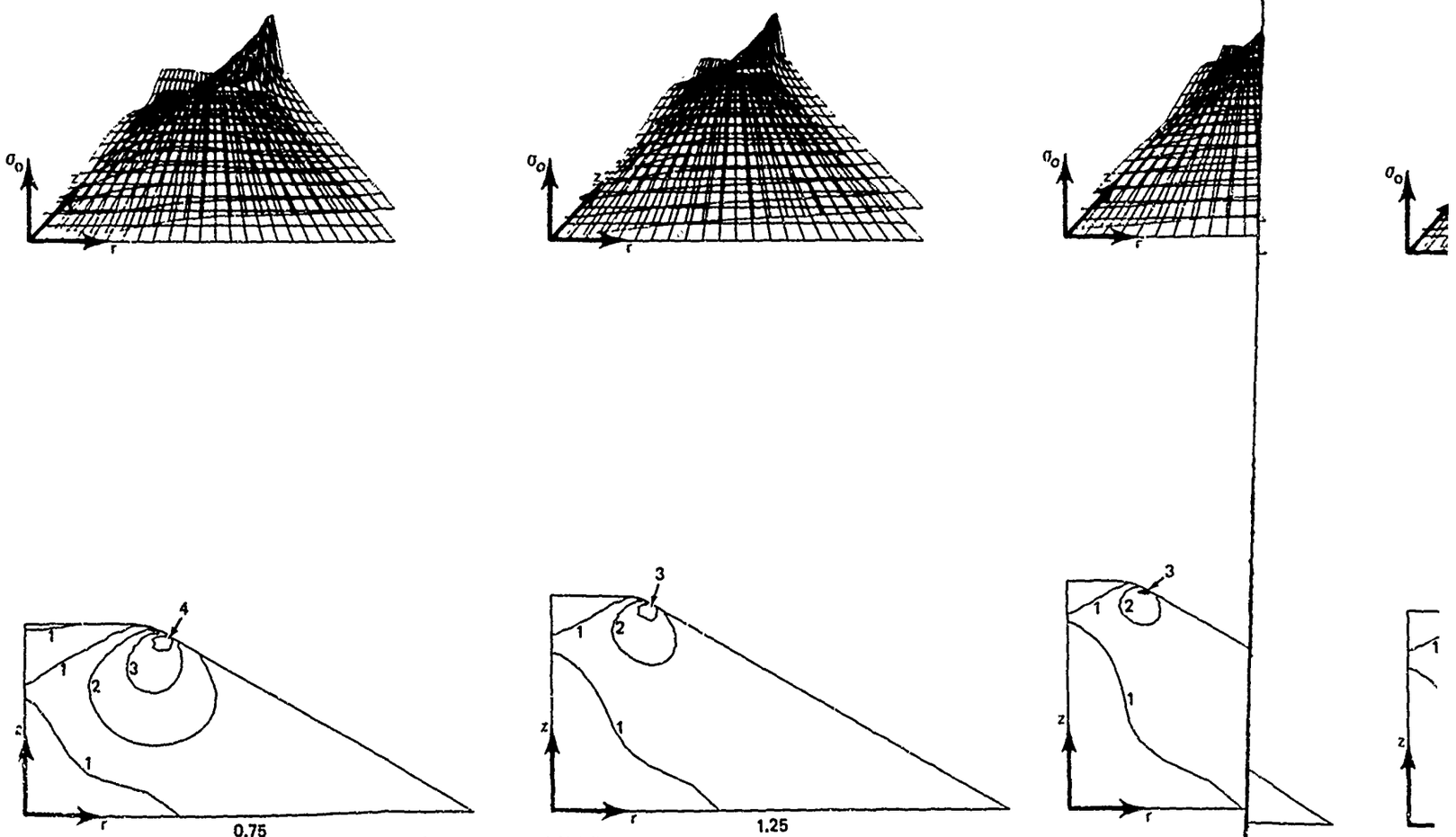

σ_o = (contour number) (0.25)

Thickness/Minor Diameter Ratio, t/d

Figure 10. Effective stress contour and surface plots for 120° angle and fixed boundary condition.

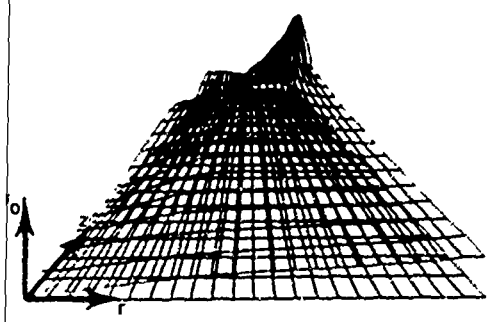

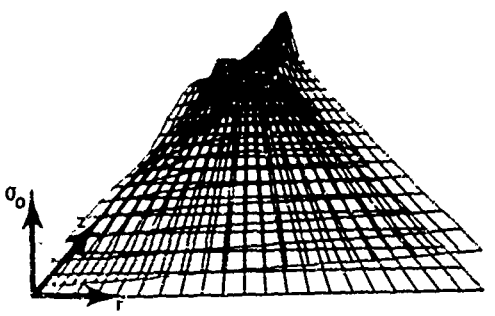

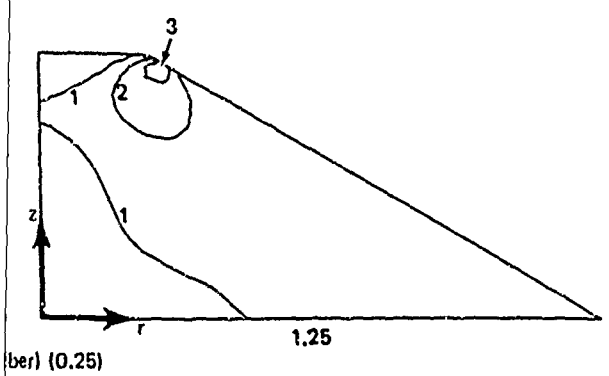

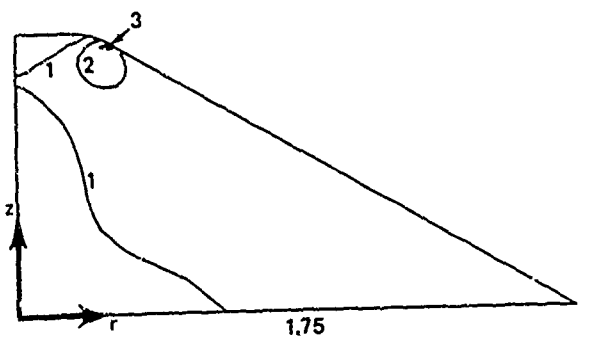

ber) (0.25)

neter Ratio, t/d

s for 120^{0} angle and fixed boundary condition.

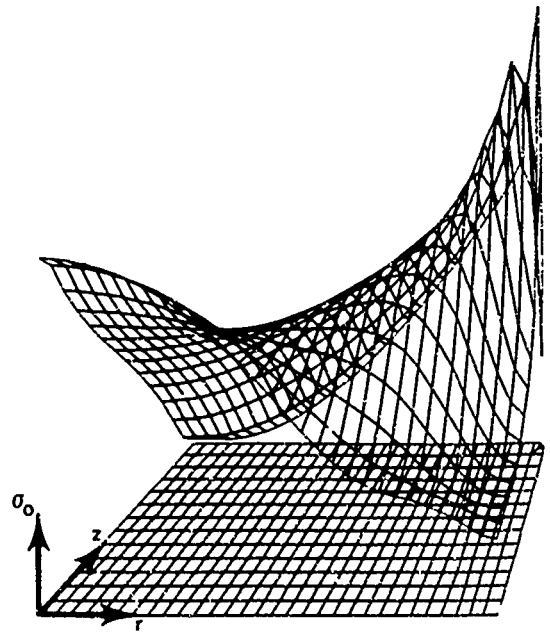

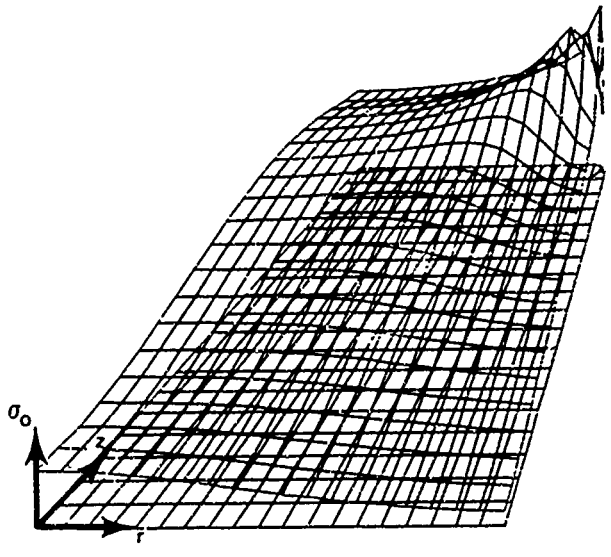

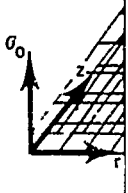

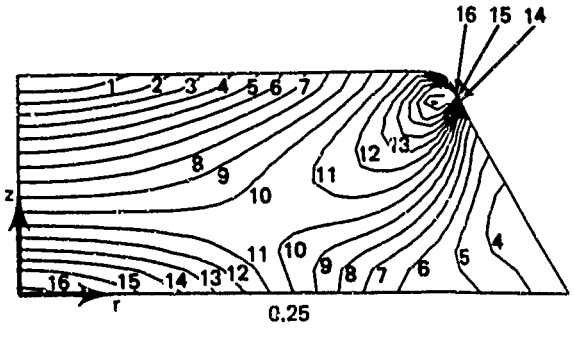

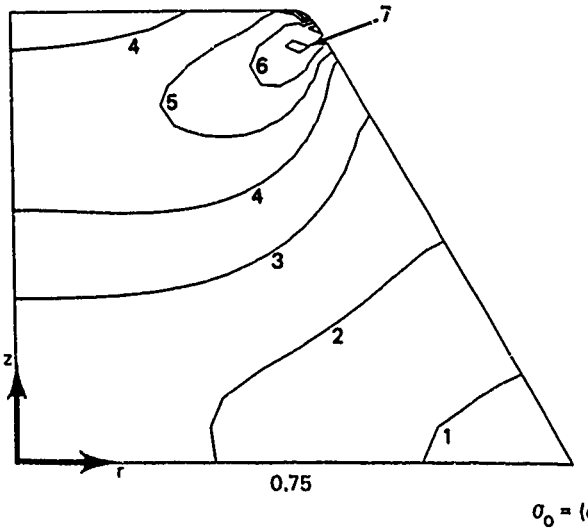

σ_o = (contour number) (0.25

Thickness/Minor Diameter Ratio

Figure 11. Effective stress contour and surface plots for 60°

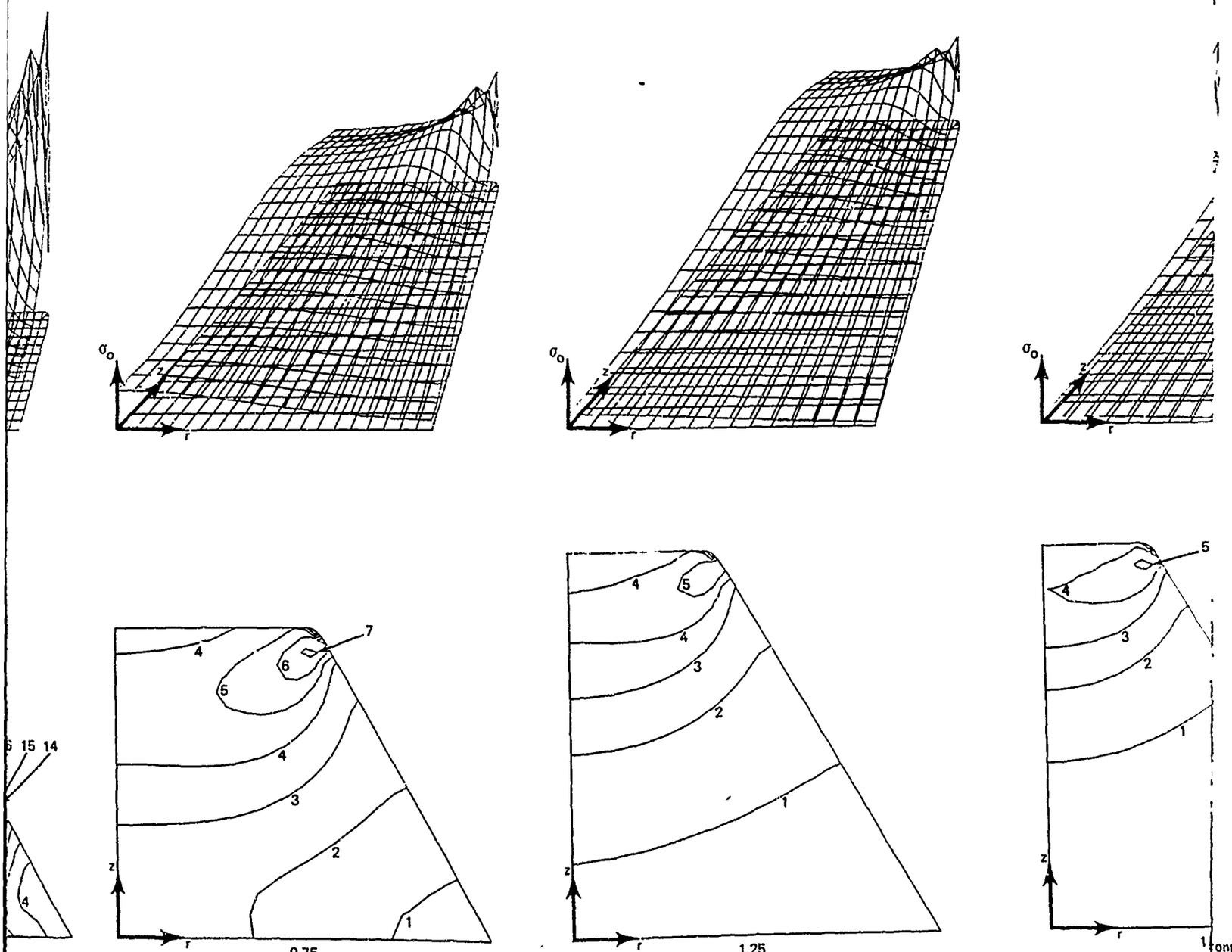

Figure 11. Effective stress contour and surface plots for 60° angle and free boundary condition.

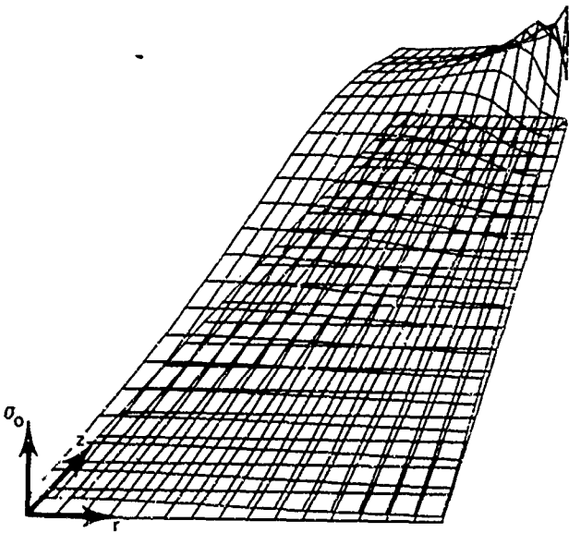

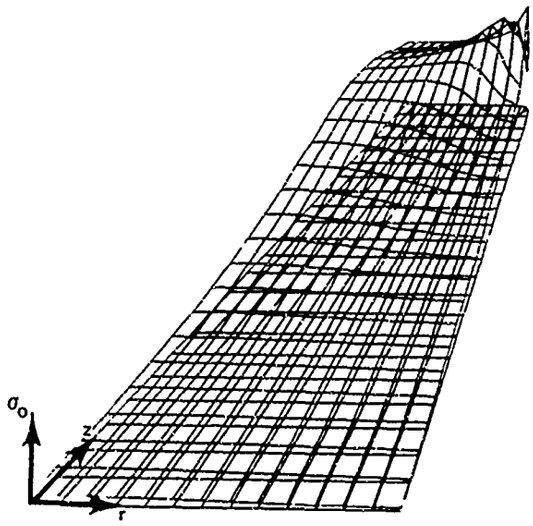

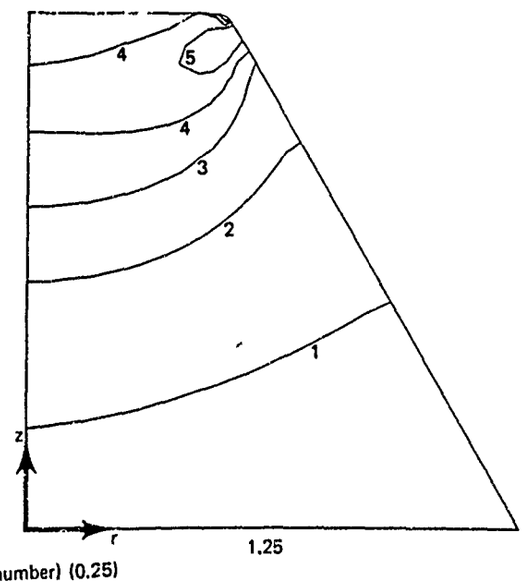

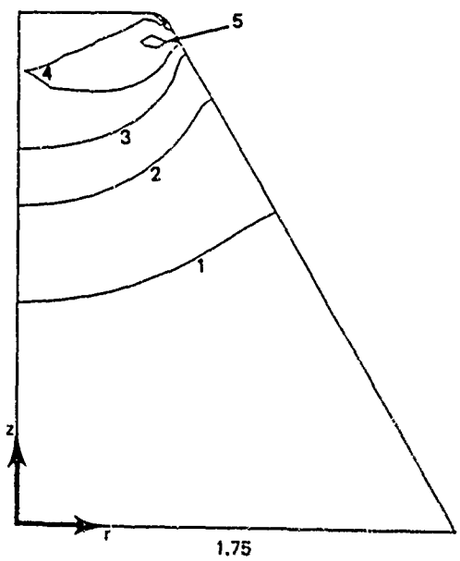

ontour number) (0.25)

Minor Diameter Ratio, t/d

rface plots for 60° angle and free boundary condition.

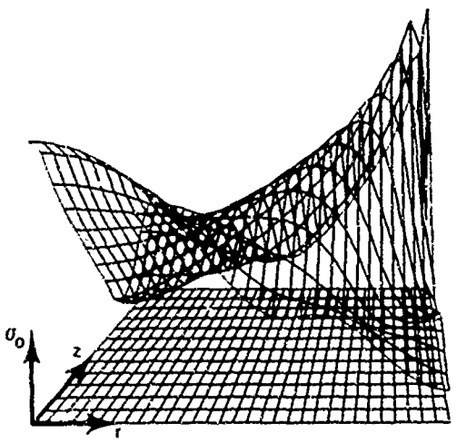

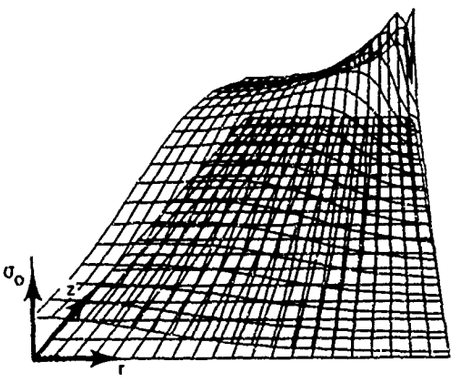

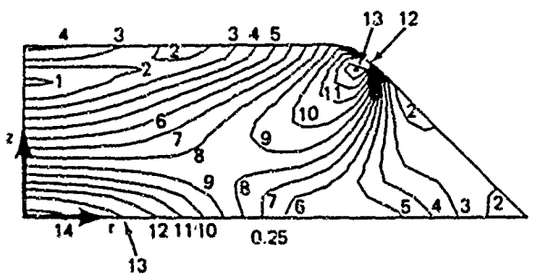

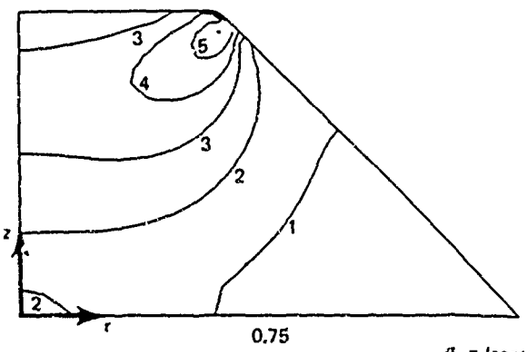

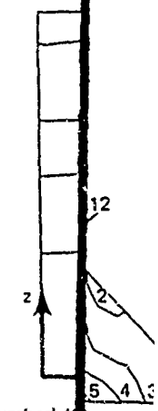

σ_o = (contour number) (

Thickness/Minor Diameter R

Figure 12. Effective stress contour and surface plots for S

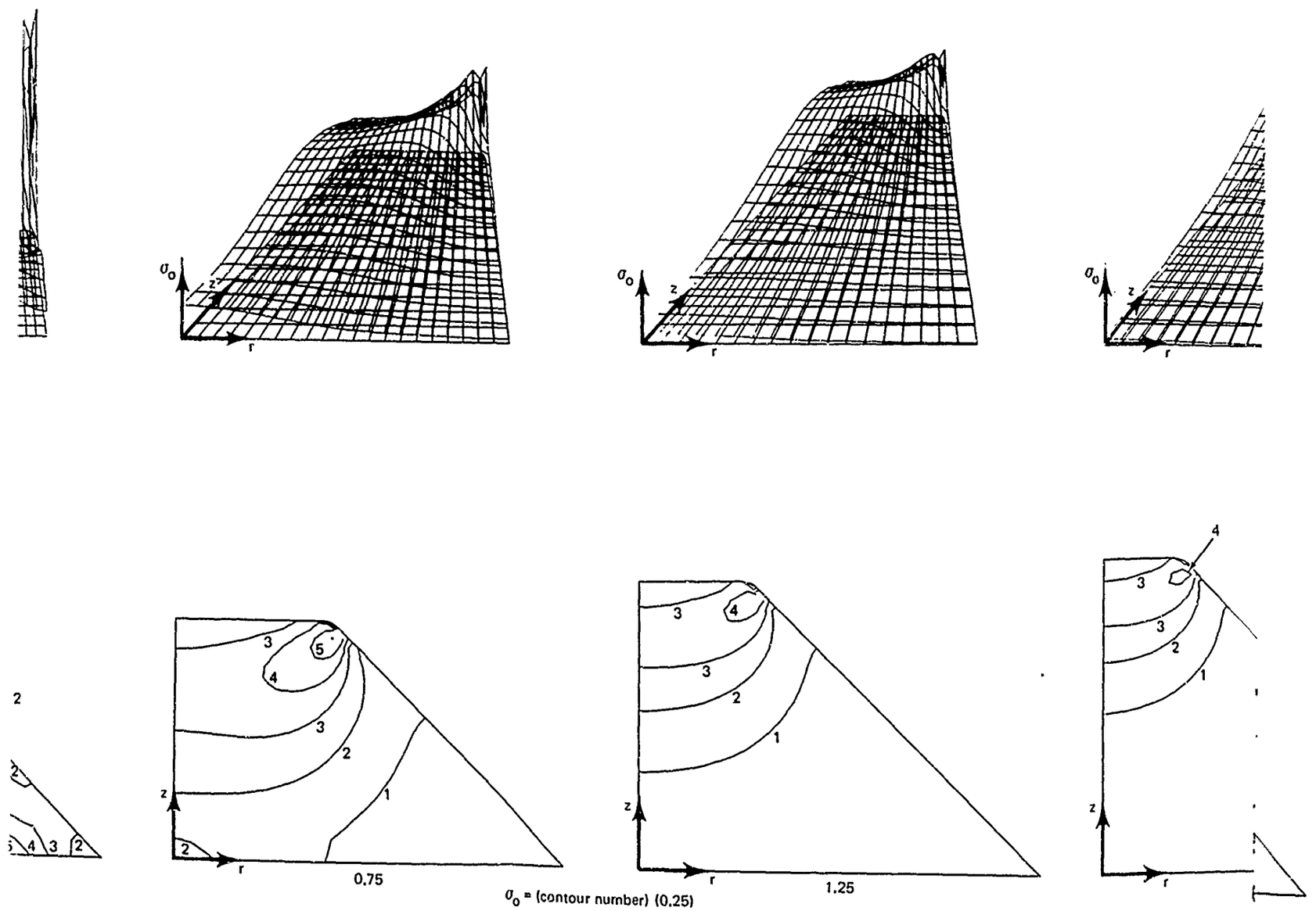

Figure 12. Effective stress contour and surface plots for 90° angle and free boundary condition.

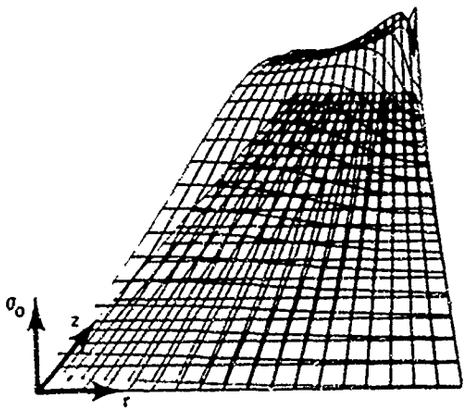

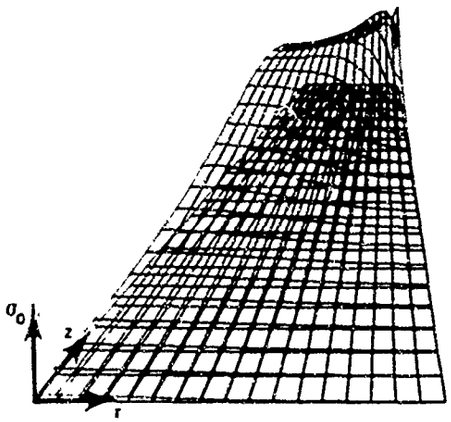

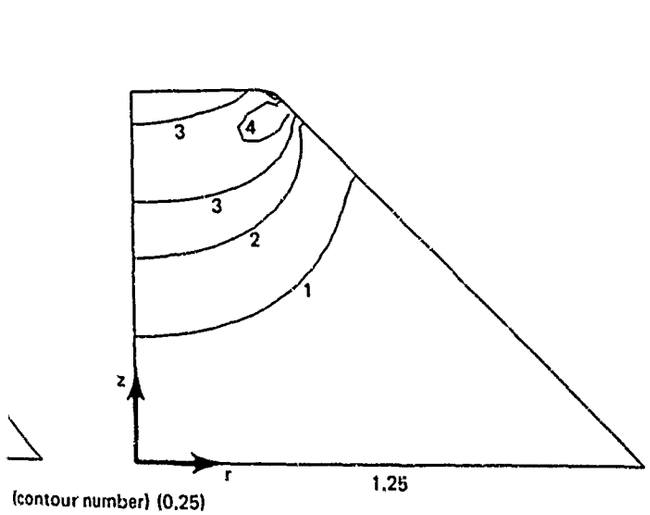

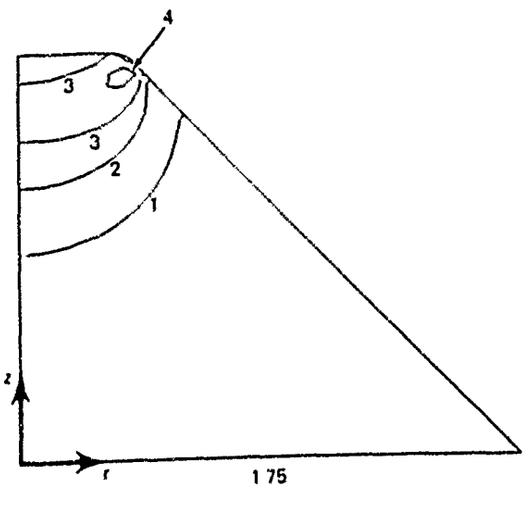

(contour number) (0.25)

ss/Minor Diameter Ratio, t/d

surface plots for 90° angle and free boundary condition.

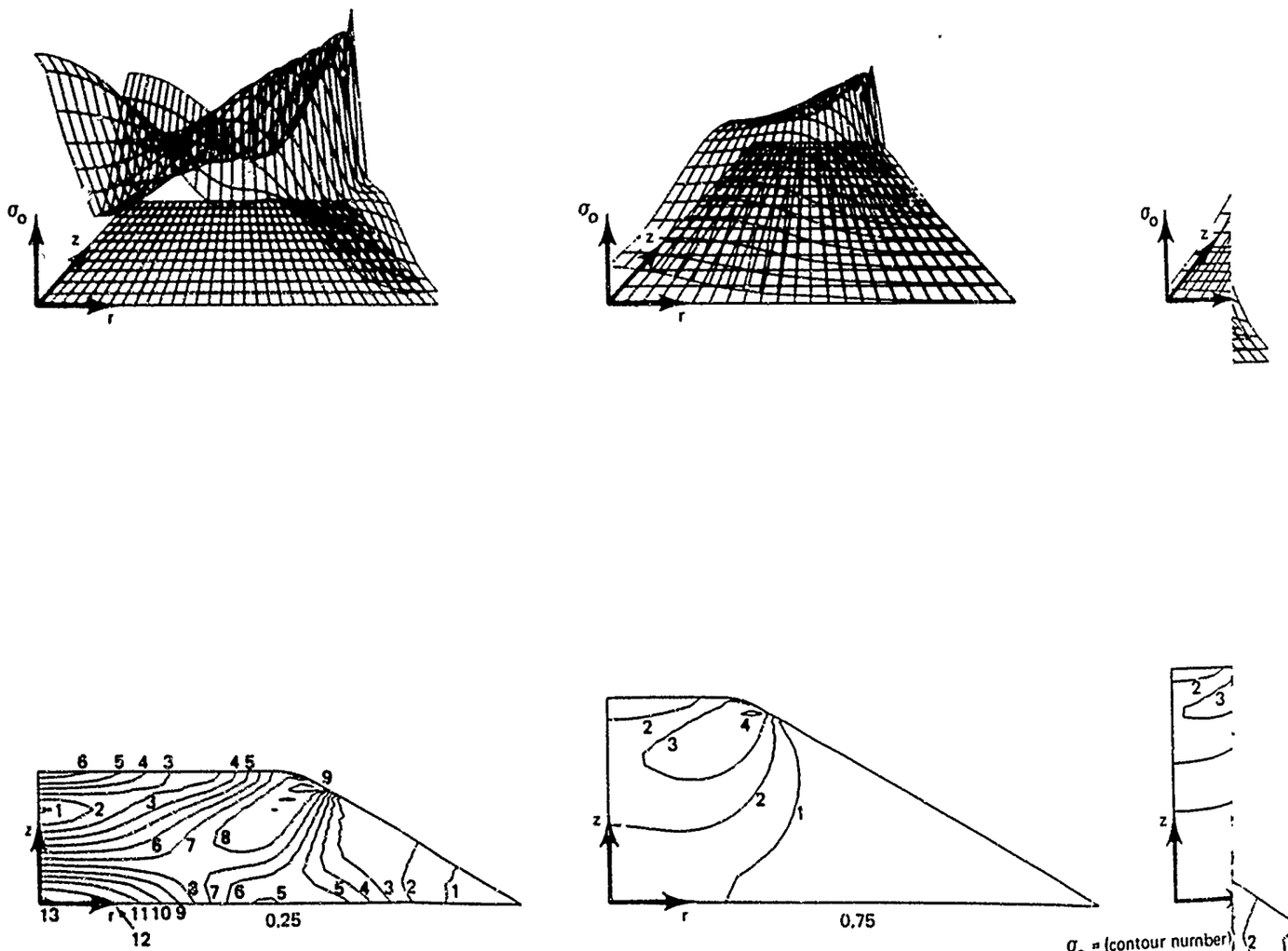

Figure 13. Effective stress contour and surface plots fo

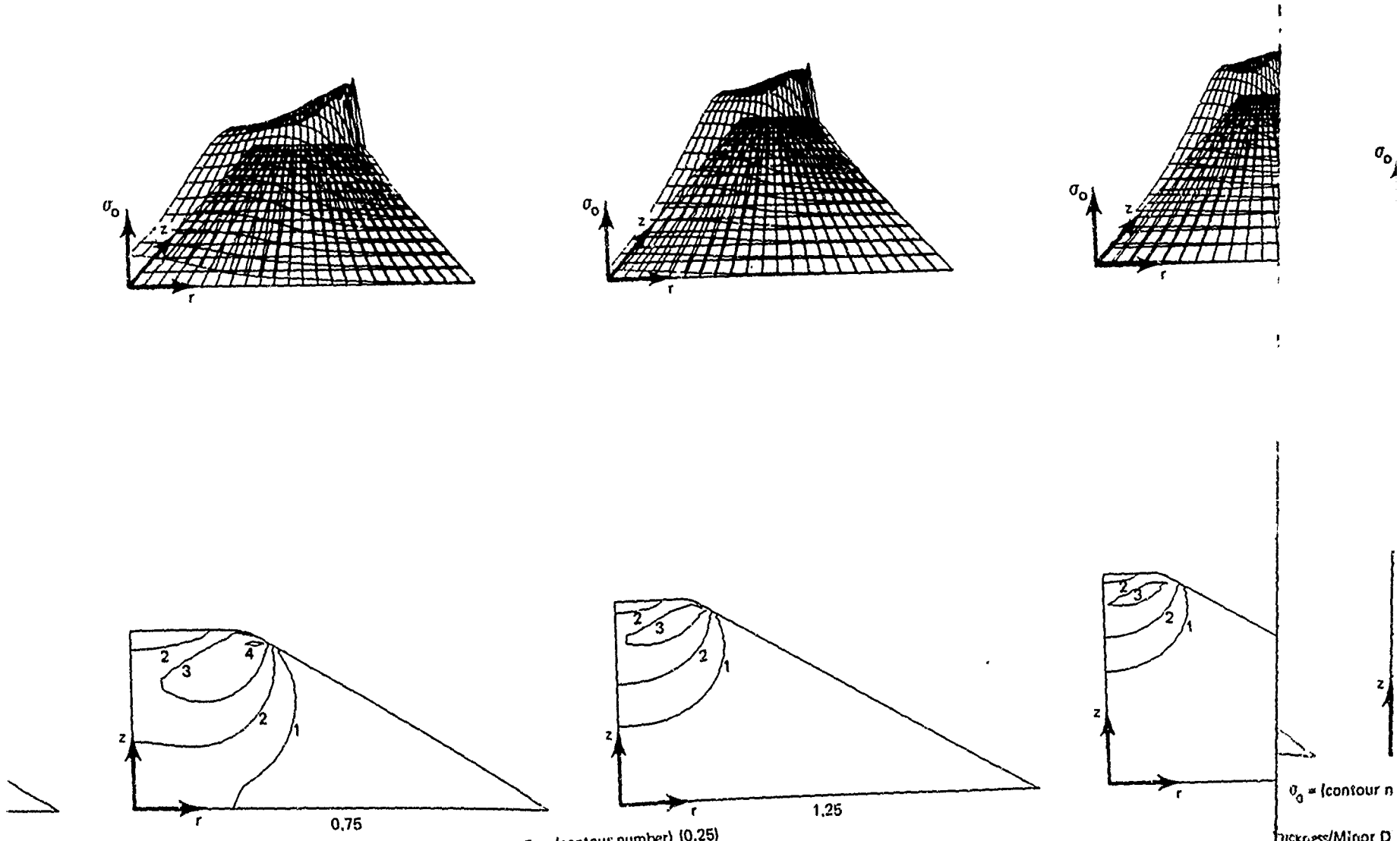

Figure 13. Effective stress contour and surface plots for 120° angle and free boundary condition.

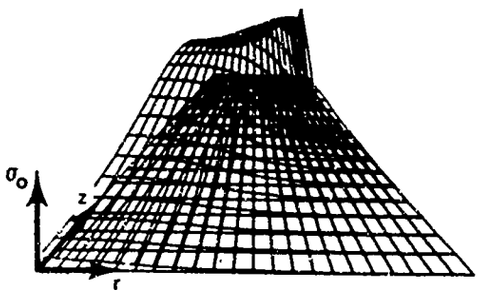

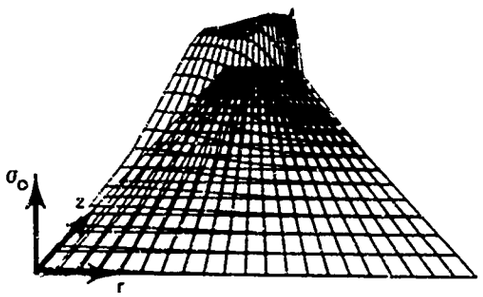

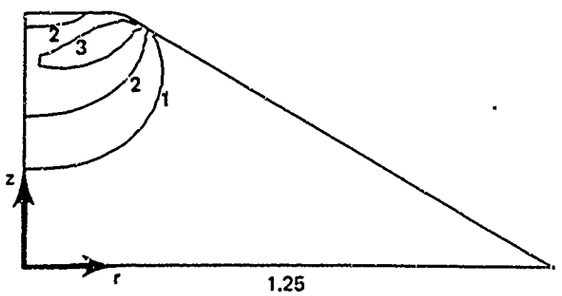

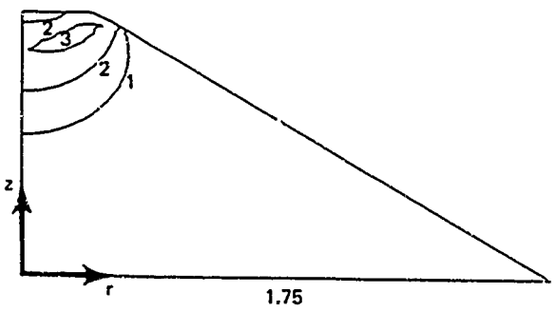

ntour number) (0.25)

Minor Diameter Ratio, t/d

face plots for 120° angle and free boundary condition.

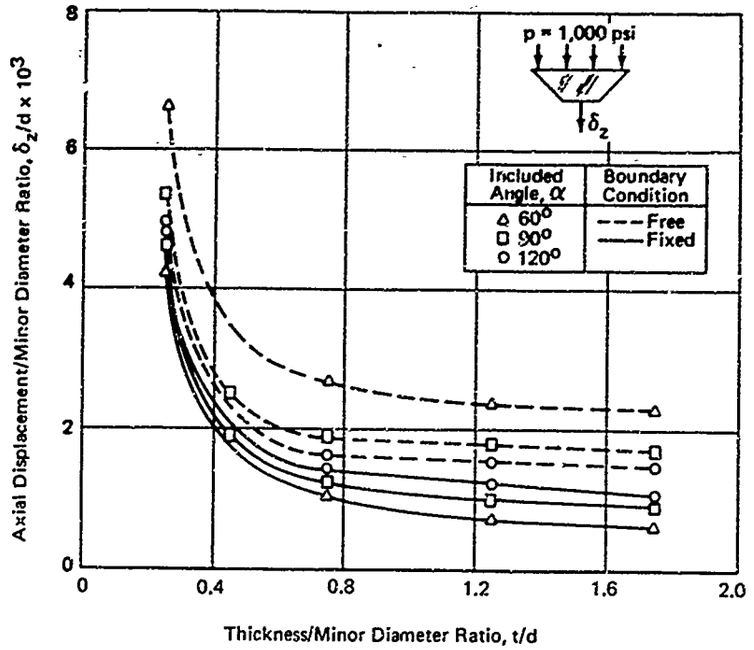

Figure 14. Instantaneous axial displacements at center of low-pressure face.

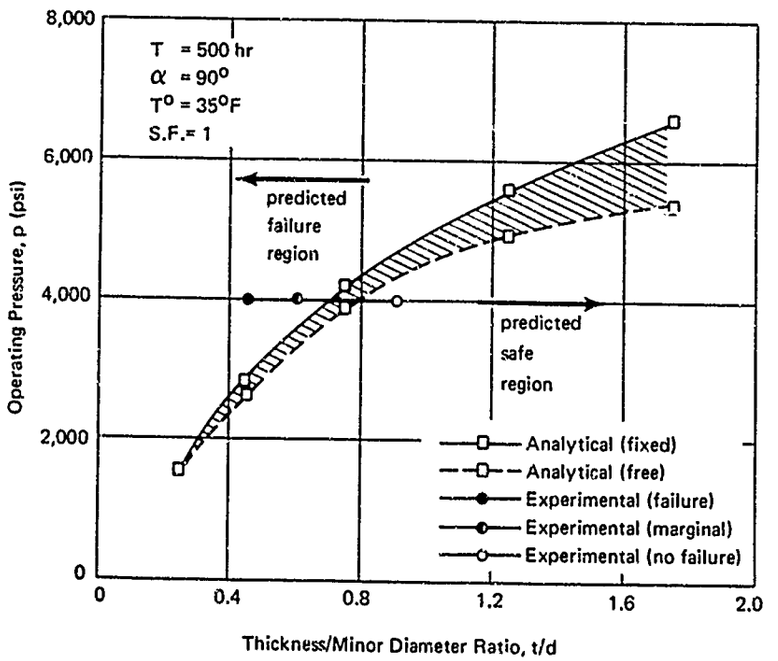

Figure 15. Comparison of experimental and analytical results.

Figure 16 compares the instantaneous displacements at the center of the low-pressure face for both the experimental and analytical work. The two analytical cases (fixed and free) successfully bracketed the experimental results. The smooth surface finish of 32 rms on the viewport flanges, in combination with the liberal use of silicone grease at the viewport-flange interface, resulted in the experimental displacements approaching the analytical free boundary condition.

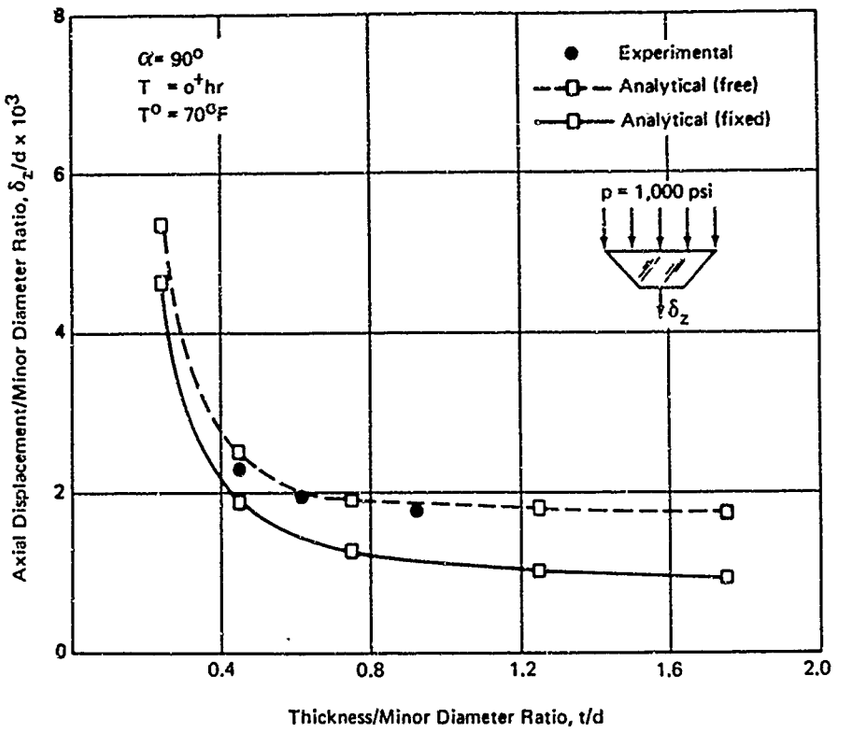

Figure 16. Comparison of experimental and analytical displacements.

Discussion

When comparing the design curves in this report with those in Reference 2, one notices a distinct difference. The curves in Reference 2, based on ultimate strength tests, indicate an exponential increase of strength

with respect to increases in the t/d ratio. This is understandable because the strength is based solely on physically forcing the material through the flange opening. Ultimate strength tests give an indication of the catastrophic load but do not indicate at what pressure the viewport fails to fulfill its function of providing visibility.

The design curves in this report, however, are based on the visibility aspect of the viewports and show that the operating pressure or depth is limited by the yield strength of the material. As exhibited by Figures 8 through 13, the peak effective stress asymptotically approaches a finite maximum value as the t/d ratio is increased.

No extensive creep data exist at temperatures other than room temperature. One can, however, get a comparison between 35 and 70°F tests on viewports by comparing experimental displacement results of the t/d = 0.45 viewport in the main test, and the t/d = 0.45 viewport with O-ring in Appendix A. The displacement at 70°F with a time period of 500 hours was 7% greater than the displacement at 35°F for the same length of time, and after 4,800 hours the displacement was 20% greater.

Figure 17 together with Table 3 compare the analytical results of this study with the present viewport designs in operational submersibles. A load duration time of 24 hours was chosen to include the emergency time of an average vehicle. From Figure 17 it appears that many of the present designs are conservative, which was probably due to lack of structural analysis at the time of design.

FINDINGS

Within the scope of this investigation, the following findings appear to be valid:

1. Based on both experimental and analytical results, the strength of a viewport increases with an increase in either the t/d ratio and/or the included angle for limits of 0.25 to 1.75 and 60° to 120°, respectively.

2. The maximum effective stress for a tensile region always occurs at the center of the low-pressure face with a fixed boundary condition.

3. The maximum effective stress for a compressive region always occurs at the corner of the low-pressure face with a free boundary condition.

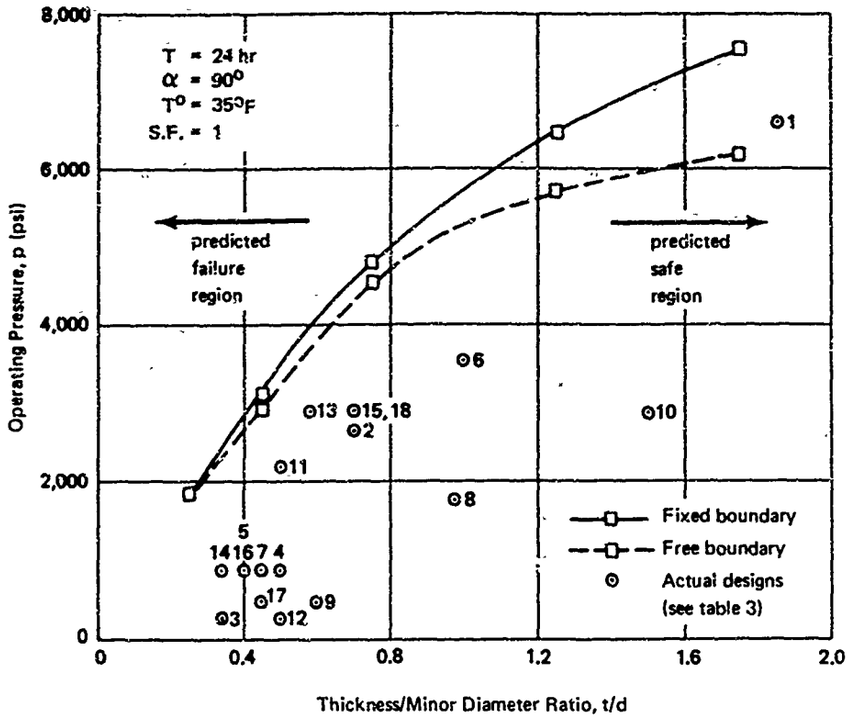

Figure 17. Comparison of analytical results and operational designs.

Table 3. Submersible Viewport Designs in Figure 17

(Extract from Reference 2.)

Identification Number	Submersible Name	Operating Depth (ft)
1	ALUMINAUT	15,000
2	ALVIN	6,000
3	ASHERAH	600
4	BEN FRANKLIN	2,000
5	DEEP JEEP	2,000
6	DEEP QUEST	8,000
7	DEEPSTAR 2000	2,000
8	DEEPSTAR 4000	4,000
9	DIVING SAUCER	1,000
10	DOWB	6,500
11	DSRV	5,000
12	PAULO I	600
13	PISCES IV	6,500
14	ROUGHNECK	2,000
15	SEA CLIFF	6,500
16	STAR III	2,000
17	SURV	1,000
18	TURTLE	6,500

4. In the actual viewport, a sharply spiked stress concentration exists at the low-pressure face corner which results in rounding of the sharp corner.

5. The transition to the dominance of flexural bending behavior occurs at about t/d = 0.6.

6. The stress distribution for conical frustums is independent of elastic modulus and only slightly dependent on Poisson's ratio, thus, the structural design curves are generally applicable to materials other than acrylic.

7. A conventional O-ring design with the groove located in the viewport conical face satisfactorily fulfills the requirements for viewport sealing (Appendix A).

DESIGN RECOMMENDATIONS

The purpose of this section is to provide the designer with the necessary information to design a vehicle viewport accurately, quickly, and safely. The type of analysis used in this section was experimentally verified as previously described.

In order to design a conical acrylic vehicle viewport, the designer must have available such information as: t/d ratio, included angle, elevation of viewport in flange, method of sealing, and flange surface finish. The design requirements would, of course, include the operating pressure, ambient temperature, and maximum length of dive.

This section of the report deals with design curves for viewport dimensions and recommendations for elevation of viewport in flange. Design recommendations for the flange surface finish are in Reference 5, and an analysis of the viewport sealing problem is in Appendix A of this report. Annealing instructions for the viewport may be found in Appendix B or Reference 11.

Design Curves

Material. Figure 18 represents the material facet of the design or the relationship between the yield stress of acrylic and time. A more detailed discussion of the origin of these curves is presented in Appendix C. The figure contains both tensile and compressive curves. The yield strengths can be seen to reduce to about 50% of the instantaneous value after 500 hours.

These curves are only for room temperature, but a temperature of 35°F will increase the yield strength by about 20% according to References 4 and 10. The strength is, of course, much lower with a higher temperature and, therefore, temperatures considerably above room temperature should be avoided.

Figure 18 is used concomitantly with Figure 19 for calculating design strength.

Structure. Figure 19 represents the structural facet of the design. The curves include the parameters: t/d ratio, included angle, safety factor, yield stress, and operating pressure. The t/d ratios range from 0.25 to 1.75 while the included angles range from 60° to 120°.

The curves are based on a finite element stress analysis. With four t/d ratios, three included angles, and two boundary conditions (fixed and free), there were a total of 24 computer runs.

Figure 19a represents the maximum effective stress in the compression-compression-compression octant and the worst of the two boundary conditions, the free case. This point always occurred at the low-pressure face corner for the complete range of t/d ratios and angles. This is attributed to the plugging action creating a higher effective stress at this point.

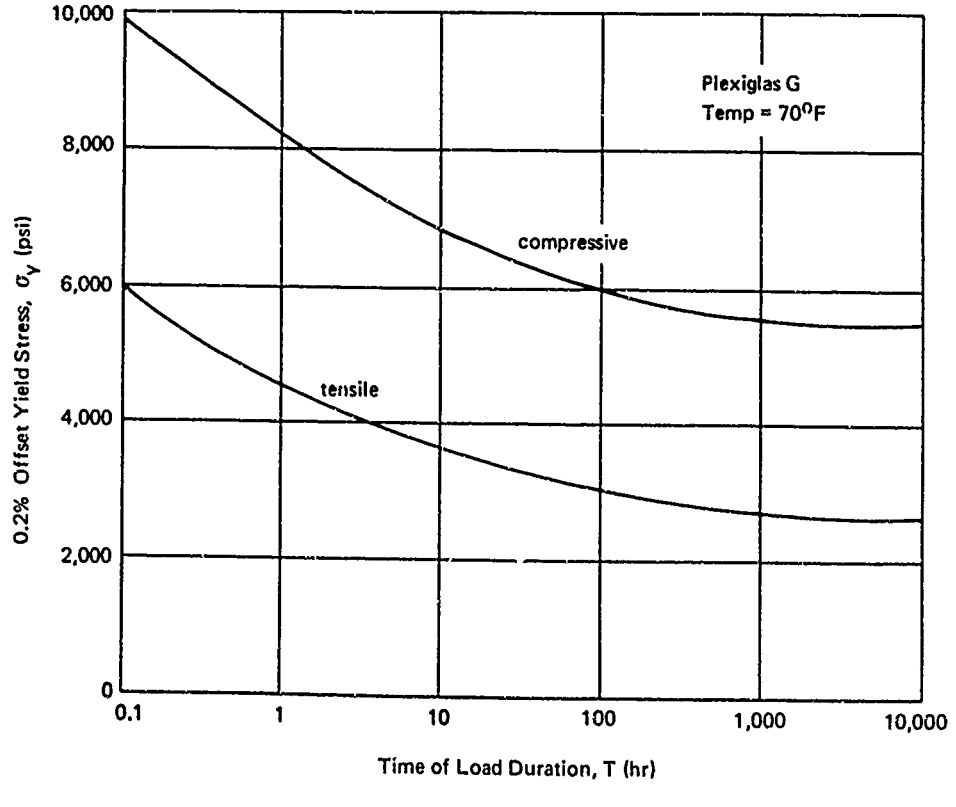

Figure 18. Yield stress-time curves for acrylic plastic.

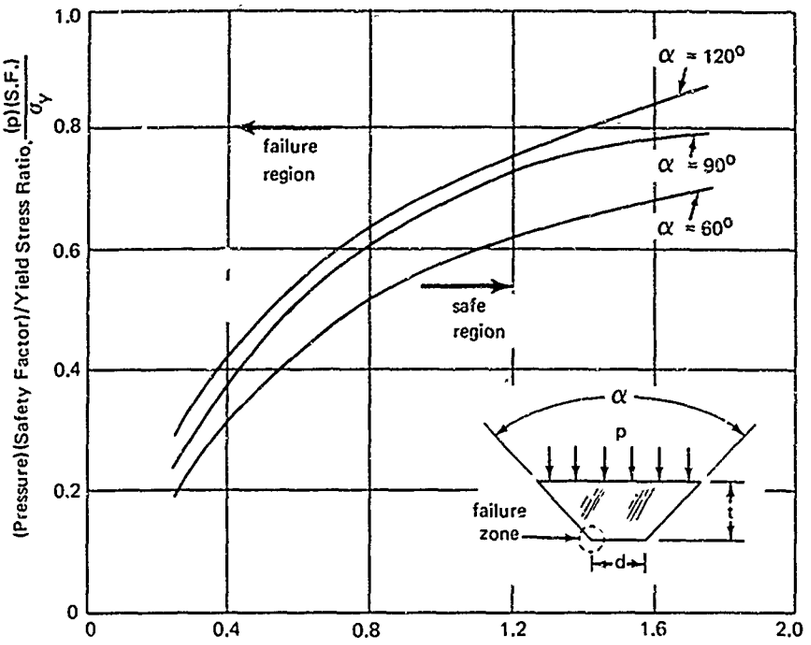

(a) Compressive region.

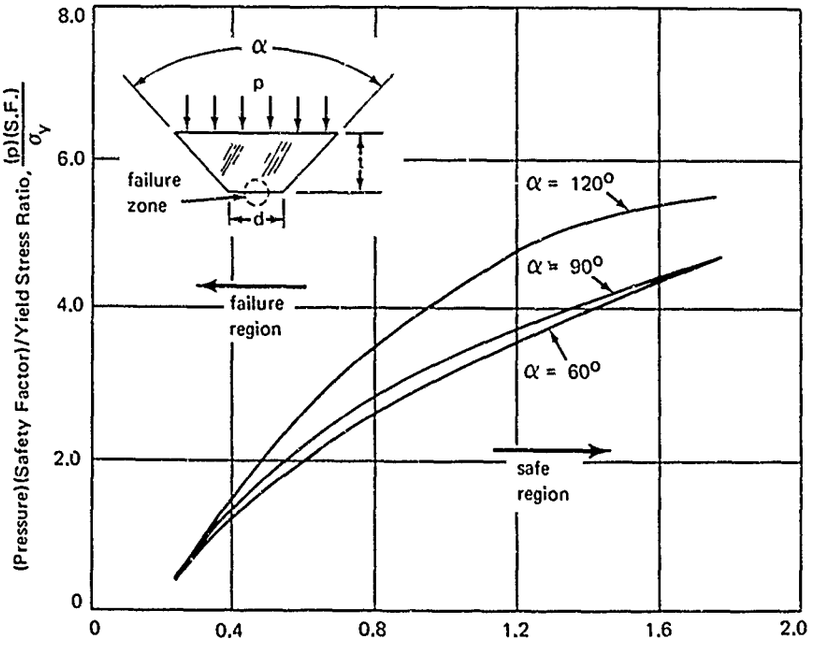

(b) Tensile region.

Figure 19. Design curves for conical acrylic viewports.

Figure 19b represents the maximum effective stress in the tension-tension quadrant due to the worst boundary condition, the fixed case. This point always occurred at the center of the low-pressure face for the complete range of the variables. The fixed boundary case was the worst due to the increase in flexural bending.

Example

To indicate how the design curves may be used, a hypothetical case is considered. Suppose the design requirements are as follows:

Maximum operating pressure = 2,000 psi
Maximum temperature = 70°F
Safety factor = 1.5
Length of dive* = 100 hours
Included angle = 90°
Minor diameter = large as possible

To properly design this viewport, the first step is to find out what t/d ratio is necessary. From Figure 18 with an abscissa value of 100 hours, the following results are obtained:

compressive yield stress = 6,000
tensile yield stress = 3,000

Proceeding to Figures 19a and 19b, and calculating the ordinate value for each curve

compressive $\frac{(p)\ (S.F.)}{\sigma_y} = \frac{(2{,}000)\ (1.5)}{6{,}000} = 0.5$

tensile $\frac{(p)\ (S.F.)}{\sigma_y} = \frac{(2{,}000)\ (1.5)}{3{,}000} = 1.0$

Using the above ordinate values, the following t/d ratios were taken off the abscissa:

from Figure 19a t/d = 0.58
from Figure 19b t/d = 0.34

---

* This assumes that there is adequate relaxation time between dives.

To safely withstand the operating requirements, a t/d ratio of 0 58 or larger would be used. Since the minor diameter is to be as large as possible and commercial acrylic sheets come in thicknesses up to 4 inches

$$t/d = 0.58$$

$$\therefore d = \frac{t}{0.58} = \frac{4}{0.58} = 6.9 \text{ inches}$$

The largest minor diameter would be 6.9 inches.

The elevation, h, (see Figure 2) of the viewport in the flange is another important aspect of the total viewport design. Using a t/d ratio of 0.58 on the abscissa of Figure 14, a value for the ordinate is obtained

from Figure 14 (free boundary) $\quad \frac{\delta_z}{d} = 0.0021$ inch per 1,000 psi

It is recommended by the authors that the viewport be elevated five times the analytical (free case) displacement

$$h = 5\delta_z = (5)\left(\frac{0.0021}{1{,}000}\right)(6.9)(2{,}000) = 0.145 \text{ inch}$$

For safe operation of the viewport, a minimum elevation of 0.15 inch should be used in this particular design to insure adequate distance to the end of the conical surface, again recognizing the fact that any significant elevation above this achieves nothing (stress distribution remains the same) and, in fact, only adds additional flange material (i.e., weight) to the vehicle.

Figure 19 provides for the use of a safety factor in designing conical viewports. Safety factors are utilized when a designer cannot control all of the many extraneous variables during fabrication and service that might affect his original design. In view of the in-depth research for both the structure and the material properties contained in this report, and the reproducibility of commercial Plexiglas, the authors feel that a safety factor of 1.5 is more than adequate if all other design recommendations contained herein are followed.

ACKNOWLEDGMENT

Mr. John McKay conducted the experimental tests and reduced the experimental data used in this study

Appendix A

INVESTIGATION OF A VIEWPORT SEAL DESIGN

INTRODUCTION

A necessary, although oftentimes neglected, function of a viewport design is that of maintaining waterproof integrity at all times. Even very small leaks would be detrimental in a habitat (long term submergence) because of the large accumulation over a long length of time, not to mention the psychological effects on the occupants. Waterproof integrity is accomplished by a viewport seal system which must function in two environments: (1) at the surface both before and after dives (low pressure), and (2) at the operating depth (high pressure).

The objective of this appendix is to (1) review and evaluate existing methods of sealing submersible (short term submergence) viewports, but with regard to the additional habitat functional requirements, and (2) investigate both experimentally and analytically the most promising of the designs.

BACKGROUND

To provide waterproof integrity, the first viewport seal designs relied on a lapped-joint seal between the viewport and flange as shown in Figure A-1a. Achievement of the seal is by 80 to 90% contact surface area, which requires surface finishes in the 8 to 32 rms range. This design maintained a seal at the lapped joint for both low-pressure and high-pressure sealing. Sometimes a flat gasket is used for padding between the retainer ring and viewport.

The next design was the gasket seal as shown in Figure A-1b. This particular design relied on a gasket located at the perimeter of the high-pressure face for low-pressure sealing and on the lapped joint for high-pressure sealing.

A similar design, as shown in Figure A-1c, had an O-ring located at the corner of the viewport high-pressure face. Here again the low-pressure sealing was accomplished by the O-ring and the high-pressure sealing by the lapped joint.

The design shown in Figure A-1d is currently being used for submersibles. Here both high-pressure and low-pressure sealing is accomplished by the O-ring seal.

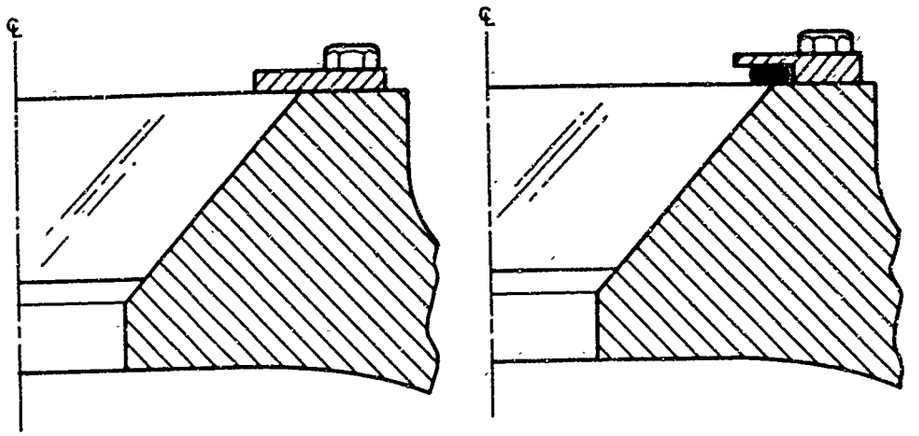

(a) Lapped-joint seal.

(b) Gasket seal.

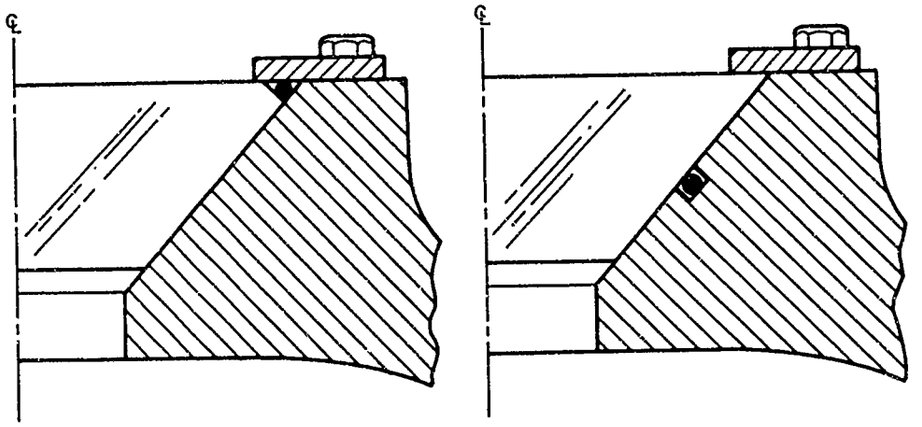

(c) O-ring seal no. 1.

(d) O-ring seal no. 2.

Figure A-1. Current viewport seal designs.

Submersible designs are not necessarily acceptable for habitat designs because of the more stringent functional requirement due to creep. It would, therefore, be worthwhile investigating a new seal design which would meet the requirements and still reduce cost without compromising the structural integrity of the viewport. A new design or variation of the seal in Figure A-1d is shown in Figure A-2. It is a conventional circular O-ring in a rectangular groove located on the conical face of the viewport. Note that all five designs discussed require retainer rings.

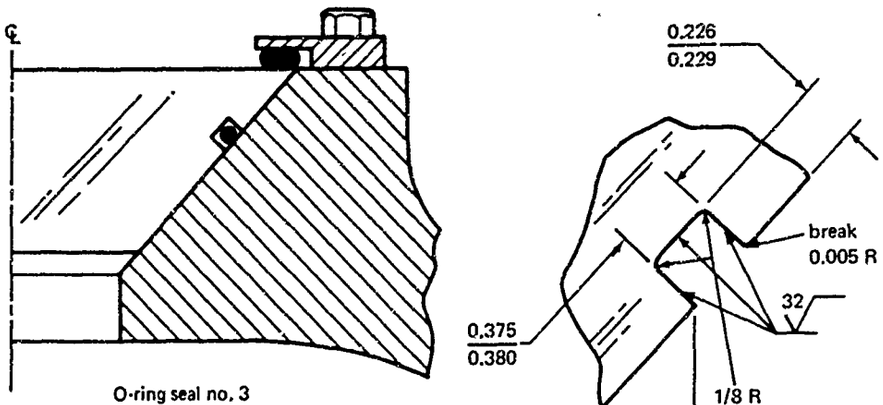

Figure A-2. Recommended viewport seal design.

COMPARISON OF DESIGNS

The five seal designs described may be compared in three different areas: (1) operation, (2) economy, and (3) structure.

Operation

Functional requirements for viewport seal systems include sealing under all conditions. As previously observed in the main body of this report, creep occurs in the viewport after a long term submergence. Even after returning to the surface, the viewport does not immediately return to its

original position. Therefore, the first three seal designs, a, b, and c, in Figure A-1, would find it difficult to efficiently seal after the habitat surfaces. Neither the retainer ring, gasket, nor O-ring seal no. 1, respectively, would be able to follow the creep displacement of the viewport; the necessary compression of the components for sealing would be lost These designs function perfectly for submersibles because their dive times are short, thus minimizing the effects of creep.

O-ring seal no. 2 and O-ring seal no. 3 are both able to follow the displacement of the viewport and to maintain the seal. A compressible gasket might be employed at the retainer ring-viewport interface, not as a seal, but as a spring to maintain pressure on the viewport for low-pressure sealing. Operationally, an O-ring that is stretched around the viewport (O-ring seal no. 3) is much easier to work with than the reverse (O-ring seal no. 2). The design in Figure A-2 appears to exhibit operational advantages over the other four designs.

The success of such a seal system (Figure A-2) has already been proven under long term tests in the ocean. Jenkins and Reinhart[12] tested such a design, a conventional O-ring seal in an angular flange, for 189 days at a depth of 5,900 feet in the Pacific Ocean. The O-ring gland materials were carbon steel, aluminum, and clad steel. The O-ring material was nitrile (Buna N) with a hardness of 90 Shore A durometer. The lubrication was petroleum based, although a silicone grease is recommended to preclude any deleterious effect on the acrylic. Results of the tests indicated: (1) no deterioration of the O-ring material, (2) no significant change in O-ring hardness or resilience, (3) no significant amount of water absorption by the O-ring, and (4) no leakage past the seal system.

Economy

The total cost of a viewport assembly could be reduced if an O-ring seal was used rather than a lapped-joint seal. Lapped-joint seals are extremely expensive due to: (1) manual lapping of viewport, (2) tight tolerances on dimensions, (3) additional machining for smooth surface finishes, and (4) absence of interchangeability of viewports. Even for low-pressure sealing, seal systems a, b, and c in Figure A-1 require tight tolerances to insure that the viewport seats at the correct level in the flange.

O-ring seals no. 2 and no. 3 on the other hand, can seal anywhere on the faying surfaces so the tolerances need not be so tight. Between the two designs, no. 2 and no. 3, the latter appears to be the more economical. In initial fabrication, it would be more economical to cut the groove in the easily machined acrylic. Also, if the flange is to be clad for corrosion purposes, the process is more economical if it is not necessary to contend with

an O-ring groove. Since the flange is usually welded to the steel pressure hull, it would be cheaper to replace a damaged O-ring groove in the viewport as opposed to a damaged one in the flange.

Structure

With the design in Figure A-2 exhibiting advantages both operationally and economically, it remains only a question of whether the viewport can structurally withstand the stress concentration due to the presence of the O-ring groove. The earlier seal designs in Figure A-1 did not structurally affect the viewport. Designers probably did not use the design in Figure A-2 because of the unknown effects of the stress concentration; there was no thorough stress analysis until Reference 5 was completed.

The possibility does exist with O-ring seal no. 2 in Figure A-1, that the softer acrylic will creep down into the O-ring groove in the flange and cause an extremely high stress concentration that could be catastrophic with long term loading.

The O-ring groove in the viewport seal design of Figure A-2 was located near the high-pressure face because the results discussed in the main text of this report indicated that the stress distribution was nearly hydrostatic in this area. The rest of this appendix is concerned only with the design in Figure A-2 and the structural response of the viewport to the presence of the O-ring groove.

SCOPE OF INVESTIGATION

To thoroughly determine the structural effect of the groove on the viewport, both an experimental and analytical phase were conducted on the design shown in Figure A-2.

Experimental Phase

The viewport used to test the O-ring design was very similar to the $t/d = 0.45$ viewports used in the main text and is shown in Figure A-3. The temperature during the test was maintained between 65 and 75°F because this would impose a more severe test than a lower temperature. While the pressure was held at 4,000 psi, the displacements at the center of the low-pressure face were recorded until the displacements became asymptotic within the measurement accuracy. The machining procedure, pressure vessel type, and testing procedures are all discussed in Appendix B.

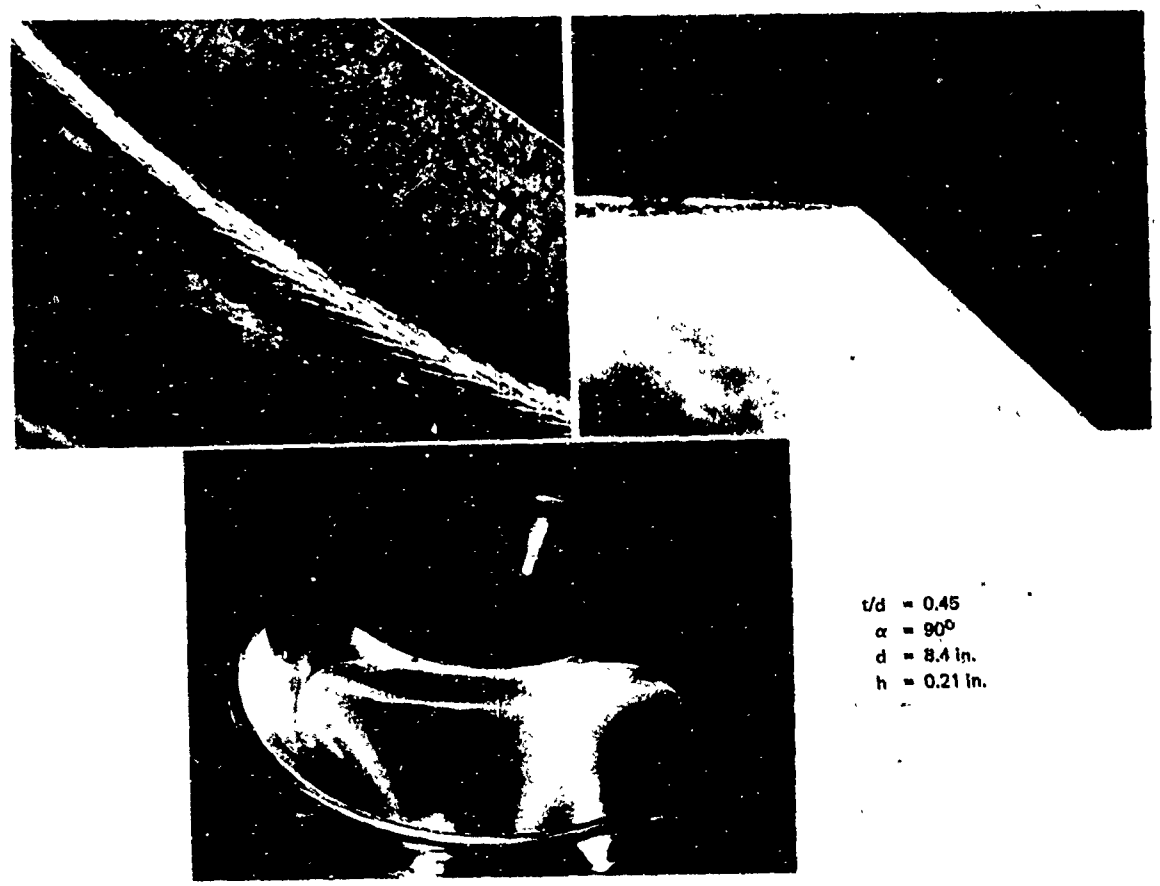

Figure A-3. Post-test physical condition of t/d = 0.45 viewport with O-ring after 200 days.

Analytical Phase

The viewport was simulated using the finite element method to obtain effective stress values at critical points for later analysis. The mesh contained 664 nodal points and 610 elements. Both the free and fixed boundary conditions were used in this analysis.

RESULTS

Experimental

The viewport with the O-ring was loaded at 4,000 psi for a total time of 200 days before the creep leveled off. Post-test observations, as shown in Figure A-3, indicated rounding of the corner and presence of cracks. Inspection of the O-ring groove, however, found no crazing or cracks whatsoever. Figure A-4 presents the absolute displacement at the center of the low-pressure face versus time in days. Creep accounted for 35% of the total displacement at 200 days. Even with this much displacement the O-ring did seal when the dive was completed and the viewport was relaxing.

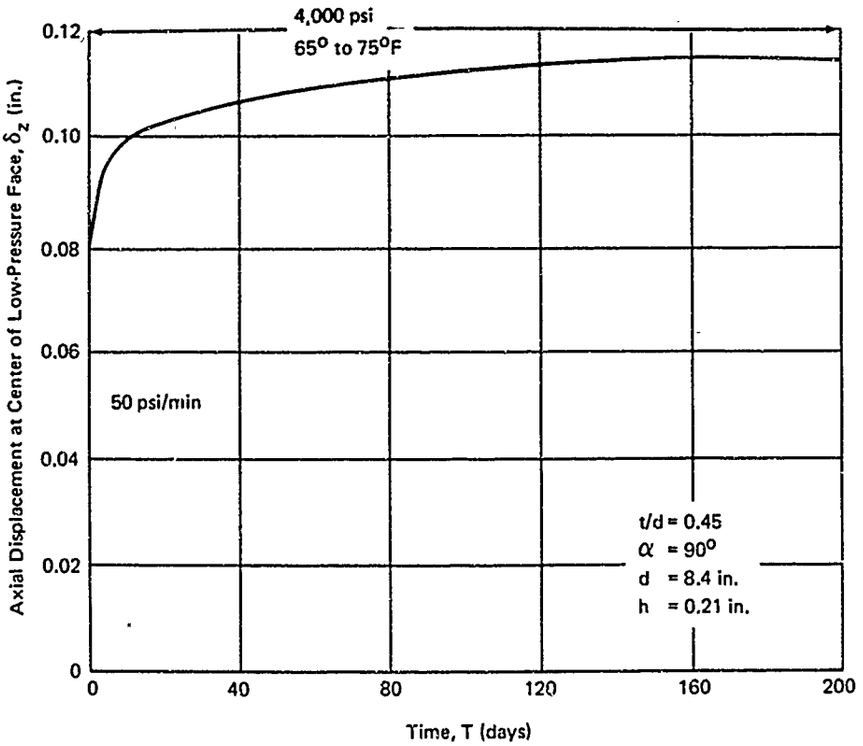

Figure A-4. Displacement response of viewport with recommended seal design.

Analytical

Figure A-5 shows the resulting contour plot of effective stresses for the viewport with the O-ring. Two stress concentrations are clearly found: (1) at the low-pressure face corner, and (2) at the O-ring groove. Table A-1 summarizes the data at the critical locations and indicates that the maximum effective stress value around the O-ring groove is only about one-half that at the low-pressure face corner. The boundary condition essentially created no difference in the stresses around the O-ring groove.

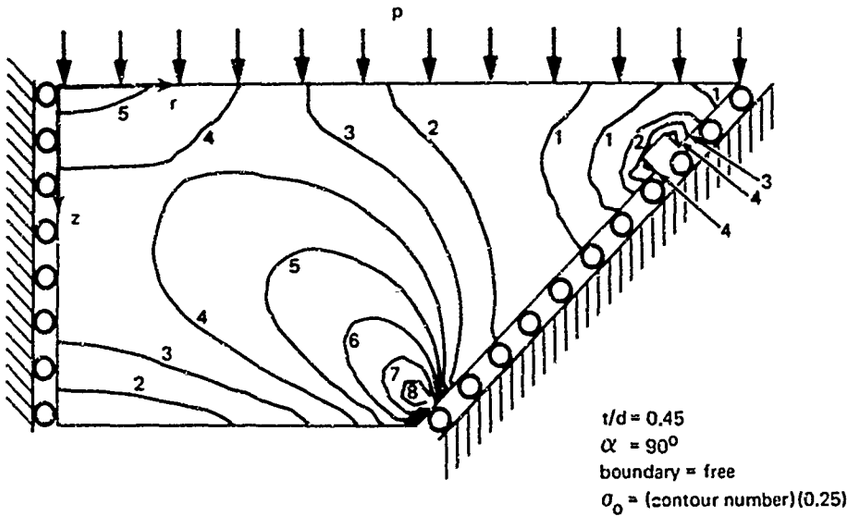

Figure A-5. Effective stress contour plot for 90° angle and free boundary condition with O-ring groove.

Table A-1. Effective Stress, σ_o, for Viewport With O-Ring Groove

Location	Boundary Condition	
	Fixed	Free
Maximum at O-ring groove (compressive)	1.15	1.41
Center of low-pressure face (max tension)	0.728	no tensile stresses
Low-pressure face corner (max compressive)	2.51	2.58

DISCUSSION

The experimental results and the analytical results had excellent agreement. Even when the viewport failed at the low-pressure face corner, there was no failure at the O-ring groove. The design recommendations (Figures 18 and 19a) of this report predicted failure for this viewport and, as shown in Figure A-3, failure occurred.

It might also be interesting to note the flexural behavior of this viewport as shown in Table A-1. For the free boundary condition, no tensile stresses appeared at the center of the low-pressure face as they did for the fixed boundary case.

Although minimum research time negated any investigation of mesh-size influence on the O-ring groove, the results were in agreement with the experimental results. Also, the analytical simulation of the groove was a worst case solution. This means there was no rounding of the corners in the simulated model while in the experimental case the corners had a 1/8-inch radius.

FINDING

A conventional O-ring design with the groove located in the conical face of the viewport (Figure A-2) satisfactorily fulfills the requirements for viewport sealing in three ways: operationally, economically, and structurally.

Appendix B

EQUIPMENT AND PROCEDURE FOR EXPERIMENTAL PHASE

INTRODUCTION

Information relative to the design and operation of equipment for the simulated operational tests on full-scale viewports is contained in this appendix. The testing requirements were as follows:

1. Test at least three sizes of full-scale viewports
2. Pressure range, 0 to 4,000 psi
3. Temperature range, 35^{o} to 70^{o}F
4. Test time, 1 year
5. Cycling to simulate dives of an undersea vehicle

Due to the size of the viewports and the length of time of the tests, a decision was made to design pressure vessels and a refrigeration system specifically for these tests. As a result, pressure vessels with other capabilities would not be tied up for a year.

HIGH PRESSURE SYSTEM

Pressure Vessels

The pressure vessel design was as shown in Figure B-1. This particular design yielded the following advantages:

1. Efficiency—each vessel tested two viewports at one time.
2. Safety—low volume of fluid to negate "bomb" danger.
3. Economy—materials and fabrication costs were low.
4. Ease of operation—simplicity and compactness of design allows ease in pressure and temperature cycling.
5. True simulation—low-pressure face exposed to constant room temperature while high-pressure face exposed to simulated cycling of temperature and pressure.

There were two possible disadvantages to the design. (1) opening and closing of a vessel was time consuming and (2) the O-ring extruded when operated to any reasonable pressure and required replacement after each test. These disadvantages are not severe because the system is for long term operation, not day-to-day operation. A typical pressure vessel consisted of two 32-inch-diameter steel flanges as shown in Figure B-1 The conical surfaces of the flanges were machined to a 32 rms finish. The three vessels had through-hole nominal diameters of 4, 6, and 8 inches.

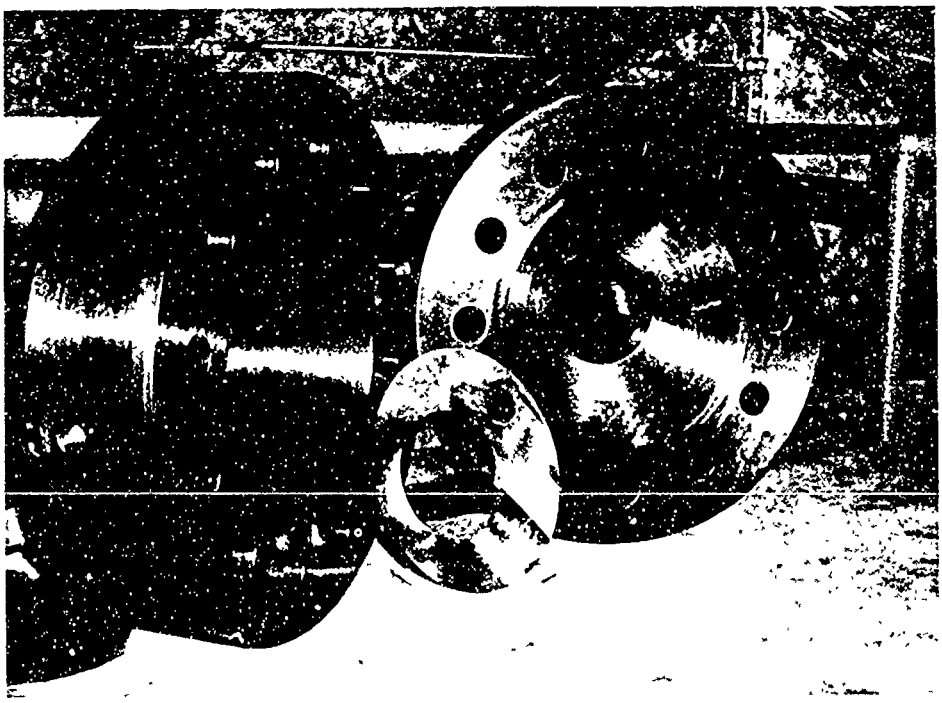

Figure B-1. Typical pressure vessel flanges with an 8-inch minor diameter viewport.

High-Pressure Pump

The high-pressure pump was an air-driven double-acting piston type rated for 20,000 psi Tubing made of 1/4-inch diameter, 316 stainless steel connected the pump to the accumulator

Accumulator

The air/water accumulator provided a means of storing energy in the high-pressure system to maintain a constant pressure in the vessels The vessels were all connected to a common manifold, thus, pressure cycling was identical for all three vessels

REFRIGERATION SYSTEM

A refrigeration system was necessary in this study to aid in simulating actual environmental conditions. Located on the pressure vessels were Plate-Coil heat transfer units as shown in Figure B-2a. The single, embossed units were rolled to the vessel diameter to insure adequate heat transfer between the vessels and the units. Two units which were connected together by a jumper hose were necessary for one vessel. A heat transfer cement, Thermon T-3, was used between the vessel and heat transfer units to increase the overall heat transfer coefficient. Sheets of an elastomeric insulation, Armaflex, were used on top of the heat transfer units as shown in Figure B-2b. Glycol brine was circulated through the refrigeration system. Cooling was provided by a 5-ton-capacity air-cooled chiller. Temperature measurements were taken at both the inlet and outlet of the chiller.

INSTRUMENTATION SYSTEM

Dial indicators, as shown in Figure B-3, were utilized on each of the six viewport faces to measure absolute displacement of the center of the face with respect to the pressure vessel. Lufkin dial indicators with graduations of 0.001 inch were used. The averages of the displacement readings for the three pairs of viewports in the pressure vessels were calculated and are presented in Figure 7 of this report.

Pressure gages with a range of 5,000 psi were the high-pressure measuring system, while a 50-psi gage was used on the no-load part of the cycle. Here it was necessary to maintain a 1 to 5-psi load to keep the viewport in position.

VIEWPORTS

The seven viewports in this study (including one used in the O-ring test) were machined from a 4-foot by 5-foot by 4-inch cast sheet of Plexiglas G acrylic plastic. The viewports were rough machined and then annealed in accordance with the manufacturer's recommendations[11] as follows:

Section Thickness (in.)	Annealing Temp (^{o}F)	Time (hr)	Cooling Rate (^{o}F/hr)
4	175	22	5

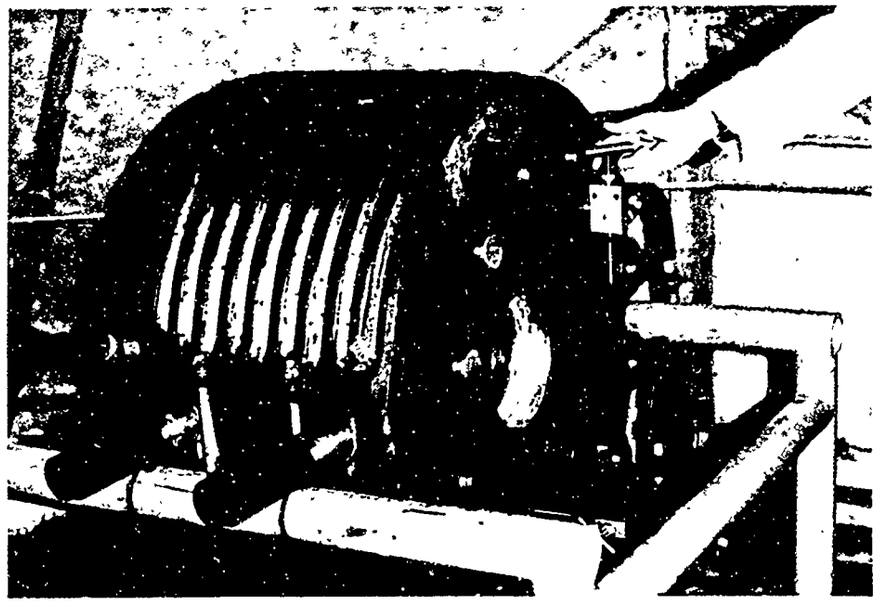

(a) Heat transfer units installed on pressure vessel.

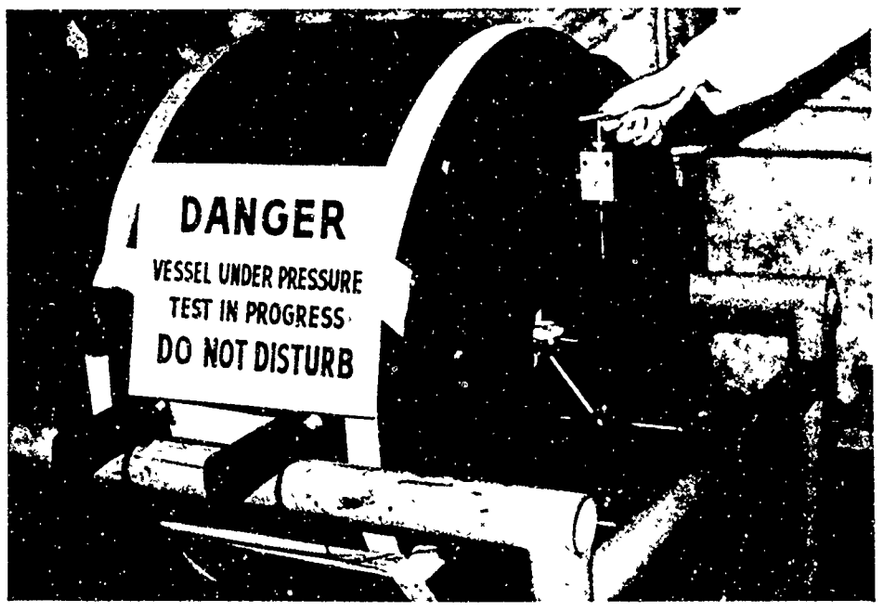

(b) Pressure vessel with installed insulation.

Figure B-2. Typical pressure vessel with refrigeration system.

Upon completion of initial anneal, the viewports were machined to final dimensions and annealed again. The viewports were polished to an optical finish before testing to facilitate post-test observations of possible cracks.

Figure B-3. Experimental test setup.

All minor diameters of the viewports were designed larger than the penetrations in the pressure vessel to elevate the viewport in its seat in order to avoid the stress concentration at the break of the conical surface.

Because the test occurred over such a length of time, it was necessary to insure accuracy of results. Therefore, two viewports of the same dimensions were tested at the same time to provide redundancy to the test.

TEST PROCEDURE

The conical surfaces of the viewports were first coated with Dow Corning No. 4 silicone grease, a lubricant which will not attack the acrylic plastic. After the six viewports were placed in the three vessels, the vessels were filled with tap water. Initially, the pressure was raised to 2,000 psi and quickly returned to 0 psi. This procedure seated the viewports, squeezed out a majority of the excess grease, and allowed the dial indicators to be zeroed. Subsequently, the pressure and temperature were changed simultaneously

from 0 to 4,000 psi and 70 to 35°F, respectively. This portion of the cycle represented the dive of the vehicle. Upon completing the desired loading time of 500 hours, the pressure and temperature were simultaneously changed from 4,000 to 0 psi and 35 to 70°F, respectively.

The displacements at the center of the low-pressure face were taken twice a day except for weekends and holidays. The morning and the afternoon were chosen for the displacement recordings because the minimum and maximum pressures for each working day corresponded with the minimum and maximum temperature fluctuations for the 24 hours of the day.

Appendix C

FAILURE CRITERION APPLIED TO CONICAL ACRYLIC VIEWPORTS

A FAILURE CRITERION

This appendix outlines the development of a rational yield-failure theory utilized in the design guidelines of this report.

In keeping with the yield-failure definition set forth in this report, two entities must be completely described. First, the location and relative magnitude of the maximum effective stress, σ_o, must be evaluated; and second, the material yield strength, σ_y, must be determined. Unfortunately, acrylic exhibits time dependency, consequently, both of the above entities are functions of time, i.e., loading history. Because of the infinite variety of possible loading histories, the general design procedure would be to choose the most unfavorable loading history to account for all other less severe cases.

For the special case of acrylic viewports, the most detrimental loading history would be represented by a step loading raised immediately to maximum operational depth and held there for the given duration. Moreover, if acrylic was purely viscoelastic, the stress distribution in the viewport at time $T = 0^+$, is identical to the distribution resulting from an elastic analysis and represents the most unfavorable distribution in terms of the high magnitudes and stress concentrations. As time progresses, stress relaxation occurs relieving and redistributing high stress concentrations. Thus, in terms of the viscoelastic behavior, the elastic solution ($T = 0^+$) may be conservatively used to determine the maximum stress concentrations and assume these magnitudes constant with time rather than decreasing. Actually, the conservative assumption of constant viewport stresses is quite accurate due to the phenomenon that the elastic stresses of conical frustums are independent of Young's modulus and only slightly dependent on Poisson's ratio. Hence, in view of the correspondence principle, which relates elastic and viscoelastic solutions, time would have very little effect on the viscoelastic stresses. In light of the above, one can rationally accept the stresses resulting from an elastic analysis (approximated by the finite element technique) as the governing stresses throughout the loading duration, providing there is adequate recovery time between loadings.

The effect of time on the material yield stress, σ_Y, which has been observed to decrease as loading time progresses,is next considered A graphical relationship of this is presented in Figure 18 in the Design Recommendation portion of this report. At this point, a qualitative outline is presented, illustrating the origination of the graph.

Consider the typical creep data shown in a of Figure C-1 where each curve represents the strain-time relation for a given level of stress. If a particular time, T_1, is selected and corresponding values of stress and strain are plotted as shown in b of Figure C-1, an isochronous stress-strain relationship results. Because time has been held constant, any curvature in the stress-strain relation is due to either yielding or nonlinearity of the material. Curvature arising solely from nonlinearity does not limit the yield-strength of the material as previously defined, however, existing creep data for acrylic does not contain unloading histories and permanent set records, thus rendering it impossible to separate the effect of nonlinearity from yielding. Therefore, it was conservatively assumed that all curvature was due to yielding and that the yield strength at time T_1 was defined as the 0.2% offset strain intersect of the isochronous stress-strain relation. Following the above procedure for several different times of interest, a curve can be generated as in c of Figure C 1 which establishes the yield-stress versus load-time relationship. The graph of this relationship for acrylic, displayed in Figure 18, was derived from creep data obtained from three sources [10,13,14] For some loading durations, creep data were nonexistent for Plexiglas G, but were approximated by engineering judgments of creep data on Plexiglas I-A

A STRESS SINGULARITY AND THE ANALYTICAL TOOL (FINITE ELEMENT)

In modeling the viewport by the finite element technique, a preliminary investigation was conducted to determine an adequate number of quadrilateral elements to represent the system It can be shown by variational theorems that the finite element solution approaches the exact solution as the number of elements approach infinity Of practical importance, the convergence of the finite element model can be determined by comparing stresses obtained from a coarse mesh with those obtained from a finer mesh. In so doing, it was discovered that about 400 elements was a sufficient number, such that, further increase in the number of elements did not appreciably alter the numerical values of stresses at a given point. This held true throughout the entire cross section except for one very notable

point, namely, a minute region in the neighborhood of the low-pressure face corner. At this particular location all stresses were becoming exceedingly higher as the number of elements were increased. Further subdivision in this corner revealed that these stresses were becoming arbitrarily high, suggesting that the corner point stresses would approach infinitely high values if the subdividing process continued. In witness of this phenomenon, Figure C-2 portrays the computed effective stress as a surface over the cross section of a typical viewport in which the corner has been finely subdivided. This representation readily depicts the singular nature of this stress concentration as a Dirac spike. It was hypothesized that this spike has physical significance and that it is not simply an error emanating from the numerical technique involved. In support of this contention, it was observed that all experimental viewports exhibited a minute permanent plastic deformation at this corner even for moderate loads.

Taking the cue from experimental observations, the corner of the analytical model was "rounded" in an attempt to model the plastic deformation occurring in the actual viewport. Furthermore, care was taken to determine what effect various amounts of "rounding" had on the resulting stresses. It was discovered that the percentage of area removed did not alter stress values significantly providing the percentage of deformation (percentage of area removed) was greater than about 0.02%. Figure C-3 illustrates this relationship where it is seen that the relative maximum effective stress stabilizes for deformation percentages above 0.02%, *independent of the mesh size.* In view of this, it was hypothesized that in a physical case the viewport would deform approximately 0.02% to relieve the Dirac spike stress concentration. This contention was supported by the percentage of deformation measured in the viewport shown in Figure 4 of this report.

In summary, the philosophy to be adopted in comparing the analytical and experimental results is that, under initial loading, the actual viewport will undergo minute local yielding which results in deformation at the low-pressure face corner, to relieve itself of the spiked stress concentration. This results in a "modified" structure which, when analyzed, does not display the Dirac spike stress concentration, but rather a realistic stress concentration with some finite value. Thus, from the analytical standpoint, the initial yielding problem is dismissed by beginning the analysis with the modified structure (deformed corner). Accordingly, the failure definition applies to the modified structure for both fixed and free boundary condition.

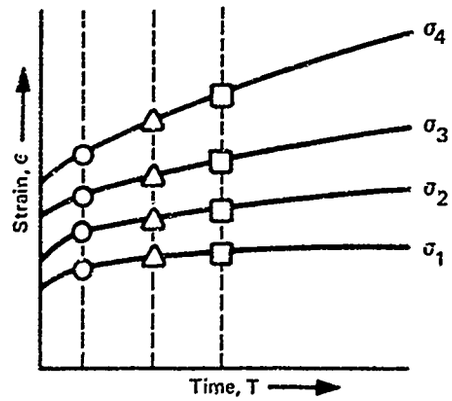

(a) Creep curves.

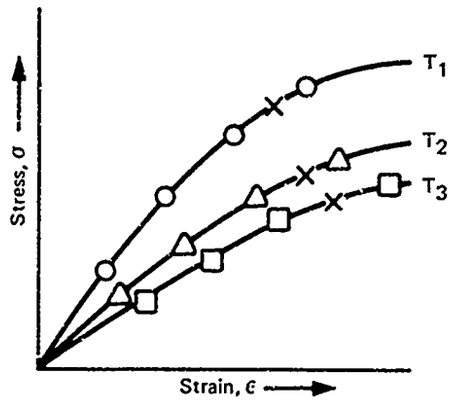

(b) Isochronous curves.

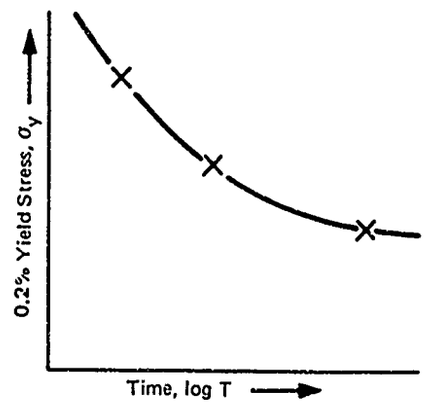

(c) Yield stress-time curve.

Figure C-1. Material property curves for acrylic plastic.

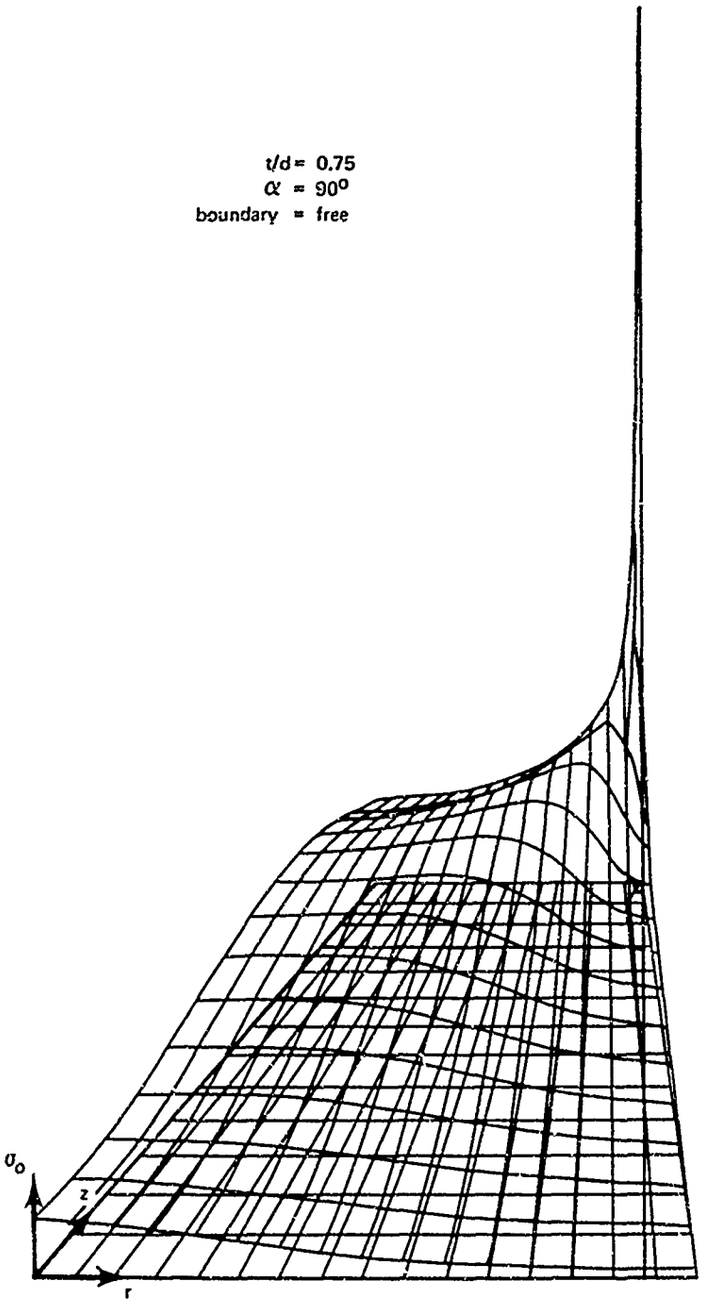

Figure C-2. Effective stress surface plot for sharp corner.

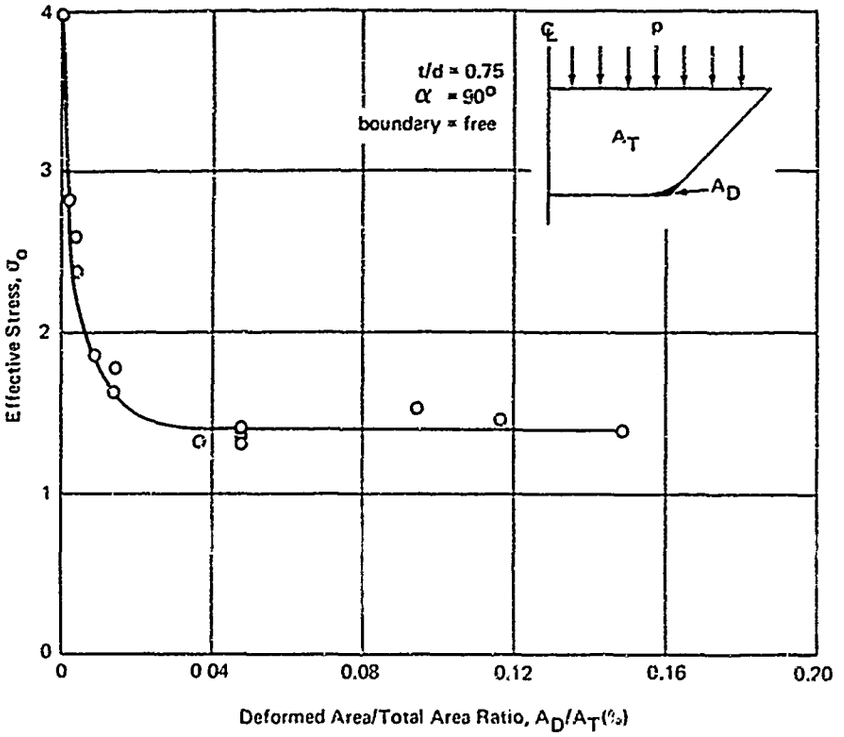

Figure C-3. Effective stress variation at low-pressure face corner.

REFERENCES

1. A. Piccard. Earth, sky and sea. New York, Oxford University Press, 1956.

2. M. R. Snoey and J. D. Stachiw. "Windows and transparent hulls for man in hydrospace," in A critical look at marine technology; transactions of the 4th annual MTS conference & exhibit, Washington, D.C , July 8-10, 1968. Washington, D.C., Marine Technology Society, 1968, pp. 419-463.

3. Allied Research Associates, Inc. Technical Report ARA 350-3 Tests of acrylic deep submergence windows under simulated operational conditions, by R. Winter and J. Pozerycki. Concord, Mass., Sept. 1968 (Contract no N00024-67-C-5351) (AD 848287)

4. Naval Ship Research and Development Center. Technical Report 2944 Evaluation of full-scale DSRV-1 acrylic windows under external pressure, by M. A. Krenzke, M C Breiter, and L N. Gifford. Washington, D C , Jan 1969 (AD 849354)

5. Naval Civil Engineering Laboratory. Technical Report R-675 Stress analysis of a conical acrylic viewport, by M. R Snoey and J E Crawford Port Hueneme, Calif , Apr 1970

6 A Nadai Theory of flow and fracture of solids, vol 1 New York, McGraw-Hill, 1950

7 General Electric Company Advanced Technology Laboratories Report No 61GL181 The effects of biaxial stresses on the deformation and fracture of polymethylmethacrylate, by R L Thorkildsen and W V Olszewski, Schenectady, N.Y , Apr 1962.

8 Army Missile Command Physical Sciences Laboratory. Report No RR-TR-64-15 Combined stress properties for acrylic tube specimens, by R E. Ely Redstone Arsenal, Ala., Aug. 1964. (AD 450662)

9 E L Wilson. "Structural analysis of axisymmetric solids," American Institute of Aeronautics and Astronautics, Journal, vol. 3, no 12, Dec. 1965, pp. 2269-2274

10 Armed Forces Supply Support Center. Military Handbook MIL-HDBK-17 Plastics for flight vehicles, pt. 2 Transparent glazing materials. Washington, D C., Aug. 1961.

11. Rohm and Haas Company. Publication no. PL-28n. PLEXIGLAS design and fabrication data, Rev. ed. Philadelphia, Pa., Sept. 1964.

12 Naval Civil Engineering Laboratory. Technical Note N-1072: Seal systems in hydrospace, Phase III: Effects of long-term hydrospace exposure on seal system integrity. 189 days at 5900 feet, by J. F. Jenkins and F. M. Reinhart Port Hueneme, Calif., Jan. 1970.

13. J. Marin and Y. Pao. "On the accuracy of extrapolated creep-test relations for plexiglas subjected to various stresses," American Society of Mechanical Engineers, Transactions, vol. 74, Oct. 1952, pp. 1231-1240.

14. Rohm and Haas Company. PLEXIGLAS handbook for aircraft engineers, 2nd ed Philadelphia, Pa., 1952, pp. 15-16.

LIST OF SYMBOLS

A_D, A_T	Deformed and total areas of viewports, $in.^2$
D	Diameter of high-pressure face, in.
d	Diameter of low-pressure face, in.
h	Elevation of viewport in flange, in.
p	Pressure applied to viewport, psi
r	Radial coordinate, in.
S.F.	Safety factor
T	Time, indicated units
T^o	Temperature, ^oF
t	Thickness of viewport, in.
z	Axial coordinate, in.
α	Included angle of conical viewport, degrees
δ_z	Axial displacement of viewport, in.
ϵ	Strain, in./in.
θ	Tangential coordinate, degrees
$\sigma_1, \sigma_2, \sigma_3$	Principal stresses per unit of applied pressure, psi/psi
σ_o	Effective stress per unit of applied pressure, psi/psi
σ_y	Yield stress, psi

DISTRIBUTION LIST

SNDL Code	No. of Activities	Total Copies	
–	1	20	Defense Documentation Center
FKAIC	1	10	Naval Facilities Engineering Command
FKNI	10	10	NAVFAC Engineering Field Divisions
FKN5	9	9	Public Works Centers
FA25	1	1	Public Work Center
–	11	11	RDT&E Liaison Officers at NAVFAC Engineering Field Divisions and Construction Battalion Centers
–	310	310	NCEL Special Distribution List No. 9 for persons and activities interested in reports on Deep Ocean Studies

Unclassified

Security Classification

DOCUMENT CONTROL DATA - R & D

Security classification of title, body of abstract and indexing annotation must be entered when the overall report is classified)

1 ORIGINATING ACTIVITY (Corporate author) Naval Civil Engineering Laboratory Port Hueneme, California 93041	2a. REPORT SECURITY CLASSIFICATION Unclassified 2b. GROUP

3 REPORT TITLE

STRUCTURAL DESIGN OF CONICAL ACRYLIC VIEWPORTS

4 DESCRIPTIVE NOTES (Type of report and inclusive dates)
Final; April 1967—April 1969

5 AUTHOR(S) (First name, middle initial, last name)

M. R. Snoey and M. J. Katona

6 REPORT DATE June 1970	7a. TOTAL NO OF PAGES 57	7b NO OF REFS 14
8a. CONTRACT OR GRANT NO b PROJECT NO YF 38.535.005.01.005 c. d.	9a. ORIGINATOR'S REPORT NUMBER(S) TR-686 9b. OTHER REPORT NO(S) (Any other numbers that may be assigned this report)	

10 DISTRIBUTION STATEMENT

This document has been approved for public release and sale; its distribution is unlimited.

11 SUPPLEMENTARY NOTES	12 SPONSORING MILITARY ACTIVITY Naval Facilities Engineering Command Washington, D. C. 20390

13 ABSTRACT

The purpose of this report is to establish a rational engineering approach for the design of conical acrylic viewports. To achieve this goal, a time-dependent, yield-failure criterion was developed and utilized in the analysis of a variety of viewport configurations. Specifically, a range of thickness/minor diameter (t/d) ratios from 0.25 to 1.75 and included angles from 60° to 120° were analyzed by the finite element technique. Using the viewport structural analysis in conjunction with the yield-failure criterion for acrylic, time-dependent operating depths were determined as a function of viewport configuration.

Paralleling the above, an experimental investigation was performed to validate the analytical results. Six full-scale viewports were tested for a year under simulated operational conditions that included simultaneous cycling of pressure and temperature, 0 to 4,000 psi and 70 to 35°F, respectively.

Comparison of analytical and experimental results indicated excellent agreement for the physical location of viewport failure at specified loading histories.

Design recommendations are presented in the form of design curves which enable the design of a conical acrylic viewport for a specified operating pressure and duration under load. To complete the recommendations, design information is given also on sealing with a conventional O-ring, as well as guidelines for elevating a viewport in its flange.

DD FORM NO. 1473 (PAGE 1)

S/N 0101-807-6801

Unclassified

Security Classification

14 KEY WORDS	LINK A		LINK B		LINK C	
	ROLE	WT	ROLE	WT	ROLE	WT
Acrylic plastic						
Plexiglas						
Undersea vehicles						
Design curves						
Habitats						
Viscoelastic						
Submersibles						
O-ring seal						
Finite element						
Pressure cycling						
Deep submergence						
Stress analysis						
Yield failure criterion						
Windows						
Failure theory						
Hydrostatic pressure test.						
Pressure vessels						
Conical viewports						